AD_____

Award Number: DAMD17-99-1-9272

TITLE: Resources for Precision Analysis of Human Breast Cancer

PRINCIPAL INVESTIGATOR: Doctor Peter H. Watson

CONTRACTING ORGANIZATION: University of Manitoba
Winnipeg, Manitoba R3E 0W3 Canada

REPORT DATE: August 2002

TYPE OF REPORT: Final

PREPARED FOR: U.S. Army Medical Research and Materiel Command
Fort Detrick, Maryland 21702-5012

DISTRIBUTION STATEMENT: Approved for Public Release;
Distribution Unlimited

REPORT DOCUMENTATION PAGE

Form Approved
OMB No. 074-0188

1. AGENCY USE ONLY (Leave blank)	2. REPORT DATE	3. REPORT TYPE AND DATES COVERED
	August 2002	Final (15 Jul 99 - 15 Jul 02)

4. TITLE AND SUBTITLE
Resources for Precision Analysis of Human Breast Cancer

5. FUNDING NUMBERS
DAMD17-99-1-9272

6. AUTHOR(S)
Doctor Peter H. Watson

7. PERFORMING ORGANIZATION NAME(S) AND ADDRESS(ES)
University of Manitoba
Winnipeg, Manitoba R3E 0W3 Canada

E-Mail: pwatson@cc.umanitoba.ca

8. PERFORMING ORGANIZATION REPORT NUMBER

9. SPONSORING / MONITORING AGENCY NAME(S) AND ADDRESS(ES)
U.S. Army Medical Research and Materiel Command
Fort Detrick, Maryland 21702-5012

10. SPONSORING / MONITORING AGENCY REPORT NUMBER

11. SUPPLEMENTARY NOTES

12a. DISTRIBUTION / AVAILABILITY STATEMENT
Approved for Public Release; Distribution Unlimited

12b. DISTRIBUTION CODE

13. Abstract ***(Maximum 200 Words)*** *(abstract should contain no proprietary or confidential information)*
This US Army academic award has guaranteed ongoing protection and a balance of 75/25% of my time for research/clinical activities. This has ensured my continued active contribution to breast cancer research through specific projects underway in my laboratory as well as through efforts to maintain and improve on resources that offer appropriately processed, relevant and pathologically defined tissue samples to other investigators. This award has allowed the PI to 1) continue to advance research projects that are currently ongoing in the laboratory focusing on the role of the psoriasin and lumican genes, the identification and study of additional novel genes associated with progression of pre-invasive DCIS to invasive disease, and 2) continue to direct the Manitoba Breast Tumor Bank and offer clinical pathology expertise and advice to many investigators who seek access to appropriate tissues to test their ideas.

14. SUBJECT TERMS
breast cancer, ductal carcinoma in-situ, tumor bank

15. NUMBER OF PAGES
268

16. PRICE CODE

17. SECURITY CLASSIFICATION OF REPORT	18. SECURITY CLASSIFICATION OF THIS PAGE	19. SECURITY CLASSIFICATION OF ABSTRACT	20. LIMITATION OF ABSTRACT
Unclassified	Unclassified	Unclassified	Unlimited

TABLE OF CONTENTS

Front cover	*1*
SF298	*2*
Table of Contents	*3*
Introduction	*4*
Body	*5-24*
Key Research Accomplishments	*25-26*
Reportable Outcomes	*27-32*
Conclusions	*33-34*
References	*35-37*
Appendices	*38-268*

"Resources for precision analysis of human breast cancer" - Dr Peter H. Watson

INTRODUCTION.

The past decade has seen dramatic progress in our understanding of the basic cell and molecular biology of breast cancer. However, the translation of this basic science knowledge and ideas has been impeded by the limited numbers of clinician-scientists with skills to effectively collaborate with basic scientists and to accurately interpret tissue pathology, quality and the cellular composition of heterogeneous tissue samples subjected to molecular study. Beyond this there is the problem of access to appropriate human tissue samples. The PI's overall goal is the improvement in our current ability to predict individual risk of development of invasive disease and to predict further progression of invasive disease in terms of resistance to therapies. The specific aims of the PI are 1) continue to advance the two general avenues of research that are currently ongoing in the laboratory and which have direct relevance to important clinical problems in the management of early pre-invasive disease and the therapy of later advanced disease, 2) continue to direct the Manitoba Breast Tumor Bank and offer clinical pathology expertise and advice to many investigators who seek access to appropriate tissues to test their ideas, and 3) to work with others to develop and analyze new tissue resources such as those based on collection of pre-invasive lesions and tissue samples and collection of tumor samples associated with clinical trials.

BODY OF REPORT

The accomplishments over the three years of this award are summarized in four sections with reference to the tasks defined in the original statement of work (entered in italics in each section).

Task 1. To develop the National Clinical Trial Tumor Bank Module

- *Complete supervision of collection of material from recently completed NCIC-CTG Trials and conduct histological analysis of all samples (months 0-12)*
- *Continue and refine prospective collection mechanism from collaborating centers (months 0-24)*
- *Travel to new centers in Canada to discuss protocols and enrol in the network (months 0-24)*

Years 1,2,3.

The PI has worked closely with Dr K. Pritchard (breast site group chair for the NCIC-clinical trials group, NCIC-CTG) and other colleagues across Canada, funded jointly by a grant from the NCIC (1997-2000) to develop an NCIC clinical trial breast tumor bank. The PI also served as Chair of the NCIC-CTG biological studies section 1998-1999 and is currently on the executive of the section. The PI assisted in writing and representing at a site visit, Kingston Dec'98) the relevant components of the renewal of the NCIC-CTG major program grant application to the NCIC. This successfully secured funding for the CTG to support administrative functions associated with Tissue Banking. The studies section functions through regular conference calls and annual meetings. The initial focus was on collection of paraffin tissue blocks associated with the completed MA5 trial and has been subsequently extended to involve retrospective collection from MA12 and prospective collection from all ongoing breast cancer trials. We have also sought to collect frozen tissue blocks, and collected frozen tissues from 11 MA5, 54 MA12 (both completed trials) and 25 MA14 (currently ongoing trial). The low yield for MA5 was not unexpected but

we had anticipated more cases from the more recently completed MA12 trial. The gap between our expectation and the actual yield reflects an uphill battle that we have faced with the rapid discontinuation of the frozen tissue estrogen receptor (ER) and progesterone receptor (PR) labs across the country, as ER and PR began to be measured by immunohistochemical techniques. The PI also contributed to an unsuccessful application from the CTG to the Canada Foundation for Innovation (submitted Jan 1999), to seek more substantial funds for Tumor Banking within the CTG. Additional activity related to network development is described below.

Task 2. To develop the Pre-neoplastic Tissue Tumor Bank Module

- *Continue supervision of database of Manitoba Breast Surgical Events and collection of representative paraffin blocks from collaborating pathology centers (months 0-36)*
- *Continue to direct accrual of tissue samples and data from collaborating center in Warsaw and conduct histological analysis of all samples (months 0-36)*
- *Travel to Warsaw to discuss protocols and collection system (months 0-12 and 24-36)*

Years 1,2,3

The first objective in this task was to continue to expand on the Manitoba Breast Surgical Events Database (MBED) in order to create a virtual database of patients with breast lesions including preneoplastic and preinvasive lesions within paraffin blocks stored in clinical pathology departments. Initiated in 1996, it now comprises a virtual database linked to specific paraffin blocks in the archives of 8 pathology departments linked by a common laboratory program. As of June 2002 this database contained 17,744 events on approximately 12,540 patients. This represents a steady rate of case accrual since our last audit in July 2001 with approximately 2,590 new events and 1,740 new patients. These events include

a spectrum of pathological changes limited to only normal tissue, fibrocystic changes, ductal hyperplasia, atypical ductal hyperplasia, in-situ carcinoma, and also cases with invasive carcinoma and combinations of pre-invasive lesions. In time we will create a large dataset of pre-neoplastic lesions in paraffin blocks and a small but invaluable 'longitudinal' dataset comprised of lesions in breast biopsies associated with later higher grade lesions or invasive tumors in the same patients 'captured' in the Tumor Bank.

A second objective was to further augment the ability of the tumor bank to support research into pre-neoplastic and pre-invasive disease by accruing frozen tissues containing these lesions (in addition to paraffin block tissues encompassed by the MBED). Given the very focal nature of such lesions, they can only be collected as frozen tissue by systematic accrual and careful analysis of tissues from areas adjacent to breast tumors. However, this simple strategy, though once feasible, is now very hard to apply in North America where changes in surgical and pathology practice dictate that limited tissue is resected and the peripheral tissue surrounding the tumor is destined for paraffin blocks, required for clinical assessment of margin status. Therefore we have tried to forge collaborations with pathology departments in countries where clinical practice still allows extensive sampling from larger specimens. Our initial goal was to establish such a collaboration with a center in Poland but after a promising start and collection of approximately 100 cases we could not sustain interest. We therefore considered several alternatives and the PI then visited the 2nd affiliated hospital, Wuhan, Hubei Province, China in 1999. The PI discussed plans to collaborate with the director of this center and the head of dept of Pathology. However, due to the scarcity of electrical power and cold storage, we have been unable to proceed with this collaboration in the absence of specific funding. A third approach has been through close colleagues at the University of Manitoba to establish a new potential linkage with a center in Kunming, China. Assurance of ethical review has been obtained from the president of the hospital and a formal letter of invitation to visit and

establish a collaboration with the 1st Peoples Hospital of Yunnan Province is in hand. The next steps will be a) pilot shipments of cases and review to assess the feasibility of instituting a sampling protocol and shipment of samples from China to Winnipeg, b) local ethics review by the Ethics Review Board at the University of Manitoba, and c) securing funding from a granting agency.

Task 3. To direct the NCIC-Manitoba Breast Tumor Bank

- *Continue to direct accrual of primary tumor tissue samples and data and conduct histological analysis of all samples (months 0-36)*
- *Continue to provide advice to external applicants to the Bank (months 0-36)*
- *Continue to supervise the review of applications, and undertake review and selection of appropriate cases for each study (months 0-36)*

Years 1,2,3

The Manitoba Breast Cancer Database (MBCD) section of the Bank now contains over 4500 fully processed cases (662 A category cases, 1490 B category cases, 2204 C category cases, 141 D category cases, 67 N category cases) and many further samples collected and partially processed in reserve to maintain the 'stocks'. All cases are associated with a database comprising pathological data derived from uniform assessment of the tissue blocks and clinical staging. A subset (all A&B cases) is also associated with complete clinical follow-up.

The Bank has provided support to researchers for more than 40 projects conducted in research laboratories across North America. The total aggregate of cases utlized and sections released in support of

these projects is 7,497 cases and 73,790 tissue sections. Over the past 3 years (mid-1999 to mid-2002) the Tumor Bank has utilized 2,879 cases and released 26,261 sections.

Over this period the Manitoba Breast Tumor Bank has acquired a national and international reputation as a unique resource and for its contribution to cancer research. This statement is supported in part by the wide geography of requests and reputation of users and recognition in national cancer research forums (eg "CBCRI Reasons for Hope conference, Quebec City 2001" and the "Future of Health Research and Economic Development in Western Canada", workshop sponsored by Western Economic Development Agency, Chair Dr Henry Friesen, 2001).

Tasks 1,2,3. Additional activities relevant to these tasks

In addition to continued direction of the Manitoba Breast Tumor Bank, the PI has been actively engaged as both an advocate and external consultant at both National and International levels. These activities are summarized as follows;

The NCIC 'tumor bank' program initially funded 4 Tumor Banks from 1993 (Breast, Lung, Brain, Sarcoma), all through regular operating grants. NCIC subsequently became uncomfortable with the mechanism of funding and review of this type of research infrastructure and engaged the Tumor Bank groups in discussions to identify a way to alter NCIC's commitment to these currently established Banks. A Tumor Bank Working Group was chaired by the PI from spring 1999 and these discussions led to a report (May 1998) with recommendations for a way that NCIC could alter the funding model in such a way that NCIC-Banks could evolve into a network of self sustaining enterprises. Nevertheless the NCIC Board decided to cease funding Tumor Banks as of June 30, 2001. The failure to convince the NCIC

board to maintain NCIC's involvement may have reflected several factors; the different interests and resources available to different Tumor Bank groups, the reluctance of investigators primarily skilled in research to accept the increased challenge and burden of securing income to provide these resources, and the reality that the transformation of a Tumor Bank into a self sustaining enterprise would require significant personal costs in individual research time and priorities.

While NCIC did not act on the Tumor Bank Working Group report, it has served as a template for two subsequent Canadian Provincial based Tumor Bank initiatives, for which the PI has served as an external consultant. The first of these is in British Columbia where the PI served a as a consultant to the Western Economic Development Agency (spring 2001) and assisted in their decision to fund a Provincial Tumor Tissue Resource within the British Columbia Cancer Agency (BCCA, coordinating P.I., Dr Simon Sutcliffe, 2002) http://www.bccancer.bc.ca/ABCCA/NewsCentre/2002BCCancerAgencyNews/20020216AllanRockandStephenOwenJoinBCCAandGenyousLifeSciencesToAnnounceAWorldClassCancerResource.htm. The second of these is in Ontario where the PI also served as an external consultant and assisted in the development of the Tumor Bank component within the Ontario Cancer Research Network (http://www.est.gov.on.ca/english/ar/nr_intro.cfm?news_id=212&body=yes). This involved assisting in proposals to the Ontario Government (coordinated by Mr Pat Lafferty, PriceWaterhouseCoopers LLP, in spring 2001) and subsequently working with the director Dr Bob Philips and contributing to a workshop (May 2002). The PI has also served as an external scientific advisor to the Clinical Breast Care Project developed by the Walter Reed US Army Center, and in this role attended the first CBCP offsite meeting Dec 2001.

The withdrawal of the NCIC from funding Tumor Banks in 2000 may also in part have reflected an anticipation that such infrastructure costs for cancer research would be better and more appropriately funded by other agencies including the newly created Canadian Institutes of Health Research (CIHR) and the Canadian Foundation for Innovation (CFI). However the CFI has evolved to focus on capital infrastructure such as equipment and buildings rather than operating funds and the CIHR has taken time to develop. The PI submitted a grant to the CIHR (multiuser equipment and maintenance competition, fall 2001) seeking support for the Manitoba Breast Tumor Bank and although successful in obtaining new equipment funding was not successful in obtaining operating funds. Nevertheless the Cancer Institute of the CIHR has sought further input on this and other issues through a Needs, Gaps and Opportunities (NGOA) RFA. The PI and collaborators (D. Bannerjee BC and D. Demetrik Alberta) applied for and were awarded a grant (March 2002-Jan 2003) to address this issue again through a national workshop. The PI has subsequently contributed to a series of conference call based discussions (March 2002-present) with a working group including representatives (Carlow, R. Deeley) of the Canadian Provincial Cancer Agencies (CAPCA), CIHR (P. Branton), the BCCA (V. Ling) and OCRN (B. Philips) to explore the best way to proceed on this front.

The PI has also continued to publish on the issue of the importance of Tumor Banking. (1)

Task 4. To direct the research program in our laboratory

- *Continue to direct laboratory studies to understand and identify markers of risk of progression from pre-invasive to invasive disease and examine the role of specific genes, including the psoriasin and lumican genes in conferring this risk (months 0-36)*

- *Continue to direct laboratory studies to understand and identify markers of resistance to endocrine therapy and examine the role of estrogen receptor variants and their influence on determination of ER/PR status and response to therapy. (months 0-36)*

Over the past 3 years these specific goals have evolved into four broad projects within the laboratory as well as several relevant collaborations as described below;

Psoriasin (S100A7) related projects.

Using our microdissection approach we had previously identified Psoriasin (S100A7) as differentially expressed between in-situ (DCIS) and invasive carcinoma. We had also shown that expression is relatively low in normal tissue and ductal hyperplasia, increased in atypical hyperplasia and highest in DCIS.

1. We have continued to study the psoriasin (S100A7) gene and have developed two anti-psoriasin polyclonal antibodies (a chicken IgY and a rabbit IgG). Antibody specificity was confirmed by analysis of transfected cell lines and the strong correlation between RT-PCR / in-situ hybridization detected levels of mRNA and western blot / immunohistochemistry detected protein. We observed that psoriasin protein, studied by immunohistochemistry in skin and breast tumors, is localized predominantly (but not exclusively) to epithelial cells, and we were intrigued to find that it appears to localize to both cytoplasm and nuclei (the latter most prominent in breast tumor cells). While there is evidence that secreted psoriasin can act as a chemotactic factor for CD-4 positive lymphocytes in psoriatic skin lesions, an intracellular biological function is unknown. Therefore, we became interested to pursue the possible intracellular role and interactions of psoriasin. To identify interacting proteins we used the yeast 2-hybrid assay to screen a normal breast cell library. From the first screen we have

identified 4 positive clones. At the time the first two genes were both recently identified components of the centrosome, RanBPM and spindle pole body protein hGCP3, while the other two cDNAs were Jab1, a transcription factor binding protein, and a gene of unknown function (CXX-1).

2. We initially pursued the potential interaction with RanBPM. RanBPM, a novel Ran binding protein, was found to specifically interact with psoriasin and this interaction was confirmed in vitro by co-immunoprecipitation. RT-PCR analysis of RanBPM mRNA expression in cell lines (n=13) shows that RanBPM is widely expressed in different cell types and that expression is higher in tumor compared to normal breast epithelial cell lines. RanBPM mRNA is also frequently expressed in invasive breast carcinomas (n=64) and a higher psoriasin/RanBPM ratio is associated with both ER negative ($p<0.0001$) and PR negative status ($p<0.001$), and inflammatory cell infiltrates ($p<0.0001$) within the tumor. These findings support the hypothesis that psoriasin may interact with RanBPM to influence microtubule functions that may contribute to breast tumor progression. (manuscript submitted). (2)
3. We have next examined the potential interaction with Jab1 and the effect of psoriasin on invasive breast tumor cells. We found that psoriasin physically interacts with Jab1 (c-jun activation-domain binding protein 1) in the yeast two-hybrid assay and confirmed this by co-immunoprecipitation assay in breast cells. Furthermore sequence analysis and additional yeast 2-hybrid experiments have also shown that this interaction involves a region within psoriasin that contains a Jab1 binding domain that is also present in other Jab1 interacting proteins. Psoriasin transfected MDA-MB-231 breast cancer cells also showed increased nuclear Jab1 and demonstrated several features consistent with an alteration in Jab1 activity including an increase in AP-1 activity, increased expression of AP-1 and HIF-1 dependent genes (VEGF and MMP13 and CAIX), and reduced expression of the cell-cycle inhibitor p27Kip1. Psoriasin overexpression in MDA-MB-231 cells was also associated with alteration of cellular functions that are associated with increased malignancy, including increased growth,

decreased adhesion and increased invasiveness in-vitro as well as increased tumorigenicity in-vivo in nude mice. We conclude that intracellular psoriasin influences breast cancer progression and that this may occur through stimulation of Jab1 activity. (3)

4. We have examined the persistence of psoriasin expression in a set of carefully selected invasive tumors that exhibited a range of types, grades and ER status. Psoriasin was significantly associated with poor prognostic markers including ER and PR negative ($p<0.0001$, $p=0.0003$) and lymph node positive status ($p=0.035$). Psoriasin protein expression is also associated with inflammatory infiltrates (all tumors excluding medullary where inflammation is a diagnostic criteria, $p=0.0022$). These results suggest that while psoriasin is often highly expressed in pre-invasive ductal carcinoma in-situ (DCIS), persistent psoriasin expression occurs in some invasive carcinomas and is associated with poor prognostic factors. (4)
5. We have gone on to examine psoriasin expression by immunohistochemistry in a cohort of 122 estrogen receptor negative invasive ductal carcinomas to determine any relationship with outcome and survival. Psoriasin expression was observed in 64/122 cases (52%) but was not correlated with other prognostic factors (including PR, size, grade, and nodal status) within this cohort. However, in univariate analysis psoriasin expression was associated with a shorter time to progression ($p<0.04$) and poor survival ($p<0.03$). In multivariate analysis psoriasin also emerged as independent indicator of time to progression (hazard ratio 1.98: 95% C.I. 1.13-5.46, $p=0.017$) and survival (hazard ratio 2.06: 95% C.I. 1.12-3.79 , $p=0.021$). These results suggest that psoriasin expression may be associated with a worse prognosis in estrogen receptor negative invasive ductal carcinomas and raise the possibility that psoriasin expression may also be an indicator of risk of progression in DCIS. (5)

Lumican related projects.

Using our microdissection approach we had previously identified lumican mRNA as differentially expressed between the stroma adjacent to pre-invasive and central invasive components of early breast tumors. RT-PCR and in situ hybridization study confirmed the presence of lumican mRNA in fibroblast-like cells within stroma of most tumors, with highest levels adjacent to in-situ components and beyond the invasive edge. Higher expression in the invasive tumor was also associated with poor prognostic markers.

1. Further study of lumican and other members of the small leucine-rich proteoglycan (SLRP) gene family in breast tissues was completed (in collaboration with Dr Peter Roughley, Montreal) to explore their relative role in breast tumor progression. Lumican and decorin were found to be expressed by similar fibroblast-like cells and are relatively abundant, while biglycan and fibromodulin are only detected occasionally and at low levels in breast tissues. However, while lumican mRNA expression was significantly increased in tumors ($n=34$, $p<0.0001$), decorin mRNA was decreased ($p=0.0002$) in neoplastic relative to adjacent normal stroma. This was accompanied by similar changes in both lumican ($p=0.0122$) and decorin (similar trend but p=ns) proteins. Alteration of lumican expression in breast tumor stroma may also be manifested by discordance between mRNA and protein localization in some tumors, where some areas (mostly central regions) can demonstrate mRNA expression by in-situ hybridization but no detectable protein in parallel sections assessed both by immunohistochemistry and microdissection in combination with western blot. (6)
2. We have gone on to examine the prognostic significance of lumican and decorin in a cohort of 140 invasive breast carcinomas by western blot analysis. All cases selected were axillary lymph node negative and treated by adjuvant endocrine therapy, as these represent early stage invasive disease and it is also in this subset of breast cancers that EGFR expression has been shown to be predictive of

outcome. The latter criteria is significant as it is believed that decorin is a natural ligand for EGFR and related growth factor receptors. Lumican and decorin expression was highly correlated ($r=0.45$, $p<0.0001$), but while low levels of lumican were associated with large tumor size ($p=0.0496$), negative estrogen receptor ($p=0.0024$) and negative progesterone receptor status ($p=0.0116$), and increased host inflammatory response ($p=0.0077$), low decorin levels were associated only with large tumor size ($p=0.0496$). However, using univariate analysis, low levels of lumican and decorin were both associated with a shorter time to progression ($p=0.0013$, $p=0.0262$) and poorer survival ($p=0.001$, $p=0.0076$). In multivariate analysis using the Cox regression model, low decorin was also shown to be an independent predictive factor for recurrence (hazard ratio 2.25: 95% C.I. 1.0-5.0, $p=0.047$) and survival (hazard ratio 3.39: 95% C.I. 1.2-9.6, $p=0.021$). These results suggest that low levels of SLRPs in breast tumors may be associated with a worse prognosis in lymph node negative invasive breast carcinomas and warrant further study with larger patient cohorts (manuscript submitted). (7)

Our work with the SLRPs has specifically interested us in identification of alterations in other intracellular factors. In a collaboration led by Dr Charis Eng, Ohio State Univ., we have begun to examine the existence and role of LOH (loss of heterozygosity) in stroma as opposed to the epithelial elements of breast cancer. Application of lazer capture microdissection to tissue samples in both laboratories and analysis in the Eng lab of 13 microsatellite markers has demonstrated that LOH can occur in stroma. (8,9)

<u>Ductal Carcinoma in-situ (DCIS) and markers of risk related projects.</u>

To address the critical issue of the biology of early breast tumor progression and improved determination of risk of progression in pre-invasive lesions, we have applied microdissection approaches in combination

with our uniquely designed tissue resource and molecular methodologies, in order to directly identify alterations that mark and may contribute to the development and progression of pre-invasive lesions.

1. We have microdissected and screened 10 invasive tumors using Research Genetics Array filters, combined with Pathways computer analysis software and identified a number of cDNA's that are differentially expressed between adjacent in-situ and invasive elements within the same tumor. Further assessment to identify patterns of highly and/or consistently differentially expressed cDNA's (ie those overexpressed in 3 or more DCIS/invasive tumor pairs) has found that 36 cDNAs are consistently differentially overexpressed in the DCIS versus invasive component. These 36 candidate cDNAs emerged from out of approximately 5000 ESTs and known genes included on the filter array (amongst which approximately 1500 were considered to be expressed above background level). Additional analysis has also found the following; a) the number of cDNAs overexpressed in DCIS vs invasive elements is higher in cases where there is necrosis in the DCIS component (mean # cDNAs = 135 in necrosis+ve DCIS versus 70 in necrosis –ve DCIS, p=0.0325 t-test) and b) the number of cDNAs is also higher in cases where the invasive component is high nuclear grade (mean #cDNAs = 112 where the invasive component is high nuclear grade versus 51 in low/intermediate nuclear grade, p=0.0104, t-test). Work is still in progress to confirm differential expression of these 36 candidates by other techniques including in-situ hybridization and RT-PCR.
2. To identify molecular alterations underlying the morphological features that separate low from high grade DCIS we have compared gene expression within this total cohort of 10 cases of DCIS (6 high and intermediate-grade DCIS with necrosis and 4 low-grade DCIS without necrosis). A set of 42 cDNAs, from a group of 1,500, has been identified that were consistently differentially

expressed and whose expression profile clustered with DCIS grade. Amongst this set, the angio-associated migratory protein (AAMP) was identified as a gene that is consistently higher in high grade DCIS and that is also induced by hypoxia in the T47D breast cancer cell line. Differential expression was confirmed by in situ hybridization and quantitative RT-PCR analysis of 37 DCIS. AAMP mRNA was associated with high and intermediate-grade DCIS (p=0.0155) and DCIS with necrosis (p=0.023). However, no relationship was observed between AAMP and angiogenesis, and its functional role in tumorigenesis and breast cancer progression remains to be determined.(10)

In collaboration with Adrian Harris's group, University of Oxford who are leaders in the field of tumor hypoxia and angiogenesis we are also currently examining the role of other hypoxia regulated genes as markers of progression in DCIS and early invasive breast cancer. This is particularly relevant because necrosis, which is thought to be an indicator of severe hypoxia in-vivo is also a marker of high risk of progression of DCIS to recurrence and invasive disease.

3. In one aspect of these studies we have focused on the carbonic anhydrase genes, CAIX and CAXII that influence intra- and extra- cellular pH and ion transport in varied biological processes, are also regulated by hypoxia and are HIF-1 dependent in cell lines including breast cancer cells (11). We then went on to show that expression of CAIX in particular, is associated with necrosis in vivo in both breast and other tumor types. Furthermore, in a cohort of 104 invasive breast cancers, CAIX expression was an independent predictor of recurrence free and overall survival (12). By contrast, factors related to differentiation appear to dominate regulation of CAXII in-vivo, and paradoxically high overall expression of CAXII is a good prognostic marker within the same tumor cohort, at least in univariate analysis (13). Next we examined the expression of CAIX and XII in 68 cases of

ductal carcinoma in-situ (DCIS; 39 pure DCIS and 29 DCIS associated with invasive carcinoma). As in invasive disease, CA IX was associated with necrosis (p=0.0053) and high grade (p=0.012). In contrast, CA XII was associated with the absence of necrosis (p=0.036) and low grade (p=0.012) but was occasionally observed to be induced adjacent to necrosis within high grade lesions. Assessment of mammographic calcification showed that CA XII expression was also associated with the absence of calcification (n=43, p=0.0083) (14). Our results demonstrate that induction of CA IX and CA XII occurs in regions adjacent to necrosis in DCIS. Furthermore, these data suggest that hypoxia may be a dominant factor in the regulation of CA IX, and that factors related to differentiation, as determined by tumor grade, dominate the regulation of CA XII. The associations of CAIX with an aggressive phenotype and outcome in invasive tumors suggest that it may be important as a predictor in DCIS and also as a target for therapy through the development of selective inhibitors of carbonic anhydrases, since the latter have recently been shown to prevent tumor invasion.

4. To further explore the relevance of hypoxia, we examined a series of 59 breast tumors to assess the relation between necrosis and hypoxia. Hypoxia was detected by coincident induction of hypoxia induced transcription factor HIF1 and the downstream genes CA IX and GLUT1 that are involved in the hypoxic response. Expression within tumor cells of all three markers was infrequent in 28 tumors with no necrosis. Among 31 tumors with necrosis the co–expression of all three markers was present in 7/31 (23%), while no hypoxia markers were expressed in 5/31 (16%) of tumors. The frequency of HIF1 expression (29%) was significantly lower than CAIX and GLUT1, which were frequently expressed (74% and 71% respectively) and strongly correlated to each other. Our results support the hypothesis that hypoxia is frequently but not always associated with necrosis in invasive breast tumors. Future studies to explore this relationship in DCIS and the discordance

between expression of HIF1 and downstream genes, may provide useful information for categorizing acute and chronic hypoxia as well as severity of hypoxia (manuscript in preparation).

5. To explore the relationship between apoptosis and necrosis we have examined expression of two cell death related genes in breast cell lines and tumors. Analysis of human carcinoma cell lines showed that both NIP3 and NIX are regulated in many tumour types, as well as in endothelial cells and macrophages. Regulation was hypoxia inducible factor-1 (HIF-1)-dependent, and HIF-1 expression was suppressed by von Hippel-Lindau protein (pVHL) in normoxic cells. Northern blotting and in situ hybridization analysis revealed that these factors are highly expressed in human tumours compared to normal tissue, and that NIP3 is upregulated in peri-necrotic regions of the tumour (15). In a subsequent study we have analysed 58 samples of DCIS (including low, intermediate and high grade, with or without associated invasive carcinoma) for expression of NIP3 and NIX mRNAs, and for markers of tumour environment such as vascular endothelial growth factor, necrosis, macrophages and blood vessels. We found that expression of NIP3, but not NIX, indicates the presence of a high grade, necrotic DCIS, which is likely to be associated with invasive carcinoma. These studies have showed that hypoxia regulates a specific necrosis pathway and may be a key drive to tumour evolution, including progression of DCIS. (16)

<u>ER related projects.</u>

Basic research into the mechanisms which underlie the clinical evolution of breast cancer from hormone dependent to hormone independent growth has identified alterations in specific components of the mechanism of estrogen action which may shortcircuit the requirement for estrogen and so contribute to 'hormonal progression'. Our aim has been to determine the in-vivo existence and the clinical relevance of these potential mechanisms, focusing on alterations at the level of the estrogen receptor (ER). Over the

past 3 years (1999-2002) we have made the following progress, much of it in close collaboration with Dr L C. Murphy's laboratory in our research group;

1. We have now shown that discrepancies in ER status determined by immunohistochemical assay (ER-IHA) can occur between different ER antibodies and that this may be attributable to the expression of truncated ERα variant proteins. (17)
2. To assess alternative indirect methods to assess ER status (from ligand binding and immunohistochemical assay) we have examined the application of Infrared (IR) spectroscopy applied to tissue sections to provide a molecular fingerprint of the tissue. In a cohort of 77 breast tumors and using a multivariate pattern recognition strategy to analyze IR spectra we have shown IR patterns relate to different biological characteristics of tumors and can predict both grade and ER status. (18)
3. To assess whether ERα variant expression measured in the primary tumor will reflect that seen in the metastasis we have examined synchronous primary and metastatic tumors (n=15) and found similar patterns and levels of truncated and deleted ERα mRNA variant expression, suggesting that altered expression of ERα is an event that occurs early in tumorigenesis. (19)
4. To assess the level of estrogen receptor (ER)-beta mRNA in tumors, we have examined the level of ER-β mRNA and found that this can be significantly lower in PR+ tumors compared with PR- tumors (p=0.036) but that no association with ER status (determined by ligand binding assay) is seen, suggesting the possibility that expression of ER-β in human breast tumors may be an additional marker of endocrine therapy responsiveness. Finally we have found that changes in the relative expression of ER-beta1, -beta2, and -beta5 variant mRNAs also occur (study cohort n=53) during breast tumorigenesis and tumor progression. (20,21)

5. We have also begun to assess the expression several steroid receptor associated molecules, including the RNA activator (SRA). In a cohort of 27 breast tumors, we found that SRA expression was similar in ER+/PR+ and in ER-/PR- tumors, but was significantly ($p < 0.05$) lower than in ER+/PR- and ER-/PR+ tumors. A variant form of SRA was also found and correlated with grade in breast tumor tissues ($r = 0.53$, $n = 27$, $p= 0.004$). The expression of a specific repressor of estrogen receptor activity (REA) was also investigated in 40 human breast tumor biopsy samples and was found to be positively correlated with estrogen receptor (ER) levels ($r = 0.3231$; $P = 0.042$) and also significantly higher in ER+ compared with ER- tumors ($p = 0.04$), with no significant differences associated with PR status. REA was also inversely correlated with tumor grade ($r = -0.4375$; $P = 0.005$). Expression of SRA and AIB1 and REA was also compared between normal and neoplastic tissues. While SRA and AIB1 were increased in tumors ($p<0.01$) REA was no different. However the AIB1:REA, SRA:REA, and SRA:AIB1 ratios were higher in tumors. These observations implicate changes in the expression of SRA, AIB1 and REA molecules as an additional factor in breast tumor progression and possibly alteration in response to endocrine therapy (22,23,24).
6. The role of altered MAP kinase expression was investigated using immunohistochemistry and specific antibodies which specifically detect the dually phosphorylated forms of erk 1 and 2. Active MAP kinase expression was detected in approximately 48% of primary human breast tumors, and was found to be significantly increased in the tumors compared to their matched adjacent normal breast tissues (Wilcoxon matched pairs statistical test, $P = 0.027$). No statistically significant correlations were found with grade, cellular composition, ER or PR status. However, a significant positive correlation ($r = 0.38$, $P = 0.0044$, $n = 55$) was obtained between active MAP kinase expression and the presence of lymph node metastases. Moreover, a statistically significant increase in the level of active MAP kinase (Wilcoxon matched pairs test, $P = 0.0098$) was found in concurrent lymph node metastases compared to their matched primary

breast tumors. These data support the hypothesis that active MAP kinase may be a marker of breast cancer metastasis and have a functional role in the metastatic process. We also investigated the possibility that active MAP kinase may be a marker of endocrine resistance. However, no statistically significant difference in detection or level of active MAP kinase expression was found in the primary tumors of node negative patients who later were found to respond to tamoxifen treatment (tamoxifen sensitive) or not respond to tamoxifen treatment (tamoxifen resistant). Therefore, active MAP kinase was unlikely to be a marker of endocrine sensitivity, or involved in de novo tamoxifen resistance. (25)

Collaborations

Access to the Manitoba Breast Tumor Bank resource and our tissue expertise is in no way dependent on establishing direct collaborations with the PI. Nevertheless some investigators have sought formal collaborations or assistance in detailed study design and analysis, and the PI also collaborates with colleagues within the University of Manitoba Breast Cancer Research Group on other projects. In the past 3 years this has resulted in the following additional abstracts and publications;

1. Regulation and Role of Hypoxia-Inducible Tumor-Associated Carbonic Anhydrases in Human Breast Cancer - Charles Clifton Wykoff, Peter H. Watson, Stephen K. Chia, Helen Turley, Kevin C. Gatter, Peter J. Ratcliffe, Adrian L. Harris, John Radcliffe Hospital, Oxford, UK; University of Manitoba, Winnipeg, Canada; British Columbia Cancer Agency, Vancouver, Canada; Wellcome Trust Centre for Human Genetics, Oxford, UK. Poster Session #3370, **AACR 2001**

2. Differential Gene Expression Analysis of Microdissected Ductal Carcinoma in Situ (DCIS) of the Breast - Adewale Adeyinka, Ethan D. Emberley, Charles C. Wykoff, Adrian L. Harris, Leigh C. Murphy, Peter H. Watson, University of Manitoba, Winnipeg, MB, Canada; John Radcliffe Hospital, Oxford, UK. Poster Session #310, **AACR, 2001**

3. T. Toyama, H. Iwase, P. Watson, H. Muzik, E. Saettler, A. Magliocco, L. DiFrancesco, P. Forsyth, I. Garkavtsev, S. Kobayashi, and K. Riabowol. Suppression of ING1 expression in sporadic breast cancer. **Oncogene** 18 (37):5187-5193, 1999.

4. W. R. Zeng, P. Watson, J. Lin, S. Jothy, R. Lidereau, M. Park, and A. Nepveu. Refined mapping of the region of loss of heterozygosity on the long arm of chromosome 7 in human breast cancer

defines the location of a second tumor suppressor gene at 7q22 in the region of the CUTL1 gene. **Oncogene** 18 (11):2015-2021, 1999.

5. H. Dotzlaw, E. Leygue, P. Watson, and L. C. Murphy. The human orphan receptor PXR messenger RNA is expressed in both normal and neoplastic breast tissue. **Clin.Cancer Res**. 5 (8):2103-2107, 1999.

6. E. Leygue, H. Dotzlaw, P. H. Watson, and L. C. Murphy. Altered expression of exon 6 deleted progesterone receptor variant mRNA between normal human breast and breast tumour tissues. **Br.J.Cancer** 80 (3-4):379-382, 1999.

7. B. Lu, H. Dotzlaw, E. Leygue, L. J. Murphy, P. H. Watson, and L. C. Murphy. Estrogen receptor-alpha mRNA variants in murine and human tissues. **Mol.Cell Endocrinol**. 158 (1-2):153-161, 1999.

8. J. W. Clark, L. Snell, R. P. Shiu, F. W. Orr, N. Maitre, C. P. Vary, D. J. Cole, and P. H. Watson. The potential role for prolactin-inducible protein (PIP) as a marker of human breast cancer micrometastasis. **Br.J.Cancer** 81 (6):1002-1008, 1999.

9. Myal Y, Blanchard A, Watson P, Corrin M, Shiu R, Iwasiou B. Detection of genetic point mutations by PNA-mediated PCR clamping usig paraffin embedded specimens. **Anal. Biochem**. 285:169-172, 2000

10. Lee J, Weber M, Mejia S, Bone E, Watson P, Orr W. A matrix metalloproteinase inhibitor, batimastat, retards the development of osteolytic bone metastases by MDA-MB-231 human breast cancer cells in Balb C nu/nu mice. **Eur J Cancer**. Jan;37(1):106-113. 2001

11. Yu-Hua Tseng, David Vicent, Jianhua Zhu, Yulian Niu, Adewale Adeyinka, Julie S. Moyers, Peter H. Watson and C. Ronald Kahn. Regulation of growth and tumorigenicity of breast cancer cells by the low molecular weight GTPase RAD and NM23. **Cancer Research** 1;61(5):2071-9. 2001

12. Miksicek RJ, Myal Y, Watson PH, Walker C, Murphy LC, Leygue E: Identification of a novel breast- and salivary gland-specific, mucin- like gene strongly expressed in normal and tumor human mammary epithelium. **Cancer Res** 62:2736-2740. 2002,

13. Expression of BAG-1 correlates with Bcl-2, p53, differentiation, estrogen and progesterone receptor in invasive breast carcinoma Shou-Ching Tang, Jessalyn Beck, Garry Chernenko, Sean Murphy, Desmond Robb, Peter Watson, Mahmoud Khalifa, Memorial University of Newfoundland, St. John's, NF, Canada; University of Manitoba, Winnipeg, MB, Canada. Abstract #227, **AACR 2002.**

14. Microarray analysis of differentially expressed genes during mouse mammary gland involution Nicole DeCorby, Peter Watson, Adewale Adeyinka, Molly Pind, Janini Balasubramaniam, Yvonne Myal, University of Manitoba, Winnipeg, MB, Canada. Abstract #2253, **AACR 2002.**

KEY RESEARCH ACCOMPLISHMENTS

In the 3 year period July 1999 – July 2002 the PI has contributed through studies in his own laboratory and with others to the following accomplishments;

Major Accomplishments

1. Fostering Tumor Banking through;
    - Continued operation and development of the Manitoba Breast Tumor Bank
    - Continued involvement at a national and international level as a consultant and advocate for Tumor Banking
2. Establishing the potential importance of psoriasin in breast cancer through;
    - identification of its association with properties associated with increased malignancy in breast cells and with poor relapse free and overall survival in breast tumors.
    - Discovery of a mechanism for these effects through interaction with the multifunctional transcription activator Jab1. This raises the possibility that future therapies aimed at modulating Psoriasin-Jab1 interaction and activity may influence early breast cancer progression.
3. Establishing the potential importance of Lumican and Decorin in breast cancer through;
    - Identification of Lumican and Decorin as the most abundant among the small leucine rich proteoglycan (SLRP) genes in breast tissues,
    - Demonstration that their expression is altered in breast tumors and that low levels of these extracellular proteins may be predictive of outcome in node negative invasive breast cancer.

Other Accomplishments (including collaborative accomplishments)

4. Establishing that the carbonic anhydrases genes CAIX and CAXII and hypoxia regulated, that expression of both may be predictive of outcome in invasive breast cancer, and that the altered expression of both occurs between low and high grade DCIS (in collaborative studies)

5. Observation that discrepancies in ER status determined by immunohistochemical assay and ligand binding assay may be attributable to the expression of truncated ERα variant proteins

6. Demonstration that altered expression of ER-beta and steroid receptor cofactor molecules can occur in breast tumors and therefore should be considered as factors that may influence response to therapies.

7. Establishing that an interaction occurs in-vitro and in-vivo between Psoriasin and a novel nuclear and centrosomal protein, RanBPM.

8. Establishing that the Angio-Associated Migratory Protein (AAMP) is hypoxia regulated and that the altered expression of AAMP occurs between low and high grade DCIS

9. Demonstrating that loss of heterozygosity (LOH) can not only occur in stroma adjacent to invasive carcinoma but that this LOH can be associated with clinical-pathological prognostic factors.

REPORTABLE OUTCOMES

PAPERS

1. Huang, E. Leygue, H. Dotzlaw, L. C. Murphy, and P. H. Watson. Influence of estrogen receptor variants on the determination of ER status in human breast cancer. **Breast Cancer Res.Treat.** 58 (3):219-225, 1999.

2. M. Jackson, J. R. Mansfield, B. Dolenko, R. L. Somorjai, H. H. Mantsch, and P. H. Watson. Classification of breast tumors by grade and steroid receptor status using pattern recognition analysis of infrared spectra. **Cancer Detect Prev.** 23 (3):245-253, 1999.

3. S. Al Haddad, Z. Zhang, E. Leygue, L. Snell, A. Huang, Y. Niu, T. Hiller-Hitchcock, K. Hole, L. C. Murphy, and P. H. Watson. Psoriasin (S100A7) expression and invasive breast cancer. **Am.J.Pathol.** 155 (6):2057-2066, 1999.

4. J. W. Clark, L. Snell, R. P. Shiu, F. W. Orr, N. Maitre, C. P. Vary, D. J. Cole, and P. H. Watson. The potential role for prolactin-inducible protein (PIP) as a marker of human breast cancer micrometastasis. **Br J Cancer** 81 (6):1002-1008, 1999.

5. E. Leygue, R. E. Hall, H. Dotzlaw, P. H. Watson, and L. C. Murphy. Oestrogen receptor-alpha variant mRNA expression in primary human breast tumours and matched lymph node metastases. **Br J Cancer** 79 (5-6):978-983, 1999.

6. H. Dotzlaw, E. Leygue, P. H. Watson, and L. C. Murphy. Estrogen receptor-beta messenger RNA expression in human breast tumor biopsies: relationship to steroid receptor status and regulation by progestins. **Cancer Res.** 59 (3):529-532, 1999.

7. E. Leygue, H. Dotzlaw, P. H. Watson, and L. C. Murphy. Expression of estrogen receptor beta1, beta2, and beta5 messenger RNAs in human breast tissue. **Cancer Res.** 59 (6):1175-1179, 1999.

8. E. Leygue, H. Dotzlaw, P. H. Watson, and L. C. Murphy. Expression of the steroid receptor RNA activator in human breast tumors. **Cancer Res.** 59 (17):4190-4193, 1999.

9. H. Dotzlaw, E. Leygue, P. Watson, and L. C. Murphy. The human orphan receptor PXR messenger RNA is expressed in both normal and neoplastic breast tissue. **Clin.Cancer Res.** 5 (8):2103-2107, 1999.

10. E. Leygue, H. Dotzlaw, P. H. Watson, and L. C. Murphy. Altered expression of exon 6 deleted progesterone receptor variant mRNA between normal human breast and breast tumour tissues. **Br J Cancer** 80 (3-4):379-382, 1999.

11. B. Lu, H. Dotzlaw, E. Leygue, L. J. Murphy, P. H. Watson, and L. C. Murphy. Estrogen receptor-alpha mRNA variants in murine and human tissues. **Mol.Cell Endocrinol.** 158 (1-2):153-161, 1999.

12. W. R. Zeng, P. Watson, J. Lin, S. Jothy, R. Lidereau, M. Park, and A. Nepveu. Refined mapping of the region of loss of heterozygosity on the long arm of chromosome 7 in human breast cancer defines

the location of a second tumor suppressor gene at 7q22 in the region of the CUTL1 gene. **Oncogene** 18 (11):2015-2021, 1999.

13. T. Toyama, H. Iwase, P. Watson, H. Muzik, E. Saettler, A. Magliocco, L. DiFrancesco, P. Forsyth, I. Garkavtsev, S. Kobayashi, and K. Riabowol. Suppression of ING1 expression in sporadic breast cancer. **Oncogene** 18 (37):5187-5193, 1999.

14. Leygue E, Snell L, Dotzlaw H, Hole K, Hiller-Hitchcock T, Murphy LC, Roughley PJ, Watson PH. Lumican and decorin are differentially expressed in human breast carcinoma. **J Pathology**. Nov;192(3):313-20. 2000

15. Murphy LC, Simon SL, Parkes A, Leygue E, Dotzlaw H, Snell L, Troup S, Adeyinka A, Watson PH. Altered expression of estrogen receptor coregulators during human breast tumorigenesis. **Cancer Research** Nov 15;60(22):6266-71. 2000.

16. S. L. Simon, A. Parkes, E. Leygue, H. Dotzlaw, L. Snell, S. Troup, A. Adeyinka, P. H. Watson, and L. C. Murphy. Expression of a repressor of estrogen receptor activity in human breast tumors: relationship to some known prognostic markers. **Cancer Res.** 60 (11):2796-2799, 2000.

17. C.C. Wykoff, N.J.P. Beasley, P.H. Watson, KJ Turner, J. Pastorek, GD Wilson, H. Turley PH Maxwell, P. Ratcliffe, A.L. Harris. Hypoxia induced regulation of tumor associated carbonic anhydrases. **Cancer Research** Dec 15;60(24):7075-83. 2000

18. Myal Y, Blanchard A, Watson P, Corrin M, Shiu R, Iwasiou B. Detection of genetic point mutations by PNA-mediated PCR clamping usig paraffin embedded specimens. **Anal. Biochem**. 285:169-172, 2000

19. Lee J, Weber M, Mejia S, Bone E, Watson P, Orr W. A matrix metalloproteinase inhibitor, batimastat, retards the development of osteolytic bone metastases by MDA-MB-231 human breast cancer cells in Balb C nu/nu mice. **Eur J Cancer**. Jan;37(1):106-113. 2001

20. Yu-Hua Tseng, David Vicent, Jianhua Zhu, Yulian Niu, Adewale Adeyinka, Julie S. Moyers, Peter H. Watson and C. Ronald Kahn. Regulation of growth and tumorigenicity of breast cancer cells by the low molecular weight GTPase RAD and NM23. **Cancer Research** 1;61(5):2071-9. 2001

21. Charles C. Wykoff, Nigel Beasley, Peter H. Watson, Stephen K. Chia, Ruth English, Jaromir Pastorek, William S. Sly, Peter Ratcliffe, and Adrian L. Harris "Expression of the Tumor Associated Carbonic Anhydrases IX and XII in Ductal Carcinoma In-Situ (DCIS) of the Breast." **Am J Pathology** 158(3):1011-9.2001

22. N.J.P. Beasley, C.C. Wykoff, P.H. Watson, R. Leek, H. Turley, K. Gatter, J. Pastorek, G.J. Cox, P. Ratcliffe, A.L. Harris. Carbonic Anhydrase IX expression in Head and Neck Squamous Cell Carcinoma and its relationship to hypoxia, necrosis and microvessel density. **Cancer Research.** 1;61(13):5262-7. 2001

23. Stephen K. Chia, Charles C. Wykoff, Peter H. Watson, Cheng Han, Russell D. Leek, Jaromir Pastorek, Kevin C. Gatter, Peter Ratcliffe and Adrian L. Harris "Prognostic Significance of a Novel

Hypoxia Regulated Marker –Carbonic Anhydrase IX in Invasive Breast Carcinoma." **J Clin Oncology** 19(16):3660-8, 2001

24. Sowter HM, Ratcliffe PJ, Watson P, Greenberg AH, Harris AL. HIF-1-dependent regulation of hypoxic induction of the cell death factors BNIP3 and NIX in human tumors. **Cancer Res.** 2001 Sep 15;61(18):6669-73

25. Kurose K, Hoshaw-Woodard S, Adeyinka A, Lemeshow S, Watson PH, Eng C. Genetic model of multi-step breast carcinogenesis involving the epithelium and stroma: clues to tumour-microenvironment interactions. **Hum Mol Genet.** 2001 Sep 1;10(18):1907-13.

26. Turner KJ, Crew JP, Wykoff CC, Watson PH, Poulsom R, Pastorek J, Ratcliffe PJ, Cranston D, Harris AL: The hypoxia-inducible genes VEGF and CA9 are differentially regulated in superficial vs invasive bladder cancer. **Br J Cancer** 2002, 86:1276-1282.29.

27. Miksicek RJ, Myal Y, Watson PH, Walker C, Murphy LC, Leygue E: Identification of a novel breast- and salivary gland-specific, mucin- like gene strongly expressed in normal and tumor human mammary epithelium. **Cancer Res** 2002, 62:2736-2740.

28. Adeyinka A, Nui Y, Cherlet T, Snell L, Watson PH, Murphy LC: Activated Mitogen-activated Protein Kinase Expression during Human Breast Tumorigenesis and Breast Cancer Progression. **Clin Cancer Res** 2002, 8:1747-1753.

PAPERS – submitted

1. Adewale Adeyinka, Ethan Emberley, Yulian Niu, Linda Snell, Leigh C. Murphy, Heidi Sowter, Charlie Wykoff, Adrian Harris, and Peter H. Watson Angio-Associated Migratory Cell Protein (AAMP) mRNA is a hypoxia-regulated protein associated with necrosis and is differentially expressed between High-grade and Low-grade Ductal Carcinoma In Situ (DCIS) of the Breast. Submitted to Int J Cancer
2. Sandra Troup, Cal Roskelley, Shukti Chakravarti, Peter J. Roughley, Leigh C. Murphy, Peter H. Watson. Reduced expression of the small leucine-rich proteoglycans, Lumican and Decorin, is associated with poor outcome in node negative invasive breast cancer. Submitted to Clinical Cancer Research
3. Keisuke Kurose, Stacy Hoshaw-Woodard, Adewale Adeyinka, Stan Lemeshow, Peter Watson and Charis Eng. Differential alterations in the epithelial and stromal compartments of breast cancers correlate with grade and nodal involvement. Submitted
4. Peter H. Watson, Stephen K. Chia, Charles C. Wykoff, Cheng Han, Russell D. Leek, Sly, Kevin C. Gatter, Peter Ratcliffe, and Adrian L. Harris "Carbonic Anhydrase XII is a marker of good prognosis in Invasive Breast Carcinoma." Submitted
5. Ladislav Tomes, Yulian Niu, Sandra Troup, Jaromir Pastorek, Adrian Harris, Peter H. Watson. Relationship between necrosis and immunohistochemical markers of hypoxia in invasive breast carcinoma. Submitted to J. Pathology

6. Ethan D. Emberley, A. Kate Hole , R. Daniel Gietz, J. Darren Campbell , Kent T. HayGlass , Leigh C. Murphy, Peter H. Watson. Psoriasin Interacts with RanBPM in Human Breast Cancer Cells. Submitted.
7. Ethan D. Emberley, Yulian Niu, Etienne Leygue, Ladislav Tomes, R. Daniel Gietz, Leigh C. Murphy, Peter H. Watson. Intracellular psoriasin interacts with Jab1 and influences breast cancer progression. Submitted to PNAS
8. Ethan D. Emberley, Yulian Niu, Catherine Njue, Erich V. Kliewer, Leigh C. Murphy, and Peter H. Watson. Psoriasin (S100A7) expression is associated with poor outcome in estrogen receptor negative invasive breast cancer. Submitted to Clin Cancer Research.
9. Salem Alowami, Gefei Qing, Ethan Emberley, Linda Snell, and Peter H. Watson. Psoriasin (S100A7) expression is altered during skin tumorigenesis. Submitted to J Path.
10. Heidi M. Sowter, Peter J. Ratcliffe, Peter Watson, Arnold H. Greenberg and Adrian L. Harris HIF-1-dependent regulation of hypoxic induction of the cell death factors BNIP3 and NIX in human tumours. Submitted.

CHAPTERS

1. Watson PH, Hiller T, Snell LS, Murphy LC, Leygue E, Dotzlaw H, "microdissection RT-PCR analysis of gene expression" in "Expression Genetics: Differential Display". Editors Arthur and Michael McClelland Eaton Publishing. 1999

2. Shiu R., Dubik D., Venditti J., Sparling J, Iwasiow B., Watson P., "Estrogen and c-myc oncogene actions in human breast cancer." In Proceedings of the the 3rd International Symposium on hormonal carcinogenesis. Editors JJ Liu, SA Li, J Darling. Springer Verlag. New York. NY. 1999.

3. Murphy LC, Leygue E, Dotzlaw H, Coutts A, Liu B, Huang A, Watson P. "Multiple facets of the estrogen receptor in human breast cancer". Endocrine OncologyEditor SP Ethier, Humana Press. , Chapter 2, pages 17-34, 2000 .

4. Watson PH. "The importance of tumor banking: bridging no-mans-land in cancer research". Expert Rev. Anticancer Ther. 2(1) 1-3, 2002

5. Murphy LC, Watson P. Steroid receptors in human breast tumorigenesis and breast cancer progression. Biomedicine and Pharmacotherapy. 56:65-77. Invited review. 2002.

ABSTRACTS

1. Lee B, Bowden G, Troup S, Watson P. Shiu RPC, Myal Y. Molecular and functional studies on the mosue submaxillary gland protein. The 16th International conference on oral biology, Virginia, 2000.

2. Peter H. Watson, Leigh C. Murphy, Etienne Leygue, Tamara Hiller-Hitchcock, Kate Hole, Sahar Al-Haddad, Zi Zhang, Linda Snell. Identification of markers of the invasive phenotype in human breast cancer. USAMRMC Era of Hope. Atlanta, June 2000.

3. Ethan D. Emberley[1]*, A. Kate Hole[1], R. Daniel Gietz[2], Leigh C. Murphy[2] and Peter H. Watson[1]. Interaction of the Differentially Expressed S100A7 Gene With Centrosomal Proteins., San Antonio Dec 2000.

4. Charles Clifton Wykoff, Peter H. Watson, Stephen K. Chia, Helen Turley, Kevin C. Gatter, Peter J. Ratcliffe, Adrian L. Harris, Poster Session - 3370 - Regulation and Role of Hypoxia-Inducible Tumor-Associated Carbonic Anhydrases in Human Breast Cancer Abstract # 3370 AACR 2001

5. Adewale Adeyinka, Ethan D. Emberley, Charles C. Wykoff, Adrian L. Harris, Leigh C. Murphy, Peter H. Watson, Differential Gene Expression Analysis of Microdissected Ductal Carcinoma in Situ (DCIS) of the Breast. Abstract # 310 AACR, 2001

6. Adeyinka A, Emberley E, Murphy LC, Watson PH. Differential Gene Expression Analysis of Microdissected Ductal Carcinoma In Situ of The Breast. CBCRI reasons for hope. May 2001

7. Emberley E, Murphy LC, Geitz RD, Watson PH. Role of RanBPM in breast cancer. CBCRI Reasons for Hope, May 2001

8. Keisuke Kurose, Satoshi Matsumoto, Kristie Gilley, Heather Dziema, Manju Prasad, Stacy Hoshaw-Woodard, Adewale Adeyinka, Stanley Lemeshow, Peter H. Watson, Charis Eng, Differential genetic alterations in the epithelial and stromal compartments of breast cancers correlate with grade and lymph node involvement. Abstract #4172, AACR 2002.

9. Sandra Troup, Catherine Njue, Erich V. Kliewer, Michelle Parisien, Cal Roskelley, Shukti Chakravarti, Peter J. Roughley, Leigh C. Murphy, and Peter H. Watson, Reduced expression of the small leucine-rich proteoglycans, lumican and decorin, is associated with poor outcome in node negative invasive breast cancer. Abstract LB159, AACR 2002.

10. Nicole DeCorby, Peter Watson, Adewale Adeyinka, Molly Pind, Janini Balasubramaniam, Yvonne Myal, Microarray analysis of differentially expressed genes during mouse mammary gland involution. Abstract #2253, AACR 2002.

PRESENTATIONS

1. Institute of Molecular Medicine, John Radcliffe Hospital, University of Oxford, UK. "Microdissecting elements of progression in breast cancer" Nov 1999

2. Cancer Care Manitoba, "Invasive phenotype in breast cancer", Winnipeg, Feb 2000

3. USAMRMC Era of Hope Breast Cancer conference, "Identification of markers of the invasive phenotype", Atlanta June 2000

4. Manitoba Laboratory Congress (MCMLS), "The role of tumor banks in research", Winnipeg, Oct 2000

5. FASEB 2001, "Microdissecting breast cancer tumor banks" Orlando Florida, March 2001

6. CBCRI Reasons for Hope conference, "Invasion genes in DCIS, - the real McCoy", Quebec City, May 2001

7. Manitoba Institute of Cell Biology, retreat "Genes involved in invasion of breast cancer" Oct 2001.

DATABASES

- NCIC-Manitoba Breast Tumor Bank – continued operation and development of a unique tissue resource and provision of cases to external investigators across North America

FUNDING

Operating Grants awarded;

- NCIC/CBCRI, "The role of Psoriasin in progression of early breast cancer", $109,000 pa, 2000-2003 (renewal)
- MRC, "The role of the small leucine rich proteoglycan in human breast cancer", $120,000pa, 2000-2003 (renewal)
- NCIC/CBCRI Streams of Excellence, group grant, "The role of extracellular matrix in mediating risk of breast cancer", $60,000 pa, 2000-2003
- MRC group grant, "Markers of Breast cancer progression", core grant, 2000.
- CIHR grant (PI Dr L.C. Murphy, co-PI Dr Watson) –"mechanisms of estrogen dependence and independence in human breast cancer", $117,000, July 2001-2004

Equipment and Workshop Grants awarded:

- CIHR, Needs Gaps and Opportunities RFA, "Tumor Banking in no-mans land", $80,000, 2002
- CIHR, Multiuser Equipment Grant, "Manitoba Breast Tumor Bank", $35,000, 2002.

Travel Grants awarded:

- Detweiler Travel Fellowship, Royal College of Physicians & Surgeons of Canada
- Burroughs Welcome Fund, Travel Fellowship

CONCLUSIONS

Importance & Implications: It is anticipated that the many studies that will be conducted by the users of the Manitoba Tumor Bank, will be facilitated and enhanced by access to histologically defined tissues containing invasive and pre-invasive breast lesions. This will lead to the identification of biological markers and cellular alterations that are directly relevant to the prediction of the natural history of onset and the later response to treatment of breast cancer. This knowledge will in turn ultimately contribute to strategies to predict and reduce risk of breast cancer or to circumvent resistance and improve on current treatments for invasive and metastatic disease. Our own research studies described above will also hopefully contribute to this knowledge.

Summary analysis of task related accomplishments:

- Tumor Bank related Tasks.
  - Task 1, to develop a National Clinical Trial Tumor Bank, has been successfully completed in collaboration with colleagues within the NCIC-CTG.
  - Task 2, to develop a Pre-neoplastic Tumor Bank Module, has been partially successful, in that continued development of a paraffin block 'virtual bank' has continued as planned, however despite significant effort we have still to secure an ongoing collaboration to enable us to develop a frozen tissue bank.
  - Task 3, to direct the Manitoba Breast Tumor Bank has been successfully completed with ongoing support by multiple users and projects.
  - Underlying all three of these Tasks is the issue of sustained support and funding for Tumor Bank infrastructure which remains an ongoing challenge that the PI has worked towards with mixed

success. On the one hand several major research funding agencies have either withdrawn or continued to stand back from involvement in direct support for this critical infrastructure. However the PIs efforts have contributed to an emergence of provincial support for Tumor Banking in Canada and renewed interest by national agencies (including CIHR and CAPCA) in linkage of these intiatives.

❖ Research related Tasks.

- Task 4 revolved around the PI's own research program. Successful renewal of operating grant funding from the CIHR and CBCRI in July 2000 provided the foundation for continued discovery of differentially expressed genes associated with the early stages of breast tumor progression and improved understanding of the biological role and functional importance of novel genes. These studies have included further work identifying roles in early breast tumor progression for psoriasin, lumican&decorin, CAIX&CAXII and the AAMP genes.
- Our work on psoriasin (S100A7) has been particularly stimulating. We had previously identified a highly expressed gene in DCIS, and in the past 3 years have shown that overexpression in breast cells can foster invasion and other aspects of tumor progression both in-vitro and in-vivo, shown that overexpression in invasive breast tumors is associated with markers of poor prognosis, short relapse free and overall survival, and identified potential mechanisms of action through interaction with Jab1 and RanBPM.
- The relationship between expression of psoriasin and these other potential markers and the risk of recurrence and progression of DCIS remains to be tested as does further exploration of the biological function and roles of different interacting pathways in the process of early progression.

REFERENCES

1. Watson PH. "The importance of tumor banking: bridging no-mans-land in cancer research". Expert Rev. Anticancer Ther. 2(1) 1-3, 2002

2. Ethan D. Emberley, A. Kate Hole , R. Daniel Gietz, J. Darren Campbell , Kent T. HayGlass , Leigh C. Murphy, Peter H. Watson. Psoriasin Interacts with RanBPM in Human Breast Cancer Cells. Submitted.

3. Ethan D. Emberley, Yulian Niu, Etienne Leygue, Ladislav Tomes, R. Daniel Gietz, Leigh C. Murphy, Peter H. Watson. Intracellular psoriasin interacts with Jab1 and influences breast cancer progression. Submitted to PNAS

4. S. Al Haddad, Z. Zhang, E. Leygue, L. Snell, A. Huang, Y. Niu, T. Hiller-Hitchcock, K. Hole, L. C. Murphy, and P. H. Watson. Psoriasin (S100A7) expression and invasive breast cancer. Am. J. Pathol. 155 (6):2057-2066, 1999.

5. Ethan D. Emberley, Yulian Niu, Catherine Njue, Erich V. Kliewer, Leigh C. Murphy, and Peter H. Watson. Psoriasin (S100A7) expression is associated with poor outcome in estrogen receptor negative invasive breast cancer. Submitted to Clin Cancer Research.

6. Leygue E, Snell L, Dotzlaw H, Hole K, Hiller-Hitchcock T, Murphy LC, Roughley PJ, Watson PH. Lumican and decorin are differentially expressed in human breast carcinoma. J Pathology. Nov;192(3):313-20. 2000

7. Sandra Troup, Cal Roskelley, Shukti Chakravarti, Peter J. Roughley, Leigh C. Murphy, Peter H. Watson. Reduced expression of the small leucine-rich proteoglycans, Lumican and Decorin, is associated with poor outcome in node negative invasive breast cancer. Submitted to Clinical Cancer Research

8. Kurose K, Hoshaw-Woodard S, Adeyinka A, Lemeshow S, Watson PH, Eng C. Genetic model of multi-step breast carcinogenesis involving the epithelium and stroma: clues to tumour-microenvironment interactions. Hum Mol Genet. 2001 Sep 1;10(18):1907-13.

9. Keisuke Kurose, Satoshi Matsumoto, Kristie Gilley, Heather Dziema, Manju Prasad, Stacy Hoshaw-Woodard, Adewale Adeyinka, Stanley Lemeshow, Peter H. Watson, Charis Eng, Differential genetic alterations in the epithelial and stromal compartments of breast cancers correlate with grade and lymph node involvement. Abstract #4172, AACR 2002.

10. Adewale Adeyinka, Ethan Emberley, Yulian Niu, Linda Snell, Leigh C. Murphy, Heidi Sowter, Charlie Wykoff, Adrian Harris, and Peter H. Watson Angio-Associated Migratory Cell Protein (AAMP) mRNA is a hypoxia-regulated protein associated with necrosis and is differentially expressed between High-grade and Low-grade Ductal Carcinoma In Situ (DCIS) of the Breast. Submitted to Int J Cancer

11. C.C. Wykoff, N.J.P. Beasley, P.H. Watson, KJ Turner, J. Pastorek, GD Wilson, H. Turley PH Maxwell, P. Ratcliffe, A.L. Harris. Hypoxia induced regulation of tumor associated carbonic anhydrases. Cancer Research Dec 15;60(24):7075-83. 2000

12. Stephen K. Chia, Charles C. Wykoff, Peter H. Watson, Cheng Han, Russell D. Leek, Jaromir Pastorek, Kevin C. Gatter, Peter Ratcliffe and Adrian L. Harris "Prognostic Significance of a Novel Hypoxia Regulated Marker –Carbonic Anhydrase IX in Invasive Breast Carcinoma." J Clin Oncology 19(16):3660-8, 2001

13. Peter H. Watson, Stephen K. Chia, Charles C. Wykoff, Cheng Han, Russell D. Leek, Sly, Kevin C. Gatter, Peter Ratcliffe, and Adrian L. Harris "Carbonic Anhydrase XII is a marker of good prognosis in Invasive Breast Carcinoma." Submitted

14. Charles C. Wykoff, Nigel Beasley, Peter H. Watson, Stephen K. Chia, Ruth English, Jaromir Pastorek, William S. Sly, Peter Ratcliffe, and Adrian L. Harris "Expression of the Tumor Associated Carbonic Anhydrases IX and XII in Ductal Carcinoma In-Situ (DCIS) of the Breast." Am J Pathology 158(3):1011-9.2001

15. Sowter HM, Ratcliffe PJ, Watson P, Greenberg AH, Harris AL. HIF-1-dependent regulation of hypoxic induction of the cell death factors BNIP3 and NIX in human tumors. Cancer Res. 2001 Sep 15;61(18):6669-73

16. Heidi M. Sowter, Peter J. Ratcliffe, Peter Watson, Arnold H. Greenberg and Adrian L. Harris HIF-1-dependent regulation of hypoxic induction of the cell death factors BNIP3 and NIX in human tumours. Submitted.

17. Huang, E. Leygue, H. Dotzlaw, L. C. Murphy, and P. H. Watson. Influence of estrogen receptor variants on the determination of ER status in human breast cancer. Breast Cancer Res.Treat. 58 (3):219-225, 1999.

18. M. Jackson, J. R. Mansfield, B. Dolenko, R. L. Somorjai, H. H. Mantsch, and P. H. Watson. Classification of breast tumors by grade and steroid receptor status using pattern recognition analysis of infrared spectra. Cancer Detect.Prev. 23 (3):245-253, 1999.

19. E. Leygue, R. E. Hall, H. Dotzlaw, P. H. Watson, and L. C. Murphy. Oestrogen receptor-alpha variant mRNA expression in primary human breast tumours and matched lymph node metastases. Br.J.Cancer 79 (5-6):978-983, 1999.

20. H. Dotzlaw, E. Leygue, P. H. Watson, and L. C. Murphy. Estrogen receptor-beta messenger RNA expression in human breast tumor biopsies: relationship to steroid receptor status and regulation by progestins. Cancer Res. 59 (3):529-532, 1999.

21. E. Leygue, H. Dotzlaw, P. H. Watson, and L. C. Murphy. Expression of estrogen receptor beta1, beta2, and beta5 messenger RNAs in human breast tissue. Cancer Res. 59 (6):1175-1179, 1999.

22. E. Leygue, H. Dotzlaw, P. H. Watson, and L. C. Murphy. Expression of the steroid receptor RNA activator in human breast tumors. Cancer Res. 59 (17):4190-4193, 1999.

23. S. L. Simon, A. Parkes, E. Leygue, H. Dotzlaw, L. Snell, S. Troup, A. Adeyinka, P. H. Watson, and L. C. Murphy. Expression of a repressor of estrogen receptor activity in human breast tumors: relationship to some known prognostic markers. Cancer Res. 60 (11):2796-2799, 2000.

24. Murphy LC, Simon SL, Parkes A, Leygue E, Dotzlaw H, Snell L, Troup S, Adeyinka A, Watson PH. Altered expression of estrogen receptor coregulators during human breast tumorigenesis. Cancer Research Nov 15;60(22):6266-71. 2000.

25. Adeyinka A, Nui Y, Cherlet T, Snell L, Watson PH, Murphy LC: Activated Mitogen-activated Protein Kinase Expression during Human Breast Tumorigenesis and Breast Cancer Progression. Clin Cancer Res 2002, 8:1747-1753.

APPENDICES

A. Table 1, Users and Projects supported by the NCIC-Manitoba Breast Tumor Bank. (1 page)

B. Papers

- Huang, E. Leygue, H. Dotzlaw, L. C. Murphy, and P. H. Watson. Influence of estrogen receptor variants on the determination of ER status in human breast cancer. **Breast Cancer Res.Treat.** 58 (3):219-225, 1999.
- M. Jackson, J. R. Mansfield, B. Dolenko, R. L. Somorjai, H. H. Mantsch, and P. H. Watson. Classification of breast tumors by grade and steroid receptor status using pattern recognition analysis of infrared spectra. **Cancer Detect Prev**. 23 (3):245-253, 1999.
- S. Al Haddad, Z. Zhang, E. Leygue, L. Snell, A. Huang, Y. Niu, T. Hiller-Hitchcock, K. Hole, L. C. Murphy, and P. H. Watson. Psoriasin (S100A7) expression and invasive breast cancer. **Am.J.Pathol.** 155 (6):2057-2066, 1999.
- J. W. Clark, L. Snell, R. P. Shiu, F. W. Orr, N. Maitre, C. P. Vary, D. J. Cole, and P. H. Watson. The potential role for prolactin-inducible protein (PIP) as a marker of human breast cancer micrometastasis. **Br J Cancer** 81 (6):1002-1008, 1999.
- E. Leygue, R. E. Hall, H. Dotzlaw, P. H. Watson, and L. C. Murphy. Oestrogen receptor-alpha variant mRNA expression in primary human breast tumours and matched lymph node metastases. **Br J Cancer** 79 (5-6):978-983, 1999.
- H. Dotzlaw, E. Leygue, P. H. Watson, and L. C. Murphy. Estrogen receptor-beta messenger RNA expression in human breast tumor biopsies: relationship to steroid receptor status and regulation by progestins. **Cancer Res.** 59 (3):529-532, 1999.
- E. Leygue, H. Dotzlaw, P. H. Watson, and L. C. Murphy. Expression of estrogen receptor beta1, beta2, and beta5 messenger RNAs in human breast tissue. **Cancer Res.** 59 (6):1175-1179, 1999.
- E. Leygue, H. Dotzlaw, P. H. Watson, and L. C. Murphy. Expression of the steroid receptor RNA activator in human breast tumors. **Cancer Res.** 59 (17):4190-4193, 1999.
- H. Dotzlaw, E. Leygue, P. Watson, and L. C. Murphy. The human orphan receptor PXR messenger RNA is expressed in both normal and neoplastic breast tissue. **Clin.Cancer Res.** 5 (8):2103-2107, 1999.
- E. Leygue, H. Dotzlaw, P. H. Watson, and L. C. Murphy. Altered expression of exon 6 deleted progesterone receptor variant mRNA between normal human breast and breast tumour tissues. **Br J Cancer** 80 (3-4):379-382, 1999.

- B. Lu, H. Dotzlaw, E. Leygue, L. J. Murphy, P. H. Watson, and L. C. Murphy. Estrogen receptor-alpha mRNA variants in murine and human tissues. **Mol.Cell Endocrinol**. 158 (1-2):153-161, 1999.

- W. R. Zeng, P. Watson, J. Lin, S. Jothy, R. Lidereau, M. Park, and A. Nepveu. Refined mapping of the region of loss of heterozygosity on the long arm of chromosome 7 in human breast cancer defines the location of a second tumor suppressor gene at 7q22 in the region of the CUTL1 gene. **Oncogene** 18 (11):2015-2021, 1999.

- T. Toyama, H. Iwase, P. Watson, H. Muzik, E. Saettler, A. Magliocco, L. DiFrancesco, P. Forsyth, I. Garkavtsev, S. Kobayashi, and K. Riabowol. Suppression of ING1 expression in sporadic breast cancer. **Oncogene** 18 (37):5187-5193, 1999.

- Leygue E, Snell L, Dotzlaw H, Hole K, Hiller-Hitchcock T, Murphy LC, Roughley PJ, Watson PH. Lumican and decorin are differentially expressed in human breast carcinoma. **J Pathology**. Nov;192(3):313-20. 2000

- Murphy LC, Simon SL, Parkes A, Leygue E, Dotzlaw H, Snell L, Troup S, Adeyinka A, Watson PH. Altered expression of estrogen receptor coregulators during human breast tumorigenesis. **Cancer Research** Nov 15;60(22):6266-71. 2000.

- S. L. Simon, A. Parkes, E. Leygue, H. Dotzlaw, L. Snell, S. Troup, A. Adeyinka, P. H. Watson, and L. C. Murphy. Expression of a repressor of estrogen receptor activity in human breast tumors: relationship to some known prognostic markers. **Cancer Res.** 60 (11):2796-2799, 2000.

- C.C. Wykoff, N.J.P. Beasley, P.H. Watson, KJ Turner, J. Pastorek, GD Wilson, H. Turley PH Maxwell, P. Ratcliffe, A.L. Harris. Hypoxia induced regulation of tumor associated carbonic anhydrases. **Cancer Research** Dec 15;60(24):7075-83. 2000

- Myal Y, Blanchard A, Watson P, Corrin M, Shiu R, Iwasiou B. Detection of genetic point mutations by PNA-mediated PCR clamping usig paraffin embedded specimens. **Anal. Biochem**. 285:169-172, 2000

- Lee J, Weber M, Mejia S, Bone E, Watson P, Orr W. A matrix metalloproteinase inhibitor, batimastat, retards the development of osteolytic bone metastases by MDA-MB-231 human breast cancer cells in Balb C nu/nu mice. **Eur J Cancer**. Jan;37(1):106-113. 2001

- Yu-Hua Tseng, David Vicent, Jianhua Zhu, Yulian Niu, Adewale Adeyinka, Julie S. Moyers, Peter H. Watson and C. Ronald Kahn. Regulation of growth and tumorigenicity of breast cancer cells by the low molecular weight GTPase RAD and NM23. **Cancer Research** 1;61(5):2071-9. 2001

- Charles C. Wykoff, Nigel Beasley, Peter H. Watson, Stephen K. Chia, Ruth English, Jaromir Pastorek, William S. Sly, Peter Ratcliffe, and Adrian L. Harris "Expression of the Tumor Associated Carbonic Anhydrases IX and XII in Ductal Carcinoma In-Situ (DCIS) of the Breast." **Am J Pathology** 158(3):1011-9.2001

- N.J.P. Beasley, C.C. Wykoff, P.H. Watson, R. Leek, H. Turley, K. Gatter, J. Pastorek, G.J. Cox, P. Ratcliffe, A.L. Harris. Carbonic Anhydrase IX expression in Head and Neck Squamous Cell Carcinoma and its relationship to hypoxia, necrosis and microvessel density. **Cancer Research.** 1;61(13):5262-7. 2001

- Stephen K. Chia, Charles C. Wykoff, Peter H. Watson, Cheng Han, Russell D. Leek, Jaromir Pastorek, Kevin C. Gatter, Peter Ratcliffe and Adrian L. Harris "Prognostic Significance of a Novel Hypoxia Regulated Marker –Carbonic Anhydrase IX in Invasive Breast Carcinoma." **J Clin Oncology** 19(16):3660-8, 2001

- Sowter HM, Ratcliffe PJ, Watson P, Greenberg AH, Harris AL. HIF-1-dependent regulation of hypoxic induction of the cell death factors BNIP3 and NIX in human tumors. **Cancer Res.** 2001 Sep 15;61(18):6669-73

- Kurose K, Hoshaw-Woodard S, Adeyinka A, Lemeshow S, Watson PH, Eng C. Genetic model of multi-step breast carcinogenesis involving the epithelium and stroma: clues to tumour-microenvironment interactions. **Hum Mol Genet.** 2001 Sep 1;10(18):1907-13.

- Turner KJ, Crew JP, Wykoff CC, Watson PH, Poulsom R, Pastorek J, Ratcliffe PJ, Cranston D, Harris AL: The hypoxia-inducible genes VEGF and CA9 are differentially regulated in superficial vs invasive bladder cancer. **Br J Cancer** 2002, 86:1276-1282.29.

- Miksicek RJ, Myal Y, Watson PH, Walker C, Murphy LC, Leygue E: Identification of a novel breast- and salivary gland-specific, mucin- like gene strongly expressed in normal and tumor human mammary epithelium. **Cancer Res** 2002, 62:2736-2740.

- Adeyinka A, Nui Y, Cherlet T, Snell L, Watson PH, Murphy LC: Activated Mitogen-activated Protein Kinase Expression during Human Breast Tumorigenesis and Breast Cancer Progression. **Clin Cancer Res** 2002, 8:1747-1753.

C. Chapters

- Watson PH, Hiller T, Snell LS, Murphy LC, Leygue E, Dotzlaw H, "microdissection RT-PCR analysis of gene expression" in "Expression Genetics: Differential Display". Editors Arthur and Michael McClelland Eaton Publishing. 1999

- Murphy LC, Leygue E, Dotzlaw H, Coutts A, Liu B, Huang A, Watson P. "Multiple facets of the estrogen receptor in human breast cancer". Endocrine OncologyEditor SP Ethier, Humana Press. , Chapter 2, pages 17-34, 2000 .

- Watson PH. "The importance of tumor banking: bridging no-mans-land in cancer research". Expert Rev. Anticancer Ther. 2(1) 1-3, 2002

- Murphy LC, Watson P. Steroid receptors in human breast tumorigenesis and breast cancer progression. Biomedicine and Pharmacotherapy. 56:65-77. Invited review. 2002.

Manitoba Breast Tumor Bank

Table of Users

	REQUESTOR	AFFILIATION	STUDY PURPOSE	INITIAL TISSUE REQUESTED	1st Date Tissue Released
1	Dr. Catalena Birek	U of M - oral biology	Use as controls to compare to salivary gland tmrs	3 frozen sects from normal, prim & met tiss blocks	94-09-13
2	Dr. Ted Bradley	Montreal Cancer Institute	Determine expression of RARb isoforms in breast compared - norm.	16c + 10-20 tmrs & 35 norm. breast tiss. B-class - frozen sections	94-08-11
3	Dr. Jim Davie	U of M Biochemistry	Identification of Nuclear matrix proteins in breast cancer	40 C-class cases	94-01-06
4	Dr. Joanne Emmerman	U of BC Anatomy	Analysis of breast ca cells in primary culture	10 breast cancer cases	95-03-14
5	Dr. Mike Jackson	NRC - Winnipeg	IR studies	100 tumors - X2, 20um of frozen sects.	94-05-04
6	Dr. Etienne Leygue	U of M Biochemistry & Molecular Biology	Molecular Mechanisms of Progression in Human breast cancer	15 tumors - 5 sections & also 25 tumors - 5 sections	95-03-27
7	Dr. Bill Muller	McMaster University	Analysis of HER2/neu mutations in breast cancer	90 C-Class breast tumor samples	93-12-01
8	Dr. L. Murphy & Dr. P.Watson	U of M Pathology & Biochemistry	ER variant expression in breast tumors- study1	100 primary tmrs (B-class) - paraffin & frozen sects	95-08-24
9	Dr. L. Murphy & Dr. P.Watson	U of M Pathology & Biochemistry	ER variant expression in breast tumors-study 2	Additional material 193 B cases & 50 cases	97-06-24
10	Dr. Liam Murphy	U of M Physiology	Studies on IGF-I in Human breast cancer	50 C-class specimens	94-01-05
11	Dr. Morag Park	McGill University	Prognostic significance of genotype chges in chromosome 7q31	100 primary tmrs & normal tiss (A-class) - frozen sections	94-10-25
12	Dr. Shutish C. Patel	Dept of Veterans Affairs - Medical Center	Determine the expression of apoD mRNA in primary breast tumors	50 B-class tumors	95-12-12
13	Dr. Yogesh C. Patel	McGill University	Expression & Function of Somatostatin Receptors in breast cancer	50 B-class cases - frozen sections	95-07-13
14	Dr. Leonard Pinsky	McGill University	Androgen Receptor Mutation in breast cancer-phase1	100 B-class cases - X2, 20um of frozen tissue blocks	95-05-01
15	Dr. Leonard Pinsky	McGill University	Androgen Receptor Mutation in breast cancer-phase2	Additional 25 A-class tmrs with matched normal	96-10-29
16	Dr. Michael Pollak	McGill University	Loss of IGF2 imprinting in Human breast cancer	3-4 unfixed blocks of tmr & normal tiss. - 20um frozen sects	94-07-26
17	Dr. Robert Shiu	U of M Physiology	Study of genes in hormone response in breast cancer	100 B-Class cases	94-05-08
18	Dr. Dan Skup	Montreal Cancer Institute	Role of TIMPs in breast cancer	100 primary tmrs - (B-class) - 6 frozen sects	94-05-04
19	Dr. Eva Turley	Cell Biology - MCTRF	RT-PCR, define isoforms of hyaluronan receptor termed RHAMM	100 tumors - frozen sects	95-01-24
20	Dr. Peter Watson	U of M Pathology	CD44 expression in breast tumors	100 prim. tmrs (B-class) - paraffin & frozen sects	94-06-06
21	Dr. Jim Wright	Cell Biology - MCTRF	Analyze ribonucleotide reductase gene expression	20-25 malignant samples & norm. cases - 5 slides of each	94-12-14
22	Dr. Alain Nepveu	McGill University	Study LOH & CUTL1	200 A,B,C-cases - matching tumor and normal 5-8 sections	97-02-24
23	Dr. William H. Marshall	Memorial University of Newfoundland	Determine HLA-DR4 status	100 C-cases - 5 sections	96-05-25
24	Dr. Paul Jolicoeur	Clinical Research Institute of Montreal	Screen human breast tmrs for overexpression of Mis-6	100 C-class cases	96-02-27
25	Dr. Arnold Greenberg	UofM Cell biology - MCTRF	Tissue localization of the expression of the human Nip3 protein	2 B-cases - 25 sections	97-12-11
26	Dr. Tianru Jin	The Toronto Hospital - Oncology Research Lab	Expression and function of POU homeodomain transcription factors	4 normal cases - 8 sections	97-10-23
27	Dr. Jim Stone	University of Alberta	The Role of RAS oncogenes in human breast cancers	20 B/C-class cases - 10 frozen sections of each	95-10-18
28	Dr. Tim Zacharewski	University of Western Ontario	Measurement of pS2 mRNA using a competitive RT-PCR assay	100 C-class cases - 3 frozen sections of each	97-06-25

Sorted by initial date of request

Manitoba Breast Tumor Bank **Table of Users**

29	Dr. Karl Riabowol	University of Calgary	Mutation and expression of the new tumor suppressor ING1	100 A-class cases - 6 frozen sections of each	97-05-29
30	Dr. Shou-Ching Tang	Dr. H. Bliss Murphy Cancer Centre	Prognostic Value of BAG-1 in invasive breast cancer	200 B-class cases - 3 paraffin of each	97-10-01
31	Dr. Barry Glickman	University of Victoria	Assess DNA repair gene status by the protein truncation test	10 C-class cases - 10-20 frozen sections	98-11-11
32	Dr. Matthew Ellis	Georgetown University Medical Center	Insulin-like growth factor receptors as prognostic & therapeutic response marker	250 A+/-B class cases - 3 paraffin of each	98-06-28
33	Dr. Charis Eng	Dana-Farber Cancer Institute - Boston	Modulation of PTEN expression in breast disease - Pilot study	50 C-class cases - 7 paraffin of each	98-03-03
34	Dr. Christopher Mueller	Queen's University	Screening of RDA products for sporadic breast cancer gene candidates	50 B/C-class cases - 5 frozen sections of each	98-02-23
35	Dr. Peter Roughly	McGill University		20 cases tumor and normal - 40 sections frozen	97-11-03
36	Dr. Peter Dall	Karlsruhe, Germany	CD44 expression in breast tumors	10 - 6 sections	95-03-08
37	Dr. Yvonne Myal	U of M Pathology		10 cases	97-06-23
38	Dr. John Schrader	University of British Columbia	Activating mutations or over-expression of X-Ras in breast cancer	200 C-class cases - 4 frozen sections of each	98-01-07
39	Dr. Scott Powers	Tularik Genomics	Detection of amplified loci in breast cancer	250 C-class cases - 1 frozen section each	98-01-07
40	Dr. Mark Minden	Ontario Cancer Institute - U of Toronto	WT1 expression in human breast cancer	20 B or C-class cases - 7 frozen sections each	99-01-02
41	Dr. Marc Lippman/Careen Tan	Georgetown University Medical Center	Role of EGFRvIII in human breast cancer	500 A+B-class cases - paraffin sections	98-01-12
42	Dr. Terumi Kohwi-Shigematsu	Lawrence Berkley National Lab. - U of California	Role of MAR-binding protein in breast cancer	50 A-class cases - 3-5 paraffin + 1 frozen section of each	99-01-01
43	Dr. Shafaat Rabbani	Royal Victoria Hospital	Methylation regulation of urokinase expression in hormone dependent&independent breast cancer pts	A-class cases - 4 frozen sections per grade	00-01-31
44	Dr. Sheila Drover	Memorial University of Newfoundland	Influence of HLA Class II genes on the immune response in breast cancer	130 A-class - 2 frozen sections + 80 C-class - 6+ frozen sections of each	00-02-17
45	Dr. Stephane Richard	Lady Davis Institute for Medical Research	Identification of mutations in sim-1 & sim-2 genes in breast cancer	100 A-class cases - 1 paraffin & 1 frozen section	00-05-25
46	Dr. Richard Gordon	University of Manitoba	High resolution CT mammography of breast tumors	D-class tissue block	01-05-01
47	Dr. Jorge Filmus	Sunnybrook & Women's College HSC	Identify GPC3 as a marker of breast tumor progression	20 A-class 4 frozen sections each	01-01-30
48	Dr. Luis Pardo	Max-Planck Institute for Experimental Medicine	EAG1 expression in breast cancer	150 C-class 3 paraffin sections each	01-01-16
49	Dr. Eva Turley	London Regional Cancer Centre	The role of RHAMM variants in breast cancer progression	200 B-class 4 frozen sections each	01-01-27
50	Dr. Peter Watson	University of Manitoba	The role of SLRP in breast cancer	B+C-class & MBED 227+200 approx 10 paraffin & frozen sections each	00-02-21
51	Dr. Peter Watson	University of Manitoba	The role of psoriasin in progression of early breast cancer	C-class & MBED 126+200 approx 10 paraffin & frozen sections each	00-02-21
52	Dr. Leigh Murphy	Cell Biology - CCM/Uof Manitoba	SMAD3 expression in human breast tumorigenesis & breast cancer progression	60 A-class cases + 80 B-class cases + 30 C-Class cases approx 20 frozen sections each	01-05-16
53	Dr. Etienne Leygue	U of M Biochemistry & Medical Genetics	Mammoglobin and SRA related molecules in normal & tumor human breast tissue	160+80 - A,B,C Class cases - 30 paraffin + 10 frozen sections each	01-06-08
54	Dr. Ginette Serrero	University of Maryland School of Pharmacy	Immunohistochemical determination of PCDGF expression in human breast cancer biopsies	120 B-class cases - 5 paraffin sections each	01-08-01

Sorted by initial date of request

Breast Cancer Research and Treatment **58:** 219–225, 1999.

Report

Influence of estrogen receptor variants on the determination of ER status in human breast cancer

Aihua Huang[1], Etienne Leygue[2], Helmut Dotzlaw[2], Leigh C. Murphy[2], and Peter H. Watson[1]
[1]*Department of Pathology,* [2]*Department of Biochemistry and Molecular Biology, University of Manitoba, Winnipeg, Manitoba, Canada*

Key words: estrogen receptor variant mRNAs, estrogen receptor status, immunohistochemistry, breast cancer

Summary

Determination of estrogen receptor alpha (ER) status in breast cancer is an important predictive factor for clinical response to endocrine therapy. We have recently shown that discrepancies in ER status determined by immunohistochemical assay (ER-IHA) can occur between amino-terminal (1D5) and carboxyl-terminal (AER-311) targeted ER antibodies and that those tumors which demonstrate discordance are associated with increased expression of truncated ER variant mRNAs. In this study, we have explored this observation to examine if ER variant expression can exert a direct effect on ER-IHA or whether this association is attributable to the characteristics of the antibodies. ER negative cos-1 cells were transfected with expression vectors containing wild type ER (wt-ER) and/or a frequently expressed truncated variant, ER-clone-4 variant. We found that ER-IHA performed with the same *N*- and *C*-terminal targeting ER antibodies on cos-1 cells expressing wt-ER alone demonstrated no difference in signals by western blot ($P > 0.1$). However, co-expression of wt-ER and the truncated ER-clone-4 variant, resulted in discordant IHA results with relatively higher ER-IHA H-scores from *N*-terminal antibodies ($P < 0.03$). Furthermore, re-examination of a subset of breast tumors previously studied by ER-IHA showed persistent concordance in 4/5 cases and persistent differences in 3/5 cases with a different pair of ER antibodies. We conclude that the presence of truncated ER variant proteins can interfere with the interpretation of ER status determined by IHA and that this may account for some of the inconsistencies between ER status and response to endocrine therapy.

Introduction

The measurement of estrogen receptor alpha (ER) status in breast tumors is widely used as a clinical index of potential therapeutic response to endocrine therapy. However, while up to 2/3 of breast tumors are ER positive, only 2/3 of this subset of patients will respond well to endocrine therapy [1]. Several factors have been considered in the past to account for this discrepancy, including tissue-related factors such as sampling, cellularity, and heterogeneity and biological factors such as functional status of the ER protein detected and the integrity of the downstream components of the ER signalling pathway.

More recently other potentially important biological factors that have emerged are the complexity of ER alpha gene expression as well as the recent discovery of the closely related ER beta gene that is also expressed in breast cancer tissues [2]. ER alpha gene expression is now known to be often associated with a range of ER variant mRNAs in breast tumors [3]. These ER mRNA variants include exon-deleted, exon-duplicated, or truncated ER mRNA transcripts that may encode a variety of incomplete ER-like proteins [3, 4]. Individual ER variant proteins have been demonstrated [5, 6], but in most instances may well be expressed at low levels in most tumors compared to wt-ER [4]. Nevertheless ER variant expression may be important to consider with the adoption of the IHA

as an alternative to the classical ligand binding dextran coated charcoal (DCC) assay to determine ER status [7–9]. The IHA affords the opportunity to determine ER status in paraffin tumor sections and so allows the parallel assessment of tissue factors. However, this has also meant that ER is now defined on the basis of structural epitopes as opposed to functional ligand binding. Expression of most ER variants would not be detected by the DCC assay because in many cases the predicted variant proteins have loss or disruption of the *C*-terminus and ligand binding domain (E/F region) of the protein [10]. However, the total accumulation of multiple ER-like proteins might well be expected to interfere with IHA determination of ER status, depending on the target specificity of the antibody employed. Thus, although in practice a good overall correlation between IHA and DCC exists, discrepant results occur in a proportion of tumors [8, 9, 11–13]. These discrepancies are not only between IHA and DCC assays [8, 9], but also between IHA performed with different antibodies on the same tumors [11–13]. While tissue related factors can be invoked to account for some of the former discrepancies, differences between comparable IHAs scored on the same areas within serial sections [11] are more difficult to explain.

In order to understand such discrepancies we have recently examined ER mRNA variant expression and shown that those variants that specifically encode putative truncated ER-like proteins, are preferentially expressed in these 'IHA-discordant' cases [14]. This suggests that ER variant proteins encoded by ER variant mRNAs may contribute to discrepancies in ER status determined by IHA using different antibodies. In this study, we have now compared the signal intensities of different ER targeted antibodies and used these to examine experimentally the direct effect of truncated ER variant expression on the determination of wild type ER (wt-ER) status by IHA.

Materials and methods

ER expression vectors and transfection assays

Wt-ER (HEGO, kindly provided by Dr P. Chambon) was cloned into the vector pSG5 and expression was driven by an SV40 promotor. Truncated ER-clone-4 was cloned into the pcDNA3.1 vector (Invitrogen) and expression was driven by a CMV promotor. ER-negative cos-1 cells were grown in DMEM supplemented with 5% (v/v) fetal bovine serum. The cells were transiently transfected with either pHEGO, pER-clone-4, or both expression plasmids in varying proportions (5 μg total plasmid, as described in Figure 2). After 48 h, transfected cells were harvested for immunoblotting or fixed for immunohistochemical assay. All transfections were done in 60-mm dishes (for western blot samples) or in chamber slides (for immunohistochemistry samples) in parallel and using the superfect transfection system (Qiagen, CA) as described by the manufacturer. Plasmid pCH110 (encoding β-galactosidase protein, Pharmacia) was co-transfected and galactosidase activity was determined by standard methods to control for and confirm transfection efficiency (25–35% cells positive).

Western blot analysis

Whole cell extracts were prepared from cells transfected with wt-ER, ER-clone-4, or both plasmids. Cells were washed with chilled phosphate-buffered saline (PBS), scraped, collected in PBS, and centrifuged at 1000 g for 5 min at 4°C, and cell pellets were re-suspended in 200 μl of 50 mM Tris–HCl, 20 mM EDTA, 5% sodium dodecyl sulphate (SDS), 1 mM phenylmethylsulphonyl fluoride (PMSF), 5 mM β-glycerophosphate, and 1 mM aprotinin. Protein concentration was determined by the Bio-Rad (Hercules, CA) protein assay kit as described by the manufacturer. Twenty-five micrograms of protein was separated on a 10% SDS-polyacrylamide gel and transferred to nitrocellulose. Western blot analysis to detect ER present in different transfected cells was carried out with ER-specific mouse monoclonal antibodies 1D5 (DAKO, Canada) or AER314 raised against *N*-terminal epitopes and AER311 or AER320 (Neomarkers, CA) raised against *C*-terminal epitopes (at 1/1000 dilution for all antibodies) of the wild type protein (Figure 1D). The second antibody used was a horseradish peroxidase (HRP)-conjugated goat anti-mouse antibody (Hyclone Laboratories, Logan, UT, USA). Visualization was accomplished using the Supersignal detection system (Pierce, USA) according to the manufacturer's instructions. Densitometry on western blot signals was performed using a video-computer image analysis system (M4, Imaging Research, St Catherines, Ontario). Western blot experiments were performed at least in triplicate on independent cell transfections. Statistical comparisons were assessed by the student *t*-test.

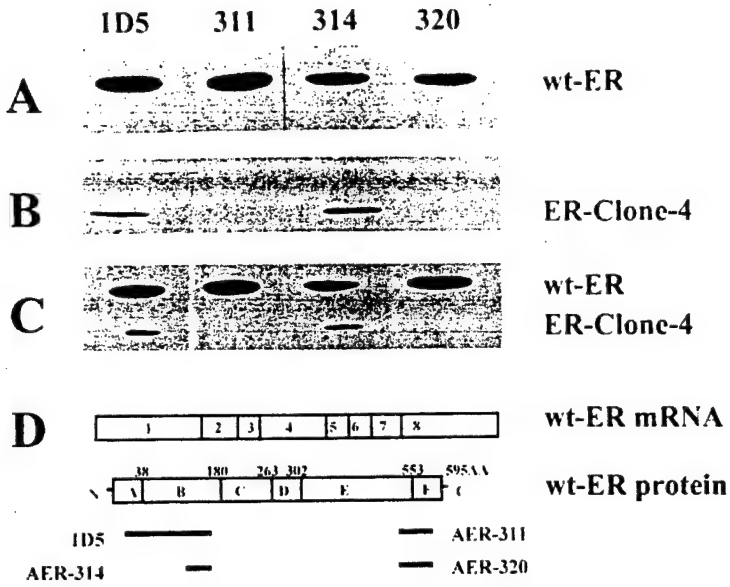

Figure 1. Western blot analysis of estrogen receptor expression detected with different antibodies in cos-1 cells following transient transfection with ER and/or ER-clone-4 variant. Twenty five micrograms of whole cell extract protein prepared from transfected cos-1 cells were loaded in each lane and separated by 0.1% SDS-10% PAGE. (A) Cos-1 cells transfected with 5 μg wt-ER plasmid. (B) Cos-1 cells transfected with 5 μg ER-clone-4, (C) cos-1 cells transfected with both wt-ER and ER-clone-4 (0.5 and 4.5 μg). Monoclonal antibodies used to detect ER proteins were 1D5 or AER314, and AER311 or AER320, which target epitopes within the *N*-terminal and *C*-terminal of the ER protein, respectively (D).

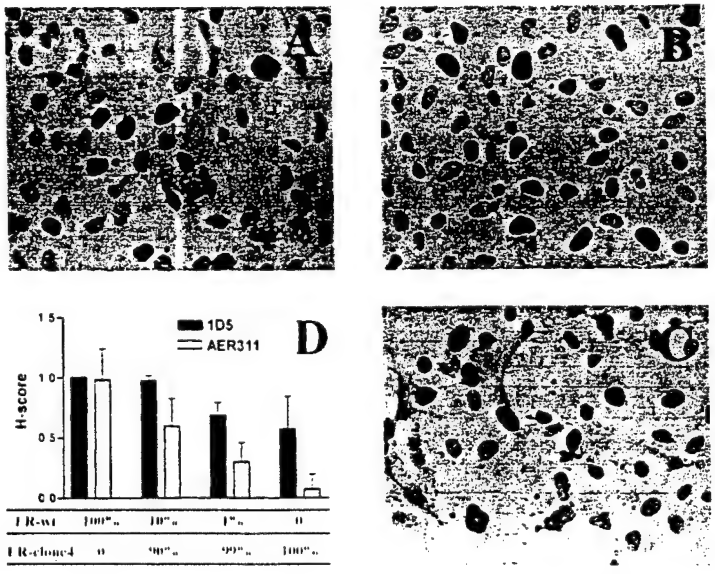

Figure 2. Immunohistochemical detection of estrogen receptor-like protein in transfected cos-1 cells. IHA-1D5 assay (A, B) and IHA-AER311 assay (C) were conducted on cells transfected with either ER-wt alone (A), or co-transfected with ER-wt and ER-clone-4 (ratio 1%:99%, B&C). The graph (D) summarizes the H-score values obtained by either IHA-1D5 or IHA-AER311 applied to cos-1 cells transfected with ER-wt and ER-clone-4 in different proportions. Each bar represents the mean and standard deviation relative to 1D5 H-score applied to ER-wt transfected cells derived from 7 (ER-wt alone) or 3 (all other) independent transfection experiments.

Immunohistochemistry

In parallel experiments, cos-1 cells were grown in chamber slides (Nalge Nunc, Intl., Il, USA). Transfections were performed as above. Cells were fixed in 2% paraformaldehyde–PBS for 30 min and washed twice with PBS for 2 min. Then IHA was performed as described previously [11]. Briefly, the slides were incubated in 10% goat serum in PBS for 20 min to block non-specific binding. Primary antibody 1D5 or AER311 (at 1/50 dilution for both) was added and incubation carried out overnight at 4°C, followed by two washes in PBS for 5 min. The second antibody (biotinylated goat anti-mouse IgG, Vector Labs, CA) was used at 1:200 dilution in PBS for 45 min at room temperature. After a rinse in PBS, the slides were incubated in AB Complex (Elite kit, Vector Labs) at 1:100 dilution for 45 min. The label was developed using diaminobenzidine/hydrogen peroxide and slides were then lightly counterstained with methyl green, dehydrated, cleared, and mounted.

Human breast tumor specimens (10 cases) were obtained from the NCIC-Manitoba Breast Tumor Bank. Formalin fixed and paraffin embedded tissue blocks were sectioned to provide serial sections from tumors and examined by IHA using the same protocol except that a different pair of ER antibodies (AER314 and AER320, Neomarkers, CA) were used.

Semi-quantitative H-scoring for all IHA experiments was done as previously described [11]. Brown immunoreactivity of cell nuclei was taken as positive and the proportion of negative cells (P_0) and those staining at low (P_1), moderate (P_2), or high (P_3) levels of intensity were scored. The score for each section (H-score = $[(0 \times P_0) + (1 \times P_1) + (2 \times P_2) + (3 \times P_3)] \times 100$) was calculated from the mean of $\times 5$ representative high power fields (Leica DMRB, $\times 40$ objective). For transfection experiments where non-specific background was uniformly higher than in tumor sections, only P_2 and P_3 values entered into the final H-score. Initial IHA experiments were also analyzed with the video-densitometry system as above, to compare with and validate the H-scoring quantification. All IHA slides were coded and assessment was done without knowledge of the antibody, transfection conditions, or tumor identity. As described previously [11], tumors which exhibited an H-score difference of >50 between IHA assays performed with different ER antibodies on serial sections were classified as 'IHA-discordant'.

Results

Comparison of ER antibodies

A panel of ER antibodies directed to different epitopes was tested by IHA and western blot assay in parallel, applied to an ER-negative cos-1 cell line transfected with wt-ER. Cos-1 cells were selected as ER mRNA or protein expression is undetectable in these cells (unpublished data) to avoid the possibility of endogenous ER and ER variant expression present in many breast cell lines. All antibodies detected a 65 kDa protein on western blot (Figure 1A) and comparison using a video-densitometry system showed that there was no significant difference between the signals obtained with 1D5 and AER311 antibodies (optical density units mean^{SD} for 1D5 = $0.79^{0.22}$ vs mean^{SD} AER311 = $0.78^{0.19}$; $n = 4$, $P > 0.1$). IHA was performed in parallel on transfected cells using these antibodies at the same relative concentrations. These were also the concentrations that we had previously used to study breast tumors. Initially IHA was assessed by both video-densitometry and semi-quantitative H-score (applied independently and without knowledge of the antibody) and it was found that these provided comparable results ($n = 10, r = 0.96, p = 0.004$, data not shown). Subsequently all IHA signals were quantitated by H-score. Positive immunoreactivity in approximately 30% of nuclei was seen with IHA-1D5 and IHA-AER311 with no significant difference in ER levels (H-score 1D5 $\text{mean}^{SD} = 63^{8}$; AER311 $\text{mean}^{SD} = 60^{17}$, $n = 7$, $P > 0.1$, Figure 2D).

Effect of modulation of ER variant expression on IHA

The ER-clone-4 variant was used for these experiments as this variant is predicted to encode a *C*-terminally truncated ER-like protein and has previously been shown to be frequently expressed in breast tumors [14–16]. Following transfection of ER-clone-4 alone, a single 24 kDa protein was detected by western blot analysis (Figure 1B) and positive nuclear staining was only seen by IHA using *N*-terminal antibodies (1D5 and AER314). However, *C*-terminal antibodies (AER311 and AER320) failed to detect it on western blot (Figure 1B & C) or IHA (Figure 2D). IHA was then performed using the same protocol as used in our previous study of breast tumors applied to cells following co-transfection with ER-clone-4 variant and wt-ER to obtain different proportions of ER variant expression relative to wt-ER. A consistently lower signal

Table 1. Immunohistochemical determination of ER level in tumors with different ER antibodies

			H-scores					
#	ER	PR	1D5	AER311	1D5 ↔ 311	AER314	AER320	314 ↔ 320
1	69	18	200	100	**100–**	150	80	**70–**
2	7	26	134	14	**120–**	180	90	**90–**
3	33	21	182	88	**94–**	110	60	**50–**
4	140	101	160	66	**94–**	125	100	25–
5	19	10	190	20	**170–**	90	80	10–
6	39	44	132	128	4–	105	140	35+
7	79	22	124	138	14+	150	170	20+
8	85	125	120	150	30+	150	150	0
9	27	10	228	200	28–	165	135	25–
10	24	59	128	104	24–	150	50	**100–**

Columns are as follows; #: case number; ER/PR: estrogen/progesterone receptor levels in fmol/mg protein as determined by DCC assay; 1D5, AER311, AER314, AER320: H-score values for ER levels determined by IHA using the corresponding antibody; 1D5 ↔ 311, 314 ↔ 320: Difference in H-score values with each antibody pair, with higher or lower values with *C*-terminal antibody shown as + or −, respectively, and 'IHA-discordant'; H-Scores (difference ≥50) shown in bold and 'IHA-consistent' H-Scores (<50) shown in regular typeface.

intensity for transfected ER-clone-4 relative to wt-ER was obtained with the *N*-terminal antibodies that was probably attributable to differences in efficiency between the expression plasmids (Figure 1). Nevertheless we observed that while both 1D5 and AER311 antibodies recognized wt-ER on western blot (Figure 1C) and gave similar H-score values with wt-ER alone, a significant and increasing discordance in IHA H-score occurred between *N*-terminal and *C*-terminal antibodies as the relative proportion of ER-clone-4 variant increased ($P < 0.03$, *t*-test, Figure 2D).

ER-IHA on breast tumors

We then investigated the reproducibility of our original observation in breast tumors. A different pair of antibodies was selected for repeat IHA assay (AER314 and AER320 targeting *N*- and *C*-terminal ER epitopes, respectively) as these were found to give similar results in cos-1 cells following wt-ER transfection and western blot analysis (AER314 $\text{mean}^{SD} = 0.67^{0.28}$ vs AER320 $\text{mean}^{SD} = 0.65^{0.22} n = 4$, $P > 0.1$) and IHA (data not shown). The original tissue blocks were available on a subset of 10 cases that were all ER/PR positive by DCC assay (and therefore expressing wild type ER and likely to also express a range of ER variants). All five tumors that had previously been classified as 'IHA-discordant' by our previous definition (H-score difference >50) showed lower H-scores by IHA-AER320 as compared to IHA with the matching AER314 antibody. In 3/5 the lower H-score was sufficient to remain classified as 'IHA-discordant' (Table 1). In contrast, amongst an equal number of cases previously classified as 'IHA-consistent', 4/5 showed equivalent H-scores and remained classified as 'IHA-consistent' with AER320. In 1/5 of the latter cases the IHA was discordant.

Discussion

Multiple ER alpha mRNA variants are expressed in normal breast tissue and in breast tumors [3]. However, in considering the role of ER variants in breast cancer, it has been argued that expression of ER mRNA variants may not be important on the basis that expression may not change during tumorigenesis and that the evidence to date for expression of specific variant proteins that might play a role in hormonal progression is limited [17, 18]. Nevertheless, studies founded on histologically characterized tissue sections have clearly shown that certain mRNA variants are differentially expressed between normal and neoplastic tissues and also between tumors [19, 20]. Differential expression has also been found in association with contrasting responses to estrogen and resistance to tamoxifen in cell lines [21–24] and parameters of hormone response and prognosis *in vivo* [16, 25]. Overexpression of an ER mRNA variant deleted in exon 5 (D5-ER) has also been shown to occur in certain tamoxifen resistant tumors [26] and has been used successfully to predict reponse to hormonal therapy of

hepatocellular carcinoma [27]. It is also conceivable that ER variants might exert indirect functional effects through competition with wt-ER for ER binding proteins [28] or with proteins involved in interactions with antiestrogens [29].

Although expression of specific variant proteins has not yet been proven in breast tumors, partly because it has been difficult to develop antibodies that will distinguish variants, expression of ER-like variant proteins expressed recombinantly can be demonstrated *in vitro* and in breast cell lines [21, 22]. In some cases these variant proteins have been shown to possess either hormone independent and constitutive activity or to exert a dominant negative influence on estrogen regulated target genes in *ex vitro* models. At the same time our own data suggest that previous attempts to demonstrate these proteins *in vivo* may have been hampered by the fact that, although total expression of ER variants of all forms may be significant, many individual variants such as D5-ER may be expressed at only low levels in breast tissues [4]. Furthermore, our recent observation that discordant immunostaining with ER antibodies correlates with the total overall expression of mRNA variants encoding out-of-frame proteins (i.e. predicted to encode *C*-terminally truncated ER-like proteins) also supports the view that ER-like variant proteins are present *in vivo* [11, 14]. In the latter study, we examined ER expression in breast tumors by DCC and IHA using both '*N*-terminal' (1D5) and '*C*-terminal' (AER-311) targeting ER alpha antibodies. The IHA provided similar results to the DCC assay in terms of overall ER status. However, the ER-IHA levels assessed in almost 25% of tumors were discordant (H-score difference of >50) between these different antibodies, even when scored on the same areas within serial sections [11]. Further analysis of these 'IHA-discordant' cases by RT-PCR assays [4, 20] showed that those ER mRNA variants that encode putative truncated ER-like proteins, were preferentially expressed in 'IHA-discordant' cases [14].

However, although the antibodies we used provided similar signal intensities by IHA on strongly ER positive tumors, and in many tumors the IHA signals were concordant [11], it remained possible that the discordant IHA signals might be explained by different antibody affinities. Furthermore, the principle that ER variants may interfere with IHA results had not previously been tested experimentally. Our results here show that the 1D5 and AER-311 antibodies can provide similar signal intensities of wt-ER by both western blot and IHA when used at the same relative concentrations as in our previous study [11]. But the relative IHA signal intensity obtained with these antibodies changes and becomes discordant with increasing expression of a truncated ER variant protein alongside the wt-ER. IHA consistency or inconsistency is also apparently quite reproducible when tumor blocks that have previously been studied by IHA and RT-PCR are re-examined using a different pair of matched ER monoclonal antibodies targeting similar *N*- and *C*-terminal epitopes. The degree of reproducibility between IHA with different pairs of antibodies in the small subset of cases available for reexamination should be considered against the fact that although RT-PCR assays using primers to span regions of deletion [4] can detect most exon-deleted ER mRNA variants, many of which encode putative truncated proteins, the spectrum of truncated ER mRNA variants analogous to the frequently expressed ER clone 4 is more difficult to study and is currently unknown [4, 15]. Therefore, given also that the precise epitopes recognized by the ER antibodies used are unknown, it is possible that additional truncated mRNA variants are expressed in particular cases, similar to ER-clone-4, that would remain undetected by the RT-PCR assays we have previously used [15, 16].

In summary, we have shown that ER status determined by IHA can be directly influenced by expression of a *C*-terminally truncated ER variant and that discordant IHA results in tumors using different ER antibodies are reproducible. We conclude that ER variant mRNA's and their putative variant proteins may interfere with the interpretation of ER status assessed by IHA and that this may underlie some of the inconsistencies in determination of ER status in breast tumors [30]. It should be emphasized that the clinical significance of discordance in IHA, in terms of assignment of IHA status, remains to be tested, but is likely to affect only a small subset of breast tumors. The relationship between ER variant expression, 'IHA-discordant' status, and clinical response to endocrine therapy remains to be determined.

Acknowledgement

This work was supported by grants from the Canadian Breast Cancer Research Initiative (CBCRI) and the U.S. Army Medical Research and Materiel Command (USAMRMC). The Manitoba Breast Tumor Bank is supported by funding from the National Cancer Institute of Canada (NCIC). EL is a USAM-

RMC postdoctoral fellow. LCM is a Medical Research Council of Canada (MRC) Scientist. PHW is an MRC Clinician-Scientist.

References

1. McGuire WL: Hormone receptors: their role in predicting response to endocrine therapy. Semin Oncol 5: 428–433, 1978
2. Dotzlaw H, Leygue E, Watson PH, Murphy LC: Expression of estrogen receptor-beta in human breast tumors. J Clin Endocrinol Metab 82: 2371–2374, 1997
3. Murphy LC, Leygue E, Dotzlaw H, Douglas D, Coutts A, Watson PH: Oestrogen receptor variants and mutations in human breast cancer. Ann Med 29: 221–234, 1997
4. Leygue E, Huang A, Murphy L, Watson P: Prevalence of estrogen receptor variant mRNAs in human breast cancer. Cancer Res 56: 4324–4327, 1996
5. Park W, Choi JJ, Hwang ES, Lee JH: Identification of a variant estrogen receptor lacking exon 4 and its coexpression with wild-type estrogen receptor in ovarian carcinomas. Clin Cancer Res 2: 2029–2035, 1996
6. Desai AJ, Luqmani YA, Walters JE, Coope RC, Dagg B, Gomm JJ, Pace PE, Rees CN, Thirunavukkarasu V, Shousha S, Groome NP, Coombes R, Ali S: Presence of exon 5-deleted oestrogen receptor in human breast cancer: functional analysis and clinical significance. Brit J Cancer 75: 1173–1184, 1997
7. Taylor CR.: Paraffin section immunocytochemistry for estrogen receptor. Editorial Cancer 77: 2419–2422, 1996
8. Allred DC, Bustamante MA, Daniel CO, Gaskill HV, Cruz AJ: Immunocytochemical analysis of estrogen receptor in human breast carcinomas. Evaluation of 130 cases and review of the literature regarding concordance with biochemical assay and clinical relevance. Arch Surg 125: 107–113, 1990
9. Alberts SR, Ingle JN, Roche PR, Cha SS, Wold LE, Farr GH, Krook JE, Wieland HS: Comparison of estrogen receptor determinations by a biochemical ligand assay and immunohistochemical staining with monoclonal antibody ER1D5 in females with lymph node positive breast carcinoma entered on two prospective clinical trials. Cancer 78: 764–772, 1996
10. Dowsett M, Daffada A, Chan CMW, Johnston SRD: Oestrogen receptor mutants and variants in breast cancer. Euro J Cancer 33: 1177–1183, 1997
11. Huang A, Pettigrew N, Watson P: Immunohistochemical assay for estrogen receptors in paraffin wax sections of breast carcinoma using a new monoclonal antibody. J Pathol 180: 223–227, 1996
12. Pertschuk LP, Feldman JG, Kim YD, Braithwaite L, Schneider F, Braverman AS, Axiotis C: Estrogen receptor immunocytochemistry in paraffin embedded tissues with ER1D5 predicts breast cancer endocrine response more accurately than H222Spγ in frozen sections or cytosol-based ligand-binding assays. Cancer 77: 2514–2519, 1996
13. Nedergaard L, Christensen L, Rasmussen BB, Jacobsen GK: Comparison of two monoclonal antibodies for the detection of estrogen receptors in primary breast carcinomas. Pathol Res Pract 192: 983–988, 1996
14. Huang A, Leygue E, Snell L, Murphy L, Watson P: Expression of estrogen receptor variant mRNAs and determination of estrogen receptor status in human breast cancer. Am J Pathol 150: 1827–1833, 1997
15. Dotzlaw H, Alkhalaf M, Murphy L: Characterization of estrogen receptor variant mRNAs from breast cancers. Mol Endocrinol 6: 773–785, 1992
16. Murphy LC, Hilsenbeck SG, Dotzlaw H, Fuqua SAW: Relationship of clone 4 estrogen receptor variant messenger RNA expression to some known prognostic variables in human breast cancer. Clin Cancer Res 1: 155–159, 1995
17. Pfeffer U, Fecarotta E, Arena G, Forlani A, Vidali G: Alternate splicing of the estrogen receptor primary transcript normally occurs in estrogen receptor positive tissues and cell lines. J Steroid Biochem 56: 99–105, 1996
18. Gotteland M, Desauty G, Delarue JC, Liu L, May E: Human estrogen receptor messenger RNA variants in both normal and tumor tissues. Mol Cell Endocrinol 112: 1–13, 1995
19. Leygue E, Watson P, Murphy L: Estrogen receptor variants in normal human mammary tissue. J Natl Cancer Inst 88: 284–290, 1996
20. Leygue E, Murphy L, Watson P: Triple primer polymerase chain reaction: a new way to quantify truncated mRNA expression. Am J Pathol 148: 1097–1103, 1996
21. Castles CG, Fuqua SAW, Klotz DM, Hill SM.: Expression of a constitutively active estrogen receptor variant in the estrogen receptor-negative BT-20 human breast cancer cell line. Cancer Res 53: 5934–5939, 1993
22. Pink JJ, Wu SQ, Wolf DM, Bilimoria MM, Jordan VC: A novel 80 kDa human estrogen receptor containing a duplication of exons 6 and 7. Nucleic Acids Res 4: 962–969, 1996
23. Madsen MW, Reiter BE, Lykkesfeldt AE: Differential expression of estrogen receptor mRNA splice variants in the tamoxifen resistant human breast cancer cell line, MCF-7/TAMR-1 compared to the parental MCF-7 cell line. Mol Cell Endocrinol 109: 197–207, 1995
24. Castles CG, Klotz DM, Fuqua SAW, Hill SM: Coexpression of wild type and variant estrogen receptor mRNAs in a panel of human breast cell lines. Br J Cancer 71: 974–980, 1995
25. Fuqua SAW, Chamness GC, McGuire WL: Estrogen receptor mutations in breast cancer. J Cell Biochem 51: 135–139, 1993
26. Daffada AA, Johnston SR, Smith IE, Detre S, King N, Dowsett M: Exon 5 deletion variant estrogen receptor messenger RNA expression in relation to tamoxifen resistance and progesterone receptor/pS2 status in human breast cancer. Cancer Res 55: 288–293, 1995
27. Villa E, Dugani A, Fantoni E, Camellini L, Buttafoco P, Grottola A, Pomper G, Santis MD, Ferrari A, Manenti F: Type of estrogen receptor determines response to antiestrogen therapy. Cancer Res 56: 3883–3885, 1996
28. Halachmi S, Marden E, Martin G, Mackay H, Abbondanza C, Brown M: Estrogen receptor associated proteins: possible mediators of hormone induced transcription. Science 264: 1455–1458, 1994
29. Yang NN, Venugopalan M, Hardikar S, Glasebrook A: Identification of an estrogen response element activated by metabolites of estradiol and raloxifene. Science 273: 1222–1225, 1996
30. Stierer M, Rosen H, Weber R, Hanak H, Auerbach L, Spona J, Tuchler H. Comparison of immunohistochemical and biochemical measurement of steriod receptors in primary breast cancer: Evaluation of discordant findings. Breast Cancer Res Treat 50: 125–134, 1998

Address for offprints and correspondence: Dr. Peter Watson, Department of Pathology, Faculty of Medicine, D212-770 Bannatyne Ave, University of Manitoba, Winnipeg, MB, R3E 0W3, Canada; *Tel:* (204)-789-3435; *Fax:* (204)-789-3931; *E-mail:* pwatson@cc.umanitoba.ca

Cancer Detection and Prevention, 23(3):245–253 (1999)

Classification of Breast Tumors by Grade and Steroid Receptor Status Using Pattern Recognition Analysis of Infrared Spectra

Michael Jackson, Ph.D.,[a] James R. Mansfield, M.Sc.,[a] Brion Dolenko, M.Sc.,[a] Rajmund L. Somorjai, Ph.D.,[a] Henry H. Mantsch, Ph.D.,[a] and Peter H. Watson, M.D.[b]

[a]Institute for Biodiagnostics, National Research Council Canada, Winnipeg, Manitoba, Canada; and [b]Department of Pathology, Faculty of Medicine, Health Sciences Center, University of Manitoba, Winnipeg, Manitoba, Canada

Address all correspondence and reprint requests to: Michael Jackson, Ph.D., Institute for Biodiagnostics, National Research Council Canada, 435 Ellice Ave., Winnipeg, Manitoba, Canada, R3B 1Y6.

Accepted for publication January 26, 1999.

ABSTRACT: Infrared (IR) spectroscopy applied to tissue sections yields complex spectra that provide a molecular fingerprint of the tissue. We have studied a cohort of 77 breast tumors by IR spectroscopy to develop an objective method for the assignment of grade of breast tumors. Although the major variations between spectra from different tumors were in absorptions arising from triglycerides (adipose tissue) and collagen, subtle changes in spectra could be detected that were independent of cellularity and tissue composition. Using a specific multivariate pattern recognition strategy to associate these changes in spectra with different tumor grades, we then were able to accurately reclassify tumors by grade (87% accuracy; $\kappa = 0.835$). A similar approach allowed classification of steroid receptor status (93% accuracy; $\kappa = 0.852$). We conclude that IR spectroscopy may have clinical utility in the objective assignment of breast tumor grade.

KEY WORDS: breast cancer grade, classification strategy, diagnosis, estrogen receptors, Fourier transform infrared spectroscopy, multivariate analysis, progesterone receptors.

I. INTRODUCTION

The clinical management of breast cancer patients is guided by several clinical and pathological measures of tumor growth, hormone response, and metastatic potential.[1] These indicators include tumor size, histologic type, grade, stage, and the presence of steroid receptors.[2,3] However, an increasing proportion of cases now present at an earlier stage as axillary node negative or preinvasive *in situ* disease where determination of the likelihood of local or distant recurrence becomes even more dependent on assessment of the inherent biology of the tumor.[2] Improvement in the accuracy of this assessment may in part come from better methods for the determination and integration of known prognostic factors. Amongst these, tumor grade has been shown by some to be an excellent indicator of biological potential.[4] However, reliable assessment of tumor grade has been hindered in the past by difficulties in determining reproducible criteria and the problem of interobserver variability.[5]

In search of improved benchmarks by which to measure characteristics within tumor tissue that would allow accurate assignment into grade categories, we have used Fourier transform infrared (FTIR) spectroscopy to assess frozen breast tumor sections. FTIR spectroscopy is based upon the absorption of infrared (IR) light by covalent bonds as they vibrate. The frequency of light that is absorbed depends upon the nature of the bond between the atoms (e.g., C-C versus C=C), the atoms involved in the bond (e.g., C=C versus C=O), the type of vibration (e.g., bending versus stretching), and factors such as the strength of any hydrogen bonding interactions. Furthermore, as with other forms of optical spectroscopy, the amount of light absorbed by a vibrating bond is linearly related to concentration. The infrared spectrum of a sample is therefore a direct indicator of its chemi-

0361-090X/99/$14.00

cal composition. In biological systems, functional groups that strongly absorb infrared light include C=O, N-H, C-H, and P=O groups. The intensity of the absorption bands in the infrared spectrum of a tissue sample therefore provides information concerning lipid, protein, and nucleic acid content of the sample, whereas the frequency of the absorption provides information relating to structure/conformation and intermolecular interactions. In other words, the infrared spectrum of tissues provides information that reflects the biochemistry of the tissue.

If the infrared spectrum of a tissue sample can provide information with regard to tissue biochemistry, then the changes in tissue biochemistry accompanying a disease process should be reflected in changes in the infrared spectrum of the diseased tissue. We have recently demonstrated that this is indeed so, identifying spectroscopic features characteristic of Alzheimer's disease,[6] chronic lymphocytic leukemia,[7] multiple sclerosis,[8] and scar formation in ventricular tissue following infarction.[9] By extension, it is reasonable to speculate that tumors of differing grades will also show different spectroscopic features, in principle allowing characterization of tumor spectra by grade.

IR spectra are thus characterized by a high information content that can be viewed and analyzed from different perspectives. In this respect IR spectroscopy is not unlike light microscopy, but this information relates directly to tissue biochemistry. We have therefore investigated the possibility of using FTIR spectroscopy to derive parameters from tumor sections analogous to but more objective than light microscopic tumor grade. This was achieved using a novel, multivariate classification (pattern recognition) strategy specifically developed to deal with complex spectra.

II. MATERIALS AND METHODS

A. Sample Preparation and Data Acquisition

A cohort of 77 cases of invasive ductal breast carcinomas for which full historical data (including case records, slides, paraffin blocks, and tumor tissue) was available was selected for study from the Manitoba Breast Tumor Bank. These were chosen primarily on the basis of tumor grade to provide three equivalent groups at each of three grade levels. All tumors were graded uniformly by a single pathologist according to the Nottingham grading system[4] applied to an H&E section from a formalin-fixed and paraffin-embedded tissue block. Additional criteria included good histologic tissue quality and the presence of invasive tumor in >30% of the surface of the block selected for study. In all cases, the percentage of tumor cells, normal ducts/lobules, fibrous stroma, and fat was also estimated and scored as a percentage of the surface area of the tissue section to allow analysis of the effect of cellularity and stromal compostion and interpretation of spectra. The estrogen and progesterone receptor status was assessed by ligand binding assay performed on an adjacent portion of tumor tissue and shown to be positive for 45 and 49 tumors, respectively. Tumors were considered estrogen and/or progesterone receptor positive if the receptor concentration was greater than 3 fg/mg or 15 fg/mg, respectively. Thin frozen sections (10 μm) were then obtained in each case from frozen tissue blocks that corresponded to tissue immediately adjacent and mirror image to the paraffin sections.[10] Frozen sections were transported in dry ice to the laboratory and rapidly removed from their containers using cooled forceps, transferred to a CaF_2 window having a specially machined 10 μm depression, covered with a second CaF_2 window and mounted in a demountable cell holder. The use of a window with a machined depression ensured that when the tissue is lightly compressed during cell assembly, a constant sample thickness is obtained. The cell holder was placed in a Digilab FTS 60 A Fourier transform infrared spectrometer (Digilab Laboratories, Cambridge, MA) equipped with a liquid nitrogen–cooled mercury cadmium telluride detector and continuously purged with dry air. For each sample, 256 interferograms were collected, signal averaged, and Fourier transformed to generate spectra with a nominal resolution of 2 cm^{-1}. Absorptions from the CaF_2 windows and residual water vapour were interactively subtracted from all spectra.

B. Data Processing

Given the complex manner in which biochemical information is encoded in the spectra, in addition to

traditional methods of spectral analysis, we have developed a new and specific strategy to extract the information relevant for classification of tumor spectra. The strategy was implemented in three stages: (i) a preprocessing stage in which the spectral subregions most useful for classification were determined,[11] (ii) regional classification, and (iii) aggregation of classifier outcomes.[12,13] Particular emphasis has been placed on developing robust, reliable classifiers. This was achieved by a specific cross-validation methodology, based on bootstrapping,[14] applied at each of the three stages. For further details, see Appendix 1. To ensure that classification was not based upon variations in sample thickness, spectra were normalized with repect to integrated area prior to analysis.

III. RESULTS

Infrared spectra of sections from three low-grade breast tumors (Nottingham grade score: 3–5) normalized with respect to maximum absorption intensity are shown in Figure 1. The most noticeable feature of each spectrum is the complexity, with prominent absorptions in almost all regions of the spectrum. The region between 2700 and 3100 cm^{-1} is populated by absorptions arising from C-H vibrations of lipids, proteins and DNA.[15–17] Obvious differences exist in both the absolute and relative intensities of these absorptions in the three spectra, which must be related to compositional differences among the three tumors. The absolute intensity of each of the C-H stretching absorptions increases progressively from Figure 1A to Figure 1C, indicating increasing concentrations of fatty acyl chains. In addition, the relative intensity of the absorptions at around 2950 to that at 2920 cm^{-1} changes. In Figure 1A, the relative intensity is highest (similar to that seen for pure phospholipid systems), progressing to the lowest relative intensity in Figure 1(C) (similar to that seen for isolated proteins). These results suggest that the tissue section giving rise to Figure 1C is lipid/acylglyceride rich, the one giving rise to Figure 1A is protein rich, and the one giving rise to Figure 1B contains significant amounts of both lipids and/or acylglyceride and protein.

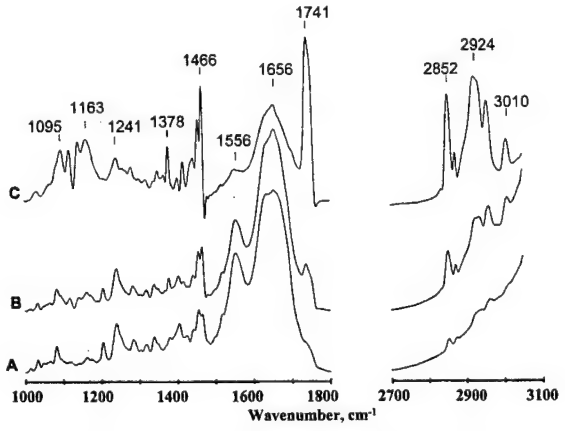

FIGURE 1. Infrared spectra of 10-μm sections of low-grade (Nottingham grade 3–5) breast tumors.

Variations in lipid/acylglyceride and protein content are confirmed by analysis of spectra between 1000 and 1800 cm^{-1}. Absorptions at 1741, 1466, 1378, 1163, and 1095 cm^{-1} in Figure 1C arise from C=O, CH_2, CH_3, and C-O-C vibrations of phospholipids and/or acylglycerides.[15–17] Phospholipids exhibit two intense absorptions at 1240 and 1080 cm^{-1}, arising from PO_2^- vibrations of phosphodiester groups.[15] These characteristic absorptions are absent in Figure 1, suggesting that the material giving rise to the intense C-H, C=O, and C-O-C absorptions is predominantly acylglyceride rather than phospholipid. This observation is supported by the known storage of fatty acids in the breast as acylglycerides. The intensity of the acylglyceride absorptions in Figure 1C is much greater than that seen in Figure 1A, with the intensity in Figure 1B again being intermediate.

The intensity of the strong absorption at 1656 cm^{-1}, termed the amide I absorption and arising from C=O vibrations of the amide groups of polypeptide backbones, also varies between tissue sections. This variation suggests that different tumor sections have different protein content. In addition to changes in intensity, differences in the shape of the amide I are also apparent. A distinct absorption is apparent at around 1634 cm^{-1} in Figure 1A, which is reduced in intensity in Figure 1B and completely absent from Figure 1C. As the position of amide I absorptions is sensitive to protein conformation,[18] this implies conformational changes in tissue proteins or the expression of a new set of proteins. Changes in intensity in the 1634 cm^{-1} region of the spectrum of cancerous tissue have been suggested to arise from an altered proportion of β-sheet secondary structures in such tissue. However, we have shown that such spectral changes in a variety of tissues can be explained based

on an increase in the type I collagen content of tissue—for example, in the rat myocardium following an infarct.[9] In addition, the presence of collagen was accompanied by the appearance of absorptions at 1033, 1082, 1204, 1240, 1280, and 1338 cm^{-1}. Similar absorption bands can easily be identified in Figure 1 A and B, suggesting that the altered shape and increased intensity of the amide I absorptions in Figure 1 A and B is indeed related to the presence of type I collagen in these tumor sections.

Based upon these results, human breast tumors appear to fall into three classes upon visual inspection of their IR spectra: class I, characterized by high acylglyceride content and little collagen; class II, characterized by the presence of appreciable amounts of both acylglyceride and collagen; class III, characterized by large amounts of collagen and little or no acylglyceride. The differences among these three classes do not arise as a result of the disease being at different stages in the different tumors, as the tumors were matched with respect to grade, but result from normal spatial variations in the composition of breast tissue.

IV. DISCUSSION

Given that breast tumors of similar grade show such large spectral variation as a consequence of normal variations in histology, this raises the question, Can one detect the much less pronounced changes in the spectrum expected as a consequence of the progression of the disease? Many spectral changes expected to accompany disease progression may be masked by variations in acylglyceride and/or collagen content. For example, progression to a high-grade tumor is accompanied by the appearance of nuclear abnormalities (e.g., altered chromosomal structure, increased DNA content). The infrared absorption bands most useful in studies of DNA arise from the stretching vibrations of phosphodiester groups seen at 1080 and 1240 cm^{-1}. Since this region of the spectrum is dominated by absorptions from both collagen (see Figure 1A) and acylglycerides (see Figure 1C), the changes in cellular DNA that accompany disease progression may be masked by the large changes in collagen and acylglyceride content which are possible between tumors. Changes in protein expression accompanying the disease process, expected to be manifested in changes in the amide I absorption, may be masked by differences in collagen content. Finally, changes in cell membrane properties that would be manifested as changes in C-H absorptions may be masked by differences in acylglycerides content. These problems are highlighted in a number of studies which have attempted to interpret differences among spectra of normal and neoplastic colon,[19] bladder,[20] skin,[21] and breast tissue[22,23] in terms of such differences in DNA hydrogen bonding interactions and membrane and protein structural properties. However, inspection of the data presented in these studies clearly indicates that the changes the authors describe are in fact related to changes in collagen (colon, bladder, and skin) or adipose tissue content (breast).

An alternative approach to visual discrimination among spectra of tumors of different grade is to use the power of modern classification methods, which can assess variations in many variables simultaneously. In the case of spectra, these variables may include the absolute intensity of one or more absorptions, the position of one or more absorptions, the relative intensities of two absorptions, the width of one or more absorptions, the relative width of two absorptions, and so on. To decode complex information from spectra, typically at least 10 such variables are required to adequately describe differences between groups of measurements. This is a particularly challenging task when the changes under investigation are subtle and masked by other, nonspecific features such as noise and redundant or irrelevant information. However, such subtle changes in spectra can indeed be detected by multivariate pattern recognition methods, including hierarchical clustering, linear discriminant analysis, and artificial neural network analysis.[24,25] Such multivariate methods are powerful tools for identifying patterns that characterize different classes of spectra (hence the term "pattern recognition") based upon the comparison of a large number of variables that describe the spectra (hence the term "multivariate").

Multivariate pattern recognition methods are divided into "unsupervised" and "supervised" categories. The former, such as hierarchical clustering or fuzzy clustering, classify spectra based upon the degree of their overall similarity, and require no training. We have recently successfully applied such techniques to the classification of control and Alzheimer's-diseased central nervous system tissue,[24,25] and

benign and leukemic leukocytes.[7] However, in the present study application of cluster analysis produced two distinct groups of spectra, corresponding to spectra containing either significant contributions from collagen or from adipose tissue (not shown), with no correlation between these two clusters and any clinical criteria (e.g., tumor grade).

The lack of success of such unsupervised methods, which are generally driven by gross differences, is not surprising given the fact that the changes expected as a result of the clinical condition are subtle compared to the large changes resulting from normal histologic variation. Supervised pattern recognition methods make use of the fact that the investigator often has available a substantial amount of biochemical or clinical information concerning the samples from which the spectra were obtained. In short, we have in our possession the "class identities" of the samples with which to train our classifier. This trained classifier is then used to predict the class identity of unknown samples. We have previously applied such methods with great success to the classification of spectra of synovial fluid samples from control and arthritic joints.[26,27] We applied these more discriminatory supervised pattern recognition methods to our data. Unfortunately, even this approach was less than satisfactory, and we had to develop the novel classification strategy described in the Appendix.

Tumors were graded using the Nottingham scale[4] and classified as low grade (score: 3–5), intermediate grade (score: 6–7), or high grade (score 8–9).[8,9] The results of application of our robust classification strategy to spectra based upon tumor grade are presented in Table I. Numbers in rows represent the results of histopathological classification of the tumors, whereas numbers in columns represent the classification predicted by the trained classifier. Numbers on the diagonal (in bold italics) show the number of correctly classified spectra. Thus, for 21 tumors pathologically classified as low grade, 19 (90.5%) gave rise to spectra which could be correctly classified as arising from low-grade tumors. For intermediate-grade tumors, the accuracy of the classification was significantly reduced, only 26 of 34 spectra (76.5%) were correctly classified. In fact, perhaps not surprisingly, the accuracy of the classification of the intermediate-grade tumors was lowest of the three classifications attempted. It is interesting, however, that the classifier always misclassified intermediate-grade tumors as high-grade tumors, and never as low-grade tumors. All 22 high-grade tumors were correctly classified. The overall accuracy of the method was 87%, with 67 of 77 tumors correctly classified. Also included in Table I is κ, a chance-corrected measure of agreement, which indicates the probability that the tumor grade predicted by this method agrees with the clinical diagnosis. If the prediction was generated at random, the agreement measure would be zero, whereas for perfect classification the value would be unity. The agreement measure for this data set is 0.835.

The Nottingham grade is derived from a composite score of several quite different parameters that can be assessed under a light microscope. These include assessment of the arrangement of cells in tubule formations, nuclear morphology, and mitotic activity, and can be time-consuming to assess if done properly by counting mitoses in multiple fields. Nevertheless tumor grade as assessed in this fashion has been shown to be able to classify tumors into categories that show distinct biological potential as indicated by patient survival rates. However, as reviewed by Robbins et al.[5] concordance in grading score between pathologists in published series can range from 54 to 78%. Reproducibility between pathologists at differ-

TABLE I
Results of Classification of Breast Tumor Spectra by Grade

	L	I	H	% accuracy	SP (%)	PPV (%)
L	***19***	1	1	90.5	100	100
I	0	***26***	8	76.5	97.6	94.1
H	0	0	***22***	100	85.9	77.9

Note: Numbers in rows represent the pathological classification of tumors; results in columns are the calculated classifications. L = low grade; I = intermediate grade; H = high grade; SP = specificity; PPV = positive predictive value. Bold italics indicate correct classifications. See text for more details. Overall accuracy = 87%, κ = 0.835.

TABLE II
Results of Classification of Breast Tumor Spectra According to Estrogen Receptor Presence (+ve) or Absence (–ve)

	+ve	–ve	% accuracy	SP (%)	PPV (%)
+ve	***16***	2	88.9	96.3	96.0
–ve	1	***26***	96.3	88.9	89.2

Note: SP = specificity; PPV = positive predictive value. Numbers in rows represent the immunological classification of tumors; results in columns are the calculated classifications. Bold italics indicate correct classifications. See text for more details. Overall accuracy = 93.3%; $\kappa = 0.852$.

TABLE III
Results of Classification of Breast Tumor Spectra According to Progesterone Receptor Presence (+ve) or Absence (–ve)

	+ve	–ve	% accuracy	SP (%)	PPV (%)
+ve	***23***	1	95.8	84.0	85.7
–ve	4	***21***	84.0	95.8	95.3

Note: SP = specificity; PPV = positive predictive value. Numbers in rows represent the immunological classification of tumors; results in columns are the calculated classifications. Bold italics indicate correct classifications. See text for more details. Overall accuracy = 89.8%; $\kappa = 0.798$.

ent centers is of particular concern in the assessment of clinical trial results.[2,5,10] Even though a more standardized approach to grading of breast tumors may now be gaining acceptance, concordance among expert groups of pathologists in grading standard formalin-fixed paraffin-embedded sections remains below 75%, even after training.[5] Therefore, our results, which show a high degree of concordance between a single pathologist and FTIR spectroscopic grade, suggest that this new methodology may provide an alternative approach to microscopic grading and improved standardization of a valuable prognostic parameter. It should be made clear however, that the present study was based on a tumor series that had been selected to provide approximately equivalent representation of low, intermediate and high grade tumors. Previous studies of unselected cases may have included relatively few low-grade tumors for which the degree of concordance between pathologists is higher.[5]

We also examined the relationship between infrared spectra and steroid receptor status. The results of our classification of tumors based upon the ER/PR status is presented in Tables II and III. For estrogen receptors, correct classification as either receptor positive or negative was achieved for 93.3% of tumors ($\kappa = 0.852$), with classification of estrogen negative tumors being superior to classification of receptor positive tumors (88.9 vs. 96.3%). This situation was reversed for progesterone receptors, with 95.8% of receptor-positive tumors being correctly classified compared with 84% of receptor-negative tumors, and the overall accuracy of prediction was slightly reduced (89.8%; $\kappa = 0.798$). It should be stressed that it is unlikely that steroid receptors *per se* are being detected, as the concentration of the receptors (fg/mg tissue) is significantly below the detection limit of infrared spectroscopy. Rather, it is most likely the consequences of the presence or activation of the receptors, such as protein phosphorylation, that are being detected.

The spectral regions selected as the most diagnostic for the prediction of tumor grade and hormone receptor status are shown as the shaded areas superimposed over class average spectra (produced by calculating the arithmetic mean of all spectra in each class) in Figure 2 and Figure 3. For the prediction of tumor grade, diagnostic subregions were only found in the low-frequency (1077–1258 cm^{-1}) region of the

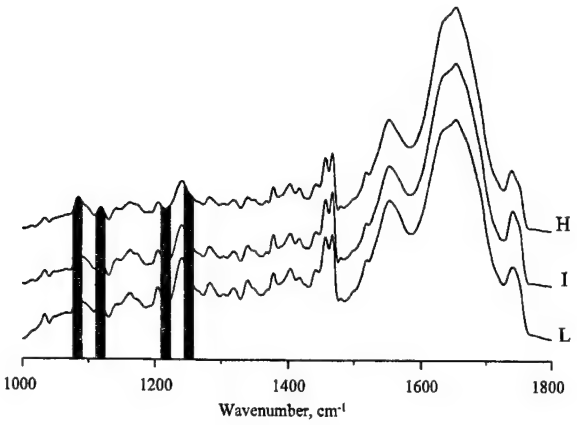

FIGURE 2. Class average infrared spectra of low- (L, Nottingham grade 3–5), intermediate- (I, Nottingham grade 6–7), and high- (H, Nottingham grade 8–9) grade breast tumors. Regions selected for use by the multivariate analysis strategy are indicated by shaded areas.

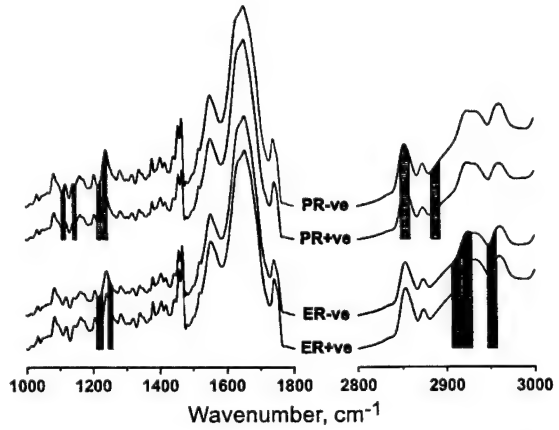

FIGURE 3. Class average spectra of estrogen receptor positive (ER+ve) and negative (ER-ve) and progesterone receptor positive (PR+ve) and negative (PR-ve) breast tumors. Regions selected for use by the multivariate analysis strategy are indicated by shaded areas.

spectrum. In contrast, the prediction of estrogen and progesterone receptor status required subregions in both high- and low-frequency regions of the spectrum (see Figure 3). Although it is difficult to determine exactly the biochemical significance of the spectral regions selected, three interesting points emerge. 1 Classification of tumors by grade, which is strongly influenced by assessment of nuclear size and morphology, was optimal using only spectral regions in which absorptions from nucleic acids are typically found (although as stressed above, collagen and adipose tissue also absorb strongly in these spectral regions). 2 Classification of tumors by receptor status required more spectral regions (i.e., more information) than prediction of tumor grade. 3 Different spectral subregions were selected for classification of tumors by grade, estrogen receptor status, and progesterone receptor status, indicating that, as expected, different biochemical events were detected in each case.

In summary we have shown that infrared spectroscopy, combined with appropriate multivariate classification methods and strategies, can be used to reliably determine the grade of human breast tumors and to classify tumors according to hormone receptor status with an accuracy of about 90%. Tumor grade and receptor status can be obtained from the same spectrum. A number of steps may be taken to improve accuracy. Most obviously, increasing the size of our database should improve accuracy of prediction. An alternative approach to the characterization of sections of breast tumors is the analysis of materials extracted from tumors. This approach has met with some success in the prediction of the biological potential of breast tumors based upon FTIR spectra of extracted DNA.[28,29] However, the extraction of DNA is time-consuming, and the structure (and thus spectroscopic properties) of the DNA may be modified during extraction. In contrast, the method described here requires no extraction and is rapid, requiring only 2–3 min to perform.

The major advantage of this novel approach to the classification of breast tumors will be standardization. The method can readily be trained on data that represented a consensus diagnosis based upon the classifications of a board of pathologists. An instrumental method using such trained data would then in essence provide practitioners with a reliable diagnosis based upon this consensus, and different laboratories analyzing the same tissue sample using such an instrument would achieve the same diagnosis. Thus, variability is removed, and consistent and reliable classification/prediction may be achieved. The clinical utility of such a technique warrants further investigation.

REFERENCES

1. McGuire WL. Prognostic factors for recurrence and survival in human breast cancer. Breast Cancer Res Treat 1987; 10: 5–9.

2. McGuire WL, Clark GM. Prognostic factors and treatment decisions in axillary-node-negative breast cancer. N Engl J Med 1992; 326:1756–1761.
3. Simpson JF, Page DL. Prognostic value of histopathology in the breast. Semin Oncol 1992; 19:254–262.
4. Elston CW, Ellis IO. Pathological prognostic factors in breast cancer. I. The value of histological grade in breast cancer: Experience from a large study with long-term follow-up. Histopathol 1991; 19:403–410.
5. Robbins P, Pinder S, de Klerk N, et al. Histological grading of breast carcinomas. A study of interobserver agreement. Hum Pathol 1995; 26:873–879.
6. Choo LP, Wetzel DL, Halliday WC, et al. In situ characterisation of β-amyloid in Alzheimer's diseased tissue by synchrotron Fourier transform infrared spectroscopy. Biophys J 1996; 71:1672–1679.
7. Schultz CP, Liu KZ, Johnston JB, et al. Study of chronic lymphocytic leukemia by FT-IR spectroscopy and cluster analysis. Leuk Res 1996; 20:649–655.
8. Choo LP, Jackson M, Halliday WC, et al. Infrared spectroscopic characterisation of multiple sclerosis plaques in the human central nervous system. Biochim Biophys Acta 1993; 1182:333–337.
9. Liu KZ, Jackson M, Sowa MG, et al. Modification of the extracellular matrix following myocardial infarction monitored by FTIR spectroscopy. Biochim Biophys Acta 1996; 1315:73–77.
10. Stenkvist B, Westman-Naeser S, Vegelius J, et al. Analysis of reproducibility of subjective grading systems for breast carcinoma. J Clin Pathol 1979; 32:979–985.
11. Somorjai RL, Dolenko B. Split and merge: A new composite strategy for classifying spectra. In: European Society for Magnetic Resonance in Medicine and Biology, 13th Annual Meeting, Prague. New York: Chapman & Hall; 1996; 323–324.
12. Somorjai RL, Nikulin AE, Pizzi N, et al. Computerized consensus diagnosis: A classification strategy for the robust analysis of MR spectra. I. Application to ^{1}H spectra of thyroid neoplasms. Magn Reson Med 1995; 33:257–263.
13. Wolpert DH. Stacked generalization. Neural Networks 1992; 5:241–259.
14. Efron B, Tibshirani RJ. An introduction to the bootstrap. In: Monographs on statistics and applied probability. Vol. 57. New York: Chapman & Hall; 1993.
15. Jackson M, Mantsch HH. Biomembrane structure from FT-IR spectroscopy. Spectrochimica Acta Rev 1993; 15:53–69.
16. Jackson M, Mantsch HH. FTIR spectroscopy in the clinical sciences. In: Clarke RJH, Hester RE, eds. Biomedical applications of spectroscopy. London: John Wiley & Sons; 1996: 185–215.
17. Jackson M, Mantsch HH. Biomedical infrared spectroscopy. In: Mantsch HH, Chapman D, eds. Infrared spectroscopy of biomolecules. New York: Wiley-Liss; 1996:311–340.
18. Jackson M, Mantsch HH. The use and misuse of FTIR spectroscopy in the determination of protein secondary structure. CRC Crit Rev Biochem Mol Biol 1995; 30:95–120.
19. Rigas B, Morgello S, Goldman IS, et al. Human colorectal cancers display abnormal Fourier transform infrared spectra. Proc Natl Acad Sci U S A 1990; 87:8140–8144.
20. Lin AY, Liang RC, Hsu HS, et al. Evidence of possible carcinogenesis during conformational changes in bladder mucosa induced by bladder outlet obstruction. Cancer Lett 1995; 79:221–226.
21. Wong PTT, Goldstein SM, Grekin RC, et al. Distinct infrared spectroscopic patterns of human basal cell carcinoma. Cancer Res 1993; 53:762–765.
22. Wallon J, Yan SH, Tong J, et al. Identification of breast carcinomatous tissue by near infrared reflectance spectroscopy. Appl Spectrosc 1994; 48:190–193.
23. Meurens M, Wallon J, Tong J, et al. Breast cancer detection by Fourier transform infrared spectrometry. Vibrational Spectrosc 1996; 10:341–346.
24. Choo LP, Mansfield JR, Pizzi N, et al. Infrared spectra of human central nervous system tissue: Diagnosis of Alzheimer's disease by multivariate analyses. Biospectroscopy 1995; 1:141–148.
25. Pizzi N, Choo LP, Mansfield JR, et al. Neural network classification of infrared spectra of control and Alzheimer's diseased tissue. Art Int Med 1995; 7:67–69.
26. Shaw RA, Kotowich S, Eysel HH, et al. Classification of arthritic disorders based upon near infrared spectra. Rheumatol Int 1995; 15:159–166.
27. Eysel HH, Jackson M, Nikhulin A, et al. A novel, non-subjective diagnostic test for arthritis utilising FTIR spectroscopy and multivariate classification. Biospectroscopy 1997; 3:161–167.
28. Malins DC, Polissar NL, Nishikida K, et al. The etiology and prediction of breast cancer. Cancer 1995; 75:503–517.
29. Malins DC, Polissar NL, Gunselman SJ. Tumour progression to the metastatic state involves structural modifications in DNA markedly different from those associated with primary tumour formation. Proc Natl Acad Sci U S A 1996; 93: 14047–14052.
30. McLachlan GJ. Discriminant analysis and statistical pattern recognition. New York: John Wiley; 1992.

APPENDIX 1

For most classification studies the standard linear discriminant analysis (LDA) method[30] with the leave-one-out cross validation works well (with the proviso that the data were appropriately preprocessed). LDA is the classifier of choice due to its simplicity and speed. It explicitly determines the boundaries (defined by the equations for the linear combinations of attributes) that best separate the classes. Class assignment of any given spectrum involves computing its distance from all class centroids (i.e., the representative class average spectra) and allocating it to the class whose centroid is nearest. The "resubstitution" error (rE) is calculated by using all data to determine the optimum

LDA classifier. rE tends to be optimistically low, especially when the number of sample per class is small. The remedy is to make the classifier more realistic and robust with respect to classification error by cross-validation. One common cross-validation technique is called "leave-one-out" (LOO). It works by sequentially omitting one of the n samples, training a classifier using the remaining $n - 1$, assigning the sample that was left out of the training, and carrying out this process for all n samples. The average error committed by these n classifiers is never less than rE, and is a more realistic estimate of the true error rate. However, especially when n is relatively small and the number of spectra per class is widely different, LOO can be unreliable and still too optimistic. The more realistic approach of partitioning the n spectra into a "training" and a "test" set, optimizing the classifier on the training set and validating its classification power on the test set, can exacerbate the reliability problem, since we now use only $\sim n/2$ of the already few n samples. Furthermore, classification of a new sample, not in the original n, would involve assigning it to all $\sim n/2$-trained classifiers. This implies that these classifiers would have to be always available, creating awkward storage problems. The cross-validation approach we have implemented is designed to remedy these problems. It is a type of "bootstrapping" methodology. It consists of repeatedly partitioning, with replacement, the data into approximately equal-sized random training and test subsets. For each of the random training subsets, an optimal classifier is produced, and its accuracy validated on the random test subset. The process is repeated a number of times (25 times at the less critical preprocessing stages, 250 times for the final classifiers). The ultimate classifier is the average of these individual component classifiers. This approach eliminates storage problems, while effectively using all n samples. Its expected classification accuracy can be validated by how well it does on the entire n samples. Although any classifier could be used, LDA, because of its speed and robustness, was the choice for all classifiers, at all stages.

Preprocessing was found to be essential for developing reliable classifiers. The preprocessing method selects relevant features from the spectra by an optimal region selection (ORS) algorithm developed in-house.[11] ORS starts at one end of an N-point spectrum by selecting a window consisting of $M << N$ adjacent data points. Typically, $M = 10$–12. LDA with bootstrapping (25 random samples) is carried out with these M points as local attributes, and the average classification accuracy on the test subsets is recorded. The window is advanced by $M/2$ data points along the spectrum and the process repeated. When the spectra are fully traversed, the nonoverlapping subregions are sorted in decreasing order of accuracy. If the best subregion found satisfies a prescribed accuracy (typically $\geq 90\%$), the subregion selection process is terminated. This happens rarely, and thus the next stage is initiated. The best 6–8 subregions (comprising $6 \times M - 8 \times M$ data points) are tested in all possible combinations (i.e., all pairs, triplets, etc.). The most parsimonious combination (least number L of subregions, $L \leq 8$) that satisfies the accuracy criterion provides the feature set for our final classifier. Typically, $L = 3$–6 combined subregions ($3 \times M - 6 \times M$ data points) are found optimal. The final step is the verification of the accuracy and robustness of the ultimate classifier, using the derived attributes. This is done by carrying out 250 bootstrap steps and creating the averaged classifier. If even this process does not yield a satisfactory classifier, we invoke our classifier aggregation stage,[12] computerized consensus diagnosis (CCD). The idea behind CCD is to combine differently the L optimal subregions (i.e., $L \times M$ data points, $L = 3$–6) found earlier. Our implementation of classifier aggregation is called stacked generalization (SG).[13] SG works by presenting sequentially to classifier j the corresponding M attributes of a given spectrum and recording the C class assignment probabilities p_i^j, $i = 1,2,...,C$, $j = 1,2,...,L$, $\Sigma_i p_i^j = 1$ (C is the number of classes, L the number of classifiers). These $C \times L$ probabilities serve as the new input attributes to a higher level classifier. At this ultimate stage, 250 bootstrap samples are taken again to produce the final robust classifier. Note that SG generally reduces the total number of attributes, since $C < M$. In addition, the class assignment probabilities tend to be much less ambiguous, i.e., fewer spectra are classified ambiguously (unreliably).

American Journal of Pathology, Vol. 155, No. 6, December 1999

Psoriasin (S100A7) Expression and Invasive Breast Cancer

Sahar Al-Haddad,* Zi Zhang,* Etienne Leygue,† Linda Snell,* Aihua Huang,* Yulian Niu,* Tamara Hiller-Hitchcock,* Kate Hole,* Leigh C. Murphy,† and Peter H. Watson*

Departments of Pathology and Biochemistry and Molecular Biology,† University of Manitoba, Faculty of Medicine, Winnipeg, Manitoba, Canada*

Alteration of psoriasin (S100A7) expression has previously been identified in association with the transition from preinvasive to invasive breast cancer. In this study we have examined persistence of psoriasin mRNA and protein expression in relation to prognostic factors in a cohort of 57 invasive breast tumors, comprising 34 invasive ductal carcinomas and 23 other invasive tumor types (lobular, mucinous, medullary, tubular). We first developed an IgY polyclonal chicken antibody and confirmed specificity for psoriasin by Western blot in transfected cells and tumors. The protein was localized by immunohistochemistry predominantly to epithelial cells, with both nuclear and cytoplasmic staining, as well as occasional stromal cells in psoriatic skin and breast tumors; however, *in situ* hybridization showed that psoriasin mRNA expression was restricted to epithelial cells. In breast tumors, higher levels of psoriasin measured by reverse transcriptase-polymerase chain reaction and Western blot (93% concordance) were significantly associated with estrogen and progesterone receptor-negative status ($P < 0.0001$, $P = 0.0003$), and with nodal metastasis in invasive ductal tumors ($P = 0.035$), but not with tumor type or grade. Psoriasin expression also correlated with inflammatory infiltrates (all tumors excluding medullary, $P = 0.0022$). These results suggest that psoriasin may be a marker of aggressive behavior in invasive tumors and are consistent with a function as a chemotactic factor. *(Am J Pathol 1999, 155:2057–2066)*

Earlier diagnosis of breast cancer has increased the need for the identification of molecular alterations that might serve as tissue markers to predict the risk of progression to metastatic disease. Among the most important of these alterations are likely to be those associated with the development of the invasive phenotype and the transition from preinvasive to invasive cancer with the capability for subsequent metastasis.

We have recently identified psoriasin (S100A7) as a gene that is frequently overexpressed in preinvasive ductal carcinoma *in situ* (DCIS) relative to adjacent invasive carcinoma, suggesting a role in breast tumor progression.[1] Other members of the S100 gene family of calcium-binding proteins have been implicated in a range of biological processes, including tumor metastasis.[2] In particular, S100A2 has been shown to be down-regulated in breast tumor cells relative to their normal epithelial cell counterparts,[3] whereas up-regulation of S100A4 has been strongly implicated in breast tumor metastasis.[4–6] In the latter case this may reflect the ability of S100A4 to influence cell motility,[7] the cytoskeleton[6,8,9] or cell adhesion molecules.[10] Psoriasin was initially identified as a highly abundant protein belonging to the S100 gene family,[11] expressed by abnormally proliferating keratinocytes in psoriatic epidermis.[12,13] It has subsequently been shown to be a secreted protein that can exert an effect as a chemotactic factor for inflammatory cells.[14,15] However, the function of psoriasin in breast cancer remains to be determined.[16] In this study we have developed a psoriasin-specific antibody and evaluated the persistence of psoriasin expression in invasive breast tumors with different invasive and metastatic potential as well as host inflammatory response.

Materials and Methods

Human Breast Tissues and Cell Lines

All breast tumor cases used for this study were selected from the NCIC–Manitoba Breast Tumor Bank (Winnipeg, Manitoba, Canada). As has previously been described,[17] tissues accrue to the Bank from cases at multiple centers within Manitoba and are rapidly collected and processed to create matched formalin-fixed embedded and frozen tissue blocks for each case, with mirror-image surfaces

Supported by grants from the Medical Research Council of Canada (MRC) and the U.S. Army Medical Research and Materiel Command (USAMRMC). The Manitoba Breast Tumor Bank is supported by funding from the National Cancer Institute of Canada (NCIC). P. H. W. is an MRC Clinician-Scientist; L. C. M. is an MRC Scientist; E. L. is a recipient of a USAMRMC Postdoctoral Fellowship. T. H.-H. is a recipient of an MRC studentship award.

Accepted for publication August 24, 1999.

Address reprint requests to Dr. Peter Watson, Department of Pathology, D212-770 Bannatyne Ave., University of Manitoba, Winnipeg, MB R3E OW3, Canada. E-mail: pwatson@cc.umanitoba.ca.

oriented by colored inks. The histology of every sample in the Bank is uniformly interpreted in hematoxylin/eosin (H&E)-stained sections from the face of the paraffin tissue block by a pathologist. This information is available in a computerized database along with relevant pathological and clinical information and was used as a guide for the selection of specific paraffin and frozen blocks from cases for this study. For each case interpretations included an estimate of the cellular composition (including the percentage of invasive epithelial tumor cells, collagenous stroma, and fatty stroma), tumor type, and tumor grade for ductal tumors (Nottingham score).[18,19] The inflammatory host response was scored semiquantitatively on a scale of 1 (low) to 5 (high). Steroid receptor status was determined for all cases by ligand binding assay performed on an adjacent portion of tumor tissue. Tumors with estrogen and progesterone receptor levels above 20 fmol/mg and 15 fmol/mg of total protein, respectively, were considered ER- or PR-positive.

Two cohorts of tumors were selected. The first cohort comprised 35 invasive ductal carcinomas selected to include six subgroups differing with respect to estrogen receptor status (ER-positive and ER-negative) and tumor grade (low, intermediate, high). Additional selection criteria also included high tissue quality, presence of invasive tumor within >35% of the cross section of the frozen block for invasive ductal cases, and minimal (<5%) normal or *in situ* epithelial components. The second cohort comprised 23 invasive tumors selected to include four subgroups of different tumor types[18] that vary in differentiation and metastatic potential, including invasive lobular (six), medullary (five), tubular (six), and colloid (six). Similar secondary criteria were also used for this cohort.

For analysis of antibody specificity and for positive controls for tumor assays, MCF7 human breast cancer cells obtained from the American Type Culture Collection (Manassas, VA) were used. MCF7 cells were grown as previously described under normal conditions in the presence of 5% fetal bovine serum, to provide a negative control.[20] Alternatively MCF7 cells were subjected to estrogen-deprived conditions in the presence of charcoal-stripped serum before stimulation by estradiol (10^{-8} mol/L) for 48 hours before harvesting to induce psoriasin expression and provide a positive control. As an additional positive control MDA-MB-231 human breast cancer cells were transfected with a plasmid containing the cytomegalovirus (CMV) promotor adjacent to the psoriasin cDNA (Hiller-Hitchcock T, Leygue E, Cummins-Leygue C, Murphy LC, Watson PH, manuscript in preparation), and stable transfectants (CL7FD3 cell clone) expressing psoriasin mRNA were also used.

Antibody Reagents

A psoriasin-specific chicken IgY polyclonal antibody was generated by immunization of chickens with a 14-amino acid peptide corresponding to the carboxy terminus of psoriasin (KQSHGAAPCSGGSQ; Bionostics, Toronto, and Aves Labs). A >90% pure IgY fraction from chicken egg yolk was obtained in phosphate-buffered saline (PBS) and then further purified by passing it over a psoriasin peptide affinity column made by binding the synthetic peptide to N-hydroxy-succinimide-activated Sepharose 4B (Pharmacia Biotech), according to the manufacturer's instructions. The bound IgY was then eluted with 5.0 mol/L sodium thiocyanate, followed by dialysis against PBS. Additional antibodies used included a commercial anti-S100 antibody (Sigma, St. Louis, MO) as well as a rabbit polyclonal antibody, raised against the recombinant protein (kindly provided by Prof J. Celis, University of Aarhus, Aarhus, Denmark).

Western Blot Analysis

For tumors, multiple sections (10–20 × 20 μm) were cut from the face of frozen tissue blocks immediately adjacent to the face of the matching paraffin block.[17] For cell lines, trypsinized cell pellets were obtained from breast cancer cell lines (grown to ~80% confluence). Total protein lysates were extracted from both the cell line pellets and frozen tissue sections, using Tri-reagent (Sigma), as described by the manufacturer. The recovered protein was dissolved in SDS isolation buffer (50 mmol/L Tris, pH 6.8, 20 mmol/L EDTA, 5% sodium dodecyl sulfate (SDS), 5 mmol/L β-glycerophosphate) and a cocktail of protease inhibitors (Boehringer Mannheim, Laval, PQ). Protein concentrations were determined using the Micro-BCA protein assay kit (Pierce, Rockford, IL). Sixty micrograms of total protein lysates were run on a 16.5% sodium dodecyl sulfate-polyacrylamide gel electrophoresis (SDS-PAGE) mini gel, using Tricine SDS-PAGE to separate the proteins,[21] and then transferred to 0.2-μm Nitrocellulose (Bio-Rad, Mississauga, ON). After blocking in 10% skimmed milk powder in Tris-buffered saline-0.05% Tween (TBST buffer), blots were incubated with chicken IgY anti-psoriasin antibody (~15 μg/ml in TBST), followed by incubation with secondary antibody, rabbit IgG anti-chicken IgY conjugated to horseradish peroxidase (1:5000 dilution in TBST; Jackson ImmunoResearch Laboratories), and visualization by incubation with Supersignal (Pierce), per the manufacturer's instructions. Exposed x-ray films were photographed, and the band intensities were determined by video image analysis, using MCID M4 software (Imaging Research, ST. Catherine's, ON). All signals were adjusted with reference to the psoriasin-transfected MDA-MB-231 cell control (CL7FD3), run on each blot.

Immunohistochemistry

Immunohistochemistry was performed on 5-μm paraffin-embedded breast tumor tissue sections from tissue blocks fixed in 10% neutral buffered formalin for 18–24 hours. After deparaffinizing, clearing, and hydrating to PBS buffer (pH 7.4) containing 0.05% Tween 20 (Mallinckrodt), the sections were pretreated with hydrogen peroxide (3%) for 10 minutes to remove endogenous peroxidases, and nonspecific binding was blocked with normal rabbit serum (1:50; Sigma). Primary chicken IgY

anti-psoriasin antibody (1:500 dilution in PBS) was applied for 1 hour at 37°C followed by washing and incubation with the secondary antibody, peroxidase-conjugated affinity purified rabbit anti-chicken (1:200 dilution), for 1 hour at room temperature. Detection was performed with 3,3′-diaminobenzidine tetrahydrochloride peroxidase substrate (Sigma) and counterstaining with methyl green (2%), followed by dehydration, clearing, and mounting. A positive tissue control and a negative reagent control (normal rabbit serum only/no primary antibody) were run in parallel in all experiments. Immunostaining was scored semiquantitatively by assessing the average signal intensity (on a scale of 0 to 3) and the proportion of tumor cells showing a positive nuclear signal (0, none; 0.1, less than one-tenth; 0.5, less than one-half; 1.0 greater than one-half). The intensity and proportion scores were then multiplied to give an overall score, and tumors with a score equal to or higher than 1.0 were deemed positive.

In Situ *Hybridization*

In situ hybridization was performed on paraffin sections (5 μm) according to a previously described protocol.[1] Linearized psoriasin plasmid cDNA (1.0 μg/μl) was used to generate UTP^{S35}-labeled sense and antisense RNA probes with the Riboprobe System (Promega, Madison, WI) according to the manufacturer's instructions. Sense and antisense probes were equalized by diluting 1×10^6 cpm/μl in hybridization solution. These were then applied to paraffin sections (approximately 30 μl of probe per section) that had undergone postfixation with 4% paraformaldehyde (pH 7.4) in PBS and further pretreatments with triethanolamine/acetic anhydride and proteinase K before hybridization. Sections were then coverslipped, sealed, and incubated overnight in a humid chamber at 42°C. After coverslip removal, sections underwent incubation in posthybridization solution and buffered RNase A (20 μg/ul), followed by several washes in descending dilutions of standard saline citrate buffer to remove weakly bound nonspecific label. After dehydration in ethanol containing 300 mmol/L ammonium acetate, the sections were coated in NTB-2 Kodak emulsion, subsequently developed after various time intervals from 2 to 5 weeks, and counterstained with Lee's methylene blue and basic fuchsin. Psoriasin expression was assessed by bright-field microscopic examination at low power (10× objective) magnification with reference to the negative sense and positive control tumor sections run with each batch. Levels were scored semiquantitatively as previously described[22] by assessing the average signal intensity (on a scale of 0 to 3) and the proportion of tumor cells showing a positive signal (0, none; 0.1, less than one-tenth; 0.5, less than one-half; 1.0 greater than one-half). The intensity and proportion scores were then multiplied to give an overall score, and tumors with a score equal to or higher than 1.0 were deemed positive.

Reverse Transcriptase-Polymerase Chain Reaction Analysis

Reverse transcriptase-polymerase chain reaction (RT-PCR) was performed based on extracted RNA (600 ng) that was reverse transcribed in a total volume of 20 μl as described previously.[1] Briefly, reverse transcription was completed with the following reaction mixture: for each sample, 200 ng (2 μl of 0.1 μg/μl) of total RNA was added to 16 μl of RT mix (4 μl of 5× RT buffer; 1 μl of each of dATP, dCTP, dGTP, and dTTP, all at 2.5 mmol/L; 2 μl of 0.1% bovine serum albumin; 2 μl of 0.1 mol/L dithiothreitol; 1 μl of 0.25 mol/L random hexamer primer; 2 μl of dimethyl sulfoxide (DMSO), and 1 μl of 200 units/μl of Moloney murine leukemia virus reverse transcriptase) and incubated at 37°C for 1.5 hours. Each PCR was performed in 50-μl volume, using 1 μl of the completed RT reaction (cDNA); 30.8 μl of sterile water; 5 μl of 10× PCR buffer; 5 μl of 25 mmol/L $MgCl_2$; 200 mmol/L each of dATP, dCTP, dGTP, and dTTP; 1 μl of DMSO; 1 unit of Taq DNA polymerase; and 0.5 μl of 50 mmol/L PCR primers. The psoriasin primers were sense (5′-AAG AAA GAT GAG CAA CAC-3′) and antisense (5′-CCA GCA AGG ACA GAA ACT-3′) corresponding to the cDNA sequence,[13] or alternatively, PCR was performed with GAPDH primers, sense (5′-ACC CAC TCC TCC ACC TTT G-3′) and antisense (5′-CTC TTG TGC TCT TGC TGG G-3′).[23] For PCR amplification the reaction comprised an initial step of 5 minutes at 94°C, and then 45 cycles (30 seconds at 94°C, 30 seconds at 56°C, 30 seconds at 72°C) for psoriasin or 35 cycles (45 seconds at 93°C, 45 seconds at 58°C, 30 seconds at 72°C) for GAPDH. PCR products of the two genes amplified from the same RT reaction were loaded into the same wells onto a 1.5% agarose gel before electrophoresis and ethidium bromide staining to visualize psoriasin (246 bp) and GAPDH (198 bp) cDNAs under UV illumination.

Preliminary experiments were performed with cell line and tumor RNA samples to establish the appropriate RNA input and PCR cycle number conditions to achieve amplification with both psoriasin and GAPDH primers in the linear range in a typical sample. Tumors from each cohort were processed as a batch, from frozen sectioning to RNA extraction, reverse transcription in triplicate, and then duplicate PCRs from each RT reaction. For each batch controls included RT-negative and RNA-negative controls and both psoriasin-positive (estradiol-stimulated MCF7) and psoriasin-negative (untransfected, wild-type MDA-MB-231 cells) RNA controls. All primary tumor PCR signals were assessed in gels and autoradiographs by video image capture and with a MCID-M4 image analysis program. Psoriasin expression was standardized to GAPDH expression assessed from the same RT reaction in separate PCR reactions and run in parallel on the same gel, and the mean of each duplicate PCR was then expressed relative to the levels in the MCF7 cell line standard. The invasive tumor component within each section was also assessed in the adjacent mirror image paraffin section, and the percentage area occupied by tumor was

used to correct for differences in epithelial cell content of the tumor sections used for RNA extraction.

Statistical Analysis

For analysis of associations, standardized psoriasin mRNA levels were used either as a continuous variable or transformed into low- or high-expression categories, using a level of one relative density unit. This cutpoint was selected to correspond to the lowest level at which protein could be detected by Western blot. Correlations with estrogen (ER) and progesterone (PR) receptor levels and inflammation were tested using Spearman's test. Associations with categorical variables were tested by either Mann-Whitney or analysis of variance tests for selected dependent variables, or unpaired *t-test for independent variables, or a* χ^2 *test.*

Results

Characterization of Psoriasin-Specific Antibody

Multiple S100 proteins are expressed in individual tissues and cells. To specifically distinguish psoriasin expression within archival formalin-fixed and paraffin-embedded tissues we raised a polyclonal antibody in chicken against a synthetic peptide that corresponded to the COOH terminus of psoriasin. This 14-amino acid region was selected on the basis of very low homology to other S100 proteins. Western blot analysis of an MDA-MB-231 breast cell line transfected with a plasmid incorporating psoriasin cDNA under the control of a CMV promotor (and known to express psoriasin mRNA by Northern blot; unpublished data) and breast tumors showed a single band corresponding to a protein of approx 11.7 kd with the chicken IgY antibody (Figure 1A). This signal could be completely inhibited by preincubation of the primary antibody with psoriasin synthetic peptide (data not shown) and was absent from the wild-type and vector-alone transfected MDA-MB-231 control cells. By comparison, a commercial anti-S100 antibody (Sigma), known to detect several S100 proteins in MDA-MB-231 cells,[24] weakly recognized the same 11.7-kd protein in transfected cells as well as several other S100 proteins in most samples (Figure 1B). Both antibodies reacted with additional higher molecular mass bands in tumor samples. However, specificity of the 11.7-kd psoriasin signal was further confirmed by Western blot using another anti-psoriasin polyclonal rabbit antibody previously raised against a recombinant psoriasin protein (data not shown).

Localization of Cellular Expression of Psoriasin

To assess cellular localization of psoriasin we studied paraffin-embedded tissue blocks from breast, skin, and larynx by immunohistochemistry. The breast tumors studied possessed either high (six cases) or low (seven cases) levels of psoriasin mRNA and total protein expression (determined by Western blot and RT-PCR analysis of

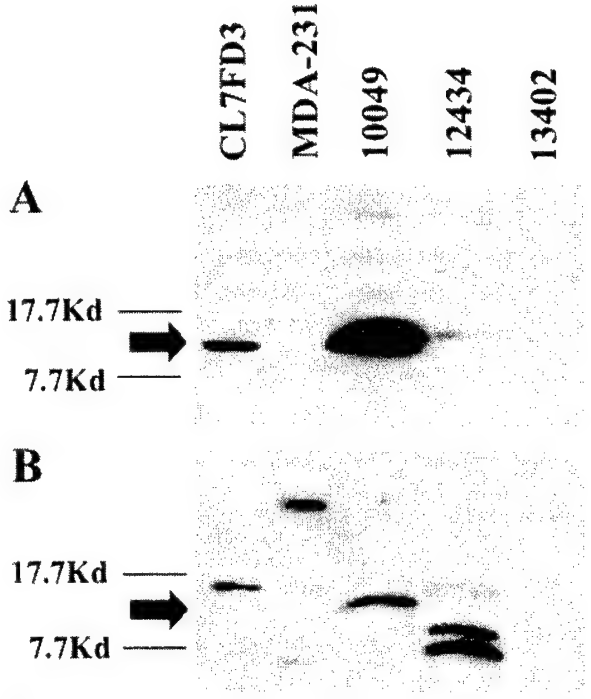

Figure 1. Western blot analysis of cell lines and tumors to demonstrate anti-psoriasin IgY antibody specificity. **A:** A protein band (approx 11.7 kd) detected using a chicken IgY anti-psoriasin antibody in a psoriasin-transfected MDA-MB-231 breast cell line and two tumors (10049, 12434), but absent in tumor 13402 and wild-type MDA-MB-231 cells. **B:** Detection of several S100-like proteins, using a commercial polyclonal S100 antibody applied to the same samples, in addition to weak detection of the same (approx 11.7 kd) protein band seen in **A**.

protein and RNA extracted from sections cut from the adjacent mirror-image frozen tissue blocks). Skin biopsies from the margins of two psoriatic lesions and a squamous carcinoma of larynx were also studied, as psoriasin was originally identified as a highly expressed protein in psoriatic skin and has also been identified as an expressed sequence tag in a cDNA library from laryngeal squamous carcinoma (http://www.ncbi.nlm.nih.gov/UniGene/Hs.112408). All cases were subjected to both immunohistochemistry and *in situ* hybridization on adjacent paraffin sections, and both signals were assessed independently, using a semiquantitative scoring system as described in Materials and Methods.

In breast tumors psoriasin protein was detected predominantly within epithelial tumor cells and was localized within both tumor cell nuclei as well as cytoplasm. Psoriasin was also present within some stromal cells and in some cases also on the luminal aspects of endothelial cells within small vessels (Figure 2). However, *in situ* hybridization demonstrated that mRNA expression was limited to epithelial tumor cells in all cases (Figure 2). The nuclear immunohistochemical staining was completely abolished by competition with the immunizing peptide and was not present in tumors that were negative for psoriasin but showed additional immunoreactive bands on Western blot (eg, see case 13402, Figure 1, and case 8840, Figure 4). Immunohistochemistry and Western blot were concordant in 12/13 cases. In one case Western blot analysis was negative and weak focal staining was

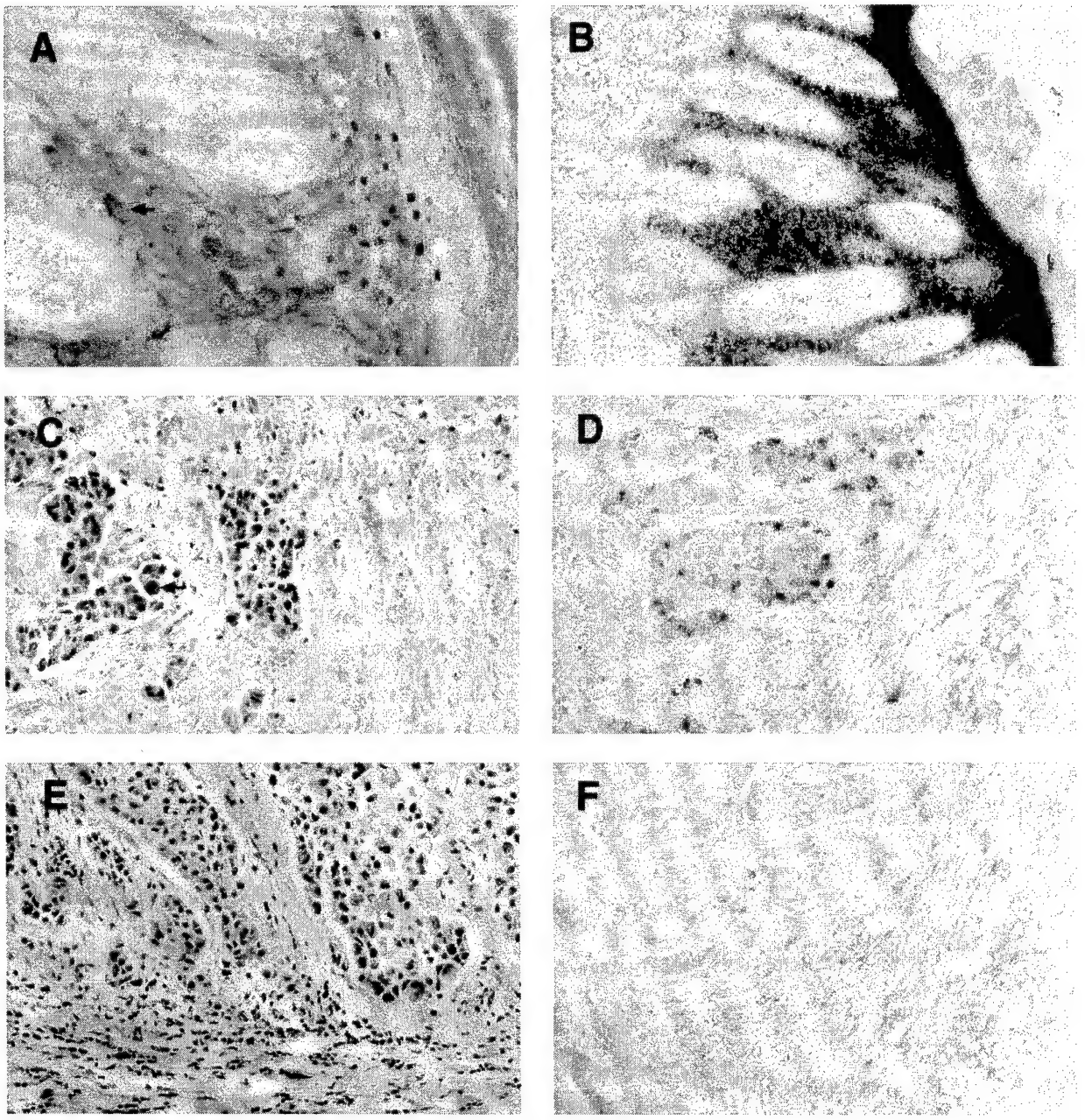

Figure 2. Immunohistochemical and *in situ* hybridization analysis of the cellular distribution and patterns of expression of psoriasin within psoriatic skin and breast carcinoma. Psoriasin protein is localized in hyperplastic epidermis of skin to both nuclei (**A**, **white arrow**) and cytoplasm (**A**, **black arrow**) of keratinocytes. Similar nuclear and cytoplasmic staining is seen in breast epithelial tumor cells (**C**, **black arrow**; case 8965). Psoriasin protein is also detected within occasional stromal inflammatory cells (**C**, **white arrow**). **E:** H&E-stained section from the same region of the tumor shown in **C**. Psoriasin mRNA expression in skin is restricted to epithelial cells in suprabasal layers of epidermis (**B**) and scattered invasive epithelial tumor cells in breast tumors (**D**), detected using antisense probe (**B** and **D**) compared to sense probe (**F**). Original magnification for all panels at the microscope, ×200.

seen by immunohistochemistry. Specificity of the nuclear signal was further confirmed by the fact that the presence of immunohistochemically detected protein expression, assessed on the basis of nuclear staining, was highly concordant (92%) with expression detected by *in situ* hybridization mRNA.

In skin, immunohistochemical staining was localized to keratinocytes within the mid to upper zones of the epidermis of skin showing psoriasiform hyperplasia. These keratinocytes corresponded to the cells that also showed mRNA expression by *in situ* hybridization in adjacent sections (Figure 2). The adjoining normal skin was negative. Occasional positive immunohistochemical staining, but no mRNA signal, was also observed in stromal cells in the dermis underlying the psoriatic lesion. As seen in breast tumor cells, psoriasin protein was localized both to the nucleus and cytoplasm within keratinocytes (Figure 2). The same nuclear and cytoplasmic localization was also detected in a squamous laryngeal carcinoma (data not shown). However, the polyclonal rabbit anti-psoriasin

antibody previously shown to provide immunofluorescent staining in frozen skin sections[13,25] did not detect any signal on paraffin sections from skin or breast. Additional experiments were performed with the chicken IgY anti-psoriasin antibody on skin and breast tumor sections in which immunohistochemical conditions (microwave *versus* protease antigen retrieval) and tissue treatment/fixation conditions (formalin *versus* alcohol *versus* paraformaldehyde *versus* frozen) were varied, and nuclear localization persisted under all conditions (data not shown).

Expression of Psoriasin mRNA in Invasive Breast Tumors

The changes in psoriasin expression previously observed in association with the transition from *in situ* to invasive carcinoma suggested a functional role in the early stages of progression. However, alteration of psoriasin expression in normal skin has also been associated with abnormal keratinocyte differentiation. To examine further the relationship of psoriasin with differentiation and invasiveness, we used RT-PCR and Western blot to examine psoriasin mRNA and protein levels in a cohort of invasive tumors. These tumors included several different tumor types and a range of differentiation, as determined by tumor grade and estrogen receptor status (Table 1).

Psoriasin mRNA was detected in all tumors by RT-PCR, but the levels varied considerably and were mostly low (Figure 3). Within the invasive ductal subgroup there was no significant difference in psoriasin expression with tumor grade. There was also no significant difference between tumor size or type, although there was a trend toward lower levels of expression in both well-differentiated tumor types, tubular and mucinous carcinomas, whereas lobular and medullary carcinomas showed a trend toward higher expression than invasive ductal tumors. However, higher levels of psoriasin mRNA expression showed a significant inverse correlation with both ER and PR levels ($r = -0.66$, $P = 0.0001$; $r = -0.47$, $P = 0.0003$, Spearman) and with ER and PR negative status (ER-ve *vs.* ER+ve; $n = 28$ *vs.* 29, mean (SD) 1.032 (0.7) *vs.* 0.32 (0.36), $P < 0.0001$ Mann-Whitney; PR-ve *vs.* PR+ve, $n = 25$ *vs.* 32, 1.05 (0.72) *vs.* 0.37 (0.40), $P < 0.0001$) in all tumors and within the invasive ductal subgroup. Psoriasin expression was also higher in axillary node-positive cases in all tumors (mean (SD) = 0.86 (0.73) *vs.* 0.59 (0.66), and the difference was statistically significant for the invasive ductal subgroup (mean (SD) = 0.88 (0.79) *vs.* 0.38 (0.28), $P = 0.035$, *t*-test). These relationships with ER, PR, and nodal status (Table 2) were also evident and remained statistically significant after correction of psoriasin levels for the relative tumor cell content, assessed as a percentage within the paraffin sections adjacent to the frozen tissue sections studied.

Psoriasin protein was detected by Western blot analysis in 10 tumors (Table 1 and Figure 4). These tumors (six ductal, two lobular, two medullary) corresponded to those with the highest mRNA levels observed by RT-PCR (above 1.0 arbitrary expression units). Also consistent with RT-PCR analysis, Western blot-positive invasive ductal tumors were also significantly associated with ER-negative ($P < 0.0001$) and PR-negative ($P < 0.0012$) and node-positive ($P = 0.0143$) status (Table 2).

The relationship between psoriasin mRNA and protein expression and host inflammatory response was also examined (Table 2). Psoriasin mRNA showed a significant positive correlation in the entire cohort ($n = 57$, $r = 0.47$, $P = 0.0002$), in the entire cohort excluding the medullary carcinoma subgroup, which includes inflammatory infiltrates as a diagnostic criterion ($n = 52$, $r = 0.42$, $P = 0.0022$), and within the invasive ductal subgroup alone ($n = 34$, $r = 0.39$, $P = 0.023$). Cases with Western blot-detectable psoriasin protein also showed increased inflammatory infiltrates, both in the entire cohort (mean (SD) = 3.6 (1.1) *vs.* 2.3 (1.2), $P = 0.004$) and in the entire cohort excluding the medullary subgroup (mean (SD) = 3.3 (0.89) *vs.* 2.1 (0.98), $P = 0.007$).

Discussion

We have developed a psoriasin-specific antibody and confirmed its specificity as well as its ability to detect the psoriasin protein in formalin-fixed and paraffin-embedded specimens. We have shown that there is a high concordance between psoriasin mRNA and protein levels in invasive tumors, and persistance of psoriasin expression at higher levels is significantly associated with poor prognostic markers, including ER- and PR-negative and lymph node-positive status. Psoriasin expression within breast tumor cells is also associated with inflammatory infiltrates.

Indirect support for a role for S100 genes in breast tumor progression is provided by several observations. Disruption of calcium signaling pathways has been implicated as a central mechanism in tumorigenesis and specifically in the process of invasion and metastasis.[26] Moreover, the chromosomal location of the S100 gene family lies in a region of chromosome 1 that frequently (>50%) shows loss of heterozygosity in invasive tumors.[27] Furthermore, several S100 genes are expressed in breast cell lines and tumors and are known to manifest alteration of their expression in association with tumorigenesis and progression.[11,24] In particular, S100A2 and S100A4 have been identified to be differentially expressed between normal and neoplastic cells[3,28,29] and up-regulated in metastatic as compared to nonmetastatic cells in both mouse and rat mammary tumor cell lines.[5,30] *In vivo* studies of breast tumors have also shown a correlation between high levels of S100A4 expression, nodal metastasis, and ER-negative status.[31] More direct evidence has emerged from modulation of S100A4 expression in transfected cell lines that have shown that overexpression of S100A4 can also induce the metastatic phenotype in mouse, rat, and human cells.[4,6,32] Furthermore, there is evidence that S100A4 may exert its effect on cell cytoskeleton[8,9] and motility,[7] and it has also been demonstrated that up-regulation of S100A4 in mouse tumor cell lines can down-regulate expression of E-

Table 1. Clinicopathological Parameters, Histological Composition of the Tumor Section, and Psoriasin Expression in 57 Invasive Breast Carcinomas Assessed by RT-PCR and Western Blot

	Clinicopathological parameters							Psoriasin		
TB#	Type	ER	PR	GrSc	Size	NS	Inf	RT-PCR	RT-PCR/Inv%	WB
11549	muc	194	133		3	–	2	0.06	0.15	–
10515	muc	341	176		3	–	1	0.08	0.14	–
9948	muc	46	22		6.5	–	1	0.10	0.16	–
10582	muc	109	62		2.3	na	1	0.14	0.34	–
8832	muc	295	177		4	–	2	1.94	2.77	–
8021	muc	331	328		2.3	–	2	0.11	0.15	–
11387	tub	105	35		3.5	na	2	0.09	0.29	–
9483	tub	56	0		1.2	–	2	0.09	0.91	–
11651	tub	67	24		2.2	–	3	0.23	0.77	–
8814	tub	232	103		2	–	2	0.44	1.45	–
8720	tub	29	73		2	–	1	0.52	5.21	–
12072	tub	8.3	5		2.3	+	3	0.67	1.34	–
13041	med	3.4	9		2	–	5	0.40	0.49	–
13153	med	4.9	2.4		3	na	5	0.61	0.76	–
11867	med	1.4	9		1.6	+	5	1.60	2.67	+
13058	med	4.6	12		2.8	–	5	1.63	2.04	–
12434	med	1	1.3		1.2	–	5	1.63	3.27	+
8639	ilc	52	83		na	–	1	0.20	0.67	–
8799	ilc	111	139		6	+	2	0.31	3.15	–
8993	ilc	142	528		8	+	1	0.52	0.86	–
9801	ilc	2.1	9.8		na	–	3	0.56	1.60	–
8921	ilc	2.3	8.9		8	–	2	2.07	3.77	+
8961	ilc	0.7	3.4		2.5	–	3	2.34	5.84	+
9000	idc	392	596	7	2.5	–	1	0.07	0.09	–
13402	idc	49	35	4	2.8	–	2	0.07	0.17	–
11971	idc	97	25	4	1.5	–	2	0.13	0.42	–
8684	idc	74	43	7	5	+	1	0.14	0.35	–
12853	idc	17.3	83	9	4.8	+	4	0.15	0.22	–
8840	idc	74	68	7	1.8	+	3	0.17	0.37	–
8834	idc	10	147	5	2	–	2	0.17	0.34	–
8674	idc	16.7	4.5	9	na	–	2	0.19	0.35	–
12037	idc	225	144	4	3.5	+	2	0.20	0.40	–
12868	idc	93	141	9	3.5	na	1	0.21	0.28	–
8599	idc	58	81	4	3.5	–	1	0.24	0.79	–
10105	idc	0.9	3.8	9	3	+	4	0.24	0.40	–
7928	idc	33	72	5	3	+	2	0.27	0.67	–
13414	idc	15.5	59	5	4.1	–	2	0.28	0.56	–
11343	idc	78	44	4	na	–	3	0.29	0.73	–
10644	idc	130	4.7	9	3.2	+	2	0.32	0.81	–
10137	idc	42	26	7	1.8	–	1	0.44	0.89	–
10064	idc	0.8	4.6	9	2.5	na	2	0.53	0.88	–
11769	idc	1.1	3.5	7	na	–	3	0.56	0.80	–
8932	idc	114	27	4	2	–	1	0.56	1.13	–
10906	idc	46	6.6	9	4.5	na	5	0.58	0.64	–
8789	idc	0.8	0.4	7	na	na	3	0.66	1.64	–
10150	idc	70	42	7	na	–	1	0.67	1.68	–
11459	idc	3.6	98	5	4.6	+	3	0.67	0.96	–
13191	idc	17.2	9.2	9	3.2	–	2	0.69	0.87	–
10124	idc	1.9	12.9	9	3	–	4	1.00	1.42	–
8830	idc	0.7	8	9	6	+	4	1.06	1.32	+
8790	idc	6	50	5	1.5	+	2	1.07	3.58	–
11118	idc	6.6	11.8	5	8.5	+	2	1.10	2.20	–
12715	idc	1.5	16	7	3	na	3	1.24	2.06	+
9631	idc	0.7	4.5	9	na	+	4	1.32	3.10	+
8965	idc	0.4	9.9	7	na	+	4	1.85	2.64	+
10049	idc	0.8	14	9	3.7	+	4	2.01	5.04	+
8704	idc	0.7	3.5	7	3.5	+	2	2.60	6.50	+

TB, tumor bank case number; type, mucinous (muc), tubular (tub), medullary (med), lobular (ilc), ductal (idc); ER, PR, estrogen/progesterone receptor levels (fmol/mg protein); GrSc, Nottingham grade score; Size, tumor size (cms); NS, nodal status, positive (+), negative (−), not available (na); Inf, estimate of inflammatory infiltrate, low (1) to high (5). RT-PCR, psoriasin mRNA level determined by RT-PCR; RT-PCR/Inv%, psoriasin mRNA level determined by RT-PCR and adjusted for the percentage tumor cell content of the tissue section (as described in Materials and Methods); WB, psoriasin protein level determined by Western blot.

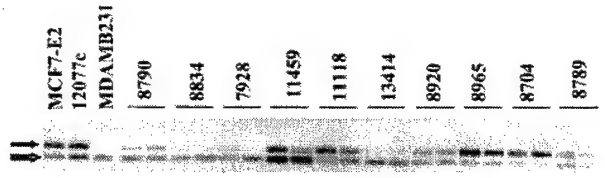

Figure 3. RT-PCR analysis of psoriasin mRNA expression in invasive breast tumors. Psoriasin (**upper black arrow**) and GAPDH (**lower open arrow**) from duplicate PCRs of 10 representative tumors. Control lanes include estradiol-treated MCF7-E2 cells, a tumor control 12077c, and wild-type MDA-MB-231 cells.

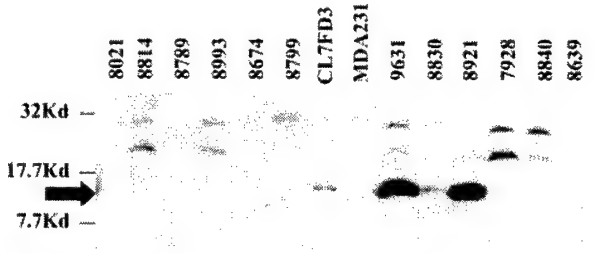

Figure 4. Western blot analysis of psoriasin protein expression in invasive breast tumors. Psoriasin (**black arrow**) is detected in 3/12 representative tumors and within the positive control (CL7FD3).

cadherin and disturb the intracellular distribution of B-catenin.[10]

A possible role for psoriasin (S100A7) in breast cancer first emerged when it was also identified as a cDNA down-regulated in a nodal metastasis relative to a primary breast tumor.[33] Nevertheless, the significance of the initial observation was unclear because of the fact that expression was only detectable in a small proportion of cells within invasive primary tumors studied by *in situ* hybridization and overall could be detected in only 18% of primary tumor specimens assessed by Northern analysis. An explanation for this paradox became apparent when psoriasin was also identified by us as a gene that is particularly highly expressed in the ductal epithelial cells of preinvasive ductal carcinoma *in situ*,[1] which can be present as a significant component with invasive tumor specimens. We have now shown that when higher levels of psoriasin expression persist within invasive tumors, this correlates with indicators of increased metastatic potential. It should be noted that the strong relationship with ER status is compatible with studies of S100A4[31] and the *in vitro* observation[33] (and our unpublished data) that psoriasin is regulated by estradiol in MCF7 cells. Although it is interesting that the nature of this correlation is different between the *in vitro* and *in vivo* situations, similar differences have been found with other genes in breast tumors,[34] suggesting that additional external factors may influence psoriasin regulation *in vivo*.

Although the biological effect of alteration of psoriasin in breast tumors is currently unknown, it is interesting to speculate from this pattern of expression that psoriasin may be important in the invasive phenotype.[16] This role might be mediated through an indirect influence on the effector cells of the host immune response or perhaps through a more direct influence on the epithelial tumor cell. The first hypothesis is supported by the correlation seen here with the degree of host inflammatory cell response within breast tumors and the previous evidence that implicates psoriasin as a chemotactic factor.[14] However, psoriasin protein was only detected in approximately 50% of medullary and ductal tumors with marked inflammatory responses. The second hypothesis is supported by our observation that psoriasin may not only be secreted[13,15] but also can be localized in both nuclear and cytoplasmic compartments in normal skin and breast tumors. Although further studies beyond immunohistochemistry are necessary to confirm this observation, the pattern of expression is consistent between cells in two

Table 2. Relationship between Psoriasin Expression and Prognostic and Tissue Factors

		All				IDC			
		n	Low Ps	High Ps		*n*	Low Ps	High Ps	
ER	–	28	14	4	$P = 0.0001$	19	10	9	$P = 0.0019$
	+	29	28	1		15	15	0	
PR	–	25	13	12	$P = 0.001$	15	8	7	$P = 0.018$
	+	32	29	3		19	17	2	
NS	–	30	24	6	ns ($P = 0.095$)	14	13	1	$P = 0.0002$
	+	19	11	8		15	8	7	
INFL	Low	34	29	5	$P = 0.049$	20	17	3	ns ($P = 0.07$)
	High	18	11	7		14	8	6	
Size	<2	12	9	3		6	5	1	
	2–5	29	22	7	ns	18	14	4	ns
	≥5	7	4	3		3	1	2	
Grade	Low					12	10	2	
	Mod					10	7	3	ns
	High					12	8	4	
Type	idc	34	25	9					
	ilc	6	4	2					
	med	5	2	3	ns				
	muc	6	5	1					
	tub	6	6	0					

ER, PR, estrogen/progesterone receptor status; NS, nodal status; INFL, inflammatory infiltrate; Size, tumor size (cms); Grade, Nottingham grade; Type, mucinous (muc), tubular (tub), medullary (med), lobular (ilc), ductal (idc); Low Ps/High Ps, low/high psoriasin mRNA level determined by RT-PCR (cutpoint values used as described in Materials and Methods). *P* values determined by χ^2 or ANOVA tests. ns, not significant.

closely related epithelia, epidermis and breast ductal epithelium, and the detection of nuclear and cytoplasmic signal was unrelated to tissue fixation or immunohistochemistry protocol, which may effect staining with some antibodies.[35,36] Dual localization and alteration of the subcellular localization with disease has also been observed with another S100 related keratinocyte protein, profilaggrin, expressed in the epidermis.[2,37] Similarly, altered cellular distribution of proteins such as BRCA1 and B-catenin are also recognized to be an important aspect of tumor progression.[38–40] Furthermore, other S100 proteins have previously been associated with both extracellular and intracellular actions,[41] and previous studies have also indicated potential interactions for S100A4 with both cytoskeletal[8,9] and nuclear[42] proteins. It has also recently been shown that other secreted S100 proteins can be localized to cytoplasm and nucleus,[43,44] and specifically S100A2 has been found in breast cell nuclei, whereas S100A6 localizes to the cytoplasm[24]; however, the functional significance of these findings remains unknown.

In conclusion, we have shown that expression of psoriasin (S100A7) mRNA and protein correlates with indicators of poor prognosis in invasive breast tumors, including ER, PR, and nodal status, but is not related to differentiation, as manifested by invasive tumor type or grade. The relationship observed between psoriasin and the inflammatory response is also compatible with a role as a chemotactic factor; however, the possibility of additional intracellular functions is raised by the presence of its nuclear localization in both skin and breast tumors. Further studies will be necessary to confirm the latter observation and pursue the biological functions of psoriasin in relation to breast tumor progression.

Acknowledgments

The authors thank Prof. J. E. Celis (University of Aarhus, Aarhus, Denmark) for kindly providing anti-psoriasin antibody and Helmut Dotzlaw and Caroline Cummins-Leygue for assistance with cell transfections. We also thank Bionostics, North York, for assistance with antibody production. The tissues used in this study were provided by the Manitoba Breast Tumor Bank, which is funded by the National Cancer Institute of Canada.

References

1. Leygue E, Snell L, Hiller T, Dotzlaw H, Hole K, Murphy LC, Watson PH: Differential expression of psoriasin messenger RNA between in situ and invasive human breast carcinoma. Cancer Res 1996, 56:4606–4609
2. Schafer BW, Heizmann CW: The S100 family of EF-hand calcium-binding proteins: functions and pathology. Trends Biochem Sci 1996, 21:134–140
3. Lee SW, Tomasetto C, Swisshelm K, Keyomarsi K, Sager R: Down-regulation of a member of the S100 gene family in mammary carcinoma cells and reexpression by azadeoxycytidine treatment. Proc Natl Acad Sci USA 1992, 89:2504–2508
4. Lloyd BH, Platt-Higgins A, Rudland PS, Barraclough R: Human S100A4 (p9Ka) induces the metastatic phenotype upon benign tumour cells. Oncogene 1998, 17:465–473
5. Sherbet GV, Lakshmi MS: S100A4 (MTS1) calcium binding protein in cancer growth, invasion and metastasis. Anticancer Res 1998, 18: 2415–2421
6. Grigorian M, Ambartsumian N, Lykkesfeldt AE, Bastholm L, Elling F, Georgiev G, Lukanidin E: Effect of mts1 (S100A4) expression on the progression of human breast cancer cells. Int J Cancer 1996, 67:831–841
7. Ford HL, Salim MM, Chakravarty R, Aluiddin V, Zain SB: Expression of Mts1, a metastasis-associated gene, increases motility but not invasion of a nonmetastatic mouse mammary adenocarcinoma cell line. Oncogene 1995, 11:2067–2075
8. Bastholm L, Elling F, Georgiev G, Lukanidin EKM, Tarabykina S, Bronstein I, Maitland N, Lomonosov M, Hansen K, Georgiev G, Lukanidin E: Metastasis-associated Mts1 (S100A4) protein modulates protein kinase C phosphorylation of the heavy chain of nonmuscle myosin. J Biol Chem 1998, 273:9852–9856
9. Ford HL, Zain SB: Interaction of metastasis associated Mts1 protein with nonmuscle myosin. Oncogene 1995, 10:1597–1605
10. Keirsebilck A, Bonne S, Bruyneel E, Vermassen P, Lukanidin E, Mareel M, Van Roy F: E-cadherin and metastasin (mts-1/S100A4) expression levels are inversely regulated in two tumor cell families. Cancer Res 1998, 58:4587–4591
11. Borglum AD, Flint T, Madsen P, Celis JE, Kruse TA: Refined mapping of the psoriasin gene S100A7 to chromosome 1cen-q21. Hum Genet 1995, 96:592–596
12. Hoffmann HJ, Olsen E, Etzerodt M, Madsen P, Thogersen HC, Kruse T, Celis JE: Psoriasin binds calcium and is upregulated by calcium to levels that resemble those observed in normal skin. J Invest Dermatol 1994, 103:370–375
13. Madsen P, Rasmussen HH, Leffers H, Honore B, Dejgaard K, Olsen E, Kiil J, Walbum E, Andersen AH, Basse B, et al.: Molecular cloning, occurrence, and expression of a novel partially secreted protein "psoriasin" that is highly up-regulated in psoriatic skin. J Invest Dermatol 1991, 97:701–712
14. Jinquan T, Vorum H, Larsen CG, Madsen P, Rasmussen HH, Gesser B, Etzerodt M, Honore B, Celis JE, Thestrup-Pedersen K: Psoriasin: a novel chemotactic protein. J Invest Dermatol 1996, 107:5–10.
15. Celis JE, Rasmussen HH, Vorum H, Madsen P, Honore B, Wolf H, Orntoft TF: Bladder squamous cell carcinomas express psoriasin and externalize it to the urine. J Urol 1996, 155:2105–2112
16. Watson PH, Leygue ER, Murphy LC: Psoriasin (S100A7). Int J Biochem Cell Biol 1998, 30:567–571
17. Hiller T, Snell L, Watson PH: Microdissection RT-PCR analysis of gene expression in pathologically defined frozen tissue sections. Biotechniques 1996, 21:38–40
18. Ellis IO, Galea M, Broughton N, Locker A, Blamey RW, Elston CW: Pathological prognostic factors in breast cancer. II. Histological type. Relationship with survival in a large study with long-term follow-up. Histopathology 1992, 20:479–489
19. Elston CW, Ellis IO: Pathological prognostic factors in breast cancer. I. The value of histological grade in breast cancer: experience from a large study with long-term follow-up. Histopathology 1991, 19:403–410
20. Leygue ER, Watson PH, Murphy LC: Estrogen receptor variants in normal human mammary tissue. J Natl Cancer Inst 1996, 88:284–290
21. Schagger H, von Jagow G: Tricine-sodium dodecyl sulfate-polyacrylamide gel electrophoresis for the separation of proteins in the range from 1 to 100 kDa. Anal Biochem 1987, 166:368–379
22. Leygue E, Snell L, Dotzlaw H, Hole K, Hiller-Hitchcock T, Roughley PJ, Watson PH, Murphy LC: Expression of lumican in human breast carcinoma. Cancer Res 1998, 58:1348–1352
23. Ercolani L, Florence B, Denaro M, Alexander M: Isolation and complete sequence of a functional human glyceraldehyde-3-phosphate dehydrogenase gene. J Biol Chem 1988, 263:15335–15341
24. Ilg EC, Schafer BW, Heizmann CW: Expression pattern of S100 calcium-binding proteins in human tumors. Int J Cancer 1996, 68: 325–332
25. Ostergaard M, Rasmussen HH, Nielsen HV, Vorum H, Orntoft TF, Wolf H, Celis JE: Proteome profiling of bladder squamous cell carcinomas: identification of markers that define their degree of differentiation. Cancer Res 1997, 57:4111–4117
26. Kohn EC, Liotta LA: Molecular insights into cancer invasion: strategies for prevention and intervention. Cancer Res 1995, 55:1856–1862
27. Munn KE, Walker RA, Varley JM: Frequent alterations of chromosome

1 in ductal carcinoma in situ of the breast. Oncogene 1995, 10:1653–1657
28. Wicki R, Franz C, Scholl FA, Heizmann CW, Schafer BW: Repression of the candidate tumor suppressor gene S100A2 in breast cancer is mediated by site-specific hypermethylation. Cell Calcium 1997, 22: 243–254
29. Ebralidze A, Tulchinsky E, Grigorian M, Afanasyeva A, Senin V, Revazova E, Lukanidin E: Isolation and characterization of a gene specifically expressed in different metastatic cells and whose deduced gene product has a high degree of homology to a Ca^{2+}-binding protein family. Genes Dev 1989, 3:1086–1093
30. Barraclough R, Rudland PS: The S-100-related calcium-binding protein, p9Ka, and metastasis in rodent and human mammary cells. Eur J Cancer 1994, 30A:1570–1576
31. Albertazzi E, Cajone F, Leone BE, Naguib RN, Lakshmi MS, Sherbet GV: Expression of metastasis-associated genes h-mts1 (S100A4) and nm23 in carcinoma of breast is related to disease progression. DNA Cell Biol 1998, 17:335–342
32. Grigorian MS, Tulchinsky EM, Zain S, Ebralidze AK, Kramerov DA, Kriajevska MV, Georgiev GP, Lukanidin EM: The mts1 gene and control of tumor metastasis. Gene 1993, 135:229–238
33. Moog-Lutz C, Bouillet P, Regnier CH, Tomasetto C, Mattei MG, Chenard MP, Anglard P, Rio MC, Basset P: Comparative expression of the psoriasin (S100A7) and S100C genes in breast carcinoma and co-localization to human chromosome 1q21–q22. Int J Cancer 1995, 63:297–303
34. Yarden RI, Lauber AH, El Ashry D, Chrysogelos SA: Bimodal regulation of epidermal growth factor receptor by estrogen in breast cancer cells. Endocrinology 1996, 137:2739–2747
35. Scully R, Ganesan S, Brown M, De Caprio JA, Cannistra SA, Feunteun J, Schnitt S, Livingston DM: Location of BRCA1 in human breast and ovarian cancer cells (technical comments). Science 1996, 272:123–124.
36. Chen Y, Chen P-L, Riley DJ, Lee W-H, Allred DC, Osborne CK: Location of BRCA1 in human breast and ovarian cancer cells (technical comments). Science 1996, 272:125–126
37. Ishida-Yamamoto A, Takahashi H, Presland RB, Dale BA, Iizuka H: Translocation of profilaggrin N-terminal domain into keratinocyte nuclei with fragmented DNA in normal human skin and loricrin keratoderma. Lab Invest 1998, 78:1245–1253
38. Wilson CA, Ramos L, Villasenor MR, Anders KH, Press MF, Clarke K, Karlan B, Chen JJ, Scully R, Livingston D, Zuch RH, Kanter MH, Cohen S, Calzone FJ, Slamon DJ: Localization of human BRCA1 and its loss in high-grade, non-inherited breast carcinomas. Nature Genet 1999, 21:236–240
39. Chen Y, Chen CF, Riley DJ, Allred DC, Chen PL, Von Hoff D, Osborne CK, Lee WH: Aberrant subcellular localization of BRCA1 in breast cancer. Science 1995, 270:789–791
40. Sheng H, Shao J, Williams CS, Pereira MA, Taketo MM, Oshima M, Reynolds AB, Washington MK, DuBois RN, Beauchamp RD: Nuclear translocation of beta-catenin in hereditary and carcinogen-induced intestinal adenomas. Carcinogenesis 1998, 19:543–549
41. Hessian PA, Edgeworth J, Hogg N: MRP-8 and MRP-14, two abundant Ca(2+)-binding proteins of neutrophils and monocytes. J Leukoc Biol 1993, 53:197–204
42. Albertazzi E, Cajone F, Lakshmi MS, Sherbet GV: Heat shock modulates the expression of the metastasis associated gene MTS1 and proliferation of murine and human cancer cells. DNA Cell Biol 1998, 17:1–7
43. Yang Q, O'Hanlon D, Heizmann CW, Marks A: Demonstration of heterodimer formation between S100B and S100A6 in the yeast two-hybrid system and human melanoma. Exp Cell Res 1999, 246:501–509
44. Mandinova A, Atar D, Schafer BW, Spiess M, Aebi U, Heizmann CW: Distinct subcellular localization of calcium binding S100 proteins in human smooth muscle cells and their relocation in response to rises in intracellular calcium. J Cell Sci 1998, 111:2043–2054

British Journal of Cancer (1999) 81(6), 1002–1008

Article no. bjoc.1999.0799

The potential role for prolactin-inducible protein (PIP) as a marker of human breast cancer micrometastasis

JW Clark[1], L Snell[1], RPC Shiu[2], FW Orr[1], N Maitre[3], CPH Vary[4], DJ Cole[3] and PH Watson[1]

Department of [1]Pathology and [2]Physiology, D212-770 Bannatyne Avenue, University of Manitoba, Faculty of Medicine, Winnipeg, Manitoba, Canada, R3E 0W3; [3]Department of Surgery and [4]Center for Molecular Biology, Medical University of South Carolina, 171 Ashley Ave, Charleston, SC 29425, USA

Summary The prolactin-inducible protein (PIP/GCPD15) is believed to originate from a limited set of tissues, including breast and salivary glands, and has been applied as a clinical marker for the diagnosis of metastatic tumours of unknown origin. We have investigated the potential role of PIP mRNA as a marker of human breast cancer metastasis. Using reverse transcription polymerase chain reaction and Southern or dot blot analysis, PIP mRNA was detected in 4/6 breast cell lines, independent of oestrogen receptor (ER) status. In breast primary tumours ($n = 97$), analysed from histologically characterized sections, PIP mRNA was detected in most cases. Higher PIP mRNA levels correlated with ER$^+$ ($P = 0.0004$), progesterone receptor positive (PR$^+$) ($P = 0.0167$), low-grade ($P = 0.0195$) tumours, and also PIP protein levels assessed by immunohistochemistry ($n = 19$, $P = 0.0319$). PIP mRNA expression was also detectable in 11/16 (69%) of axillary node metastases. PIP mRNA expression, however, was also detected in normal breast duct epithelium, skin, salivary gland and peripheral blood leucocyte samples from normal individuals. We conclude that PIP mRNA is frequently expressed in both primary human breast tumours and nodal metastases. However, the presence of PIP expression in skin creates a potential source of contamination in venepuncture samples that should be considered in its application as a marker for breast tumour micrometastases. © 1999 Cancer Research Campaign

Keywords: breast cancer; micrometastases; reverse transcription polymerase chain reaction; prolaction inducible protein; genetic marker

Detection of breast cancer micrometastases based on specific genetic markers may provide useful information to guide early therapeutic decisions. Immunohistochemical (IHC) and reverse transcription polymerase chain reaction (RT-PCR) methods offer the potential of improved sensitivity for detection of micrometastatic carcinoma cells that are missed by conventional histopathological examination (Raj et al, 1998; Pelkey et al, 1996; Lockett et al, 1998). Various biological markers have been proposed for the detection of breast cancer cells using these techniques, including keratin 19, muc1, EMA, CEA, HCG (Hoon et al, 1996; Tsuchiya et al, 1996; Mori et al, 1996; Schoenfeld et al, 1997). However, the frequency of expression of these markers is often related to tumour differentiation and is not always confined to breast tissue (Zippelius et al, 1997). Another promising breast specific marker is prolactin inducible protein (PIP) which is also known as gross cystic disease fluid protein-15 (GCDFP-15) (Haagensen et al, 1990; Wick et al, 1989; Murphy et al, 1987). IHC studies have previously shown that PIP is frequently expressed in human breast carcinomas and is comparatively specific for breast cancer (Wick et al, 1998; Wick et al, 1989; Mazoujian et al, 1983). While PIP expression is found to occur in tumours arising from skin and salivary gland, distinction from breast cancer is rarely a clinical issue and PIP protein has already found practical application as a marker for the recognition of breast origin of metastatic tumours (de Almeida & Pestana 1992; Fiel et al, 1996; Ormsby et al, 1995; Monteagudo et al, 1991). However, PIP is a secreted protein that is readily detectable in benign breast cyst fluid and plasma, which may impact on the significance of IHC detection of the protein (Haagensen et al, 1990). We have recently used PIP alongside other markers to explore its value in detection of breast micrometastases (Lockett et al, 1998a; Lockett et al, 1998b), however, the incidence and pattern of PIP expression at the level of RT-PCR is not known. Our purpose in this study was to evaluate the potential of PIP mRNA as a marker for the detection of breast cancer cells by assessing the frequency of PIP mRNA expression in human breast cell lines and in breast tumors in relation to tissue composition and pathology.

Received 10 December 1998
Revised 12 May 1999
Accepted 13 May 1999

Correspondence to: PH Watson

MATERIALS AND METHODS

Human cell lines

The human breast cancer cell lines (T47D, ZR 75, MDA-MB-231, BT 474 and MCF-7) and the normal human breast cell line, HBL-100, were obtained from the American Type Culture Collection (ATCC, Rockville, MD, USA). All cell lines were cultured as described previously in Dulbecco's modified Eagle's medium (DMEM) containing 10% fetal bovine serum (FBS), 1% 1 mg ml^{-1} insulin, 1% 35% (w/v) glucose, 1% penicillin–streptomycin and 1% L-glutamine. Cells were harvested with 5% trypsin (v/v) from culture flasks.

Human tissue samples

A cohort of 97 primary breast tumour samples was obtained from the Manitoba Breast Tumor Bank located in the Department of Pathology, Faculty of Medicine, University of Manitoba. The cohort was selected initially on the basis of oestrogen receptor

(ER) status so as to ensure a wide range of ER levels to determine any correlation between ER status and PIP expression. The tumour bank collected all breast tumour specimens on ice which were then bisected to provide mirror image tissues for formalin-fixed, paraffin-embedded blocks and matching frozen tissue blocks stored at –70°C (Hiller et al, 1996). The pathological and histological parameters (including tumour type, grade, invasive and normal cell content) were then assessed uniformly by one pathologist in sections from the paraffin block and entered into a database enabling selection by specific criteria (Watson, 1996). Tumour grading was performed using the Nottingham system (Elston & Ellis, 1991) and steroid receptor levels were measured by ligand binding assay performed on an adjacent piece of tumour tissue. ER and progesterone receptor (PR) values above 3 fmol mg^{-1} and 15 fmol mg^{-1} total protein respectively were deemed positive. A second cohort of five primary tumours was also selected from the tumour bank on the basis of association with matching frozen tissue in the bank from a synchronous nodal metastasis.

A third cohort of axillary lymph node samples from 32 patients with metastatic breast tumours undergoing breast cancer surgery was obtained from the Department of Surgery at the Medical University of South Carolina. These samples were collected prospectively from patients with primary tumours associated with a range of clinical stages (12 stage I, 12 stage II, eight stage III) and included 16 samples from patients who were histologically node-positive and 16 from patients who were node-negative. Immediately after resection, the axillary lymph node specimens were identified and separated from the specimen by a pathologist. All lymph nodes > 1 cm were bisected, with half of the node sent for routine histological evaluation and the other half for RT-PCR screening. The RT-PCR screened lymph nodes were snap frozen at –70°C until being processed to extract total RNA.

Normal tissue samples from several potential sites of breast tumour metastasis were also obtained from the Manitoba Breast Tumor Bank. Normal human peripheral blood lymphocytes (PBL) were isolated from 5 ml blood samples drawn from each of 11 healthy volunteers (females and males, 22–29 years old). The red blood cells in each 5 ml samples were lysed by adding 25 ml of lysing reagent (140 mM NH_4Cl_2 and 17 mM Tris, pH 7.6) and leaving the mixture to incubate for 10 min at 37°C. This was followed by centrifugation at 2000 rpm for 10 min to pellet white blood cells, removal of the supernatant and re-suspension of PBLs in PBS.

Sensitivity assay

To determine the sensitivity of the RT-PCR assay, T47D human breast cancer cells (PIP^+) were diluted into a background of MDA-MB-231 cells (PIP^-) so as to obtain a range of concentrations of PIP^+ cells from 1 to 1000 cells in 10^6 PIP^- cells prior to RNA extraction and RT-PCR assay. Cell numbers were determined by directly counting aliquots of cells in suspension under a microscope using a haemocytometer.

RNA extraction and RT-PCR

Total RNA from all tumour, tissue and cell pellet samples was isolated using similar commercial extraction reagents, either Tri-reagent or Tri-zol reagents and protocols according to the manufacturer's instructions (Molecular Research Center Inc, Cincinnati, OH, USA and BRL). RNA samples were quantified by performing spectrophotometry. Samples were presumed to be free of DNA and proteins if the OD 260/280 ratio was 1.6–1.8. All RNA samples were stored at –70°C until further use.

Reverse transcription of mRNA to cDNA was performed as previously described (Hiller et al, 1996) with the following modifications. All PCR primers were designed to cross intron–exon boundaries. The PIP primers were sense (5′-GCTCAGGACAA-CACTCGGAA-3′) and antisense (5′-ATAACATCAACGACG-GCTGC-3′) corresponding to positions 107 and 356 of the cDNA sequence (Murphy et al, 1987), and GAPDH primers were sense (5′-ACCCACTCCTCCACCTTTG-3′) and antisense (5′-CTCT-TGGCTCTTGCTGGG-3′) (Ercolani et al, 1988). Preliminary experiments were performed with cell line and tumour RNA samples to establish the appropriate RNA input and PCR cycle number conditions to achieve amplification with both PIP and gluceraldehyde 3-phosphate dehydrogenase (GAPDH) primers in the linear range in a typical sample. Amplification of GAPDH or actin was then performed in duplicate samples, for every experimental sample, to provide an internal indicator as to the quality of the cDNA of each sample. The PCR consists of an initial 5-min preheating step at 94°C, followed by repeated cycles of a 1-min denaturing step at 94°C, a 1-min primer annealing step at 54°C, and a 90 s elongation step at 72°C. Cycle numbers to achieve amplification in the linear range were 40 for PIP and 35 for GAPDH and actin. Once thermal cycling was completed, samples underwent one final elongation step at 72°C for 7 min. Tumours were processed in batches of 12 samples, from frozen sectioning to RNA extraction, RT in triplicate and PCR. For each batch controls included RT- and RNA-controls, and both PIP^+ (T47D) and PIP^- (MDA-MB-231) RNA controls. All primary tumour PCR signals were assessed in gels and autoradiographs by video image capture and computer analysis using MCID-M4 Imaging Research Inc, version 2.0 image analysis program. PIP expression was standardized to GAPDH expression assessed in separate PCR reactions from the same RT reaction and run in parallel on the same gel and then expressed relative to the levels in the T47D cell line standard. To correct for any differences in processing between gels PIP levels were further standardized to a set of PCR product standards incorporated into each gel.

Southern and dot blot analysis

For Southern blot analysis following PCR amplification, PCR products were loaded into a 1% agarose gel. After electrophoresis the gel was exposed to ethidium bromide, illuminated with ultraviolet light and photographed. For hybridization, gels were denatured in 0.5 M sodium hydroxide (NaOH), 1 M sodium chloride (NaCl) for 30 min at room temperature and neutralized for 30 min in 1.5 M Tris–HCl pH 7.4, 3 M NaCl. PCR product cDNA was then transferred to Zeta-Probe membrane according to the Zeta-Probe protocol (Bio-Rad Laboratories, Hercules, CA, USA) and membranes were then dried in an 80°C oven for 30 min. For probing membranes were prehybridized with 10 ml of hybridization solution (50 ml of formamide, 12 ml of 1 M Na_2HPO_4, 5 ml of 5 M NaCl, 7 g of sodium dodecyl sulphate (SDS), and 200 µl of 0.5 M EDTA in 100 ml with ddH_2O) at 42°C for 2 h with agitation. Hybridization was then conducted at 42°C for 24 h with a hPIP cDNA probe (Murphy et al, 1987) ^{32}P labelled by the random priming method and purified with a NICK chromatography column (Pharmacia Biotech, Inc.). Hybridization membranes were washed at room temperature for 1 h in a solution of 2 × SSC

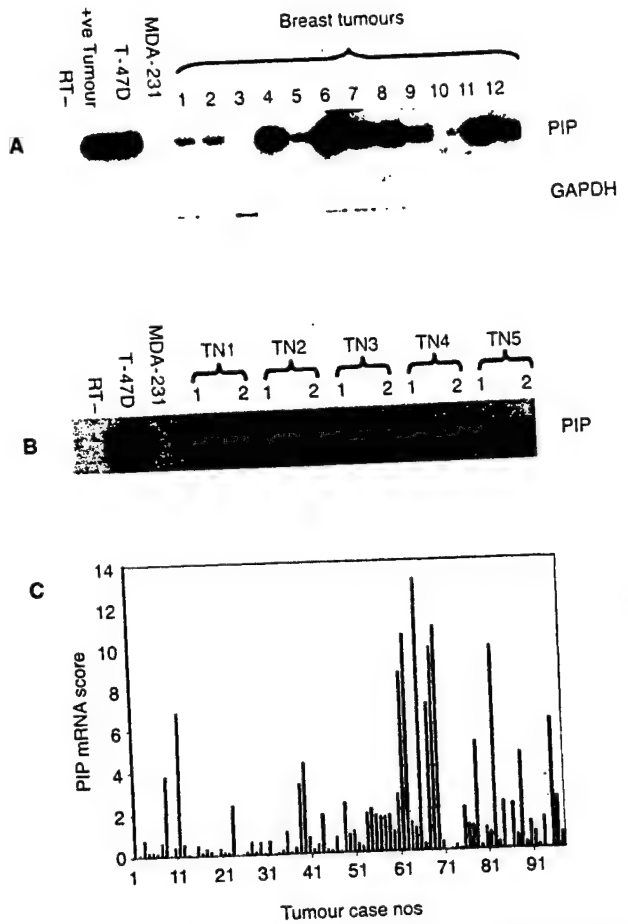

Figure 1 PIP mRNA expression in breast tumours. The upper panels show a representative set of 12 primary tumours (**A**) and a set of five cases (**B**, TN 1–5) comprising primary breast tumours (1) and their corresponding nodal metastases (2) analysed for PIP mRNA levels by RT-PCR – Southern blot. Corresponding GAPDH levels, determined as described in Materials and Methods relative to T47D cells and a reference tumour (positive controls) and MDA-MB-231 cells (negative control) are also shown. T47D RNA subjected to reverse transcription reaction without RT-enzyme and subsequent PCR is also shown (RT-control). In the lower panel the chart shows a graphical representation of the level of PIP mRNA expression in tumours relative to ER status (**C**). Tumour case numbers 1–30 are ER– (< 3 fmol mg^{-1} protein), 31–49 are ER low positive (3–20 fmol mg^{-1} protein) and 50–97 are ER high positive (> 20 fmol mg^{-1} protein)

Table 1 Relationship between mean PIP mRNA levels in primary breast tumours and prognostic parameters

		n	Mean	(s.d.)	*P*-value
ER	–ve	30	0.69	(1.4)	0.0004
	+ve	67	2.12	(3)	
PR	–ve	52	1.04	(1.8)	0.0167
	+ve	45	2.42	(3.3)	
Grade	low	16	2.59	(3.5)	
	mod	41	1.83	(2.9)	0.0195
	high	40	1.16	(1.9)	
Nodal status	+ve	37	2.09	(3.3)	NS
	–ve	42	1.18	(1.8)	
	unknown	18			
Size	<2 cm	14	2.39	(4.5)	
	2–5 cm	45	1.36	(2.1)	NS
	> 5 cm	16	1.33	(1.9)	
	Unknown	22			

PIP mRNA score (mean and s.d.) shown was derived as described in Materials and Methods. *P*-values correspond to Spearman correlation test

Table 2 PIP RT-PCR screening of axillary lymph nodes compared to routine histopathology

		Pathology		
		+ve	–ve	Total
RT-PCR	+ve	11 (69%)	6 (37%)	17 (53%)
	–ve	5 (31%)	10 (63%)	15 (47%)
	Total	16 (50%)	16 (50%)	32 (100%)

(standard saline citrate) and 0.1% SDS, then 1 h in 0.5 × SSC and 0.1% SDS, and 1 h in a 65°C waterbath in 0.1 × SSC and 0.1% SDS. Bands were then visualized after autoradiography for 2–6 h.

For dot blot analysis, 1 µl of each PCR reaction sample was deposited on a strip of Sure Blot Hybridization Membrane (Oncor, Gaithersburg, MD, USA) and left to dry for 5 min. The membrane was incubated for 5 min in a solution of 0.2 M NaOH at room temperature after which the strip was incubated for another 30 min at 56°C in Blocking Buffer (0.2% I-Block; Tropix, Bedford, MA, USA), 1 × PBS, 0.5% SDS). The same PIP cDNA probe (Murphy et al, 1987) was labelled using alkaline phosphatase as previously described (Vary et al, 1996) and then added to the same tube at a 1:3000 dilution of stock (50 ng ml^{-1}) and hybridized for 15 min. The membrane was then washed 3 times for 10 min in Wash Buffer (10 × PBS, 0.5% SDS) and twice in AMPPD Buffer (1 mM magnesium chloride hexahydrate, 0.1 M diethanolamine, pH 10). Finally, the membrane was incubated 30 min in the dark with 1% CSPD (Tropix, Bedford, MA, USA) in AMPPD buffer. Dots were visualized by exposure to 4× autoradiography film for 10 min.

Immunohistochemistry and in situ hybridization

Immunohistochemical detection of PIP expression was performed using a commercially available monoclonal antibody (Signet Laboratories Inc, Dedham, MA, USA) and protocol as recommended. PIP was assessed in paraffin sections from a subset of 19 primary tumours, selected to correspond to a wide range of PIP mRNA levels as determined by the RT-PCR assay based on frozen tissue sections from the same cases. PIP protein was scored by estimating the average signal intensity (on a scale of 0–3) and the proportion of cells showing a positive signal and scored as 0 (none), 0.1 (less than one-tenth), 0.5 (less than one-half), or 1.0 (greater than one-half). The intensity and proportion scores were then multiplied to give an overall score. In situ hybridization was performed as previously described (Leygue et al, 1996) on 5-µm paraffin sections from normal and tumour tissue with both sense and antisense PIP riboprobes synthesized using UTP (^{35}S) to label the probes using Riboprobe^R Systems (Promega, Madison, WI, USA) according to the manufacturer's instructions.

RESULTS

Analysis of sensitivity and PIP expression in cell lines

Multiple experiments were performed to determine the threshold for detection of PIP^+ cells in a background of PIP^- cells, using the

Table 3 Correlation between PIP protein and mRNA expression in a subset of 19 tumours

Case no.	Int %	PIP IHC	PIP RT-PCR
11913	[0 × 0]	0	0.023
11365	[1 × 0.1]	0.1	0.030
11657	[1 × 0.1]	0.1	0.048
10927	[1 × 0.5]	0.5	0.073
10970	[0 × 0]	0	0.170
11097	[2 × 0.5]	1	0.205
11836	[1 × 0.1]	0.1	0.350
11909	[2 × 1]	2	0.415
11526	[1 × 1]	1	0.469
10975	[2 × 1]	2	0.748
11341	[2 × 1]	2	0.964
11729	[1 × 0.1]	0.1	1.180
11339	[0 × 0]	0	1.840
11603	[3 × 0.1]	0.3	2.020
11288	[1 × 0.5]	0.5	2.470
11010	[2 × 1]	2	2.718
11903	[2 × 0.5]	1	4.320
11734	[1 × 1]	1	4.610
11152	[2 × 1]	2	6.190

Int = intensity, % = percentage of positive staining cells, PIP IHC = PIP protein score derived as described in Materials and Methods from the product of intensity and proportion of positive cells by immunohistochemistry assay, PIP RT-PCR = PIP mRNA score as described in Materials and Methods.

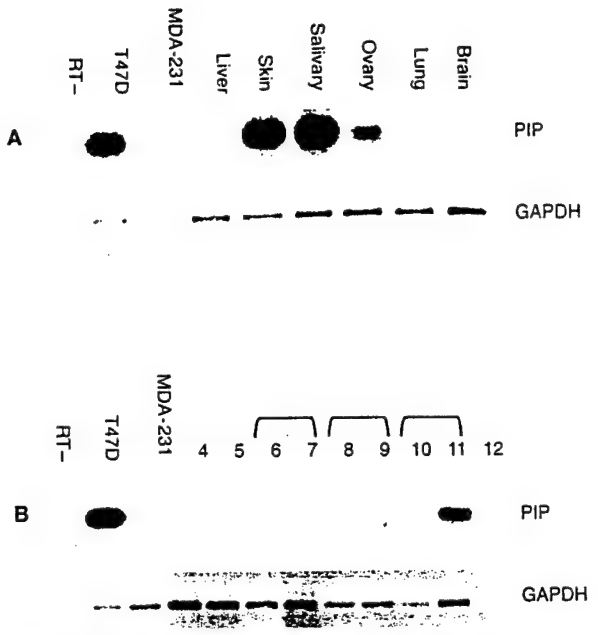

Figure 2 PIP mRNA expression in normal tissues. The upper panel shows PIP levels in a set of normal tissues that are sites of breast cancer metastasis (**A**) and the lower panel shows normal peripheral blood lymphocytes isolated from venepuncture samples from five individuals (**B**). Lanes are as follows: lane 4 normal male; lane 5 normal female, lanes 6 & 7, 8 & 9 and 10 & 11 are from three normal females on two separate occasions each, lane 12, RNA minus PCR control

RT-PCR/Southern blot assay. In different experiments the detection limit varied between 10 and 50 PIP^+ cells in a background of 1×10^6 PIP^- cells in different experiments (data not shown).

Of the six human breast cell lines (T47D, ZR 75, BT 474, MCF-7, MDA-MB-231 and HBL-100) that were analysed, four showed positive expression of PIP mRNA (data not shown). The rank order of expression amongst the PIP^+ cell lines was: T47D > ZR 75 > HBL-100 > BT 474.

Analysis of PIP mRNA expression in human breast tumours

PIP mRNA expression in 97 primary tumours was assessed by three independent RT and PCR reactions and expressed as a PIP mRNA score. This was calculated from the mean intensity of PIP mRNA signals for each tumour, standardized to the GAPDH signal from three separate PCR reactions performed on the same RT reactions and then standardized to the reference PIP signal as determined in the T47D cell line (Figure 1). PIP was negative or very low (< 5% of the T47D level) in eight tumours (8% cases). Amongst the PIP^+ tumours, 37 (38% cases) expressed PIP at levels between 5% and 50% of that of the T47D cell, 30 (31% of cases) expressed PIP at levels that were similar, between 50% and 200%, and 22 (23% of cases) expressed PIP at higher levels. Further analysis of PIP expression levels in relation to clinical-pathological factors found a significant correlation between higher levels of PIP expression in the primary tumours and higher ER ($P = 0.0004$, $r = 0.32$) and PR levels ($P = 0.0167$, $r = 0.24$) and lower Nottingham tumour grade score ($P = 0.0195$, $r = 0.24$, Spearman correlation test). Similar analysis of these same parameters as discontinuous variables was performed and confirmed these associations. Mean (s.d.) PIP mRNA levels were higher in ER^- ($n = 67$, $2.12^{(3.01)}$) versus ER^- ($n = 30$, $0.69^{(1.39)}$) tumours ($P = 0.0004$ Mann–Whitney test), PR^+ ($n = 45$, $2.42^{(3.33)}$) versus PR^- ($n = 52$, $1.04^{(1.78)}$ tumours ($P = 0.001$). PIP mRNA levels also increased from well differentiated to poorly differentiated tumours when assessed as three grade categories, although these differences fell short of achieving statistical significance (low-grade, $n = 16$, $2.59^{(3.49)}$, moderate-grade, $n = 41$, $1.83^{(2.92)}$, high-grade, $n = 40$, $1.15^{(1.95)}$, $P = 0.099$ ANOVA test). No relationship was seen between PIP mRNA expression and tumour size or nodal status (Table 1).

In five additional cases with matching primary and nodal metastasis tissue, analysis confirmed that PIP expression is conserved at similar levels between primary and metastatic cells (Figure 1B). Furthermore, RT-PCR analysis of lymph nodes from three patients undergoing elective carotid endarterectomy without any current or prior history of cancer was negative. Detection of PIP mRNA expression was also performed on axillary lymph nodes from 32 different patients using the same RT-PCR assay but with minor modifications to the method of detection. This assay used the same PCR assay and primers and PIP cDNA probe, but detection was performed by use of a non-radioactive alkaline phosphatase labelling method for the probe applied to a dot blot for detection of the PCR product. Overall PIP mRNA was detected in 17/32 lymph nodes (53%) and increasing PIP positivity reflected the tumour stage with 2/12 (17%) stage I cases positive compared to 9/12 (75%) stage II and 6/8 (75%) of stage III cases positive by RT-PCR assay. Amongst the subset of cases that were positive by histology, 11/16 (69%) were also positive by PIP RT-PCR and 5/16 (31%) were negative for PIPmRNA. Amongst the lymph nodes that were negative by histology, 6/16 (37%) were PIP RT-PCR positive (Table 2).

Immunohistochemistry and in situ hybridization

PIP mRNA levels determined by RT-PCR assay was compared to protein levels assayed in a subset of 19 cases by immunohisto-

chemistry (Table 3). PIP mRNA level correlated well with protein level ($r = 0.493$, $P = 0.0319$, Spearman test) and using cut-off points of < 5% PIPmRNA score and < 0.1 for PIP IHC score there was also 89% concordance. Additional study by in situ hybridization was performed on one tumour and one normal breast tissue which confirmed previous observations that PIP mRNA expression was confined to epithelial cells but showed that PIP mRNA is also expressed by both normal and neoplastic epithelia ils (data not shown).

Analysis of PIP expression in normal human tissues

PIP mRNA was expressed at comparable levels to the T47D breast tumour cell in several normal tissues examined including skin salivary gland and ovary (Figure 2A). Very low levels of PIP expression were observed in lung, whereas brain and liver were negative. Immunohistochemistry analysis of skin demonstrated that PIP protein expression was confined to sweat gland-like structures in the dermis. Also mRNA analysis of PBLs from 11 normal people that were analysed, all were PIP⁻ on at least one occasion (Figure 2B). Repeat samples from three individuals showed positive signals on other occasions that could not be explained as systematic contamination at the RT-PCR step.

DISCUSSION

We have shown that PIP mRNA is frequently expressed by primary breast tumours, although higher levels of expression occur in well-differentiated and ER/PR⁺ tumours. Nevertheless, PIP mRNA expression is also often conserved within the corresponding lymph node metastases. Given confirmation of the relative specificity for breast tissue that has also previously been established at the protein level by immunohistochemical studies (Wick et al, 1989), it is clear that PIP mRNA expression is a potential marker for breast micrometastasis. The presence of occasional positive signals in morphologically normal breast epithelium and in peripheral blood samples from normal individuals also indicates that, in common with most other markers, there is a need for caution in the application of PIP as a single marker for metastatic disease.

Many recent studies have concentrated on either IHC or RT-PCR assays to detect specific markers that may indicate the presence of micrometastatic disease. It is clear, however, that several pitfalls need to be considered in the practical application of individual markers (Dingemans et al, 1997). For example, while IHC assay allows morphological confirmation of the origin of positive signals it may detect some secreted proteins beyond the context of the known cell of origin. In contrast, RT-PCR may be more sensitive but does not allow direct confirmation of a positive signal in the context of the appropriate cell morphology. RT-PCR assay can also face problems that could arise from the presence of pseudogene DNA sequences and low levels of background gene expression in target tissues (Bostick et al, 1998; Lopez-Guerrero et al, 1997; Zippelius et al 1997). Improvement in specificity, rather than sensitivity, is needed. Amongst the several markers that have been used for the detection of breast micrometastases, keratin 19 and muc1 have been the most widely used (Noguchi et al, 1996; McGuckin et al, 1996). Improvements in specificity might best be achieved through a combination of these with other markers (Min et al, 1998) and a composite of technical approaches to their detection, refined still further by an appreciation of the limitations of individual markers (Zippelius et al 1997).

This study is aimed at establishing the potential of PIP as a supplementary breast tumour cell marker. The GCDFP-15/PIP gene encodes a protein that is found in high concentrations in gross cystic disease of breast and in fluids of normal apocrine glands such as sweat, tears and seminal fluid (Haagensen et al, 1990). Given the low incidence and clinical distinctiveness of tumours arising from other source tissues, PIP/GCDFP-15 protein has already been considered as a breast cell specific marker, complementary to keratin (de Almeida & Pestana 1992). This potential is based on the fact that PIP expression can be detected by IHC in up to 76% of breast carcinomas (Wick et al, 1989) and there is a high degree of concordance between PIP expression in 1° primary carcinomas and nodal metastases (Mazoujian et al, 1989). Expression of this marker has been associated with apocrine differentiation, but there is not a direct concordance with Muc1 (Soomro & Shousha, 1992). While IHC, in situ hybridization and Northern analysis have all found expression at a similar frequency (Murphy et al, 1987; Pagani et al, 1994), the prevalence and specificity of PIP mRNA for breast cancer at the sensitivity level of RT-PCR has not been established. Using RT-PCR we have found expression of PIP mRNA is readily detectable in most human breast cell lines and breast tumours. This is more frequent than previous IHC studies, which have reported the proportion of PIP positivity between 55% and 72% (Wick et al, 1989; Mazoujian et al, 1983). Not only is RT-PCR recognized as a highly sensitive technique but it is clear that, in this study, the very high frequency of PIP mRNA expression could in some cases be partly attributable to weak signals that originated only within residual normal breast elements. Consistent with this conclusion is the fact that a minor component of histologically detectable normal epithelium was found to be present within some (15%) of the 97 cases studied, which also mostly showed low levels of PIP expression. We estimate therefore that the true frequency of PIP mRNA positive primary tumours is approximately 85% of cases. This is consistent with our data where PIP mRNA expression was detected in approximately 70% nodal metastases (Table 2) and that of others (Mazoujian et al, 1989) and the fact that PIP expression is often conserved between primary and nodal metastases (Figure 1B), as also documented by others (Mazoujian et al, 1989; Wick et al, 1998). The presence of PIP mRNA in lymph nodes that are histologically negative (on the basis of assessment of a single haematoxylin and eosin (H&E)-stained diagnostic section) may suggest the presence of occult metastases (Ferrari et al, 1997). Previous studies have found micrometastases up to 25% lymph nodes from breast cancer patients when this is pursued intensively by histology and immunohistochemistry applied to serial sections, (McGuckin et al, 1996) and in 15–25% of cases when RT-PCR analysis is applied using other tumour markers such as muc1 (Noguchi et al, 1994) or β-human chorionic gonadotrophin (Hoon et al 1996). More sensitive nested-RT-PCR assays to detect both prostate-specific antigen and prostate-specific membrane antigen in histologically negative lymph nodes from prostate cancer patients have found positive tumour marker expression in up to 79% of histologically negative cases. Nonetheless, as with other current markers, the possibility of ectopic expression within normal tissues in some patients remains to be ruled out (Ferrari et al 1997).

While normal PBL samples taken from healthy individuals were all usually negative, positive results were also obtained from

independent samples taken from the same individuals. It is already known that PIP protein is present at relatively high levels in some tissues other than breast, including skin, sweat glands and salivary gland (Viacava et al, 1998; Wick et al, 1998). It therefore seems possible that these false-positive results are attributable to contamination from PIP expressing cells from sweat glands in the skin, removed during venepuncture. If this interpretation is correct then this problem might be minimized in any similar future study of PIP by obtaining several blood samples at each venapuncture and retaining only the final sample for analysis (de Graaf et al, 1997).

In this uniformly assessed tumour cohort increased PIP mRNA expression was significantly associated with low-grade and ER and PR positivity, both features that could be interpreted to indicate either biological potential or cellular differentiation. However, while PIP was not correlated with other indicators of biological potential such as tumour size or nodal status, PIP expression has previously been associated with cellular differentiation. PIP mRNA in vitro in breast cells in culture is highest in well-differentiated ER^+ cells where PIP expression has also been shown to be influenced by steroid hormones (Murphy et al, 1987) and expression in non-neoplastic and neoplastic breast tissues in vivo has been associated with specific morphological features of apocrine cellular differentiation (Haagensen et al, 1990). It should be noted that while our results are in agreement with the trends seen in other recent studies (Hall et al, 1998; Bundred et al, 1990), previous IHC studies, several larger than the present one (Mazoujian et al, 1989; Wick et al, 1989), have not established an association with these parameters. However, levels of PIP protein in breast cancer tissue, unlike PIP mRNA, may be affected by the fact that PIP is a secreted protein that is present at high levels in breast duct secretions and the serum and so can originate from adjacent breast tissues or other tissue normal tissues (Haagensen et al, 1990; Manni et al, 1984).

We conclude that the PIP gene has potential as a marker of breast micrometastasis. This is supported by the following attributes: (1) PIP is expressed by most primary breast tumours, (2) expression is often conserved in nodal metastases, and (3) this gene is not expressed in several tissues that are often targets of breast tumour metastasis. In common with several other genes proposed as tumour markers, our results demonstrate the potential for false-negative and false-positive results. The impact of this on the clinical identification of true micrometastases should be recognized and strategies developed to minimize these errors through parallel assessment of unrelated tumour markers.

ACKNOWLEDGEMENTS

This work was supported by grants from the Medical Research Council of Canada (MRC) and the Canadian Breast Cancer Research Initiative. The Manitoba Breast Tumor Bank is supported by funding from the National Cancer Institute of Canada (NCIC). PHW is an MRC Scientist.

REFERENCES

Bostick PJ, Chatterjee S, Chi DD, Huynh KT, Giuliano AE, Cote R and Hoon DS (1998) Limitations of specific reverse-transcriptase polymerase chain reaction markers in the detection of metastases in the lymph nodes and blood of breast cancer patients. *J Clin Oncol* **16**: 2632–2640

Bundred NJ, Stewart HJ, Shaw DA, Forrest AP and Miller WR (1990) Relation between apocrine differentiation and receptor status, prognosis and hormonal response in breast cancer. *Eur J Cancer* **26**: 1145–117

de Almeida PC and Pestana CB (1992) Immunohistochemical markers in the identification of metastatic breast cancer. *Breast Cancer Res Treat* **21**: 201–210

de Graaf H, Maelandsmo GM, Ruud P, Forus A, Oyjord T, Fodstad O and Hovig E (1997) Ectopic expression of target genes may represent an inherent limitation of RT-PCR assays used for micrometastasis detection: studies on the epithelial glycoprotein gene EGP-2. *Int J Cancer* **72**: 191–196

Dingemans AM, Brakenhoff RH, Postmus PE and Giaccone G (1997) Detection of cytokeratin-19 transcripts by reverse transcriptase-polymerase chain reaction in lung cancer cell lines and blood of lung cancer patients [see comments]. *Lab Invest* **77**: 213–220

Elston CW and Ellis IO (1991) Pathological prognostic factors in breast cancer. I. The value of histological grade in breast cancer: experience from a large study with long-term follow-up. *Histopathology* **19**: 403–410

Ercolani L, Florence B, Denaro M and Alexander M (1988) Isolation and complete sequence of a functional human glyceraldehyde-3-phosphate dehydrogenase gene. *J Biol Chem* **263**: 15335–15341

Ferrari AC, Stone NN, Eyler JN, Gao M, Mandeli J, Unger P, Gallagher RE and Stock R (1997) Prospective analysis of prostate-specific markers in pelvic lymph nodes of patients with high-risk prostate cancer [see comments]. *J Natl Cancer Inst* **89**: 1498–1504

Fiel MI, Cernaianu G, Burstein DE and Batheja N (1996) Value of GCDFP-15 (BRST-2) as a specific immunocytochemical marker for breast carcinoma in cytologic specimens. *Acta Cytol* **40**: 637–641

Haagensen DE, Jr, Dilley WG, Mazoujian G and Wells SA, Jr (1990) Review of GCDFP-15. An apocrine marker protein. *Ann NY Acad Sci* **586**: 161–173

Hall RE, Clements JA, Birrell SN and Tilley WD (1998) Prostate-specific antigen and gross cystic disease fluid protein-15 are co-expressed in androgen receptor-positive breast tumours. *Br J Cancer* **78**: 360–365

Hiller T, Snell L and Watson PH (1996) Microdissection RT-PCR analysis of gene expression in pathologically defined frozen tissue sections. *Biotechniques* **21**: 38–40, 42, 44

Hoon DS, Sarantou T, Doi F, Chi DD, Kuo C, Conrad AJ, Schmid P, Turner R and Guiliano A (1996) Detection of metastatic breast cancer by beta-hCG polymerase chain reaction. *Int J Cancer* **69**: 369–374

Leygue E, Snell L, Hiller T, Dotzlaw H, Hole K, Murphy LC and Watson PH (1996) Differential expression of psoriasin messenger RNA between in situ and invasive human breast carcinoma [published erratum appears in Cancer Res 1997 Feb 15; 57(4): 793]. *Cancer Res* **56**: 4606–4609

Lockett MA, Baron PL, PH, OB, Elliott BM, Robison JG, Maitre N, Metcalf JS and Cole DJ (1998*a*) Detection of occult breast cancer micrometastases in axillary lymph nodes using a multimarker reverse transcriptase-polymerase chain reaction panel. *J Am Coll Surg* **187**: 9–16

Lockett MA, Metcalf JS, Baron PL, PH, OB, Elliott BM, Robison JG and Cole DJ (1998*b*) Efficacy of reverse transcriptase-polymerase chain reaction screening for micrometastic disease in axillary lymph nodes of breast cancer patients. *Am Surg* **64**: 539–543; discussion 543–544

Lopez-Guerrero JA, Bolufer-Gilabert P, Sanz-Alonso M, Barragan-Gonzalez E, Palau-Perez J, De la Rubia-Comos J, Sempere-Talens A and Bonanad-Boix S (1997) Minimal illegitimate levels of cytokeratin K19 expression in mononucleated blood cells detected by a reverse transcription PCR method (RT-PCR). *Clin Chim Acta* **263**: 105–116

Manni A, Santen RJ, Boucher AE, Lipton A, Harvey H, Drago J, Rohner T, Haagensen D, Glode M and Santner SJ (1984) Evaluation of CEA and GCDFP-15 plasma level during hormonally induced cancer stimulation. *Anticancer Res* **4**: 141–144

Mazoujian G, Bodian C, Haagensen DE, Jr and Haagensen CD (1989) Expression of GCDFP-15 in breast carcinomas. Relationship to pathologic and clinical factors. *Cancer* **63**: 2156–2161

Mazoujian G, Pinkus GS, Davis S and Haagensen DE, Jr (1983) Immunohistochemistry of a gross cystic disease fluid protein (GCDFP-15) of the breast. A marker of apocrine epithelium and breast carcinomas with apocrine features. *Am J Pathol* **110**: 105–112

McGuckin MA, Cummings MC, Walsh MD, Hohn BG, Bennett IC and Wright RG (1996) Occult axillary node metastases in breast cancer: their detection and prognostic significance. *Br J Cancer* **73**: 88–95

Min CJ, Tafra L and Verbanac KM (1998) Identification of superior markers for polymerase chain reaction detection of breast cancer metastases in sentinel lymph nodes [In Process Citation]. *Cancer Res* **58**: 4581–4584

Monteagudo C, Merino MJ, LaPorte N and Neumann RD (1991) Value of gross cystic disease fluid protein-15 in distinguishing metastatic breast carcinomas

among poorly differentiated neoplasms involving the ovary. *Hum Pathol* **22**: 368–372

Mori M, Mimori K, Ueo H, Karimine N, Barnard GF, Sugimachi K and Akiyoshi T (1996) Molecular detection of circulating solid carcinoma cells in the peripheral blood: the concept of early systemic disease. *Int J Cancer* **68**: 739–743

Murphy LC, Lee-Wing M, Goldenberg GJ and Shiu RP (1987*a*) Expression of the gene encoding a prolactin-inducible protein by human breast cancers in vivo: correlation with steroid receptor status. *Cancer Res* **47**: 4160–4164

Murphy LC, Tsuyuki D, Myal Y and Shiu RP (1987*b*) Isolation and sequencing of a cDNA clone for a prolactin-inducible protein (PIP). Regulation of PIP gene expression in the human breast cancer cell line, T-47D. *J Biol Chem* **262**: 15236–15241

Noguchi S, Aihara T, Nakamori S, Motomura K, Inaji H, Imaoka S and Koyama H (1994) The detection of breast carcinoma micrometastases in axillary lymph nodes by means of reverse transcriptase-polymerase chain reaction. *Cancer* **74**: 1595–1600

Noguchi S, Aihara T, Motomura K, Inaji H, Imaoka S and Koyama H (1996) Detection of breast cancer micrometastases in axillary lymph nodes by means of reverse transcriptase-polymerase chain reaction. Comparison between MUC1 mRNA and keratin 19 mRNA amplification. *Am J Pathol* **148**: 649–656

Ormsby AH, Snow JL, Su WP and Goellner JR (1995) Diagnostic immunohistochemistry of cutaneous metastatic breast carcinoma: a statistical analysis of the utility of gross cystic disease fluid protein-15 and estrogen receptor protein. *J Am Acad Dermatol* **32**: 711–716

Pagani A, Sapino A, Eusebi V, Bergnolo P and Bussolati G (1994) PIP/GCDFP-15 gene expression and apocrine differentiation in carcinomas of the breast. *Virchows Arch* **425**: 459–465

Pelkey TJ, Frierson HF Jr and Bruns DE (1996) Molecular and immunological detection of circulating tumor cells and micrometastases from solid tumors. *Clin Chem* **42**: 1369–1381

Raj GV, Moreno JG and Gomella LG (1998) Utilization of polymerase chain reaction technology in the detection of solid tumors. *Cancer* **82**: 1419–1442

Schoenfeld A, Kruger KH, Gomm J, Sinnett HD, Gazet JC, Sacks N, Bender HG, Luqmani Y and Coombes RC (1997) The detection of micrometastases in the peripheral blood and bone marrow of patients with breast cancer using immunohistochemistry and reverse transcriptase polymerase chain reaction for keratin 19. *Eur J Cancer* **33**: 854–861

Soomro S and Shousha S (1992) Monoclonal antibody B72.3 immunostaining of breast carcinoma. Patterns of staining and relationship to mucin content and GCDFP-15 reactivity. *Arch Pathol Lab Med* **116**: 32–35

Tsuchiya A, Sugano K, Kimijima I and Abe R (1996) Immunohistochemical evaluation of lymph node micrometastases from breast cancer. *Acta Oncol* **35**: 425–428

Vary CP, Carmody M, LeBlanc R, Hayes T, Rundell C and Keilson L (1996) Allele-specific hybridization of lipoprotein lipase and factor-V Leiden missense mutations with direct label alkaline phosphatase-conjugated oligonucleotide probes. *Genet Anal* **13**: 59–65

Viacava P, Naccarato AG and Bevilacqua G (1998) Spectrum of GCDFP-15 expression in human fetal and adult normal tissues. *Virchows Arch* **432**: 255–260

Watson PH, Snell L and Parisien M (1996) The NCIC-Manitoba Breast Tumor Bank: a resource for applied cancer research. *Cmaj* **155**: 281–283

Wick MR, Lillemoe TJ, Copland GT, Swanson PE, Manivel JC and Kiang DT (1989) Gross cystic disease fluid protein-15 as a marker for breast cancer: immunohistochemical analysis of 690 human neoplasms and comparison with alpha-lactalbumin. *Hum Pathol* **20**: 281–287

Wick MR, Ockner DM, Mills SE, Ritter JH and Swanson PE (1998) Homologous carcinomas of the breasts, skin, and salivary glands. A histologic and immunohistochemical comparison of ductal mammary carcinoma, ductal sweat gland carcinoma, and salivary duct carcinoma. *Am J Clin Pathol* **109**: 75–84

Zippelius A, Kufer P, Honold G, Kollermann MW, Oberneder R, Schlimok G, Riethmuller G and Pantel K (1997) Limitations of reverse-transcriptase polymerase chain reaction analyses for detection of micrometastatic epithelial cancer cells in bone marrow. *J Clin Oncol* **15**: 2701–2708

British Journal of Cancer (1999) 79(5/6), 978–983

Article no. bjoc.1998.0156

Oestrogen receptor-α variant mRNA expression in primary human breast tumours and matched lymph node metastases

E Leygue[1], RE Hall[2], H Dotzlaw[1], PH Watson[3] and LC Murphy[1]

[1]Department of Biochemistry and Molecular Biology, University of Manitoba, Winnipeg, MB, Canada; [2]Department of Surgery, Flinders University of South Australia, Bedford Park, SA, Australia; [3]Department of Pathology, University of Manitoba, Winnipeg, MB, Canada

Summary We have shown previously that the relative expression of a truncated oestrogen receptor-α variant mRNA (ER clone 4) is significantly increased in axillary node-positive primary breast tumours compared with node-negative tumours. In this study, we have examined the relative expression of clone 4-truncated, exon 5-deleted and exon 7-deleted oestrogen receptor-α variant mRNAs in 15 primary breast tumour samples and in synchronous axillary lymph node metastases. Overall, there were no significant differences between the primary tumours and the matched metastases in the relative expression of these three specific variant mRNAs. Furthermore, the pattern of all deleted oestrogen receptor-α variant mRNAs appeared conserved between any primary and its matched secondary tumour.

Keywords: oestrogen receptor-α variants; breast cancer; metastasis

Multiple oestrogen receptor-α (ER) mRNA species have been identified in human breast cancer samples (Dowsett et al, 1997; Murphy et al, 1997*a*, *b*). The significance of these variant transcripts remains unclear. Although the ability to detect variant ER proteins encoded by such variant transcripts remains controversial (Park et al, 1996; Desai et al, 1997; Huang et al, 1997), alteration of expression of some variant ER mRNAs has been found to occur during both breast tumorigenesis (Leygue et al, 1996*a*, *b*) and breast cancer progression. With regard to the latter, we showed previously that the expression of the truncated, clone 4 variant (C4) ER mRNA (Dotzlaw et al, 1992) was significantly increased relative to wild-type (WT) ER mRNA in a group of primary breast tumours with multiple poor prognostic features compared with a group of primary breast tumours with good prognostic features (Murphy et al, 1995). The 'poor' prognostic features were defined as the presence of lymph node metastases at the time of surgery, large tumour size, lack of progesterone receptor (PR) expression and high S-phase fraction, while 'good' prognostic features were lack of nodal involvement, small tumour size, PR positivity and low S-phase fraction. In the same study, the relative expression of clone 4 ER variant mRNA was significantly higher in primary breast tumours that were PR– than in those that were PR+ (Murphy et al, 1995). This suggested that altered ER variant expression may be a marker of a more aggressive phenotype and lack of endocrine sensitivity in human breast cancer. As a prerequisite to addressing such a possibility, we have investigated the pattern of ER variant expression in a cohort of primary tumours and their matched, concurrent lymph node metastases.

Received 20 April 1998
Revised 3 July 1998
Accepted 14 July 1998

Correspondence to: LC Murphy

MATERIALS AND METHODS

Tumour selection and RNA isolation

Sections from 15 frozen primary human breast tumour samples and their matched frozen lymph node metastases were provided by the Manitoba Breast Tumour Bank (Winnipeg, MB, Canada). For the primary tumour samples, the ER levels, determined by ligand-binding assays, ranged from 0.8 fmol mg^{-1} protein to 89 fmol mg^{-1} protein with a median value of 17.5 fmol mg^{-1} protein. Thirteen tumours were ER+ and two were ER– (ER+ was defined as >3 fmol mg^{-1} protein). PR levels determined by ligand-binding assays ranged from 2.9 fmol mg^{-1} protein to 112 fmol mg^{-1} protein with a median value of 12.6 fmol mg^{-1} protein. Nine tumours were PR+ and 6 were PR– (PR+ was defined as > 10 fmol mg^{-1} protein). ER and PR values were available for only four of the lymph node metastases and the ER and PR status as defined by ligand binding did not differ from their matched primary tumour. RNA was extracted from the sections using Trizol reagent (Gibco/BRL, Ontario, Canada) according to the manufacturer's instructions.

For validation of triple-primer polymerase chain reactions (TP-PCR) by comparison with RNAase protection assays, a second cohort of human breast tumour specimens (25 cases) was also obtained from the Manitoba Breast Tumour Bank. Twenty of these tumours were ER+, as determined by ligand-binding assay, with values ranging from 4.5 to 311 fmol mg^{-1} protein (median 93 fmol mg^{-1}). The five remaining cases were ER–, with values ranging from 0 to 1.8 fmol mg^{-1} protein (median 0.9 fmol mg^{-1}). Total RNA was extracted from frozen tissues using guanidinium

thiocyanate as previously described (Murphy and Dotzlaw, 1989). The integrity of the RNA was confirmed by denaturing gel electrophoresis as previously described (Murphy and Dotzlaw, 1989).

RNAase protection assay

Antisense riboprobes spanning the point at which the C4 ER mRNA sequence diverges from the WT ER mRNA sequence (Dotzlaw et al, 1992) were synthesized as previously described (Dotzlaw et al, 1990). The level of C4 ER mRNA and WT ER mRNA in 10 µg of total RNA was determined using an RNAase Protection Assay kit (RPA II, Ambion, Austin, TX, USA) following the manufacturer's instructions. Briefly, RNA was denatured at 80°C for 5 min in the presence of 5×10^5 d.p.m. ^{32}P-labelled riboprobe, then hybridized at 42°C for 16 h. Following RNAase digestion, samples were electrophoresed on 6% acrylamide gels containing 7 M urea, dried and autoradiographed.

To quantify C4 and WT ER mRNAs within breast tumour samples, a standard curve was established in each assay. C4 and WT ER mRNAs (30, 125, 500 pg C4 RNA and 125, 500, 2000 pg WT ER RNA) synthesized using T7 RNA polymerase were purified on a Sephadex G-50 column and quantitated spectrophotometrically. WT ER RNA was transcribed from linearized pHEO, which contains the entire WT ER coding sequence but is missing the 3′-untranslated portion of the ER mRNA [(kindly provided by P Chambon, Strasbourg, France (Green et al, 1986)]. Full-length C4 RNA was transcribed from linearized pSK-C4 (Dotzlaw et al, 1992). Standard RNAs were analysed together in the same assay as the breast tumour mRNAs. Bands corresponding to the C4 ER mRNA and WT ER mRNA protected fragments were excised from the gel and counted after addition of 5 ml scintillant (ICN Pharmaceuticals, Inc., Irvine, CA, USA) in a scintillation counter (Beckman Instruments, Inc., Fullerton, CA, USA). For each sample, absolute amounts of C4 and WT ER mRNA were determined from the standard curve.

Reverse transcription, PCR and triple-primer (TP) PCR

For each sample, 1 µg of total RNA was reverse transcribed in a final volume of 15 µl as described previously (Leygue et al, 1996*a*). One microlitre of the reaction mixture was taken for subsequent amplification.

The primers and PCR conditions for the long-range PCR were as previously described (Leygue et al, 1996*c*). The primers and PCR conditions for measuring the relative expression of exon 5-deleted and exon 7-deleted ER transcripts relative to WT ER transcripts were as previously described (Leygue et al, 1996*a*).

The TP-PCR conditions were similar to those previously described (Leygue et al, 1996*b*) with minor modifications. ERU (5′-TGTGCAATGACTATGCTTCA-3′, sense, located in WT ER exon 2: 792–811, as numbered in Green et al, 1986) and ERL (5′-GCTCTTCCTCCTGTTTTTAT-3′, antisense, located in WT ER exon 3; 940–921) primers allowed amplification of a 149-bp fragment corresponding to WT ER mRNA. The C4-specific primer (C4L, 5′-TTTCAGTCTTCAGATACCCCAG-3′, antisense; 1336–1315, as numbered in Dotzlaw et al, 1992) spans the only region of the C4 unique sequence that does not have any homology with repetitive LINE-1 sequences (Dotzlaw et al, 1992). ERU and C4L allowed amplification of a 536-bp fragment corresponding specifically to C4 ER variant mRNA.

PCR amplifications were performed in a final volume of 10 µl in the presence of 20 mM Tris-HCl (pH 8.4), 50 mM potassium chloride, 2 mM magnesium chloride, 0.2 mM dATP, 0.2 mM dTTP, 0.2 mM dGTP, 0.2 mM dCTP, 4 ng µl^{-1} of each primer (ERU, ERL and C4L), 0.2 units of *Taq* DNA polymerase (Gibco-BRL) and 1 µCi of [α-^{32}P] dCTP (3000 Ci mmol^{-1}, ICN Pharmaceuticals, Irvine, CA, USA). Each PCR consisted of 30 cycles (1 min at 94°C, 30 s at 60°C and

Figure 1 (**A**) Autoradiogram of long-range RT-PCR (Leygue et al, 1996*c*) results from two samples of primary breast tumours (P) and their matched concurrent lymph node metastase (M). WT ER is the expected product corresponding to the WT ER mRNA; D7 is the expected product corresponding to the exon 7-deleted ER variant mRNA; D4 is the expected product for the exon 4-deleted ER mRNA; D3-4 is the expected product for the exon 3+4-deleted ER mRNA; D4/7 is the expected product for the exon 4+7-deleted ER mRNA. (**B**) Autoradiogram of RT-PCR results from two samples of primary breast tumours (P) and their matched concurrent lymph node metastase (M). D5 is the expected product corresponding to the exon 5-deleted ER variant mRNA. WT ER is the expected product corresponding to the WT ER mRNA. (**C**) Autoradiogram of RT-PCR results from two samples of primary breast tumours (P) and their matched concurrent lymph node metastase (M). D7 is the expected product corresponding to the exon 7-deleted ER variant mRNA. WT ER is the expected product corresponding to the WT ER mRNA. (**D**) Autoradiogram of TP-PCR results from two samples of primary breast tumours (P) and their matched concurrent lymph node metastase (M). C4 is the expected product corresponding to the clone 4 ER variant mRNA. WT ER is the expected product corresponding to the WT ER mRNA. *Band coamplified with C4 and WT ER and shown to correspond to an exon 2-duplicated ER variant mRNA

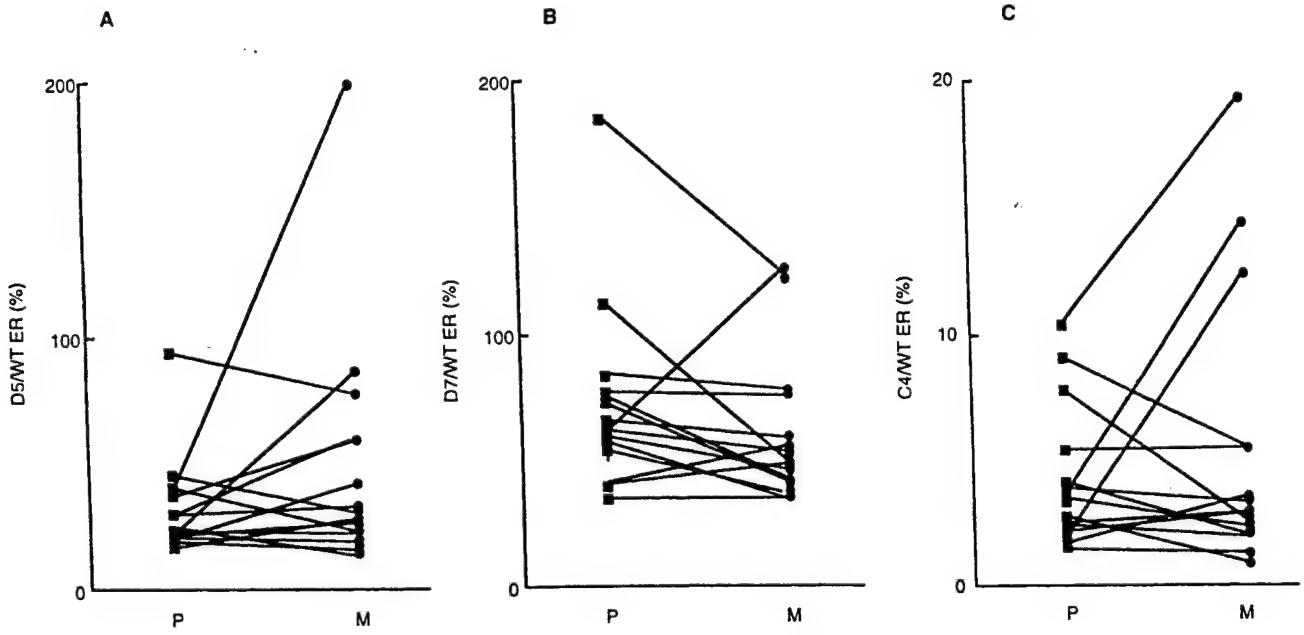

Figure 2 (**A**) Quantitative comparison of the relative expression of exon 5-deleted variant ER mRNA in primary (P) human breast tumours and their concurrent matched lymph node metastases (M). For each sample, the mean of three independent measures of exon 5-deleted ER relative expression expressed as a percentage of the corresponding WT ER signal was determined as described in the Materials and methods section. (**B**) Quantitative comparison of the relative expression of exon 7-deleted variant ER mRNA in primary (P) human breast tumours and their concurrent matched lymph node metastases (M). For each sample, the mean of three independent measures of exon 7-deleted ER relative expression expressed as a percentage of the corresponding WT ER signal was determined as described in the Materials and Methods section. (**C**) Quantitative comparison of the relative expression of clone 4 variant ER mRNA in primary (P) human breast tumours and their concurrent matched lymph node metastases (M). For each sample, the mean of three independent measures of clone 4 relative expression expressed as a percentage of the corresponding WT ER signal was determined as described in the Materials and Methods section

1 min at 72°C) using a thermocycler (Perkin Elmer). Four microlitres of the reaction mix was then denatured by addition of 6 µl of 80% formamide buffer and boiling before electrophoresis on 6% polyacrylamide gels containing 7 M urea (PAGE). Following electrophoresis, the gels were dried and exposed to Kodak XAR Film at –70°C with two intensifying screens for 2 h.

Quantification of RT-PCR and TP-PCR

Bands corresponding to the variant ER mRNA and WT ER mRNA were excised from the gel and counted after addition of 5 ml of scintillant in a scintillation counter. The variant signal was expressed as a percentage of the WT ER signal. It should be noted that the percentage obtained reflects the relative ratio of the variant to WT ER RT-PCR product and does not provide absolute initial mRNA levels. Validation of this approach was described previously (Daffada et al, 1994, 1995; Leygue et al, 1996*a*, *b*). At least two independent PCR assays were performed for each sample in the comparison of RNAase protection assay with TP-PCR assays. For assessment of matched primary and secondary breast tumour samples, at least two and in most cases three independent PCR reactions were performed and the mean determined.

The statistical significance of differences in the relative levels of expression of any single ER mRNA variant between primary tumour and lymph node metastasis was determined using the Wilcoxon signed-rank test.

RESULTS

Determination of the pattern of exon-deleted ER variant mRNA expression

Multiple ER variant mRNAs have been shown to be expressed in any one breast tissue sample (Leygue et al, 1996*a*; Murphy et al, 1997*a*, *b*). To investigate the pattern of multiple exon-deleted ER variant expression between primary breast tumours and their matched lymph node metastases, a long-range RT-PCR approach was used. This approach, based on the competitive amplification of wild-type and exon-deleted ER variant cDNAs, using primers annealing within exons 1 and 8, allows the evaluation of the relative pattern of expression of all exon-deleted ER variant transcripts present in any individual sample (Leygue et al, 1996*c*; Fasco. 1997). Typical results are shown in Figure 1A. The pattern of deleted ER mRNA expression between any one primary tumour and its matched lymph node metastasis was conserved.

Determination of the relative expression of exon 5-deleted and exon 7-deleted ER variant mRNA expression

Using a previously validated semiquantitative PCR approach (Leygue et al, 1996*a*), the measurement of the relative expression of specific individual exon-deleted ER variant mRNAs was also undertaken. Specifically, the relative expressions of exon 5-deleted

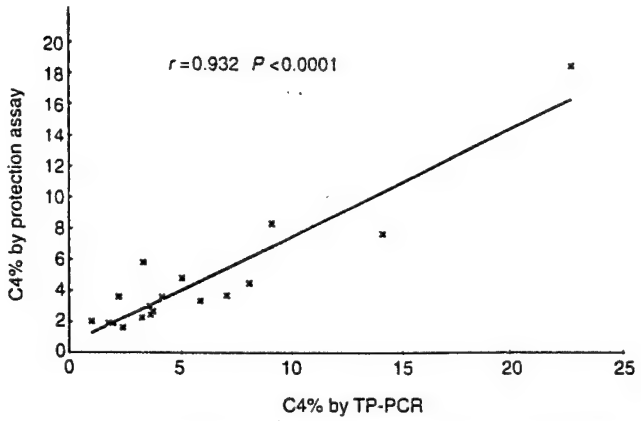

Figure 3 Linear regression analysis of clone 4 expression (expressed as a percentage of the corresponding WT ER expression) as determined by TP-PCR vs standardized RNAase protection assay in 18 human breast tumours

ER cDNA (Figure 1B) using primers in exons 4 and 6, and exon 7-deleted ER cDNA (Figure 1C), using primers in exons 5 and 8, were measured. The median value for the relative expression of the exon 5-deleted ER for the primary tumours was 23.1% (range 17.3–94.3%) and the median value for the matched lymph node metastases was 31.3% (range 14.9–200%). The scatter plot for these results is shown in Figure 2A. The median relative expression of the exon 7-deleted ER for primary tumours was 65% (range 39.3–184.9%) and the median value for the matched lymph node metastases was 52.5% (range 35.5–126%). The scatterplot of these results is shown in Figure 2B. There were no statistically significant differences in the relative expression of either exon-deleted ER mRNA between primary and concurrent metastatic tumours.

Comparison of RNAase protection assay and triple-primer PCR assay for determination of the relative expression of clone 4 truncated ER variant mRNA expression

Another frequently expressed ER variant, which would not be detected in the above assays, is the C4 ER mRNA. This variant was previously found to be significantly elevated in a group of primary breast tumours with poor prognostic features that included concurrent lymph node metastases, compared with a group of primary tumours with good prognostic variables that included lack of concurrent nodal metastases (Murphy et al, 1995). Therefore, it was relevant to determine the level of C4 ER variant expression in primary breast tumours and their matched, concurrent lymph node metastases.

In this previous study, we used RNAase protection assays to measure WT and variant ER mRNA expression (Murphy et al, 1995). However, in order to conduct this study using smaller tissue samples (in particular from nodal metastases) and to ensure a close correlation with the histological composition of the tissue, we used a previously described TP-PCR assay (Leygue et al, 1996*b*) to measure the relative expression of C4 ER mRNA. To facilitate comparison of the current data with our earlier study (Murphy et al, 1995), it was necessary to compare the RNAase protection assay with the TP-PCR assay, before proceeding to analyse the primary and secondary breast tumour samples for C4 mRNA expression by TP-PCR.

RNA from 25 human breast tumours, selected to represent a wide range of ER status by ligand-binding assay (Table 1), was

Table 1 C4 and WT ER mRNA expression in 25 human breast tumours, as determined by RNAase protection assay and TP-PCR

Sample no.	Ligand binding	RNAase protection			TPPCR
	ER (fmol mg^{-1})	C4 (pg 10 μg^{-1})	WT ER (pg 10 μg^{-1})	C4 (%)	C4 (%)
5	0.0	ND	ND	–	1.7
3	0.4	ND	ND	–	2.6
1	0.9	ND	ND	–	3.1
24	1.2	6.2	105.1	5.9	3.3
4	1.8	ND	ND	–	3.7
23	4.5	10.0	54.3	18.4	22.7
8	5.8	ND	26.8	–	2.8
7	6.3	ND	224.6	–	3.4
2	8.7	ND	9.0	–	2.2
19	10.0	22.6	902.9	2.5	3.6
10	17.8	5.3	146.4	3.6	4.1
13	25.0	2.3	112.0	2.0	1.0
15	44.0	5.0	148.5	3.4	5.9
22	57.0	11.8	153.6	7.7	14.1
11	90.0	2.5	129.1	1.9	1.7
21	96.0	9.6	263.4	3.6	2.2
14	105.0	4.6	94.4	4.9	5.0
17	111.0	26.7	320.3	8.3	9.1
9	121.0	4.6	277.7	1.7	2.4
6	146.0	2.0	105.0	1.9	1.9
18	198.0	15.8	422.0	3.7	7.0
20	236.0	8.8	288.4	3.0	3.5
12	289.0	3.6	80.5	4.5	8.0
16	304.0	38.8	1440.8	2.7	3.7
25	311.0	83.9	3651.0	2.3	3.2

ND, not detected.

analysed in a standardized RNAase protection assay in order to determine the absolute amount of C4 and WT ER mRNAs within each sample. The signals corresponding to C4 and WT ER mRNAs were quantified as described in Materials and Methods. In each assay, known amounts of synthetic WT ER and C4 mRNAs were analysed in parallel in order to establish a standard curve allowing the determination of absolute levels of C4 and WT ER mRNAs, expressed as pg 10 μg^{-1} RNA (Table 1). Because of the very low C4 protected fragment signal (≤ 15 d.p.m.) in seven tumours, it was not possible to determine confidently the absolute amount of C4 mRNA in these samples (not detected, ND). All C4-negative tumours by RNAase protection assay were from tumours with ER values lower than 10 fmol mg^{-1} protein, as determined by ligand-binding assay. The absolute amounts of C4 and WT ER mRNAs in the remaining 18 tumours, as determined by RNAase protection assay, varied from 2 to 83.9 pg 10 μg^{-1} RNA and from 9 to 3651 pg 10 μg^{-1} RNA respectively. For each sample, the C4 mRNA signal was expressed as a percentage of WT ER mRNA signal (Table 1).

C4 ER mRNA relative expression was determined by TP-PCR within the same 25 RNA samples as described in Materials and Methods. Both C4 and WT ER cDNAs signals were detected in all 25 tumours studied, independent of their ER status as determined by ligand-binding assay. C4 and WT ER signals were quantified as described in Materials and Methods. The signal corresponding to C4 was expressed as a percentage of the WT ER signal. Table 1 presents the average of a least two independent TP-PCR experiments. Linear regression analysis (Figure 3) shows a highly significant correlation between C4 mRNA relative expression as

determined by RNAase protection assay (in the 18 tumours in which a C4 signal was detectable) and C4 mRNA relative expression determined by TP-PCR ($r = 0.932$, $P < 0.0001$). Interestingly, an additional band was also observed in most of the samples using the TP-PCR assay (see asterisk, Figure 1D). This band was identified after subcloning and sequencing to be a product of an exon 2-duplicated ER variant mRNA. The intensity of the signal obtained from this exon 2-duplicated ER band paralleled that of the WT ER band, and the co-amplification of the exon 2-duplicated ER variant mRNA using TP-PCR did not interfere with the relationship between TP-PCR and RNAase protection assay.

Determination of the relative expression of clone 4 truncated ER variant mRNA expression

The above TP-PCR assay was used to compare the relative expression of C4 and WT ER expression in the matched breast cancer samples (Figure 1D). The median relative expression of the C4 ER for the primary tumours was 3.5% (range 1.6–10.5%) and the median value for the matched lymph node metastases was 3.1% (range 1.0–19.4%). A scatterplot of the results is shown in Figure 2C. There is no statistically significant difference in the relative expression of C4 ER variant expression between primary breast tumours and their concurrent lymph node metastases by Wilcoxon rank-sum analysis. Interestingly, although not statistically significant, we found that the median level of C4 expression in ER+ PR– primary tumours, 3.7% (range 2.5–7.9%, $n = 5$), was approximately 50% higher than the median level of C4 expression in ER+ PR+ primary tumours, which was 2.4% (range 1.6–10.5%, $n = 8$). Such a trend would be consistent with our previous results in which C4 expression was higher in PR– primary breast tumours than in PR+ primary tumours.

DISCUSSION

The data presented in this study provide evidence that both the overall pattern of ER variant expression and the relative level of expression of three individual ER variants are conserved in primary breast tumours and their matched, concurrent lymph node metastases.

The observations presented in this manuscript, showing a conserved pattern and similar relative expression of ER variants between primary tumours and their concurrent lymph node metastases, would be consistent with previous observations that little change of ER status can be found between primary human breast tumours and their concurrent lymph node metastases or their distant metastases (Hahnel and Twaddle, 1985; Robertson, 1996). These findings are not inconsistent with our previously published data, which showed that the relative expression of one ER variant was significantly increased in primary tumours with poor prognostic characteristics, which included having concurrent lymph node metastases, as compared with primary tumours without concurrent lymph node metastases (Murphy et al, 1995). It should be stressed that all the primary tumours in the current study had concurrent lymph node metastases, a major feature of poor prognosis in breast cancer, and most likely resembled our previously described poor prognostic group (Murphy et al, 1995). Therefore in primary tumours that have concurrent lymph node metastases and have detectable levels of C4 ER variant as well as other variant ER mRNAs, mRNA levels do not significantly change between primary tumours and their concurrent lymph node metastases. These data do not, however, shed any light on whether tumours with good prognostic features, as previously described (Murphy et al, 1995), that have a relatively low level of C4 ER variant mRNA subsequently develop higher levels when recurrent disease develops. Although this issue remains to be investigated, our earlier observation of higher relative C4 ER mRNA expression in PR– primary tumours compared with PR+ primary tumours appeared to be conserved in the present cohort, although the numbers were low and the difference did not reach statistical significance. As quantitative differences in the expression of several ER variants have been shown to occur in primary breast tumours compared with normal human breast tissues (Leygue et al, 1996*a*, *b*), as well as between good vs poor prognosis primary breast tumours, the current data suggest that alterations in ER variant expression and any role this may have in altered oestrogen signal transduction probably occurs early in tumorigenesis and well before the acquisition of the ability to metastasize. This is consistent with previous data supporting the concept of an early involvement of perturbations of oestrogen signal transduction and the development of hormone independence in breast tumorigenesis (Khan et al, 1994; Schmitt, 1995). It remains therefore to be determined if altered ER variant expression can predict tumour recurrence and progression in node-negative breast cancers.

To our knowledge, this study is the first to compare an already established quantitative approach, such as the RNAase protection assay, with an RT-PCR based approach in the study of ER variant mRNA expression. Earlier studies have utilized either the RNAase protection assay or RT-PCR only. Considering the potential clinical relevance of the measurement of the relative level of ER variants with respect to WT ER within human breast tissue samples and the sensitivity of an RT-PCR based approach, such a comparative study was deemed necessary. Furthermore, our data provide validation for comparing previous data obtained using a non-amplification-dependent RNAase protection assay with the current data obtained using an amplification-dependent TP-PCR assay.

The lack of sensitivity of the RNAase protection assay for a subset of tumours with very low (<10 fmol mg^{-1}) ER values by ligand-binding assay is an important limiting factor. It effectively means that, in a screening study, ER-negative tumours (< 3 fmol mg^{-1} protein), as well as ER-positive tumours with ER values lower than 10 fmol mg^{-1}, as measured by ligand-binding assay, cannot be reliably assessed for C4 ER variant mRNA expression by RNAase protection assay. This, together with the relatively large amount of RNA needed to perform an RNAase protection analysis, severely limits the usefulness of a standardized RNAase protection assay in such screening studies. The low amount of starting material needed, together with the higher sensitivity observed (samples C4 ER variant negative by RNAase protection assay had detectable levels of C4 ER variant and WT ER mRNA by TP-PCR) make TP-PCR an attractive alternative to the RNAase protection assay in studies in which such factors are limiting.

In conclusion, the current investigation extends our previous studies on the relationship of ER variant expression and progression in human breast cancer. The data presented show that both the pattern and level of expression of ER variants are conserved between matched primary breast tumours and their concurrent lymph node metastases. Therefore, any alteration in ER variant expression that could be a marker of altered ER signal transduction and breast cancer progression probably occurs before breast cancer cells acquire the ability to metastasize.

ACKNOWLEDGEMENTS

This work was supported by the US Army Medical Research and Materiel Command (USAMRMC), grant number DAMD17-95-1-5015. The Manitoba Breast Tumour Bank is supported by funding from the National Cancer Institute of Canada (NCIC). LCM is a Medical Research Council of Canada (MRC) Scientist, PHW is a MRC Clinician-Scientist, EL is a recipient of a USAMRMC Postdoctoral Fellowship (DAMD17-96-1-6174), RH was supported by a University of Manitoba Visiting Scientist Award.

REFERENCES

Daffada AA, Johnston SR, Nicholls J and Dowsett M (1994) Detection of wild type and exon 5-deleted splice variant oestrogen receptor (ER) mRNA in ER-positive and -negative breast cancer cell lines by reverse transcription/polymerase chain reaction. *J Mol Endocrinol* **13**: 265–273

Daffada AA, Johnston SR, Smith IE, Detre S, King N and Dowsett M (1995) Exon 5 deletion variant estrogen receptor messenger RNA expression in relation to tamoxifen resistance and progesterone receptor/pS2 status in human breast cancer. *Cancer Res* **55**: 288–293

Desai A, Luqmani Y, Coope R, Dagg B, Gomm J, Pace P, Rees C, Thirunavukkarasu V, Shousha S, Groome N, Coombes R and Ali S (1997) Presence of exon 5 deleted oestrogen receptor in human breast cancer: functional analysis and clinical significance. *Br J Cancer* **75**: 1173–1184

Dotzlaw H, Miller T, Karvelas J and Murphy LC (1990) Epidermal growth factor gene expression in human breast cancer biopsy samples: relationship to estrogen and progesterone receptor gene expression. *Cancer Res* **50**: 4204–4208

Dotzlaw H, Alkhalaf M and Murphy LC (1992) Characterization of estrogen receptor variant mRNAs from human breast cancers. *Mol Endocrinol* **6**: 773–785

Dowsett M, Daffada A, Chan C and Johnston S (1997) Oestrogen receptor mutants and variants in breast cancer. *Eur J Cancer* **33**: 1177–1183

Fasco M (1997) Quantitation of estrogen receptor mRNA and its alternatively spliced mRNAs in breast tumor cells and tissues. *Anal Biochem* **245**: 167–178

Green S, Walter P, Kumar V, Krust A, Bornert J, Argos P and Chambon P (1986) Human estrogen receptor cDNA: sequence, expression, and homology to v-erb-A. *Nature* **320**: 134–139

Hahnel R and Twaddle E (1985) The relationship between estrogen receptors in primary and secondary breast carcinomas and in sequential primary breast carcinomas. *Breast Cancer Res Treat* **5**: 155–163

Huang A, Leygue E, Snell L, Murphy LC and Watson P (1997) Expression of estrogen receptor variants mRNAs and determination of estrogen status in human breast cancer. *Am J Pathol* **150**: 1827–1833

Khan SA, Rogers MA, Obando JA and Tamsen A (1994) Estrogen receptor expression of benign breast epithelium and its association with breast cancer. *Cancer Res* **54**: 993–997

Leygue ER, Watson PH and Murphy LC (1996*a*) Estrogen receptor variants in normal human mammary tissue. *J Natl Cancer Inst* **88**: 284–290

Leygue E, Murphy LC, Kuttenn F and Watson P (1996*b*) Triple primer polymerase chain reaction. A new way to quantify truncated mRNA expression. *Am J Pathol* **148**: 1097–1103

Leygue E, Huang A, Murphy LC and Watson P (1996*c*) Prevalence of estrogen receptor variant messenger RNAs in human breast cancer. *Cancer Res* **56**: 4324–4327

Murphy LC and Dotzlaw H (1989) Variant estrogen receptor mRNA species detected in human breast cancer biopsy samples. *Mol Endocrinol* **3**: 687–693

Murphy LC, Hilsenbeck SG, Dotzlaw H and Fuqua SAW (1995) Relationship of clone 4 estrogen receptor variant messenger RNA expression to some known prognostic variables in human breast cancer. *Clin Cancer Res* **1**: 155–159

Murphy LC, Dotzlaw H, Leygue E, Douglas D, Coutts A and Watson P (1997*a*). Estrogen receptor variants and mutations: a review. *J Steroid Biochem Mol Biol* **62**: 363–372

Murphy LC, Leygue E, Dotzlaw H, Douglas D, Coutts A and Watson P (1997*b*) Oestrogen receptor variants and mutations in human breast cancer. *Ann Med* **29**: 221–234

Park W, Choi J, Hwang E and Lee J (1996) Identification of a variant estrogen receptor lacking exon 4 and its coexpression with wild type estrogen receptor in ovarian carcinomas. *Clin Cancer Res* **2**: 2029–2035

Robertson J (1996) Oestrogen receptor: a stable phenotype in breast cancer. *Br J Cancer* **73**: 5–12

Schmitt F (1995) Multistep progression from an oestrogen dependent growth towards an autonomous growth in breast carcinogenesis. *Eur J Cancer* **12**: 2049–2052

[CANCER RESEARCH 59, 529–532, February 1, 1999]

Advances in Brief

Estrogen Receptor-β Messenger RNA Expression in Human Breast Tumor Biopsies: Relationship to Steroid Receptor Status and Regulation by Progestins[1]

Helmut Dotzlaw, Etienne Leygue, Peter H. Watson, and Leigh C. Murphy[2]

Departments of Biochemistry and Molecular Biology [H. D., E. L., L. C. M.] and Pathology [P. H. W.], Faculty of Medicine, University of Manitoba, Winnipeg, Manitoba, R3E 0W3 Canada

Abstract

When the level of estrogen receptor (ER)-β mRNA in tumors, determined by reverse transcription-PCR, was assessed according to either ER status or PR status alone, determined by ligand binding assays, the level of ER-β mRNA was significantly lower in PR+ tumors compared with PR− tumors ($P = 0.036$), and no association with ER status was found. Subgroup analysis showed that ER-β mRNA expression in ER+/PR+ breast tumors was significantly less than in ER+/PR− ($P = 0.009$), ER−/PR+ ($P = 0.029$), and ER−/PR− ($P = 0.023$) groups. Interestingly, the ER-β mRNA expression was specifically decreased by progestin in T-47D breast cancer cells. The data suggest the possibility that expression of ER-β in human breast tumors is a marker of endocrine therapy responsiveness.

Introduction

Both estrogen and antiestrogen can mediate transcriptional activity via the recently identified ER[3]-β (1–3). Recently, we have shown the presence of ER-β mRNA in both normal and neoplastic human breast tissues (4, 5). Furthermore, the relative expression of ER-α and ER-β mRNA changes between normal human breast tissues and their concurrent matched ER+ breast tumors (6), suggesting that altered expression of ER-α and ER-β occurs and may be functionally involved in breast tumorigenesis. Interestingly, it also seemed that the level of ER-β mRNA varied among breast tumors but was not correlated with the expression of ER-α (4), although the two receptor mRNAs were often coexpressed in the same tumor. These observations raised the question of whether the expression of ER-β in breast tumors was correlated with known prognostic and endocrine treatment response markers. In this study, the relationship of ER-β mRNA expression to ER and PR status, as determined by ligand binding analysis, was investigated.

Materials and Methods

Materials. All cell culture reagents were obtained from Life Technologies, Inc. (Burlington, Ontario). MPA and dexamethasone were purchased from Sigma Chemical Co. (St. Louis, MO). R5020 and Org 2058 were purchased from Amersham Corp. (Oakville, Canada). RU 486 was a gift from Roussel Uclaf (Romainville, France). [α-^{32}P]dCTP was purchased from ICN (Montreal, Quebec).

Human Breast Tumors. Forty invasive ductal carcinomas were selected from the National Cancer Institute of Canada-Manitoba Breast Tumor Bank (Winnipeg, Manitoba, Canada). The cases were selected for ER and PR status as determined by ligand binding assays. Ten tumors were classified as ER+/PR+ (ER range, 50–127 fmol/mg protein; PR range, 105–285 fmol/mg protein); 10 tumors were classified as ER+/PR− (ER range, 59–156 fmol/mg protein; PR range, 5–10 fmol/mg protein); 10 tumors were ER−/PR− (ER range, 0–2 fmol/mg protein; PR range, 0–10 fmol/mg protein); and 10 tumors were classified as ER−/PR+ (ER range, 5–9 fmol/mg protein; PR range, 51–271 fmol/mg protein). These tumors spanned a wide range of grade (grade 4–9), determined using the Nottingham grading system.

Cell Culture. T-47D human breast cancer cells were obtained from Dr. D. Edwards (University of Colorado, Denver, CO). The cells were grown in DMEM supplemented with 5% fetal bovine serum, 100 nM glutamine, 0.3% (v/v) glucose, and penicillin/streptomycin, as previously described (7). Cells were plated at 1 times 10^6 in 100-mm dishes and 2 days later were treated as indicated in the text. The steroids and other compounds were added directly from 1000 times stock solutions in ethanol to achieve the concentrations indicated. The cells were harvested at the times indicated by scraping with a rubber policeman. After centrifugation, the cell pellet was frozen and stored at −70°C until RNA was isolated.

RNA Extraction and RT-PCR Conditions. Total RNA was extracted from 20-μm frozen tissue sections (5 sections/tumor) or frozen cell pellets using Trizol reagent (Life Technologies, Inc., Grand Island, NY), according to the manufacturer's instructions. Total RNA (1 μg) was reverse transcribed in a final volume of 25 μl, as previously described (4).

The primers used consisted of ER-β-U primer (5′-GTCCATCGCCAGTTATCACATC-3′; sense; located in ER-β 130-151) and ER-β-L primer (5′-GCCTTACATCCTTCACACGA-3′; antisense; located in ER-β 371-352). Nucleotide positions given correspond to published sequences of the human ER-β cDNA (2). PCR amplifications were performed, and PCR products were analyzed as previously described, with minor modifications (4). Briefly, 1 μl of reverse transcription mixture was amplified in a final volume of 15 μl, in the presence of 1.5 μCi [α-^{32}P]dCTP (3000 Ci/mmol), 4 ng/μl ER-β-U/ER-β-L, and 0.3 units of Taq DNA polymerase (Life Technologies, Inc.). Each PCR consisted of 30 cycles (30 s at 94°C, 30 s at 60°C, and 30 s at 72°C). PCR products were then separated on 6% polyacrylamide gels containing 7M urea. After electrophoresis, the gels were dried and autoradiographed. Amplification of the ubiquitously expressed *GAPDH* cDNA was performed in parallel, and PCR products were separated on agarose gels stained with ethidium bromide, as previously described (4). PCR products were subcloned and sequenced, as previously described (4).

Quantification and Statistical Analysis. Quantification of signals was carried out by excision of the band corresponding to ER-β cDNA, addition of scintillant, and scintillation counting. Three independent PCRs were performed. To control for variations between experiments, a value of 100% was assigned to the case exhibiting the highest signal measured, and all signals were expressed as a percentage of this signal. In parallel, *GAPDH* cDNA was amplified and, after analysis of PCR products on prestained agarose gels, signals were quantified by scanning using NIH Image 161/ppc software. Each *GAPDH* signal was also expressed as a percentage of the highest signal observed in the experiment. Two independent PCRs were performed. For each sample, the average of the ER-β signal was then expressed as a percentage of the average *GAPDH* signal. The statistical significance of any differences of

Received 10/30/98; accepted 12/17/98.

The costs of publication of this article were defrayed in part by the payment of page charges. This article must therefore be hereby marked *advertisement* in accordance with 18 U.S.C. Section 1734 solely to indicate this fact.

[1] Supported by grants from the Canadian Breast Cancer Research Initiative and the United States Army Medical Research and Materiel Command (USAMRMC). The Manitoba Breast Tumor Bank is supported by funding from the National Cancer Institute of Canada. L. C. M. is a Medical Research Council of Canada (MRC) Scientist. P. H. W. is a MRC Clinician-Scientist. E. L. is a recipient of a USAMRMC Postdoctoral Fellowship.

[2] To whom requests for reprints should be addressed, at The University of Manitoba, Department of Biochemistry and Molecular Biology, 770 Bannatyne Avenue, Winnipeg, Manitoba, R3E OW3 Canada. Phone: 204-789-3233; Fax: 204-789-3900; E-mail: lcmurph@cc.umanitoba.ca.

[3] The abbreviations used are: ER, estrogen receptor; MPA, medroxyprogesterone acetate; GAPDH, glyceraldehyde-3-phosphate dehydrogenase; PR, progesterone receptor; RT-PCR, reverse transcription-PCR.

the mean ER-β mRNA level between groups was determined using the Mann-Whitney test (two-tailed).

Results

Measurement of ER-β mRNA Expression in Primary Human Breast Tumors with Different ER and PR Status. Previous data have suggested that the level of ER-β mRNA varied widely in human breast tumor samples (4), which raised the question of whether the expression of ER-β in breast tumors was correlated with the known prognostic and treatment response variables, ER and PR status. Four groups, containing 10 breast tumor samples each, were identified according to their ER/PR status, as defined by ligand binding analysis (see "Materials and Methods"). ER-β mRNA levels were measured by RT-PCR and normalized to the *GAPDH* mRNA level, as measured in parallel by RT-PCR. The primers used in this analysis are located in exons 1 and 2 (Fig. 1*A*) of the human *ER-β* gene (2, 8) and would, therefore, measure the wild-type human ER-β mRNA and all ER-β mRNA variants so far documented (5, 9, 10). Examples of the results obtained are shown in Fig. 1*B*. The results obtained for all tumors assayed are shown in Fig. 1*C*, arranged in groups according to the ER/PR status of the tumor, as measured by ligand binding analysis.

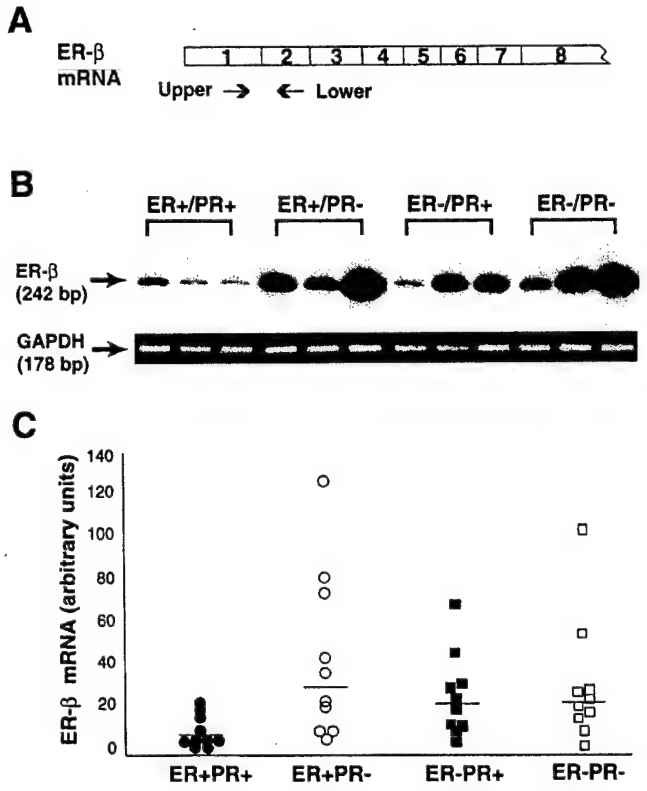

Fig. 1. *A*, schematic diagram of the human ER-β cDNA showing the priming sites of the *upper* and *lower* primers used for the analysis of ER-β mRNA by RT-PCR. *B*, expression of ER-β mRNA in human breast tumor biopsy samples, according to ER and PR status determined by ligand binding assay. *Top*, an autoradiogram of the RT-PCR assays for *ER-β* mRNA obtained from representative samples of tumors that were classified as *ER+/PR+*, *ER+/PR−*, *ER−/PR+*, and *ER−/PR−*, as described in "Materials and Methods." *Bottom*, the ethidium bromide-stained gel of the RT-PCR analysis of *GAPDH* mRNA run in parallel for the same samples. *C*, quantification of ER-β mRNA expression within human breast tumors classified according to ER and PR status, as determined by ligand binding assay. Total RNA, extracted from the tumors, was reverse transcribed, PCR-amplified, and PCR products were separated on acrylamide gel as described in "Materials and Methods." Signals have been quantified and normalized, as indicated in "Materials and Methods." ●, ER+/PR+ tumors; ○, ER+/PR− tumors; ■, ER−/PR+ tumors; □, ER−/PR− tumors. *Horizontal line*, the median value in each group.

Table 1 *Summary of ER-β mRNA levels according to steroid receptor status*

ER/PR status	Number[a]	ER-β mRNA level (mean ± SE)	Statistical significance[b]
A. ER+/PR+	10	11 ± 7.2	
B. ER+/PR−	10	45 ± 12	A *vs.* B, $P = 0.009$
C. ER−/PR+	10	26 ± 6	A *vs.* C, $P = 0.029$
D. ER−/PR−	10	31 ± 9.3	A *vs.* D, $P = 0.023$
E. ER+	20	28 ± 7.2	
F. ER−	20	28 ± 5.4	E *vs.* F, NS
G. PR+	20	19 ± 3.5	
H. PR−	20	38 ± 7.7	G *vs.* H, $P = 0.036$

[a] Number of tumors/group.
[b] Mann-Whitney test (two-tailed).
[c] NS, not significant.

The level of ER-β mRNA in ER+/PR+ breast tumors was significantly less than in all other groups (see Table 1), with no significant differences seen among the ER+/PR−, ER−/PR+, or ER−/PR− groups. When the level of ER-β mRNA in tumors was assessed according to either ER status or PR status alone, as defined by ligand binding analysis, the level of ER-β mRNA was significantly lower in PR+ tumors compared with PR− tumors (Table 1, *G versus H*; $P = 0.036$), with no significant differences associated with ER status alone (Table 1, *E versus F*; $P = 0.323$).

Spearman correlation analysis showed no significant correlations of the level of ER-β mRNA with grade, age, nodal status, or the percentage of normal duct and lobular epithelium, stromal or fat cell content within the tissue section analyzed. However, an inverse relationship was found when the level of ER-β mRNA was correlated with the absolute level of PR, as measured by ligand binding analysis ($r = -0.31$; $P = 0.052$), consistent with the data when analyzed using clinically relevant cut-off values for both ER and PR status as shown above.

Regulation of Steady-state Levels of ER-β mRNA by Progestins in T-47D Human Breast Cancer Cells. The relationship of the level of ER-β mRNA with PR status in human breast tumor biopsies suggested the hypothesis that ER-β expression may be regulated by progestins. This hypothesis was investigated using the PR+ T-47D human breast cancer cell line in culture. The steady-state level of ER-β mRNA was found to decrease after treatment with 10 nM MPA (Fig. 2*A*). A significant decrease was observed at 6 hours after MPA treatment, and the levels remained decreased for up to 48 hours after treatment. The effect of MPA on the steady-state levels of ER-β mRNA in T-47D cells was first seen with 1 nM MPA and was maximal between 10 and 100 nM MPA (Fig. 2*B*). The progestin specificity of this response was assessed by treating T-47D cells for 24 hours with MPA, Org 2058, dexamethasone, and the antiprogestin RU 486 (Fig. 3, *A* and *B*). Both 10 nM MPA and 10 nM of the synthetic progestin Org 2058 significantly decreased the steady-state levels of ER-β mRNA, whereas little, if any, effect was observed with 100 nM of the synthetic glucocorticoid, dexamethasone. Antiprogestin/anti-glucocorticoid RU 486 (500 nM) had little, if any, effect by itself, but inhibited the down-regulation by 10 nM MPA on the level of ER-β mRNA. It was concluded that progestins can down-regulate the steady-state levels of ER-β mRNA and that an antiprogestin can inhibit this effect in T-47D human breast cancer cells.

Discussion

It was previously documented that the level of ER-β mRNA expression in human breast tumors varied widely (4, 8). This raised the question of whether the expression of ER-β in breast tumors was correlated with known prognostic and treatment-response markers. The measurement of both ERs and PRs in human breast biopsies is routinely used to provide both prognostic and treat-

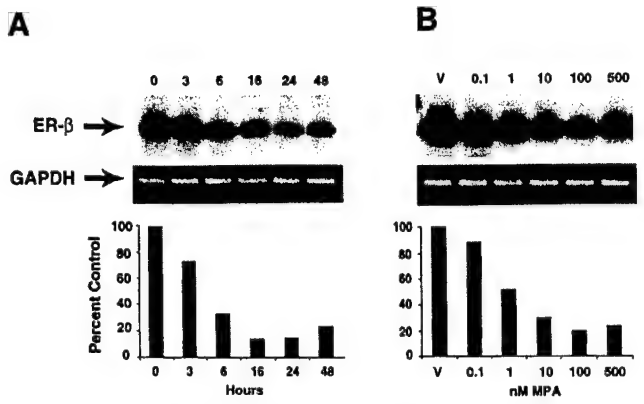

Fig. 2. *A*, time-dependent down-regulation of ER-β mRNA expression in T-47D human breast cancer cells. *Top*, an autoradiogram of *ER-β* mRNA levels determined by RT-PCR after treatment with 10 nM MPA for the indicated time periods. *Middle*, the ethidium bromide-stained gel of the RT-PCR analysis of *GAPDH* mRNA run in parallel for the same samples. *Bottom*, the results presented as a histogram after quantification and normalization of the ER-β signal, as described in "Materials and Methods." This experiment was replicated twice. *B*, dose-dependent down-regulation of ER-β mRNA expression in T-47D human breast cancer cells. *Top*, an autoradiogram of ER-β mRNA levels determined by RT-PCR after treatment with vehicle alone (*V*) and varying concentrations of MPA for 24 h. *Middle*, the ethidium bromide-stained gel of the RT-PCR analysis of *GAPDH* mRNA run in parallel for the same samples. *Bottom*, the results presented as a histogram after quantification and normalization of the ER-β signal, as described in "Materials and Methods."

ment-response information (11). Because ER-β is structurally and functionally related to ER-α (1–3, 12), it was relevant to determine whether the expression of ER-β was related to the ER and PR status of the tumor, as defined by ligand binding assays. Our analysis established that the expression of ER-β mRNA was inversely correlated with PR status generally. Although there was no significant correlation between ER-β mRNA levels and ER status overall, a significant difference in ER-β mRNA levels in those tumors that were ER+/PR+ (lowest expression) and those tumors that were ER−/PR+ (higher expression) was observed. This could be interpreted to mean that both ER status and PR status could influence ER-β mRNA expression. However, the differences observed could also be explained by the significant difference in the absolute level of PR expression between the two groups (PR levels determined by ligand binding assays expressed as mean ± SE, 190 ± 24 fmol/mg protein *versus* 97 ± 21 fmol/mg protein, in ER+/PR+ and ER−/PR+ groups, respectively). This would be consistent with the inverse correlation that was seen with ER-β mRNA and the absolute levels of PR determined by ligand binding analysis, considering all groups together.

These data suggested the possibility that the expression of ER-β may be regulated by progestins. In T-47D cells (which express ER-α, ER-β, and PR), the steady-state level of ER-β mRNA was specifically decreased by progestin treatment in a time- and dose-dependent manner. Our data support the hypothesis that the progestin effect is mediated by PR, however, our data do not address whether this occurs via a transcriptional or post-transcriptional mechanism. Interestingly, progestins are known to also decrease the steady-state levels of ER-α mRNA and protein in T-47D cells (13). Therefore, PR is able to regulate the expression of both ER-α and ER-β in human breast cancer cells in a similar fashion. However, the interaction of PR and the two distinct ERs is likely to be different. It has been well documented that there is a general positive correlation between ER and PR levels, as determined by ligand binding assays in human breast tumors (11). ER status, as determined by ligand binding, correlates well with both immunological detection of the ER-α protein (14) and ER-α mRNA detection (15). Such data together with other studies (6) suggest that the ER level in breast tumors, as determined by ligand binding in most cases, is due to ER-α. Furthermore, ER-β mRNA is the predominant ER mRNA in MDA MB 231 human breast cancer cells (4) and these cells are known to be ER negative by ligand binding assay providing further evidence for the lack of interference of ER-β expression in the determination of ER status by ligand binding assay in the majority of human breast tumors. Interestingly, a significant level of ER-β-like mRNA in human breast cancer cell lines and possibly, therefore, breast tumors may be represented by exon 8 deleted variants (10), which most likely encode nonestrogen binding ER-β variant proteins, which could not contribute to ER ligand binding assays. Therefore, the available data suggest that the previously observed positive correlation of ER and PR in human breast tumors is due to ER-α expression, underscoring the difference in the relationship of ER-α and ER-β with PR in human breast cancer tissue.

Our data are the first to identify a correlation between ER-β mRNA expression and a known prognostic and treatment-response marker in human breast cancer biopsies. The inverse relationship between PR (a good prognostic variable and a marker of response to endocrine therapies) and ER-β suggests that although ER-β is often down-regulated in human breast tumors compared with normal human breast tissue (6), its maintainance and/or increased expression in some breast tumors may correlate with a poorer prognosis and the likelihood of failure of response to endocrine therapies such as antiestrogens. This remains to be tested in samples of breast tumors from patients known to have responded or not to have responded to endocrine therapies, in clinical trials. Furthermore, a functional involvement of ER-β in this phenotype remains to be determined. Interestingly, although no agonist activity of tamoxifen-like antiestrogens can be measured through ER-β in a recombinant expression system using

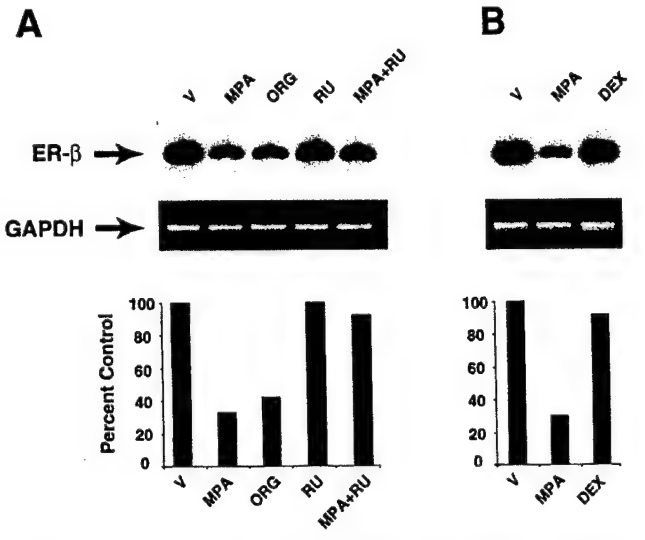

Fig. 3. *A*, steroid specificity of the down-regulation of ER-β mRNA expression in T-47D human breast cancer cells. *Top*, an autoradiogram of *ER-β* mRNA levels determined by RT-PCR after 24 h of treatment with vehicle alone (*V*), 10 nM MPA (MPA), 10 nM Org2058 (*ORG*), 500 nM RU 486 (*RU*), and 10 nM MPA + 500 nM RU 486 (*MPA+RU*). *Middle*, the ethidium bromide-stained gel of the RT-PCR analysis of *GAPDH* mRNA run in parallel for the same samples. *Bottom*, the results presented as a histogram after quantification and normalization of the ER-β signal, as described in "Materials and Methods." This experiment was replicated twice. *B*, steroid specificity of the down-regulation of ER-β mRNA expression in T-47D human breast cancer cells. *Top*, an autoradiogram of ER-β mRNA levels determined by RT-PCR after 24 h of treatment with vehicle alone (*V*), 10 nM MPA (MPA), and 10 nM dexamethasone (*DEX*). *Middle*, the ethidium bromide-stained gel of the RT-PCR analysis of *GAPDH* mRNA run in parallel for the same samples. *Bottom*, the results presented as a histogram after quantification and normalization of the ER-β signal, as described in "Materials and Methods."

transient transfection and a classical ERE-reporter gene (3), all classes of antiestrogens bound to ER-β result in the transcriptional activation of AP-1-driven reporter genes, again in a transient recombinant model system (12). Because AP-1-regulated genes are often associated with growth and proliferation (16–18), it is tempting to speculate that increased expression of ER-β in human breast tumors could play a role in tamoxifen resistance in the small number of tumors that appear to proliferate in response to tamoxifen (19, 20).

Acknowledgments

We thank Caroline Cumins-Leygue and Helen Bergen for laboratory assistance with the cell culture.

References

1. Kuiper, G., Enmark, E., Pelto-Huikko, M., Nilsson, S., and Gustafsson, J-A. Cloning of a novel estrogen receptor expressed in rat prostate and ovary. Proc. Natl. Acad. Sci. USA, *93:* 5925–5930, 1996.
2. Mosselman, S., Polman, J., and Dijkema, R. ER-β: identification and characterization of a novel human estrogen receptor. FEBS Lett., *392:* 49–53, 1996.
3. Tremblay, G., Tremblay, A., Copeland, N., Gilbert, D., Jenkins, N., Labrie, F., and Giguere, V. Cloning, chromosomal localization, and functional analysis of the murine estrogen receptor β. Mol. Endocrinol., *11:* 353–365, 1997.
4. Dotzlaw, H., Leygue, E., Watson, P., and Murphy, L. Expression of estrogen receptor-β in human breast tumors. J. Clin. Endocrinol. Metab., *82:* 2371–2374, 1997.
5. Lu, B., Leygue, E., Dotzlaw, H., Murphy, L. J., Murphy, L. C., and Watson, P. H. Estrogen receptor-β mRNA variants in human and murine tissues. Mol. Cell. Endocrinol., *138:* 199–203, 1998.
6. Leygue, E., Dotzlaw, H., Watson, P., and Murphy, L. Altered estrogen receptor α and β mRNA expression during human breast tumorigenesis. Cancer Res., *58:* 3197–3201, 1998.
7. Alkhalaf, M., and Murphy, L. C. Regulation of c-jun and jun-B by progestins in T-47D human breast cancer cells. Mol. Endocrinol., *6:* 1625–1633, 1992.
8. Enmark, E., Pelto-Huikko, M., Grandien, K., Lagercrantz, S., Lagercrantz, J., Fried, G., Nordenskjold, M., and Gustafsson, J-A. Human estrogen receptor β gene structure, chromosomal localization and expression pattern. J. Clin. Endocrinol. Metab., *82:* 4258–4265, 1997.
9. Vladusic, E., Hornby, A., Guerra-Vladusic, F., and Lupu, R. Expression of estrogen receptor β messenger RNA variant in breast cancer. Cancer Res., *58:* 210–214, 1998.
10. Moore, J., McKee, D., Slentz-Kesler, K., Moore, L., Jones, S., Horne, E., Su, J-L., Kliewer, S., Lehmann, J., and Wilson, T. Cloning and characterization of human estrogen receptor β isoforms. Biochem. Biophys. Res. Commun., *247:* 75–78, 1998.
11. Ravdin, P., Green, S., Dorr, T., McGuire, W., Fabian, C., Pugh, R., Carter, R., Rivkin, S., Borst, J., Belt, R., Metch, B., and Osborne, C. Prognostic significance of progesterone receptor levels in estrogen receptor-positive patients with metastatic breast cancer treated with tamoxifen: results of a prospective Southwest Oncology Group study. J. Clin. Oncol., *10:* 1284–1291, 1992.
12. Paech, K., Webb, P., Kuiper, G., Nilsson, S., Gustafsson, J., angst, Kushner, P. J., and Scanlan, T. S. Differential ligand activation of estrogen receptors ERα and ERβ at AP1 sites. Science (Washington DC) *277:* 1508–1510, 1997.
13. Read, L., Greene, G., and Katzenellenbogen, B. Regulation of estrogen receptor messenger ribonucleic acid and protein levels in human breast cancer cell lines by sex steroid hormones, their antagonists and growth factors. Mol. Endocrinol., *3:* 295–304, 1989.
14. McClelland, R., Berger, U., Miller, L., Powles, T., and Coombes, R. Immunocytochemical assay for estrogen receptor in patients with breast cancer: relationship to biochemical assay and outcome of therapy. J. Clin. Oncol., *4:* 1171–1176, 1986.
15. May, E., Mouriesse, H., May-Leven, F., Contesso, G., and Delarue, J. A new approach allowing an early prognosis in breast cancer: the ratio of estrogen receptor (ER) ligand binding activity to the ER-specific mRNA level. Oncogene, *4:* 1037–1042, 1989.
16. Umayahara, Y., Kawamori, R., Watada, H., Imano, E., Iwama, N., Morishima, T., Yamasaki, Y., Kajimoto, Y., and Kamada, T. Estrogen regulation of the insulin-like growth factor I gene transcription involves an AP-1 enhancer. J. Biol. Chem., *269:* 16433–16442, 1994.
17. Weisz, A., and Bresciani, F. Estrogen regulation of proto-oncogenes coding for nuclear proteins. Crit. Rev. Oncog., *4:* 361–388, 1993.
18. Piechaczyk, M., and Blanchard, J. c-fos protooncogene regulation and function. Crit. Rev. Oncol. Hematol., *17:* 93–131, 1994.
19. Howell, A., Dodwell, D., Anderson, H., and Redford, J. Response after withdrawal of tamoxifen and progestogens in advanced breast cancer. Ann. Oncol., *3:* 611–617, 1992.
20. Howell, A., Defriend, D., Robertson, J., Blamey, R., and Walton, P. Response to a specific antioestrogen (ICI182780) in tamoxifen resistant breast cancer. Lancet, *345:* 29–30, 1995.

[CANCER RESEARCH 59, 1175–1179, March 15, 1999]

Advances in Brief

Expression of Estrogen Receptor β1, β2, and β5 Messenger RNAs in Human Breast Tissue[1]

Etienne Leygue,[2] Helmut Dotzlaw, Peter H. Watson, and Leigh C. Murphy

Departments of Biochemistry and Molecular Biology [E. L., H. D., L. C. M.] and Pathology [P. H. W.], University of Manitoba, Faculty of Medicine, Winnipeg, Manitoba R3E OW3, Canada

Abstract

A triple-primer PCR assay was developed, based on the coamplification of estrogen receptor (ER)-β1, -β2, and -β5 cDNAs, to investigate the relative expressions of the corresponding mRNAs in breast cancer lines and in 53 independent breast tumors. The expression of ER-β2 and ER-β5 mRNAs was higher than that of ER-β1 mRNA in both cancer cell lines and breast tumors. In breast tumors, increases in the ER-β2:ER-β1 and ER-β5:ER-β1 mRNA expression ratios were observed, which positively correlated with the level of tumor inflammation and tumor grade, respectively. A trend toward an increase of these ratios was also found in tumors, as compared to the normal adjacent breast tissue available for 13 cases. Our data suggest that changes in the relative expression of ER-β1, -β2, and -β5 mRNAs occur during breast tumorigenesis and tumor progression.

Introduction

Estrogens regulate the growth and development of normal human mammary tissue and are also involved in breast tumor progression (1). Indeed, estrogens are thought to promote the growth of breast tumors through their mitogenic effects on breast cancer cells. The ability of antiestrogens such as tamoxifen or raloxifene to inhibit estrogenic action provides the basic rationale for the use of endocrine therapies. Estrogen action is believed to be mediated mainly through two ERs[3]: ER-α (2) and ER-β1 (3, 4). These two receptors, which are encoded by two different mRNAs containing eight exons each (5, 6), belong to the steroid/thyroid/retinoic acid receptor superfamily (7). ER-α and ER-β1 share the same structural and functional domain composition (8), defined as region A–F (Fig. 1*A*). The A–B regions contain the NH_2-terminal transactivation function (AF-1) of the receptors, whereas the C region of the molecule contains the DNA binding domain. The ligand binding domain and the second transactivation function (AF-2) are located within the E region of the receptors. The receptors, once bound to the ligand, are subject to conformational changes that result in complexes containing dimers of receptors/hormones that recognize estrogen-responsive elements located upstream of target genes. Interactions between ERs and accessory proteins ultimately lead to the modification of the transcription of these genes (9). The ER-ligand complexes can also interact with c-*fos*/c-*jun* complexes to modify the transcription of target genes through AP1 enhancer elements (10, 11). Differential activation of ER-α and ER-β1 by the antiestrogen 4-hydroxytamoxifen, determined by activation of estrogen response element-regulated reporter genes, and differential activation of AP1-regulated reporter genes by the two ERs have been observed (11, 12). Also, because heterodimerization of ER-α and ER-β1 has also been shown, putative cross-talk between the two signaling pathways is possible (4, 13).

Several variant forms of ER-α and ER-β1 mRNAs have been identified (for reviews see Refs. 14–17). Among them, exon-deleted variant mRNAs, which would encode ER-like proteins missing some of the functional domains of the wild-type receptors, could interfere with ER-α and/or ER-β1 signaling pathways. Indeed, exon 5- and exon 7-deleted ER-α variant proteins have been shown, *in vitro*, to exhibit a constitutive transcriptional (18) and a dominant negative activity (19) on ER-α, respectively. More recently, an ER-β2 variant, deleted of regions encoded by ER-β1 exon 8 sequences, has been shown to heterodimerize with both ER-β1 and ER-α and to inhibit ER-α DNA binding capability (20, 21). The ability of ER-α variants to potentially interfere with the ER-α signaling pathways raised the question of their possible involvement in mechanisms underlying breast tumorigenesis and tumor progression. Although much data have been published documenting the differential expression of ER-α variants at different stages of breast cancer progression (14), no studies have been performed comparing the relative expression of ER-β variant mRNAs in human breast tissue. We have developed a TP-PCR assay to evaluate the relative expression of ER-β1, -β2, -β4, and ER-β5 variant mRNAs. As shown in Fig. 1*A*, ER-β2, -β4, and -β5 variant mRNAs do not contain exon 8 ER-β1 sequences but share similar 3′ end sequences. This assay was used to evaluate the relative expression of ER-β1, -β2, and -β5 mRNA within breast tumors ($n = 53$) and, in some cases ($n = 13$), within adjacent normal breast tissue.

Materials and Methods

Human Breast Tissues and Tumor Cell Lines. Fifty-three cases were selected from the National Cancer Institute of Canada-Manitoba Breast Tumor Bank (Winnipeg, Manitoba, Canada). As reported previously, all cases in the bank have been processed to provide paraffin-embedded tissue blocks and mirror-image frozen tissue blocks (22). Histopathological analysis was performed on H&E-stained sections from the paraffin tissue block to estimate, for each case, the proportions of tumor and normal epithelial cells, fibroblasts, and fat as well as to determine the levels of inflammation and Nottingham grade scores (23). The age of the patients ranged between 39 and 87 years ($n = 53$, median = 67 years). Tumors spanned a wide range of ER (from 0 to 159 fmol/mg protein, $n = 53$, median = 9 fmol/mg protein) and PR (ranging from 0 to 285 fmol/mg protein, $n = 53$, median = 10 fmol/mg protein) levels, as measured by ligand binding assay. These tumors also covered a wide spectrum of grades (Nottingham grading scores from 1 to 9, $n = 47$, median = 7). Inflammation levels were assessed for 51 cases by scoring the extent of lympho-histocystic infiltrates throughout the section using a semiquantitative scale from 0 (low to minimal infiltration) to 5 (marked infiltrate). For 13 cases, matched adjacent normal tissue blocks were also available. The characteristics of this subset of 13 tumors were as follows: ER status ranged from 0 to 159 fmol/mg protein (median = 3.5 fmol/mg protein), PR status ranged from 4.9 to 134 fmol/mg protein (median = 8.5), Nottingham grade scores ranged from 5 to 9 (median = 7), inflammation levels ranged from 1 to 5 (median = 3), and patients were between 39 and 75 years old (median age = 54 years).

MDA-MB-231, MDA-MB-468, ZR-75, BT-20, T-47D, and MCF-7 breast

Received 12/21/98; accepted 1/27/99.

The costs of publication of this article were defrayed in part by the payment of page charges. This article must therefore be hereby marked *advertisement* in accordance with 18 U.S.C. Section 1734 solely to indicate this fact.

[1] This work was supported by grants from the Canadian Breast Cancer Research Initiative and United States Army Medical Research and Materiel Command Grant DAMD17-95-1-5015. The Manitoba Breast Tumor Bank is supported by funding from the National Cancer Institute of Canada. P. H. W. is a Medical Research Council of Canada Clinician-Scientist, L. C. M. is an Medical Research Council Scientist, and E. L. is a recipient of a United States Medical Research and Materiel Command Postdoctoral Fellowship (Grant DAMD17-96-1-6114).

[2] To whom requests for reprints should be addressed, at Department of Biochemistry and Molecular Biology, University of Manitoba, Winnipeg, Manitoba, R3E OW3, Canada. Phone: (204) 789-3812; Fax: (204) 789-3900; E-mail: eleygue@cc.umanitoba.ca.

[3] The abbreviations used are: ER, estrogen receptor; TP-PCR, triple-primer PCR; PR, progesterone receptor.

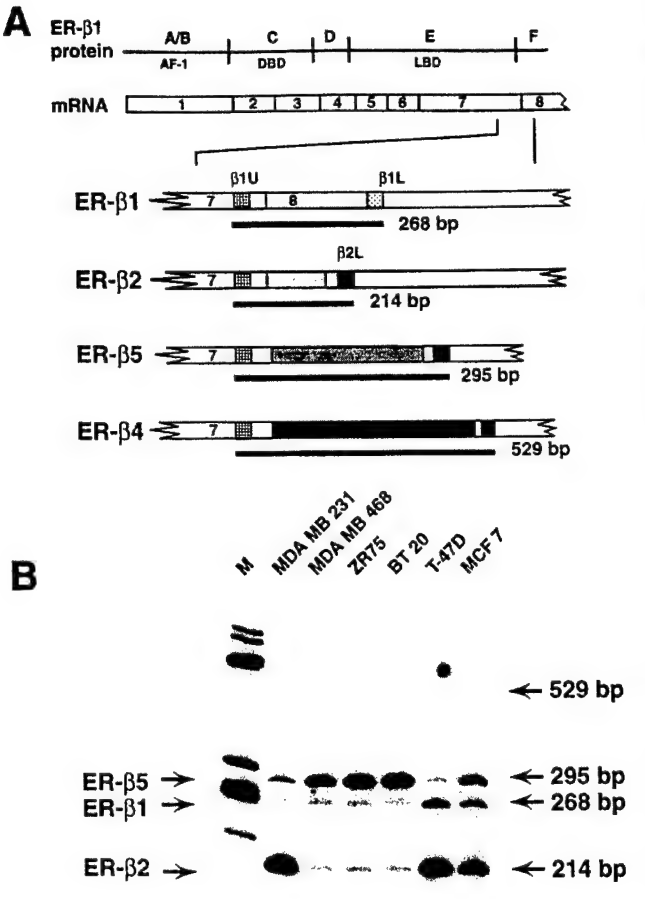

Fig. 1. Presentation of the TP-PCR assay and relative expression of ER-β1, -β2, -β4, and ER-β5 mRNAs in breast cancer cell lines. *A*, structural and functional domains (AF) of the ER-β1 protein (*AF-1*, transactivation function 1; *DBD* and *LBD*, DNA and ligand binding domains, respectively) are shown together with the corresponding exonic structure (*exons 1–8*) of the ER-β1 mRNA. Common sequences (□) and specific sequences (□) are depicted for each cDNA (β1, β2, β4, and β5). ER-β1U (■), ER-β1L (□), and ER-β2L (■) primer annealing sites are also represented. The sizes of the possible PCR products (*black bars*) obtained after TP-PCR are indicated. *B*, breast cancer cell line (MDA-MB-231, MDA-MB-468, ZR-75, BT-20 T-47D, and MCF-7) poly(A) mRNAs were reverse-transcribed, TP-PCR was performed, and PCR products were separated on an acrylamide gel, as described in "Materials and Methods." PCR products migrating at apparent sizes of 295, 268, and 214 bp have been subcloned, sequenced, and identified as corresponding to ER-β5, -β1, and -β2 mRNAs, respectively. *Lane M*, molecular size markers (φx174 RF DNA/Hae III fragments; Life Technologies, Inc.).

cancer cells were grown and poly(A) mRNA was obtained as described previously (24). Total RNA was extracted from frozen breast tissue sections using Trizol reagent (Life Technologies, Inc., Grand Island, NY) according to the manufacturer's instructions, and quantified spectrophotometrically. One μg of total RNA was reverse-transcribed in a final volume of 25 μl as described previously (25).

Primers and PCR Conditions. The primers used consisted of ER-β1U primer (5′-CGATGCTTTGGTTTGGGTGAT-3′; sense, located in exon 7, positions 1400–1420, GenBank accession no. AB006590), ER-β1L primer (5′-GCCCTCTTTGCTTTTACTGTC-3′; antisense, located in exon 8, positions 1667–1648, GenBank accession no. AB006590), and ER-β2L (5′-CTTTAGGCCACCGAGTTGATT-3′; antisense, located in ER-β2 extrasequences, positions 1933–1913, GenBank accession no. AF051428). PCR amplifications were performed, and PCR products were analyzed as described previously, with minor modifications (25). Briefly, 1 μl of reverse transcription mixture was amplified in a final volume of 15 μl, in the presence of 1 μCi of [α-^{32}P]dCTP (3000 Ci/mmol), 4 ng/μl each primer (ER-β1U, ER-β1L, and ER-β2L), and 0.3 unit of Taq DNA polymerase (Life Technologies, Inc.). Each PCR consisted of 30 cycles (30 s at 60°C, 30 s at 72°C, and 30 s at 94°C). PCR products were then separated on 6% polyacrylamide gels containing 7 M urea. Following electrophoresis, the gels were dried and autoradiographed. Amplification of the ubiquitously expressed *glyceraldehyde-3-phosphate dehydrogenase* cDNA was performed in parallel, and PCR products, separated on agarose gels, were stained with ethidium bromide as described previously (25). Identity of PCR products was confirmed by subcloning and sequencing, as reported previously (25).

TP-PCR Validation. The first series of experiments, performed using cDNAs prepared from breast cancer cell line mRNA, showed that ER-β1, -β2, and -β5 cDNAs can be coamplified, and they led to the production of three PCR products that were subcloned and sequenced as described previously (25). Spiked cDNA preparations containing 1 fg of purified PCR products, corresponding to ER-β1 and -β5 mRNAs, were amplified together with increasing amounts of ER-β2 PCR product (0, 0.2, 0.4, 1, 4, and 8 fg) in a single PCR tube using the three primers (ER-β1U, ER-β1L, and ER-β2L), as described above. Similar experiments were performed using constant amounts of ER-β1 and ER-β2 or of ER-β2 and ER-β5, with increasing amounts of ER-β5 or ER-β1 PCR products, respectively. In parallel, preparations containing 1 fg of each PCR product alone were also amplified. In every case, PCR products were separated on 6% polyacrylamide gels containing 7 M urea. Following electrophoresis, the gels were dried and autoradiographed. Signals were quantified by excision of the appropriate bands and counting in a scintillation counter (Beckman). For each sample, ER-β1, -β2, and -β5 signals were expressed as a percentage of the sum of all signals measured (ER-β1 + ER-β2 + ER-β5 signals). Experiments have been performed in duplicate and the mean of the relative signals calculated. For each ER-β isoform, regression analyses between the relative signal obtained and the relative initial input (*i.e.*, ER-β isoform input expressed as a percentage of ER-β1 + ER-β2 + ER-β5 input) were performed using GraphPad Prism software.

Quantification and Statistical Analyses. To quantitate the relative expression of ER-β1, -β2, and -β5 mRNAs within each breast tissue sample, we used the TP-PCR described above. Quantification of ER-β1, -β2, and -β5 signals was carried out by excision of the bands and scintillation counting. For each sample, ER-β1, -β2, and -β5 signals were expressed as a percentage of the sum of all signals measured (ER-β1 + ER-β2 + ER-β5 signals). Three independent PCRs were performed and the mean of the relative expressions was calculated. Differences between ER-β1, -β2 and -β5 relative expression within the cohort studied were tested using the Wilcoxon signed rank test (two-tailed). Correlations with tumor characteristics were tested by calculation of the Spearman coefficient (r).

Results

Validation of TP-PCR as an Approach to Evaluate the Relative Expression of ER-β1, -β2, and -β5 mRNAs. We established previously that TP-PCR provided a reliable method to investigate the expression of a truncated mRNA relative to the wild-type mRNA expression within small breast tissue samples (25). In its initial design, the TP-PCR assay relied on the coamplification of one truncated and a wild-type cDNA molecule using three primers in the PCR. The upper primer recognized both sequences, whereas the two lower primers recognized the variant and the wild-type sequences, respectively. We have shown that the final ratio between the two coamplified products was linearly related to the initial cDNA input (25).

As shown Fig. 1*A*, ER-β1, -β2, -β4, and -β5 mRNAs all have exon 7 sequences but differ from each other in the following sequences. Interestingly, comparison of the sequences revealed that ER-β2, -β4, and -β5 mRNAs have sequence similarities within their 3′ extremities. Therefore, it was possible to use TP-PCR to investigate the relative expression of these variants. Three primers were designed (ER-β1U, ER-β1L, and ER-β2L) that recognized exon 7 sequences common to all transcripts, ER-β1 exon 8-specific sequences, and sequences shared by ER-β2, -β4, and ER-β5 mRNAs, respectively (Fig. 1*A*). As shown in Fig. 1*A*, the expected PCR products resulting from the coamplification of the corresponding cDNAs are different in size and can be easily distinguished on an acrylamide gel.

The assay was used initially to determine the expression of ER-β1, -β2, -β4, and -β5 mRNAs in several different human breast cancer cell lines (Fig. 1*B*). Three bands migrating at apparent sizes of 268, 214, and 295 bp were observed in all samples. Subcloning and

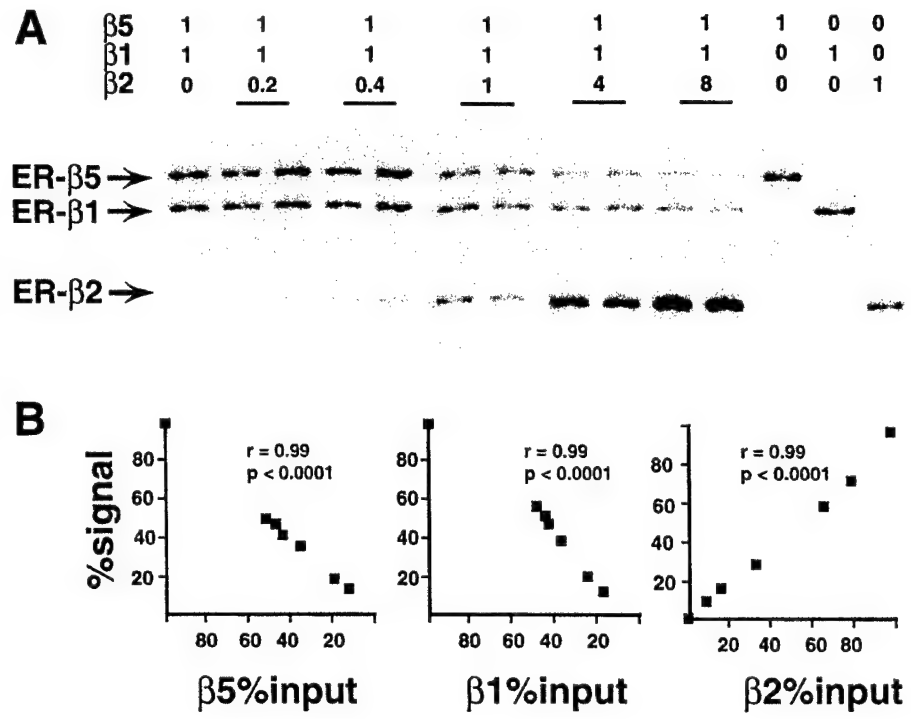

Fig. 2. TP-PCR validation. *A*, spiked cDNA preparations, containing various amounts [indicated *above* the autoradiogram] of ER-β5, -β1, and -β2 purified PCR products (β5, β1, and β2) were amplified by TP-PCR, and PCR products were separated on an acrylamide gel, as specified in "Materials and Methods." The autoradiogram shows the PCR products obtained. *B*, signals corresponding to ER-β5, -β1, and -β2 PCR products have been quantified in each lane, as described in "Materials and Methods." For each ER-β isoform, the relative signal observed (percentage signal, expressed as a percentage of the sum: β1 + β2 + β5 signals) is presented as a function of the initial relative cDNA input (percentage input, expressed as a percentage of the sum: β1 + β2 + β5 inputs). The regression coefficient (*r*) and *P* of the associations are also presented.

sequencing of these bands confirmed their identity as ER-β1, -β2, and -β5 cDNAs, respectively (data not shown). We were unable to detect a product of 529 bp, which would correspond to the ER-β4 PCR product. Interestingly, in all tumor cell lines, the ER-β1 signal was lower than the ER-β2 and/or ER-β5 signals (Fig. 1*B*).

Because TP-PCR performed using these primers produced three PCR products, instead of the two PCR products obtained in the original published validation studies (25), it was necessary to establish the quantitative relationship between the signals obtained and the initial target concentrations. To address this issue, spiked DNA preparations containing equal amounts of ER-β1 and ER-β5 PCR products and increasing amounts of ER-β2 PCR products were amplified (Fig. 2*A*). The relative signals of ER-β1, -β2, and -β5 have been measured and expressed as a percentage of the sum of the signals measured, as described in "Materials and Methods." As expected, in the absence of ER-β2, only two bands, corresponding to ER-β1 and ER-β5 PCR products, are observed. The relative signals of ER-β1 and ER-β5 decreased, whereas the ER-β2 relative signal increased linearly with increasing ER-β2 input. Indeed, for each ER-β isoform, regression analysis showed a linear correlation between the relative signal of the PCR product measured and its relative input (Fig. 2*B*). Similar results were obtained when experiments were performed using constant amounts of ER-β1 and ER-β2 with increasing amounts of ER-β5 PCR products or using constant amounts of ER-β2 and ER-β5 with increasing amounts of ER-β1 (data not shown). It should be noted that the amplification of similar amounts of the three molecules led to the production of three bands of similar intensities (Fig. 2*A*). It should also be stressed that the ER-β5:ER-β1 ratio was not affected by increasing amounts of ER-β2 and that the ER-β2:ER-β5 and ER-β5:ER-β2 ratios varied as a linear function of the initial ER-β2:ER-β5 and ER-β5:ER-β2 input ratios, respectively (data not shown). We concluded that the TP-PCR assay, performed under the described conditions, provided a reliable method with which to compare breast tissue samples for their relative expression of ER-β1, -β2, and -β5 mRNAs.

Comparison of the Relative Expression of ER-β1, -β2, and -β5 mRNAs in Breast Tumor Tissues. To determine whether alterations occur in the balance between ER-β1, -β2, and -β5 mRNAs during breast tumor progression, the relative expression of these transcripts was measured in primary breast tumor tissues from 53 different patients, using the TP-PCR assay described above. These tumors presented a wide spectrum of ER and PR statuses, as determined by ligand binding assay, and also spanned a wide range of grades and inflammation levels (for a more detailed description of the cohort characteristics, see "Materials and Methods"). Total RNA was extracted from frozen tissue sections and reverse-transcribed as described in "Materials and Methods." TP-PCR was then performed. Examples of the results obtained are shown in Fig. 3*A*. Three PCR products migrating at apparent sizes of 268, 214, and 295 bp were obtained. These PCR products were shown by cloning and sequencing to correspond to ER-β1, -β2, and ER-β5 cDNAs, respectively. As in our preliminary study performed in human breast cancer cell lines, no band of 529 bp was detected, which would correspond to ER-β4 PCR product. Amplification of the ubiquitously expressed *glyceraldehyde-3-phosphate dehydrogenase* cDNA, performed to check the integrity of each cDNA studied, revealed similar amounts of cDNA in all samples (data not shown). ER-β1, -β2, and -β5 signals obtained in three independent TP-PCRs were quantified as described in "Materials and Methods." For each sample, the percentage of each band relative to the sum of the signals obtained has been calculated. The medians of ER-β1, -β2, and -β5 relative expression within tumors, sorted according to their grade or to the level of inflammation, are presented in Fig. 3*B*. The ER-β1 relative signal was found to be significantly lower than ER-β2 (Wilcoxon sign rank test, $n = 53$, $P = 0.0002$) and ER-β5 (Wilcoxon sign rank test, $n = 53$, $P = 0.004$) signals. A trend toward a higher expression of ER-β2 as compared to ER-β5 was also observed but did not reach statistical significance (Wilcoxon sign rank test, $n = 53$, $P = 0.09$).

Possible associations between ER-β1, -β2, or -β5 signals and tumor characteristics were then investigated. ER-β1 relative expression was found (Fig. 3*B*) to be inversely related to the grade of the tumor ($n = 47$, Spearman $r = -0.33$, $P = 0.02$) and the level of inflammation ($n = 51$, Spearman $r = -0.28$, $P = 0.04$). No other associations were found between ER-β1 expression and ER status, PR status, or age of the patients. ER-β2 mRNA expression increased

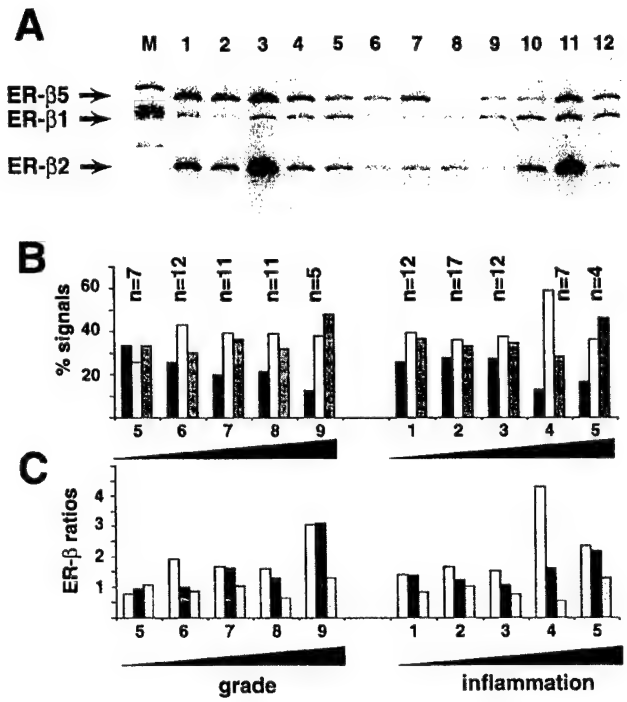

Fig. 3. TP-PCR analysis of the relative expression of ER-β1, -β2, and -β5 mRNAs within a cohort of 53 independent breast tumors. Total RNA was extracted from 53 breast tumors, reverse-transcribed, and analyzed by TP-PCR, as described in "Materials and Methods." PCR products were separated on acrylamide gels. *A*, autoradiogram showing the results obtained for 12 cases (*Lanes 1–12*). *Lane M*, molecular weight marker ϕx174 RF DNA/*Hae*III fragments. *B*, ER-β1, -β2, and -β5 signals have been quantified and expressed relatively to the sum of the signals obtained, as described in "Materials and Methods." Tumors have been sorted according to their Nottingham grade scores (*5–9*) or to their levels of inflammation (*1–5*). For each group, the number of patients (*n*) and the medians of the relative expression of ER-β1 (■), -β2 (□), and -β5 (▦) signals are indicated. *C*, for each group, the number of patients (*n*) and the median of ER-β2:ER-β1 (□), ER-β5:ER-β1 (■) and ER-β5:ER-β2 (□) signal ratios are indicated.

significantly with the levels of inflammation (n = 52, Spearman r = 0.28, P = 0.04). No other associations were found between ER-β2 and ER-β5 and other characteristics.

Because the ratio between two signals was related to the respective proportion of the two corresponding cDNAs, we also addressed the question of the expression of ER-β2 and ER-β5 relative to ER-β1. The medians of the ER-β2:ER-β1, ER-β5:ER-β1, and ER-β5:ER-β2 ratios within tumors, sorted according to their grade or to the level of inflammation, are presented in Fig. 3*C*. ER-β5 and ER-β2 expression relative to ER-β1 were found positively associated with the tumor grade (n = 47; Spearman r = 0.29, P = 0.04; and Spearman r = 0.28, P = 0.05, respectively). In addition, one should note that ER-β2 expression relative to ER-β1 expression correlated (n = 52, Spearman r = 0.34, P = 0.01) with levels of inflammation. ER-β2 and ER-β5 expression relative to each other did not correlate with grade, degree of inflammation, or any other tumor characteristics. No correlations were found between the content of the tissue sections analyzed, *i.e.*, percentage of normal cells, tumor cells, fibroblasts, or fat, and ER-β1, -β2, and -β5 mRNA relative expression (data not shown).

ER-β1, -β2, and -β5 mRNA Expression within Matched Normal and Tumor Compartments. To determine whether changes in the expression of ER-β1, -β2, and -β5 mRNAs occur during breast tumorigenesis, we compared the relative expression of these transcripts between normal breast tissue and matched adjacent tumors. Normal adjacent breast tissue was available for 13 cases belonging to the cohort described earlier in the text. The characteristics of this tumor subset are detailed in "Materials and Methods." Total RNA was extracted, and following reverse transcription, TP-PCR was performed as described in "Materials and Methods." Typical results are shown in Fig. 4*A*. Quantification of the signals was performed as described above. Fig. 4*B* shows the relative expression within tumor and adjacent normal breast tissues of ER-β1 mRNA. A trend toward a lower ER-β1 signal (9 of 13 cases, Wilcoxon sign rank test, P = 0.06) in the tumor compartment compared to the normal adjacent components was observed. In contrast, trends toward higher expression of ER-β2 (Fig. 4*C*) and ER-β5 (Fig. 4*D*) mRNAs relative to ER-β1 mRNA were observed in tumor compartments (8 of 13 cases, Wilcoxon sign rank test, P = 0.10; and 9 of 13 cases, Wilcoxon sign rank test, P = 0.06, respectively).

Discussion

To evaluate the relative expression of ER-β1, -β2, and -β5 mRNAs within small frozen sections of human breast tissues, we have developed an assay based on the coamplification of the corresponding cDNAs in a single tube, using three primers in the PCR. The quantitative aspect of this assay was validated using preparations containing known amounts of target cDNA. The TP-PCR approach appeared to be a reliable approach to estimate not only the relative expression of each variant within the population of ER-β molecules measured (*i.e.*, ER-β1, -β2, and ER-β5 mRNAs) but also the proportion of each

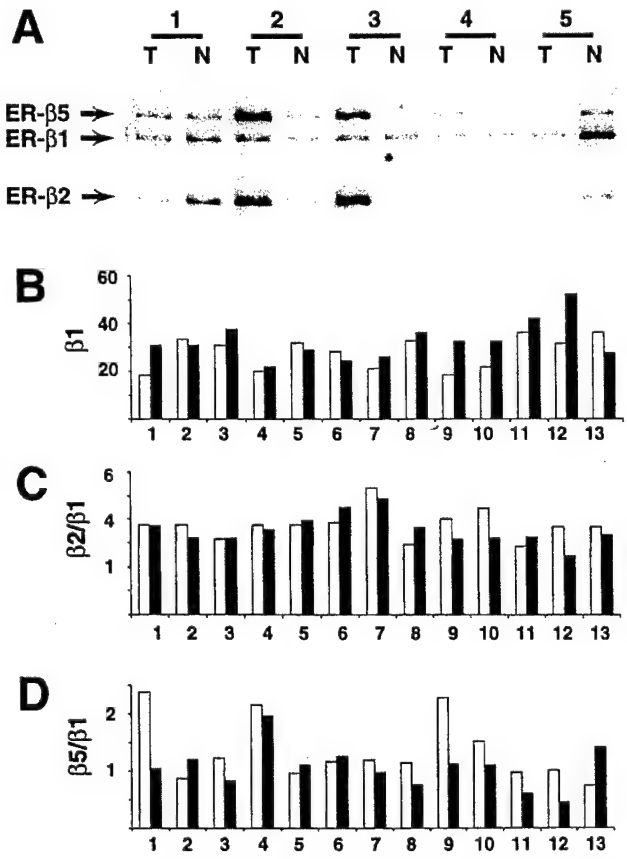

Fig. 4. TP-PCR analysis of the relative expression of ER-β1, -β2, and -β5 mRNAs within matched normal and tumor compartments of human breast tumors. Total RNA was extracted from 13 breast tumors (*Lanes T*) and adjacent normal breast tissues (*Lanes N*), reverse transcribed and analyzed by TP-PCR as described in "Materials and Methods." PCR products were separated on acrylamide gels. *A*, autoradiogram showing the results obtained for five cases (*1–5*). *B*, ER-β1, -β2, and -β5 signals have been quantified and expressed relatively to the sum of the signals obtained, as described in "Materials and Methods." For each case (*1–13*), the relative percentages of ER-β1 in tumor (□) and normal (■) components are shown. *C*, for each case (*1–13*), the ER-β2:ER-β1 ratios in tumor (□) and normal (■) components are shown. *D*, for each case (*1–13*), the ER-β5: ER-β1 ratios in tumor (□) and normal (■) components are shown.

RNA relative to one another. One should note that the set of primers used would detect ER-β4 variant mRNA. However, this variant was not detected in any breast sample or tumor cell line studied. This might result from either a lower efficiency of amplification of this specific variant in our PCR conditions or a lower relative expression of ER-β4 mRNA as compared to ER-β1, -β2, and -β5. A low expression of ER-β4 mRNA would be consistent with data obtained on breast cancer cell lines by Moore *et al.* (20).

Our data show that ER-β1, -β2, and -β5 mRNAs are coexpressed in human breast cancer cells grown in culture. These data confirm the previous observation of Moore *et al.* (20). These authors however, did not address the question of the relative expression of these mRNAs. Striking differences in the pattern of expression of ER-β1, -β2, and -β5 mRNAs were found between breast cancer cell lines. If these differences in expression are conserved at the protein level, one might hypothesize that ER-β signaling pathways, which likely result from the balance between the different forms, vary in these cells. To date, multiple ER-β-like mRNAs that could encode different proteins that would be difficult to distinguish from each other by Western blot analysis have been described. For example, ER-β1 protein (5) and ER-β2 protein (20) have theoretical molecular masses of 54.2 kDa and 55.5 kDa, respectively. Most likely, antibodies specifically recognizing the different ER-β proteins would be the best approach to address the question of the relative expression of ER-β proteins within breast cancer cells. Higher ER-β2 and ER-β5 expression as compared to ER-β1 expression was observed in breast cancer cell lines. This suggests that the respective participation of ER-β2 and ER-β5 variants in ER-β signaling pathways within breast cancer cells might be as significant as or more significant than that of ER-β1.

As observed in breast cancer cell lines, ER-β1, -β2, and -β5 mRNAs were detected in human breast tumors. Consistent with the observations in breast cancer cell lines, ER-β2 and ER-β5 mRNAs were more highly expressed than ER-β1 mRNA in these tissues. However, even though this observation may result directly from the expression of different ER-β isoforms in breast cancer cells, it may also be a consequence of the heterogeneity of the cell populations expressing ER-β molecules and present in different proportions within the tumor sample analyzed. Indeed, because lymphocytes have previously been shown to express ER-β1, -β2, and -β5 mRNAs, one could speculate that infiltrating lymphocytes within the tumor might contribute to the higher level of ER-β2 mRNA expression in tumors with higher inflammation levels. Techniques such as *in situ* hybridization or immunocytochemistry, designed to distinguish between the different ER-β isoforms, are needed to address the question of the cellular origin of ER-β isoform expressions *in vivo*.

We observed an inverse relationship between the relative expression of ER-β1 mRNA and tumor grade. It has been shown that the Nottingham grade provides a useful marker of the length of disease free interval and overall survival (23). We have also observed a decrease of the relative expression of ER-β1 in tumor *versus* normal adjacent components. Taken together, these data suggest that changes in the relative expression of ER-β1, -β2, and -β5 mRNAs occur during breast tumorigenesis and tumor progression. Whether these changes are a cause or a consequence of tumorigenesis remains to be elucidated.

In conclusion, we have developed a TP-PCR assay allowing the investigation of the relative expression of ER-β1, -β2, and -β5 mRNA in human breast tissues. In these tissues, ER-β1 mRNA appeared to have the lowest level of expression when compared to the two other isoforms detected. We found that the relative expression of ER-β1 was inversely related to the grade of the tumor, suggesting that it could be used as a marker of tumor progression. Moreover, a lower relative expression of ER-β1 was observed in tumor *versus* adjacent normal breast tissues, suggesting that changes in the expression of ER-β isoforms occur during breast tumorigenesis. The cellular origin of the expression of ER-β1, -β2, and -β5 in breast tumor tissue *in vivo* remains to be determined, as does the putative role of the different ER-β variant forms in the mechanisms underlying tumorigenesis and tumor progression.

Acknowledgments

We thank Caroline Cumins-Leygue and Helen Bergen for laboratory assistance with the cell culture.

References

1. Vorherr, H. (ed.). Breast Cancer. Baltimore: Urban and Schwarzenberg Press, 1980.
2. Green, S., Walter, P., Kumar, V., Krust, A., Bornert, J. M., Argos, P., and Chambon, P. Human oestrogen receptor cDNA: sequence, expression and homology to v-erb-A. Nature, (Lond.) *320:* 134–139, 1986.
3. Mosselman, S., Polman, J., and Dijkema, R. ER β: identification and characterization of a novel human estrogen receptor. FEBS Lett., *392:* 49–53, 1996.
4. Ogawa, S., Inoue, S., Watanabe, T., Hiroi, H., Orimo, A., Hosoi, T., Ouchi, Y., and Muramatsu, M. The complete primary structure of human estrogen receptor β (hER β) and its heterodimerization with ER α *in vivo* and *in vitro*. Biochem. Biophys. Res. Commun., *243:* 129–132, 1998.
5. Enmark, E., Pelto-Huikko, M., Grandien, K., Lagercrantz, S., Lagercrantz, J., Fried, G., Nordenskjold, M., and Gustafsson, J. A. Human estrogen receptor beta-gene structure, chromosomal localization, and expression pattern. J. Clin. Endocrinol. Metab., *82:* 4258–4265, 1997.
6. Ponglikitmongkol, M., Green, S., and Chambon, P. Genomic organization of the human oestrogen receptor gene. EMBO J., *7:* 3385–3388, 1988.
7. Evans, R. M. The steroid and thyroid receptor super-family. Science (Washington DC), *240:* 889–895, 1988.
8. Kumar, V., Green, S., Stack, G., Berry, M., Jin, J. R., and Chambon, P. Functional domains of the human estrogen receptor. Cell, *51:* 941–951, 1987.
9. Shibata, H., Spencer, T. E., Onate, S. A., Jenster, G., Tsai, S. Y., Tsai, M. J., and O'Malley, B. W. Role of co-activators and co-repressors in the mechanism of steroid/thyroid receptor action. Rec. Prog. Horm. Res., *52:* 141–164, 1997.
10. Umayahara, Y., Kawamori, R., Watada, H., Imano, E., Iwama, N., Morishima, T., Yamasaki, Y., Kajimoto, Y., and Kamada, T. Estrogen regulation of the insulin-like growth factor I gene transcription involves an AP-1 enhancer. J. Biol. Chem., *269:* 16433–16442, 1994.
11. Paech, K., Webb, P., Kuiper, G. G., Nilsson, S., Gustafsson, J., Kushner, P. J., and Scanlan, T. S. Differential ligand activation of estrogen receptors ERα and ERβ at AP1 sites. Science (Washington DC), *277:* 1508–1510, 1997.
12. Watanabe, T., Inoue, S., Ogawa, S., Ishii, Y., Hiroi, H., Ikeda, K., Orimo, A., and Muramatsu, M. Agonistic effect of tamoxifen is dependent on cell type, ERE-promoter context, and estrogen receptor subtype: functional difference between estrogen receptors α and β. Biochem. Biophys. Res. Commun., *236:* 140–145, 1997.
13. Cowley, S. M., Hoare, S., Mosselman, S., and Parker, M. G. Estrogen receptors α and β form heterodimers on DNA. J. Biol. Chem., *272:* 19858–19862, 1997.
14. Murphy, L. C., Leygue, E., Dotzlaw, H., Douglas, D., Coutts, A., and Watson, P. H. Estrogen receptor variants and mutations. Ann. Med., *29:* 221–224, 1997.
15. Vladusic, E. A., Hornby, A. E., Guerra-Vladusic, F. K., and Lupu, R. Expression of estrogen receptor β messenger RNA variant in breast cancer. Cancer Res., *58:* 210–214, 1998.
16. Lu, B., Leygue, E., Dotzlaw, H., Murphy, L. J., Murphy, L. C., and Watson, P. H. Estrogen receptor-β mRNA variants in human and murine tissues. Mol. Cell. Endocrinol., *138:* 199–203, 1998.
17. Shupnik, M. A., Pitt, L. K., Soh, A. Y., Anderson, A., Lopes, M. B., and Laws, E. R., Jr. Selective expression of estrogen receptor α and β isoforms in human pituitary tumors. J. Clin. Endocrinol. Metab., *83:* 3965–3972, 1998.
18. Fuqua, S. A. W., Fitzgerald, S. D., Chamness, G. C., Tandon, A. K., McDonnell, D. P., Nawaz, Z., O'Malley, B. W., and McGuire, W. L. Variant human breast tumor estrogen receptor with constitutive transcriptional activity. Cancer Res., *51:* 105–109, 1991.
19. Wang, Y., and Miksicek, R. J. Identification of a dominant negative form of the human estrogen receptor. Mol. Endocrinol., *5:* 1707–1715, 1991.
20. Moore, J. T., McKee, D. D., Slentz-Kesler, K., Moore, L. B., Jones, S. A., Horne, E. L., Su, J. L., Kliewer, S. A., Lehman, J. M., and Willson, T. M. Cloning and characterization of human estrogen receptor β isoforms. Biochem. Biophys. Res. Commun., *247:* 75–78, 1998.
21. Ogawa, S., Inoue, S., Watanabe, T., Hiroi, H., Orimo, A., Hosoi, T., Ouchi, Y., and Muramatsu, M. Molecular cloning and characterization of human estrogen receptor βcx: a potential inhibitor of estrogen action in human. Nucleic Acids Res., *26:* 3505–3512, 1998.
22. Hiller, T., Snell, L., and Watson, P. H. Microdissection RT-PCR analysis of gene expression in pathologically defined frozen tissue sections. Biotechniques, *21:* 38–44, 1996.
23. Elston, C. W., and Ellis, I. O. Pathological prognostic factors in breast cancer. Histopathology, *19:* 403–410, 1991.
24. Dotzlaw, H., Alkhalaf, M., and Murphy, L. C. Characterization of estrogen receptor variant mRNAs from human breast cancers. Mol. Endocrinol., *6:* 773–785, 1992.
25. Leygue, E., Murphy, L. C., Kuttenn, F., and Watson, P. H. Triple primer PCR: a new way to quantify truncated mRNA expression. Am. J. Pathol., *148:* 1097–1103, 1996.

[CANCER RESEARCH 59, 4190–4193, September 1, 1999]

Advances in Brief

Expression of the Steroid Receptor RNA Activator in Human Breast Tumors[1]

Etienne Leygue,[2] Helmut Dotzlaw, Peter H. Watson, and Leigh C. Murphy

Departments of Biochemistry and Molecular Biology [E. L., H. D., L. C. M.] and Pathology [P. H. W.], University of Manitoba, Faculty of Medicine, Winnipeg, Manitoba, R3E OW3, Canada

Abstract

The expression of the recently described steroid receptor RNA activator (*SRA*) was measured by semiquantitative reverse transcription-PCR within 27 independent breast tumors, spanning a wide spectrum of grade and estrogen receptor (ER) and progesterone receptor (PR) levels. Subgroup analysis showed that *SRA* expression was similar in ER+/PR+ (median = 65.5, $n = 8$) and in ER−/PR− (median = 94.6, $n = 5$) tumors. Interestingly, *SRA* expression in these two subgroups was significantly (Mann-Whitney rank-sum test, $P < 0.05$) lower than that observed in ER+/PR− (median = 156.4, $n = 6$) and ER−/PR+ (median = 144.8, $n = 8$) tumors. A variant form of *SRA*, presenting a deletion of 203 bp within the *SRA* core sequence, was also observed in breast tumor tissues. The relative expression of this new *SRA* isoform correlated with tumor grade (Spearman coefficient $r = 0.53$, $n = 27$, $P = 0.004$). These data suggest that changes in the expression of *SRA*-related molecules occur during breast tumor progression.

Introduction

Estrogens, through their mitogenic action on breast epithelial cells, regulate the growth and the development of normal as well as neoplastic human mammary tissue (1). The ability of antiestrogens such tamoxifen or raloxifene to antagonize this estrogenic action provides the basic rationale for endocrine therapy and prevention (for review see Ref. 2). Estrogen action is mainly mediated through two ERs,[3] ER-α and ER-β (3–5), which belong to the steroid/thyroid/retinoic acid receptors superfamily (6) and act as ligand-dependent transcription factors. The mechanisms by which steroid receptors modulate the transcription of target genes is under extensive investigation (7). Once bound to the ligand, the receptors undergo conformational changes and dimers of receptors recognize specific regulatory DNA sequences upstream of target genes. Activated receptors, through interactions with coactivator proteins, direct the assembly and the stabilization of a preinitiation complex that will ultimately conduct the transcription of these genes (see Ref. 8 and references therein). To an already long list of nuclear receptor coactivators (8), which includes the p160 proteins (such as SRC-1 and AIB1), Lanz *et al.* (9) recently added the *SRA*. *SRA* differs from other coactivators in two main ways. (*a*) *SRA* transcripts do not appear to be translated, and therefore, this coactivator acts as an RNA and not as a protein. Lanz *et al.* (9) showed that *SRA* exists in a ribonucleoprotein complex that contains SRC-1 and is recruited by steroid receptors. (*b*) *SRA* appears to be actually specific for steroid receptors. Indeed, most of the receptor-interacting factors, such as SRC-1 or TIF2/hSRC-2, interact with and coactivate both class I and class II nuclear receptors (9). Because of the importance of ER signaling pathways in the mechanisms underlying breast tumor progression, it was important to establish whether *SRA* could be expressed in breast tumors. If so, it was also of interest to determine whether the expression of *SRA* was related to known markers of endocrine sensitivity and prognostic markers. We have selected a subset of breast cancer cases to look for possible correlations between *SRA* expression and already established predictive and/or prognostic factors, such as grade, ER, and PR status (10).

Materials and Methods

Human Breast Tumors. Twenty-seven cases were selected from the National Cancer Institute of Canada-Manitoba Breast Tumor Bank (Winnipeg, Manitoba, Canada). The cases were selected according to their ER and PR status, as determined by ligand binding assay. Tumors were classified as ER−/PR+ ($n = 8$; ER range, 5–9 fmol/mg protein; PR range, 51–271 fmol/mg protein), ER+/PR− ($n = 6$; ER range, 59–151 fmol/mg protein; PR range, 5–10 fmol/mg protein), ER−/PR− ($n = 5$; ER range, 0–2 fmol/mg protein; PR range, 0–8 fmol/mg protein), and ER+/PR+ ($n = 8$; ER range, 50–127 fmol/mg protein; PR range, 101–285 fmol/mg protein). These tumors covered a wide spectrum of grade (grades 4–9), determined using the Nottingham grading system (11). Patients were 49–87 years old.

RNA Extraction and RT-PCR. Total RNA was extracted from frozen breast tissue sections using Trizol reagent (Life Technologies, Inc., Grand Island, NY) according to the manufacturer's instructions and quantified spectrophotometrically. One μg of total RNA was reverse-transcribed in a final volume of 25 μl, as described previously (12).

Primers and PCR Conditions. The primers used consisted of *SRA*coreU primer (sense, 5′-AGGAACGCGGCTGGAACGA-3′, positions 35–53; GenBank accession no. AF092038) and *SRA* core L primer (antisense, 5′-AGTCTGGGGAACCGAGGAT-3′, positions 696–678; GenBank accession no. AF092038). PCR amplifications were performed and PCR products analyzed as described previously (12), with minor modifications. Briefly, 1 μl of reverse transcription mixture was amplified in a final volume of 15 μl, in the presence of 1.5 μCi of [α-^{32}P]dCTP (3000 Ci/mmol), 4 ng/μl each primer, and 0.3 unit of Taq DNA polymerase (Life Technologies, Inc.). Each PCR consisted of 30 cycles (30 s at 60°C, 30 s at 72°C, and 30 s at 94°C). PCR products were then separated on 6% polyacrylamide gels containing 7 M urea. Following electrophoresis, the gels were dried and exposed for 1 h to a Molecular Imager-FX Imaging screen (Bio-Rad, Hercules, CA). Amplification of the ubiquitously expressed *GAPDH* cDNA was performed in parallel and PCR products separated on agarose gels stained with ethidium bromide as described previously (12). Identity of PCR products was confirmed by subcloning and sequencing, as reported previously (13).

Quantification of *SRA* Expression. Exposed screens were scanned using a Molecular Imager-FX (Bio-Rad), and the intensity of the *SRA* corresponding signal was measured using Quantity One software (Bio-Rad). Three independent PCRs were performed. To control for variations between experiments, a value of 100% was arbitrarily assigned to the *SRA* signal of one particular tumor (tumor 14) measured in each set of PCR experiments, and all signals were expressed as a percentage of this signal. In parallel, *GAPDH* cDNA was amplified and following analysis of PCR products on prestained agarose gels, signals were quantified by scanning using NIH Image 161/ppc software. Three

Received 6/16/99; accepted 7/20/99.

The costs of publication of this article were defrayed in part by the payment of page charges. This article must therefore be hereby marked *advertisement* in accordance with 18 U.S.C. Section 1734 solely to indicate this fact.

[1] This work was supported by grants from the Canadian Breast Cancer Research Initiative and the United States Army Medical Research and Materiel Command. The Manitoba Breast Tumor Bank is supported by funding from the National Cancer Institute of Canada. P. H. W. is a Medical Research Council of Canada Scientist, L. C. M. is a Medical Research Council of Canada Scientist, and E. L. is a recipient of a United States Army Medical Research and Materiel Command Postdoctoral Fellowship.

[2] To whom requests for reprints should be addressed, at Department of Biochemistry and Molecular Biology, University of Manitoba, Winnipeg, Manitoba R3E OW3, Canada. Phone: (204) 789-3812; Fax: (204) 789-3900; E-mail: eleygue@cc.umanitoba.ca.

[3] The abbreviations used are: ER, estrogen receptor; SRA, steroid receptor RNA activator; PR, progesterone receptor; RT-PCR, reverse transcriptase-PCR; GAPDH, glyceraldehyde-3-phosphate dehydrogenase.

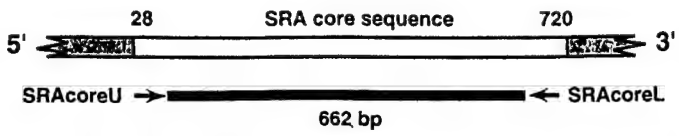

Fig. 1. *SRA* structure and primer presentation. *SRA* isoforms identified to date (9) differ in their 5′ and 3′ terminal regions (▨) but present an identical nucleotide sequence (□) in between (*SRA* core sequence, bases 28 to 720). *SRA*coreU and *SRA*coreL primers anneal with *SRA* core sequences and allow the amplification of a 662-bp fragment.

independent PCRs were performed. Each *GAPDH* signal was also expressed as a percentage of the signal observed in the tumor 14. For each sample, the average of *SRA* signal was then expressed as a percentage of the *GAPDH* signal (arbitrary units).

Quantification of *SRA*-Del Relative Expression. It has previously been shown that the coamplification of a wild-type and a deleted variant cDNA resulted in the amplification of two PCR products, the relative signal intensity of which provided a reliable measurement of the relative expression of the deleted variant (13, 14). For each sample, *SRA*-Del corresponding signal was measured using Quantity One software (Bio-Rad) and expressed as a percentage of the corresponding *SRA* signal. For each case, three independent assays were performed, and the mean was determined.

Statistical Analysis. Differences between tumor subgroups were tested using the two-sided Mann-Whitney rank sum test. Correlation between *SRA* expression and tumor characteristics was tested by calculation of the Spearman coefficient *r*.

Results

Detection of *SRA* and a Variant mRNA Deleted Form (*SRA*-Del) in Human Breast Tumor Tissues. The existence of three different *SRA* mRNAs have been reported (9). The sequences of these isoforms differ in their 5′- and 3′-terminal regions but are identical within their central region, called the core (Fig. 1). To investigate the expression of all described *SRA* isoforms in human breast tumor tissues, we designed primers to amplify a 662-bp fragment encompassing almost all of the *SRA* core region. Total RNA was extracted from 27 human breast tumors and reverse-transcribed, and PCR amplification was performed as described in the "Materials and Methods" using SRA core primers. A 662-bp fragment was obtained in all samples. However, the intensity levels varied from one sample to another (Fig. 2*A*). This fragment was sequenced and corresponded to the *SRA* core region. The differences in *SRA* expression were unlikely to result from different cDNA input, as shown by the similar intensities of *GAPDH* signal obtained after amplifying *GAPDH* mRNA in parallel using the same cDNAs (Fig. 2*B*). An additional fragment, migrating at an apparent size of 459 bp was also observed in most samples. Sequencing analysis revealed that this band corresponded to a variant form of *SRA* (referred to as *SRA*-Del) deleted in 203 bp between positions 155 and 357 (corresponding to GenBank accession no. AF092038).

The Expression of *SRA* Correlates with ER and PR Levels in Subgroups of Human Breast Tumors. For each case, the *SRA*-corresponding signal was quantified and expressed in arbitrary units, as described in "Materials and Methods." Results obtained from the 27 cases, grouped according to their ER and PR levels, as determined by ligand binding analysis, are presented Fig. 3*A*. When the cohort of cases was considered as a whole ($n = 27$), no correlation was observed between *SRA* expression and ER or PR levels. Indeed, similar levels of *SRA* were found in ER+/PR+ (median = 65.5, $n = 8$) and ER−/PR− (median = 94.6, $n = 5$) tumors (Fig. 3*A*). However, when only ER− tumors were considered ($n = 13$), a trend toward a positive correlation between *SRA* expression and PR levels was observed (Spearman coefficient $r = 0.527$, $P = 0.064$). *SRA* expression was higher in ER−/PR+ ($n = 8$, median = 144.8) than it was in ER−/PR− tumors (Fig. 3*A*); this difference was statistically significant (two-sided Mann-Whitney rank sum test, $P = 0.045$). In contrast, within ER+ cases ($n = 14$), *SRA* expression negatively correlated with PR levels (Spearman coefficient $r = -0.810$, $P = 0.0004$). *SRA* expression was higher (two-sided Mann-Whitney rank sum test, $P = 0.001$) in ER+/PR− ($n = 6$, median = 156.4) than it was in ER+/PR+ cases. In a similar way, *SRA* expression correlated positively (Spearman coefficient $r = 0.735$, $P = 0.009$) and negatively (Spearman coefficient $r = -0.532$, $P = 0.033$) with ER levels in PR− ($n = 11$) and PR+ ($n = 16$) cases, respectively. *SRA* levels were higher in ER+/PR− than in ER−/PR− tumors (two-sided Mann-Whitney rank sum test, $P = 0.017$) and in ER−/PR+ than in ER+/PR+ cases (two-sided Mann-Whitney rank sum test, $P = 0.047$). *SRA* levels of expression did not correlate with tumor grade scores (Fig. 3*B*).

The Expression of *SRA*-Del Correlates with Breast Tumor Grade Scores. For each case, *SRA*-Del signal was measured and expressed relative to the corresponding *SRA* signal, as described in the "Materials and Methods." *SRA*-Del relative signal did not correlate with ER or PR levels when the cohort of cases was considered as a whole or when ER−, ER+, and PR− subgroups were analyzed. Interestingly, *SRA*-Del expression positively correlated (Spearman coefficient $r = 0.512$, $P = 0.042$) with PR levels in PR+ subgroup ($n = 16$). However, no statistically significant differences (Fig. 4*A*) were observed between ER−/PR+ ($n = 8$, median = 2.346), ER+/PR− ($n = 6$, median = 2.561), ER−/PR− ($n = 5$, median = 6.571) and ER+/PR+ ($n = 8$, median = 3.528). By contrast, *SRA*-Del levels strongly correlated (Spearman coefficient $r = 0.530$, $P = 0.004$) with Nottingham grade scores within the whole cohort ($n = 27$). The level of expression of *SRA* was significantly higher (two-sided Mann-Whitney rank sum test, $P < 0.05$) in tumors of high grade ($n = 7$, median = 6.572) than it was in tumors of low ($n = 4$, median = 2.192) or intermediate ($n = 9$, median = 2.588) grade (Fig. 4*B*).

Discussion

Using primers annealing with the core region of the three previously described *SRA* isoforms (9), we have investigated *SRA* expression in 27 independent breast tumors by means of semiquantitative RT-PCR. These *SRA* isoforms, although different in their 5′- and 3′-terminal regions, are all able to coactivate steroid receptor. Indeed,

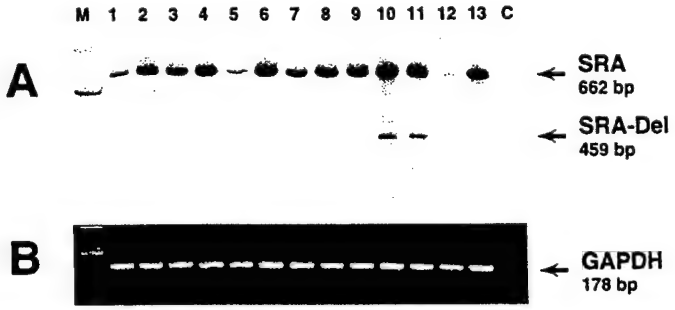

Fig. 2. Detection of *SRA* in human breast tumors by RT-PCR. Total RNA was extracted from 27 breast tumors, reverse-transcribed, and analyzed by PCR as described in "Materials and Methods." PCR products were separated on 6% acrylamide gels. Gels were dried and exposed 1 h to a Molecular Imager-FX Imaging screen. Screens were then scanned using a Molecular Imager-FX. *A*, computerized image showing the results obtained for 13 cases (*Lanes 1–13*). *Lane M*, molecular weight marker (ϕx174 RF DNA/*Hae*III fragments). *Lane C*, control lane, no cDNA added in the PCR. Sequencing analysis of PCR fragments revealed that the 662-bp (*SRA*) and 459-bp (SRA-Del) fragments corresponded to *SRA* and to a variant *SRA* isoform deleted in sequences from position 155 to 357 (GenBank accession no. AF092038), respectively. *B*, ethidium bromide-stained gel of the RT-PCR analysis of *GAPDH* mRNA run in parallel for the same samples.

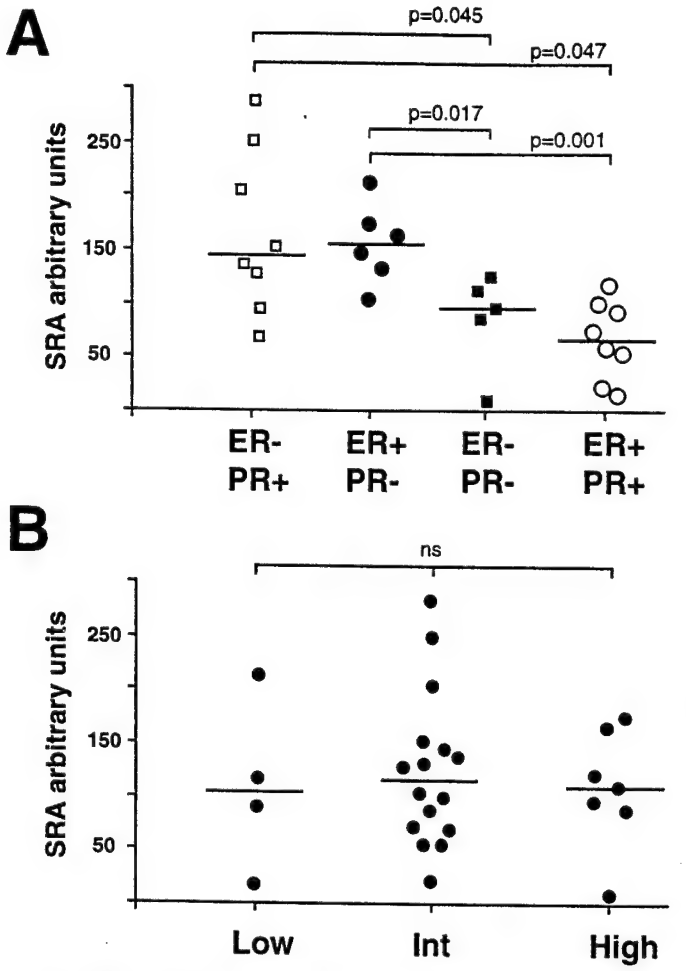

Fig. 3. Subgroup analysis of *SRA* expression within 27 human breast tumors. For each case, *SRA* expression was quantified and expressed in arbitrary units as described in "Materials and Methods." *A*, tumors were grouped according to their ER and PR status, as determined by ligand binding assay. □, ER−/PR+ tumors; ●, ER+/PR− tumors; ■, ER−/PR− tumors; and ○, ER+/PR+ tumors. *B*, tumors were grouped according to their grade: low (Nottingham grading scores 4–5), intermediate (Nottingham grading scores 6–7), and high (Nottingham grading scores 8–9). The *horizontal line* represents the median value in each group. *P*s (two-sided Mann-Whitney rank sum test) are indicated when subgroups were statistically different. *ns*; no statistically significant differences were found between subgroups.

SRA core region was found to be necessary and sufficient for the coactivation properties of *SRA* isoforms (9). Therefore, although PCR performed using primers spanning the *SRA* core region is likely to recognize several different *SRA*-like molecules, the signal obtained corresponds to molecules that should all have essentially the same function, *i.e.*, coactivation of steroid receptors.

The expression of *SRA* did not correlate with ER or PR status when the cohort was considered as a whole. This differs from what has been observed for another coactivator, *AIB1*. Indeed, Anzick *et al.* (15) first showed that a strong expression of *AIB1* that resulted from *AIB1* gene amplification was observed in ER+ but not in ER− breast cancer cell lines. More recently, Bautista *et al.* (16) reported that *AIB1* gene amplification correlated with ER and PR positivity. Our results suggest that the pattern of expression of *SRA* is more complex. Indeed, we found that *SRA* expression could correlate positively or negatively with ER and PR levels, depending on the subgroup considered. The general trend appeared to be that, in tumors expressing a low level of one receptor (ER or PR), a positive correlation was found between *SRA* expression and the second receptor (PR or ER). Inversely, in tumors highly expressing one receptor (ER or PR), *SRA* expression negatively correlated with the level of expression of the second receptor (PR or ER). At this stage of the knowledge of *SRA* biological function, the interpretation of such an observation is difficult. Indeed, *SRA* has been shown to be able to coactivate both ER and PR (9). Moreover, progestins are known to decrease the steady state levels of ER-α mRNA and protein, whereas estrogens increase PR expression (17, 18). Therefore, all combinations and cross-talk appear possible. One could speculate that increased levels of *SRA* in ER−/PR+ cases could partially be responsible, by "boosting" the activity of the weakly expressed ER, of the expression of PR in these tumors. Inversely, in the same ER−/PR+ cases, the strong *SRA* expression could be responsible for an increased down-regulation of ER by PR. Our results suggest that *SRA* expression varies from one particular tumor to another. Changes in *SRA* expression can be associated with known prognostic and predictive factors such as ER and PR in particular tumor subgroups. The question of a direct involvement of *SRA* in the hormonal status changes occurring during breast tumor progression remains unanswered. Also of interest is the fact that *SRA* interacts with the activation function 1 of the steroid receptors (9). Activation function 1 is thought to mediate the agonistic effect of antiestrogens such hydroxytamoxifen (19). This agonistic action of antiestrogens is believed to be involved in part in the mechanisms underlying hormone

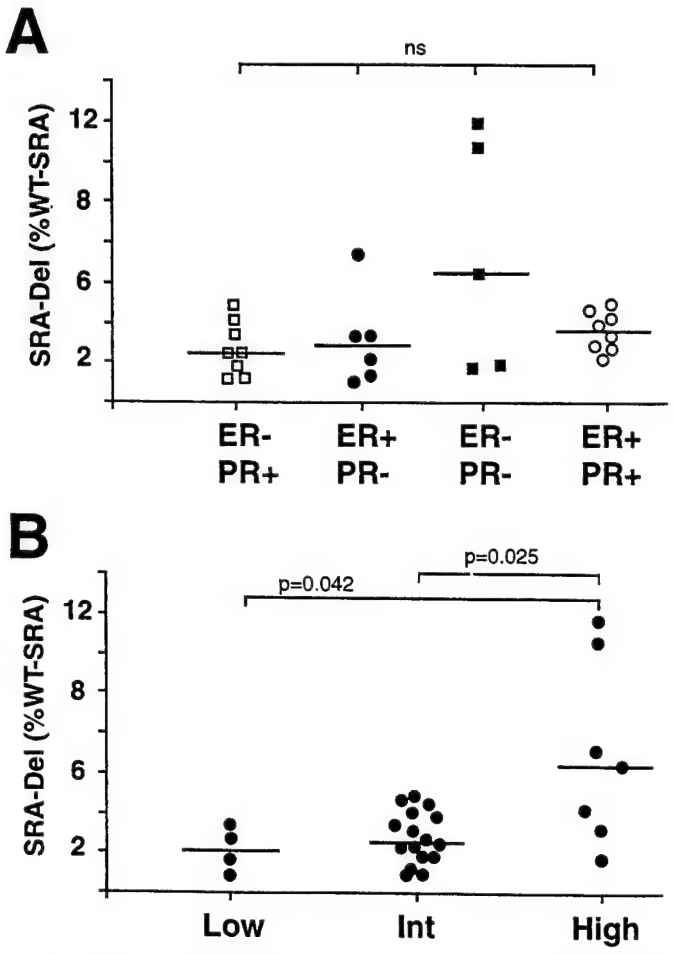

Fig. 4. Subgroup analysis of *SRA*-Del relative expression within 27 human breast tumors. For each case, SRA-D3 expression relative to *SRA* was quantified as described in "Materials and Methods." *A*, tumors were grouped according to their ER and PR status, as determined by ligand binding assay. □, ER−/PR+ tumors; ●, ER+/PR− tumors; ■, ER−/PR− tumors; and ○, ER+/PR+ tumors. *B*, tumors were grouped according to their grade: low (Nottingham grading scores 4–5), intermediate (Nottingham grading scores 6–7), and high (Nottingham grading scores 8–9). The *horizontal line* represents the median value in each group. *P*s (two-sided Mann-Whitney rank sum test) are indicated when subgroups were statistically different. *ns*; no statistically significant differences were found between subgroups.

resistance in breast cancer. One could speculate that the level of *SRA* expression might, therefore, modulate and predict the response of a given tumor to hormone therapy. This hypothesis appears to be refuted by the observation of similar levels of *SRA* in ER+/PR+ and ER−/PR− tumors. But ER+/PR+ tumors, as opposed to ER−/PR− tumors, are likely to respond to endocrine therapy and prevention (see Ref. 2 and references therein). In these cases, the differences in ER levels rather than in *SRA* expression are more likely involved in the mechanisms underlying endocrine sensitivity. On the other hand, the observation of a higher *SRA* expression within ER−/PR+ cases, which are more likely to respond to hormone therapy than ER−/PR− tumors (see Ref. 20 and references therein), would be consistent with the hypothesis of a possible involvement of *SRA* in these mechanisms under some circumstances. One should also note that Berns *et al.* (21) recently reported that, although no correlation was found between the expression of *SRC-1* and ER status, a high expression of this coactivator indicated a favorable response to tamoxifen of patients with recurrent breast cancer. This issue can only be addressed in studies performed on tumors from patients that did and did not respond to endocrine therapy.

We have identified in breast tumor cases a new *SRA* isoform deleted in sequences from nucleotide 155 to 357 (*SRA*-Del). Interestingly, sequence comparison using the BLAST algorithm and the human EST database showed that this deleted *SRA* isoform has already been found in a pooled cDNA library containing cDNAs from melanocyte, fetal heart, and pregnant uterus (GenBank accession no. AA426601). Because uterus is another steroid target tissue, it could be hypothesized that the source of *SRA*-Del in this pooled library was, indeed, uterus. Even though the structure of the *SRA* gene has not yet been published, *SRA*-Del appears to correspond to a perfect exon-3 deleted *SRA* variant. *SRA* gene has recently been located on chromosome 5q31.3-32.[4] Sequence analysis of the corresponding DNA sequence (chromosome 5, BAC clone 319C17; GenBank accession no. AC005214) revealed that the fragment from nucleotide 155 to 357 corresponds to the third *SRA* exon. The putative function of *SRA*-Del remains to be determined. One should, however, note that a recombinantly developed *SRA* mutant, deleted of the region 3′ of a *Bbs*I site (position 341) and, therefore, partially deleted of exon 3 sequences, did not coactivate steroid receptors (9). Moreover, exon 3 deletion introduces a shift in the open reading frames, suggested by Lanz *et al.* (9), and could lead to a premature termination of the putative SRA proteins. One could, therefore, hypothesize that *SRA*-Del might interfere with *SRA* activity. The resulting modifications of the steroid receptor signaling pathways could confer a more aggressive behavior to the tumors expressing higher levels of *SRA*-Del. The positive correlation between *SRA*-Del levels and tumor grade scores would be consistent with this hypothesis.

Interestingly, modifications of the long arm of the chromosome 5 have been reported in breast tumors. Indeed, Hermsen *et al.* (22) found a frequent chromosomal gain in 5q within a subset of 53 lymph node-negative breast carcinoma, whereas Schwendel *et al.* (23) observed a frequent loss of this region in 39 invasive breast carcinomas. Moreover, among *BRCA1* mutation carriers, loss of 5q was observed more frequently than in the control patient (24). One could, therefore, speculate that the loss of *SRA* is selected for during tumor progression in cells lacking *BRCA1* functional gene. Whether changes in *SRA* expression result from chromosomal abnormalities remains to be determined.

In conclusion, we have shown that *SRA* is expressed in breast tumors and that its expression correlates with ER and PR levels in particular tumor subgroups. We speculate that changes in *SRA* expression could be involved in the mechanisms underlying tumor progression and hormone resistance.

References

1. Vorherr, H. (ed.). Breast Cancer. Baltimore: Urban and Schwarzenberg Press, 1980.
2. Jordan, V. C., and Morrow, M. Tamoxifen, Raloxifene, and the prevention of breast cancer. Endocr. Rev., *20:* 253–278, 1999.
3. Green, S., Walter, P., Kumar, V., Krust, A., Bornert, J. M., Argos, P., and Chambon, P. Human oestrogen receptor cDNA: sequence, expression and homology to v- erb-A. Nature (Lond.), *320:* 134–139, 1986.
4. Mosselman, S., Polman, J., and Dijkema, R. ER β: identification and characterization of a novel human estrogen receptor. FEBS Lett., *392:* 49–53, 1996.
5. Ogawa, S., Inoue, S., Watanabe, T., Hiroi, H., Orimo, A., Hosoi, T., Ouchi, Y., and Muramatsu, M. The complete primary structure of human estrogen receptor β (hER β) and its heterodimerization with ER α *in vivo* and *in vitro*. Biochem. Biophys. Res. Commun., *243:* 129–132, 1998.
6. Evans, R. M. The steroid and thyroid receptor super-family. Science (Washington DC), *240:* 889–895, 1988.
7. Shibata, H., Spencer, T. E., Onate, S. A., Jenster, G., Tsai, S. Y., Tsai, M. J., and O'Malley, B. W. Role of co-activators and co-repressors in the mechanism of steroid/thyroid receptor action. Rec. Prog. Horm. Res., *52:* 141–164, 1997.
8. McKenna, N. J., Lanz, R. B., and O'Malley, B. W. Nuclear receptor coregulators: cellular and molecular biology. Endocr. Rev., *20:* 321–344, 1999.
9. Lanz, R. B., McKenna, N. J., Onate, S. A., Albrecht, U., Wong, J., Tsai, S. Y., Tsai, M-J., and O'Malley, B. W. A steroid receptor coactivator, *SRA*, functions as an RNA and is present in an SRC-1 complex. Cell, *97:* 17–27, 1999.
10. Henderson, I. C., and Patek, A. J. The relationship between prognostic and predictive factors in the management of breast cancer. Breast Cancer Res. Treat., *52:* 261–288, 1998.
11. Elston, C. W., and Ellis, I. O. Pathological prognostic factors in breast cancer. Histopathology, *19:* 403–410, 1991.
12. Leygue, E., Murphy, L. C., Kuttenn, F., and Watson, P. H. Triple primer PCR: a new way to quantify truncated mRNA expression. Am. J. Pathol., *148:* 1097–1103, 1996.
13. Leygue, E., Watson, P. H., and Murphy, L. C. Estrogen receptor variants in normal human mammary tissue. J. Natl. Cancer Inst., *88:* 284–290, 1996.
14. Daffada, A. A. I., Johnston, S. R. D., Nicholls, J., and Dowsett, M. Detection of wild type and exon 5-deleted splice variant oestrogen receptor (ER) mRNA in ER-positive and -negative breast cancer cell lines by reverse transcription/polymerase chain reaction. J. Mol. Endocrinol., *13:* 265–273, 1994.
15. Anzick, S. L., Kononen, J., Walker, R. L., Azorsa, D. O., Tanner, M. M., Guan, X. Y., Sauter, G., Kallioniemi, O. P., Trent, J. M., and Meltzer, P. S. AIB1, a steroid receptor coactivator amplified in breast and ovarian cancer. Science (Washington DC), *277:* 965–968, 1997.
16. Bautista, S., Valles, H., Walker, R. L., Anzick, S., Zeillinger, R., Meltzer, P., and Theillet, C. In breast cancer, amplification of the steroid receptor coactivator gene *AIB1* is correlated with estrogen and progesterone receptor positivity. Clin. Cancer Res., *4:* 2925–2929, 1998.
17. Read, L., Greene, G., and Katzenellenbogen, B. Regulation of estrogen receptor messenger ribonucleic acid and protein levels in human breast cancer cell lines by sex steroid hormones, their antagonists and growth factors. Mol. Endocrinol., *3:* 295–304, 1989.
18. Berkenstam, A., Glaumann, H., Martin, M., Gustafsson, J. A., and Norstedt, G. Hormonal regulation of estrogen receptor messenger ribonucleic acid in T47Dco and MCF-7 breast cancer cells. Mol. Endocrinol., *3:* 22–28, 1989.
19. Berry, M., Metzger, D., and Chambon, P. Role of the two activating domains of the oestrogen receptor in the cell-type and promoter-context dependent agonistic activity of the anti-oestrogen 4-hydroxytamoxifen. EMBO J., *9:* 2811–2818, 1990.
20. Osborne, C. K. Steroid hormone receptors in breast cancer management. Breast Cancer Res. Treat., *51:* 227–238, 1998.
21. Berns, E. M., Van Staveren, I. L., Klijn, J. G., and Foekens, J. A. Predictive value of SRC-1 for tamoxifen response of recurrent breast cancer. Breast Cancer Res. Treat., *48:* 87–92, 1998.
22. Hermsen, M. A., Baak, J. P., Meijer, G. A., Weiss, J. M., Walboomers, J. W., Snijders, P. J., and van Diest, P. J. Genetic analysis of 53 lymph node-negative breast carcinomas by CGH and relation to clinical, pathological, morphometric, and DNA cytometric prognostic factors. J. Pathol., *186:* 356–362, 1998.
23. Schwendel, A., Richard, F., Langreck, H., Kaufmann, O., Lage, H., Winzer, K. J., Petersen, I., and Dietel, M. Chromosome alterations in breast carcinomas: frequent involvement of DNA losses including chromosomes 4q and 21q. Br. J. Cancer, *78:* 806–811, 1998.
24. Tirkkonen, M., Johannsson, O., Agnarsson, B. A., Olsson, H., Ingvarsson, S., Karhu, R., Tanner, M., Isola, J., Barkardottir, R. B., Borg, A., and Kallioniemi, O. P. Distinct somatic genetic changes associated with tumor progression in carriers of *BRCA1* and *BRCA2* germ-line mutations. Cancer Res., *57:* 1222–1227, 1997.

[4] http://www.ncbi.nlm.nih.gov/genemap/loc.cgi?ID=12637.

The Human Orphan Receptor PXR Messenger RNA Is Expressed in Both Normal and Neoplastic Breast Tissue[1]

Helmut Dotzlaw, Etienne Leygue, Peter Watson, and Leigh C. Murphy[2]

Departments of Biochemistry and Molecular Biology [H. D., E. L., L. C. M.] and Pathology [P. W.], University of Manitoba, Winnipeg, Manitoba, Canada R3E 0W3

ABSTRACT

The expression of PXR mRNA and a variant PXR mRNA, deleted in 111 nucleotides in the ligand-binding domain, was detected by reverse transcription-PCR amplification in both normal and neoplastic human breast tissues. The level of PXR mRNA did not differ between breast tumors and their adjacent matched normal breast tissues. However, the expression of PXR mRNA did vary among breast tumors. A statistically significant inverse relationship was found between the level of PXR mRNA expression and estrogen receptor (ER) status, as defined by ligand binding analysis. The level of PXR mRNA expression in ER+ tumors (median = 22.4, $n = 15$) was significantly lower ($P = 0.04$) than the level of PXR mRNA expression in ER− tumors (median = 46.7, $n = 15$). No relationship with progesterone receptor status was found. These data raise the possibility that PXR has a role in human breast tissues.

INTRODUCTION

A novel orphan receptor, PXR, activated by pregnanes, was originally cloned from a mouse liver cDNA library (1). Its human "homologue," hPXR, has been recently cloned from a human liver cDNA library (2). This orphan receptor can be activated by natural and synthetic pregnenolone derivatives as well as the antiglucocorticoid/antiprogestin RU-486. A possible target gene of hPXR is *CYP3A*,[3] which is thought to have a role in the biotransformation of many drugs (2). Also, the CYP3A enzymes have been implicated as major players in the metabolism of the clinically useful antiestrogens tamoxifen and toremifene (3–5). Although the major site of expression of hPXR and CYP3A enzymes is the liver, CYP3A enzymes have also been found in human breast cancer tissue (6, 7). Because these enzymes are involved in the metabolism of several antihormonal agents used in the treatment of breast cancer and because their potential transcriptional regulator, hPXR, can be activated by another endocrine agent (*i.e.*, RU-486), we considered the possibility that the presence of such a pathway in breast cancers may have an influence on the efficacy of some endocrine therapies. To determine the potential existence of such a pathway in human breast cancer, we have investigated the expression of hPXR mRNA in both normal and neoplastic human breast tissue.

MATERIALS AND METHODS

Materials. All cell culture reagents were obtained from Life Technologies, Inc. (Burlington, Ontario, Canada). [α-^{32}P]dCTP was purchased from ICN (Montreal, Quebec, Canada).

Human Breast Tissues. Thirteen cases were selected from the NCIC-Manitoba Breast Tumor Bank (Winnipeg, Manitoba, Canada). For each case, matched adjacent normal and tumor frozen tissue blocks were available. The quality of each block was determined by the histopathological assessment of sections from adjacent mirror image paraffin-embedded tissue blocks, as described previously (8). The presence of normal ducts and lobules and the absence of any atypical lesion were confirmed in all normal tissue specimens. Histopathological analysis was performed on H&E-stained sections from the paraffin tissue block to estimate, for each case, the proportions of tumor and normal epithelial cells, fibroblasts, and fat as well as to determine the levels of inflammation and Nottingham grade scores. Six tumors were ER− (ER < 3 fmol/mg protein), with PR values ranging from 4.9 to 11.2 fmol/mg protein, as measured by ligand binding assay. Seven tumors were ER+ (ER values ranging from 3.5 to 134 fmol/mg protein), with PR values ranging from 5.8 to 134 fmol/mg protein. These tumors spanned a wide range of grade (grade 5–9), determined using the Nottingham grading system.

In a second experiment, 40 invasive ductal breast carcinomas were selected from the NCIC-Manitoba Breast Tumor Bank (Winnipeg, Manitoba, Canada). The cases were selected for ER and PR status, as determined by ligand binding assays. Ten tumors were classified as ER+/PR+ (ER range, 50–127 fmol/mg protein; PR range, 105–285 fmol/mg protein), 10 tumors were classified as ER+/PR− (ER range, 59–156 fmol/mg protein; PR range, 5–10 fmol/mg protein), 10 tumors were ER−/PR− (ER range, 0–2 fmol/mg protein; PR range, 0–10 fmol/mg protein), and 10 tumors were classified as ER−/PR+ (ER range, 5–9 fmol/mg protein; PR range, 51–271 fmol/mg protein).

Received 2/23/99; revised 5/3/99; accepted 5/4/99.

The costs of publication of this article were defrayed in part by the payment of page charges. This article must therefore be hereby marked *advertisement* in accordance with 18 U.S.C. Section 1734 solely to indicate this fact.

[1] This work was supported by grants from the Canadian Breast Cancer Research Initiative and the United States Army Medical Research and Materiel Command. The Manitoba Breast Tumor Bank is supported by funding from the NCIC. L. C. M. is a Medical Research Council of Canada Scientist, P. W. is a Medical Research Council of Canada Clinician-Scientist, and E. L. is a recipient of a United States Army Medical Research and Materiel Command Postdoctoral Fellowship.

[2] To whom requests for reprints should be addressed. Phone: (204) 789-3233; Fax: (204) 789-3900; E-mail: lcmurph@cc.umanitoba.ca.

[3] The abbreviations used are: CY3PA, cytochrome P450 monooxygenase 3A4; NCIC, National Cancer Institute of Canada; ER, estrogen receptor; PR, progesterone receptor; GAPDH, glyceraldehyde-3-phosphate dehydrogenase; RT-PCR, reverse transcription-PCR.

Ligand Binding Assays for ER and PR. Available steroid receptors were assayed using a single saturating dose of [^{3}H]ligand plus 500-fold excess of unlabeled ligand and incubated overnight at 4°C, and the bound and free steroids were separated using the charcoal-dextran method. ER and PR concentrations were expressed as fmol of steroid specifically bound per mg of cytosol protein, as described previously (9).

Cell Culture. Human breast cancer cells were grown in DMEM supplemented with 5% fetal bovine serum, 100 nM glutamine, 0.3% (v/v) glucose, and penicillin/streptomycin, as described previously (10). The cells were grown until they were ~80% confluent, and they were harvested by scraping with a rubber policeman. After centrifugation, the cell pellet was frozen and stored at −70°C until RNA was isolated.

RNA Extraction and RT-PCR conditions. Total RNA was extracted from 20-μm frozen tissue sections (15 and 5 sections for normal and tumor breast tissue, respectively) or frozen cell pellets using Trizol reagent (Life Technologies, Inc., Grand Island, NY), according to the manufacturer's instructions. One μg of total RNA was reverse-transcribed in a final volume of 25 μl, as described previously (11).

The primers used consisted of hPXR-U primer (sense, 5′-CAAGCGGAAGAAAAGTGAACG-3′; nucleotides 678–698 of *hPXR*) and hPXR-L primer (antisense, 5′-CTGGTC-CTCGATGGGCAAGTC-3′; nucleotides 1119–1099 of *hPXR*). The nucleotide positions given correspond to published sequences of the human PXR cDNA (2). PCR amplifications were performed, and PCR products were analyzed as described previously, with modifications (11). Briefly, 1 μl of reverse transcription mixture was amplified in a final volume of 15 μl, in the presence of 1.5 μCi of [α-^{32}P]dCTP (3000 Ci/mmol), 4 ng/μl hPXR-U/hPXR-L, and 0.4 unit of Hot Start Taq DNA polymerase (Qiagen, Mississauga, Ontario, Canada). Each PCR consisted of 20 min at 95°C, followed by 35 cycles of 30 s at 94°C, 30 s at 60°C, and 30 s at 72°C. PCR products were then separated on 6% polyacrylamide gels containing 7 M urea. Following electrophoresis, the gels were dried and autoradiographed. Amplification of the ubiquitously expressed *GAPDH* cDNA was performed in parallel, and PCR products were separated on agarose gels stained with ethidium bromide, as described previously (11). PCR products were subcloned and sequenced as described previously (11).

Quantification and Statistical Analysis. Quantification of signals was carried out by excision of the bands corresponding to hPXR cDNAs (wild-type and variant cDNAs), addition of scintillant, and counting. Three independent PCRs were performed. To control for variations between experiments, a value of 100% was assigned to the sum of hPXR-related signals (wild-type plus variant, when present) measured in one of the tumor samples arbitrarily chosen (case 1) and used as the reference in all individual PCR assays. For each sample, the sum of hPXR-related signals (wild-type plus variant, when present) was expressed as the percentage of the case 1 value. In parallel, *GAPDH* cDNA was amplified, and following analysis of PCR products on prestained agarose gels, signals were quantified by scanning using NIH Image 161/ppc software. Two independent *GAPDH* PCRs were performed. Each *GAPDH* signal was also expressed as a percentage of the *GAPDH* value measured in case 1. For each sample, the average of the hPXR values was then expressed as a percentage of the average of the *GAPDH* signals. Only samples (n = 13 for the tumor and matched normal experiment; n = 30 for the ER/PR tumor experiment), which demonstrated a reproducible wild-type hPXR signal (present or absent, see "Results"), were included in the statistical analysis. Differences in hPXR mRNA expression between groups were tested using the Mann-Whitney rank sum test (two-sided).

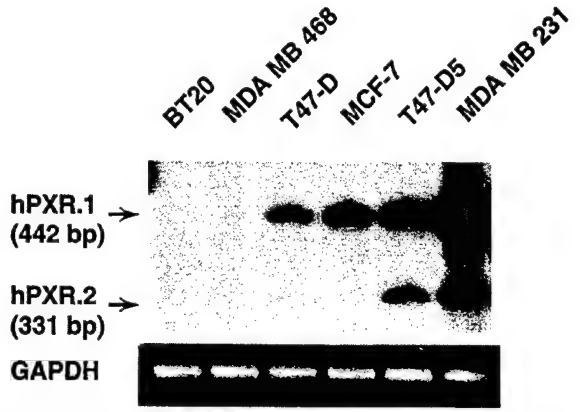

Fig. 1 Expression of hPXR mRNA and a variant hPXR mRNA in human breast cancer cell lines. *Top*, total RNA was extracted from six human breast cancer cell lines. Radiolabeled RT-PCR products using primers for human PXR and 35 cycles of PCR, separated by 6% PAGE containing 7 M urea, are shown. The hPXR.1 or wild-type product is 442 bp. The hPXR.2 or variant product is 331 bp. *Bottom*, amplification of *GAPDH* in the same six human breast cancer cell lines. The *GAPDH* PCR product was visualized by ethidium bromide staining of agarose gels.

RESULTS

Expression of hPXR mRNA and a Variant hPXR mRNA in Human Breast Cancer Cell Lines. A RT-PCR approach was used to determine whether mRNA for hPXR was expressed in human breast cancer cell lines. In several human breast cancer cell lines, an expected 442-bp product was detected in T-47D, MCF-7, T-47D-5, and MDA-MB-231 but not in BT20 or MDA-MB-468 human breast cancer cells (Fig. 1). The ER− MDA-MB-231 cell line expressed the highest level of hPXR mRNA. However, the expression of hPXR mRNA was not related to the absolute ER status of the cell line in this small set of cell lines because both ER+ (T-47D and MCF-7) and ER− (MDA-MB-231) cells expressed hPXR mRNA. In some cell lines (T-47D-5 and MDA-MB-231), a smaller-sized PCR product of 331 bp was observed. Both of these PCR products were cloned and sequenced. The larger 442-bp product had a nucleotide sequence that was identical to that previously published for the human PXR cDNA (2). The 331-bp product was deleted in 111 nucleotides, which correspond to nucleotides 823–933 of the hPXR cDNA, as numbered in Lehmann *et al.* (2). This is an in-frame deletion in which 37 amino acids (residues 174–210) are deleted in the putative ligand-binding domain (Fig. 2). The protein predicted to be encoded by this variant hPXR mRNA, assuming there are no other alterations in

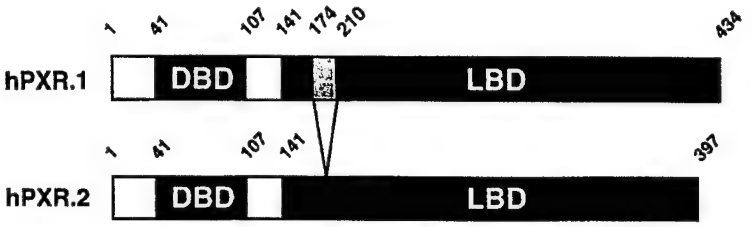

Fig. 2 Diagrammatic representation of the protein predicted to be encoded by the variant hPXR mRNA. hPXR.1 represents the wild-type human PXR (2). hPXR.2 represents the deleted PXR variant. *Numbers* represent the amino acid residues. *DBD*, DNA-binding domain; *LBD*, ligand-binding domain.

the mRNA, would be 397 amino acids, unlikely to bind ligand or have a markedly altered ligand profile compared to that of the "wild-type" hPXR (1). This variant human hPXR mRNA has not been reported previously and is similar but not identical to the mouse PXR.2, which contains an in-frame 123-nucleotide deletion predicting a 41-amino acid deletion in a similar region of the ligand-binding domain (1).

Identification of hPXR mRNA and a Variant hPXR mRNA in Human Breast Tissues. A RT-PCR approach was used to determine whether hPXR mRNA was expressed in human breast tissues *in vivo* (Fig. 3). The expected PCR products corresponding to the wild-type hPXR and the deleted hPXR cDNAs were detected in both normal and neoplastic human breast tissues. The normal tissues corresponded to the matched adjacent normal breast tissue of each breast tumor examined. Using parallel PCRs for the ubiquitous *GAPDH* mRNA for normalization, it appeared that the levels of hPXR and its deleted variant mRNA varied among the samples, but there were no quantitative differences seen between the normal tissues and their matched breast tumor samples (Fig. 3). Overall, there were no obvious differences in the pattern of hPXR mRNA expression between any one matched normal sample and its corresponding tumor, although the expression of the variant hPXR was not always seen (Fig. 3, *Lanes 5*, *6*, and *8*).

Relationship of hPXR mRNA Expression with ER and PR Status in Primary Human Breast Tumors. To address the question of whether the expression of hPXR in breast tumors could potentially influence the efficacy of endocrine therapy, we investigated the relationship of hPXR mRNA expression to the known prognostic and treatment response variables, ER and PR. Four groups of breast tumor samples were identified according to their ER/PR status, as defined by ligand binding analysis (see "Materials and Methods"). hPXR mRNA levels were measured by RT-PCR and normalized to the *GAPDH* mRNA level, as measured in parallel by RT-PCR. Results obtained are shown in Fig. 4. Only samples ($n = 13$ for the tumor and matched normal experiment; $n = 30$ for the ER/PR tumor experiment) that demonstrated a reproducible wild-type hPXR signal (present or absent, see "Materials and Methods") were included in the statistical analysis. Furthermore, total hPXR-like PCR products (wild-type plus the variant) in any sample were used in the quantification of hPXR mRNA expression for statistical analysis. A statistically significant inverse relationship was found between the level of hPXR mRNA expression and ER status, as defined by ligand binding analysis. The level of hPXR mRNA expression in ER− tumors (median = 46.7, $n = 15$) was significantly higher ($P = 0.04$) than the level of hPXR mRNA expression in ER+ tumors (median = 22.4, $n = 15$), as shown in Fig. 4*B*. No relationship with PR status was found.

Spearman correlation analysis showed no significant correlations of the level of hPXR mRNA with grade, age, nodal status, or the percentage of normal duct and lobular epithelium, stromal, or fat cell content within the tissue section analyzed. However, consistent with the above results (for which clinically relevant cutoff values for both ER and PR status were applied), a trend toward an inverse relationship was found between hPXR mRNA expression and the absolute level of ER, as measured by ligand binding analysis (Spearman $r = -0.50$, $P = 0.07$).

DISCUSSION

The data presented here provide evidence that the novel nuclear orphan receptor hPXR is expressed in both normal and neoplastic human breast tissues. As yet, there are no available antibodies to the hPXR protein to complement this investigation. Recombinantly expressed hPXR protein has been shown to activate transcription of reporter genes through a response element conserved in the promoter of the *CYP3A* genes (1, 2), suggesting the possibility that hPXR might be a transcriptional regulator of CYP3A enzyme expression (2). Because these CYP3A enzymes have also been found in human breast cancer tissues (6, 7), we hypothesized that hPXR/CYP3A-regulated pathways might play a role in human breast cancer.

The CYP3A enzymes, the expression of which is likely to be modulated, at least in part, by hPXR, are known to be involved in the metabolism of a wide range of xenobiotics, natural and synthetic steroids, and antisteroids, including tamoxifen and toremifene (3–5, 12, 13). Our observation that hPXR is expressed in both normal and neoplastic breast tissue opens the possibility that local metabolism and the factors regulating local metabolism may have a role in the responsiveness of human breast cancers to endocrine therapies. Indeed, altered uptake and retention of tamoxifen and possible altered local metabolism have been suggested as possible mechanisms of tamoxifen resistance in some human breast cancers (14, 15). Also, the antiglucocorticoid/antiprogestin compound RU-486 was shown to be a relatively potent activator of hPXR (1). RU-486 has shown some efficacy as an endocrine therapy in human breast cancer (16); therefore, the interaction of RU-486 with PXR in human breast tissues, both normal and neoplastic, might be important to assess with respect to drug resistance and/or drug interactions.

Although the natural ligand for hPXR is unknown, the observations that high concentrations of several natural hormones, *e.g.*, pregnenolone and progesterone, and synthetic preg-

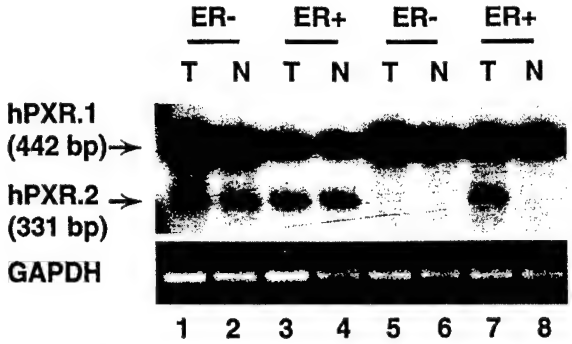

Fig. 3 Expression of hPXR mRNA and a variant hPXR mRNA in human breast tumor biopsies and their matched normal adjacent breast tissues. *Top*, total RNA was extracted from human breast cancer biopsy samples (*Lanes T*) and their matched adjacent normal breast tissues (*Lanes N*). Radiolabeled RT-PCR products using primers for human PXR and 35 cycles of PCR, separated on 6% PAGE containing 7 M urea, are shown. The hPXR.1 or wild-type product is 442 bp. The hPXR.2 or variant product is 331 bp. Both ER+ and ER− tumors were analyzed. *Bottom*, amplification of *GAPDH* in the same human breast tissue samples. The *GAPDH* PCR product was visualized by ethidium bromide staining of agarose gels.

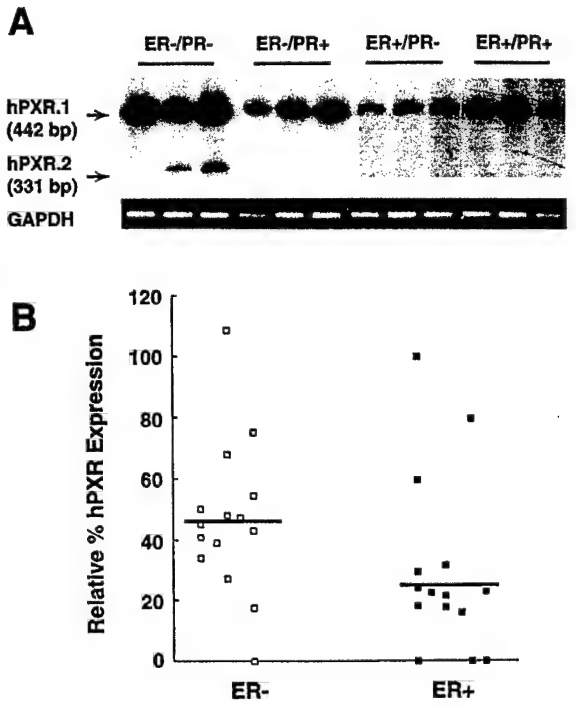

Fig. 4 Relationship of expression of hPXR-like mRNA to ER and PR status in human breast tumors. *A*, total RNA was extracted from human breast cancer biopsy samples of known ER (+ or −) and PR (+ or −) status, as defined by ligand-binding assays. Radiolabeled RT-PCR products using primers for human PXR and 35 cycles of PCR, separated on 6% PAGE containing 7 M urea, are shown. The hPXR.1 or wild-type product is 442 bp. The hPXR.2 or variant product is 331 bp. *Bottom*, amplification of *GAPDH* in the same human breast cancer biopsy samples. The *GAPDH* PCR product was visualized by ethidium bromide staining of agarose gels. *B*, relative PXR signals quantified as described in "Materials and Methods" are presented for ER− and ER+ breast tumors. The median of the values obtained in each group is indicated by a *solid line*.

nenolone derivatives, such as pregnenolene 16α-carbonitrile, can activate hPXR have led to its being named the pregnane X receptor (1). It is unlikely that the concentrations required for any of these individual compounds that activate hPXR *in vitro* could be achieved in the circulation under physiological conditions; tissue accumulation levels and the possible additive effects of the various potential ligand activators of this receptor, which is activated by a wide spectrum of compounds, are unknown.

Our interest is in factors that could influence responsiveness to the so-called endocrine or hormonal therapies in human breast cancers, and we, therefore, investigated the relationship of hPXR expression to ER and PR status, which are known markers of treatment response to endocrine therapies and are also used as prognostic markers in human breast cancer (17). We observed that, in human breast tumors, the expression of hPXR was inversely correlated with the expression of ER, suggesting that hPXR-mediated pathways might be more active in breast tumors which are less likely to respond to endocrine therapies. This remains to be tested in samples of breast tumors from patients with known responses to endocrine therapies in clinical trials.

We have also investigated whether altered expression of hPXR occurs between matched normal and neoplastic breast tissues from histopathologically defined tissue sections. In this study, we found no significant difference in hPXR expression between matched normal and neoplastic breast tissues. The ER status of these normal tissues was not determined; however, given that normal tissue is often ER− and ER+ cells are a minor component (18) and that the epithelial cell content among the typical relatively sparse ducts and lobular units found in normal tissue is lower than in tumor sections (13.5 ± 6.6% *versus* 40.4 ± 13.6%, respectively, in this study), these results suggest that average hPXR expression is, in fact, high in normal epithelia, which is consistent with the inverse relationship between ER status and hPXR seen in tumors. This interpretation suggests that hPXR is not significantly altered during tumorigenesis but may show changes in relation to altered differentiation and phenotype in tumors.

This is the first description of a human PXR variant mRNA that contains an in-frame deletion of 111 nucleotides corresponding to a deletion of nucleotides 823–933 of the wild-type hPXR mRNA and is most likely generated by an alternative splicing mechanism. This variant is similar but not identical to mouse PXR.2, which contains an in-frame 123-nucleotide deletion in a similar region of the ligand-binding domain (1). The mouse PXR.2, compared to the mouse PXR.1, showed a markedly reduced profile with respect to the agents that could activate the wild-type receptor in transient transfection analyses (1). It is possible that the human variant PXR may display a similar profile or may be unable to bind ligand. In this study, the presence or absence of this variant hPXR mRNA was not correlated with tumorigenesis or with ER/PR status.

In conclusion, we have identified the expression of human PXR mRNA and a hPXR variant mRNA in both normal and

neoplastic human breast tissues. The expression of human PXR mRNA in breast tumors was inversely correlated with expression of ER, as determined by ligand binding assay. These data raise the possibility that hPXR may play a role in human breast tissues.

ACKNOWLEDGMENTS

We thank Caroline Cumins-Leygue and Helen Bergen for laboratory assistance with the cell culture.

REFERENCES

1. Kliewer, S., Moore, J., Wade, L., Staudinger, J., Watson, M., Jones, S., McKee, D., Oliver, B., Willson, T., Zetterstrom, R., Perlmann, T., and Lehmann, J. An orphan nuclear receptor activated by pregnanes defines a novel steroid signaling pathway. Cell, *92:* 73–82, 1998.

2. Lehmann, J., McKee, D., Watson, M., Willson, T., Moore, J., and Kliewer, S. The human orphan nuclear receptor PXR is activated by compounds that regulate *CYP3A4* gene expression and cause drug interactions. J. Clin. Invest., *102:* 1016–1023, 1998.

3. Mani, C., Gelboin, H., Park, S., Pearce, R., Parkinson, A., and Kupfer, D. Metabolism of the antimammary cancer antiestrogenic agent tamoxifen. 1. Cytochrome P-450-catalyzed *N*-demethylation and 4-hydroxylation. Drug Metab. Dispos., *21:* 645–656, 1993.

4. Berthou, F., Dreano, Y., Belloc, C., Kangas, L., Gautier, J-C., and Beaune, P. Involvement of cytochrome P450 3A enzyme family in the major metabolic pathways of toremifene in human liver microsomes. Biochem. Pharmacol., *47:* 1883–1895, 1994.

5. Mani, C., Pearce, R., Parkinson, A., and Kupfer, D. Involvement of cytochrome P4503A in catalysis of tamoxifen activation and covalent binding to rat and human liver microsomes. Carcinogenesis (Lond.), *15:* 2715–2720, 1994.

6. Huang, Z., Fasco, M., Figge, H., Keyomarsi, K., and Kaminsky, L. Expression of cytochromes P450 in human breast tissue and tumors. Drug Metab. Dispos., *24:* 899–905, 1996.

7. Smith, G., Harrison, D., East, N., Rae, F., Wolf, H., and Wolf, C. Regulation of cytochrome P450 gene expression in human colon and breast tumour xenografts. Br. J. Cancer, *68:* 57–63, 1993.

8. Hiller, T., Snell, L., and Watson, P. Microdissection/RT-PCR analysis of gene expression. Biotechniques, *21:* 38–44, 1996.

9. Murphy, L., Lee-Wing, M., Goldenberg, G., and Shiu, R. Expression of the gene encoding a prolactin-inducible protein by human breast cancers *in vivo*: correlation with steroid receptor status. Cancer Res., *47:* 4160–4164, 1987.

10. Murphy, L. C., and Dotzlaw, H. Regulation of transforming growth factor alpha and transforming growth factor β messenger ribonucleic acid abundance in T-47D, human breast cancer cells. Mol. Endocrinol., *3:* 611–617, 1989.

11. Dotzlaw, H., Leygue, E., Watson, P., and Murphy, L. Expression of estrogen receptor-β in human breast tumors. J. Clin. Endocrinol. Metab., *82:* 2371–2374, 1997.

12. Nebert, D., and Gonzalez, F. P450 genes: structure, evolution and regulation. Annu. Rev. Biochem., *56:* 945–993, 1987.

13. Juchau, M. Substrate specificities and functions of the P450 cytochromes. Life Sci., *47:* 2385–2394, 1990.

14. Osborne, C., Coronado, E., Allred, D., Wiebe, V., and DeGregorio, M. Acquired tamoxifen resistance: correlation with reduced breast tumor levels of tamoxifen and isomerization of *trans*-4-hydroxytamoxifen. J. Natl. Cancer Inst., *83:* 1477–1482, 1991.

15. Osborne, C., Wiebe, V., McGuire, W., Ciocca, D., and DeGregorio, M. Tamoxifen and the isomers of 4-hydroxytamoxifen in tamoxifen resistant tumors from breast cancer patients. J. Clin. Oncol., *10:* 304–310, 1992.

16. Goldberg, J., Plescia, M., and Anastasio, G. Mifepristone (RU 486): current knowledge and future prospects. Arch. Fam. Med., *7:* 219–222, 1998.

17. Ravdin, P., Green, S., Dorr, T., McGuire, W., Fabian, C., Pugh, R., Carter, R., Rivkin, S., Borst, J., Belt, R., Metch, B., and Osborne, C. Prognostic significance of progesterone receptor levels in estrogen receptor-positive patients with metastatic breast cancer treated with tamoxifen: results of a prospective Southwest Oncology Group study. J. Clin. Oncol., *10:* 1284–1291, 1992.

18. Petersen, O. Frequency and distribution of estrogen receptor positive cells in normal non-lactating human breast. Cancer Res., *47:* 5748–5751, 1987.

British Journal of Cancer (1999) 80(3/4), 379–382
© 1999 Cancer Research Campaign
Article no. bjoc.1998.0366

Altered expression of exon 6 deleted progesterone receptor variant mRNA between normal human breast and breast tumour tissues

E Leygue[1], H Dotzlaw[1], PH Watson[2] and LC Murphy[1]

[1]Departments of Biochemistry and Molecular Biology and [2]Pathology, University of Manitoba, Faculty of Medicine, 770 Bannatyne Avenue, Winnipeg, Manitoba, Canada R3E 0W3

Summary The progesterone receptor (PR) is an important prognostic marker in breast cancer as well as a marker of responsiveness to endocrine therapies. The presence of several exon-deleted PR variant mRNAs in both normal and neoplastic breast samples has recently been reported. Amongst them, a variant mRNA deleted in exon 6 (D6-PR mRNA) that if translated would encode a truncated PR-like protein missing the hormone binding domain and one of the transactivating domains of the wild-type PR protein. In order to determine whether changes in D6-PR variant expression could occur during tumorigenesis, its expression was investigated by reverse transcription and polymerase chain reaction in ten normal reduction mammoplasty samples, nine breast tumours with high PR levels (> 100 fmol mg^{-1} protein) and eight breast tumours with low PR levels (< 15 fmol mg^{-1} protein), as determined by ligand binding assay. The relative expression of D6-PR to wild-type PR mRNA was lower ($P < 0.01$) in normal than in all tumour breast samples. Moreover, a trend to lower ($P < 0.1$) relative D6-PR expression was observed in high PR tumours, compared to low PR tumours. These data suggest that increased expression of D6-PR occurs during tumorigenesis.

Keywords: progesterone receptor; breast cancer; tumour progression; variant mRNA

The progesterone receptor (PR) is an important prognostic marker in breast cancer (Horwitz et al, 1975). Oestrogen receptor (ER)-positive breast tumours that also contain PR are considered 'good prognosis' tumours and are likely to respond to endocrine therapies (Horwitz et al, 1978). In contrast, absence of PR often characterizes 'poor prognosis' tumours (ER + PR–) and resistance to endocrine therapy (McGuire et al, 1991).

Similar to other members of the steroid receptor superfamily, PR is divided into structural domains (A–E) (Figure 1), the functions of which are widely documented (Tsai and O'malley, 1994). Two different PR isoforms, PR-A and PR-B, that are encoded by mRNAs transcribed from the same gene under the control of two different promoters (Kastner et al, 1990), have been identified in both normal and neoplastic tissues (Figure 1). The presence of several exon-deleted PR variant mRNAs in both normal and neoplastic breast samples has recently been reported (Leygue et al, 1996*a*; Richer et al, 1998; Yeates et al, 1998). Amongst them was a variant mRNA deleted in exon 6 (D6-PR mRNA) that, if translated, would encode a PR-A-like and/or a PR-B-like protein containing a truncated E domain. This variant, missing the hormone binding domain and one of the transactivating domains (AF-2) of the wild-type (WT) PR protein, has been shown to act in-vitro as a dominant-negative transcriptional inhibitor of PR-A and PR-B isoforms (Richer et al, 1998). Because expression of analogous exon-deleted or truncated variants has been associated with tumour progression in the case of ER variant mRNAs (for review see Murphy et al, 1997), it was of interest to determine whether D6-PR variant expression was also modified during tumorigenesis. In this study, we investigated D6-PR variant expression by reverse transcription polymerase chain reaction (RT-PCR) in ten normal reduction mammoplasties samples, nine breast tumours with high PR levels (considered 'good prognostic' tumours) and eight breast tumours with low PR levels (considered 'poor prognosis' tumours).

Received 3 June 1998
Revised 28 October 1998
Accepted 4 November 1998

Correspondence to: E Leygue

MATERIALS AND METHODS

Human breast tissues

Human breast specimens (27 cases) were from the Manitoba Breast Tumor Bank (Winnipeg, Manitoba, Canada). The processing of specimens collected in the Manitoba Breast Tumor Bank has already been described (Hiller et al, 1996). Briefly, each specimen was rapidly frozen as soon as possible after surgical removal. A portion of the frozen tissue block was processed to create a paraffin-embedded tissue block matched and orientated relative to the remaining frozen block. These paraffin blocks provide high quality histologic sections, which are used for pathologic interpretation and assessment and are mirror images of the frozen sections used for RNA extractions. For each case, tumour and normal tissues were histologically characterized by observation of paraffin sections. The presence of normal ducts and lobules as well as the absence of any proliferative lesion were confirmed in all ten normal reduction mammoplasties specimens. The 17 primary invasive ductal breast carcinomas were associated with high ER levels ranging from 105 to 386 fmol mg^{-1} protein (mean = 190.7 fmol mg^{-1} protein, standard deviation (s.d.) = 58.49), as determined by ligand binding assay. Within this group,

nine tumours had a high PR level (PR > 100 fmol mg^{-1} protein, mean = 156.4 fmol mg^{-1} protein, s.d. = 28.4) and eight had a low PR level (PR < 15 fmol mg^{-1} protein, mean = 8.6 fmol mg^{-1} protein, s.d. = 4.6), as determined by ligand binding assay. The ages of patients associated with the tumour samples ranged from 37 to 91 (mean: 70 years old, s.d.: 14.4 years). For reduction mammoplasties, women were younger, with ages ranging from 19 to 41 years old (mean: 31.3 years old, s.d.: 8.3 years). Total RNA was extracted from frozen tissue and reverse transcribed in a final volume of 15 µl as previously described (Leygue et al, 1996*b*).

PCR and identification of PCR products

The primers used consisted of D6U primer (5′-CTCT-CATTCAGTATTCTTGG-3′; sense; located in PR exon 5; 2989–23008) and D6L primer (5′-TGGGTTTGACTTCGTAGC-3′; antisense; located in PR exon 7; 3262–3245). The nucleotide positions correspond to published sequences of the human PR cDNA (Kastner et al, 1990). PCR amplifications were performed and PCR products analysed as previously described, with minor modifications (Leygue et al, 1996*b*). Briefly, 1 µl of reverse transcription mixture was amplified in a final volume of 10 µl, in the presence of 10 nmol^{-1} [α-^{32}P] dCTP, 4 ng µl^{-1} of each primer and 0.3 unit of *Taq* DNA polymerase. Each PCR consisted of 40 cycles (30 s at 60°C and 30 s at 94°C). As positive controls, aliquots of plasmid DNA containing previously (Leygue et al, 1996a) subcloned WT-PR (WT cont) or exon 6-deleted PR (D6 cont) sequences were amplified in parallel. PCR products were then separated on 6% polyacrylamide gels containing 7 M urea (PAGE). Following electrophoresis, the gels were dried and autoradiographed. The PCR product corresponding in size to D6-PR was subcloned and sequenced as previously described (Leygue et al, 1996*b*).

Quantification and statistical analysis

The approach used to evaluate the exon-deleted variant mRNA expression relative to WT mRNA has been previously validated for exon-deleted ER variant mRNAs (Daffada et al, 1994; Leygue et al, 1996*b*). PCR co-amplification of WT and exon-deleted variant generates two bands whose ratio is constant with varying cycle number and is independent of initial input cDNA. This assay provides a semi-quantitative RT-PCR in which the internal control is the WT mRNA co-amplified and in which relative expression of variant mRNA can be determined for individual samples. Bands corresponding to D6-PR and WT mRNAs were excised from the gel and corresponding signals were subsequently measured after addition of 5 ml scintillant (ICN Pharmaceuticals, Inc., Irvine, CA USA) by counting. The D6-PR signal was expressed as a percentage of the WT-PR signal. For each sample, three independent assays were performed and the mean determined. The statistical significance of differences in the relative levels of expression of D6-PR mRNAs was determined using the Mann–Whitney rank-sum test (two-sided).

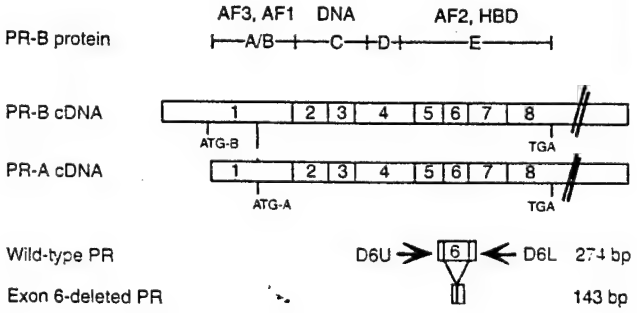

Figure 1 Schematic representation of PR-B protein, PR-B and PR-A cDNAs and primers used to co-amplify WT-PR and D6-PR variant cDNAs. PR cDNAs contain eight different exons coding for a protein divided into structural and functional domains (A–E). A/B region of the receptor contains two transactivating domains (AF3 and AF1). The C region contains the DNA binding domain whereas region E, which is involved in hormone binding, contains another transactivating domain (AF2). ATG-B and ATG-A are the translational start sites of PR-B and PR-A proteins respectively. TGA, stop codon. D6U and D6L primers allow co-amplification of 274 bp and 143 bp fragments corresponding to WT-PR and D6-PR mRNAs, respectively

RESULTS

Detection of D6-PR in all normal and tumour breast tissues

Total RNA from ten normal breast tissues and 17 breast tumour specimens was analysed by RT-PCR as described in Material and Methods using primers depicted in Figure 1. These primers were designed to allow the co-amplification of D6-PR and WT-PR mRNAs. Among the 17 tumours studied, nine had a high PR level (> 100 fmol mg protein) and eight had a low PR level (< 15 fmol mg^{-1} protein), as

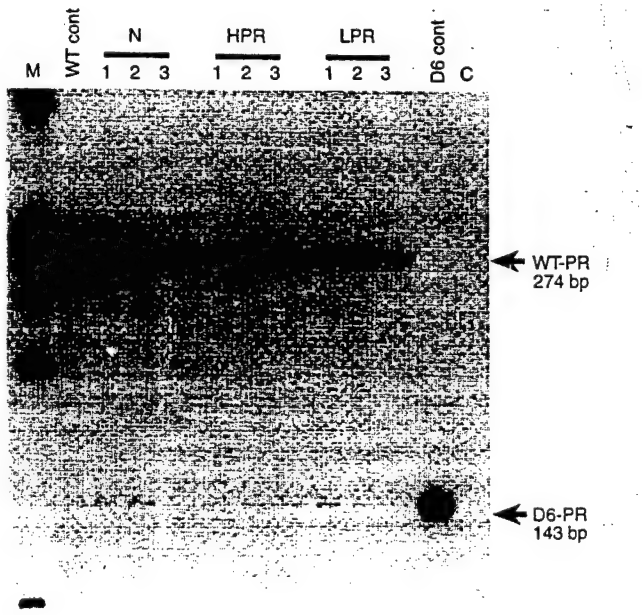

Figure 2 Detection of exon 6-deleted PR variant mRNA in all human breast samples. Total RNA extracted from normal (N1–3), high PR tumour (HPR1–3) and low PR tumour (LPR1–3) breast tissue samples was reverse transcribed and PCR-amplified as described in Material and Methods, using D6U and D6L primers. Radioactive PCR products were separated on a 6% acrylamide gel and visualized by autoradiography. Bands that migrated at 274 bp and 143 bp were identified as corresponding to WT-PR and exon 6-deleted PR variant mRNAs, respectively. Plasmids containing either WT-PR (WT cont) or exon 6-deleted PR (D6 cont) sequences were used as positive control. M: molecular weight marker (φx 174 HaeIII digest, Gibco BRL, Grand Island, NY, USA). C: no cDNA added during the PCR reaction

determined by ligand binding assay. In each sample, two major bands that corresponded in size to that expected for WT-PR and D6-PR PCR products were obtained. Figure 2 presents a typical autoradiograph after one night's exposure. It should be noted that a longer exposure or addition of intensifying screens allowed the detection of D6-PR in both lanes N3 and LPR3 (data not shown). One should also note the presence, in samples where WT-PR signal is high (such as in lane N2, Figure 2), of some minor PCR products, that are not reproducibly obtained and therefore were not further characterized. The PCR product corresponding in size to D6-PR and reproducibly obtained was subcloned and subsequently sequenced. Sequence analysis showed the expected perfect junction between exon 5 and exon 7 (data not shown).

Comparison of D6-PR variant expression in normal and tumour tissues

The D6-PR variant mRNA expression relative to WT-PR was then evaluated in each sample. It has been previously demonstrated that the co-amplification of WT and exon-deleted variant transcripts led to the synthesis of two PCR products. Further, the ratio of the signals obtained from these two products could be used to compare relative exon-deleted variant expression within samples (Daffada et al, 1994; Leygue et al, 1996*b*). The signal corresponding to D6-PR was expressed as a percentage of the WT-PR signal and the mean of three different assays calculated (Figure 3). The level of exon 6-deleted variant mRNA relative to the WT-PR mRNA was found to be significantly ($P < 0.05$) lower in normal (median = 4.8%) than in neoplastic breast tissues having either high PR or low PR (median = 9.19% and median = 25.13% respectively). The significance became higher ($P < 0.01$) when the tumour subgroups were considered together (median = 13.86%). Moreover, even though the difference did not achieve statistical significance ($0.1 < P < 0.05$), D6-PR relative expression appeared lower in tumours with high PR levels (median = 9.19%) than in tumours with low PR levels (median = 25.13%).

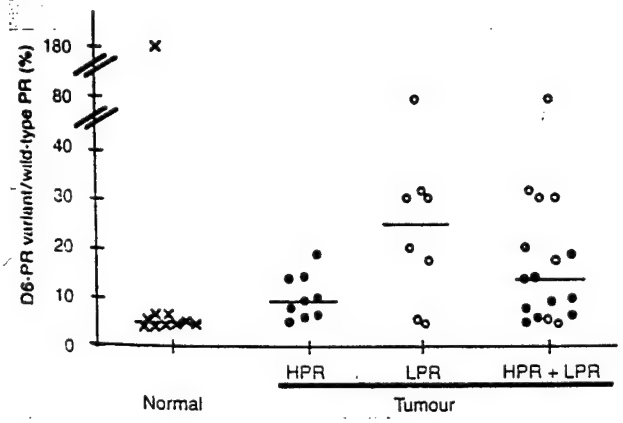

Figure 3 Comparison of D6-PR relative expression between normal and tumour samples. Total RNA extracted from ten normal breast samples (×), nine tumours with high PR (●, HPR) and eight tumours with low PR (○, LPR) was reverse transcribed and PCR-amplified as described in Material and Methods, using D6U and D6L primers. D6-PR corresponding signal was measured as described in Material and Methods and expressed as a percentage of wild-type PR corresponding signal. For each sample, the mean of three different experiments is indicated. Bars: medians

DISCUSSION

This study shows that the relative expression of D6-PR variant mRNA is altered between normal breast tissue and breast cancer tissue samples. The expression of D6-PR variant mRNA relative to WT-PR mRNA was investigated using a previously described semi-quantitative RT-PCR assay (Daffada et al, 1994; Leygue et al, 1996*b*). This assay allows the determination of the expression of PR variant mRNA relative to WT-PR mRNA using the very small amount of starting material provided by histopathologically well-characterized regions within human breast tissue.

It is important to establish whether or not this differential expression of D6-PR variant is maintained at the protein level. Anti-PR antibodies available to date (such as hPRa-7; Clarke et al, 1987), while able to recognize the predicted PR variant proteins, cannot provide any information on the unique primary sequence of the recognized molecule (Yeates et al, 1998). We are in the process of developing an antibody, raised against the predicted 12 specific C-terminal amino acids of the D6-PR protein (Leygue et al, 1996*a*) that could be used for the specific immunochemical detection of D6-PR variant protein within paraffin-embedded breast tissue sections or by Western blotting.

The recombinant D6-PR protein, has recently been shown to bind constitutively the progesterone receptor element (PRE) DNA consensus sequence and to exhibit dominant-negative activity on PR-A-and PR-B-induced transcription (Richer et al, 1998). Interestingly, a naturally occurring ER variant mRNA deleted in exon 7 and encoding an analogous truncated molecule lacking the hormone binding domain of the WT-ER can also act as a dominant-negative regulator of WT-ER, at least under some circumstances (Wang and Miksicek, 1991; Fuqua et al, 1992).

Relative levels of some of the ER variants were found to be increased during tumour progression. Exon 7-deleted variant mRNA level was shown to be higher in ER + PR – versus ER + PR + tumours (Fuqua et al, 1992). Exon 5-deleted ER variant mRNA expression was found higher in ER – PR + versus ER + PR + tumours (Fuqua et al, 1991) and was decreased in normal versus tumour breast tissues (Leygue et al, 1996*b*). It has thus been speculated that expression of these ER variants may be altered during breast tumorigenesis and progression and may have a role in progression from hormone dependence to independence in breast cancer (Murphy et al, 1997). This aspect of tumour progression consists of altered oestrogen signalling, the acquisition of resistance to the cytostatic effects of the anti-oestrogen tamoxifen and subsequently in the failure to respond to agents such progestins and probably antiprogestins (RU 486) (Horwitz et al, 1995). The apparent lower relative expression of D6-PR in normal breast samples compared to tumour tissues, as well as in high PR tumours compared to low PR tumours, is therefore of interest, since normal tissue, high PR tumours and low PR tumours may represent steps in tumour progression which correlate with increasing relative D6-PR expression. In order to clarify such issues, larger numbers of samples require screening for D6-PR expression.

The measurement of PR is an important tool in clinical decision-making with respect to prognosis and treatment of human breast cancer. Furthermore, the level of PR expression provides important clinical information as shown by Clark et al (1983). As the use of enzyme-linked immunosorbent assays (ELISA) and immunohistochemical assays for PR detection increases, it is likely that variant PR expression will interfere with these assays. Such

capability of variant forms of receptor to possibly interfere with immunohistochemical detection of the WT molecule has recently been demonstrated for ER (Huang et al, 1997 and unpublished data).

In conclusion, we show in this study that exon 6-deleted PR variant mRNA relative expression is increased during breast tumorigenesis. We speculate that PR variants may have a role in tumorigenesis and/or be a marker of breast cancer progression, as already suggested for ER variants.

ACKNOWLEDGEMENTS

This work was supported by grants from the Canadian Breast Cancer Research Initiative (CBCRI) and the US Army Medical Research and Materiel Command (USAMRMC). The Manitoba Breast Tumor Bank is supported by funding from the National Cancer Institute of Canada (NCIC). EL is a recipient of a USAMRMC Postdoctoral Fellowship, PHW is a Medical Research Council of Canada (MRC) Clinician-Scientist, LCM is an MRC Scientist.

REFERENCES

Clark GM, McGuire WL, Hubay CA, Pearson OH and Marshall JS (1983) Progesterone receptors as a prognostic factor in stage II breast cancer. *N Engl J Med* **309**: 1343–1347

Clarke CL, ZainoRJ, Feil PD, Miller JV, Steck ME, Ohlsson-Wilhem BM and Satyaswaroop PG (1987) Monoclonal antibodies to human progesterone receptor: characterization by biochemical and immunohistochemical techniques. *Endocrinology* **121**: 1123–1132

Daffada AA, Johnston SRD, Nicholls J and Dowsett M (1994) Detection of wild type and exon 5-deleted splice variant oestrogen receptor (ER) mRNA in ER-positive and -negative breast cancer cell lines by reverse transcription/polymerase chain reaction. *J Mol Endocrinol* **13**: 265–273

Fuqua SA, Fitzgerald SD, Chamness Gc, Tandon AK, McDonnell DP, Nawaz Z, O'Malley BW and McGuire WL (1991) Variant human breast tumor estrogen receptor with constitutive transcriptional activity. *Cancer Res* **51**: 105–109

Fuqua SA, Fitzgerald SD, Allred DC, Elledge RM, Nawaz Z, McDonnell DP, O'Malley BW, Greene GL and McGuire WL (1992) Inhibition of estrogen receptor action by a naturally occurring variant in human breast tumors. *Cancer Res* **52**: 483–486

Hiller T, Snell L and Watson PH (1996) Microdissection/RT-PCR analysis of gene expression. *Biotechniques* **21**: 38–44

Horwitz KB, McGuire WL, Pearson OH and Segaloff A (1975) Predicting response to endocrine therapy in human breast cancer: a hypothesis. *Science* **189**: 726–727

Horwitz KB, Koseki Y and McGuire WL (1978) Estrogen control of progesterone receptor in human breast cancer: role of estradiol and antiestrogen. *Endocrinology* **103**: 1742–1751

Horwitz KB, Tung L and Takimoto GS (1995) Novel mechanisms of antiprogestin action. *J Steroid Biochem Mol Biol* **53**: 9–17

Huang A, Leygue E, Snell L, Murphy LC and Watson PH (1997) Expression of estrogen receptor variant messenger RNAs and determination of estrogen receptor status in human breast cancer. *Am J Pathol* **150**: 1827–1833

Kastner P, Krust A, Turcotte B, Stropp U, Tora L, Gronemeyer H and Chambon P (1990) Two distinct estrogen-regulated promoters generate transcripts encoding the two functionally different human progesterone receptor forms A and B. *Embo J* **9**: 1603–1614

Leygue E, Dotzlaw H, Watson PH and Murphy LC (1996*a*) Identification of novel exon-deleted progesterone receptor variant mRNAs in human breast tissue. *Biochem Biophys Res Commun* **228**: 63–68

Leygue E, Watson PH and Murphy LC (1996*b*) Estrogen receptor variants in normal human mammary tissue. *J Natl Cancer Inst* **88**: 284–290

McGuire WL, Chamness GC and Fuqua SA (1991) Estrogen receptor variants in clinical breast cancer. *Mol Endocrinol* **5**: 1571–1577

Murphy LC, Leygue E, Dotzlaw H, Douglas D, Coutts A and Watson PH (1997) Oestrogen receptor variants and mutations in human breast cancer. *Ann Med* **29**: 221–234

Richer JK, Lange CA, Wierman AM, Brooks KM, Tung L, Takimoto GS and Horwitz KB (1998) Progesterone receptor variants found in breast cells repress transcription by wild-type receptors. *Breast Cancer Res Treat* **48**: 231–241

Tsai MJ and O'Malley BW (1994) Molecular mechanisms of action of steroid/thyroid receptor superfamily members. *Annu Rev Biochem* **63**: 451–486

Wang Y and Miksicek RJ (1991) Identification of a dominant negative form of the human estrogen receptor. *Mol Endocrinol* **5**: 1707–1715

Yeates C, Hunt SM, Balleine RL and Clarke CL (1998) Characterization of a truncated progesterone receptor protein in breast tumors. *J Clin Endocrinol Metab* **83**: 460–467

ELSEVIER

Molecular and Cellular Endocrinology 158 (1999) 153–161

MCE
Molecular and Cellular Endocrinology

www.elsevier.com/locate/mce

Estrogen receptor-α mRNA variants in murine and human tissues

Biao Lu [a], Helmut Dotzlaw [a], Etienne Leygue [a], Liam J Murphy [b], Peter H Watson [c], Leigh C Murphy [a,*]

[a] *Department of Biochemistry and Molecular Biology, University of Manitoba, 770 Bannatyne Avenue, Winnipeg, Canada R3E 0W3*
[b] *Department of Physiology, University of Manitoba, 770 Bannatyne Avenue, Winnipeg, Canada R3E 0W3*
[c] *Department of Pathology, University of Manitoba, 770 Bannatyne Avenue, Winnipeg, Canada R3E 0W3*

Received 19 January 1999; accepted 2 August 1999

Abstract

A side-by-side comparison of several normal mouse and human tissues was undertaken in order to determine if exon-deleted variant ER-α mRNAs are expressed in the mouse. The data showed that the complex pattern of ER-α alternative splicing that is detected in multiple human tissues was not apparent in murine tissues. Only low levels of an exon-4 deleted ER-α transcript were detected in murine tissues, although multiple relatively abundant exon-deleted ER-α transcripts were detected in human tissues. The data support a species-specific difference in the expression of ER-α variant mRNAs between mouse and human.

Keywords: Alternative splicing; Estrogen receptor-α; Species differences; Variant mRNAs

1. Introduction

A large body of data support the expression of multiple splice variants of the estrogen receptor-α (ER) mRNA in both normal and neoplastic human tissues (Murphy et al., 1997a,b). The most prevalent pattern of variant ER transcript is the precise deletion of one or more exons (Leygue et al., 1996a). In contrast, the expression of similar exon-deleted ER-variant transcripts in rodent tissues has not been investigated in detail. The detection of an exon-4 deleted ER mRNA species following two rounds of PCR amplification was reported using polyA + RNA isolated from hypothalamic-enriched rat brain tissue and rat uterine tissue (Skipper et al., 1993). However, it was noted in this latter study that only trace amounts of the variant ER were detected in rat uterine tissue when compared to the brain tissue. Exon-4 deleted, exon 4 + 5 deleted and exon 3 + 4 deleted ER transcripts were detected in rat aortic smooth muscle and bone cells using a similar approach of reverse transcription followed by two rounds of PCR amplification (Hoshino et al., 1995; Inoue et al., 1996). From these studies in which there was the need to use two rounds of PCR amplification for detection, it seemed that expression of ER variants in rodent tissues was less frequent and less abundant than in human tissues. However, the majority of studies in the human have been carried out in breast cancer tissues and cells, and there is some evidence to suggest that variant mRNA expression is downregulated in normal human breast tissues compared to breast tumors (Leygue et al., 1996b,c), although this is not the case for all ER-variant mRNAs (Erenburg et al., 1997). However, it was possible that the perception of a higher frequency of detection of variant ER mRNA expression in human versus rodent tissue might be a result of the more frequent study of cancerous human tissues. To our knowledge there has been no side-by-side analysis of human and rodent ER-variant expression. So to address the question of variant ER mRNA expression in rodent and human tissues we have undertaken a side-by-side comparison of several non-neoplastic murine and human tissues.

* Corresponding author. Tel.: + 1-204-7893233; fax: + 1-204-7893900.
E-mail address: lcmurph@cc.umanitoba.ca (L.C. Murphy)

0303-7207/99/$ - see front matter
PII: S0303-7207(99)00169-0

2. Materials and methods

2.1. Tissues and RNA extraction

Non-malignant human uterine hysterectomy samples were obtained from the Department of Obstetrics and Gynecology, Health Sciences Centre, Winnipeg, Canada. Total RNA was extracted using the guanidinium thiocyanate/cesium chloride method as previously described (Dotzlaw et al., 1990). Non-malignant human ovarian samples were obtained through Dr Mes-Masson and the Ovarian Tissue Bank at the Institut du Cancer de Montreal, Centre de Recherche Louis-Charles Simard, Montreal, Canada. Normal human breast tissues from reduction mammoplasties of premenopausal women were obtained through the Manitoba Breast Tumor Bank. In total six different individuals provided the tissue samples for this study. Total RNA from the ovarian and normal breast tissue samples was extracted using Trizol reagent (Gibco/BRL) according to the manufacturer's instructions, and the integrity of the RNA was confirmed by denaturing gel electrophoresis as previously described (Murphy and Dotzlaw, 1989).

Murine tissues except for mammary tissues were obtained from two female mice aged 8–9 weeks, while mammary tissues were obtained from two separate adult lactating female mice. Therefore, a total of four individual mice were used in this study. Murine studies were conducted in accordance with the principles and procedures recommended by the University of Manitoba Animal Care Review Board. Total RNA was extracted using Trizol reagent (Gibco/BRL) according to the manufacturer's instructions, and the integrity of the RNA was confirmed by denaturing gel electrophoresis as previously described (Murphy and Dotzlaw, 1989).

2.2. RT-PCR and primers

Total RNA (1.5 μg per reaction) was reverse transcribed as previously described (Dotzlaw et al., 1997). One microliter of this reaction was amplified by PCR incorporating ^{32}P in a final volume of 10 μl, and 4 μl of this reaction separated on 6% denaturing polyacrylamide gels and autoradiographed as previously described (Dotzlaw et al., 1997). Routinely PCR was carried out for 35 cycles, where one cycle consisted of 1 min 94°C (denaturation), 1 min 60°C (annealing), and 2 min 72°C (extension).

To avoid confusion with respect to the numbering of exons and to facilitate comparisons of the human and murine ER-α primer sets, all mER-αexons are defined in this report by analogy to the human ER-αexon/intron structure (see Fig. 1). Primer design was facilitated by the use of the software programs OLIGO (version 4.0s, National Biosciences Inc., Plymouth, MN, USA) and Amplify (version 1.2, Genetics, University of Wisconsin, Madison, WI).

2.2.1. Mouse ER-α exon 1 and 8 primer set

mER 1–8 (sense) 5′-GCC GCC TTC AGT GCC AAC AG-3′ (priming site in exon 1, nucleotides 461–480 as numbered in reference (White et al., 1987)); mER 1–8 (antisense) 5′-AGG AAT GTG CTG AAG TGG AG-3′ (priming site in exon 8, nucleotides 1918–1937 (White et al., 1987)).

2.2.2. Mouse ER-α exon 2 and 5 primer set

mER 2–5 (sense) 5′-GCA GTA ACG AGA AAG GAA AC-3′ (priming site in exon 2, nucleotides 702–721 as numbered in reference (White et al., 1987)); mER 2–5 (antisense) 5′-CGA GAC CAA TCA TCA GAA TC-3′ (priming site in exon 5, nucleotides 1357–1376 (White et al., 1987)).

2.2.3. Mouse ER-α exon 4 and 7 primer set

mER 4–7 (sense) 5′-ATC AAC TGG GCA AAG AGA GT-3′ (priming site in exon 4, nucleotides 1275–1293 (White et al., 1987)); mER 4–7 (antisense) 5′-TCA AGG TGC TGG ACA GM AC-3′ (priming site in exon 7, nucleotides 1582–1601 (White et al., 1987)).

2.2.4. Mouse ER-α exon 6 and 8 primer set

mER 6–8 (sense) 5′-AGG GTG AAG AGT TTG TGT GC-3′ (priming site in exon 6, nucleotides 1524–1543 (White et al., 1987)); mER 6–8 (antisense) 5′-AGG AAT GTG CTG AAG TGG AG-3′ (priming site in exon 8, nucleotides 1918–1937 (White et al., 1987)).

2.2.5. Human ER-α exon 1 and 8* primer set

hER-α 1–8* (sense) 5′-TGC CCT ACT ACC TGG AGA ACG-3′ (priming site in exon 1, nucleotides 615–637 (Green et al., 1986)); hER-α 1–8* (antisense) 5′-GCC TCC CCC GTG ATG TAA-3′ (priming site in exon 8, nucleotides 1995–1978 (Green et al., 1986)).

2.2.6. Human ER-α exon 2 and 6 primer set

hER-α 2–6 (sense) 5′-AGG GTG GCA GAG AAA GAT-3′ (priming site in exon 2, nucleotides 708–725 as numbered in reference (Green et al., 1986)); hER-α 2–6 (antisense) 5′-ATG CGG AAC CGA GAT GAT GTA GC-3′ (priming site in exon 6, nucleotides 1520–1542 (Green et al., 1986)).

2.2.7. Human ER-α exon 4 and 6 primer set

hER-α 4–6 (sense) 5′-CAG GGG TGA AGT GGG GTC TGC TG-3′ (priming site in exon 4, nucleotides 1060–1082 (Green et al., 1986)); hER-α 4–6 (antisense) 5′-ATG CGG AAC CGA GAT GAT GTA GC-3′ (priming site in exon 6, nucleotides 1520–1542 (Green et al., 1986)).

2.2.8. Human ER-α exon 5 and 8 primer set

hER-α 5–8 (sense) 5′-TCC TGA TGA TTG GTC TCG TCT GG-3′ (priming site in exon 5, nucleotides 1389–1411 (Green et al., 1986)); hER-α 5–8 (antisense) 5′-CAG GGA TTA TCT GAA CCG TGT GG-3′ (priming site in exon 8, nucleotides 2035–2057 (Green et al., 1986)).

2.3. Southern blot analysis

Ten microlitres of non-radioactive PCR products were subjected to Southern blotting as previously described (Murphy and Dotzlaw, 1989) and the resulting blots were hybridized with mER-α cDNA (kindly provided by Dr K Korach, NIEHS, North Carolina) labeled with ^{32}P by nick-translation as previously described (Murphy and Dotzlaw, 1989). The mER-α cDNA used, contained the entire coding sequences and represented nucleotides 177–2061 (White et al., 1987; Couse et al., 1995).

PCR products from human and murine tissue were subcloned into the cloning vector, pGEM-T Easy (Promega) following the manufacturer's instructions. Double stranded DNA from at least two independent clones from each tissue was sequenced using a T7 Sequencing kit (Pharmacia) following the manufacturer's protocol. All RT-PCRs were carried out at least three times for each sample analyzed.

3. Results

Previously, we have used a long range RT-PCR approach to examine the pattern and relative frequency of expression of all exon-deleted ER-variant mRNAs as long as they also contain the primer sequences located in exons 1 and 8 (Leygue et al., 1996a). Long range RT-PCR was carried out using mouse primer set 1–8 (see Fig. 1A) with murine RNA and human primer set 1–8* (see Fig. 1B) with human RNA. Although these primer sets are not exactly the analogous sequences between the two species they are similar in that they both prime within the first and last protein coding exons of the appropriate species ER cDNA (Fig. 1). The results shown in Fig. 2 indicate that one RT-PCR product of 1477 bp is detected in RNA isolated from

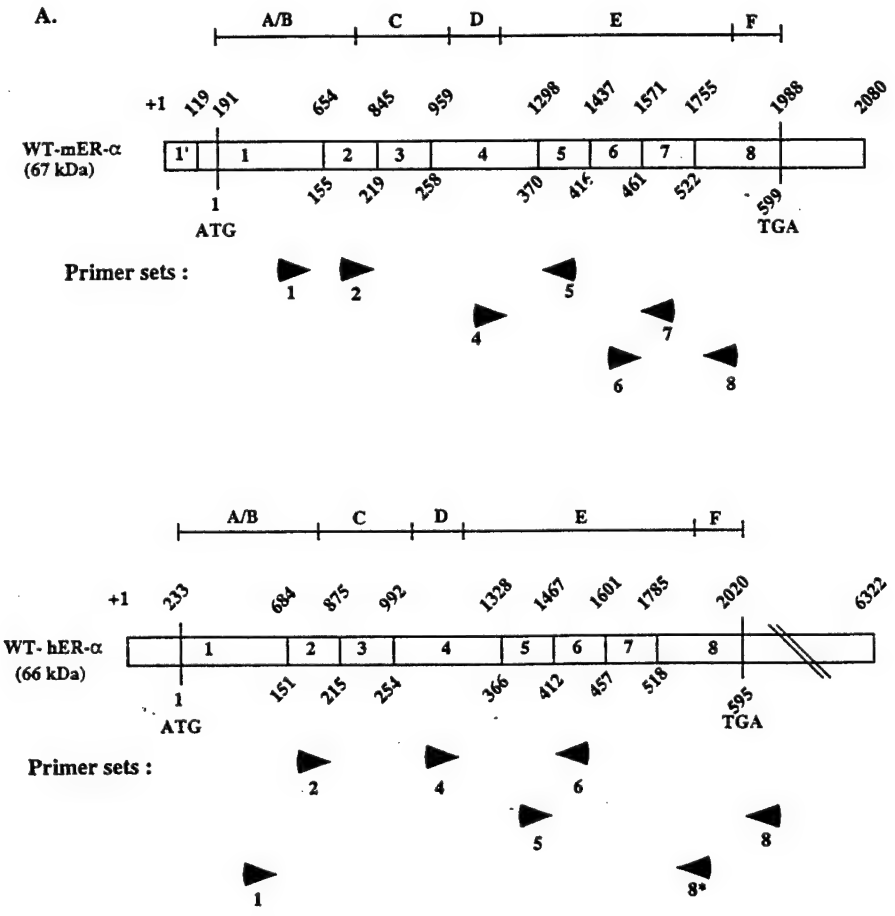

Fig. 1. (A) Schematic diagram of the wild-type murine ER-α cDNA showing the positions of the various primer sets used in PCR amplification. (B) Schematic diagram of the wild-type human ER-α cDNA showing the positions of the various primer sets used in PCR amplification.

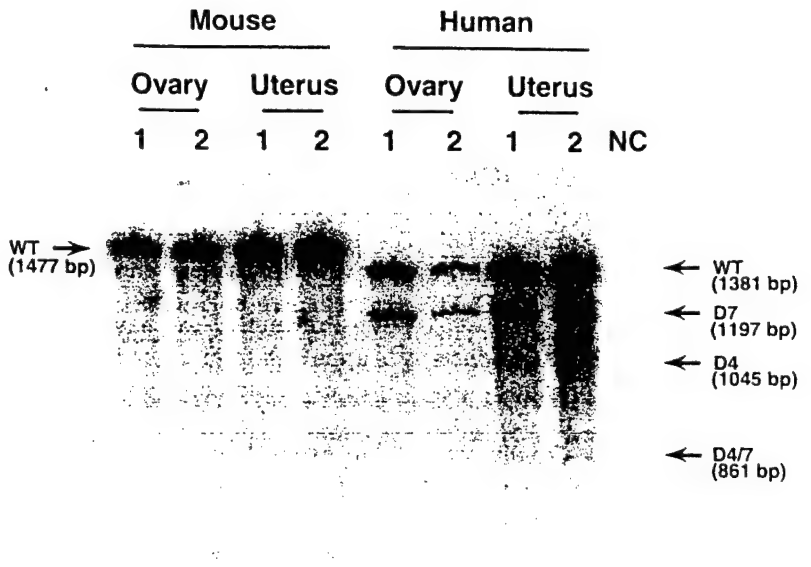

Fig. 2. Long range RT-PCR assay of ER-α mRNA in murine ovarian and uterine tissues, and human ovarian and uterine tissues. Total RNA extracted from two samples of each tissue was reverse transcribed and PCR amplified incorporating ^{32}P-dCTP and using primers as shown in Fig. 1A: for the mouse primers 1 and 8: Fig. 1 B: for the human primers 1 and 8*. The PCR products were separated on a 6% denaturing polyacrylamide gel, dried and exposed to X-ray film overnight with a screen. The PCR product migrating at 1477 bp is the murine wild-type ER-αcDNA. The PCR products migrating at 1381 bp, 1197 bp, 1045 bp, and 861 bp are the human wild-type, exon-7 deleted, exon-4 deleted, and exon 4 + 7 deleted ER-α cDNAs, respectively. NC, negative control.

murine ovarian and uterine tissues, this is the expected product for the wild-type murine ER mRNA. No other RT-PCR products are detected in murine tissues, suggesting that little or no ER deletion variant mRNAs are expressed in murine tissues. In contrast, in human ovarian and uterine tissues several smaller RT-PCR products are clearly detected together with the 1381-bp RT-PCR product expected for the wild-type human ER mRNA. In human tissues an abundant 1197-bp RT-PCR product is detected which corresponds to an exon-7 deleted ER mRNA, a less abundant 1045-bp RT-PCR product is detected which corresponds to an exon-4 deleted ER mRNA and a less abundant 861-bp RT-PCR is detected which corresponds to an exon 4 + 7 deleted ER mRNA. These data suggest that if murine tissues express ER-deleted variant mRNA their relative abundance compared to wild-type ER mRNA is very low, especially when compared to that seen in human tissues, although levels of wild-type ER mRNA within any one tissue e.g. uterus, are similar between the two species analyzed in this study. To further investigate possibly very low levels of expression of murine ER-αexon deleted transcripts, a series of primers were designed to amplify overlapping but smaller regions of the coding sequences of murine ER-α cDNA (Fig. 1A). Exon 2–5 primers amplified an expected 675-bp product from cDNA prepared from total RNA isolated from several estrogen target tissues, murine mammary gland, ovary, and uterus (Fig. 3, top panel). Similarly, exon 4–7 primers amplified an expected 327-bp product (Fig. 3, middle panel) and exon 6–8 primers amplified an expected 414-bp product (Fig. 3, bottom panel). All these products are the predicted size for the wild-type murine ER-αmRNA, although theoretically the wild-type product could also include

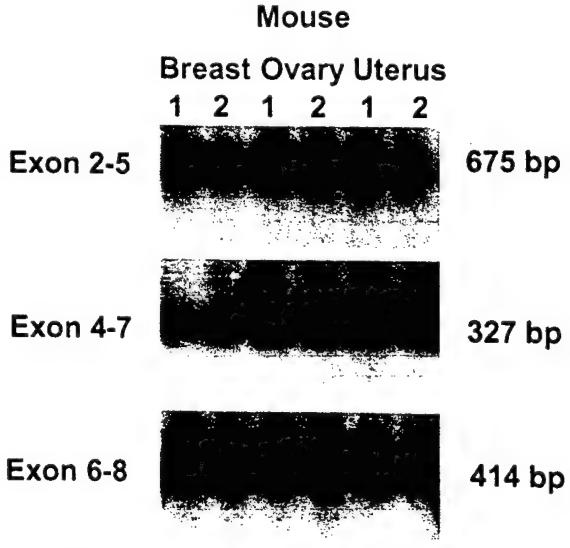

Fig. 3. Detection of wild-type ER-αmRNA in murine mammary, ovarian and uterine tissues. Total RNA extracted from two samples of each tissue was reverse transcribed and PCR amplified using primers as shown in Fig. 1A. An aliquot of each PCR reaction was Southern blotted and hybridized with radiolabeled murine ER-α cDNA (White et al., 1987). The blot was exposed to X-ray film for 4 h with a screen. The PCR products migrating at sizes of 675 bp using primer set exon 2–5, 327 bp using primer set exon 4–7 and 414 bp using primer set exon 6–8 were subsequently cloned and sequenced and identified as being wild-type murine ER-α cDNA.

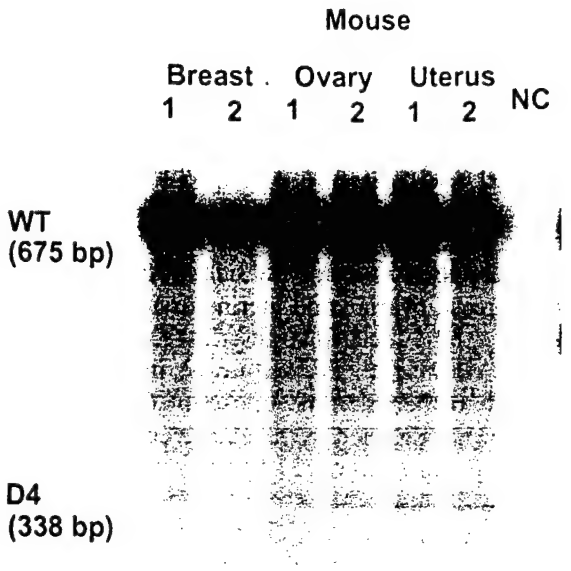

Fig. 4. Detection of wild-type and exon-4 deleted ER-α mRNA in murine mammary, ovarian, and uterine tissues. Total RNA extracted from two samples of each tissue was reverse transcribed and using primer set exon 2–5 (see Fig. 1A) PCR amplified incorporating ^{32}P-dCTP. The PCR products were separated on a 6% denaturing polyacrylamide gel, dried and exposed to X-ray film for 2 days with a screen. The PCR products migrating at 675 bp and 338 bp were cloned and sequenced and confirmed to be wild-type and exon-4 deleted murine ER-α cDNAs, respectively. NC, negative control.

products of ER-like mRNAs which are deleted in regions outside those bounded by the PCR primer set. The specificity of all these RT-PCR products was determined by Southern blotting and hybridization with a radiolabeled murine ER-α cDNA probe (Fig. 3). Therefore, these experiments detected little, if any, smaller sized PCR products which would be supportive of the expression of variant murine ER-αmRNA species deleted in exonic sequences. These data are consistent with those obtained using the long range RT-PCR approach (Fig. 2) but are in contrast to the detection of variant human ER-α mRNA species in human breast tumors using a similar technique (Green et al., 1986).

The experiments were repeated using a radiolabeled PCR technique with no detection of deleted murine ER-αmRNA species (Figs. 4, 7 and 8) except when using the exon 2-5 primer set. As shown in Fig. 4, a low-abundance PCR product of 338-bp and some other bands were detected in murine mammary gland, ovary and uterus only after a long exposure of the gel to X-ray film (2 days compared to 4–8 h exposure for detection of human ER variants). The 338-bp product was that expected for an exon-4 deleted ER cDNA and this was confirmed by cloning and sequencing. Other low-abundance PCR products were also detected between the wild-type PCR product and the exon-4 deleted PCR product, however, these bands did not correspond to the expected size of any exon-deleted product and were not further characterized following our failure to successfully clone these products despite the parallel success with cloning the exon-4 deleted product. Since the exon-4 deleted ER transcript had been identified previously in rat brain (Skipper et al., 1993) we analyzed RNA isolated from murine brain and several other tissues (Fig. 5). A prominent 675-bp RT-PCR product was detected in most tissues which was consistent with a wild-type murine ER-αmRNA. A

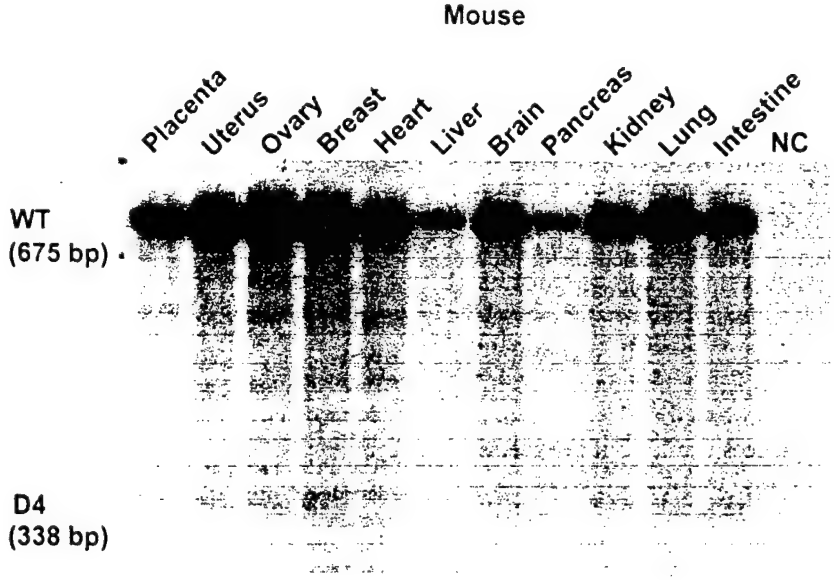

Fig. 5. Detection of wild-type and exon-4 deleted ER-α mRNA in multiple murine tissues. Total RNA extracted from multiple murine tissues, as shown, was reverse transcribed and using primer set exon 2–5 (see Fig. 1A) PCR amplified incorporating ^{32}P-dCTP. The PCR products were separated on a 6% denaturing polyacrylamide gel, dried and exposed to X-ray film for 2 days with a screen. The PCR products migrating at 675 bp and 338 bp are wild-type and exon-4 deleted murine ER-α cDNAs, respectively. NC, negative control.

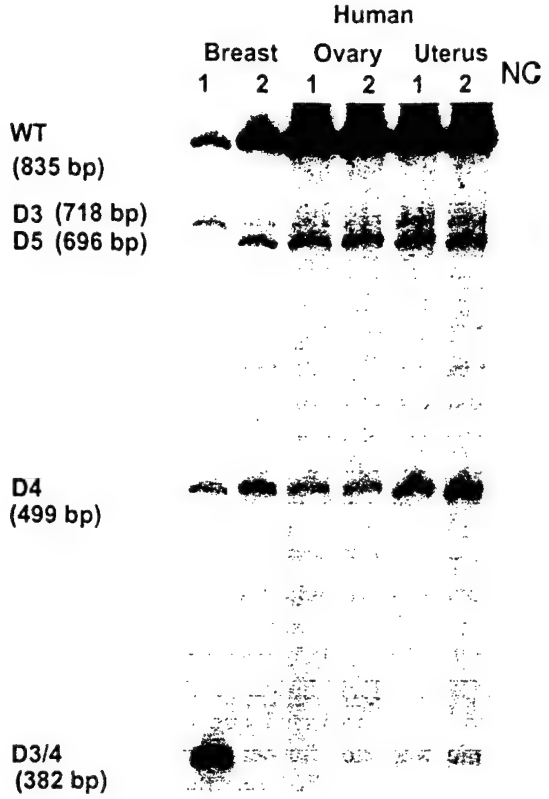

Fig. 6. Detection of wild-type and exon-deleted ER-α mRNAs in non-neoplastic human mammary, ovarian and uterine tissues. Total RNA extracted from two samples of each human tissue was reverse transcribed and using primer set exon 2–6 (see Fig. 1B) PCR amplified incorporating ^{32}P-dCTP. The PCR products were separated on a 6% denaturing polyacrylamide gel, dried and exposed to X-ray film for 6–8 h with a screen. The PCR products migrating at sizes of 835 bp, 718 bp, 696 bp, 499 bp, and 382 bp were cloned and sequenced and confirmed to be wild-type, exon-3 deleted, exon-5 deleted, exon-4 deleted, and exon 3 + 4 deleted human ER-αcDNAs, respectively. NC, negative control.

338-bp PCR product consistent with an exon-4 deleted murine ER-α transcript and other uncharacterized bands were detected in most tissues only after prolonged exposure to X-ray film (2 days), suggesting extremely low relative levels. These data again appeared to be in marked contrast to data obtained using human breast cancer tissues (Leygue et al., 1996a).

For a more direct comparison we therefore, determined the expression of exon-deleted transcripts in RNA isolated from non-neoplastic human tissues using primer sets designed to amplify overlapping smaller regions of the coding sequences similar but not identical to those investigated in the murine experiments described above. Primer set 2–6 (Fig. 6) resulted in detectable RT-PCR products, after a few hours of exposure to X-ray film, of 718 bp (exon-3 deleted), 696 bp (exon-5 deleted), 499 bp (exon-4 deleted), and 382 bp (exons 3 + 4 deleted), as well as the expected 835-bp product corresponding to the wild-type human ER-α mRNA, in the human breast, ovarian, and uterine tissues examined. In the two human breast tissues studied there appears to be both differences in the type of ER-α deletion variants seen as well as differences in the relative expression of some of the variants. The reasons for and the significance of these differences are unknown.

Primer sets designed to specifically detect an exon-5 deleted transcript relative to the wild-type ER-α transcript were used to compare side-by-side murine and human breast, ovarian and uterine tissues. Fig. 7 shows that an exon-5 deleted transcript (344 bp, bottom panel) is relatively highly expressed in human tissues compared to the wild-type transcript (483 bp, bottom panel) but not detected in the equivalent murine tissues (Fig. 7, top panel shows 327 bp for wild-type transcript only).

Fig. 8 shows that an RT-PCR product consistent with an exon-7 deleted ER-αmRNA (484-bp product, Fig. 8 bottom panel) is easily detected in human tissues together with the expected wild-type product (669 bp,

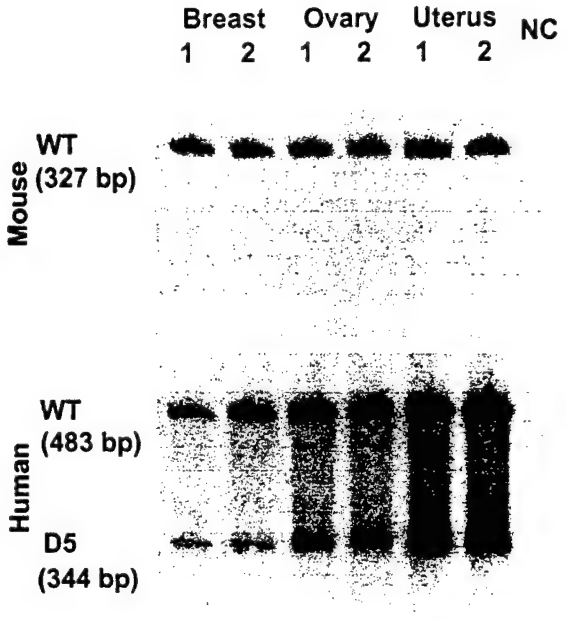

Fig. 7. Comparison of detection of exon-5 deleted ER-αcDNA in human and murine tissues. Primers specifically designed to detect only the wild-type and an exon-5 deleted ER-αcDNAs were used to PCR amplify incorporating ^{32}P-dCTP reverse transcribed RNA isolated from both human and murine mammary, ovarian, and uterine tissues. Primer set exon 4–7 was used in murine samples (see Fig. 1A) and primer set exon 4–6 was used in the human samples (Fig. 1B). The PCR products were separated on a 6% denaturing polyacrylamide gel, dried and exposed to X-ray film for 4 h with a screen. The results for the mouse are shown in the top panel and the results for the human are shown in the bottom panel. The 327 bp product in murine samples represents the wild-type ER-αcDNA. The faint band below the wild-type product is unknown. It is not that expected for an exon-5 deleted product and has not been successfully cloned and sequenced. The results for human tissues are shown in the lower panel. The 483-bp and the 344-bp products are the human wild-type and exon-5 deleted (D5)ER-αcDNAs, respectively.

Fig. 8. Comparison of detection of exon-7 deleted ER-αcDNA in human and murine tissues. Primers specifically designed to detect only the wild-type and an exon-7 deleted ER-αcDNAs were used to PCR amplify incorporating ^{32}P-dCTP reverse transcribed RNA isolated from both human and murine mammary, ovarian and uterine tissues. Primer set exon 6–8 was used in murine samples (see Fig. 1A) and primer set exon 5–8 was used in the human samples (Fig. 1B). The PCR products were separated on a 6% denaturing polyacrylamide gel, dried and exposed to X-ray film for 4 h with a screen. The results for the mouse are shown in the top panel and the results for the human are shown in the bottom panel. The 414-bp product in murine samples represents the wild-type ER-α cDNA. The results for human tissues are shown in the lower panel. The 669-bp and the 484-bp products are the human wild-type and exon-7 deleted (D7) ER-α cDNAs, respectively.

Fig. 8 bottom panel). Interestingly, in the two human breast tissue samples there appear to be differences in the relative expression of the ER-α deletion variant, consistent with that observed in Fig. 6. The significance of this difference between two individuals is unknown. However, only the expected wild-type product (414 bp, Fig. 8 top panel) was detected in murine tissues.

4. Discussion

The data presented above provide evidence that extensive alternative splicing of the estrogen receptor-α gene may be species-specific. Our data show little, if any, evidence in murine tissues for the high level or the complex pattern of ER alternative splicing that is detected in human tissues (Murphy et al., 1997b).

Little is known about the mechanisms underlying species-specific alternative splicing. However, several splicing signals (Balvay et al., 1994; Cooper and Mattox, 1997), in particular exonic splicing elements (Coulter et al., 1997) and different levels of some splicing factors (Manley and Tacke, 1996; Morrison et al., 1997) are likely to be involved. An investigation of murine ER-α and human ER-α exonic sequences for putative purine rich and A/C rich exonic splicing enhancer sequences (Cooper and Mattox, 1997; Coulter et al., 1997) showed no major differences in frequency of detection. Differences in intronic splicing elements of the ER-α between mouse and human cannot be assessed at this time because no intronic sequence information is available for the murine ER-α and little intronic sequence information except for the intron/exon boundaries of the human ER-α is available (Ponglikitmongkol et al., 1988).

Although only a handful of publications exist in which species-specific alternative splicing of a gene has been described (Hendriks et al., 1990; Conboy et al., 1992; Will et al., 1995; Fulop et al., 1996; Oakley et al., 1996; Hirano et al., 1998; Laurell et al., 1997; Lu et al., 1998), two of these are also members of the steroid hormone receptor gene family. This may suggest that species-specific alternative splicing is a relatively common phenomenon within the steroid hormone receptor gene family. We found previously that an ER-β mRNA containing 54 nucleotides inserted between exon 5 and 6 sequences is found at high levels in multiple murine tissues but is not detected in the equivalent human tissues (Lu et al., 1998). In addition, alternative splicing of exon 9α/9β Of the glucocorticoid receptor is only detected in human tissues (Oakley et al., 1996, 1997) and is not detected in any murine tissues studied (Otto et al., 1997). Both IκBβ1 and IκBβ2 alternatively spliced isoforms are found in human cells but only IκBβ1 was detected in murine cells (Hirano et al., 1998). As well in the mouse BRCA1 gene there is no homologue of the human exon 1β suggesting that there is no murine equivalent to the human BRCA1 β transcript (Xu et al., 1997). In contrast alternative spliced forms of the tumor suppressor p53 mRNA have only been detected in murine tissues and not human tissues (Will et al., 1995). Such data suggest either that mice and humans developed different mechanisms for whatever functions the alternative spliced products in the human subserve, or that species-specific functions exist. Interestingly, functional differences between murine wild-type ER-α and human wild-type ER-α have now been reported (Curtis et al., 1997). For example, the murine ER-α displays differential induction of the lactoferrin gene when liganded with modified diethystilbestrol agonists, however, the human ER-α was found to be activated by all these compounds with respect to activation of the lactoferrin promoter (Curtis et al., 1997). Furthermore, the activity of tamoxifen-like antiestrogens is quite different in the mouse compared to the human in particular with regard to agonist activity in the uterus (Martin and Middleton, 1978). However, a functional role(s) of ER-α variants in human estrogen signal transduction remains to be determined.

The identification of possible differences in the relative expression of variants and the type of variant expression between the two human breast tissue samples is potentially interesting. It is unclear why this difference within a single tissue occurs, and it is unclear how frequently such differences occur because only two samples have been studied. It is interesting, that there may be different variants under different physiological or perhaps pathophysiological conditions, which was one of the reasons to study variants in an animal model, which could be easily manipulated. Our data suggest that the mouse or rat may not be useful for such studies. Two individual mice were used in the uterine and ovarian study and the stage of estrous cycle for these was not noted. Two separate lactating female mice were used for the mammary tissue study but non-lactating tissue was not investigated. We cannot therefore, completely exclude the possibility that ER-α deletion variant mRNAs in the mouse are expressed in tissues at defined developmental stages or under specific pathophysiological conditions not investigated in this study. We think this is unlikely, but if so, would again underscore differences between human and rodent tissues, because ER-α deletion variants are found in human uterus in both pre- and post-menopausal uterine samples with no statistically significant differences in their levels of expression (Rice et al., 1997; Rey et al., 1998).

In conclusion, our data would be consistent with a species-specific difference in the expression of ER-α deletion variant mRNAs between murine and human tissues. However, we cannot exclude the possibility that ER-α deletion variant mRNAs in the mouse may be expressed in tissues at defined developmental stages or under specific pathophysiological conditions not investigated in this study. Irrespective of this, our data suggest that depending on the functional significance of ER-α deletion variants, extrapolation of results of some estrogen related studies in the mouse model to the human may be problematic.

Acknowledgements

This work was supported by the US Army Medical Research and Materiel Command (USAMRMC). The Manitoba Breast Tumor Bank is supported by funding from the National Cancer Institute of Canada (NCIC). LCM is a Medical Research Council of Canada (MRC) Scientist, PHW is a MRC Clinician Scientist, EL is a recipient of a USAMRMC Postdoctoral Fellowship.

References

Balvay, L., Pret, A.-M., Libri, D., Helfman, D., Fiszman, M., 1994. Splicing of the alternative exons of chicken, rat and *Xenopus* β tropomyosin transcripts requires class-specific elements. J. Biol. Chem. 269, 19675–19678.

Conboy, J., Cox, T., Bottomley, S., Bawden, M., May, B., 1992. Human erythroid 5-aminolevulinate synthase: gene structure and species-specific differences in alternative RNA splicing. J. Biol. Chem. 267, 18753–18758.

Cooper, T., Mattox, W., 1997. The regulation of splice-site selection, and its role in human disease. Am. J. Hum. Genet. 61, 259–266.

Coulter, L., Landree, M., Cooper, T., 1997. Identification of a new class of exonic splicing enhancers by in vivo selection. Mol. Cell. Biol. 17, 2143–2150.

Couse, J., Curtis, S., Washburn, T., Lindzey, J., Golding, T., Lubahn, D., et al., 1995. Analysis of transcription and estrogen insensitivity in the female mouse after targeted disruption of the estrogen receptor gene. Mol. Endocrinol. 9, 1441–1454.

Curtis, S., Shi, H., Teng, C., Korach, K., 1997. Promoter and species-specific differential estrogen mediated gene transcription in the uterus and cultured cells using structurally altered agonists. J. Mol. Endocrinol. 18, 203–211.

Dotzlaw, H., Miller, T., Karvelas, J., Murphy, L.C., 1990. Epidermal growth factor gene expression in human breast cancer biopsy samples: relationship to estrogen and progesterone receptor gene expression. Cancer Res. 50, 4204–4208.

Dotzlaw, H., Leygue, E., Watson, P., Murphy, L., 1997. Expression of estrogen receptor-beta in human breast tumors. J. Clin. Endocrinol. Metabol. 82, 2371–2374.

Erenburg, I., Schachter, B., Lopez, R.M.y., Ossowski, L., 1997. Loss of an estrogen receptor isoform (ER-alpha deleted 3) in breast cancer and the consequences of its reexpression: interference with estrogen-stimulated properties of malignant transformation. Mol. Endocrinol. 11, 2004–2015.

Fulop, C., Cs-szabo, G., Glant, T., 1996. Species-specific alternative splicing of the epidermal growth factor-like domain 1 of cartilage aggrecan. Biochem. J. 319, 935–940.

Green, S., Walter, P., Kumar, V., Krust, A., Bornert, J., Argos, P., 1986. Human estrogen receptor cDNA: sequence, expression, and homology to v-erb-A. Nature 320, 134–139.

Hendriks, W., Weetink, H., Voorter, C., Sanders, J., Bloemendal, H., Jong, W.d., 1990. The alternative splicing product αAins-crystallin is structurally equivalent to αA and αB subunits in the rat- α-crystallin aggregate. Biochim. Biophys. Acta 1037, 58–65.

Hirano, F., Chung, M., Tanaka, H., Maruyama, N., Makino, I., Moore, D., et al., 1998. Alternative splicing variants of IκBβ establish differential NF-κB signal responsiveness in human cells. Mol. Cell. Biol. 18, 2596–2607.

Hoshino, S., Inoue, S., Hosoi, T., Saito, T., Ikegami, A., Kaneki, M., et al., 1995. Demonstration of isoforms of the estrogen receptor in the bone tissues and in osteoblastic cells. Calcif. Tissue Int. 57, 466–468.

Inoue, S., Hoshino, S., Miyoshi, H., Akishita, M., Hosoi, T., Orimo, H., et al., 1996. Identification of a novel isoform of estrogen receptor, a potential inhibitor of estrogen action, in vascular smooth muscle cells. Biochem. Biophys. Res. Commun. 219, 766–772.

Laurell, H., Grober, J., Vindis, C., Lacombe, T., Dauzats, M., Holm, C., et al., 1997. Species-specific alternative splicing generates a catalytically inactive form of human hormone sensitive lipase. Biochem. J. 328, 137–143.

Leygue, E., Huang, A., Murphy, L., Watson, P., 1996a. Prevalence of estrogen receptor variant messenger RNAs in human breast cancer. Cancer Res. 56, 4324–4327.

Leygue, E., Murphy, L., Kuttenn, F., Watson, P., 1996b. Triple primer polymerase chain reaction: a new way to quantify truncated mRNA expression. Am. J. Pathol. 148, 1097–1103.

Leygue, E.R., Watson, P.H., Murphy, L.C., 1996c. Estrogen receptor variants in normal human mammary tissue. J. Natl. Cancer Inst. 88, 284–290.

Lu, B., Leygue, E., Dotzlaw, H., Murphy, L., Murphy, L., Watson, P., 1998. Estrogen receptor-beta mRNA variants in human and murine tissues. Mol. Cell. Endocrinol. 138, 199–203.

Manley, J., Tacke, R., 1996. SR proteins and splicing control. Genes. Dev. 10, 1569–1579.

Martin, L., Middleton, E., 1978. Prolonged oestrogenic and mitogenic activity of tamoxifen in the ovariectomized mouse. J. Endocrinol. 78, 125–129.

Morrison, M., Harris, K., Roth, M., 1997. *smg* mutants affect the expression of alternatively spliced SR protein mRNAs in *Caenorhabditis elegans*. Proc. Natl. Acad. Sci. USA 94, 9782–9785.

Murphy, L.C., Dotzlaw, H., 1989. Variant estrogen receptor mRNA species detected in human breast cancer biopsy samples. Mol. Endocrinol. 3, 687–693.

Murphy, L., Leygue, E., Dotzlaw, H., Douglas, D., Coutts, A., Watson, P., 1997a. Oestrogen receptor variants and mutations in human breast cancer. Ann. Med. 29, 221–234.

Murphy, L., Dotzlaw, H., Leygue, E., Douglas, D., Coutts, A., Watson, P., 1997b. Estrogen receptor variants and mutations: a review. J. Steroid Biochem. Mol. Biol. 62, 363–372.

Oakley, R., Sar, M., Cidlowski, J., 1996. The human glucocorticoid receptor isoform: expression, biochemical properties, and putative function. J. Biol. Chem. 271, 9550–9559.

Oakley, R., Webster, J., Sar, M., Jr, C.P., Cidlowski, J., 1997. Expression and subcellular distribution of the β-isoform of the human glucocorticoid receptor. Endocrinology 138, 5028–5038.

Otto, C., Reichardt, H., Schutz, G., 1997. Absence of glucocorticoid receptor-beta in mice. J. Biol. Chem. 272, 26665–26668.

Ponglikitmongkol, M., Green, S., Chambón, P., 1988. Genomic organization of the human oestrogen receptor gene. EMBO. J. 7, 8885–8888.

Rey, J., Pujol, P., Dechaud, H., Edouard, E., Hedon, B., Maudelonde, T., 1998. Expression of oestrogen receptor-alpha splicing variants and oestrogen receptor-beta in endometrium of infertile patients. Mol. Hum. Reprod. 4, 641–647.

Rice, L.W., Jazaeri, A.A., Shupnik, M.A., 1997. Estrogen receptor mRNA splice variants in pre- and postmenopausal human endometrium and endometrial carcinoma. Gynecol. Oncol. 65, 149–157.

Skipper, J.K., Young, L.J., Bergeron, J.M., Tetzlaff, M.T., Osborn, C.T., Crews, D., 1993. Identification of an isoform of the estrogen receptor messenger RNA lacking exon four present in the brain. Proc. Natl. Acad. Sci. USA 90, 7172–7175.

White, R., Lees, J., Needham, M., Parker, M., 1987. Structural organization and expression of the mouse estrogen receptor. Mol. Endocrinol. 1, 735–744.

Will, K., Warnecke, G., Bergmann, S., Deppert, W., 1995. Species- and tissue-specific expression of the C-terminal alternatively spliced form of the tumor suppressor p53. Nucleic. Acid. Res. 23, 4023–4028.

Xu, C., Chambers, J., Solomon, E., 1997. Complex regulation of the BRCA1 gene. J. Biol. Chem. 272, 20994–20997.

Oncogene (1999) 18, 5187–5193

http://www.stockton-press.co.uk/onc

Suppression of *ING1* expression in sporadic breast cancer

Tatsuya Toyama[1], Hirotaka Iwase[3], Peter Watson[4], Huong Muzik[2], Elizabeth Saettler[1], Anthony Magliocco[5], Lisa DiFrancesco[6], Peter Forsyth[2], Igor Garkavtsev[1,7] Shunzo Kobayashi[3] and Karl Riabowol*[,1]

[1]*Departments of Biochemistry & Molecular Biology and Oncology and Southern Alberta Cancer Research Centre, Faculty of Medicine, The University of Calgary, 3330 Hospital Drive, NW, Calgary, Alberta T2N 4N1, Canada;* [2]*Department of Clinical Neuroscience, Faculty of Medicine, The University of Calgary, 3330 Hospital Drive, NW, Calgary, Alberta T2N 4N1, Canada;* [3]*Department of Surgery II, Nagoya City University Medical School, 1 Kawasumi, Mizuho-cho, Mizuho-ku, Nagoya 467-8601, Japan;* [4]*Department of Pathology, Faculty of Medicine, The University of Manitoba, D212-770 Bannatyne Avenue, Winnipeg, Manitoba R3E 0W3, Canada;* [5]*Department of Pathology, College of Medicine, The University of Saskatchewan, Royal University Hospital, 103 Hospital Drive, Saskatoon, Saskatchewan S7N 0W8, Canada;* [6]*Department of Pathology, Foothills Hospital, 1403–29 Street, NW, Calgary, Alberta T2N 2T9, Canada*

Down regulation of the *ING1* candidate tumour suppressor promotes growth in soft agar and focus formation *in vitro* and tumour formation *in vivo*. *ING1* encodes a nuclear, cell cycle-regulated protein, over-expression of which efficiently blocks cell growth and is capable of inducing apoptosis in different experimental systems. Here we present the first report of *ING1* mutation and expression analysis in a total of 452 cancer samples. One germline missense alteration and three germline silent alterations were detected in 377 primary breast cancers while marked (2–10-fold) decreases in *ING1* mRNA expression were seen in 44% of primary breast cancers and in ten of ten breast cancer cell lines examined. Furthermore, the majority of breast cancers (58%) showing decreased *ING1* expression had metastasized to regional lymph nodes whereas only 9% of cancers with elevated *ING1* expression, compared to adjacent normal tissues, were metastatic. Thus, *ING1* mutation is very rare in breast or ovarian cancers, however, repression of *ING1* expression frequently accompanies tumour development of breast cancer.

Keywords: *ING1*; tumour suppressor gene; breast cancer; SSCP; mutation; expression

Introduction

Tumour suppressor genes play important roles in the regulation of cell growth and differentiation. Characterization of various human cancers on the basis of molecular genetics has indicated involvement of altered tumour suppressor genes in the genesis and progression of carcinoma (Devilee, 1994). We have recently cloned a novel growth inhibitor and candidate tumour suppressor gene called *ING1* using a method that combined PCR-mediated subtractive hybridization of cDNAs (Lisitsyn *et al.*, 1993) from normal and cancerous cells with adaptor-mediated enrichment (Diatchenko *et al.*, 1996) and an *in vivo* selection assay (Garkavtsev *et al.*, 1996). The *ING1* gene localized to chromosome 13q33–34 (Garkavtsev *et al.*, 1997b), a site that has been implicated in the progression of various tumours (Maestro *et al.*, 1996; Motomura *et al.*, 1988; Mostert *et al.*, 1996; Yang-Feng *et al.*, 1992). It also appears to have a role in programmed cell death as its expression confers sensitivity to apoptosis whereas antisense *ING1* protects cells from apoptosis in different experimental systems (Helbing *et al.*, 1997). Expression of *ING1* is also regulated through the cell cycle and its growth inhibitory effects are abrogated by SV40 large T antigen (Garkavtsev and Riabowol, 1997).

Recently, *ING1* protein ($p33^{ING1}$) has been reported to cooperate directly with p53 in growth regulation by modulating the ability of p53 to act as a transcriptional activator (Garkavtsev *et al.*, 1998). The biological effects of increasing and decreasing *ING1* expression and the involvement of $p33^{ING1}$ in the p53 signalling pathway indicate that *ING1* may be a tumour suppressor, and that functional loss of *ING1* might contribute to tumorigenesis.

BRCA1 and *BRCA2* contribute to a significant fraction of familial breast and ovarian cancers, and breast cancers, respectively. However, they undergo mutation at very low rates in sporadic breast and ovarian cancers which suggests that functional inactivation of additional genes also contributes to the genesis and development of these cancer types. To test this idea, we have examined both the mutational status and expression levels of *ING1* in primary human breast and ovarian cancers.

Results

Infrequent alterations of the ING1 *gene in primary breast and ovarian cancers, and breast cancer cell lines*

Since there is some indication that different factors predispose towards breast cancer in different populations, we have examined the mutational status of *ING1* in a number of tumours, initially screening for mutation in 240 primary breast cancer tissues from Japanese patients, 137 from Canadian patients, ten breast cancer cell lines of various origin, and 65 primary ovarian cancer tissues using PCR–SSCP

*Correspondence: K. Riabowol
[7]Current address: Genome Therapeutics Inc., 100 Beaver Street, Waltham, Massachusetts, MA 02154-8440, USA
Received 10 November 1998; revised 14 April 1999; accepted 14 April 1999

analysis. DNA sequence was determined for any PCR product that showed a variant pattern by SSCP analysis, and DNA from corresponding normal lymphocytes was also examined to determine whether this variant was a somatic or germline alteration. One germline missense alteration and three germline silent alterations were detected in primary breast cancers (Table 1). The tumour DNA from the missense alteration case had a C-to-T transition at the first nucleotide of codon 95, which results in a Proline to Serine substitution (Figure 1). This alteration was also present in the corresponding normal lymphocyte DNA from this patient indicating that this alteration was germline. The age of cancer onset for this patient was 38 years, and the tumour was aggressive, being classified as clinical stage III (Japanese Breast Cancer Society, 1992). Elevated levels of mutant p53 were not detected immunohistochemically, c-*erb*B-2 and *int-2* expression showed no amplification by Southern blot analysis, however, the expression of RB was very low in this tumour and c-*myc* was also amplified (Yamashita *et al*., 1993). No family history of cancers was evident.

Table 1 *ING1* germline alterations in breast cancers

Codon	*Nucleotide change*	*Effect on coding* *Consequence*	*sequence*	*Frequency*
95	CCC→TCC	Pro→Ser	missense	0.2% (1/442)
188	TCG→TCA	Ser→Ser	silent	4.1% (18/442) 7.5% (18/240)[a]
166	CGG→CGA	Arg→Arg	silent	0.2% (1/442)
228	TGT→TGC	Cys→Cys	silent	0.2% (1/442)

[a]The percentage in Japanese patients

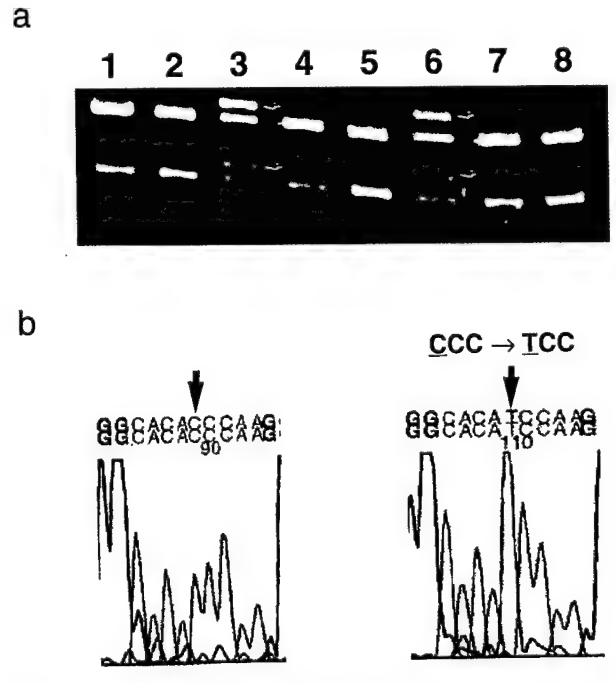

Figure 1 PCR–SSCP analysis and sequence of germline missense alteration. (**a**) results of PCR–SSCP analysis. Note the bands of altered mobility in lanes 3 and 6 (arrows) which represent a germline silent and a germline missense alteration, respectively. (**b**) the *ING1* sequence of tumour and corresponding normal lymphocyte DNA in a germline missense alteration case (right). The control is unrelated normal lymphocyte DNA (left)

Eighteen of 240 Japanese breast cancer patients (7.5%) had a G-to-A substitution at the third nucleotide of codon 188, which represented a serine to serine silent germline alteration (Table 1). Interestingly, we could not detect this alteration in

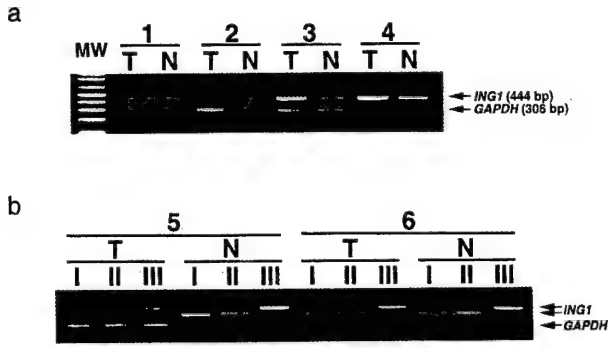

Figure 2 *ING1* mRNA expression analysis in selected samples. (**a**) *ING1* mRNA expression levels in tumour (T) and in matched adjacent normal mammary (N) tissues were monitored by 'primer dropping' RT–PCR which includes internal controls (*GAPDH*) for RNA integrity, RT and amplification efficiency in every sample (Wong *et al*., 1994). Tumour tissues in case 1 and 2 demonstrated decreased expression of *ING1* compared with matched normal mammary tissues and tumour samples were overloaded to highlight the degree of suppression of *ING1* expression. Case 3 and 4 showed increased *ING1* expression in tumour tissue. Lane MW shows molecular weight markers. (**b**) examples of RT–PCR signals generated from all *ING1* primers used. Expression is considered reduced in tumour *versus* matched normal tissue of both paired samples. I: *ING1* primers that span an intron, II: *ING1-B* primers than span an intron, III: primers that amplify within a single conserved exon

Table 2 Relationship between *ING1* mRNA expression levels and clinicopathologic features

	Decrease[a]	*No change*	*Increase*[a]	*Total*	P *value*
Mean age ± SD (year)	58.6 ± 13.4	60.5 ± 11.8	62.5 ± 22.0	60.3 ± 15.1	NS
Tumour size					
⩽2 cm	6	3	2	11	NS
2 cm to 5 cm	10	12	8	30	
>5 cm	4	1	1	6	
unknown	1	0	0	1	
Lymph nodes[b]					
positive	11	9	1	21	0.0182[c]
negative	8	7	10	25	
unknown	2	0	0	2	
Sub-type					
ductal	19	15	11	45	NS
lobular	2	1	0	3	
ER					
positive	14	11	8	33	NS
negative	7	5	3	15	
PgR					
positive	9	9	5	23	NS
negative	12	7	6	25	
Histologic grade					
grade I	4	0	2	6	NS
grade II	4	10	5	19	
grade III	13	6	3	22	
unknown	0	0	1	1	
Total	21 (44%)	16 (33%)	11 (23%)	48 (100%)	

[a]The *ING1* mRNA expression in tumour sample decreases, or increases modestly compared with matched normal mammary tissue. [b]Pathological metastasis status to regional lymph nodes. [c]Increased cases *versus* decreased cases. Data analysed by Fisher's exact probability test

Canadian patients. Other silent germline alterations were a G-to-A substitution at the third nucleotide of codon 166 (arginine to arginine) and a T-to-C substitution at the third nucleotide of codon 228 (cysteine to cysteine). These alterations were also detected in Japanese patients only. No alterations

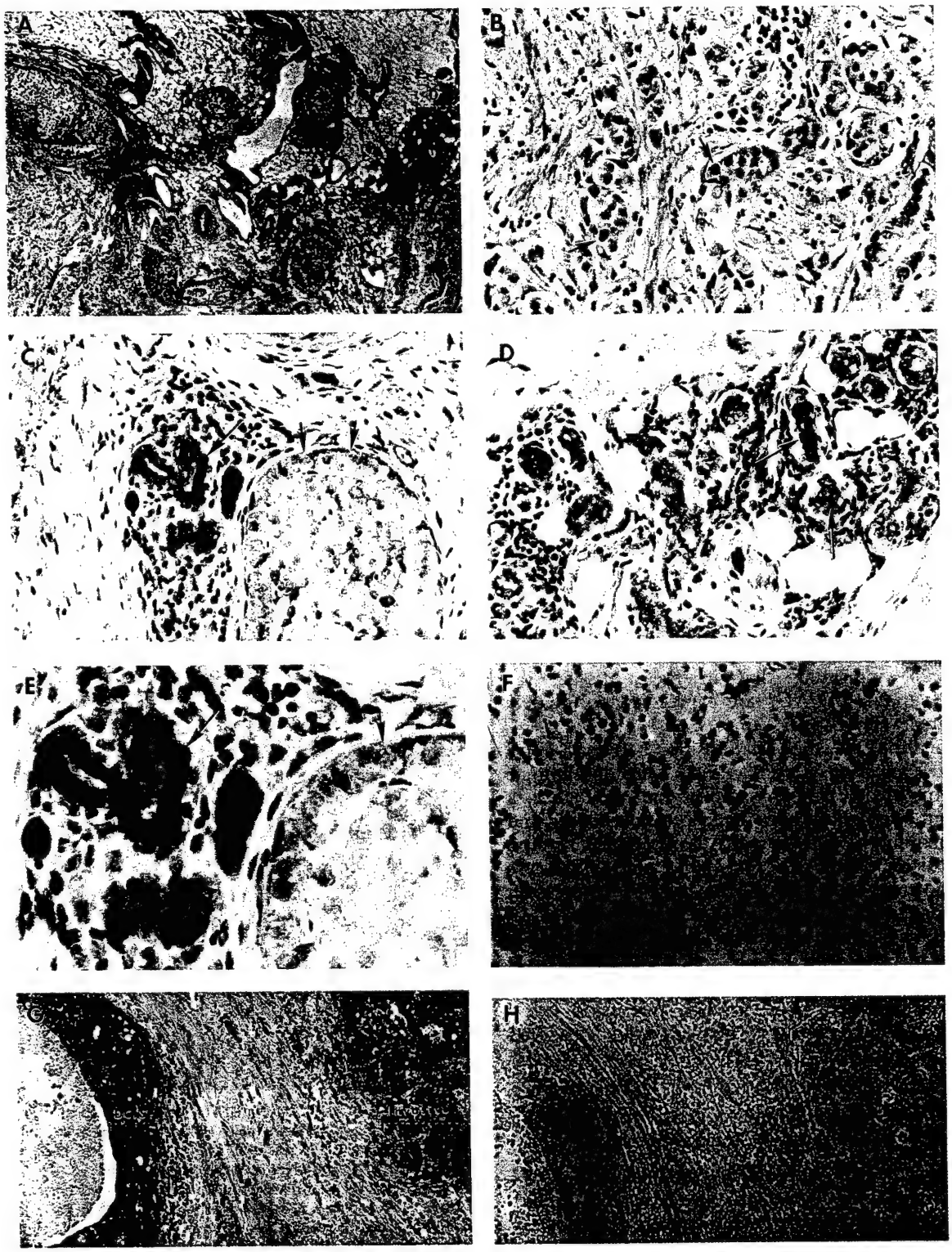

Figure 3 *In situ* hybridization analysis of *ING1* mRNA expression in primary breast cancer samples. (**a**–**e** and **g**) show the results of *in-situ* hybridization with antisense *ING1* mRNA probe. (**f** and **h**) are negative controls showing the results of hybridizing sections consecutive to (**b** and **g**) with no probe and sense probe, respectively. (**b**–**d**) show higher magnifications of the areas indicated as 'B', 'C' and 'D' in (**a**) respectively and (**e**) is a higher magnification of (**c**). (**b**–**d**) show invasive lesion, DCIS (right short arrows) plus normal mammary gland (left long arrow), and normal mammary gland alone, respectively. As shown in **b**–**e**, *ING1* mRNA expression is lower in breast cancer cells (short arrows in (**b**), (**c**) and (**e**) compared to adjacent normal mammary epithelial cells (long arrows in (**c**–**e**)). Note that cells staining positively for *ING1* stain brown and nuclei are stained blue with hematoxilyn in (**a**–**e**) as described in Materials and methods. (**g**) shows that lower levels of *ING1* are often observed in invasive components of breast cancer compared to DCIS components. Note positive cells stain brown in (**g**) and nuclei were not stained (as described in Materials and methods). Magnifications, (**a**) × 40, (**b**–**d**) and (**f**) × 200, (**e**) × 400, (**g** and **h**) × 100

were detected in breast cancer cell lines and in the 65 ovarian cancer tissues examined.

Decreased levels of ING1 *mRNA are frequently seen in breast cancer cell lines and in primary breast cancers*

The expression levels of *ING1* mRNA were examined in 48 randomly selected paired samples of primary breast cancer tissues and matched adjacent normal breast tissues from the NCIC Manitoba Breast Tumour Bank, and in ten breast cancer cell lines by RT–PCR. PCR primers were designed to span an intron sequence in order to eliminate the potential contribution of genomic DNA. Our results show that *ING1* mRNA expression was decreased (2–10-fold) in 44% (21/48) of breast cancer tissues compared to adjacent normal tissues while 33% (16/48) of tumours showed levels similar to control sample and 23% (11/48) showed increases in *ING1* mRNA (Figure 2a). Recently, additional splicing variants of *ING1* have been identified by our and other groups (in preparation). We therefore designed another two sets of primers including one to amplify a commonly expressed splicing variant we call *ING1-B* (GenBank accession AF044076) and one that amplifies within a single exon conserved in all known splicing variants. Results from RT–PCR of *ING1-B* show that approximately 80% (37/48) of paired breast samples show results that parallel those found for *ING1* while the remaining samples show slight variations. Results using primers to amplify total *ING1* transcripts also show very similar results (Figure 2b) indicating that in breast tissue, the different variants of *ING1* are expressed coordinately in the great majority of samples.

Examination of the relationship between *ING1* mRNA expression levels and clinicopathologic factors of breast cancer samples indicated that a significant correlation between expression levels and the probability of metastasis to regional lymph nodes existed (Table 2). Only one of 11 tumours (9%) showing increased *ING1* mRNA expression had metastasized to lymph nodes whereas 11 of 19 cases (58%) showing decreased expression of *ING1* exhibited metastasis to lymph nodes (increased cases *vs* decreased cases: $P=0.0182$). No significant associations between *ING1* mRNA expression levels and other clinicopathologic features were observed (Table 2).

Decreased levels of ING1 *mRNA are also observed in breast cancer tissues using* in situ *hybridization*

To confirm by an independent method that *ING1* mRNA expression decreased in advanced breast cancers compared to early stage cancers and normal tissues, we performed non-radioisotopic *in situ* hybridization on breast cancer samples. As shown in Figure 3a–f, *ING1* mRNA levels are clearly decreased in breast cancer cells relative to adjacent normal mammary epithelial cells. Decreased levels of *ING1* mRNA expression were also observed in invasive components of breast cancer compared to DCIS as illustrated in a separate experiment shown in Figure 3g and h.

Levels of ING1 *mRNA reflect protein levels*

We examined both ING1 protein and mRNA expression in ten independent samples derived from breast cancer cell lines by Western blotting analysis and RT–PCR, respectively. As shown in Figure 4a,

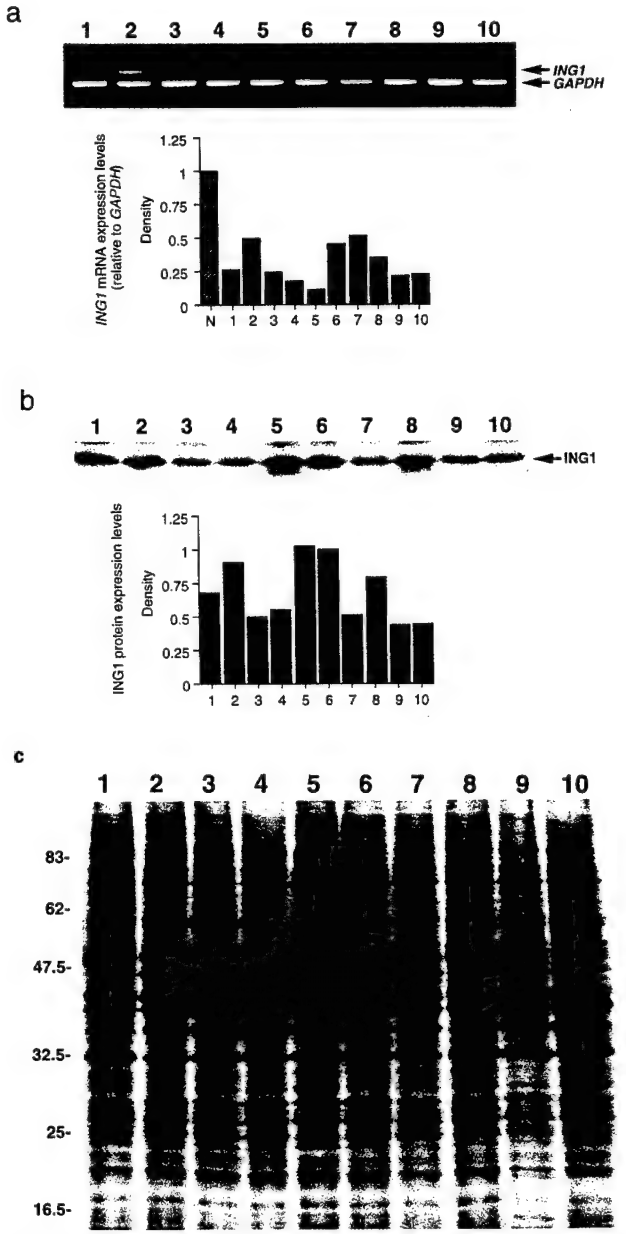

Figure 4 Expression levels of *ING1* mRNA and protein in breast cancer cell lines. (**a**) results of *ING1* mRNA expression analysis in breast cancer cell lines. All breast cancer cell lines showed decreased *ING1* mRNA expression compared to the average expression level seen in 48 independently analysed normal breast tissues (N) and to a normal breast cell line (Hs578 Bst) (data not shown). The relative mRNA expression levels in breast cancer cell lines are shown with the densitometric reading in the corresponding histograms below. N: mean value for normal tissues, 1: BT-20, 2: BT-474, 3: MCF-7, 4: SK-BR-3, 5: BT-483, 6: MDA-MB-435S, 7: MDA-MB-468, 8: T-47D, 9: Hs 578T, 10: ZR 75-1. (**b**) the results of ING1 protein expression analysis using a mouse monoclonal antibody (Garkavtsev *et al*., 1997a) against ING1 in a Western immunoblot of the same panels of breast cancer cell lines as in panel (**a**). (**c**) Coomassie brilliant blue-stained gel of samples run in parallel as loading controls. Lanes are the same as in panels (**a**) and (**b**). The pattern of protein molecular weight standards (kDa) is indicated on the left side of the gel

expression levels of *ING1* mRNA varied between samples and were much lower than the average level seen in different control samples (hatched bar N). Although the average protein expression level of normal breast samples is not demonstrated in Figure 4b, our data shows that the relative levels of polypeptide recognized by an ING1 monoclonal antibody (Garkavtsev *et al.*, 1997a) in these samples are very similar to the relative levels of mRNA seen in the majority of samples (compare the pattern of bar graphs in Figure 4a,b).

Discussion

This study has established several facts about the *ING1* candidate tumour suppressor. First, the *ING1* gene is mutated very rarely in primary breast or ovarian cancers and breast cancer cell lines. Second, expression of the gene is reduced in a high proportion of breast tumours (44%) and in all breast cancer cell lines examined. Third, ING1 protein levels parallel the levels of mRNA seen in most breast cancer cells. Fourth, *ING1* expression levels correlate strongly with metastasis, with primary tumours showing reduced levels of *ING1* being metastatic at a frequency at least sixfold greater than these showing increased levels of *ING1* (57% *vs* 9%, respectively).

We screened for mutation of the *ING1* gene in 377 primary breast cancer tissues, ten breast cancer cell lines and 65 primary ovarian cancer tissues. One germline missense and three germline silent alterations were detected in primary breast cancers. A germline missense alteration showed a C-to-A transition resulting in a proline to serine substitution. This change would be predicted to have severe effects upon protein conformation making it more likely that this is a germline mutation rather than a very rare polymorphism. However, we cannot exclude the possibility that this nucleotide change is a polymorphism because the biological effect caused by this alteration has not yet been determined. Although we examined a total of 442 breast or ovarian cancer tissues and ten breast cancer cell lines and the resulting data suggest that *ING1* alterations occur with very low frequency, this is a minimal estimate. PCR–SSCP analysis is reported to be less than 100% sensitive for mutation detection (Vidal-Puig and Moller, 1994) and *ING1* has two splicing variants which have one large conserved common exon. The common exon accounts for approximately 75 and 85% of coding region for *ING1* and *ING1-B*, respectively. In this study, primers for PCR–SSCP analysis were designed within the common exon, therefore our data likely underestimates the contribution of *ING1* mutations to the overall incidence of breast and ovarian cancers. Determination of the genetic structure of the *ING1* gene and analysis of the entire coding region is presently being undertaken and will help to refine our estimates of mutation rate.

Although the mutation rate is very low, the frequency of down regulation of *ING1* in tumours is very substantial, similar to those described for *BRCA1* (Thompson *et al.*, 1995; Dobrovic and Simpfendorfer, 1997; Magdinier *et al.*, 1998; Rice *et al.*, 1998; Sourvinos and Spandidos, 1998) and $p16^{INK4A}$ (Merlo *et al.*, 1995; Brenner *et al.*, 1996; Herman *et al.*, 1995). Furthermore, down regulation of *ING1* was observed in all breast cancer cell lines examined (ten of ten). Using *in situ* hybridization, down regulation of *ING1* mRNA was also observed in breast cancer cells while normal mammary epithelial cells expressed *ING1* mRNA at higher levels, and lower levels of *ING1* were observed in invasive components of breast cancer compared to DCIS (Figure 3) in the majority of samples analysed. These data suggest that down regulation of *ING1* expression accompanies, and may contribute to the process of cancer development.

From analysis of the mRNA expression levels of the *ING1* gene, we noted an interesting correlation between the level of *ING1* expression and aggressiveness of the tumour as judged by whether the tumour had metastasized. Although we have no evidence that *ING1* plays a role in metastasis *per se*, observations have been made linking *BRCA1* levels to neoplastic progression. For example, *BRCA1* mRNA is expressed at several-fold higher levels in normal mammary tissues than in invasive breast cancer tissues, although higher levels of *BRCA1* mRNA expression were observed in DCIS samples than in normal mammary tissues (Thompson *et al.*, 1995). While the explanation of the finding that expression levels of *BRCA1* are increased in DCIS is unclear, one possibility is that normally functioning *BRCA1* may be an active inhibitor of neoplastic progression in breast epithelial cells and the increased expression of *BRCA1* in DCIS could be a response to genetic alterations that predispose to develop invasive breast cancer. Our data for *ING1* expression are similar to those reported for *BRCA1* expression (Thompson *et al.*, 1995). We observed that expression levels of *ING1* are increased in some breast cancers, and that 91% (10/11) of them showed no lymph node metastasis. If the above-mentioned hypothesis regarding *BRCA1* is accurate, *ING1* in these breast cancers also could be responsive to genetic alterations that predispose to develop more advanced breast cancer.

We have shown previously in different human cell types that the levels of *ING1* mRNA are a good predictor of protein levels (Garkavtsev and Riabowol, 1997). However, since tumour cells can show uncoupling of mRNA and protein levels for different genes, we examined both ING1 protein and mRNA expression in ten breast cancer cell lines. Our data shows that the relative levels of ING1 protein expression in these samples are very similar to the relative levels of *ING1* mRNA seen in the majority of cell lines corroborating earlier observations that ING1 protein levels are regulated primarily at the level of transcription (Garkavtsev and Riabowol, 1997).

The mechanism by which *ING1* inhibits growth and possibly contributes to breast cancer progression through reduced expression is presently unknown, however $p33^{ING1}$ has recently been reported to be essential for p53 function (Garkavtsev *et al.*, 1998). *ING1* appears to be able to also exert cellular effects independently of *p53* since a role in apoptosis was observed in the absence of transcriptionally active *p53* (Helbing *et al.*, 1997). Thus, decreased expression of *ING1* mRNA in breast cancers may contribute to both altered cell growth control through involvement of $p33^{ING1}$ in the p53 signalling pathway and to resistance to apoptosis by p53-independent mechanisms.

Materials and methods

Tumour tissues and cell lines

Tumour tissues and matched normal lymphocytes or adjacent normal mammary tissues were obtained from Nagoya City University Hospital, the University of Saskatchewan Hospital, Calgary Foothills Hospital, and from the Manitoba Breast Tumour Bank. Breast cancer cell lines (BT-20, BT-474, MCF-7, SK-BR-3, BT-483, MDA-MB-435S, MDA-MB-468, T-47D, Hs 578T, ZR 75-1) were grown in Dulbecco's modified Eagle's medium with 10% FBS or in RPMI 1640 with 10% FBS in 5% CO_2, and were harvested for RNA, DNA or protein by standard methods.

DNA and RNA extractions

For DNA extraction, samples were homogenized and suspended in STE buffer (100 mM Tris-HCl (pH 8.0), 10 mM NaCl, 1 mM EDTA (pH 8.0)) with 50 μg/ml proteinase K and 0.1% SDS at 50°C for 3–4 h. Genomic DNA was extracted using the phenol-chloroform method. Total RNA was isolated by Trizol reagent (Life Technologies, Inc., Burlington, Canada) according to the manufacturer's recommendations.

RT–PCR

ING1 mRNA expression in tumours and in normal tissues was monitored by duplex RT–PCR (Wong *et al*., 1994). Each 20 μl cDNA synthesis reaction contained 1 μg of total RNA from tumour and normal cells, buffer (10 mM Tris-HCl (pH 9.0), 50 mM KCl, 1.5 mM $MgCl_2$), 1 mM each of deoxynucleoside triphosphates, 25 units of RNAguard RNase inhibitor (Pharmacia Biotech Inc., Baie dU'rfé, Canada), 200 units of Superscript II reverse transcriptase (Life Technologies, Inc.), and 100 ng of $pd(N)_6$ random hexamer (Pharmacia). One μl of each RT reaction was amplified using 1 unit of Taq DNA polymerase (Pharmacia). Thirty-three PCR cycles for *ING1* (forward intron-spanning primer: 5′-CCGCATCTTTGCTGACCCGA-3′, reverse intron-spanning primer: 5′-GCCTTCTTCTTCTTGGGTGT-3′; forward conserved exon primer: 5′-CTGAAGGAGCTAGACGAGTG-3′, reverse conserved exon primer: 5-′-ACGCACGAGAAGTGGAACCA-3′) and for *ING1-B* (forward intron-spanning primer: 5′-CTCCATCGAGTCCCTGCCTT-3′, reverse intron-spanning primer: 5′-GCCTTCTTCTTCTTGGGTGT-3′), and 22 PCR cycles for *GAPDH* (forward primer: 5′-CGGAGTCAACGGATTTGGTCGTAT-3′, reverse primer: 5′-AGCCTTCTCCATGGTGGTGAAGAC-3′) were used for amplification consisting of 1 min at 94°C, 1 min at 62°C, 1 min at 72°C, with a 5 min extension at 72°C following the last cycle. Primers for *GAPDH* were added to PCR tubes at the end of the 11th cycle. Before RT reactions, RNase-free DNase I (Life Technologies, Inc.) was used to remove DNA contamination for conserved exon primers according to the manufacturer's instructions. Reproducibility was confirmed by processing all samples at least twice.

PCR–SSCP analysis

PCR reactions were carried out in a volume of 50 μl containing 200 ng of genomic DNA, 1.5 mM $MgCl_2$, 50 mM KCl, 10 mM Tris-HCl (pH 9.0), 0.2 mM of each deoxynucleoside triphosphates, 0.5 μM of each primer, and 1 unit Taq DNA polymerase. Thirty cycles were used for amplification consisting of 1 min at 94°C, 1 min at 60°C, 1 min at 72°C, with a 5 min extension at 72°C following the last cycle with visualization by a non-radioisotopic method as described (Iwase *et al*., 1996). Gels were electrophoresed for 1.5–4 h at 600 V, and were stained with ethidium bromide (1.0 μg/ml) for 10 min. The sequences of *ING1* primer pairs used for PCR–SSCP analysis were: primer set I (forward primer: 5′-CTGAAGGAGCTAGACGAGTG-3′ (nucleotides 201-221 (Garkavtsev *et al*., 1996)), reverse primer: 5′-GGCTTGTCAGACTGCGCTAC-3′ (nucleotides 474–494)), primer set II (forward primer: 5′-GTAGCGCAGTCTGACAAGCC-3′ (nucleotides 474–494), reverse primer: 5′-ACGCACGAGAAGTGGAACCA-3′ (nucleotides 763–783)), primer set III (forward primer: 5′-GACAACGACGAGTGCCCCAT-3′ (nucleotides 739–759), reverse primer: 5′-CTACCTGTTGTAAGCCCTCTCT-3′ (nucleotides 879–901)). Analysis of all samples showing bands of different mobilities was repeated two to four times to ensure reproducibility.

Direct sequencing of PCR products

Abnormal bands detected by PCR–SSCP analysis were cut out of gels, reamplified by PCR and purified using Geneclean II Kits (BIO 101 Inc., Vista, CA, USA). Sequencing was done using a model 373A, version 1.2.0 genetic analyser by the Southern Alberta DNA Synthesis and Sequence Facility.

In situ *hybridization*

A 987 bp *Eco*RI–*Xho*I fragment of *ING1* in plasmid pBS was used to generate antisense riboprobe with T3 RNA polymerase from template linearized with *Eco*RI, and sense riboprobe with T7 RNA polymerase and *Xho*I-digested plasmid. *In situ* hybridization was performed as described previously (Harvey *et al*., 1995; Leco *et al*., 1997). Briefly, eight micrometer paraffin-embedded breast cancer sections were dewaxed in xylene and rehydrated through a series of graded ethanol solutions. Sections were treated with proteinase K (20 μg/ml), acetylated, prehybridized, and hybridized overnight with digoxigenin-labelled probes. Hybridization was followed by RNase A treatment and four stringent washes. After this procedure, we performed two different methods as follows; (I) (Figure 3a–f): sections were incubated in 1% hydrogen peroxide to block endogenous peroxidase. To reduce nonspecific binding, they were incubated in 4% normal goat serum, and then incubated in mouse monoclonal antibody against digoxigenin (Boehringer Mannheim, Laval, Canada) overnight at 4%. Goat anti-mouse horseradish peroxidase (Pierce, Rockford, IL, USA) was used as secondary antibody. Brown colour of peroxidase was developed in DAB (Sigma, Oakville, Canada), enhanced in 0.5% copper sulphate and hematoxylin was employed as a nuclear counter stain. Sections were dehydrated and mounted in Flo-Texx mounting media (Lerner Laboratories, Pittsburgh, PA, USA) and photographed under bright field illumination. (II) (Figure 3g and h): sections were incubated in a 1:500 dilution of sheep anti-digoxigenin-alkaline phosphatase-conjugated antibody (Boehringer Mannheim) overnight. Subsequently, NBT/BCIP (Boehringer Mannheim) was added and sections were incubated in the dark. The reactions were terminated by placing sections in 10 mM Tris-HCl (pH 8.0)/10 mM EDTA (pH 8.0). After extensive washing, sections were mounted in Kaiser's mounting medium (7.7% gelatin, 54% glycerol and 0.2% phenol) and photographed under bright field illumination.

Western blotting

Breast cancer cells growing in 10 cm tissue culture dishes (approximately 3×10^6 cells per dish) were washed with ice-cold PBS, dissolved in sample buffer, and sonicated. Two sets of proteins were separated by electrophoresis through 15% SDS-polyacrylamide gels, and were stained with Coomassie brilliant blue (Bio-Rad Laboratories, Hercules, CA, USA) or transferred to PolyScreen microporous polyvinylidene difluoride membranes (NEN Life Science Products, Boston, MA, USA) for 2 h at 20 V. Membranes were blocked in PBS with 5% nonfat dried milk and 0.1% Tween-20 overnight.

Blocked membranes were incubated with an undiluted mouse p33^{ING1} monoclonal antibody hybridoma supernatant or with a 1:1000 dilution of rabbit p33^{ING1} polyclonal antibody in PBS containing 5% nonfat milk and 0.1% Tween-20 for 1 h with gentle shaking. The p33^{ING1} was then visualized as described (Garkavtsev and Riabowol, 1997).

Statistical analysis

Fisher's exact probability test was performed to estimate the correlation between the expression levels of *ING1* mRNA and clinicopathologic factors using the software StatView-J 4.02.

Abbreviations

PCR–SSCP, polymerase chain reaction-single strand conformation polymorphism; RT, reverse transcription; DCIS, ductal carcinoma *in situ*; GAPDH, glyceraldehyde-3-phosphate dehydrogenase; DAB, 3,3′ diaminobenzidine; NBT/BCIP, nitroblue tetrazolium chloride/5-bromo-4-chloro-3-idolyl-phosphate, 4-toluidine salt.

Acknowledgements

We thank Dr D Fujita for providing breast cancer cell lines, Drs RN Johnston and D Edwards for critical and insightful comments and D Boland and the SACRC Hybridoma Facility for antibody production. This work was supported by grants from the Alberta Cancer Board, the Alberta Breast Cancer Foundation/Honda Run for the Cure, and the National Cancer Institute of Canada to Karl Riabowol. The NCIC-Manitoba Breast Tumour Bank is supported by the National Cancer Institute of Canada.

References

Brenner A, Paladugu A, Wang H, Olopade O, Dreyling M and Aldaz C. (1996). *Clin. Cancer Res.*, **2**, 1993–1998.

Devilee P, Schuuring E, van de Vijver MJ and Cornelisse CJ. (1994). *Crit. Rev. Oncog.*, **5**, 247–270.

Diatchenko L, Lau Y-FC, Campbell AP, Chenchik A, Moqadam F, Huang B, Lukyanov S, Lukyanov K, Gurskaya N, Sverdlov ED and Siebert PD. (1996). *Proc. Natl. Acad. Sci. USA*, **93**, 6025–6030.

Dobrovic A and Simpfendorfer D. (1997). *Cancer Res.*, **57**, 3347–3350.

Garkavtsev I, Boland D, Mai J, Wilson H, Veillette C and Riabowol K. (1997a). *Hybridoma*, **16**, 537–540.

Garkavtsev I, Demetrick D and Riabowol K. (1997b). *Cytogen. Cell Genet.*, **76**, 176–178.

Garkavtsev I, Grigorian IA, Ossovskaya VS, Chernov MV, Chumakov PM and Gudkov AV. (1998). *Nature*, **391**, 295–298.

Garkavtsev I, Kazarov A, Gudkov A and Riabowol K. (1996). *Nature Genet.*, **14**, 415–420.

Garkavtsev I and Riabowol K. (1997). *Mol. Cell. Biol.*, **17**, 2014–2019.

Harvey MB, Leco KJ, Arcellana-Panlilio MY, Zhang X, Edwards DR and Schultz GA. (1995). *Development*, **121**, 1005–1014.

Helbing CC, Veillette C, Riabowol K, Johnston RN and Garkavtsev I. (1997). *Cancer Res.*, **57**, 1255–1258.

Herman J, Merlo A, Mao L, Lapidus R, Issa J, Davidson N, Sidransky D and Baylin S. (1995). *Cancer Res.*, **55**, 4525–4530.

Iwase H, Greenman JM, Barnes DM, Hodgson S, Bobrow L and Mathew CG. (1996). *Cancer Lett.*, **108**, 179–184.

Japanese Breast Cancer Society. (1992). *General rules for clinical and pathological recording of breast cancer*. Kanehara: Tokyo, pp. 1–14.

Leco KJ, Apte SS, Taniguchi GT, Hawkes SP, Khokha R, Schultz GA and Edwards DR. (1997). *FEBS Letts.*, **401**, 213–217.

Lisitsyn N, Lisitsyn N and Wigler M. (1993). *Science*, **259**, 946–951.

Maestro R, Piccinin S, Doglioni C, Gasparotto D, Vukosavljevic T, Sulfaro S, Barzan L and Boiocchi M. (1996). *Cancer Res.*, **56**, 1146–1150.

Magdinier F, Ribieras S, Lenoir G, Frappart L and Dante R. (1998). *Oncogene*, **17**, 3169–3176.

Merlo A, Herman JG, Mao L, Lee DJ, Gabrielson E, Burger PC, Baylin SB and Sidransky D. (1995). *Nature Med.*, **1**, 686–692.

Mostert MMC, van de Pol M, Olde Weghuis D, Suijkerbuijk RF, Geurts van Kessel AG, van Echten J, Oosterhuis JW and Looijenga LHJ. (1996). *Cancer Genet. Cytogenet.*, **89**, 146–152.

Motomura K, Nishisho I, Takai S, Tateishi H, Okazaki M, Yamamoto M, Miki T, Honjo T and Mori T. (1988). *Genomics*, **2**, 180–184.

Rice J, Massey-Brown K and Futscher B. (1998). *Oncogene*, **17**, 1807–1812.

Sourvinos G and Spandidos D. (1998). *Biochem. Biophys. Res. Commun.*, **245**, 75–80.

Thompson ME, Jensen RA, Obermiller PS, Page DL and Holt JT. (1995). *Nature Genet.*, **9**, 444–450.

Vidal-Puig A and Moller DE. (1994). *Biotechniques*, **17**, 490–492.

Wong H, Anderson WD, Cheng T and Riabowol K. (1994). *Anal. Biochem.*, **223**, 251–258.

Yamashita H, Kobayashi S, Iwase H, Itoh Y, Kuzushima T, Iwata H, Itoh K, Naitoh A, Yamashita T, Masaoka A and Kimura N. (1993). *Jpn. J. Cancer Res.*, **84**, 871–878.

Yang-Feng TL, Li S, Han H and Schwartz PE. (1992). *Int. J. Cancer*, **52**, 575–580.

Oncogene (1999) 18, 2015–2021

http://www.stockton-press.co.uk/onc

Refined mapping of the region of loss of heterozygosity on the long arm of chromosome 7 in human breast cancer defines the location of a second tumor suppressor gene at 7q22 in the region of the CUTL1 gene

Wendy Rong Zeng[1], Peter Watson[2], Jenny Lin[1], Serge Jothy[3], Rosette Lidereau[4], Morag Park[1,5] and Alain Nepveu*[,1,5]

[1]*Molecular Oncology Group, Departments of Medicine, Oncology, McGill University, Montreal, Quebec, Canada;* [2]*Department of Pathology and Physiology, Faculty of Medicine, University of Manitoba, Canada;* [3]*Department of Laboratory Medicine and Pathobiology, University of Toronto, Ontario, Canada;* [4]*Laboratoire d'Oncogénétique, Centre René Huguenin, 35 rue Daily, F-92211 St-Cloud, France;* [5]*Biochemistry (A.N.), McGill University, Montreal, Quebec, Canada*

In breast cancer, loss of heterozygosity (LOH) has been described on the long arm of chromosome 7, at band q31, suggesting the presence of a tumor suppressor gene in this region. In this study, we have identified a second region of LOH on 7q, at band 7q22. Deletion of genetic material at 7q22 was found in all tumor types and grades and was associated with increased tumor size. The region of LOH at 7q22 in every case included one or more of three polymorphic markers that are located within the CUTL1 gene. LOH of 7q22 has also been documented in the case of human uterine leiomyomas (Zeng *et al.*, 1997; Ishwad *et al.*, 1997). Interestingly, in both leiomyomas and mammary tumors induced in transgenic mice expressing the Polyomavirus (PyV) large T (LT) antigen, immunocomplexes of CUTL1 and PyV LT antigen were detected (Webster *et al.*, 1998). Altogether, genetic data in human breast cancer and biochemical analyses in breast tumors from transgenic mice suggest that CUTL1 is a candidate tumor suppressor gene.

Keywords: breast cancer; tumor suppressor gene; chromosome 7q22; CUTL1; human Cut homeobox gene; loss of heterozygosity

Introduction

Breast cancer accounts for almost 30% of cancer diagnoses and almost 20% of cancer-related deaths in women. It is the leading cause of death among women aged 40–55. In the United States, it affects more than one in ten women (Harris *et al.*, 1992). Although little is known about the etiology and pathogenesis of breast neoplasias, alterations of oncogenes and tumor suppressor genes are considered to be critical in the multistep process leading to the development of breast cancer.

In human breast cancer, genetic deletions have been demonstrated to be one of the major genetic abnormalities. LOH has been documented at several chromosomal locations, including 1p, 1q, 2p, 3p, 6q, 7q, 8q, 9q, 11p, 11q, 13q, 15q, 16q, 17p, 17q, 18p, 18q and 22q (reviewed by Bieche and Lidereau, 1995). A few of these regions of LOH have been shown to include a known tumor suppressor gene implicated in breast cancer, such as *p53* at chromosome 17q13 (Isobe *et al.*, 1986; McBride *et al.*, 1986; Miller *et al.*, 1986), *BRCA-1* at 17q21 (Miki *et al.*, 1994) and *BRCA-2* at 13q12-13 (Wooster *et al.*, 1995). Genome-wide LOH analysis to generate allelotypes of human breast cancer revealed that several chromosomal regions could be deleted in a single tumor but no common sets of deletions could be identified between different tumors (Devilee *et al.*, 1997; Kerangueven *et al.*, 1997; Larsson *et al.*, 1990; Sato *et al.*, 1990).

From cytogenetic studies, deletions within the long arm of chromosome 7 have been found in breast cancer and other types of tumors, including myeloid leukemias (reviewed in Fischer *et al.*, 1998), kidney carcinomas, colon carcinomas, ovarian carcinomas, lung carcinomas, head-and-neck carcinomas (Berker-karauzum *et al.*, 1998; Dave *et al.*, 1995; Lundgren, 1991; Lundgren *et al.*, 1992; Mertens *et al.*, 1997; Solinas-Toldo *et al.*, 1996; Storto *et al.*, 1990) and uterine leiomyomas (Ozisik *et al.*, 1993; Sargent *et al.*, 1994; Xing *et al.*, 1997). LOH analyses confirmed that genetic material on 7q is frequently deleted in breast cancer, particularly in the 7q31 region (Bieche *et al.*, 1997; Callahan *et al.*, 1993; Champeme *et al.*, 1995; Deng *et al.*, 1994; Devilee *et al.*, 1997; Kristjansson *et al.*, 1997; Lin *et al.*, 1996; Tougas *et al.*, 1996). Altogether these data have been taken to suggest that a tumor suppressor gene is located in this region, however, this gene remains to be identified.

In previous studies, the loss of heterozygosity (LOH) at 7q22 has been reported in a subset of uterine leiomyomas (Ishwad *et al.*, 1997; Zeng *et al.*, 1997), which are benign tumors of smooth muscle origin most often referred to as fibroids. The smallest commonly deleted region in leiomyomas included markers that are located within CUTL1 (Cut-like-1), a gene that is homologous to the *Drosophila melanogaster cut* gene. Genetic studies in *Drosophila melanogaster* indicated that *cut* is involved in determination and maintenance of cell identity in several tissues. CUTL1 encodes a homeodomain transcription factor that functions as a transcriptional repressor. In humans, the Cut protein was first identified as the CCAAT displacement protein (CDP), a repressor of the gp-91 phox gene in undifferentiated myeloid cells (Skalnik *et al.*, 1991). A CUTL1 cDNA was also isolated by screening a cDNA expression library within a probe derived from the

*Correspondence: A Nepveu
Received 1 June 1998; revised 29 September 1998; accepted 23 October 1998

c-Myc gene promoter (Dufort and Nepveu, 1994). The human Cut protein was shown to bind to the c-Myc promoter and repress its expression (Harada *et al.*, 1994; Mailly *et al.*, 1996). Other *cut*-related cDNAs have been isolated from several mammalian species including dog, mouse and rat and were respectively termed Clox (Cut-like homeobox), Cux-1 and Cux-2 (Cut homeobox) and CDP-2 (Andres *et al.*, 1992; Dufort and Nepveu, 1994; Neufeld *et al.*, 1992; Quaggin *et al.*, 1996; Valarche *et al.*, 1993; Yoon and Chikaraishi, 1994).

Female transgenic mice expressing the Polyomavirus (PyV) Large T (LT) antigen under the control of the mouse mammary tumor virus long terminal repeat (MMTV-LTR) frequently develop, in addition to mammary tumors, uterine leiomyomas (Webster *et al.*, 1998). Since we had identified LOH at CUTL1 in human uterine leiomyomas, we examined whether PyV LT antigen formed specific complexes not only with members of the retinoblastoma (Rb) family (p105Rb, p107, p130), but also with the mammalian Cut protein. The results of coimmunoprecipitation analyses revealed that specific complexes of Cut and PyV LT antigen could be detected in both leiomyomas and mammary tumors. The existence of such complexes suggested that the alterations in the function of the Cut protein may be an important event in the etiology of breast cancer. These results lead us to hypothesize that genetic alterations within the 7q22 region may also occur in human breast tumors. We report here that LOH at 7q22 is observed in a subset of sporadic breast cancers and is associated with increased tumor size.

Results

A subset of breast tumors exhibits LOH of 7q22 and/or 7q31

The present study was initiated following the observation that genetic material at 7q22 is deleted in a fraction of uterine leiomyomas. The smallest deleted region at 7q22 included three polymorphic markers which since then have been located within the CUTL1 gene (Figure 2) (Ishwad *et al.*, 1997; Zeng *et al.* 1997; and Zeng *et al.*, manuscript in preparation). Secondly, the product of the CUTL1 gene was found to associate with the PyV LT oncoprotein both in uterine leiomyomas and in breast tumors that arise at high frequency in MMTV-PyV LT transgenic mice (Webster *et al.*, 1998). We thus postulated that genetic alterations within the 7q22 region may occur not only in human uterine leiomyomas but also in human breast tumors.

As a first step to verify whether LOH of 7q22 may occur in breast cancer, we analysed breast tumor DNA samples that had previously been characterized regarding LOH of 7q31, the chromosomal region adjacent to 7q22. We and others have shown that within 7q22 the marker D7S518 is the most frequently deleted in uterine leiomyomas. Thus, we first asked whether breast tumors with or without LOH of 7q31 could exhibit LOH of D7S518. This marker has been mapped to intron 20 of the CUTL1 gene (Zeng *et al.*, 1997; and Zeng *et al.*, manuscript in preparation). A total of 33 pairs of samples from Bièche *et al.* (1997) study were analysed. LOH of D7S518 was found in five of ten cases with LOH of 7q31 and in one out of 23 cases without LOH of 7q31 (Table 1). A total of 63 pairs of samples from the Lin *et al.* (1996) study were analysed. Among nine pairs of samples with LOH of 7q31, seven were informative for D7S518 and four exhibited LOH of this marker (Table 1). Among 54 pairs of samples without LOH of 7q31, two had suffered LOH of D7S518. Results obtained with these two sets of samples demonstrated that among breast tumors with LOH of the 7q31 region, 53% (9/17) also exhibit LOH of the D7S518 marker in 7q22. It is likely that the deleted region in these tumors is large and encompasses both 7q22 and 7q31. On the other hand, among breast tumors without LOH of 7q31, a small fraction suffered LOH of D7SD518. Thus, LOH of D7S518 can be observed independently of LOH at 7q31. We conclude that the long arm of chromosome 7 contains at least two tumor suppressor genes that can be inactivated in breast cancers, one at 7q22 and one at 7q31.

LOH of 7q22 and 7q31 in tumors from the NCIC-Manitoba breast tumor bank

To establish the incidence and extent of 7q22 deletions, we investigated LOH of 7q22 in samples from the National Cancer Institute of Canada (NCIC)-Manitoba Breast Tumor Bank (Watson *et al.*, 1996). We have analysed 66 pairs of tumors and adjacent normal control tissues representative of all classes of breast tumors. At least three microsatellite markers within 7q22, *D7S518, D7S515 and D7S666*, were used in all cases. In a previous study, we have mapped the marker *D7S518* within an intron of the CUTL1 gene and the markers *D7S515* and *D7S666* close to the 5′ end of this gene (Zeng *et al.*, 1997). Determination of the CUTL1 exon/intron structure and DNA sequencing of the long arm of chromosome 7 has since revealed that all three markers are located within the CUTL1 gene, in introns 20, 3 and 6 respectively (Figure 2) (Zeng *et al.*, manuscript in preparation; http://www.ncbi. nlm.nih.gov, accession number AF024533 and AF047825). Tumors with LOH of one or more of these markers were then further analysed to map the boundaries of the deleted regions. The physical order of all of the microsatellite markers and CUT1 with respect to each other have previously been established (Zeng *et al.*, 1997). The number of cases studied for each marker, the number of informative

Table 1 Loss of heterozygosity of D7S518 in breast tumors with or without LOH of 7q31

Sources of samples	*7q31 status in breast cancers*	*Samples analysed*	*Informative cases for D7S518*	*LOH of D7S518*
Bièche *et al.*	LOH of 7q31	10	10	5 (50%)
Study	Retention of 7q31	23	23	1 (4%)
Lin *et al.*	LOH of 7q31	9	7	4 (57%)
Study	Retention of 7q31	54	54	2 (3.7%)

DNAs from breast cancers and matched normal tissues were amplified from patients with breast cancers using oligonucleotide primers for the polymorphic marker D7S518. The source of samples is indicated, together with the numbers of patients tested, informative patients and patients with LOH for markers on 7q31 or 7q22. The information regarding LOH at 7q31 was derived from the original studies

cases, and the number and percentage of cases that exhibit LOH are given in Table 2 and shown in Figure 2. Representative LOH results are shown in Figure 1. LOH was scored with at least one 7q22 marker in 12 of 66 (18.2%) of the tumors examined (patients 10544, 11305, 93-4635, 93-5199, 93-11232, 93-11747, 93-12017, 93-18747, 94-1663, 94-3808, 94-5629 and 94-133582, see Figure 2). The superposition of the overlapping deletions in the 12 tumors revealed two common regions of deletion, one in 7q22 and encompassing the CUTL1 gene, and one in 7q31 (Figure 2). The proximal (centromeric) and distal (telomeric) boundaries of the critical region in 7q22 were defined by breakpoints in tumors #10544, 11305, and #93-5199 that were flanked by the *D7S666* and *D7S658* markers, respectively (Figure 2). The proximal (centromeric) and distal (telomeric) boundaries of the critical region in 7q31 were flanked by the *D7S480* and *D7S650* markers, respectively (Figure 2).

Association between LOH at 7q22 and clinical parameters

To determine whether loss of genetic material at 7q22 or 7q31 may be associated with pathological features of breast tumors, we analysed available clinical data including the tumor type, grade and size, estrogen and progesterone receptor (ET and PR) status, occurrence of lymph node metastasis and age of onset. Statistical analysis was performed using the Mann–Whitney test (Mann and Whitney, 1947). We found no correlation between LOH at 7q22 and tumor type or grade, ER or PR expression, nodal status, or age of onset. However, there was a significant association (P value = 0.0082) between LOH at 7q22 and tumor size (Table 3). The average sizes of breast tumors with or without LOH at 7q22 were 4.99 and 2.93 cm respectively. The difference in size was further accentuated in the group of tumors with LOH at 7q22 but retention of 7q31 (6.5 Vs 2.99 cm; P value = 0.0074). In contrast, no significant correlation was found between LOH at 7q31 and any clinical feature.

Table 2 LOH analysis of 66 breast cancers using 11 polymorphic markers on chromosome 7

Markers	*Patients tested*	*Informative patients*	*Patients with LOH*
D7S524	12	5	2
D7S527	3	2	0
D7S518	66	59	6
D7S666	66	47	4
D7S515	66	48	8
D7S658	5	3	0
D7S471	1	1	0
D7S486	9	8	3
D7S522	66	45	3
D7S480	66	61	7
D7S650	66	48	7

DNAs from tumors and matched normal peripheral breast tissues were amplified from 66 patients with breast cancers using oligonucleotide primers for 11 polymorphic markers on chromsome 7q. The list of markers is presented, together with the numbers of patients tested, informative patients and patients with LOH for each marker. The level of informativeness observed for each of the markers in our cohort of patients was consistent with the published values

Discussion

LOH within the 7q31 region has previously reported in human breast carcinomas, and in several cases the deletions encompassed the adjacent region, 7q22 (Bieche *et al*., 1992, 1997; Champeme *et al*., 1995; Deng *et al*, 1994; Lin *et al*., 1996; Zenklusen *et al*., 1994). The results of the present study establish that in some breast tumors the loss of genetic material on the long arm of chromosome 7 can be limited to the 7q22 region. Thus, regarding chromosomal deletions on 7q, collectively the available data define three classes of breast tumors on the basis of whether the LOH region encompasses markers in only 7q22, only 7q31 or both 7q22 and 7q31 (Bieche *et al*., 1992, 1997; Champeme *et al*., 1995; Deng *et al*., 1994; Lin *et al*., 1996; Zenklusen *et al*., 1994). These results suggest that 7q contains at least two tumor suppressor genes that can be inactivated in breast cancers, one at 7q22 and one at 7q31.

Three sets of tumor samples originating from different research centers have been analysed in this study. LOH of 7q22 and 7q31 have been found in tumors from each set, however, there was considerable variation in the proportion of LOH between the three sets especially for markers at 7q31. This variation is unlikely to be due to the differences in ethnic group composition of each set since the patients in all sets were almost exclusively of Caucasian origin. We think that differences in LOH frequencies can be attributed mainly to the fact that we have been very conservative in our appreciation of LOH. In particular, we did not count as LOH any sample where both alleles in the normal control were not clear. This bias almost certainly led us to underestimate LOH frequencies.

There was no correlation between LOH at 7q22 and tumor grade, suggesting that the loss of genetic material at 7q22 is probably an early event in tumor development and, most likely, is not associated with tumor progression. On the other hand, LOH of 7q22 was associated with increased tumor size, raising the possibility that the tumor suppressor gene at 7q22 could function to restrict cellular proliferation.

The smallest commonly deleted region on 7q22 includes polymorphic markers that are all located within the CUTL1 gene. Therefore, the tumor suppressor gene at 7q22 either is CUTL1 or is located close to it. Interestingly, in breast tumors that arise in MMTV-PyV LT transgenic mice, the murine Cut protein was found to form a complex together with the PyV LT antigen (Webster *et al*., 1998). Moreover, in cotransfection studies, the CUTL1 gene product was also coimmunoprecipitated together with the SV40 Large T antigen (SV40 LT) (Martin *et al*., manuscript in preparation). At present the effect of Large T oncoproteins on Cut function is not clear. However, these viral oncoproteins have previously been found to inactivate the function of the p53 and pRB tumor suppressor proteins. Thus, interactions with these viral oncoproteins suggest that Cut proteins may play an important role in the control of cellular proliferation. This hypothesis received further support from the finding that Cut DNA binding activity is regulated in a cell-cycle dependent manner (Coqueret *et al*., 1998). Whereas Cut was expressed in all phases of the cell cycle, Cut DNA binding activity was the highest at the end of G1 and during S phase.

In conclusion, two sets of data, LOH mapping analysis and protein-protein interaction studies, strongly point towards the CUTL1 gene as a candidate tumor suppressor gene. It should be stressed, however, that the CUTL1 gene appears to cover a very large distance, over 200 Kbp, and that several introns are more than 10 Kbp (Zeng *et al.*, manuscript in preparation). It is thus possible that another transcription unit exists within the boundaries of the CUTL1 gene. In accordance with the recently

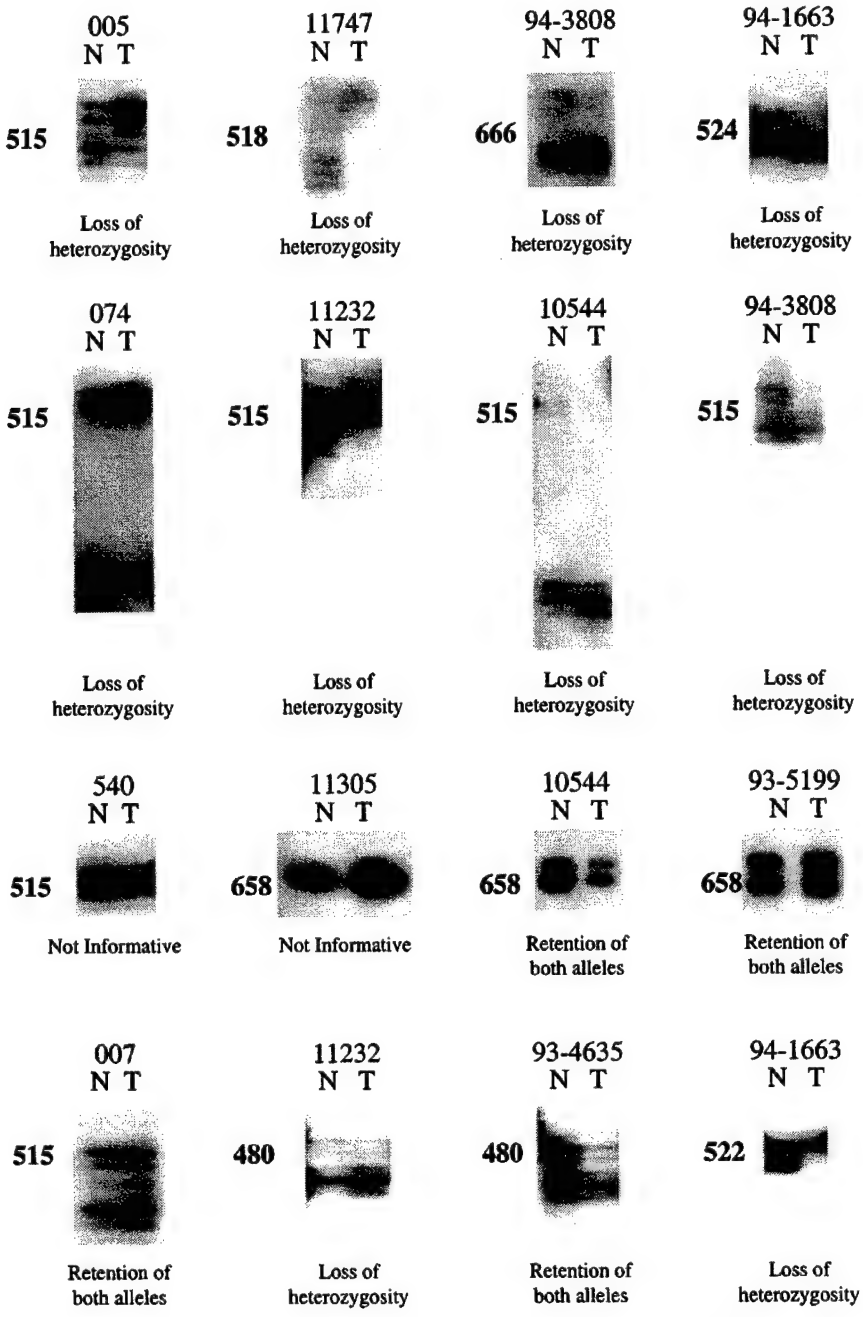

Figure 1 Representative PCR amplifications of (CA)n microsatellite repeats. DNAs from tumors (T) and matched normal breast tissues (N) were analysed from 66 patients with breast cancer. Representative PCR amplifications of (CA)n microsatellite repeats D7S518, D7S666, D7S524, D7S515, D7S522, D7S480, D7S650, D7S658 are shown. Oligonucleotide primers were used to PCR amplify the regions of DNA containing these markers, in the presence of radiolabeled dCTP. Products were denatured and separated on a standard 5% sequencing gel. A patient is considered to be informative if there are two major bands (corresponding to two alleles) in the normal DNA lane. A patient shows LOH if, in the tumor DNA lane, one of the alleles is absent or shows diminished intensity. For example, patient 10544 is informative for the marker D7S515, and shows LOH at that locus, but shows no LOH at locus D7S658 and patient 11305 is uninformative for marker D7S658

proposed rules for the definition of a tumor suppressor gene, a firm statement about the identity of the tumor suppressor gene at 7q22 will have to await the demonstration either that the remaining allele is mutated or that the function of the CUTL1 gene product is inactivated or altered in some breast tumors (Haber and Harlow, 1997). At the minimum, the fact that a polymorphic marker within CUTL1 is consistently deleted in breast tumors with LOH of 7q22 will provide a useful start point for positional cloning approaches to identify the critical tumor suppressor gene at 7q22.

Materials and methods

Specimen collection

Sixty-six pairs of samples from NCIC-Manitoba Breast Tumor Bank have been analysed in this study. All tumor samples selected from the Manitoba Breast Tumor Bank were high quality tissues selected to ensure >30% epithelial tumor component with minimal contaminating normal tissues, and matching normal tissues were also histologically verified. All tissue histological assessment was performed uniformly by a single pathologist (PW) and conducted on high quality paraffin sections from the face of the tissue block, thus ensuring consistency in assessing

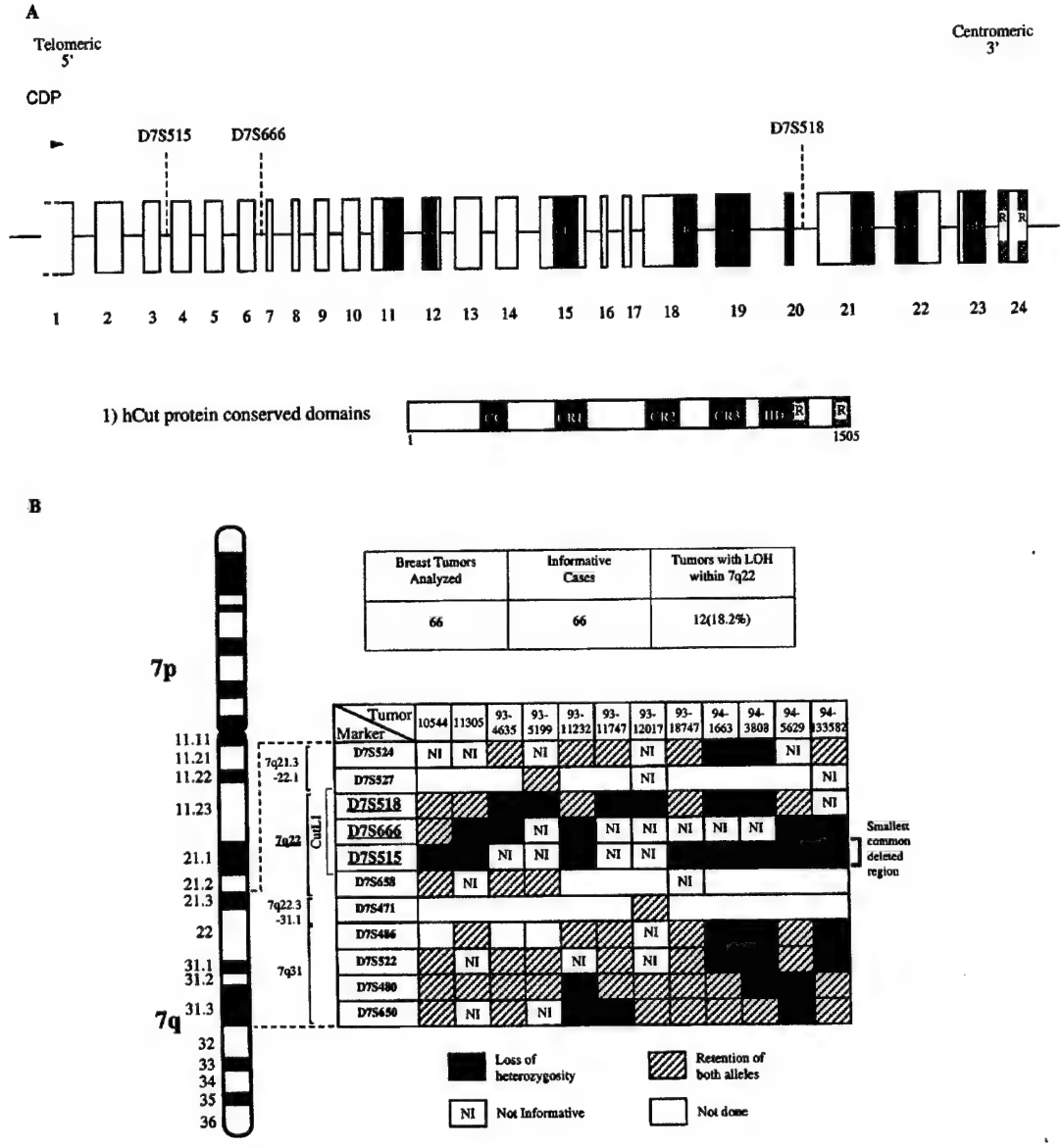

Figure 2 Mapping of LOH within 7q. (Left) Representation of human chromosome 7 including band assignments. (Right) Names of polymorphic markers used are given, along with chromosome band assignments and the position of the CUTL1 gene. Twelve columns representing 12 patients with a loss of heterozygosity on chromosome 7q22 are shown. Explanation of the symbols used is given. The smallest common deletion in these seven patients is indicated by the vertical line to the right. All 54 tumors not shown in this figure were informative for at least one marker within the critical region but failed to show LOH

Table 3 Relationship between allelic loss for loci at 7q22 and 7q31 and clinicopathological characteristics of the 66 breast tumors

Clinical-pathological characteristics		*Allelic loss for loci at 7q*					
		LOH 7q22			*LOH 7q31*		
		+	−	P *value*	+	−	P *value*
Type	Ductal	10	46		9	47	
	Lobular	1	4	ns	1	4	ns
	Other	sa	co, pa, is, is		sa	co, pa, is, is	
Grade	well	0	10		0	10	
	mod	6	22		7	21	
	poor	5	20	ns	3	22	ns
	not graded	1	2		1	2	
ER	positive	7	36	ns	8	36	ns
	negative	4	17		3	18	
PR	positive	5	24		4	23	
	negative	6	29	ns	7	31	ns
	not assayed	1	4		1	1	
LN status	positive	4	17		2	17	
	negative	8	32	ns	9	34	ns
	unknown	–	4		–	4	
Size	mean (cms)	4.99	2.93	0.0082	2.77	3.45	ns
Age	mean (yrs)	53	59	ns	55	59	ns

The statistical analysis was performed using the Mann-Whitney test. Grade = Nottingham grade, Sa = sarcoma, co = colloid carcinoma, pa = papillary carcinoma, is = predominant ductal carcinoma *in situ* with small ductal invasive foci, ns = not significant, ER = estrogen receptor, PR = progesterone receptor, LN = lymph node

histological features (Watson *et al.*, 1996). Samples from the Lin *et al.* (1996) study were obtained from two different sources: 43 from the Surgical Pathology Laboratory of the Royal Victoria Hospital, Montreal, Canada and 20 from the Mount Sinai Hospital, Toronto, Canada. Samples from the Bièche study were obtained from the Centre René Huguenin, Saint-Cloud, France (Bieche *et al.*, 1997).

Genomic DNA extraction from paraffin blocks

The basic protocol has been reported before (Watson *et al.*, 1993). Twenty μm sections were cut and placed in 1.5 ml Eppendorf tubes. This material was then subjected to two xylene washes and two ethanol washes (100 and 95%), incubated for 1–3 days in lysis buffer (800 μg/ml proteinase K, 0.1 M Tris (pH 8) and 0.004 M EDTA), followed by heat inactivation (boiling) and ethanol precipitation. The quantity or quality of DNA of 66 pairs of samples were good enough for the following microsatellite repeat analysis of all markers.

Microsatellite repeat analysis

DNA from tumors and matched control tissues were characterized by polymerase chain reaction (PCR) analysis using a pair of oligonucleotide primers for each polymorphic marker. Ten $(CA)_n$ repeat microsatellite markers on chromosome 7 were used to identify the region of loss of chromosome 7 in breast cancers: D7S524, D7S527, D7S515, D7S666, D7S518, D7S471, D7S486, D7S522, D7S480, D7S650. Information of the primer sequences and allele lengths are available in the Genome Database (GDB). Some of these markers, D7S527, D7S658 and D7S471, have been used only with a subset of samples in order to define more precisely the deleted region. To enhance the sensitivity of the assay and to limit the number of amplification cycles, radioactively labeled deoxyribonucleotides have been included in the reaction. The PCR amplification conditions were similar to that reported before (Zeng *et al.*, 1997). The $(CA)_n$ repeats were amplified by PCR in a final volume of 50 μl, containing 50 ng DNA, 1.5 mM $MgCl_2$, 5 μl standard 10 × PCR buffer (200 mM Tris-HCl pH 8.4, 500 mM KCl), 0.4 μM of each primer, 0.125 mM dNTPs, 1 μCi [α-^{32}P]dCTP and 1 unit of Taq polymerase (Gibco/BRL, Burlington, Ontario). An initial step of 5 min at 95°C was followed by 35 cycles of 1 min denaturation at 94°C 30 s of annealing at 59°C and 1.5 min of extension at 72°C, followed by a final extension step of 7 min at 72°C. Pilot experiments with different PCR cycle numbers indicated that 35 cycles was still within the linear amplification range. PCR products were separated in a 6% sequencing gel containing formamide or a conventional 6% sequencing gel.

Determination of LOH

Allelic loss was scored only on informative patients whose normal DNA samples were polymorphic at a given locus. Patients who were uninformative were not considered. LOH was identified, visually or following Phosphoimager densitometric analysis, as a loss in intensity (>50%) or complete loss of one allele in the tumor DNA when compared with the normal DNA from the same patient. All cases of LOH were confirmed by three separate experiments with two different reviewers. It is worth noting that we have been very conservative in our appreciation of LOH. In particular, we did not count as LOH any sample where both alleles in the normal control were not clear. This bias possibly led us to underestimate LOH frequencies. In certain cases, additional markers have been used in order to define more precisely the deleted region.

Acknowledgements
We are grateful to Drs Irene Andrulis and Ivan Bièche for allowing us to use samples collected respectively at the Mount Sinai Hospital in Toronto, Canada and the Centre René Huguenin, Saint-Cloud, France. Thanks are also due to Jo-Ann Bader for advice on deparaffinization, and Lam Leduy for the mapping of polymorphic markers and processing the tumors used in this study. This research was funded by an operating grant to AN from the US Army Medical Research and Materiel Command (USAMRMC) as part of the Breast Cancer Research Program (BCRP). AN is the recipient of a scholarship from Le Fonds de la Recherche en Santé du Québec. WRZ is the recipient of studentships from the Alexander McFee Studentship, the McGill University Department of Medicine Internal Studentship, and the Research Institute of the Royal Victoria Hospital Studentship.

References

Andres V, Nadal-Ginard B and Mahdavi V. (1992). *Dev.*, **116,** 321–334.
Berkerkarauzum S, Luleci G, Ozbilim G, Erdogan A, Kuzucu A *et al.* (1998). *Cancer Gene. Cytogen.*, **100,** 114–123.
Bièche I, Champeme MH, Matifas F, Hacene K, Callahan R *et al.* (1992). *Lancet*, **339,** 139–143.
Bièche I, Khodja A, Driouch K and Lidereau R. (1997). *Clin. Cancer Res.*, **3,** 1009–1016.
Bièche I and Lidereau R. (1995). *Genes, Chrom. Cancer*, **14,** 227–251.
Callahan R, Cropp C, Merlo GR, Diella F, Venesio T *et al.* (1993). *Clinica Chimica Acta*, **217,** 63–73.
Champeme MH, Bieche I, Beuzelin M and Lidereau R. (1995). *Genes Chrom. Cancer*, **12,** 304–306.
Coqueret O, Bérubé G and Nepveu A. (1998). *EMBO J.*, **17,** 4680–4694.
Dave BJ, Hopwood VL, King TM, Jiang H, Spitz MR *et al.* (1995). *Cancer Epidem. Biomarkers Prev.* **4,** 743–749.
Deng G, Chen LC, Schott DR, Thor A, Bhargava V *et al.* (1994). *Cancer Res.*, **54,** 499–505.
Devilee P, Hermans J, Eyfjord J, Boorresen AL, Liderau R *et al.* (1997). *Genes Chrom. Cancer*, **18,** 193–199.
Dufort D and Nepveu A. (1994). *Mol. Cell. Biol.*, **14,** 4251–4257.
Fischer K, Brown J, Scherer SW, Schramm P, Stewart J *et al.* (1998). *Recent Res. Cancer Res.*, **144,** 46–52.
Haber D and Harlow E. (1997). *Nature Genet.*, **16,** 320–322.
Harada R, Dufort D, Denis-Larose C and Nepveu A. (1994). *J. Biol. Chem.*, **269,** 2062–2067.
Harris JR, Lippman ME, Veronesi U and Willett W. (1992). *N. Engl. J. Med.*, **327,** 319–328.
Ishwad CS, Ferrell RE, Hanley K, Davare J, Meloni AM *et al.* (1997). *Genes Chrom. Cancer*, **19,** 156–160.
Isobe M, Emanuel BS, Givol D, Oren M and Croce CM. (1986). *Nature*, **320,** 84–85.
Kerangueven F, Noguchi T, Coulier F, Allione F, Wargniez V *et al.* (1997). *Cancer Res.*, **57,** 5469–5474.
Kristjansson AK, Eiriksdottir G, Ragnarsson G, Sigurdsson A, Gudmundsson J *et al.* (1997). *Anticancer Res.*, **17,** 93–98.
Larsson C, Bystrom C, Skoog L, Rotstein S and Nordenskjold M. (1990). *Genes Chrom. Cancer*, **2,** 191–197.
Lin JC, Scherer SW, Tougas L, Traverso G, Tsui LC *et al.* (1996). *Oncogene*, **13,** 2001–2008.
Lundgren R. (1991). *Scand. J. Urol. Nephrol.*, **136,** 1–35.
Lundgren R, Mandahl N, Heim S, Limon J, Henrikson H *et al.* (1992). *Genes Chrom. Cancer*, **4,** 16–24.
Mailly F, Berube G, Harada R, Mao PL, Phillips S *et al.* (1996). *Mol. Cell. Biol.*, **16,** 5346–5357.
Mann HB and Whitney DR. (1947). *Ann. Mathemat. Stat.*, **18,** 50–60.
McBride OW, Merry D and Givol D. (1986). *Proc. Natl. Acad. Sci. USA*, **83,** 130–134.
Mertens F, Johansson B, Hoglund M and Mitelman F. (1997). *Cancer Res.*, **57,** 2765–2780.
Miki Y, Swensen J, Shattuck-Eidens D, Futreal PA, Harshman K *et al.* (1994). *Science*, **266,** 66–71.
Miller C, Mohandas T, Wolf D, Prokocimer M, Rotter V *et al.* (1986). *Nature*, **319,** 783–784.
Neufeld EJ, Skalnik DG, Lievens PM and Orkin SH. (1992). *Nature Genet.*, **1,** 50–55.
Ozïsik YY, Meloni AM,Surti U and Sandberg AA. (1993). *Cancer Genetics & Cytogenetics* **71,** 1–6.
Quaggin SE, Vandenheuvel GB, Golden K, Bodmer R and Igarashi P. (1996). *J. Biol. Chem.*, **271,** 22624–22634.
Sargent MS, Weremowicz S, Rein MS and Morton CC. (1994). *Cancer Genetics & Cytogenetics* **77,** 65–68.
Sato T, Tanigami A, Yamakawa K, Akiyama F, Kasumi F *et al.* (1990). *Cancer Res.*, **50,** 7184–7189.
Skalnik DG, Strauss EC and Orkin SH. (1991). *J. Biol. Chem.*, **266,** 16736–16744.
Solinas-Toldo S, Wallrapp C, Muller-Pillasch F, Bentz M, Gress T *et al.* (1996). *Cancer Res.*, **56,** 3803–3807.
Storto PD, Saidman SL, Demetris AJ, Letessier E, Whiteside TL *et al.* (1990). *Genes Chrom. Cancer*, **2,** 300–310.
Tougas L, Halwani F, Tremblay G, Sampalis J, Lin J *et al.* (1996). *Clin. Investig. Med. – Medecine Clinique et Experimentale*, **19,** 222–230.
Valarche I, Tissier-Seta JP, Hirsch MR, Martinez S, Goridis C *et al.* (1993). *Development*, **119,** 881–896.
Watson PH, Safneck JR, Le K, Dubik D and Shiu RP. (1993). *J. Natl. Cancer Inst.*, **85,** 902–907.
Watson PH, Snell L and Parisien M. (1996). *Cmaj*, **155,** 281–283.
Webster MA, Martinsoudant N, Nepveu A, Cardiff RD and Muller WJ. (1998). *Oncogene*, **16,** 1963–1972.
Wooster R, Bignell G, Lancaster J, Swift S, Seal S *et al.* (1995). *Nature*, **378,** 789–792.
Xing YP, Powell WL and Morton CC. (1997). *Cancer Genetics & Cytogenetics* **98,** 69–74.
Yoon SO and Chikaraishi DM. (1994). *J. Biol. Chem.*, **269,** 18453–18462.
Zeng WR, Scherer SW, Koutsilieris M, Huizenga JJ, Filteau F *et al.* (1997). *Oncogene*, **14,** 2355–2365.
Zenklusen JC, Bieche I, Lidereau R and Conti CJ. (1994). *Proc. Natl. Acad. Sci. USA*, **91,** 12155–12158.

Journal of Pathology
J Pathol 2000; **192**: 313–320.

Original Paper

Lumican and decorin are differentially expressed in human breast carcinoma

Etienne Leygue[1], Linda Snell[2], Helmut Dotzlaw[1], Sandra Troup[2], Tamara Hiller-Hitchcock[2], Leigh C. Murphy[1], Peter J. Roughley[3] and Peter H. Watson[2]*

[1] *Department of Biochemistry and Molecular Biology, University of Manitoba, Faculty of Medicine, Winnipeg, Manitoba, Canada, R3E OW3*
[2] *Department of Pathology, University of Manitoba, Faculty of Medicine, Winnipeg, Manitoba, Canada, R3E OW3*
[3] *Genetics Unit, Shriners Hospital for Children, Montreal, Quebec, Canada, H3G 1A6*

*Correspondence to:
Dr P. H. Watson, Department of Pathology, D212-770 Bannatyne Ave, University of Manitoba, Winnipeg, Manitoba R3E OW3, Canada.
E-mail:
pwatson@cc.umanitoba.ca

Received: 22 June 1999
Revised: 1 February 2000
Accepted: 17 April 2000

Abstract

Previous studies have shown that lumican is expressed and increased in the stroma of breast tumours. Lumican expression has now been examined relative to other members of the small leucine-rich proteoglycan gene family in normal and neoplastic breast tissues, to begin to determine its role in breast tumour progression. Western blot study showed that lumican protein is highly abundant relative to decorin, while biglycan and fibromodulin are only detected occasionally in breast tissues ($n=15$ cases). Further analysis of lumican and decorin expression performed in matched normal and tumour tissues by *in situ* hybridization showed that both mRNAs were expressed by similar fibroblast-like cells adjacent to epithelium. However, lumican mRNA expression was significantly increased in tumours ($n=34$, $p<0.0001$), while decorin mRNA was decreased ($p=0.0002$) in neoplastic relative to adjacent normal stroma. This was accompanied by a significant increase in lumican protein ($n=12$, $p=0.0122$), but not decorin. Further evidence of altered lumican expression in breast cancer was manifested by discordance between lumican mRNA and protein localization in some regions of tumours but not in adjacent morphologically normal tissues. It is concluded that lumican is the most abundant of these proteoglycans in breast tumours and that lumican and decorin are inversely regulated in association with breast tumourigenesis.

Keywords: **lumican; decorin; small leucine-rich proteoglycan; breast cancer; tumour progression**

Introduction

The development and progression of breast carcinoma are caused by alterations in the expression of multiple genes, most of which are responsible for normal physiological pathways and the necessary cellular interactions to support these functions within the mammary gland. These include alterations in the interactions between the epithelial and stromal cells, which are manifested in tumours by well-recognized morphological changes known as the stromal reaction [1]. Such alterations in stromal–epithelial interactions may influence the risk of transformation of the breast epithelial cell and may contribute to the very early steps in tumourigenesis, as has recently been proposed in other systems [2]. However, the net effect of these alterations in the stroma on the later stages of tumour progression is unresolved [3].

Resolution of this issue is complicated by the recognition that the stroma is a highly complex tissue that includes a variety of different types of fibroblasts [4] and a range of proteins, glycoproteins, and proteoglycans which may play a role in tumour biology. We have recently extended this list by identifying lumican, a member of the small leucine-rich proteoglycans (SLRPs) as an mRNA that is expressed in the stroma of normal breast tissues and is overexpressed in invasive carcinomas [5]. Members of this family of proteoglycans have been implicated principally in matrix assembly and structure [6], but also more recently in the control of cell growth [7]. While studies of decorin have shown altered expression in neoplastic stroma [3], lumican has previously been studied only in the context of connective tissue and corneal disease [8,9], and the role of SLRPs in human breast cancer is relatively unexplored. To explore further the potential role of lumican and related genes in breast tumour progression, we have now examined the expression of lumican relative to that of other members of the SLRP family, decorin, biglycan and fibromodulin, at both mRNA and protein level, in normal and neoplastic breast tissues.

Materials and methods

Human breast tissues

All breast tumour cases used for this study were selected from the NCIC-Manitoba Breast Tumor Bank (Winnipeg, Manitoba, Canada). As has been previously described [10], tissues are accrued to the bank from cases at multiple centres within Manitoba, rapidly collected, and processed to create matched formalin-fixed, paraffin-embedded, and frozen tissue

blocks with the mirror image surfaces orientated by coloured inks. The histology and cellular composition of every sample in the bank are interpreted in haematoxylin and eosin (H&E)-stained sections from the face of the former tissue block.

For the initial study to compare broadly the expression of different members of the SLRP gene family, a mixed pilot cohort was selected from the Tumor Bank to include nine different invasive carcinomas, three normal tissue samples from patients with cancer, and three normal tissues from normal patients without cancer. The invasive tumours included different tumour types (five ductal, three lobular, and one tubular carcinoma), grades (four high, one moderate, four low Nottingham grades), and oestrogen receptor (ER) levels (three ER < 10 fmol/mg, three ER 10–20, three ER 39–169), and total stromal fractions ranging from 50 to 95% of the cross-sectional area. The mean patient ages were 62, 70, and 28 years for each subgroup, respectively (tumour tissues, normal tissues adjacent to tumours, and normal tissues).

For the subsequent studies to compare lumican and decorin expression, a second more defined and homogeneous cohort of 46 cases was selected to provide matching primary tumour tissues and adjacent normal tissue. This cohort included only invasive ductal carcinomas and was primarily selected to ensure availability of histologically confirmed and distinct regions comprising morphologically normal and tumour tissue elements in different blocks (12 cases, for western blot studies) or the same block (34 cases, for *in situ* hybridization studies). The subset used for western blot studies was also selected to possess equivalent cross-sectional areas [mean section area$^{(SD)}$ in tumour tissues $=0.86^{(0.44)}$ cm^2, adjacent normal tissues $=0.85^{(0.35)}$ cm^2] and stromal content [mean stromal area$^{(SD)}$ in tumour tissues $=68^{(10)}$%, adjacent normal tissues $=89^{(6)}$%] between the matching blocks and to incorporate cancer cases from both post-menopausal (six cases mean$^{(SD)}$ $=76^{(7)}$ years) and pre-menopausal patients (six cases mean$^{(SD)}$ $=44^{(3)}$ years).

Sodium dodecyl sulphate/polyacrylamide gel electrophoresis (SDS/PAGE) and immunoblotting

Total proteins were extracted from frozen tissue sections. These were cut from the face of frozen tissue blocks immediately adjacent to the face of a matching paraffin block [11] from which paraffin sections had been previously cut for pathological assessment and for *in situ* hybridization. For the first cohort of cases, an average of 20 20 μm tissue sections were cut from each typical tissue block (0.5×1.0 cm^2 cross-sectional area) and used for extraction; however, the number of tissue sections was varied for each case according to the measured area of the tissue within individual blocks, to ensure that equivalent volumes of tissue were used for the extraction, which was done as described previously [12]. For the second cohort of matching tissue samples, the same number of frozen sections (20×20 μm) was cut from the measured surface of each tissue block together with a single section from the adjacent paraffin block. This was used as a reference for composition and protein extraction was then performed on the frozen sections with equivalent volumes of extraction buffer. Proteins present in equivalent volumes of extracts were analysed by SDS/PAGE and immunoblotting, using anti-peptide antibodies specific for the carboxyl-terminal regions of the core proteins of lumican, decorin, fibromodulin, and biglycan [12–14]. The specificity of all antibodies was verified by peptide absorption and SLRP cross-reactivity analysis. Protein signals were detected by chemiluminescence and photographed prior to quantitation by video-image analysis and densitometry using an MCID M4 system and software (Imaging Research, St Catherines, Ontario, Canada). All signals were then adjusted with reference to control cartilage samples run with each blot. For the second cohort of matched tissue samples, signals were also adjusted with reference to the measured cross-sectional area and the stromal content of the tissue block to control for equivalent loading. Additional analysis was performed on all signals after further adjustment for relative stromal content of the tissue sections assessed in adjacent H&E sections.

Immunohistochemistry

Immunohistochemistry was performed on paraffin sections using the same antibody to lumican as used for immunoblotting [9,12]. Sections (5 μm thick) were obtained from paraffin-embedded tissue blocks matching the frozen tissue blocks of those cases used for reverse transcription-polymerase chain (RT-PCR) and protein analysis. After deparaffinizing, clearing, and hydrating in TBS buffer (Tris buffered saline, pH 7.6) the sections were pretreated with 3% hydrogen peroxide for 10 min to remove endogenous peroxidases and non-specific binding was blocked with normal swine serum, 1:10 (Vector Laboratories S-4000). TBS was used between steps to rinse and as a diluent. Primary antibody to lumican was applied at a 1:400 dilution overnight at 4°C, followed by biotinylated secondary swine anti-rabbit IgG, 1:200 (DAKO) for 1 h at room temperature. Tissue sections were incubated 45 min at room temperature with an avidin/biotin horseradish peroxidase system (Vectastain ABC Elite, Vector Lab.) followed by detection with DAB (diaminobenzidine), counterstaining with 2% methyl green, and mounting. A positive tissue control (colonic mucosa) and a negative reagent control (no primary antibody) were run in parallel. Immunostaining patterns and intensity were assessed by light microscopic visualization.

In situ hybridization

Paraffin-embedded 5 μm sections of breast tissues were analysed by *in situ* hybridization according to a previously described protocol [5]. For lumican, the plasmid Lumi-398, which consisted of pGEM-T plasmid (Pharmacia Biotech), containing a 398 bp portion of

lumican cDNA between bases 1332 and 1729, was used as a template to generate UTP^{S35} labelled sense and antisense riboprobes using Riboprobe Systems (Promega, Madison, WI, USA) and either the T7 or SP6 promotor at the 5′ or 3′ end of the lumican sequence according to the manufacturer's instructions. For decorin, the plasmid Dec-322 was used as a template. This consisted of pGEM-T plasmid containing a decorin insert with a comparable length (322 bp) to the lumican probe generated by PCR amplification from the decorin cDNA [12] using primers that corresponded to decorin (sense 5′-AAATGCCCAAAACTCTTCAG-3′ and antisense 5′-AAACTCAATCCCAACTTAGCC-3′) [15]. All PCR cDNAs and plasmid inserts were sequenced to confirm their identity. Levels of lumican and decorin expression were assessed in normal and tumour regions by microscopic examination at low magnification and with reference to the negative sense and positive control tumour sections. This was done as previously described [5] by scoring the estimated average signal intensity (on a scale of 0–3) and the proportion of stromal cells showing a positive signal (0, none; 0.1, less than one-tenth; 0.5, less than one-half; 1.0, greater than one-half). The intensity and proportion scores were then multiplied to give an overall score. Regions with a score lower than 1.0 were deemed negative or weakly positive.

Microdissection and protein extraction analysis

To assess protein localization within regions of tumours, two cases were selected that showed marked and well-defined regions within the same tissue section with discrepancies between mRNA and protein expression. This was determined by *in situ* hybridization and immunohistochemistry in adjacent serial sections from paraffin tissue blocks. The mirror image frozen tissue blocks to these paraffin blocks were used for microdissection as previously described [11] and protein was extracted from these histologically defined regions as described above. Briefly, thin 5 μm frozen sections were cut from the faces of the frozen tissue blocks and stained by H&E, and the relevant histological regions of approximately 1–2 mm^2 distinguished and confirmed by reference to the paraffin sections already studied. Multiple thick frozen sections (20×20 μm) were then cut, rapidly stained, and microdissected at room temperature from each section in turn, and the microdissected tissue fragments were frozen again prior to protein extraction.

Results

Identification of lumican as the most abundant SLRP in normal and neoplastic breast tissues

To determine the relative importance of altered lumican expression in breast tumourigenesis, the expression of lumican protein was compared with that of three other members of the SLRP family, decorin, fibromodulin and biglycan, by western blot in a heterogeneous panel of nine breast tumours and six normal tissues.

Lumican was highly abundant in all samples and in both neoplastic and normal tissues (Figure 1). A significant increase was seen in the mean level of lumican protein between normal and tumour [mean$^{(SD)}$ tissue adjusted optical density units, normal $= 0.43^{(0.08)}$, tumour $= 0.56^{(0.15)}$, $p = 0.026$, Mann–Whitney test]. Although an apparent difference in the level of lumican between normal samples from normal patients and normal samples adjacent to tumours was seen, this difference did not persist when the different stromal content of these samples was taken into account. Similarly, there was no difference in the levels in tumour tissues on comparing pre- and post-menopausal patients. Nevertheless, an increase in the overall molecular weight and polydiversity was noted between normal tissues and morphologically normal tissue adjacent to tumours, which might be attributable to either different age or association with tumour in the adjacent breast.

In comparison, decorin, although also present in most samples examined by western blot, was much less abundant relative to the cartilage control (Figure 1). It should be noted that the decorin (in common with biglycan and fibromodulin) signals shown in Figure 1 also required a three-fold longer chemiluminescent exposure time (9 s) than that for lumican (3 s). How-

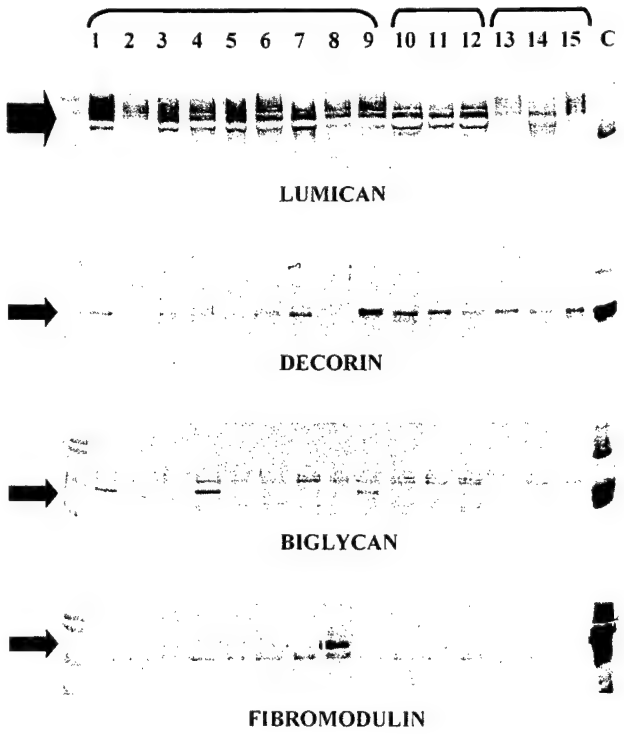

Figure 1. Immunoblotting study of lumican, decorin, biglycan, and fibromodulin protein expression in human breast tumours (lanes 1–9); normal tissues from normal patients (lanes 10–12); and normal tissues adjacent to carcinomas (lanes 13–15). All protein samples were extracted from sets of frozen tissue sections bracketed by sections assessed by H&E stain and light microscopy to confirm content. Chemiluminescent signals for decorin, biglycan, and fibromodulin required three-fold longer exposure times than that for lumican. Molecular markers (left) and cartilage control sample (right) are present in all panels

ever, in contrast to lumican, there was a marked decrease in decorin between normal and tumour samples [mean$^{(SD)}$ optical density units; normal = $0.21^{(0.06)}$, tumour = $0.13^{(0.14)}$, $p = 0.066$, Mann–Whitney test]. No difference was seen in the signals between normal samples from normal and cancer patients.

Fibromodulin expression was not detected in normal tissues and at only low levels in 3/9 tumours, where the presence of fibromodulin correlated with those tumours with the highest content of epithelial tumour cells. Biglycan was also only detected at low levels in 2/6 normal tissues and 3/9 tumours, where in contrast to fibromodulin, its presence correlated directly with those tumours with the highest content of collagenous stroma.

Lumican and decorin are differentially expressed between normal and neoplastic tissues

In order to examine further the distinct alterations in the expression of lumican and decorin, the mRNA and protein expression of both genes was examined in 46 cases by *in situ* hybridization (34 cases) and western blot (12 cases) from the second cohort of cases, comprising matched normal and tumour samples.

As previously shown, prominent lumican mRNA expression was detected, using an antisense probe, in stromal fibroblast-like cells within the tumour and immediately adjacent to invasive tumour cells. Assessment of mRNA levels using a semi-quantitative approach, as detailed in the Materials and methods section, also confirmed our previous observations [5] made on a different set of tumours, and lumican mRNA was found to be significantly elevated in the majority of tumours when levels were compared with those present in adjacent normal stroma ($p < 0.0001$, Wilcoxon test, Figures 2 and 3B). Higher levels of lumican (≥ 1) were present in tumour than in normal tissue in 26/34 cases. At the same time, decorin levels also showed a consistent and significant difference, with lower levels seen in stroma associated with tumour, relative to stroma associated with adjacent normal tissue components ($p < 0.0002$, Wilcoxon test, Figures 2 and 3C), with lower levels of decorin (≥ 1) present in tumour than in normal tissue in 22/34 cases. The pattern of expression of decorin was also identical in sections from the same cases studied with a different *in situ* hybridization riboprobe (data not shown). Although we have previously noted a relationship between lumican and poor prognostic factors, these associations were not found in the present series.

In keeping with the pattern of mRNA expression, the mean lumican protein signal assessed by western blot was also higher in 9/12 tumours relative to normal tissues [mean$^{(SD)}$ optical density units, normal = $0.22^{(0.15)}$, tumour = $0.43^{(0.19)}$, $p = 0.0122$ Wilcoxon test]. Once again, in contrast to this, decorin

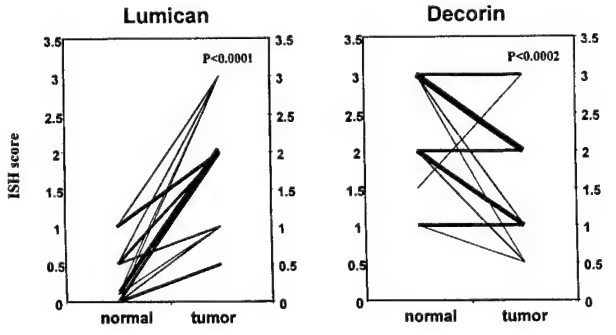

Figure 2. Lumican and decorin mRNA levels in matched normal and tumour tissues, assessed by *in situ* hybridization and semi-quantitative scoring as described in the Materials and methods section. The thickness of each line (on a scale of 1–9) corresponds to the number of cases showing the same differences in scores ($n = 34$ cases)

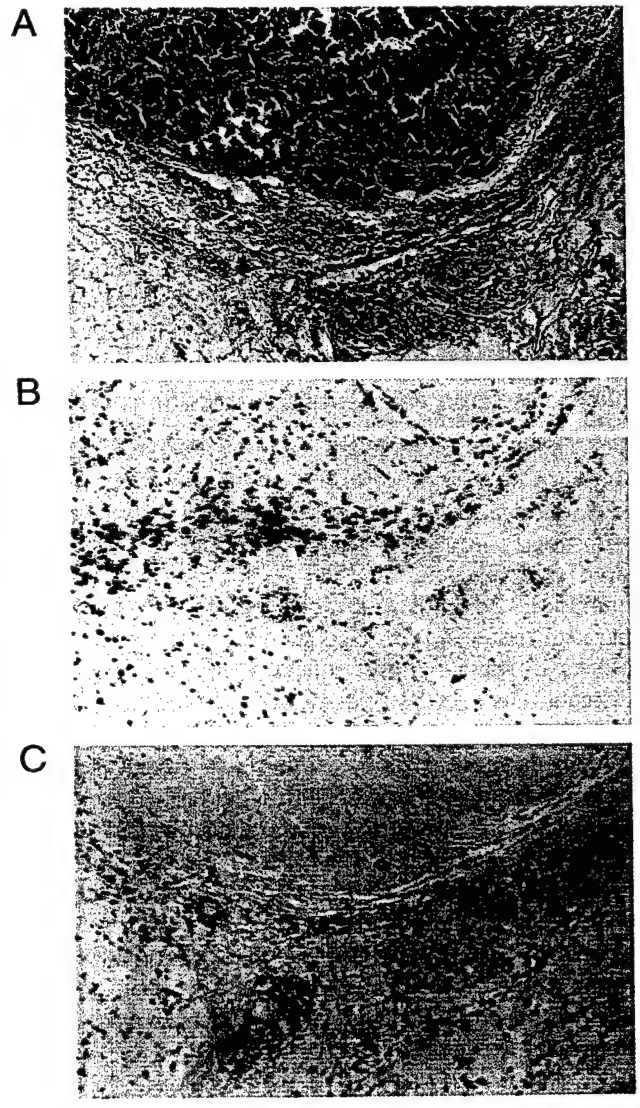

Figure 3. Lumican and decorin mRNA expression detected by *in situ* hybridization within a breast tumour section. Panel A (H&E section) shows the histology including the invasive tumour (upper area), the tumour margin (middle), and adjacent normal tissue including lobular-ductal units (lower area). Lumican expression (B) is high within the tumour and tumour margin and lower in the normal fat and collagenous stroma adjacent to the normal lobules. Decorin (C) shows high expression in the normal stroma adjacent to normal lobules and reduced expression in the tumour. ×340

protein was lower in 7/12 tumours relative to normal tissues, but in this case the differences were not statistically significant [mean$^{(SD)}$ optical density units, normal = $0.22^{(0.19)}$, tumour = $0.17^{(0.2)}$, p = ns (not significant), Wilcoxon test]. These contrasting patterns of lumican and decorin expression also persisted after standardization of western blot signals for relative stromal content (data not shown).

Lumican mRNA and protein expression can occur in different regions within breast tumours

Immunohistochemical study of the lumican distribution within the same tissues that had already been examined by *in situ* hybridization was performed using the same antibody [9,12] that had been employed for western blot analysis (Figure 4). This showed that lumican was abundant throughout the collagenous stroma of both normal and tumour sections, with prominent deposition around small vessels, breast duct, and lobular structures. There was increased deposition within the collagenous stroma of tumours, in particular at the invasive margins and in areas of dense collagen within central regions of some tumours, compared with adjacent normal tissues. However, in some cases there were distinct regions, up to 2 mm in area within the tumour sections, containing loose stroma in which there was a complete absence of lumican detectable by immunohistochemistry (Figures 4C and 4D); but the same regions showed high expression when examined for lumican mRNA by *in situ* hybridization in adjacent sections (Figures 4A and 4B). Similarly, other areas showed strong staining for lumican protein, but low levels of mRNA.

To explore the possibility that the absence of lumican expression detected by immunohistochemistry might be due to the conformation of the native protein or the binding of lumican to other proteins, resulting in the masking of the carboxy-terminal epitope, specific areas measuring approximately 1 mm^2 each were microdissected from frozen sections of two tumours and lumican protein was assessed under denaturing conditions by SDS/PAGE and western blot. In both cases, those regions with high mRNA expression and negative by immunohistochemistry were also negative by western blot, while areas showing very low mRNA expression but strong staining by immunohistochemistry were positive by western blot (Figure 5).

Discussion

We have shown that lumican is the most abundant proteoglycan in comparison with several other members of the family of small leucine-rich proteoglycans (SLRPs) in breast cancer. We have also extended our previous observations [5], based on the detection of lumican mRNA, in showing that the total lumican protein is also increased in breast tumours relative to adjacent normal tissues. Our results also demonstrate that this pattern of up-regulation of lumican in relation to breast tumourigenesis is distinct from that of the closely related decorin gene, which is inversely regulated and reduced at mRNA and to a lesser extent at protein levels, in tumour relative to adjacent normal tissue. Finally, we have shown that lumican expression in tumours may also be associated with an abnormal distribution within the stroma, manifested by discordance between mRNA and protein deposition within subregions of breast tumours.

The family of SLRPs share several common features, including a central region of leucine-rich repeats bounded by flanking cysteine residues, and localization in the extracellular matrix. The SLRPs can be separated into three subgroups that include decorin and biglycan, lumican and fibromodulin, and epiphycan and osteoglycin, which are distinguishable by amino acid homologies and also by gene structure [16]. Decorin, probably the best studied of these genes, is known to interact with a variety of extracellular matrix molecules and has been shown to be capable of influencing collagen fibril growth and assembly both *in vitro* and *in vivo* [6,7]. Decorin may also influence tumour cell growth through indirect effects on the availability of growth factors from the extracellular matrix, or directly through activation of the EGF receptor and induction of the p21 cell-cycle inhibitor [18]. In contrast, less is known about lumican and other SLRPs. However, *in vitro* and *in vivo* data indicate that lumican is also important in the regulation of collagen fibril assembly [19]. This view is supported by recent observations based on mice with homozygous deletion of the lumican gene, where loss of corneal transparency and increased skin fragility are associated with disorganized and loosely packed collagen fibres related to increased and irregular fibril size, and interfibrillar spacing, as viewed by light and electron microscopy [8].

The observation that lumican is highly abundant compared with other SLRPs in breast tumours cannot be interpreted to mean that it is necessarily the most important. This is underscored by the recent demonstration that although decorin is apparently more abundant than versican in prostate cancer tissue, only an increase in the larger chondroitin sulphate proteoglycan versican correlates with grade, and inversely with progression-free survival, in prostate cancer [20]. Similarly, the increase in lumican as seen here in association with breast tumourigenesis may be less important than the parallel decrease in decorin. It should also be noted that while the present study was focused primarily on examining the relative expression of SLRPs between matched normal and tumour tissues and was not necessarily designed to compare levels between cases, we did not observe any significant relationship between lumican or decorin and prognostic factors within this tumour cohort, as previously noted [5]. While this leaves open the question of a role for these SLRPs in later tumour progression, the implication of altered expression for the earlier stages of tumourigenesis remains intriguing. It is possible to

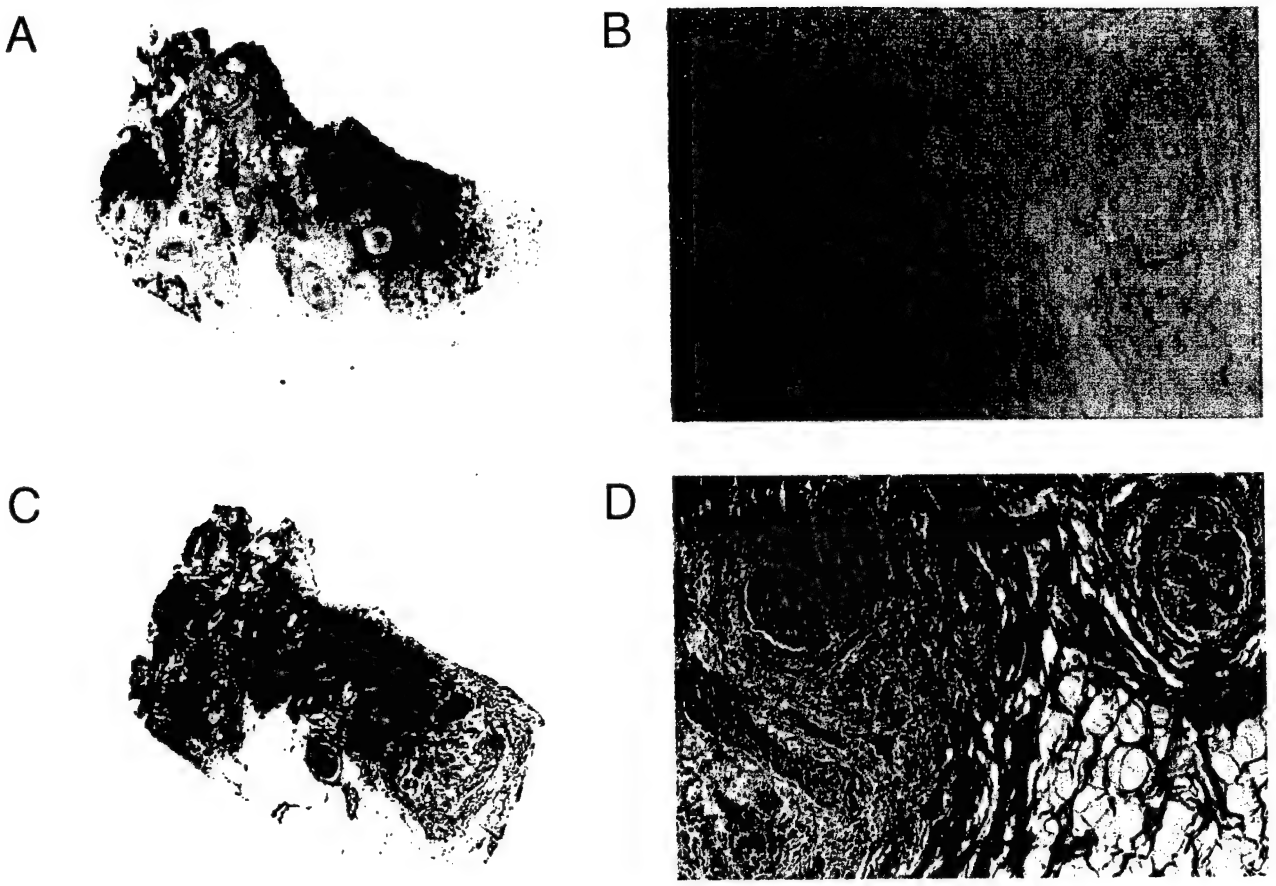

Figure 4. *In situ* hybridization and immunohistochemical study showing regional discordance in lumican mRNA (A, B) and protein expression (C, D) displayed in adjacent sections in breast tumours. Panels A and C show the overall pattern of mRNA (A, black signal) and protein (C, brown staining) within a tissue section (0.4 × 0.8 cm in size) that includes regions of *in situ* and invasive tumour (upper left and upper middle) and adjacent normal tissue (lower left and lower right). Panels B and D show a detailed microscopic view (× 400) of the cellular localization of mRNA and protein within a small region at the invasive edge within the same section (tumour component at left, normal component at right)

speculate that both induction of lumican and decrease in decorin in stromal fibroblasts within the invasive tumour may represent a positive host response, to abrogate the disorganization of collagen within the tumour stroma, encourage macrophage localization [21], and inhibit the growth of epithelial cancer cells, through the increased availability of growth factors inhibitory to breast epithelial cell growth [22]. Alternatively, these alterations may represent a negative host response contributing to early tumour development. Increased lumican mRNA expression may reflect a response to locally increased proteolysis or altered deposition of the lumican protein that is the cause of the disorganization of the collagenous stroma, which in turn facilitates tumour cell invasion. Similarly, a decrease in decorin may remove an inhibitory effect on epithelial tumour cell growth through repression of p21 [7]. A role for and the distinction between these opposing potential effects will clearly require further study.

The differences in lumican levels between normal and tumour tissues observed by both immunohistochemistry and western blot are not as marked as those seen at the level of mRNA expression. While differences in the assays may account for some of this discrepancy, it is clear that it may also be attributable to the discordance that can exist between lumican mRNA and protein expression detected by *in situ* and immunohistochemical techniques respectively, within the same regions of breast tumour stroma. A similar discordance between mRNA and protein expression has been previously observed in the course of studies on lumican and other large and small proteoglycans in different tissues. For example, in corneal development in the chicken, the mRNA levels for lumican and decorin do not always reflect the rate of synthesis of the corresponding proteins and the efficiency of translation of lumican varies over time [23]. Similar discordance between aggrecan and versican mRNA and protein has been seen in normal tendon [24], between decorin and biglycan mRNA and protein localization in normal and reactive gastric mucosa [25], and in regions of cartilage matrix around vascular channels and the growth plates of long bones in normal cartilage [26]. In this latter instance, the discordance was attributed to a high rate of breakdown and removal at these sites. This conclusion is supported by studies on endothelial cells which show that growth factors such as bFGF can increase not only both biglycan transcription and protein synthesis,

Figure 5. Lumican protein expression detected by immunohistochemistry (upper panel) and western blot (lower panel) demonstrating concordance in the assessment of protein levels in microdissected subregions within two breast tumour sections. The upper panels show IHC sections (tumour A, left; tumour B, right; scale bar = 5 mm). The mRNA and protein signals were detected by *in situ* hybridization (ISH) and immunohistochemistry (IHC) in each region in adjacent sections and ISH/IHC levels were assessed semi-quantitatively (negative, weak +, strong + +) as follows: tumour A: region 1 = + +/−, region 2 = −/+ +, region 3 (remainder of section) = +/+ +; tumour B: region 4 = +/−, region 5 = −/+ +, region 6 = + +/+ +. The lower panel shows the western blot (C = cartilage control; lanes 1–6 correspond to regions assessed and microdissected above)

but also the corresponding rate of proteolysis [27]. The absence of protein could also reflect masking of the epitope by conformational changes in the native protein, by changes in post-translational modification, or by binding to another protein. Alternatively, this could reflect reduced translation, increased breakdown, or failure to bind within the immediate stroma and rapid translocation of the protein to adjacent areas of the tissue. Our microdissection experiments, applied to small regions where lumican mRNA is highly expressed, suggest that the corresponding protein is truly absent in these areas and that epitope masking due to conformation or binding proteins is an unlikely explanation for the observation. However, it could also be the case that the necessary binding sites are not available in the immature stroma associated with rapid growth of tumours and that this allows translocation of newly synthesized lumican to binding sites in adjacent tissue.

The reciprocal nature of the changes in the expression of lumican and decorin is intriguing. Although definitive characterization of the stromal cell types awaits primary culture studies, direct comparison of *in situ* hybridization performed on serial sections suggests that expression of both genes apparently occurs in the same fibroblast-like cells in breast tissue stroma. While lumican has not previously been studied in human tumours, the expression of decorin mRNA and proteoglycans incorporating chondroitin sulphate epitopes has been shown to be increased in colon, prostate, and basal cell carcinomas [28–30], but a more recent study of multiple stromal genes in breast tumours found no difference in the levels of decorin mRNA between tumour and normal tissue, although noting increased expression in the stroma immediately adjacent to *in situ* components [31]. However, the normal tissue examined was selected to be well away from the primary tumour and this, together with differences in the method of quantitation, the definition of tumour regions, and the focus on matched samples, limits a full comparison with our observations. For example, morphologically normal tissue immediately adjacent to carcinomas may be influenced by paracrine growth factors derived from the tumour and may also harbour molecular alterations [32] that might influence local gene expression. However, similar immunohistochemical studies of breast tumours using monoclonal antibodies raised against chondroitin sulphate and dermatan sulphate small proteoglycan have shown reduced decorin expression within invasive as compared with surrounding normal stroma, consistent with our findings [33]. Decorin and other SLRPs are known to be independently regulated and mutually exclusive [26] and compensatory changes in the expression between different SLRPs have been observed [34]. However, this appears to be usually manifested by genes within subgroups of the SLRP family. At the same time, reciprocal changes in the expression between lumican and decorin have not been described in lumican or decorin 'knockout' mice [8,17]. The factors that influence altered expression of these genes in breast tumour stroma remain to be elucidated.

In summary, we have shown that lumican is highly abundant relative to decorin, biglycan, and fibro-

modulin in normal and neoplastic breast tissues. We have also shown that increased lumican protein expression and altered regional localization occur in breast tumours and that different and reciprocal alterations in expression occur between lumican and decorin. The functional significance and the role of alterations in these stromal proteoglycans in breast tumourigenesis and progression remain to be determined.

Acknowledgements

This work was supported by grants from the Medical Research Council of Canada (MRC) and the US Army Medical Research and Materiel Command (USAMRMC). The Manitoba Breast Tumor Bank is supported by funding from the National Cancer Institute of Canada (NCIC). PHW is an MRC Scientist; LCM is an MRC Scientist; and EL is a recipient of a USAMRMC Postdoctoral Fellowship. TH-H is a recipient of an MRC studentship award.

References

1. Peyrol S, Raccurt M, Gerard F, Gleyzal C, Grimaud JA, Sommer P. Lysyl oxidase gene expression in the stromal reaction to *in situ* and invasive ductal breast carcinoma. *Am J Pathol* 1997; **150**: 497–507.
2. Kinzler KW, Vogelstein B. Landscaping the cancer terrain [comment]. *Science* 1998; **280**: 1036–1037.
3. Iozzo RV. Tumor stroma as a regulator of neoplastic behavior. Agonistic and antagonistic elements embedded in the same connective tissue [editorial]. *Lab Invest* 1995; **73**: 157–160.
4. Spanakis E, Brouty-Boye D. Discrimination of fibroblast subtypes by multivariate analysis of gene expression. *Int J Cancer* 1997; **71**: 402–409.
5. Leygue E, Snell L, Dotzlaw H, *et al.* Expression of lumican in human breast carcinoma. *Cancer Res* 1998; **58**: 1348–1352.
6. Iozzo RV. The family of the small leucine-rich proteoglycans: key regulators of matrix assembly and cellular growth. *Crit Rev Biochem Mol Biol* 1997; **32**: 141–174.
7. Santra M, Mann DM, Mercer EW, Skorski T, Calabretta B, Iozzo RV. Ectopic expression of decorin protein core causes a generalized growth suppression in neoplastic cells of various histogenetic origin and requires endogenous p21, an inhibitor of cyclin-dependent kinases. *J Clin Invest* 1997; **100**: 149–157.
8. Chakravarti S, Magnuson T, Lass JH, Jepsen KJ, LaMantia C, Carroll H. Lumican regulates collagen fibril assembly: skin fragility and corneal opacity in the absence of lumican. *J Cell Biol* 1998; **141**: 1277–1286.
9. Cs-Szabo G, Melching LI, Roughley PJ, Glant TT. Changes in messenger RNA and protein levels of proteoglycans and link protein in human osteoarthritic cartilage samples. *Arthritis Rheum* 1997; **40**: 1037–1045.
10. Watson PH, Snell L, Parisien M. The NCIC-Manitoba Breast Tumor Bank: a resource for applied cancer research. *Cmaj* 1996; **155**: 281–283.
11. Hiller T, Snell L, Watson PH. Microdissection RT-PCR analysis of gene expression in pathologically defined frozen tissue sections. *Biotechniques* 1996; **21**: 38–40.
12. Grover J, Chen XN, Korenberg JR, Roughley PJ. The human lumican gene. Organization, chromosomal location, and expression in articular cartilage. *J Biol Chem* 1995; **270**: 21942–21949.
13. Roughley PJ, White RJ, Cs-Szabo G, Mort JS. Changes with age in the structure of fibromodulin in human articular cartilage. *Osteoarthritis Cart* 1996; **4**: 153–161.
14. Roughley PJ, White RJ, Magny M-C, Liu J, Pearce RH, Mort JS. Non-proteoglycan forms of biglycan increase with age in human articular cartilage. *Biochem J* 1993; **295**: 421–426.
15. Vetter U, Vogel W, Just W, Young MF, Fisher LW. Human decorin gene: intron–exon junctions and chromosomal localization. *Genomics* 1993; **15**: 161–168.
16. Hocking AM, Shinomura T, McQuillan DJ. Leucine-rich repeat glycoproteins of the extracellular matrix. *Matrix Biol* 1998; **17**: 1–19.
17. Danielson KG, Baribault H, Holmes DF, Graham H, Kadler KE, Iozzo RV. Targeted disruption of decorin leads to abnormal collagen fibril morphology and skin fragility. *J Cell Biol* 1997; **136**: 729–743.
18. Moscatello DK, Santra M, Mann DM, McQuillan DJ, Wong AJ, Iozzo RV. Decorin suppresses tumor cell growth by activating the epidermal growth factor receptor. *J Clin Invest* 1998; **101**: 406–412.
19. Ying S, Shiraishi A, Kao CW, *et al.* Characterization and expression of the mouse lumican gene. *J Biol Chem* 1997; **272**: 30306–30313.
20. Ricciardelli C, Mayne K, Sykes PJ, *et al.* Elevated levels of versican but not decorin predict disease progression in early-stage prostate cancer. *Clin Cancer Res* 1998; **4**: 963–971.
21. Funderburgh JL, Mitschler RR, Funderburgh ML, Roth MR, Chapes SK, Conrad GW. Macrophage receptors for lumican. A corneal keratan sulfate proteoglycan. *Invest Ophthalmol Vis Sci* 1997; **38**: 1159–1167.
22. Santra M, Skorski T, Calabretta B, Lattime EC, Iozzo RV. *De novo* decorin gene expression suppresses the malignant phenotype in human colon cancer cells. *Proc Natl Acad Sci USA* 1995; **92**: 7016–7020.
23. Cornuet PK, Blochberger TC, Hassell JR. Molecular polymorphism of lumican during corneal development. *Invest Ophthalmol Vis Sci* 1994; **35**: 870–877.
24. Waggett AD, Ralphs JR, Kwan AP, Woodnutt D, Benjamin M. Characterization of collagens and proteoglycans at he insertion of the human Achilles tendon. *Matrix Biol* 1998; **16**: 457–470.
25. Schonherr E, Lugering N, Stoll R, Domschke W, Kresse H. Differences in decorin and biglycan expression in patients with gastric ulcer healing. *Scand J Gastroenterol* 1997; **32**: 785–790.
26. Bianco P, Fisher LW, Young MF, Termine JD, Robey PG. Expression and localization of the two small proteoglycans biglycan and decorin in developing human skeletal and non-skeletal tissues. *J Histochem Cytochem* 1990; **38**: 1549–1563.
27. Kinsella MG, Tsoi CK, Jarvelainen HT, Wight TN. Selective expression and processing of biglycan during migration of bovine aortic endothelial cells. The role of endogenous basic fibroblast growth factor. *J Biol Chem* 1997; **272**: 318–325.
28. Adany R, Heimer R, Caterson B, Sorrell JM, Iozzo RV. Altered expression of chondroitin sulfate proteoglycan in the stroma of human colon carcinoma. Hypomethylation of PG-40 gene correlates with increased PG-40 content and mRNA levels. *J Biol Chem* 1990; **265**: 11389–11396.
29. Hunzelmann N, Schonherr E, Bonnekoh B, Hartmann C, Kresse H, Krieg T. Altered immunohistochemical expression of small proteoglycans in the tumor tissue and stroma of basal cell carcinoma. *J Invest Dermatol* 1995; **104**: 509–513.
30. Iozzo RV, Cohen I. Altered proteoglycan gene expression and the tumor stroma. *Experientia* 1993; **49**: 447–455.
31. Brown LF, Guidi AJ, Schnitt SJ, *et al.* Vascular stroma formation in carcinoma *in situ*, invasive carcinoma, and metastatic carcinoma of the breast. *Clin Cancer Res* 1999; **5**: 1041–1056.
32. Deng G, Lu Y, Zlotnikov G, Thor AD, Smith HS. Loss of heterozygosity in normal tissue adjacent to breast carcinomas. *Science* 1996; **274**: 2057–2059.
33. Nara Y, Kato Y, Torii Y, *et al.* Immunohistochemical localization of extracellular matrix components in human breast tumours with special reference to PG-M/versican. *Histochem J* 1997; **29**: 21–30.
34. Nelimarkka L, Kainulainen V, Schonherr E, *et al.* Expression of small extracellular chondroitin/dermatan sulfate proteoglycans is differentially regulated in human endothelial cells. *J Biol Chem* 1997; **272**: 12730–12737.

[CANCER RESEARCH 60, 6266–6271, November 15, 2000]

Advances in Brief

Altered Expression of Estrogen Receptor Coregulators during Human Breast Tumorigenesis[1]

Leigh C. Murphy,[2] Sharon L. R. Simon, Alicia Parkes, Etienne Leygue, Helmut Dotzlaw, Linda Snell, Sandra Troup, Adewale Adeyinka, and Peter H. Watson

Departments of Biochemistry and Medical Genetics [L. C. M., S. L. R. S., A. P., E. L., H. D.] and Pathology [L. S., S. T., A. A., P. H. W.], University of Manitoba, Faculty of Medicine, Winnipeg, Manitoba R3E OW3, Canada

Abstract

The hypothesis that altered expression of specific coactivators/repressors of the estrogen receptor occurs during human breast tumorigenesis *in vivo* is examined in this study. Using *in situ* hybridization and reverse transcription-PCR assays, the expression of two coactivators (SRA and AIB1) and one repressor (REA) of the estrogen receptor was compared between matched breast tumors and adjacent normal human breast tissue. The levels of SRA and AIB1 mRNA were increased in tumors compared with normal tissues ($n = 19$; Wilcoxon matched pairs test; $P < 0.01$). In contrast, the expression of REA mRNA was not different between tumors and normal tissues ($n = 19$; Wilcoxon; $P = 0.110$). The ratios of AIB1:REA and SRA:REA were higher (Wilcoxon; $P < 0.05$) in tumors compared with normal tissues. Furthermore, SRA:AIB1 was higher (Wilcoxon; $P = 0.0058$) in tumors compared with normal tissues. Although our study is small, these data are consistent with the above hypothesis and suggest that such alterations may have a role in the altered estrogen action occurring during breast tumorigenesis.

Introduction

During human breast tumorigenesis, enhanced activity of the ERα[3] signaling pathway is thought to occur and to be a major driving force in breast tumorigenesis. The assumption derives from the observations that only a minority of normal human breast epithelial cells have detectable ERα (7–17% ERα+ ductal epithelial cells; Ref. 1), whereas >70% of primary breast cancers are ERα+ (2). Furthermore, the majority of proliferating cells in normal human breast tissue is ERα−, and estrogen only indirectly causes proliferation in normal mammary tissues (reviewed in Ref. 3). However, estrogen can directly cause proliferation of breast cancer cells (4), and many proliferating cells in ER+ breast tumors are ERα+ (5).

Factors that enhance and repress receptor activity directly, namely coactivators and corepressors, now are considered to be important in mediating steroid receptor transcriptional activity (6). As well, experimental modulation of levels of these two classes of coregulators was shown to alter steroid receptor transcriptional activity (7, 8). These data suggest that not only are ERα levels often increased during breast tumorigenesis (9), but it is likely that other factors which modulate ERα activity might also be altered during breast tumorigenesis with an outcome of enhancement or deregulation of ERα signaling that may underlie alterations of estrogen responsiveness from indirect in normal breast epithelium to direct in ERα+ breast tumor cells. We have addressed this hypothesis by investigating the expression of two known coactivators of ERα, SRA (7) and AIB1 (10), and a repressor of ERα activity, REA (8), at the mRNA level in ER+ human breast tumors and their matched adjacent normal breast tissues. The coregulators studied were chosen because they were identified as either selective for ERs and/or steroid receptors, *e.g.*, SRA (7) and REA (8), or were identified previously to be of relevance in human breast cancer *in vivo*, *e.g.*, AIB1, which is frequently amplified in breast tumors *in vivo* (10).

Materials and Methods

Human Breast Tissues. Nineteen ER+ primary human breast tumor biopsies (ER-positivity was defined as >3 fmol/mg protein in classical ligand-binding assays) were selected from the National Cancer Institute of Canada-Manitoba Breast Tumor Bank (Winnipeg, Manitoba, Canada). The ER levels ranged from 3.7–83 fmol/mg protein and the PR levels ranged from 2.7–112 fmol/mg protein (PR-positivity was defined as >10 fmol/mg protein in classical ligand binding assays; 14 tumors were PR+, and 5 tumors were PR−). For each case, matched adjacent normal and tumor frozen tissue blocks were available. The quality of each block and the relative cellular composition was determined by the histopathological assessment of sections from adjacent mirror-image paraffin-embedded tissue blocks, as described previously (11). The presence of normal ducts and lobules as well as the absence of any atypical lesion were confirmed in all normal tissue specimens. The tumors spanned a wide range of grades (grade scores 5–9) as determined by the Nottingham grading system.

***In Situ* Hybridization.** Paraffin-embedded 5-μm breast tumor and matched adjacent normal breast tissue sections were analyzed by *in situ* hybridization according to a previously described protocol (12). The plasmid pGEM-T-SRAcore, consisting of pGEM-T-easy plasmid (Promega, Madison, WI) containing a 397-bp insert of the human SRA cDNA (from nucleotide 300 to 696, numbered according to GenBank accession no. AF092038), was used as a template to generate sense and antisense riboprobes. The plasmid pGEM-T-REA, consisting of pGEM-T-easy plasmid containing a 399-bp insert of the human REA cDNA (from nucleotide 385 to 783, numbered according to GenBank accession no. AF150962), was used as a template to generate sense and antisense riboprobes. UTP ^{35}S-labeled riboprobes were synthesized using Riboprobe Systems (Promega, Madison, WI) according to the manufacturer's instructions. Sense probes were used as controls. *In situ* hybridization and washing conditions were as described previously (12). Sections were developed using Kodak NTB-2 photographic emulsion and counterstained with Lee's stain after 2–6 weeks.

RNA Extraction and RT-PCR Conditions. Total RNA was extracted from 20-μm frozen tissue sections (20 sections/tumor; 35 sections for normal tissues) using Trizol reagent (Life Technologies, Grand Island, NY) according to the manufacturer's instructions and quantified spectrophotometrically. One μg of total RNA was reverse-transcribed in a final volume of 25 μl as described previously (13).

Primers and PCR Conditions. The primers used were: (*a*) SRAcoreU primer (5′-AGGAACGCGGCTGGAACGA-3′; sense; positions 35–53; Gen-

Received 1/6/00; accepted 10/3/00.

The costs of publication of this article were defrayed in part by the payment of page charges. This article must therefore be hereby marked *advertisement* in accordance with 18 U.S.C. Section 1734 solely to indicate this fact.

[1] Supported by grants from the Canadian Breast Cancer Research Initiative and the United States Army Medical Research and Materiel Command. The Manitoba Breast Tumor Bank is supported by funding from the National Cancer Institute of Canada. P. H. W. and L. C. M. are Medical Research Council of Canada Scientists.

[2] To whom requests for reprints should be addressed, at Department of Biochemistry and Medical Genetics, University of Manitoba, Winnipeg, MB, R3E OW3, Canada. Phone: (204) 789-3233; Fax: (204) 789-3900; E-mail: lcmurph@cc.umanitoba.ca.

[3] The abbreviations used are: SRA, steroid receptor RNA activator; AIB1, amplified in breast cancer-1; REA, repressor of estrogen receptor activity; ER, estrogen receptor; PR, progesterone receptor; RT, reverse transcription; GAPDH, glyceraldehyde-3-phosphate dehydrogenase; DCIS, intraductal carcinoma.

Bank accession no. AF092038) and SRAcoreL primer (5′- AGTCTGGG-GAACCGAGGAT-3′; antisense; positions 696–678; GenBank accession no. AF092038); (*b*) AIB1-U primer (5′-ATA CTT GCT GGA TGG TGG ACT-3′; sense; positions 110–130; GenBank accession no. AF012108) and AIB1-L primer (5′-TCC TTG CTC TTT TAT TTG ACG-3′; antisense; positions 458–438; GenBank accession no. AF012108); and (*c*) REA-U primer (5′-CGA AAA ATC TCC TCC CCT ACA-3′; sense; positions 385–405; GenBank accession no. AF150962) and REA-L primer (5′-CCT GCT TTG CTT TTT CTA CCA-3′; antisense; positions 781–761; GenBank accession no. AF150962).

Radioactive PCR amplifications for SRA were performed and PCR products were analyzed as described previously (14), with minor modifications. Briefly, 1 μl of RT mixture was amplified in a final volume of 15 μl in the presence of 1.5 μCi of [α-^{32}P]dCTP (3000 Ci/mmol), 4 ng/μl of each primer, and 0.3 unit of *Taq* DNA polymerase (Life Technologies, Inc.). For SRA, each PCR consisted of 30 cycles (30 s at 60°C, 30 s at 72°C, and 30 s at 94°C). PCR products were then separated on 6% polyacrylamide gels containing 7 M urea. After electrophoresis, the gels were dried and exposed for 2 h to a Molecular Imager-FX Imaging screen (Bio-Rad, Hercules, CA).

PCR amplifications for AIB1 and REA were performed and PCR products were analyzed as described previously (13), with minor modifications. Briefly, 1 μl of RT mixture was amplified in a final volume of 20 μl, in the presence of 4 ng/μl of each primer and 0.3 unit of *Taq* DNA polymerase (Life Technologies, Inc.).

For AIB1, each PCR consisted of 30 cycles (30 s at 55°C, 30 s at 72°C, and 30 s at 94°C). For REA, each PCR consisted of 30 cycles (30 s at 57°C, 30 s at 72°C, and 30 s at 94°C). PCR products then were separated on agarose gels stained with ethidium bromide as described previously (13). Amplification of the ubiquitously expressed *GAPDH* cDNA was performed in parallel, and PCR products were separated on agarose gels stained with ethidium bromide as described previously (13). The identity of PCR products was confirmed by subcloning and sequencing, as reported previously (15).

Quantification of SRA Expression. Exposed screens were scanned using a Molecular Imager-FX (Bio-Rad) and the intensity of the signal corresponding to SRA was measured using Quantity One software (Bio-Rad). Three independent PCRs were performed. To control for variations between experiments, a value of 100% was arbitrarily assigned to the SRA signal of one particular tumor measured in each set of PCR experiments, and all signals were expressed as a percentage of this signal. In parallel, *GAPDH* cDNA was amplified, and after analysis of PCR products on prestained agarose gels, signals were quantified by scanning using MultiAnalyst (Bio-Rad). Three independent PCRs were performed. Each *GAPDH* signal was also expressed as a percentage of the signal observed in the same tumor as above. For each sample, the average of the SRA signal was then expressed as a percentage of the *GAPDH* signal (arbitrary units).

Quantification of the Relative Expression of the Deleted SRA Variant RNA. It has been shown previously that the coamplification of a wild-type and a deleted variant SRA cDNA resulted in the amplification of two PCR products, the relative signal intensity of which provided a reliable measurement of the relative expression of the deleted variant (15). For each sample, the signal corresponding to the SRAdel was measured using Quantity One software (Bio-Rad) and expressed as a percentage of the corresponding core SRA signal. For each case, three independent assays were performed and the mean determined.

Quantification of REA and AIB1 Expression. After analysis of PCR products on prestained agarose gels, signals were quantified by scanning using MultiAnalyst (Bio-Rad). At least, three independent PCRs were performed. To control for variations between experiments, a value of 100% was arbitrarily assigned to the REA or AIB1 signal of one particular sample and all signals were expressed as a percentage of this signal. For each sample, the average of REA or AIB1 signals was then expressed as a percentage of the average of the *GAPDH* signal (arbitrary units), as described above.

Statistical Analysis. Differences between normal samples and their matched tumors were tested using the Wilcoxon matched pairs test, two-tailed. Differences between the relative expression of cofactors (*e.g.*, logAIB1:REA) obtained for matched normal and tumor compartments were also tested using the Wilcoxon matched pairs test, two-tailed. Correlation between SRA, REA, or AIB1 expression and tumor characteristics was tested by calculation of the Spearman coefficient *R*.

Results

Characterization of SRA and REA RNA Expression in Human Breast Tissues by *in Situ* Hybridization. SRA is functional as an RNA molecule (7), and because no antibodies are available for the immunohistochemical detection of REA, we have therefore used an *in situ* hybridization approach to determine the cellular localization of expression of SRA and REA RNA in human breast tissues. Fig. 1 shows examples of the results obtained. Antisense RNA probes to SRA showed a strong signal over the epithelial tumor cells of an ER+ human breast tumor section (Fig. 1*A*), with little, if any, signal obtained when sense SRA probes were used on the adjacent section of the same tumor (Fig. 1*C*). Low levels of SRA expression were detected mainly over the ductal epithelial cells of normal breast tissue from the same patient. This result paralleled that for AIB1, where it was previously shown using *in situ* hybridization that AIB1 mRNA expression was significantly increased in breast cancer cells carrying increased copies of the *AIB1* gene compared with normal breast epithelial cells, although it was not stated that these samples were from the same patient in this study (10). In contrast, when the *in situ* expression of REA mRNA was examined in an ER+ tumor and its matched adjacent normal breast tissue (Fig. 1, *D* and *E*, respectively), little difference could be seen between the signal over the epithelial breast tumor cells compared with the normal breast epithelial cells. Furthermore, little if any signal was observed when REA sense probes were used (Fig. 1*F*). These data suggested that the expression of the steroid receptor-specific coactivator, SRA, in addition to AIB1 (10) was significantly increased in breast tumor cells compared with normal breast epithelial cells, whereas the expression of a specific ER-repressor was not altered in breast tumors compared with normal breast epithelial cells. To investigate this further, we developed a semi-quantitative RT-PCR approach to measure the expression of these coregulators in multiple samples of ER+ breast tumors and their matched adjacent normal breast tissues, as described below.

Comparison of Expression of SRA and Deleted SRA in Adjacent Normal Breast Tissue and Matched Primary Breast Tumors. Previously we have detected two SRA PCR products of 662 and 459 bp in human breast tumors (14). Cloning and sequencing revealed the identity of the 662-bp fragment with the SRA core region (7) and the 459-bp fragment as a variant form of SRA deleted in 203 bp between positions 155 and 357 (numbered according to GenBank accession no. AF092038). The current analysis identified the 662-bp product in all breast tissue samples assayed. As well, a 459-bp product corresponding to the deleted SRA transcript was detected in the majority of tumors (n = 18) and normal samples (n = 17), always together with the 662-bp product (Fig. 2*A*). Therefore, core SRA is expressed in all human breast tissues, and expression of the deleted SRA is not tumor-specific.

To determine whether alterations in SRA expression occur during breast tumorigenesis, SRA RNA was measured in primary breast tumors and their adjacent matched normal breast tissues from 19 different patients (examples shown in Fig. 2*A*). The analysis was confined to tissues from women whose breast tumor was ER+ as determined by ligand-binding assays. SRA expression corrected for the *GAPDH* signal in each sample for all matched normal and tumor pairs is shown in Fig. 3*A*. The level of core SRA was significantly higher (Wilcoxon matched pairs test; P = 0.0004) in the tumors (median = 63 arbitrary units) compared with their adjacent normal tissue (median = 7 arbitrary units). When detected, expression of the deleted SRA relative to the core SRA was not significantly different between normal breast tissue and tumors (data not shown). These data suggested that core SRA expression is up-regulated, but the relative

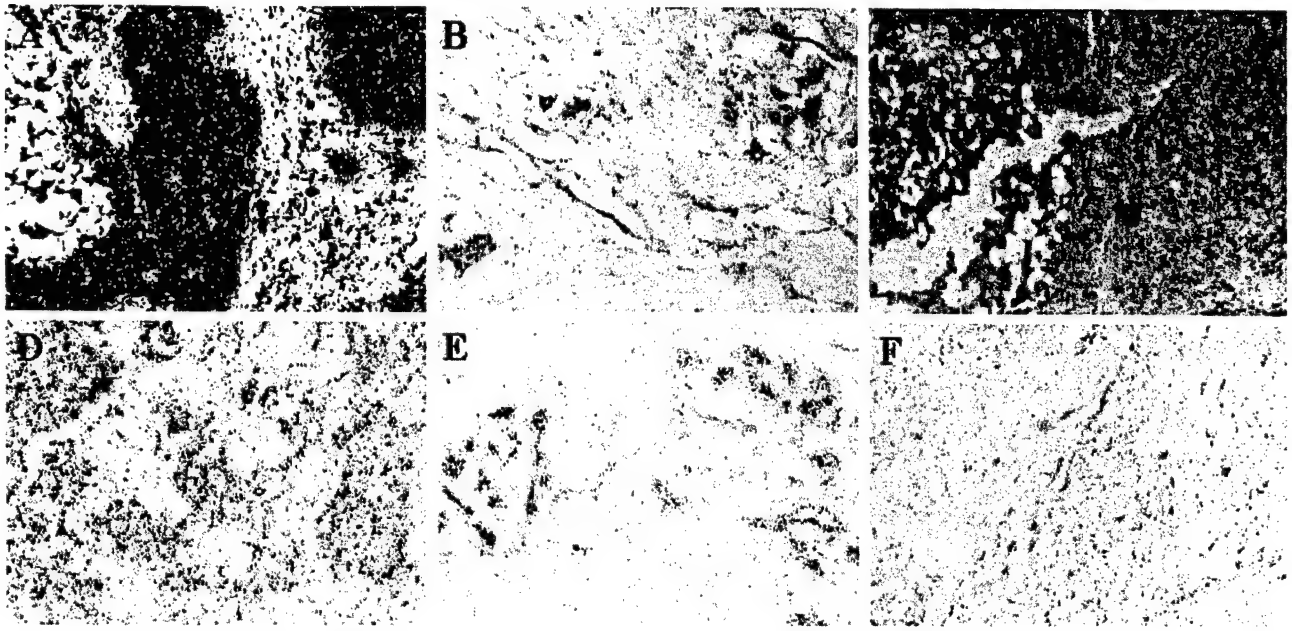

Fig. 1. *In situ* hybridization analyses of SRA and REA RNA expression in human breast tissue sections. Antisense SRA riboprobes (*A* and *B*) were used to detect SRA RNA expression in a section from an ER+ human breast tumor (*A*) and the matched normal breast tissue from the same patient (*B*). Sense SRA riboprobes were used as a specificity control, and the results from the adjacent section of the tumor shown in *A* are shown (*C*). Antisense REA riboprobes (*D* and *E*) were used to detect REA mRNA expression in a section from an ER+ human breast tumor (*D*) and the matched normal breast tissue from the same patient (*E*). Sense REA riboprobes were used as a specificity control and the results from the adjacent section of the tumor shown in *D* are shown (*F*). Magnification ×100. *Black dots/grains*, hybridization signals; *colored background*, counterstaining.

expression of a deleted SRA is not altered, during breast tumorigenesis.

The level of core SRA in the tumor cohort used in this study was not correlated with PR status, grade, tumor size, or nodal status. However, the relative expression of the deleted SRA in the tumors was positively correlated with grade score (Spearman $R = 0.556$; $P = 0.0135$) and tumor size (Spearman $R = 0.655$; $P = 0.0023$), but not with PR or nodal status. These data suggested that increased relative expression of a deleted SRA is more likely to occur in those breast tumors with characteristics of a poorer prognosis, and may be associated with breast tumor progression.

Altered Expression of AIB1 mRNA between Breast Cancer and Adjacent Matched Normal Breast Tissues. To pursue further the possibility that an imbalance in expression of activators of ER action may occur during breast tumorigenesis, we investigated in the same samples the expression of another coactivator of ER activity, AIB1 (10). AIB1 is overexpressed in several human breast tumors (10, 16), although to our knowledge measurement of its RNA expression in a series of matched normal and breast tumor tissues was not reported previously. AIB1-specific primers amplified a predicted 349-bp fragment in normal breast tissues (Fig. 2*B*), in breast tumors (Fig. 2*B*), and in breast cancer cells (data not shown). Cloning and sequencing confirmed the identity of the 349-bp PCR product with AIB1 (10). Expression of AIB1 corrected for the *GAPDH* signal in each tissue sample for all of the matched pairs is shown in Fig. 3*B*. Expression of AIB1 mRNA was significantly higher (Wilcoxon matched pairs test; $P = 0.0058$) in tumor samples (median = 67.8 arbitrary units) compared with adjacent normal tissues (median = 36.6 arbitrary units). These data are consistent with previous data (10, 16) and suggest that expression of another ER coactivator is significantly increased during breast tumorigenesis. Expression of AIB1 in this tumor cohort was not correlated with PR status, grade, tumor size, or nodal status.

Detection of REA mRNA in Normal and Neoplastic Human Breast Tissues. To determine whether alterations in expression of a corepressor, *i.e.*, REA, also occurred during breast tumorigenesis, an RT-PCR approach was developed. The REA-specific primers amplified a predicted 397-bp fragment in normal breast tissues (Fig. 2*C*), in breast tumors (Fig. 2*C*), and in breast cancer cells (data not shown). Cloning and sequencing confirmed the identity of the 397-bp PCR product as REA (8). This product was used to probe Northern blots of RNA extracted from human breast cancer cells and breast tumor biopsies. An ~1.5 kb transcript was detected, consistent with the REA mRNA described previously (data not shown; Ref. 8).

To determine whether REA expression was potentially altered during breast tumorigenesis, REA mRNA levels were measured in ER+ breast tumors and their adjacent normal breast tissues (examples in Fig. 2*C*) from the same 19 different patients described above. REA expression corrected for the *GAPDH* signal (Fig. 2*D*) in each sample for all matched pairs is shown in Fig. 3*C*. REA expression was not significantly different (Wilcoxon matched pairs test; $P = 0.110$) in the tumors (median = 84.6 arbitrary units) compared with the adjacent normal tissues (median = 69.8 arbitrary units). REA expression in the tumors was not correlated with PR status, grade, tumor size, or nodal status.

Altered Relative Expression of Coactivators and Repressors during Human Breast Tumorigenesis. The above data suggest that alterations in the relative expression of ER activators and repressor occurred during breast tumorigenesis. To address this question, the relative expression of SRA and AIB1 mRNA to REA mRNA was compared between the breast tumors and the normal tissues. Results are shown in Fig. 4. The ratio of SRA:REA (Fig. 4*A*) was significantly higher (Wilcoxon matched pairs test; $P = 0.0003$) in tumors (median = 87 arbitrary units) compared with normal tissues (median = 12 arbitrary units). Similarly, the ratio of AIB1:REA (Fig. 4*B*) was significantly higher (Wilcoxon matched pairs test; $P = 0.0414$) in

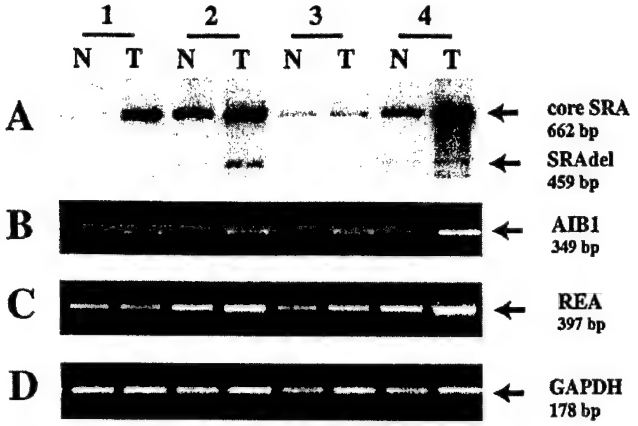

Fig. 2. *A*, detection of SRA and SRAdel in normal breast tissue adjacent to matched primary, ER+ invasive breast cancer. RNA extracted from matched breast tumors and adjacent matched normal breast tissue was extracted from 19 different patients and assayed for SRA expression using RT-PCR as described in "Materials and Methods." PCR products were separated on 6% acrylamide gels, which were dried, exposed to phosphor-imaging screens, and scanned using a Molecular Imager-FX. A digitized image showing the results obtained from four sets of normal tissue (*N*) and matched tumor tissue (*T*) is shown. *Arrows*, the expected 662-bp core SRA PCR product (SRA core, confirmed by sequence analysis) and a 459-bp deleted SRA variant PCR product (SRAdel), which was identified by sequence analysis to correspond to an SRA variant deleted in sequences from position 155 to 357 (GenBank accession no. AF092038). *B*, detection of AIB1 in normal breast tissue adjacent to matched primary, ER+ invasive breast cancer. RNA was extracted and assayed for AIB1 expression using RT-PCR as described in "Materials and Methods." After analysis of PCR products on prestained agarose gels, signals were quantified by scanning using MultiAnalyst. Ethidium bromide-stained gel of the RT-PCR analysis of four sets of normal tissue (*N*) and matched tumor tissue (*T*) is shown. *Arrows*, the expected 349-bp AIB1 PCR product (confirmed by sequence analysis). *C*, detection of REA in normal breast tissue adjacent to matched primary, ER+ invasive breast cancer. RNA was extracted and assayed for REA expression using RT-PCR as described in "Materials and Methods." After analysis of PCR products on prestained agarose gels, signals were quantified by scanning using MultiAnalyst. Ethidium bromide-stained gel of the RT-PCR analysis of four sets of normal tissue (*N*) and matched tumor tissue (*T*) is shown. *Arrows*, the expected 397-bp REA PCR product (confirmed by sequence analysis). *D*, ethidium bromide-stained gel of the RT-PCR analysis of *GAPDH* mRNA run in parallel for the same samples. *Arrow*, the expected 178-bp *GAPDH* PCR product.

tumors (median = 86.7 arbitrary units) compared with normal tissues (median = 61.3 arbitrary units). Furthermore, the ratio of SRA:AIB1 (Fig. 4*C*) was significantly higher (Wilcoxon matched pairs test; $P = 0.0058$) in tumors (median = 94.3 arbitrary units) compared with normal tissues (median = 22.8 arbitrary units), suggesting that the relative expression of ER coactivators may also change during breast tumorigenesis.

Discussion

In summary, although the RNA levels of two coactivators, SRA and AIB1, are significantly up-regulated in ER+ breast tumors compared with adjacent normal tissues, the RNA of a specific repressor of ER activity, REA exhibits no significant up-regulation during breast tumorigenesis in the same samples. These data are consistent with the hypothesis that factors enhancing ER activity are up-regulated in breast tumors, whereas factors repressing ER activity are not increased, providing a potential molecular basis for enhanced/altered estrogen action in human breast tumors. This is further supported by observations that the ratios of SRA:REA and AIB1:REA are increased in breast tumors compared with normal breast tissue. Interestingly, the increased relative expression of SRA:REA is greater (a 7.3-fold increase in median relative expression) than that for AIB1:REA (a 1.4-fold increase in median relative expression) between normal breast tissue and tumors, suggesting differentially altered expression of coactivators during breast tumorigenesis. This is supported by the observation that the ratio of SRA:AIB1 is also significantly increased in tumors (a 4.1-fold increase in median relative expression) compared with normal tissues.

SRA and AIB1 likely mediate their effects on ER activity via different mechanisms (7). SRA, unlike AIB1, functions as an RNA molecule (7). Also SRA requires the structurally and functionally distinct N-terminal/AF1 region of steroid receptors compared with AIB1, which requires the COOH-terminal/AF2 domain (6), possibly suggesting that estrogen target gene cascades could be differentially regulated by the relative expression of different coactivators. Therefore ER signaling could be altered during breast tumorigenesis. Such alterations during breast tumorigenesis are supported by the marked difference in breast epithelial growth responses to estrogen occurring during this process, *i.e.*, from indirect in normal to direct in breast cancer cells (3–5).

It is the core region of SRA that is necessary and sufficient for the coactivator activity of SRA (7). Our primers for SRA (14) will detect all SRA isoforms containing core sequences, and we assume that our measurement of all intact core SRA-like RNAs correlates with total SRA activity present in any one tissue. These primers also detect a previously described isoform of SRA (GenBank accession no. AA426601) containing a deletion of sequences within the SRA core. Deletions within the core were reported previously to result in the loss of SRA activator function (7). It is likely that this deleted variant is inactive with respect to coactivator activity and could function to alter steroid signaling in breast tumors and contribute to the more aggres-

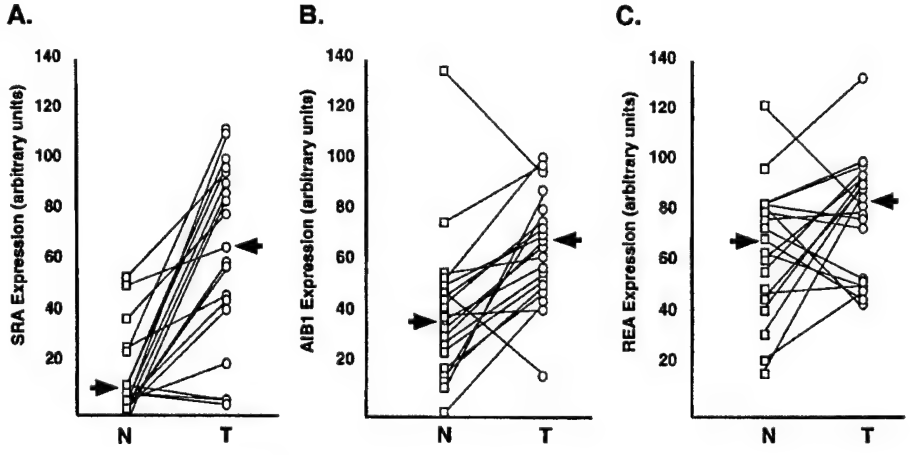

Fig. 3. Comparison of the expression of SRA, AIB1, and REA in adjacent normal breast tissue and matched primary breast tumors. For each patient ($n = 19$), SRA, AIB1, and REA expression was quantified and expressed in arbitrary units corrected for *GAPDH* signal as described in "Materials and Methods." The results are presented as a scatter graph. The normal samples are represented by □ and the tumor samples by ○. Each matched normal and tumor sample is joined by a *line*. *Arrows*, the median value in each group. *A*, the level of SRA expression in normal tissue is significantly different to the level of SRA expression in the tumor tissues (Wilcoxon matched pairs test, two-tailed; $P = 0.0004$). *B*, the level of AIB1 expression in normal tissue is significantly different from that in the tumor tissues (Wilcoxon matched pairs test, two-tailed; $P = 0.0058$). *C*, the level of REA expression in normal tissue is not significantly different from the level of REA expression in the tumor tissues (Wilcoxon matched pairs test, two-tailed; $P = 0.110$).

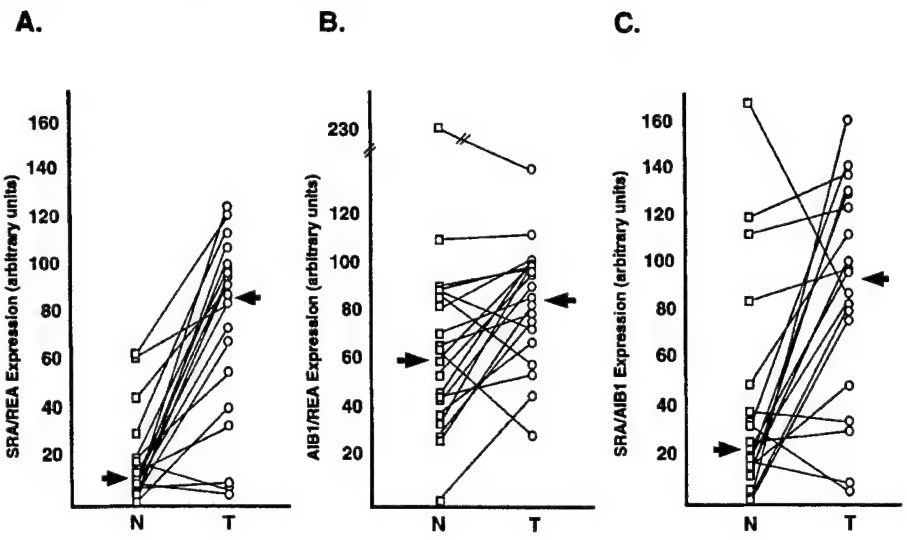

Fig. 4. Comparison of the relative expression of SRA, REA, and AIB1 in adjacent normal breast tissue and matched primary breast tumors. For each sample the expression of SRA, REA, and AIB1 has been quantified as described in "Materials and Methods," and the ratios SRA:REA (*A*), AIB1:REA (*B*), and SRA:AIB1 (*C*) have been calculated. The results are presented as a scatter graph. The normal samples are represented by □ and the tumor samples by ○. Each matched normal and tumor sample is joined by a *line*. *Arrows*, the median values in each group. *A*, the relative expression of SRA:REA expression in normal tissue is significantly different from that in the tumor tissues (Wilcoxon matched pairs test, two-tailed; $P = 0.0003$). *B*, the relative expression of AIB1:REA expression in normal tissue is significantly different from that in the tumor tissues (Wilcoxon matched pairs test, two-tailed; $P = 0.0414$). *C*, the relative expression of SRA:AIB1 expression in normal tissue is significantly different from that in the tumor tissues (Wilcoxon matched pairs test, two-tailed; $P = 0.0058$).

sive phenotype associated with poorer-prognosis tumors, which include characteristics such as high grade and large tumor size. A similar relationship of the relative expression of the deleted SRA and grade was also found in a previously described but separate breast tumor cohort (14).

Recently, REA was identified as a specific repressor of ligand-occupied ER (ERα and ERβ, but not other steroid or nuclear receptors) transcriptional activity (8). Furthermore, part of its mechanism appeared to involve competition with coactivators such as SRC-1 (6). It differed from previously identified corepressors such as N-CoR/SMRT (6) because it was selective for ER as opposed to generally effecting members of the nuclear receptor family (8). Because REA was selective for ER, it was relevant to investigate it in breast tissues. Our data suggest that REA expression is not altered in breast tumors compared with normal breast tissues.

Although the assessment of expression by RT-PCR will only allow measurement of global expression of these genes in heterogeneous tissue sections, our *in situ* hybridization data support the conclusion that the major cell type expressing SRA or REA in breast tissue is the epithelial cell, either normal or neoplastic. Previous data have confirmed that AIB1 mRNA is expressed in the epithelial component of both normal and neoplastic breast tissue (10). Therefore, our RT-PCR results likely represent expression differences in the epithelial components of the tissues examined. Furthermore, SRA, AIB1, and REA were shown to be expressed in human breast cancer cell lines in culture (7, 8, 10). Our *in situ* hybridization data are consistent with the RT-PCR data as well. Although further study is needed to confirm the relation between ER and these cofactors within individual cells, the data support the hypothesis that relative changes between coactivators (SRA and AIB1) and a corepressor (REA) can occur in breast tumorigenesis *in vivo*, an important point required to provide *in vivo* relevance for several previously published studies concerning altered coactivators and coregulators using laboratory model systems. Parallel *in situ* studies of AIB1 and REA protein levels, but not SRA (active as an RNA molecule), are required to provide unequivocal evidence of the relative changes between coactivators and corepressors during breast tumorigenesis. Unfortunately, there are presently no commercially available antibodies to REA, and available AIB1 antibodies cannot be used for immunohistochemical analysis. However, the available data based on Western blot analysis of breast and ovarian cancer cell line extracts suggest that there is a quantitative relationship between AIB1 mRNA and protein levels (17, 18).

Recently, a study was published (19) in which both ERα and the coactivator TIF2 were found to be significantly increased in intraductal carcinomas compared with normal mammary gland tissue. This study suggested as well that ERα and a general corepressor N-CoR are reduced in invasive breast cancer compared with DCIS. Although these results are consistent with our data and support the hypothesis that there may be an up-regulation of factors associated with increased ER signaling in breast tumorigenesis, the number of cases screened was small compared with our study, the normal samples and DCIS samples were not matched, *i.e.*, were not from the same patient, to the invasive breast cancer samples, and furthermore not all tumors were ER+. These factors introduce biological heterogeneity because the natural history of ER+ and ER− breast cancers is distinct, and it is likely that the factors involved in the development of ER− *versus* ER+ breast cancer are different. Also, the lack of matched samples with respect to comparisons among normal, intraductal, and invasive breast cancer introduces significant issues associated with patient-to-patient variability with respect to alterations which may be influenced by age and menopausal and other hormonal status, and may be significantly different between the groups compared and therefore confound the interpretation of the results.

We have used matched normal and breast cancer tissues as surrogates for breast tumorigenesis; however, it is acknowledged that breast tumorigenesis is a complex process, and an investigation of different morphological lesions thought to parallel the evolution of normal breast tissue to invasive breast cancer is necessary before more definite conclusions can be made. However, this study is the first, to our knowledge, that uses multiple matched samples of normal breast tissue and their ER+ tumors, and provides evidence that the relative expression of coactivators and corepressors, which are highly relevant with respect to the ER signal transduction pathway, can be significantly altered between normal human breast and breast tumors *in vivo*.

In conclusion, although our study is small, the results presented are consistent with the hypothesis that a significant up-regulation of ER signaling occurs during breast tumorigenesis in ER+ tumors. This is reflected not only in the increased expression of ERα shown previously, but now also in an increase in factors that can activate ER activity without a concomitant increase in factors that can repress ER activity. Despite the obvious need to study protein levels where appropriate, when reagents become available, the possibility now exists that an imbalance in the expression of repressors and activators of ERα can occur during human breast tumorigenesis *in vivo* and may

contribute to altered estrogen action, which is known to occur during this process.

References

1. Ricketts, D. Estrogen and progesterone receptors in normal female breast. Cancer Res., *51:* 1817–1822, 1991.
2. Osborne, C., Elledge, R., and Fuqua, S. Estrogen receptors in breast cancer therapy. Scientific American. Science Med., *3:* 32–41, 1996.
3. Woodward, T., Xie, J., and Haslam, S. The role of mammary stroma in modulating the proliferative response to ovarian hormones in the normal mammary gland. J. Mammary Gland Biol. Neoplasia, *3:* 117–131, 1998.
4. Lippman, M., and Bolan, G. Oestrogen responsive human breast cancer in long term tissue culture. Nature (Lond.), *256:* 592–593, 1975.
5. Clarke, R., Howell, A., Potten, C., and Anderson, E. Dissociation between steroid receptor expression and cell proliferation in the human breast. Cancer Res., *57:* 4987–4991, 1997.
6. McKenna, N., Lanz, R., and O'Malley, B. Nuclear receptor coregulators: cellular and molecular biology. Endocr. Rev., *20:* 321–344, 1999.
7. Lanz, R., McKenna, N., Onate, S., Albrecht, U., Wong, J., Tsai, S., Tsai, M-J., and O'Malley, B. A steroid receptor coactivator, SRA, functions as an RNA and is present in an SRC-1 complex. Cell, *97:* 17–27, 1999.
8. Montano, M., Ekena, K., Delage-Mourroux, R., Chang, W., Martini, P., and Katzenellenbogen, B. An estrogen receptor-selective coregulator that potentiates the effectiveness of antiestrogens and represses the activity of estrogens. Proc. Natl. Acad. Sci. USA, *96:* 6947–6952, 1999.
9. Leygue, E., Dotzlaw, H., Watson, P., and Murphy, L. Altered estrogen receptor α and β mRNA expression during human breast tumorigenesis. Cancer Res., *58:* 3197–3201, 1998.
10. Anzick, S., Kononen, J., Walker, R., Azorsa, D., Tanner, M., Guan, X., Sauter, G., Kallioniemi, O., Trent, J., and Meltzer, P. AIB1, a steroid receptor coactivator amplified in breast and ovarian cancer. Science (Washington DC), *277:* 965–968, 1997.
11. Hiller, T., Snell, L., and Watson, P. Microdissection/RT-PCR analysis of gene expression. Biotechniques, *21:* 38–44, 1996.
12. Leygue, E., Snell, L., Dotzlaw, H., Hole, K., Troup, S., Hiller-Hitchcock, T., Murphy, L., and Watson, P. Mammaglobin, a potential marker of breast cancer nodal metastasis. J. Pathol., *189:* 28–33, 1999.
13. Leygue, E., Murphy, L., Kuttenn, F., and Watson, P. Triple primer polymerase chain reaction. A new way to quantify truncated mRNA expression. Am. J. Pathol., *148:* 1097–1103, 1996.
14. Leygue, E., Dotzlaw, H., Watson, P., and Murphy, L. Expression of the steroid receptor RNA activator (SRA) in human breast tumors. Cancer Res., *59:* 4190–4193, 1999.
15. Leygue, E. R., Watson, P. H., and Murphy, L. C. Estrogen receptor variants in normal human mammary tissue. J. Natl. Cancer Inst., *88:* 284–290, 1996.
16. Bautista, S., Valles, H., Walker, R., Anzick, S., Zeillinger, R., Meltzer, P., and Theillet, C. In breast cancer, amplification of the steroid receptor coactivator gene *AIB1* is correlated with estrogen and progesterone receptor positivity. Clin. Cancer Res., *4:* 2925–2929, 1998.
17. Azorsa, D., and Meltzer, P. Production and characterization of monoclonal antibodies to the steroid receptor coactivator AIB1. Hybridoma, *18:* 281–287, 1999.
18. de Mora, J. F., and Brown, M. AIB1 is a conduit for kinase-mediated growth factor signaling to the estrogen receptor. Mol. Cell. Biol., *20:* 5041–5047, 2000.
19. Kurebayashi, J., Otsuki, T., Kunisue, H., Tanaka, K., Yamamoto, S., and Sonoo, H. Expression levels of estrogen receptor-α, estrogen receptor-β, coactivators and corepressors in breast cancer. Clin. Cancer Res., *6:* 512–518, 2000.

[CANCER RESEARCH 60, 2796–2799, June 1, 2000]

Advances in Brief

Expression of a Repressor of Estrogen Receptor Activity in Human Breast Tumors: Relationship to Some Known Prognostic Markers[1]

Sharon L. R. Simon, Alicia Parkes, Etienne Leygue, Helmut Dotzlaw, Linda Snell, Sandra Troup, Adewale Adeyinka, Peter H. Watson, and Leigh C. Murphy[2]

Departments of Biochemistry and Medical Genetics [S. L. R. S., A. P., E. L., H. D., L. C. M.] and Pathology [L. S., S. T., A. A., P. H. W.], Faculty of Medicine, University of Manitoba, Winnipeg, Manitoba R3E 0W3, Canada

Abstract

The expression of a specific repressor of estrogen receptor activity (REA) was investigated by a semiquantitative reverse transcription-PCR assay in 40 human breast tumor biopsy samples with respect to steroid hormone receptor status and other known prognostic variables. The data showed that REA expression was positively correlated with estrogen receptor (ER) levels as defined by ligand-binding assays (Spearman $r = 0.3231$; $P = 0.042$) and that the median level of REA mRNA was significantly (Mann-Whitney two-tailed test, $P = 0.0424$) higher in ER+ tumors (median = 94.5; $n = 30$) compared with ER− tumors (median = 64.5; $n = 10$), with no significant differences ($P = 0.4988$) associated with progesterone receptor status alone. In addition, REA expression was inversely correlated with tumor grade (Spearman $r = -0.4375$; $P = 0.0054$). When the tumors were divided into two groups based on grade, REA expression was significantly (Mann-Whitney two-tailed test, $P = 0.0024$) higher in low-grade (median = 97; $n = 16$) compared with high-grade (median = 76; $n = 23$) tumors. These results provide preliminary data suggesting that the expression of REA varies among breast tumors and is correlated with known treatment response markers and inversely correlated with a marker of breast cancer progression. REA together with ER status may be an improved marker of endocrine therapy responsiveness in human breast cancer.

Introduction

Estrogens have important roles in both normal and neoplastic mammary tissues; however, marked changes occur in estrogen action during both breast tumorigenesis and breast cancer progression (1). The mechanisms underlying altered estrogen signal transduction in target tissues is the focus of much research at present. Current concepts of estrogen action include cofactors that can either enhance or repress the transcriptional activity of the ER[3] (2). Recently, a highly specific repressor of the transcriptional activity of ligand-occupied ERs (ER-α and ER-β but not other steroid hormone receptors such as PR or type II nuclear receptors) was identified and characterized using a yeast two-hybrid system (3). Furthermore, part of its mechanism of action appeared to involve functional competition with steroid hormone receptor coactivators such as SRC-1 (2). This repressor differed from previously identified corepressors such as nuclear receptor corepressor and silencing mediator for retinoid and thyroid hormone receptor; in that it was not structurally related to either of them, it showed great selectivity for ER as opposed to other steroid hormone or non-steroid-binding members of the nuclear receptor family, and it required ER to be bound to ligand with preferential effects being seen when the ligand was an antiestrogen (3). This repressor was therefore called REA. Because REA is selective for ER, it is highly relevant to investigate the expression of this gene in human breast tissues both normal and neoplastic.

Recently we demonstrated that REA is expressed in both normal and neoplastic human breast tissues,[4] as measured by RT-PCR. Furthermore, the expression of REA was not significantly different between ER+ breast tumors and their matched adjacent normal breast tissues.[4] However, the tumor cohort in the previous study were all ER+ as determined by ligand-binding assays and did not address the question of whether REA expression in breast tumors was correlated with known prognostic and endocrine treatment response markers. In this study, we investigated the relationship of REA expression in breast tumors to ER and PR status and other known prognostic variables.

Materials and Methods

Human Breast Tumors. Forty invasive ductal carcinomas were selected from the National Cancer Institute of Canada-Manitoba Breast Tumor Bank (Winnipeg, Manitoba, Canada). The cases were selected for ER and PR status as determined by ligand-binding assays. The ER levels were 0–151 fmol/mg of protein, and 30 tumors were classified as ER+ (defined as >3 fmol/mg of protein). PR levels were 0–285 fmol/mg of protein, and 20 tumors were classified as PR+ (defined by >10 fmol/mg of protein). These tumors spanned a wide range of grade (grades 4–9), determined using the Nottingham grading system.

Cell Culture. T-47D human breast cancer cells were obtained from Dr. D. Edwards (Denver, CO), and MCF7 cells were obtained from the late Dr. W. McGuire (San Antonio, TX). T-47D cells were grown in DMEM supplemented with 5% fetal bovine serum, 100 nM glutamine, 0.3% (v/v) glucose, and penicillin/streptomycin as described previously (4). Cells were plated at 1×10^6 in 100-mm dishes and 2 days later were treated with 10 nM medroxyprogesterone acetate and harvested at various times (1–48 h). MCF7 human breast cancer cells were depleted of estrogen by passaging stock cells twice in phenol red-free DMEM supplemented with 5% twice charcoal-stripped fetal bovine serum, 100 nM glutamine, 0.3% (v/v) glucose, and penicillin/streptomycin (5% twice charcoal-stripped fetal bovine serum) as described previously (5). Cells were then plated as above in 5% twice charcoal-stripped fetal bovine serum and 2 days later treated with 10 nM estradiol-17β and harvested for analysis at various times (1–48 h). The steroids were added directly from 1000× stock solutions in ethanol to achieve the required concentrations. The cells were harvested by scraping with a rubber policeman. After centrifugation, the cell pellet was frozen and stored at −70°C until RNA was isolated.

Received 1/10/00; accepted 4/11/00.

The costs of publication of this article were defrayed in part by the payment of page charges. This article must therefore be hereby marked *advertisement* in accordance with 18 U.S.C. Section 1734 solely to indicate this fact.

[1] This work was supported by grants from the Canadian Breast Cancer Research Initiative (CBCRI) and the United States Army Medical Research and Materiel Command (USAMRMC). The Manitoba Breast Tumor Bank is supported by funding from the National Cancer Institute of Canada (NCIC). P. H. W. is a Medical Research Council of Canada (MRC) Scientist, and L. C. M. is an MRC Scientist.

[2] To whom requests for reprints should be addressed, at Department of Biochemistry and Molecular Biology, University of Manitoba, Winnipeg, MB R3E 0W3, Canada. Phone: (204) 789-3812; Fax: (204) 789-3900; E-mail: lcmurph@cc.umanitoba.ca.

[3] The abbreviations used are: ER, estrogen receptor; PR progesterone receptor; REA, repressor of estrogen receptor activity; RT-PCR, reverse transcription-PCR; GAPDH, glyceraldehyde-3-phosphate dehydrogenase.

[4] L. C. Murphy, S. L. R. Simon, A. Parkes, E. Leygue, H. Dotzlaw, L. Snell, S. Troup, A. Adeyinka, and P. H. Watson. Altered relative expression of estrogen receptor coregulators during human breast tumorigenesis, submitted for publication.

RNA Extraction and RT-PCR Conditions. Total RNA was extracted from 20-μm frozen tissue sections (20 sections per tumor) or cell pellets using Trizol reagent (Life Technologies, Grand Island, NY) according to the manufacturer's instructions and quantified spectrophotometrically. One μg of total RNA was reverse transcribed in a final volume of 25 μl as described previously (6).

Primers and PCR Conditions. The primers used were primer REAU (5′-CGA AAA ATC TCC TCC CCT ACA-3′: sense; positions, GenBank Accession No. AF150962) and primer REAL (5′-CCT GCT TTG CTT TTT CTA CCA-3′; antisense; position, GenBank Accession No. AF150962). PCR amplifications were performed and PCR products analyzed as described previously (7) with minor modifications. Briefly, 1 μl of reverse transcription mixture was amplified in a final volume of 20 μl in the presence of 4 ng/μl of each primer and 0.3 units of *Taq* DNA polymerase (Life Technologies). Each PCR consisted of 27 cycles (30 s at 57°C, 30 s at 72°C, and 30 s at 94°C) for measuring REA. PCR products were then separated on 1.8% agarose gels stained with ethidium bromide as described previously (7). Amplification of the ubiquitously expressed *GAPDH* cDNA was performed in parallel, and PCR products were separated on agarose gels stained with ethidium bromide as described previously (7). The identities of PCR products were confirmed by subcloning and sequencing, as reported previously (6).

Quantification and Statistical Analysis of REA Expression. After analysis of PCR products on prestained agarose gels, signals were quantified by scanning using MultiAnalyst (Bio-Rad, Hercules, CA). At least three independent PCRs were performed. To control for variations between experiments, a value of 100% was arbitrarily assigned to the REA signal of one particular sample and all signals were expressed as a percentage of this signal. In parallel, *GAPDH* cDNA was amplified, and after analysis of PCR products on prestained agarose gels, signals were quantified by scanning using MultiAnalyst. Three independent PCRs were performed. Each *GAPDH* signal was also expressed as a percentage of the signal observed in the same tumor. For each sample, the average of REA signal was then expressed as a percentage of the *GAPDH* signal (arbitrary units).

Correlation between REA expression and tumor characteristics was tested by calculation of the Spearman coefficient, r. Differences between tumor subgroups were tested using the Mann-Whitney rank-sum test, two-sided.

Results

Measurement of REA mRNA Expression in Primary Human Breast Tumors with Different ER and PR Status. We previously developed a semiquantitative RT-PCR approach to measure REA mRNA in small amounts of human breast tissues.[4] Cloning and sequencing confirmed the identity of the expected 397-bp PCR product as REA, and this PCR product was used to probe Northern blots of RNA extracted from human breast tumor biopsies as described previously (8). An ~1.5-kb transcript was detected, consistent with the previously described REA mRNA (Fig. 1). Varying levels of REA mRNA were detected in human breast tumor biopsy samples, which raised the question of whether the expression of REA in breast tumors was correlated with the known prognostic and treatment response variables, such as ER and PR status.

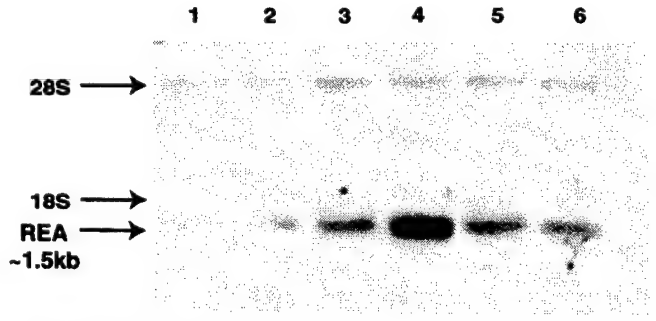

Fig. 1. Northern blot analysis of poly(A)+ enriched RNA (15 μg) isolated from several human breast cancer biopsy samples. The 397-bp REA PCR product was used to probe the Northern blot as described previously (8). Residual 28S and 18S bands are shown, as is the ~ 1.5-kb band corresponding to REA mRNA.

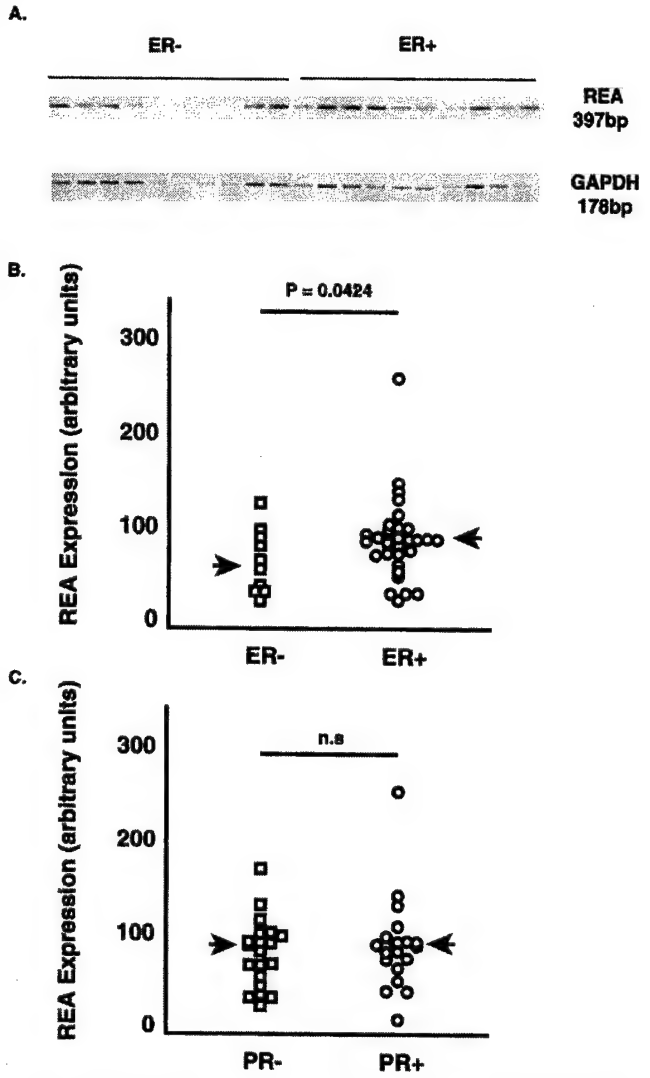

Fig. 2. *A*, RNA was extracted and assayed for REA expression using RT-PCR as described in "Materials and Methods." After analysis of PCR products on prestained agarose gels, signals were quantified by scanning using MultiAnalyst. Ethidium bromide-stained gel of the RT-PCR analysis of some ER− and ER+ breast tumors is shown (*top*). The expected 397-bp REA PCR product (confirmed by sequence analysis) is shown. Ethidium bromide-stained gel of the RT-PCR analysis of *GAPDH* mRNA run in parallel for the same samples is shown *below* the REA analysis. The expected 178-bp *GAPDH* PCR product is shown. *B*, for each tumor (n = 40), REA expression was quantified and expressed in arbitrary units corrected for *GAPDH* signal as described in "Materials and Methods." The tumors were divided into ER+ (>3 fmol/mg of protein; ○) and ER− (≤3 fmol/mg of protein; □) as defined by ligand-binding assays. The results are presented as a scatter graph. *Arrows* indicate the median value in each group. REA expression is significantly less in ER− tumors compared with ER+ tumors (Mann-Whitney two-tailed, P = 0.0424). *C*, for each tumor (n = 40), REA expression was quantified and expressed in arbitrary units corrected for *GAPDH* signal as described in "Materials and Methods." The tumors were divided into PR+ (>10 fmol/mg of protein; ○) and PR− (≤10 fmol/mg of protein; □) as defined by ligand-binding assays. The results are presented as a scatter graph. *Arrows* indicate the median value in each group. REA expression is not significantly (*n.s.*) different between PR− tumors and PR+ tumors.

Tumors were identified according to their ER or PR status as defined by ligand-binding analysis (see "Materials and Methods"). REA mRNA levels were measured by RT-PCR and normalized to the GAPDH mRNA level as measured in parallel by RT-PCR. Examples of the results obtained are shown in Fig. 2*A*. The results obtained for all tumors assayed are shown as scatter graphs in Fig. 2*B* (arranged according to ER) and Fig. 2*C* (arranged according to PR status of the

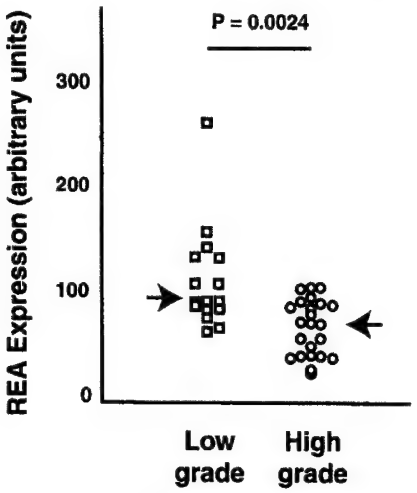

Fig. 3. For each tumor (n = 40), REA expression was quantified and expressed in arbitrary units corrected for *GAPDH* signal as described in "Materials and Methods." The tumors were divided into low-grade (Nottingham grades 3–6; □) and high-grade (Nottingham grades 7–9;○). The results are presented as a scatter graph. *Arrows* indicate the median value in each group. REA expression is significantly higher in low-grade tumors compared with high-grade tumors (Mann-Whitney two-tailed, P = 0.0024).

tumor as measured by ligand-binding analysis). When the level of REA mRNA in tumors was assessed according to either ER status or PR status alone, as defined by ligand-binding analysis, the level of REA mRNA was significantly (Mann-Whitney two-tailed test, P = 0.0424) higher in ER+ tumors (median, 94.5; n = 30) compared with ER− tumors (median, 64.5; n = 10), with no significant differences (P = 0.4988) associated with PR status alone (PR+ median, 91.5; n = 20; PR− median, 87.5; n = 20).

The relationship of the level of REA mRNA levels with ER status in human breast tumor biopsies suggested the hypothesis that REA expression may be regulated by estrogens and/or progestins. However, no effect of estrogen (10 nM estradiol-17β) on the steady-state REA mRNA levels in estrogen-depleted MCF7 cells was observed over a 48-h time span (data not shown). In addition, no effect of progestin (10 nM medroxyprogesterone acetate) treatment on REA mRNA in T-47D cells was observed over a similar time span (data not shown). It was concluded that the expression of REA mRNA was not regulated by estrogens or progestins in human breast cancer cell lines.

Correlation of REA Expression with Tumor Characteristics. Spearman analysis showed a significant correlation of the level of REA mRNA in the tumors with the level of ER as measured by ligand-binding assays (Spearman r = 0.3231; P = 0.042) but no significant correlation with the level of PR as measured by ligand-binding assays (Spearman r = 0.2777; P = 0.0841). These data are consistent with the data analyzed using clinically relevant cutoff values for ER (ER+ >3 fmol/mg of protein) and PR (PR+ >10 fmol/mg of protein) status as shown above. However, statistical significance of the correlation of REA mRNA and ER binding was lost when Spearman analysis was applied only to those tumors that were ER+ (>3 fmol/mg of protein). The level of REA mRNA was also found to be inversely correlated with tumor grade (Spearman r = −0.4375; P = 0.0054). When the tumors were divided into two groups based on grade (low, Nottingham grades 3–6; high, Nottingham grades 7–9), the level of REA mRNA (Fig. 3) was significantly (Mann-Whitney two-tailed test, P = 0.0024) higher in low-grade (median, 97; n = 16) compared with high-grade (median, 76; n = 23) tumors, which is consistent with the Spearman correlation analysis.

No significant correlations were found between the level of REA mRNA and age, nodal status, percentage of normal duct and lobular epithelium, or percentage of stromal or fat cell content within the tumor sections analyzed.

Discussion

Our data show that the level of REA mRNA in human breast tumors is significantly correlated with ER status and inversely correlated with grade. These data are the first to identify a correlation between REA mRNA expression and known prognostic and treatment response markers in human breast cancer biopsies. The positive correlation of REA and ER expression (a good prognostic variable and a marker of response to endocrine therapies) together with inverse correlation of REA expression and grade suggests that REA expression could also be a marker of good prognosis and likelihood of response to endocrine therapies such as antiestrogens. The loss of statistical significance of the correlation between ER levels and REA mRNA when only ER+ breast tumors were analyzed may be due to the reduced numbers of observations in that analysis (n = 30 compared with n = 40 for total tumor cohort) or may indicate the existence of some threshold effect associated with expression of ER and REA. This latter suggestion together with the lack of correlation of absolute ER levels and REA mRNA in ER+ tumors would be consistent with our observation that REA expression, at least at the RNA level, was found not to be regulated by estrogen.

REA has been identified as a protein that interacts in a yeast-two hybrid system with a dominant negative mutant ERα (3). It was shown to be a selective repressor of ER (both ERα and ERβ) transcriptional activity as determined in transient transfection assays using several estrogen-responsive element-containing promoters regulating a chloramphenicol acetyltransferase reporter gene. Cotransfection of a REA expression vector enhanced the potency of antiestrogens such as 4-hydroxytamoxifen and ICI 182780. Furthermore, REA competitively reversed coactivator, *i.e.,* SRC-1, transcriptional enhancement of ER activity. Together these data suggest that REA is a corepressor of ER transcriptional activity.

The current concept of the mechanism by which nuclear hormone receptors regulate gene transcription involves three main components as proposed by Katzenellenbogen *et al.* (9): the receptor, its ligands, and its coregulators. Coregulators appear to consist of at least two classes: those that enhance nuclear hormone receptor activity, referred to as coactivators, and those that repress nuclear hormone receptor activity, referred to as corepressors (2). Furthermore, it has been suggested that differences in the ratios of expression of these two different groups of coregulators may underlie altered responses to steroid hormone agonists and antagonists (10–13). More recently, we have provided the first evidence to suggest that an imbalance between factors that can enhance ER and factors that can repress ER transcriptional activity occurs during human breast tumorigenesis *in vivo*.[4] Our data showed that the levels of expression of the two ER coactivators, steroid receptor RNA activator (14) and amplified in breast cancer-1 (15), were significantly increased in ER+ breast tumors compared with their normal adjacent breast tissues, whereas the level of REA, a repressor of ER activity, was not significantly different between the tumors and normal breast tissues in the same patient cohort. However, this investigation used only ER+ breast tumors and could not address the question of REA expression in relation to steroid receptor status and other prognostic variables in breast tumors. In addition, we and others have shown that the expression of the coactivators, steroid receptor RNA activator (16) and amplified in breast cancer-1 (17), varies among breast tumors and can be correlated with steroid receptor status in some cases.

ER status itself is associated with grade, with most ER+ breast tumors being low grade and having low tumor proliferation rates,

defined by the percentage of S-phase cells (18), and this may contribute to the inverse relationship of REA with grade observed in this study. However, REA expression is more strongly inversely correlated with grade than positively with ER status; therefore, it is possible that a repressor of ER activity that can contribute to the proliferative activity of breast tumor cells could have a significant negative effect on breast cancer progression and thus functionally influence breast cancer progression. It is speculated that the coexpression of ER and REA may therefore provide better prognostic information than either alone.

ER status is also an important treatment response marker in human breast cancer (18) where the presence of ER in breast tumors increases the likelihood of response to endocrine therapies such as antiestrogens. However, a significant portion of ER+ tumors will not respond to tamoxifen initially, and of those tumors that do respond, many eventually will develop resistance to tamoxifen and other endocrine therapies (18). It has been speculated that altered relative ratios of coactivators and corepressors of ER may in part be a mechanism underlying such endocrine resistance. Direct proof of this hypothesis *in vivo* remains to be provided by measuring expression of the relevant genes in human breast tumors that are known to be clinically sensitive or resistant to tamoxifen and/or other endocrine therapies. However, the data presented here provide preliminary information that the expression of a specific repressor of ER activity varies among breast tumors and that expression is correlated with known treatment response markers and inversely correlated with a marker of breast cancer progression.

References

1. Murphy, L. Mechanisms of hormone independence in human breast cancer. In Vivo. *12:* 95–106, 1998.
2. McKenna, N., Lanz, R., and O'Malley, B. Nuclear receptor coregulators: cellular and molecular biology. Endocr. Rev. *20:* 321–344, 1999.
3. Montano, M., Ekena, K., Delage-Mourroux, R., Chang, W., Martini, P., and Katzenellenbogen, B. An estrogen receptor-selective coregulator that potentiates the effectiveness of antiestrogens and represses the activity of estrogens. Proc. Natl. Acad. Sci. USA. *96:* 6947–6952, 1999.
4. Dotzlaw, H., Leygue, E., Watson, P., and Murphy, L. Estrogen receptor-β messenger RNA expression in human breast tumor biopsies: relationship to steroid receptor status and regulation by progestins. Cancer Res., *59:* 529–532, 1999.
5. Coutts, A., Davie, J., Dotzlaw, H., and Murphy, L. Estrogen regulation of nuclear matrix-intermediate filament proteins in human breast cancer cells. J. Cell. Biochem., *63:* 174–184, 1996.
6. Dotzlaw, H., Leygue, E., Watson, P., and Murphy, L. Expression of estrogen receptor-β in human breast tumors. J. Clin. Endocrinol. Metab., *82:* 2371–2374, 1997.
7. Leygue, E. R., Watson, P. H., and Murphy, L. C. Estrogen receptor variants in normal human mammary tissue. J. Natl. Cancer Inst., *88:* 284–290, 1996.
8. Murphy, L. C., and Dotzlaw, H. Variant estrogen receptor mRNA species detected in human breast cancer biopsy samples. Mol. Endocrinol., *3:* 687–693, 1989.
9. Katzenellenbogen, J. A., O'Malley, B. W., and Katzenellenbogen, B. S. Tripartite steroid hormone receptor pharmacology: interaction with multiple effector sites as a basis for the cell- and promoter-specific action of these hormones. Mol. Endocrinol., *10:* 119–131, 1996.
10. Horwitz, K., Jackson, T., Bain, D., Richer, J., Takimoto, G., and Tung, L. Nuclear receptor coactivators and corepressors. Mol. Endocrinol., *10:* 1167–1177, 1996.
11. Smith, C., Nawaz, Z., and O'Malley, B. Coactivator and corepressor regulation of the agonist/antagonist activity of the mixed antiestrogen, 4-hydroxytamoxifen. Mol. Endocrinol., *11:* 657–666, 1997.
12. Szapary, D., Huang, Y., and Simons, S. S., Jr. Opposing effects of corepressor and coactivators in determining the dose-response curve of agonists, and residual agonist activity of antagonists, for glucocorticoid receptor-regulated gene expression. Mol. Endocrinol., *13:* 2108–2121, 1999.
13. Lavinsky, R., Jepsen, K., Heinzel, T., Torchia, J., Mullen, T., Schiff, R., Del-Rio, A., Ricote, M., Ngo, S., Gemsch, J., Hilsenbeck, S., Osborne, C., Glass, C., Rosenfeld, M., and Rose, D. Diverse signaling pathways modulate nuclear receptor recruitment of N-CoR and SMRT complexes. Proc. Natl. Acad. Sci. USA. *95:* 2920–2925, 1998.
14. Lanz, R., McKenna, N., Onate, S., Albrecht, U., Wong, J., Tsai, S., Tsai, M-J., and O'Malley, B. A steroid receptor coactivator, SRA, functions as an RNA and is present in an SRC-1 complex. Cell, *97:* 17–27, 1999.
15. Anzick, S., Kononen, J., Walker, R., Azorsa, D., Tanner, M., Guan, X., Sauter, G., Kallioniemi, O., Trent, J., and Meltzer, P. AIB1, a steroid receptor coactivator amplified in breast and ovarian cancer. Science (Washington DC), *277:* 965–968, 1997.
16. Leygue, E., Dotzlaw, H., Watson, P., and Murphy, L. Expression of the steroid receptor RNA activator (SRA) in human breast tumors. Cancer Res., *59:* 4190–4193, 1999.
17. Bautista, S., Valles, H., Walker, R., Anzick, S., Zeillinger, R., Meltzer, P., and Theillet, C. In breast cancer, amplification of the steroid receptor coactivator gene *AIB1* is correlated with estrogen and progesterone receptor positivity. Clin. Cancer Res., *4:* 2925–2929, 1998.
18. Osborne, C. Steroid hormone receptors in breast cancer management. Breast Cancer Res. Treat., *51:* 227–238, 1998.

[CANCER RESEARCH 60, 7075–7083, December 15, 2000]

Hypoxia-inducible Expression of Tumor-associated Carbonic Anhydrases[1]

Charles C. Wykoff, Nigel J. P. Beasley, Peter H. Watson, Kevin J. Turner, Jaromir Pastorek, Amen Sibtain, George D. Wilson, Helen Turley, Kate L. Talks, Patrick H. Maxwell, Christopher W. Pugh, Peter J. Ratcliffe,[2] and Adrian L. Harris

Institute of Molecular Medicine [C. C. W., N. J. P. B., K. J. T., A. L. H.] and the Nuffield Department of Clinical Laboratory Sciences [H. T., K. L. T.], John Radcliffe Hospital, Oxford OX3 9DS, United Kingdom; Department of Pathology, University of Manitoba, Winnipeg, Manitoba, R3E OW3 Canada [P. H. W.]; Institute of Virology, Slovak Academy of Sciences, 84246 Bratislava, Slovak Republic [J. P.]; Gray Laboratory Cancer Research Trust, Mount Vernon Hospital, Middlesex HA6 2JR, United Kingdom [A. S., G. D. W.]; Wellcome Trust Centre for Human Genetics, Oxford OX3 7BN, United Kingdom [P. H. M., C. W. P., P. J. R.]

ABSTRACT

The transcriptional complex hypoxia-inducible factor-1 (HIF-1) has emerged as an important mediator of gene expression patterns in tumors, although the range of responding genes is still incompletely defined. Here we show that the tumor-associated carbonic anhydrases (CAs) are tightly regulated by this system. Both *CA9* and *CA12* were strongly induced by hypoxia in a range of tumor cell lines. In renal carcinoma cells that are defective for the von Hippel-Lindau (VHL) tumor suppressor, up-regulation of these CAs is associated with loss of regulation by hypoxia, consistent with the critical function of pVHL in the regulation of HIF-1. Further studies of *CA9* defined a HIF-1-dependent hypoxia response element in the minimal promoter and demonstrated that tight regulation by the HIF/pVHL system was reflected in the pattern of CA IX expression within tumors. Generalized up-regulation of CA IX in VHL-associated renal cell carcinoma contrasted with focal perinecrotic expression in a variety of non-VHL-associated tumors. In comparison with vascular endothelial growth factor mRNA, expression of CA IX demonstrated a similar, although more tightly circumscribed, pattern of expression around regions of necrosis and showed substantial although incomplete overlap with activation of the hypoxia marker pimonidazole. These studies define a new class of HIF-1-responsive gene, the activation of which has implications for the understanding of hypoxic tumor metabolism and which may provide endogenous markers for tumor hypoxia.

INTRODUCTION

Tumor hypoxia is an important indicator of cancer prognosis; it is associated with aggressive growth, metastasis, and poor response to treatment (1, 2). Of potential importance for understanding these effects is the role of hypoxia in regulating patterns of gene expression (3–6). Studies of gene expression have defined several classes of hypoxia-inducible genes that are up-regulated in hypoxic regions of tumors and demonstrated that activation of the transcriptional complex HIF-1[3] is a key mediator of many of these effects (7–9).

Genes that are up-regulated by microenvironmental hypoxia through activation of HIF include glucose transporters, glycolytic enzymes, and angiogenic growth factors (5, 10, 11). For some HIF targets such as VEGF, a clear function in promoting tumor growth is established (12). However, the full range of HIF target genes has not yet been defined, and identification of additional genes responding to this pathway is likely to provide further insights into the consequences of tumor hypoxia and HIF activation. Indirect support for the importance of microenvironmental activation of HIF has also been provided by recent demonstrations of constitutive activation of HIF after inactivation of the VHL tumor suppressor gene (13) and amplification of the HIF response by other oncogenic mutations (14–17). Mutations in VHL cause the familial syndrome and are also found in the majority of sporadic RCCs (18). The gene product pVHL forms part of a ubiquitin-ligase complex (19, 20) that targets HIF-α subunits for oxygen-dependent proteolysis (13, 21). In VHL-defective cells, HIF-α is stabilized constitutively, resulting in up-regulation of hypoxia-inducible genes such as VEGF (13). Although the pVHL ubiquitin-ligase complex may have other targets (20) and other functions of pVHL have been proposed that may contribute to tumor suppressor effects (22, 23), these recent findings raise important questions as to the range of genes affected by constitutive HIF activation and the role of these genes in oncogenesis.

In this respect, one interesting group of genes is the tumor-associated transmembrane CAs *CA9* (24–27) and *CA12* (28, 29). CAs catalyze the reversible hydration of carbon dioxide to carbonic acid (30), providing a potential link between metabolism and pH regulation. The membrane-linked isoforms *CA9* and *CA12* were identified by RNA differential display as genes that are down-regulated by pVHL (29), although the effect of hypoxia was not examined and the mechanism of regulation was not defined. Interestingly, *CA9* can confer a variety of features of the transformed phenotype when transfected into NIH 3T3 cells (24).

In this study, we demonstrate that in contrast to constitutive up-regulation in pVHL-defective cell lines, both *CA9* and *CA12* are strongly induced by hypoxia in a broad range of other cell types. The induction of *CA9* by hypoxia was striking and has been studied in detail. We show that the *CA9* promoter is tightly regulated by a HIF-responsive HRE close to its transcriptional start site, and that the gene product is expressed in a perinecrotic manner in many types of human cancer, overlapping with VEGF mRNA and the hypoxia marker pimonidazole. In keeping with constitutive activation of HIF after inactivation of pVHL, the focal pattern of expression observed in most tumors contrasted with that observed in RCCs, where CA IX was globally up-regulated. Our findings define a new biochemical pathway that is regulated by HIF, suggest that CA IX may be a useful marker for HIF activation either by microenvironmental hypoxia or genetic events such as VHL inactivation, and provide additional insights into mechanisms by which the HIF pathway might mediate effects on tumor metabolism.

MATERIALS AND METHODS

Cell Lines. 786-0 cells expressing pVHL or empty vector were a gift from W. G. Kaelin (Dana-Farber Cancer Institute, Boston, MA). RCC4 cells expressing pVHL or empty vector and other RCC lines were as described (13). RT112 human bladder carcinoma cells were a gift from M. Knowles (Imperial Cancer Research Fund, Leeds, United Kingdom). A549, NCI-H460, HeLa, EJ28, MDA-MB-468, MDA-MB-435S, MDA-MB-231, HBL-100, T-47D, and U2 O-S lines were from American Type Culture Collection (ATCC). Cells

Received 6/13/00; accepted 10/18/00.

The costs of publication of this article were defrayed in part by the payment of page charges. This article must therefore be hereby marked *advertisement* in accordance with 18 U.S.C. Section 1734 solely to indicate this fact.

[1] This work was supported by the Wellcome Trust and the Imperial Cancer Research Fund.

[2] To whom requests for reprints should be addressed, at Wellcome Trust Centre for Human Genetics, Oxford OX3 7BN, United Kingdom. Phone: (44) 1865-287531; Fax: (44) 1865-287533; E-mail: peter.ratcliffe@imm.ox.ac.uk.

[3] The abbreviations used are: HIF-1, hypoxia-inducible factor-1; VEGF, vascular endothelial growth factor; VHL, von Hippel-Lindau; RCC, renal cell carcinoma; CA, carbonic anhydrase; *CA9*, carbonic anhydrase 9 gene (including any genomic sequence and mRNA); CA IX, carbonic anhydrase 9 protein; HRE, hypoxia response element; RPA, RNase protection assay; βgal, β-galactosidase; DFO, desferrioxamine; CHO, Chinese hamster ovary.

were grown in DMEM (Sigma) supplemented with 10% FCS (Globepharm), L-glutamine (2 μM), penicillin (50 IU/ml), and streptomycin sulfate (50 μg/ml). Studies of inducible gene expression were performed on cells approaching confluence. Parallel incubations were performed on aliquots of cells in normoxia (humidified air with 5% CO_2) and either hypoxia or DFO mesylate (100 μM; Sigma). Hypoxic conditions were generated in a Napco 7001 incubator (Precision Scientific) with 0.1% O_2, 5% CO_2, and balance N_2, unless otherwise specified. Experimental exposures were performed in normal growth medium for 16 h.

RNA Analysis. Total RNA was extracted by a modified acid/guanidinium thiocyanate/phenol/chloroform method (RNAzol B; Cinna/Biotec Laboratories), dissolved in hybridization buffer (80% formamide, 40 mM PIPES, 400 mM sodium chloride, and 1 mM EDTA, pH 8) and analyzed by RPA. To generate appropriate riboprobe templates, cDNA fragments of human *CA9* (nucleotides 3632–3771, accession number Z54349) and *CA12* (nucleotides 301–450, accession number AF037335) were amplified by PCR and ligated into pSP72 (Promega). DNA templates for generating ^{32}P-labeled RNA probes were linearized for 16 h with *Bgl*II and transcribed with SP6 RNA polymerase. For *CA9* and *CA12*, RPAs were performed on 30 μg of total RNA, using an internal control assay for U6 small nuclear RNA as described (13).

Construction of Reporter Plasmids. To generate plasmids p-506 and p-173, sequences of the *CA9* gene between −506 and +43 relative to the transcriptional start site were amplified by PCR from genomic DNA. PCR products were ligated into pGL3-basic, a promoterless and enhancerless luciferase expression vector (Promega). To generate plasmids p-36, MUT1, and MUT2, complementary oligonucleotides with ends corresponding to the 5′ restriction cleavage overhangs of *Bgl*II and *Mlu*I were annealed and ligated into *Bgl*II/*Mlu*I-digested pGL3-basic. Oligonucleotides (sense strand) were: p-36 (forward), 5′-cgcgCTCCCCCACCCAGCTCTCGTTTCCAATGCACGTACAGCCCGTACACACCG-3′; MUT1 (forward), 5′-cgcgCTCCCCCACCCAGCTCTCGTTTCCAATGCTTTTACAGCCCGTACACACCG-3′; MUT2 (forward), 5′-cgcgCTCCCCCACCCAGCTCTCGTTTCCAATGCAAGTACAGCCCGTACACACCG-3′. Nucleotides introduced for cloning are lowercase; mutations are underlined. All *CA9* promoter sequences were confirmed by dideoxy sequence analysis.

Transient Expression Assays. Cells at ~70% confluence in 60-mm dishes were transfected with 1 μg of a luciferase reporter construct and 0.4 μg of control plasmid, pCMV-βgal (Promega), using FuGENE 6 (Roche Diagnostic) according to the manufacturer's instructions. Cells were then incubated at 20% O_2 for 8 h, followed by 20% or 0.1% O_2 for 16 h.

Luciferase activity was determined in cell lysates using a commercial assay system (Promega) and a TD-20e luminometer (Turner Designs). βgal activity in cell lysates was measured using *o*-nitrophenyl-β-D-galactopyranoside as substrate in a 0.1 M phosphate buffer (pH 7.0) containing 10 mM KCl, 1 mM $MgSO_4$, and 30 mM β-mercaptoethanol. To correct for variable transfection efficiencies between experimental conditions, the luciferase:βgal ratio was determined for each sample. For cotransfection assays, cells also received 0.1–1 μg each of pCDNA3/HIF-1α or pCDNA3/HIF-2α containing the entire human HIF-1α or HIF-2α open reading frame, respectively. Transfections were balanced with various amounts of pCDNA3 (Invitrogen) and pCDNA3/HIF-α such that all cells received the same total quantity of DNA.

Cell Lysis and Immunoblotting. Whole-cell protein extracts were prepared from tissue culture cells by 10-s homogenization in denaturing conditions as described (31). Whole-cell protein extracts were prepared from tumors by fine section of frozen tissue and 30-s homogenization in denaturing conditions identical to tissue culture extracts. For Western analysis, aliquots were separated by SDS-PAGE and transferred to Immobilon-P membranes. CA IX was detected using the mouse monoclonal antihuman CA IX antibody M75 (1:50) as described (32). Horseradish peroxidase-conjugated goat-antimouse immunoglobulin (DAKO; 1:2000) was applied for 1 h at room temperature. ECL Plus (Amersham Pharmacia) was used for visualization.

Immunohistochemistry. Formalin-fixed, paraffin-embedded tissue specimens collected by standard surgical oncology procedures were obtained from the Pathology Department, John Radcliffe Hospital (Oxford, United Kingdom). Immunostaining of paraffin sections was performed after dewaxing and rehydrating 4-μm sections. For CA IX detection, endogenous peroxidase was blocked with 0.5% hydrogen peroxide in water for 30 min. To block, 10% normal human serum in TBS was applied for 15 min. M75 (see "Immunoblotting"; 1:50) was applied for 30 min at room temperature. Secondary polymer from Envision kit (DAKO) was applied for 30 min at room temperature. For pimonidazole detection, sections were digested with 0.01% Pronase (Sigma) in PBS for 30 min at 37°C. Endogenous peroxidase was blocked with 0.1% hydrogen peroxide in water for 30 min. To block, Protein Block (DAKO) was applied for 5 min. Anti-pimonidazole IgG1 antibody (Natural Pharmacia; 1:100) was applied for 1 h at room temperature. Biotinylated rabbit antimouse secondary (DAKO; 1:200) was applied for 1 h at room temperature. ABC complex horseradish peroxidase conjugate (DAKO) was applied for 1 h at room temperature. Visualization of CA IX and pimonidazole staining was by diaminobenzidine substrate. Slides were counterstained with hematoxylin before mounting in Aquamount (BDH). Substitution of primary antibody with PBS was used as a negative control for both antibodies.

CA IX and pimonidazole were studied in semiserial tissue sections. The percentage of tumor cells showing positive staining for CA IX or pimonidazole and the extent of overlap between these regions within each tissue section was assessed by light microscopy at low magnification by three observers (C. C. W., P. H. W., and H. T.) and a consensus was determined.

***In Situ* mRNA Hybridization.** Specific localization of VEGF mRNA was accomplished by *in situ* hybridization using an antisense riboprobe. Briefly, pBluescript (Stratagene) containing 517 consecutive complementary nucleotides of the $VEGF_{121}$ transcript (439 consecutive nucleotides of which are complementary to $VEGF_{165}$, $VEGF_{189}$, and $VEGF_{206}$) was linearized with *Eco*RV for 16 h at 37°C. Labeled transcripts were synthesized using T7 (antisense) and SP6 (sense) polymerase in the presence of [^{35}S]UTP (>800 Ci/mmol; Amersham Pharmacia). The methods for pretreatment, hybridization, washing, and dipping of slides in Ilford K5 for autoradiography were as described for formalin-fixed, paraffin-embedded tissue (33). The presence of hybridizable mRNA in tissue sections was established in semiserial sections using an antisense β-actin probe. Hybridizations using a sense probe were used to control for nonspecific signal. Autoradiography was at 4°C (two exposures per section for VEGF visualization at 10 and 18 days), before developing in Kodak D19 and counterstaining by Giemsa's method. Sections were examined under conventional and reflected light-/dark-field conditions.

Pimonidazole Administration. Patients with squamous or basal cell carcinomas of the skin and patients with newly diagnosed transitional cell bladder carcinoma were studied. Signed informed consent was obtained in all cases. Pimonidazole hydrochloride was selected as the hypoxia marker because of its high water solubility, chemical stability, efficient tumor uptake, and low toxicity. Patients received 500 mg/m^2 of pimonidazole hydrochloride, 1-[(2-hydroxy-3-piperidinyl)propyl]-2-nitroimidazole hydrochloride (Hypoxyprobe) in 100 ml of normal saline i.v. over 20 min. This dose is 25% of the maximum tolerated dose (34). Patients with tumors in skin underwent incisional or Trucut biopsy under local anesthetic 2–24 h after pimonidazole infusion. Patients with bladder carcinoma underwent transurethral resection of the tumor under general anesthetic 2–24 h after pimonidazole infusion. Tissue samples were immediately placed in 10% neutral buffered formalin, protected from light, and then processed into formalin blocks.

RESULTS

VHL-dependent Regulation of *CA9* and *CA12* mRNAs by Hypoxia. Expression of mRNAs encoding *CA9* and *CA12* was analyzed by RPA. To confirm the previous report of down-regulation by pVHL (29), we first examined expression in the VHL-defective RCC line RCC4 and a stable transfectant expressing a human VHL cDNA (RCC4/VHL). In normoxic cells, both mRNAs were down-regulated by pVHL. However, when cells were exposed in parallel to normoxia or hypoxia (0.1% oxygen), induction by hypoxia was observed in RCC4/VHL cells, whereas in RCC4 cells the high level of expression in normoxia was unchanged by hypoxia (Fig. 1*A*). We also examined expression in other RCC lines that are either defective (KRL140, SKRC28, UMRC2, and 786-0) or wild type (Caki-1) for VHL, and in a stable transfectant of 786-0 re-expressing wild-type pVHL (WT 8). Representative results from three cell lines are illustrated in Fig. 1*A*. In the VHL-defective cells, both *CA9* and *CA12* were constitutively expressed and unresponsive to changes in oxygen tension. In the

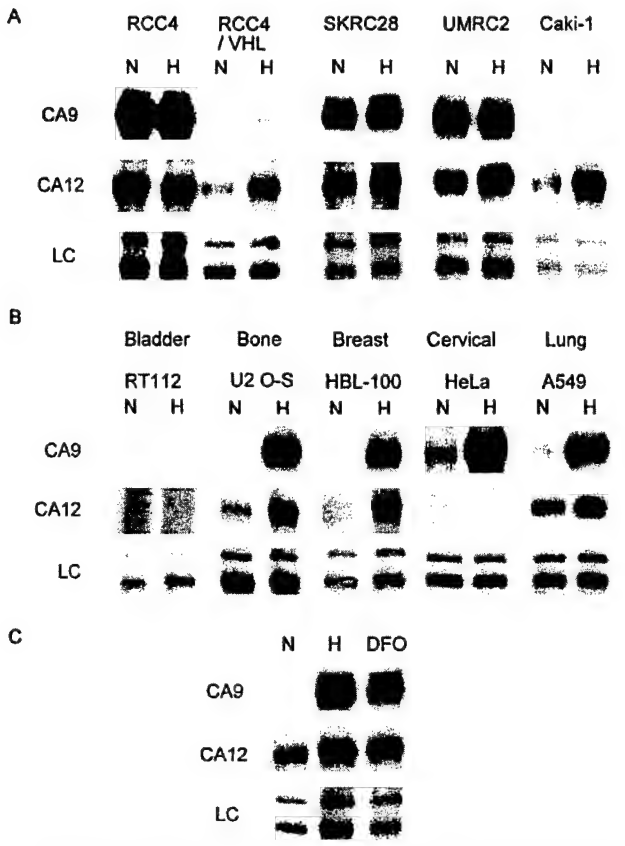

Fig. 1. Induction of *CA9* and *CA12* mRNA by hypoxia. Cells were exposed to either normoxia (*N*; 20% O_2) or hypoxia (*H*; 0.1% O_2) for 16 h. *CA9* and *CA12* mRNA was examined by RPA. *A*, induction by hypoxia in renal carcinoma-derived cell lines is VHL dependent. RCC4, SKRC28, and UMRC2 are VHL defective. RCC4/VHL is a pVHL stable transfectant of RCC4. Caki-1 is VHL competent. *B*, induction by hypoxia in nonrenal-derived cell lines from indicated tissue type. *C*, comparison of induction by hypoxia and DFO (each applied for 16 h) in A549 cells. *LC*, signal from internal control assay for the constitutively expressed U6 small nuclear RNA.

wild-type VHL cell lines, both genes, when expressed, were induced by hypoxia.

To examine regulation by hypoxia across a range of cell types, we performed RPAs for *CA9* and *CA12* on mRNA samples from normoxic and hypoxic cultures of 11 additional cell lines derived from five different tissue types: bladder (RT112 and EJ-28), bone (U2 *O*-S), breast (HBL-100, MDA-MB-435S, MDA-MB-468, MDA-MB-231, and T-47D), cervical (HeLa), and lung (A549 and NCI-H460). With the exception of bladder cell lines RT112 and EJ-28, every cell type expressed one or both CA isoforms, and in each case where expression was observed, it was induced by hypoxia. The amplitude of induction by hypoxia was particularly high for *CA9*; mRNA levels were at or below the limit of detection in normoxia, yet strikingly induced by hypoxia. Representative illustrations of one cell line from each tissue type are depicted in Fig. 1*B*. Because many hypoxia-inducible genes are up-regulated by treatment of cells with the iron chelator DFO (35), we also tested the effect of DFO and found a similar induction of both *CA9* and *CA12* mRNA (Fig. 1*C*).

***CA9* Promoter Analysis.** To investigate the unusually tight regulation of *CA9* mRNA by hypoxia, we tested for oxygen-dependent function of the *CA9* promoter. In the first set of experiments, we tested luciferase reporter genes containing ~0.5 kb of *CA9* 5′ flanking sequences (−506 to +43) and a deletion to nucleotide −173 (−173 to +43) in transiently transfected HeLa cells. Both constructs showed very low levels of activity in normoxic cells but were induced strongly by hypoxia (Fig. 2*A*). By contrast, a similar reporter linked to a minimal SV40 promoter showed no induction by hypoxia.

To test whether these responses were dependent on HIF-1, we performed further transfections using a CHO mutant cell (Ka13) that is functionally defective for the HIF-1α subunit and cannot form the HIF-1 transcriptional complex (36). In the CHO wild-type parental subline C4.5, the −173 nucleotide promoter conferred 17-fold transcriptional induction by hypoxia. In contrast, in the HIF-1α-deficient Ka13 subline, this hypoxic induction was absent (Fig. 2*B*). Cotransfection of human HIF-1α restored hypoxia-inducible activity to the *CA9* promoter in the Ka13 cells and increased normoxic activity in both C4.5 and Ka13 (Fig. 2*B*). In C4.5 and Ka13 cells at 0.1% O_2, luciferase expression was increased 1.6- and 17-fold, respectively, by cotransfection of human HIF-1α. Thus, hypoxia-inducible activity of the *CA9* promoter is completely dependent on HIF-1 and strongly influenced by the level of HIF-1α. Activity of the *CA9* promoter in Ka13 cells could also be restored by cotransfection of HIF-2α, although normoxic activity was higher and fold induction by hypoxic stimulation was reduced (data not shown).

Inspection of the *CA9* 5′ flanking sequences revealed a consensus HRE beginning 3 bp 5′ to the transcriptional start site, orientated on the antisense strand, reading 5′-TACGTGCA-3′ (Fig. 2, *left*). To test the importance of this site, we constructed a *CA9* minimal promoter containing this sequence (−36 to +14). This minimal promoter retained hypoxia-inducible activity in C4.5 cells but had no inducible activity in Ka13 cells (Fig. 2*C*). Absolute levels of activity were lower in comparison to the −173 nucleotide promoter construct, being reduced ~8 fold, indicating that although sequences −173 to −36 amplified promoter activity, responsiveness to hypoxia was conveyed by the minimal sequence containing the HRE. To confirm the importance of this HRE, two mutations were made within its core (antisense strand): a 3-bp substitution from CGT → AAA (MUT1), and a single substitution of G → T (MUT2; Fig. 2, *left*). Both mutations completely ablated hypoxia-inducible activity, although basal activity was preserved or slightly increased for MUT1 (Fig. 2*C*).

Regulation of CA IX Protein by Oxygen. As a first step toward understanding the significance of hypoxia-inducible expression of *CA9* mRNA, the effect of hypoxia was examined on CA IX protein levels in whole-cell extracts. Immunoblots of representative cells using anti-CA IX monoclonal antibody M75 are illustrated in Fig. 3*A*. Striking induction of CA IX protein by hypoxia was observed in multiple cell lines, whereas the VHL-defective RCC4 cells showed constitutive up-regulation of CA IX protein. Thus, hypoxic up-regulation of *CA9* mRNA is clearly reflected at the protein level. We next examined the response of CA IX to increasing degrees of hypoxia (Fig. 3*B*). The level of CA IX hypoxic induction after 16 h of exposure increased with decreasing oxygen tensions from 5 to 0.1%. Because the original description of CA IX was as an antigen induced by culture of cells at high density (37), we also compared the effects of culture at high density with those of hypoxia. In normoxic cultures of A549 cells, high density clearly induced CA IX, although the effect was considerably smaller than that of hypoxia (Fig. 3*C*).

CA IX Expression in Human Tumors. We next sought to determine whether regulation of *CA9* by hypoxia in tissue culture cells was reflected in patterns of expression within naturally occurring human tumors. To confirm the specificity of M75 immunostaining in our laboratory, we first compared immunohistochemical staining with CA IX immunoblot signals in pellets of cultured cells. Pellets were prepared from normoxic cultures of RCC4 and RCC4/VHL cells and processed in parallel for whole-cell protein extraction and immunohistochemistry. In keeping with the immunoblotting results, immunostaining of these sections with M75 revealed strong membrane expression of CA IX in RCC4 cells (Fig. 4*A*) and no staining in

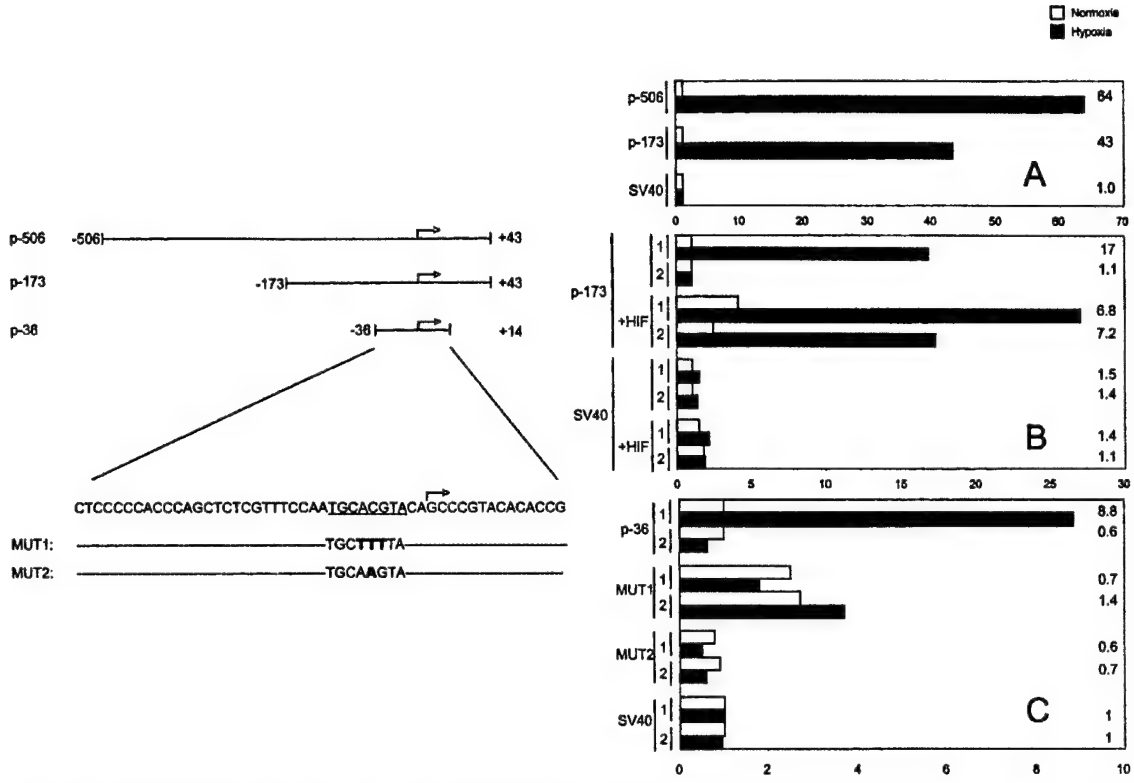

Fig. 2. Functional analysis of human *CA9* 5′-flanking sequences in transient expression assays. *Left panel*, schematic diagram of reporter genes; the indicated *CA9* wild-type and mutant sequences were inserted 5′ to a promoterless luciferase reporter gene. *Arrow*, 5′ transcriptional initiation site. *Underlined sequence*, *CA9* putative HRE. *Right panels*, reporter gene activities in transiently transfected cells. *CA9* promoter sequences are indicated to the *left* of each *column*. *SV40*, control minimal SV40 promoter. *A*, activities in normoxic and hypoxic HeLa cells. *B* and *C*, activities in wild-type CHO (C4.5) cells (*columns 1*) and HIF-1α-deficient CHO (Ka13) cells (*columns 2*). *A*, hypoxia-inducible activity of the *CA9* promoter. *B*, hypoxia-inducible activity of the *CA9* promoter is ablated in Ka13 cells. Cotransfection of HIF-1α restores induction by hypoxia in Ka13 cells and augments *CA9* promoter activity in both wild-type and Ka13 cells. In comparison, minimal effects are seen on the SV40 promoter. *C*, a minimal *CA9* promoter retains HIF-1α-dependent, hypoxia-inducible activity. Two mutations within the putative HRE, MUT1 and MUT2, completely ablate hypoxia-inducible activity, whereas basal transcription is preserved. *Columns*, mean luciferase activities corrected for transfection efficiency from a typical experiment performed in duplicate. Each duplicate experiment was repeated two to six times. Numbers to the *right* are the ratios of hypoxic to normoxic expression of the indicated reporter construct. Transfected cells were incubated at 20% O_2 for 8 h and then incubated at 20% O_2 (normoxia) or 0.1% O_2 (hypoxia) for 16 h.

normoxic RCC4/VHL cells (Fig. 4*B*). Then, we compared immunostaining and immunoblots of tissue extracts from similar regions of tumor and normal tissue in four sets of paired samples from surgical excisions of head and neck tumors. By immunostaining, CA IX expression was low or absent in normal tissue surrounding the tumors but was expressed at significant levels in each tumor specimen. Results of immunoblot analysis correlated closely with immunostaining, signals being very low or undetectable in each normal tissue sample, and correlated with the extent of CA IX immunostaining in tumor samples (data not shown).

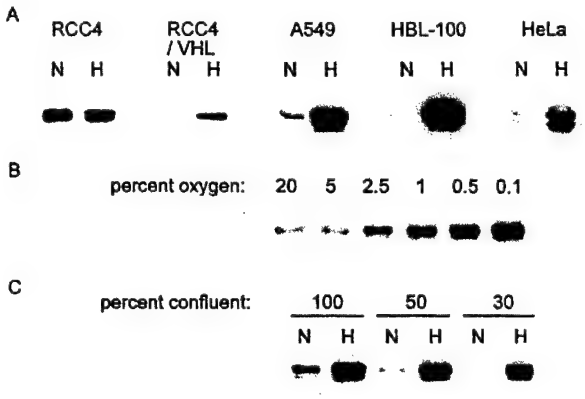

Fig. 3. Regulation of CA IX protein by hypoxia and cell density. Western blots of whole-cell extracts using anti-CA IX monoclonal antibody M75 are shown. *A*, cells exposed to either normoxia (*N*; 20% O_2) or hypoxia (*H*; 0.1%O_2) for 16 h. Expression is constitutive in the VHL-defective cell line, RCC4, but inducible by hypoxia in RCC4/VHL transfectants and a range of nonrenal cell lines. *B*, effects of graded hypoxia; A549 cells, 16 h exposure to the indicated oxygen concentration. *C*, comparison of induction by increasing cell density and hypoxia; A549 cells, 16 h exposure to hypoxia.

Of particular interest to regulation by hypoxia is the relationship of CA IX expression to zones of tumor necrosis. This was first examined in a series of nine tumors of head and neck, breast, and ovary, each of which showed well-defined zones of necrosis. Three tumors of each type were analyzed. In each specimen, a predominantly or even exclusively perinecrotic expression pattern was observed for CA IX. Representative sections from each tumor type are illustrated in Fig. 4. Expression was localized to the cellular membrane. Tracing a line from the necrotic center to adjacent viable cells revealed a gradient of CA IX expression, with the highest levels observed in cells closest to or within necrotic regions (Fig. 4, *C–F*).

Because pVHL inactivation leads to loss of *CA9* regulation by oxygen in cultured cells and is common in clear cell renal carcinoma but not other renal tumors, we next compared expression patterns in a second series of 35 clear cell renal tumors and eight papillary renal tumors. Representative sections from a clear cell and a papillary tumor are illustrated in Fig. 4, *G* and *H*. Expression patterns were markedly different. In 33 of 35 clear cell tumors, (both sporadic and derived from VHL syndrome patients), CA IX was expressed throughout

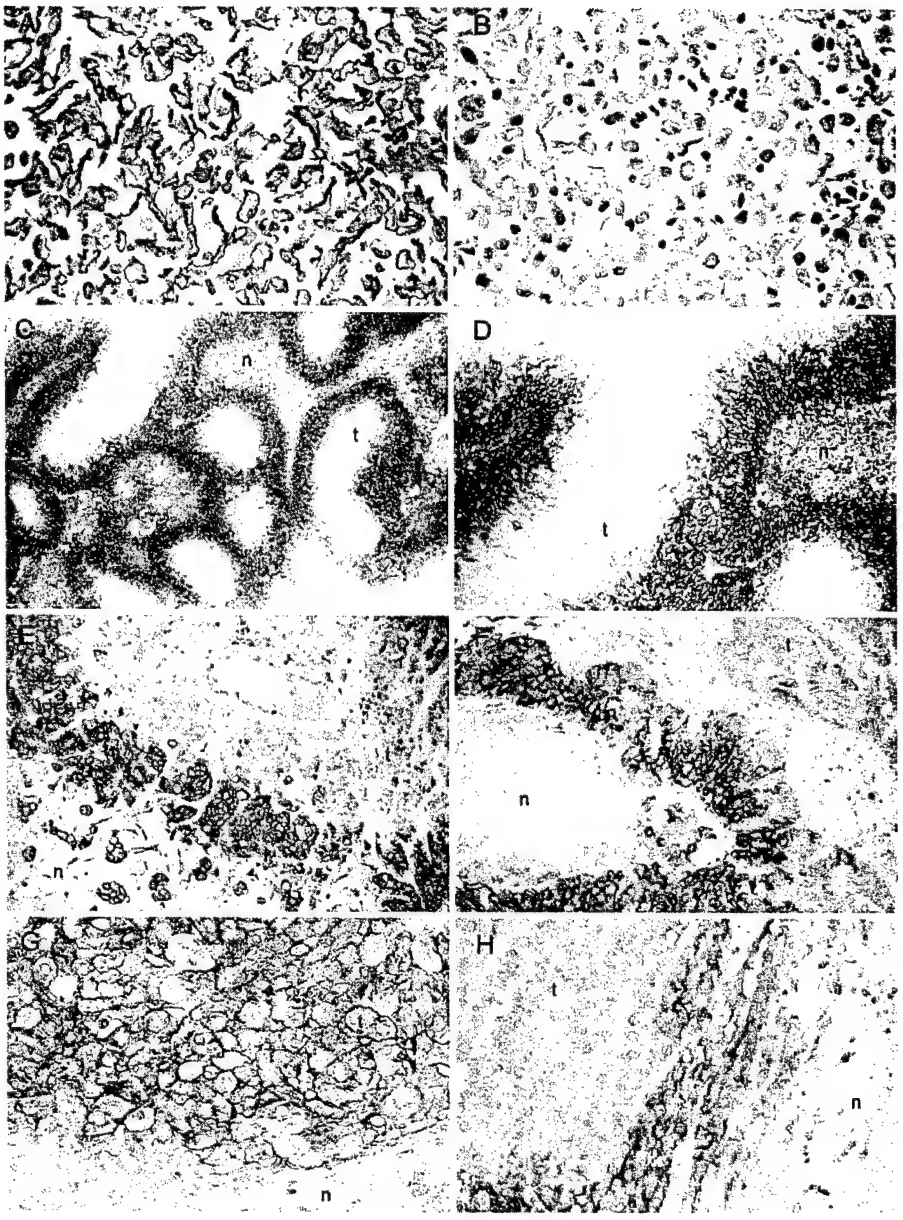

Fig. 4. Immunohistochemical analysis of CA IX expression in cell pellets and tumor biopsies. Sections were stained with anti-CA IX monoclonal antibody M75. *A* and *B*, paraffin-embedded cell pellets of normoxic RCC4 and RCC4/VHL respectively. Tumor sections showing the relationship of CA IX expression to regions of necrosis: *C* and *D*, head and neck carcinoma; *E*, breast adenocarcinoma; *F*, ovarian adenocarcinoma; *G*, clear cell renal carcinoma from a VHL syndrome patient; *H*, papillary renal carcinoma. Staining is predominantly membranous. A focal perinecrotic pattern is observed in all tumors except clear cell renal carcinomas. *n*, regions of necrosis; *t*, regions of viable tumor cells. *A*, *B*, and *D–H*, ×200; C, ×100.

tumor tissue; strong membrane staining was observed in tumor cells, regardless of proximity to necrosis or vessels (*G*). In contrast, in papillary renal tumors CA IX immunostaining was much less evident but was observed in tumors containing areas of necrosis, where, as with the nonrenal tumors, staining was strikingly focal and perinecrotic (four of eight papillary tumors contained necrosis, and all four showed focal CA IX positivity; Fig. 4*H*). Thus, the tight regulation of *CA9* expression by oxygen observed in cell culture appeared to be reflected in strikingly focal patterns of expression around areas of necrosis.

Relationship of CA IX Expression with an Endogenous and an Administered Hypoxia Marker in Human Tumors. To compare CA IX expression with potential markers of tumor hypoxia, we examined expression of VEGF mRNA and activation of the bioreductive hypoxia marker pimonidazole in relationship to CA IX staining. Serial sections of a subset of our first series of tumors were analyzed for VEGF mRNA expression by *in situ* hybridization, and CA IX expression was analyzed by immunostaining. Representative views from an ovarian and head and neck tumor sample are illustrated in Fig. 5. VEGF mRNA was expressed at varying levels throughout tumor tissue but was increased greatly in regions adjacent to necrosis. CA IX immunostaining showed strong overlap but was more tightly limited to perinecrotic regions.

For comparison of pimonidazole staining with CA IX expression, a series of 14 transitional cell bladder carcinomas and 6 squamous or basal cell skin carcinomas derived from patients who had received pimonidazole prior to surgical excision of tumor tissue was analyzed. Representative views of pimonidazole- and CA IX-stained sections are illustrated in Fig. 6, and assessment of pimonidazole and CA IX staining with corresponding overlap for each tumor biopsy are indicated in Table 1. In most tumors (16 of 20), pimonidazole staining was more extensive across tumor sections than CA IX staining, being primarily banded around necrotic areas (Fig. 6, *C* and *E*) and the periphery of papillary structures in bladder carcinomas (Fig. 6*A*).

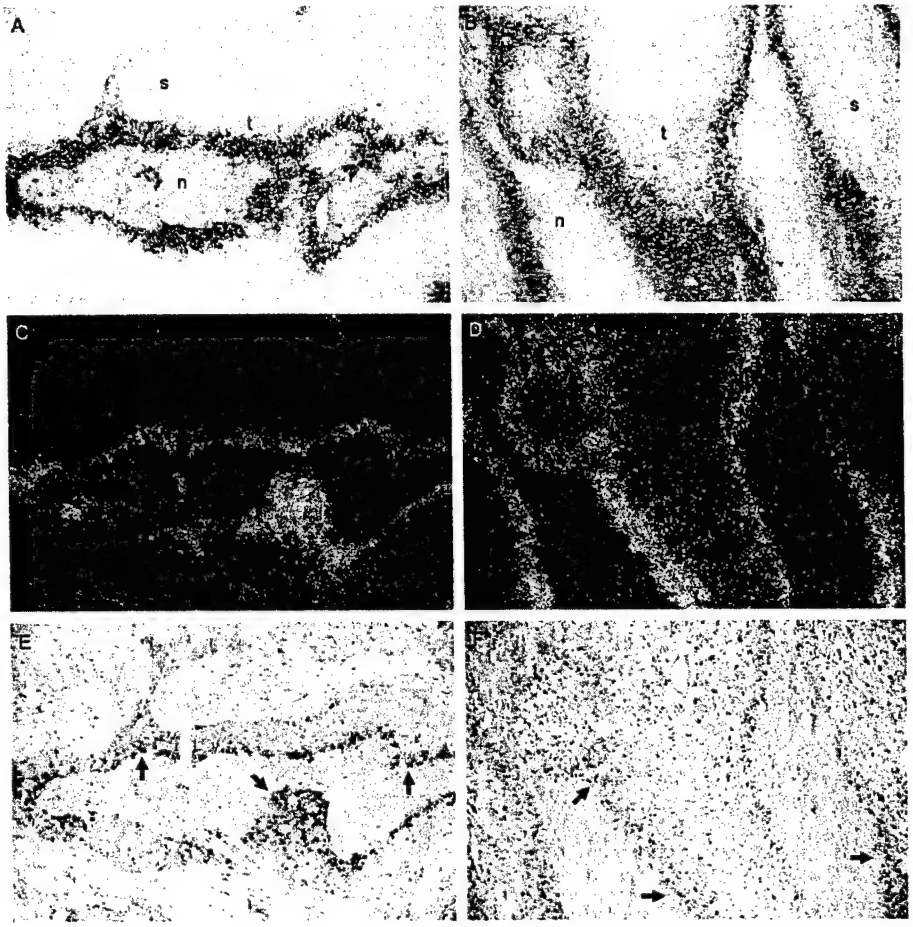

Fig. 5. Comparison of expression patterns for CA IX and VEGF in tumor biopsies. Immunohistochemical detection of CA IX using anti-CA IX monoclonal antibody M75 and *in situ* mRNA analysis of VEGF is shown. *A*, *C*, and *E*, ovarian adenocarcinoma. *B*, *D*, and *F*, head and neck carcinoma. *A* and *B*, CA IX immunostaining. *C* and *D*, dark-field views of *in situ* hybridization for VEGF mRNA on sections serial to the CA IX-immunostained sections. *E* and *F*, bright-field views of VEGF *in situ*. *Arrows* within necrotic areas (*n*) in bright-field views point toward the boundary with viable tumor cells. *s*, stroma; *t*, regions of viable tumor cells. *All panels*, ×100.

Although less extensive, the large majority of CA IX immunostaining localized within regions of pimonidazole adduct formation and was also associated with necrosis (Fig. 6, *D* and *F*) or the periphery of papillary structures in bladder carcinomas (Fig. 6*B*). Some regions containing CA IX were observed that were slightly farther removed from necrosis than regions staining positive for pimonidazole (Fig. 6, *C* and *D*). In 4 of 20 cases, CA IX staining was more extensive than pimonidazole staining. In these cases, in addition to the characteristic perinecrotic and peripheral papillary expression, a proportion of CA IX expression was not obviously associated with such regions in the plane of the section. Nevertheless, within these four tumors the pimonidazole-positive regions were consistently localized within regions of CA IX positivity, again demonstrating the overlap between these markers. Despite the relationship between pimonidazole and CA IX at the microscopic level in all tumors, we did not observe an overall correlation between the percentage of tumor stained for pimonidazole and CA IX (Table 1).

DISCUSSION

In this work, we have demonstrated that the tumor-associated CAs *CA9* and *CA12* are strongly inducible by hypoxia in a broad range of tumor cells. Our findings also explain up-regulation of these CA isoforms in VHL-defective renal tumors, indicating that they are expressed constitutively at a high level in VHL-defective cells as a consequence of constitutive activation of HIF. The work therefore extends the range of HIF target genes to a new class of molecule that may have important implications for understanding the consequences of microenvironmental tumor hypoxia, as well as the tumor-promoting effects of VHL inactivation. The regulation of *CA9* was particularly tightly controlled by oxygen, and we analyzed the hypoxia-inducible response of this gene in detail.

Studies of the *CA9* promoter demonstrated that sequences close to the transcriptional initiation site were sufficient to convey a hypoxia-inducible response, that this activity was mediated by HIF, and that it was dependent on a consensus HRE lying adjacent to the initiation site. The *CA9* promoter contains neither a TATA box nor a consensus initiator sequence at the cap site (38). The association of this unusual anatomy with tight regulation by hypoxia is therefore of interest and suggests that it may be informative to pursue the mechanism by which HIF interacts with the basal transcriptional machinery operating on this gene. Furthermore, irrespective of the mechanism, the strong inducibility conveyed by the minimal *CA9* promoter is unusual and may itself be of utility, for instance in the refinement of gene therapy vectors seeking to target therapeutic gene expression to hypoxic regions of tumors (39, 40).

Our findings also raise a number of issues relevant to recently published analyses of the *CA9* promoter that did not examine the effect of hypoxia: (*a*) they provide an explanation for the remarkably low levels of *CA9* promoter activity recently reported under standard culture conditions (41), because promoter activity is so strongly dependent on hypoxia; (*b*) they are consistent with the positive activity demonstrated for sequences −173 to +31 (41) and show that the transcriptional effects mediated by these sequences interact with the HRE in the minimal promoter to amplify the response to hypoxia; (*c*)

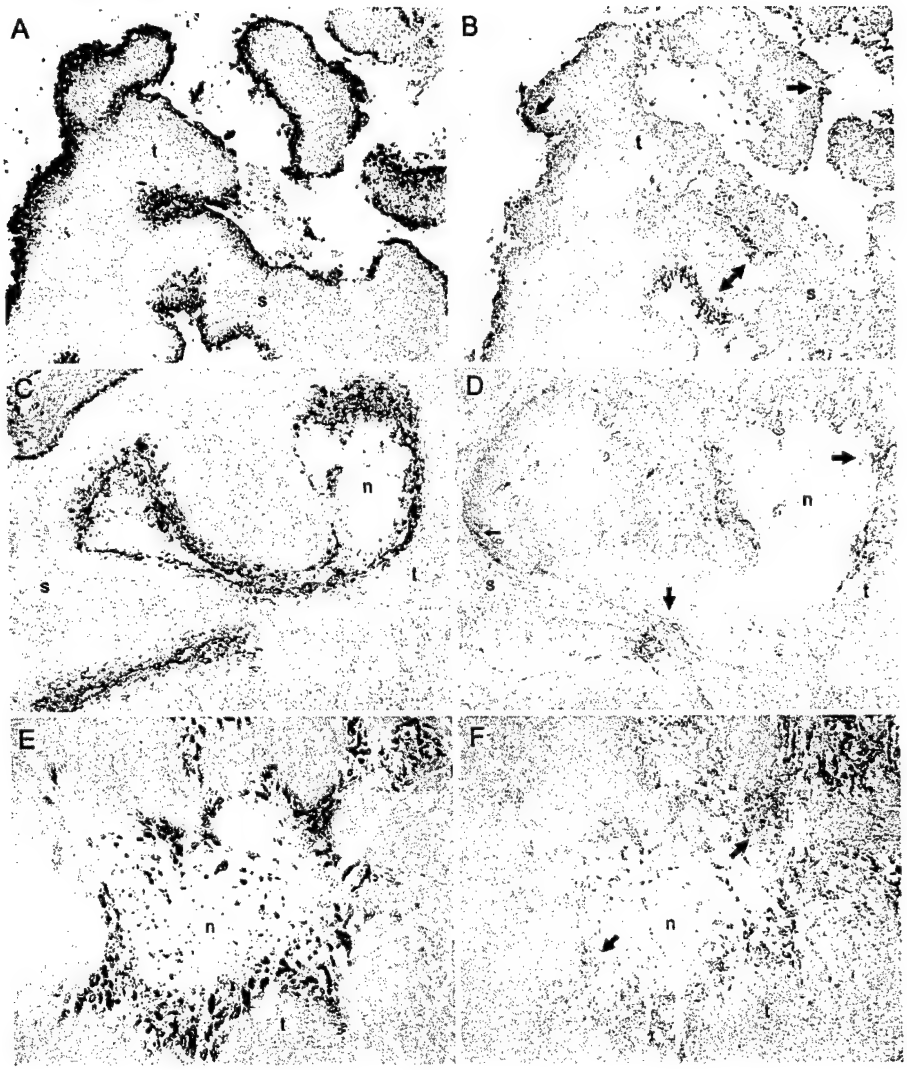

Fig. 6. Comparison of patterns of CA IX expression and pimonidazole adduct formation. *A–D*, bladder carcinomas; *E* and *F*, skin carcinoma. *Left-hand panels*, pimonidazole immunostaining. *Right-hand panels*, CA IX immunostaining on semiserial sections. *Large arrows* within CA IX-stained sections point toward regions of CA IX positivity that overlap with pimonidazole staining. *Small arrow* (*D*) highlights region of CA IX positivity farther removed from necrosis than pimonidazole-stained region. *n*, regions of necrosis; *s*, stroma; *t*, regions of viable tumor cells. *All panels*, ×50.

they are consistent with the absence of a DNase I footprint in the region of the HRE (41), because even in hypoxia it has been shown that HIF-1 binding characteristics are such that an *in vitro* footprint is not demonstrated (42); (*d*) they provide a potential explanation for the repressive effects of p53 expression on the activity of the *CA9* promoter in some cells (43), because it has been suggested that p53 can interact with the regulation of HIF-1α stability so as to reduce activity of the HIF/HRE complex (15, 16).

In tissue culture, *CA9* demonstrated a very marked difference between constitutive expression in VHL-defective RCC cells and strong induction by hypoxia in cells known or presumed to be VHL competent. This provided an opportunity to determine the extent to which these contrasting patterns of regulation in culture were reflected in patterns of expression within native tumors. In our series of renal tumors, we found a striking contrast between generalized expression in clear cell carcinomas, which are usually defective in VHL, and focal perinecrotic expression in papillary renal tumors, which are usually wild type for VHL. Notwithstanding the absence of direct ascertainment of VHL genotype in all of the tumors analyzed, this strongly suggests that effects of VHL status on HIF-dependent, hypoxia-inducible gene expression are reflected in patterns of expression within native tumors. Up-regulation by constitutively active HIF therefore provides an explanation for the utility of *CA9* as a marker for clear cell carcinoma. The pattern of diffuse expression in clear cell carcinoma is in agreement with findings of a previous analysis of CA IX expression in which the authors focused on high levels of expression in clear cell carcinoma *versus* absent expression in a variety of benign lesions and postulated that CA IX expression might be useful as a marker of malignant change (25). That study also noted focal expression in papillary renal carcinoma, although the authors did not comment on the relation to necrosis. In our studies, we found that the striking localization of focal CA IX expression to zones of necrosis is not just observed in papillary renal carcinoma but also in several series of nonrenal tumors. The pattern is similar to that first described for VEGF mRNA (5), and we compared directly the pattern of CA IX immunostaining with that of *in situ* mRNA hybridization for VEGF in several types of tumors. In this work, we used *in situ* mRNA hybridization for VEGF to localize the site of production, because, in contrast with CA IX, some isoforms of VEGF are secreted. Patterns of expression for CA IX and VEGF mRNA were clearly concordant. However, CA IX expression was more strikingly delimited, being essentially limited to regions surrounding zones of necrosis.

The concordance of hypoxia-inducible *versus* constitutive patterns of expression in tissue culture with focal perinecrotic *versus* diffuse patterns of expression in tumors strongly supports the view that the focal perinecrotic pattern of expression is driven by microenviron-

Table 1 *CA IX expression and pimonidazole activation in bladder and skin carcinomas*

Tumor type	CA IX[a]	pim[a]	Overlap[b]
Bladder	25	25	+
Bladder	25	25	+
Bladder	50	30	+ (++)
Bladder	5	50	++
Bladder	5	25	++
Bladder	5	25	++
Bladder	5	25	++
Bladder	5	25	++
Bladder	5	25	++
Bladder	5	20	++
Bladder	10	15	++
Bladder	0	25	NA
Bladder	0	5	NA
Bladder	10	0	NA
Skin	10	2	− (++)
Skin	50	15	− (++)
Skin	50	25	+ (++)
Skin	20	50	++
Skin	0	5	NA
Skin	0	0	NA

[a] Semiquantitative estimate of the percentage of tumor cells within the entire tumor section staining positive for either CA IX or pim (pimonidazole).

[b] Semiquantitative estimate of the percentage of tumor staining positive for CA IX that also stained positive for pimonidazole. Numbers in parentheses, semiquantitative estimate of the percentage of tumor staining positive for pimonidazole that also stained positive for CA IX in the four tumors in which CA IX staining was more extensive than pimonidazole staining. ++, 90–100%; +, 50–90%; −, <50%; NA, not applicable (no staining for one or both antigens).

mental hypoxia. Furthermore, the particularly tight regulation of *CA9* by hypoxia suggested that it might be useful as a hypoxia marker. It was, therefore, of interest to compare the pattern of CA IX immunostaining with staining for the hypoxia marker pimonidazole (44–46). Our analysis demonstrated clear overlap of the staining patterns, supporting expression of CA IX in hypoxic regions. Previous studies have compared the distribution of immunodetectable pimonidazole adducts with VEGF immunostaining. One study concluded that pimonidazole and VEGF displayed the same pattern of staining on adjacent sections during the angiogenesis associated with a model of liver fibrogenesis (47), whereas an earlier study emphasized the discrepancies between pimonidazole and VEGF staining, although regions of overlap were demonstrated (48). Among the explanations considered for the differences between the distribution of VEGF staining and pimonidazole adducts were regulation of VEGF by nonhypoxic stimuli and diffusion of VEGF from hypoxic sites of production. For *CA9*, basal expression in normoxic cells was lower than we have observed for VEGF, induction by hypoxia was more striking, and the protein was not secreted. Despite this, we also observed differences in pimonidazole and CA IX staining. The substantial regions of overlap presumably reflect regions where tumor hypoxia was of sufficient duration and severity to activate both markers. Regions of nonoverlap could reflect the operation of additional positive or negative influences on expression or activation or different time frames of induction or activation. For instance, pimonidazole adducts are formed over a relatively short period of time and are then long-lived (45, 46), whereas we have found that CA IX is a stable protein that, in tissue culture, accumulated over a long period of hypoxia (data not shown). Thus, CA IX induction might only be expected in regions of relatively chronic tumor hypoxia and would reflect a different hypoxic time frame from pimonidazole activation. Correlation of focal CA IX expression with direct measurements of tumor oxygenation and with clinical parameters of outcome will be of interest.

The demonstration that an extracellular CA is up-regulated by microenvironmental tumor hypoxia has potentially important implications for understanding the regulation of tumor pH and the response to hypoxia. It has been widely held that lactate production by glycolysis is a major cause of the acidic extracellular pH of tumors (49), and indeed glycolytic enzymes are induced by hypoxia (11), as is lactate production (50). However, tumors grown from mutant cells with glycolytic defects show a similar extracellular acidosis in the absence of lactate accumulation (51, 52), indicating that other mechanisms must be involved. Recently, it has been proposed that extracellular CAs could convert CO_2 diffusing from oxygenated areas to carbonic acid and promote the generation of bicarbonate and hydrogen ions (29, 52). Bicarbonate might then be exchanged for intracellular chloride, providing a mechanism for maintaining the characteristic extracellular acidosis and intracellular alkalosis that is postulated to promote tumor growth (53). Thus, it is likely that the hypoxia-inducible behavior of tumor-associated CAs could exert important biological effects through an influence on microenvironmental pH. This could have therapeutic implications because CA inhibitors have been shown to inhibit the invasion of renal cell carcinoma lines in model culture systems (54) and have synergistic effects with other chemotherapeutic agents in animal models (55). The potential for strong induction by hypoxia will now need to be considered in assessing the diagnostic and therapeutic implications of tumor-associated extracellular CAs.

ACKNOWLEDGMENTS

We thank Richard Poulsom, Rosemary Jeffery, and Jan Longcroft (Imperial Cancer Research Fund, Lincoln's Inn Fields, London, United Kingdom) for assistance with the *in situ* hybridization studies.

REFERENCES

1. Höckel, M., Schlenger, K., Aral, B., Mitze, M., Schaffer, U., and Vaupel, P. Association between tumor hypoxia and malignant progression in advanced cancer of the uterine cervix. Cancer Res., *56:* 4509–4515, 1996.
2. Brizel, D. M., Scully, S. P., Harrelson, J. M., Layfield, L. J., Bean, J. M., Prosnitz, L. R., and Dewhirst, M. W. Tumor oxygenation predicts for the likelihood of distant metastases in human soft tissue sarcoma. Cancer Res., *56:* 941–943, 1996.
3. Heacock, C. S., and Sutherland, R. M. Induction characteristics of oxygen regulated proteins. Int. J. Radiat. Oncol. Biol. Phys., *12:* 1287–1290, 1986.
4. Price, B. D., and Calderwood, S. K. Gadd45 and Gadd153 messenger RNA levels are increased during hypoxia and after exposure of cells to agents which elevate the levels of the glucose-regulated proteins. Cancer Res., *52:* 3814–3817, 1992.
5. Shweiki, D., Itin, A., Soffer, D., and Keshet, E. Vascular endothelial growth factor induced by hypoxia may mediate hypoxia-initiated angiogenesis. Nature (Lond.), *359:* 843–845, 1992.
6. Koong, A. C., Denko, N. C., Hudson, K. M., Schindler, C., Swiersz, L., Koch, C., Evans, S., Ibrahim, H., Le, Q. T., Terris, D. J., and Giaccia, A. J. Candidate genes for the hypoxic tumor phenotype. Cancer Res., *60:* 883–887, 2000.
7. Maxwell, P. H., Dachs, G. U., Gleadle, J. M., Nicholls, L. G., Harris, A. L., Stratford, I. J., Hankinson, O., Pugh, C. W., and Ratcliffe, P. J. Hypoxia inducible factor-1 modulates gene expression in solid tumors and influences both angiogenesis and tumor growth. Proc. Natl. Acad. Sci. USA, *94:* 8104–8109, 1997.
8. Carmeliet, P., Dor, Y., Herbert, J. M., Fukumura, D., Brusselmans, K., Dewerchin, M., Neeman, M., Bono, F., Abramovitch, R., Maxwell, P., Koch, C. J., Ratcliffe, P., Moons, L., Jain, R. K., Collen, D., and Keshet, E. Role of HIF-1α in hypoxia-mediated apoptosis, cell proliferation and tumour angiogenesis. Nature (Lond.), *394:* 485–490, 1998.
9. Ryan, H. E., Lo, J., and Johnson, R. S. HIF-1α is required for solid tumor formation and embryonic vascularization. EMBO J., *17:* 3005–3015, 1998.
10. Ebert, B. L., Firth, J. D., and Ratcliffe, P. J. Hypoxia and mitochondrial inhibitors regulate expression of glucose transporter-1 via distinct *cis*-acting sequences. J. Biol. Chem., *270:* 29083–29089, 1995.
11. Semenza, G. L., Roth, P. H., Fang, H-M., and Wang, G. L. Transcriptional regulation of genes encoding glycolytic enzymes by hypoxia-inducible factor 1. J. Biol. Chem., *269:* 23757–23763, 1994.
12. Kim, K. J., Li, B., Winer, J., Armanini, M., Gillett, N., Phillips, H. S., and Ferrara, N. Inhibition of vascular endothelial growth factor-induced angiogenesis suppresses tumour growth *in vivo*. Nature (Lond.), *362:* 841–844, 1993.
13. Maxwell, P., Wiesener, M., Chang, G-W., Clifford, S., Vaux, E., Cockman, M., Wykoff, C., Pugh, C., Maher, E., and Ratcliffe, P. The tumour suppressor protein VHL targets hypoxia-inducible factors for oxygen-dependent proteolysis. Nature (Lond.), *399:* 271–275, 1999.
14. Jiang, B. H., Agani, F., Passaniti, A., and Semenza, G. L. V-SRC induces expression of hypoxia-inducible factor 1 (HIF-1) and transcription of genes encoding vascular endothelial growth factor and enolase 1: involvement of HIF-1 in tumor progression. Cancer Res., *57:* 5328–5335, 1997.
15. Blagosklonny, M. V., An, W. G., Romanova, L. Y., Trepel, J., Fojo, T., and Neckers, L. p53 inhibits hypoxia-inducible factor-stimulated transcription. J. Biol. Chem., *273:* 11995–11998, 1998.

16. Ravi, R., Mookerjee, B., Bhujwalla, Z. M., Sutter, C. H., Artemov, D., Zeng, Q., Dillehay, L. E., Madan, A., Semenza, G. L., and Bedi, A. Regulation of tumor angiogenesis by p53-induced degradation of hypoxia-inducible factor 1α. Genes Dev., *14:* 34–44, 2000.
17. Zundel, W., Schindler, C., Haas-Kogan, D., Koong, A., Kaper, F., Chen, E., Gottschalk, A., Ryan, H., Johnson, R., Jefferson, A., Stokoe, D., and Giaccia, A. Loss of *PTEN* facilitates HIF-1-mediated gene expression. Genes Dev., *14:* 391–396, 2000.
18. Gnarra, J. R., Tory, K., Weng, Y., Schmidt, L., Wei, M. H., Li, H., Latif, F., Liu, S., Chen, F., Duh, F-M., Lubensky, I., Duan, D. R., Florence, C., Pozzatti, R., Walther, M. M., Bander, N. H., Grossman, H. B., Brauch, H., Pomer, S., Brooks, J. D., Isaacs, W. B., Lerman, M. I., Zbar, B., and Linehan, W. M. Mutations of the *VHL* tumour suppressor gene in renal carcinoma. Nat. Genet., *7:* 85–90, 1994.
19. Lisztwan, J., Imbert, G., Wirbelauer, C., Gstaiger, M., and Krek, W. The von Hippel-Lindau tumor suppressor protein is a component of an E3 ubiquitin-protein ligase activity. Genes Dev., *13:* 1822–1833, 1999.
20. Iwai, K., Yamanaka, K., Kamura, T., Minato, N., Conaway, R. C., Conaway, J. W., Klausner, R. D., and Pause, A. Identification of the von Hippel-Lindau tumor-suppressor protein as part of an active E3 ubiquitin ligase complex. Proc. Natl. Acad. Sci. USA, *96:* 12436–12441, 1999.
21. Cockman, M. E., Masson, N., Mole, D. R., Jaakkola, P., Chang, G. W., Clifford, S. C., Maher, E. R., Pugh, C. W., Ratcliffe, P. J., and Maxwell, P. H. Hypoxia inducible factor-α binding and ubiquitination by the von Hippel-Lindau tumor suppressor protein. J. Biol. Chem., *275:* 25733–25741, 2000.
22. Pause, A., Lee, S., Lonergan, K. M., and Klausner, R. D. The von Hippel-Lindau tumor suppressor gene is required for cell cycle exit on serum withdrawal. Proc. Natl. Acad. Sci. USA, *95:* 993–998, 1998.
23. Ohh, M., Yauch, R. L., Lonergan, K. M., Whaley, J. M., Stemmer-Rachamimov, A. O., Louis, D. N., Gavin, B. J., Kley, N., Kaelin, W. G., Jr., and Iliopoulos, O. The von Hippel-Lindau tumor suppressor protein is required for proper assembly of an extracellular fibronectin matrix. Mol. Cell, *1:* 959–968, 1998.
24. Pastorek, J., Pastorekova, S., Callebaut, I., Mornon, J., Zelnik, V., Opavsky, R., Zatovicova, M., Liao, S., Portetelle, D., Stanbridge, E., Zavada, J., Burny, A., and Kettmann, R. Cloning and characterization of MN, a human tumor-associated protein with a domain homologous to carbonic anhydrase and a putative helix-loop-helix DNA binding segment. Oncogene, *9:* 2877–2888, 1994.
25. Liao, S-Y., Aurelio, O., Jan, K., Zavada, J., and Stanbridge, E. Identification of the MN/CA9 protein as a reliable diagnostic biomarker of clear cell carcinoma of the kidney. Cancer Res., *57:* 2827–2831, 1997.
26. Saarnio, J., S, P., Parkkila, A-K., Haukipuro, K., Pastorekova, S., Pastorek, J., Kairaluoma, M., and Karttunen, T. Immunohistochemical study of colorectal tumors for expression of a novel transmembrane carbonic anhydrase, MN/CA IX, with potential value as a marker of cell proliferation. Am. J. Pathol., *153:* 279–285, 1998.
27. Vermylen, P., Roufosse, C., Burny, A., Verhest, A., Bosschaerts, T., Pastorekova, S., Ninane, V., and Sculier, J. P. Carbonic anhydrase IX antigen differentiates between preneoplastic malignant lesions in non-small cell lung carcinoma. Eur. Respir. J., *14:* 806–811, 1999.
28. Tureci, O., Sahin, U., Vollmar, E., Siemer, S., Gottert, E., Seitz, G., Parkkila, A. K., Shah, G. N., Grubb, J. H., Pfreundschuh, M., and Sly, W. S. Human carbonic anhydrase XII: cDNA cloning, expression, and chromosomal localization of a carbonic anhydrase gene that is overexpressed in some renal cell cancers. Proc. Natl. Acad. Sci. USA, *95:* 7608–7613, 1998.
29. Ivanov, S. V., Kuzmin, I., Wei, M-H., Pack, S., Geil, L., Johnson, B. E., Stanbridge, E. J., and Lerman, M. I. Down-regulation of transmembrane carbonic anhydrases in renal cell carcinoma cell lines by wild-type von Hippel-Lindau transgenes. Proc. Natl. Acad. Sci. USA, *95:* 12596–12601, 1998.
30. Sly, W. S., and Hu, P. Y. Human carbonic anhydrases and carbonic anhydrase deficiencies. Annu. Rev. Biochem., *64:* 375–401, 1995.
31. Wiesener, M. S., Turley, H., Allen, W. E., William, C., Eckardt, K-U., Talks, K. L., Wood, S. M., Gatter, K. C., Harris, A. L., Pugh, C. W., Ratcliffe, P. J., and Maxwell, P. H. Induction of endothelial PAS domain protein-1 by hypoxia: characterization and comparison with hypoxia-inducible factor-1α. Blood, *92:* 2260–2268, 1998.
32. Pastorekova, S., Zavadova, Z., Kostal, M., Babusikova, O., and Zavada, J. A novel quasi-viral agent, Ma Tu, is a two-component system. Virology, *187:* 620–626, 1992.
33. Senior, P. V., Critchley, D. R., Beck, F., Walker, R. A., and Varley, J. M. The localization of laminin mRNA and protein in the postimplantation embryo and placenta of the mouse: an *in situ* hybridization and immunocytochemical study. Development (Camb.), *104:* 431–446, 1988.
34. Kennedy, A. S., Raleigh, J. A., Perez, G. M., Calkins, D. P., Thrall, D. E., Novotny, D. B., and Varia, M. A. Proliferation and hypoxia in human squamous cell carcinoma of the cervix: first report of combined immunohistochemical assays. Int. J. Radiat. Oncol. Biol. Phys., *37:* 897–905, 1997.
35. Wang, G. L., and Semenza, G. L. Desferrioxamine induces erythropoietin gene expression and hypoxia-inducible factor 1 DNA-binding activity: implications for models of hypoxia signal transduction. Blood, *82:* 3610–3615, 1993.
36. Wood, S. M., Wiesener, M. S., Yeates, K. M., Okada, N., Pugh, C. W., Maxwell, P. H., and Ratcliffe, P. J. Selection and analysis of a mutant cell line defective in the hypoxia-inducible factor-1α subunit (HIF-1α). J. Biol. Chem., *273:* 8360–8368, 1998.
37. Zavada, J., Zavadova, Z., Pastorekova, S., Ciampor, F., Pastorek, J., and Zelnik, V. Expression of MaTu-MN protein in human tumor cultures and in clinical specimens. Int. J. Cancer, *54:* 268–274, 1993.
38. Opavsky, R., Pastoreková, S., Zelník, V., Gibadulinová, A., Stanbridge, E. J., Závada, J., Kettmann, R., and Pastorek, J. Human *MN/CA9* gene, a novel member of the carbonic anhydrase family: structure and exon to protein domain relationships. Genomics, *33:* 480–487, 1996.
39. Dachs, G. U., Patterson, A. V., Firth, J. D., Ratcliffe, P. J., Townsend, K. M. S., Stratford, I. J., and Harris, A. L. Targeting gene expression to hypoxic tumour cells. Nat. Med., *3:* 515–520, 1997.
40. Griffiths, L., Binley, K., Iqball, S., Kan, O., Maxwell, P., Ratcliffe, P., Lewis, C., Harris, A., Kingsman, S., and Naylor, S. The macrophage–a novel system to deliver gene therapy to pathological hypoxia. Gene Ther., *7:* 255–262, 2000.
41. Kaluz, S., Kaluzova, M., Opavsky, R., Pastorekova, S., Gibadulinova, A., Dequiedt, F., Kettmann, R., and Pastorek, J. Transcriptional regulation of the *MN/CA 9* gene coding for the tumor-associated carbonic anhydrase IX. Identification and characterization of a proximal silencer element. J. Biol. Chem., *274:* 32588–32595, 1999.
42. Semenza, G. L., and Wang, G. L. A nuclear factor induced by hypoxia via *de novo* protein synthesis binds to the human erythropoietin gene enhancer at a site required for transcriptional activation. Mol. Cell. Biol., *12:* 5447–5454, 1992.
43. Kaluzova, M., Pastorekova, S., Pastorek, J., and Kaluz, S. p53 tumour suppressor modulates transcription of the TATA-less gene coding for the tumour-associated carbonic anhydrase MN/CA IX in MaTu cells. Biochim. Biophys. Acta, *1491:* 20–26, 2000.
44. Arteel, G. E., Thurman, R. G., Yates, J. M., and Raleigh, J. A. Evidence that hypoxia markers detect oxygen gradients in liver: pimonidazole and retrograde perfusion of rat liver. Br. J. Cancer, *72:* 889–895, 1995.
45. Azuma, C., Raleigh, J. A., and Thrall, D. E. Longevity of pimonidazole adducts in spontaneous canine tumors as an estimate of hypoxic cell lifetime. Radiat. Res., *148:* 35–42, 1997.
46. Arteel, G. E., Thurman, R. G., and Raleigh, J. A. Reductive metabolism of the hypoxia marker pimonidazole is regulated by oxygen tension independent of the pyridine nucleotide redox state. Eur. J. Biochem., *253:* 743–750, 1998.
47. Rosmorduc, O., Wendum, D., Corpechot, C., Galy, B., Sebbagh, N., Raleigh, J., Housset, C., and Poupon, R. Hepatocellular hypoxia-induced vascular endothelial growth factor expression and angiogenesis in experimental biliary cirrhosis. Am. J. Pathol., *155:* 1065–1073, 1999.
48. Raleigh, J. A., Calkins-Adams, D. P., Rinker, L. H., Ballenger, C. A., Weissler, M. C., Fowler, W. C., Jr., Novotny, D. B., and Varia, M. A. Hypoxia and vascular endothelial growth factor expression in human squamous cell carcinomas using pimonidazole as a hypoxia marker. Cancer Res., *58:* 3765–3768, 1998.
49. Griffiths, J. R. Are cancer cells acidic? Br. J. Cancer, *64:* 425–427, 1991.
50. Heacock, C. S., and Sutherland, R. M. Enhanced synthesis of stress proteins caused by hypoxia and relation to altered cell growth and metabolism. Br. J. Cancer, *62:* 217–225, 1990.
51. Newell, K., Franchi, A., Pouyssegur, J., and Tannock, I. Studies with glycolysis-deficient cells suggest that production of lactic acid is not the only cause of tumor acidity. Proc. Natl. Acad. Sci. USA, *90:* 1127–1131, 1993.
52. Yamagata, M., Hasuda, K., Stamato, T., and Tannock, I. F. The contribution of lactic acid to acidification of tumours: studies of variant cells lacking lactate dehydrogenase. Br. J. Cancer, *77:* 1726–1731, 1998.
53. Martinez-Zaguilan, R., Seftor, E. A., Seftor, R. E., Chu, Y. W., Gillies, R. J., and Hendrix, M. J. Acidic pH enhances the invasive behavior of human melanoma cells. Clin. Exp. Metastasis, *14:* 176–186, 1996.
54. Parkkila, S., Rajaniemi, H., Parkkila, A-K., Kivela, J., Waheed, A., Pastorekova, S., Pastorek, J., and Sly, W. Carbonic anhydrase inhibitor suppresses invasion of renal cancer cells *in vitro*. Proc. Natl. Acad. Sci. USA, *97:* 2220–2224, 2000.
55. Teicher, B. A., Liu, S. D., Liu, J. T., Holden, S. A., and Herman, T. S. A carbonic anhydrase inhibitor as a potential modulator of cancer therapies. Anticancer Res., *13:* 1549–1556, 1993.

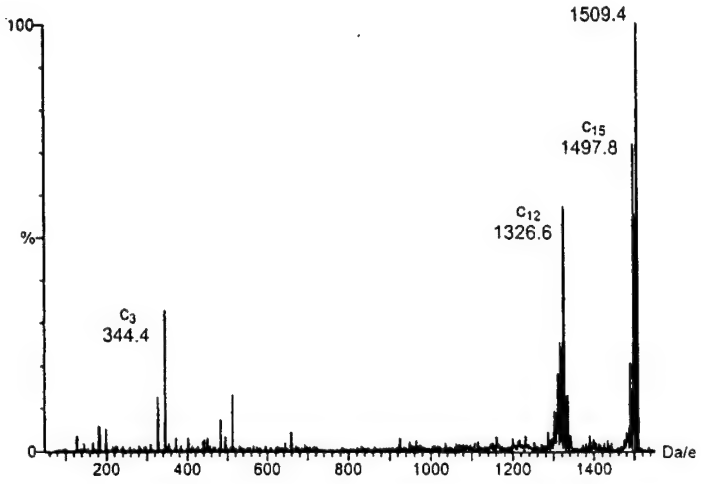

FIG. 2. Collision activated mass spectrum of the doubly charged molecular ion of C-peptide (*m/z* 1509.4). Collision gas argon at 3×10^{-3} mbar, collision energy 30 V, cone 60 V, capillary 3.5 kV, and source temperature 175°C.

fortified 1 mL of urine with 1% BSA, performed UF with Vivaspin devices (5000 MW cutoff) for 10 min at 7000*g*, added 1 mL water to the retentate (25 μL), mixed, and repeated UF so that a final retentate volume of 200 μL was reached (concentration factor, 5; purification factor, 8) (see Fig. 1). For the LC/MS analysis, we used the negative electrospray mode and monitored the collision-activated dissociation of the doubly charged molecular ion, *m/z* 1509.4 to 1326.6 (C_{12}-fragment). Two other important fragments are the C_3 (*m/z* 344.4) and C_{15}-fragment (*m/z* 1497.8). As we observed no significant ions with *m/z* >1510, we only present the spectrum in the range from *m/z* 50 to 1550 (see Fig. 2).

In conclusion, the adsorption of small proteins to BSA allows the use of UF devices for sample purification and concentration that have considerably higher nominal MW cutoffs than the MW of the analyte of interest. The method has been tested for urinary C-peptide over a concentration range from ~30 to ~170 ng/mL. In future experiments, we also hope to prove the applicability of this method for other peptides and proteins.

Acknowlegments. We acknowledge financial support by the Research Fund of the Ghent University (Grant BOF 01102096) and the National Fund for Scientific Research (Grant 3G0001096).

REFERENCES

1. Vivascience, Ltd. (1999) Vivaspin 500 μL, 2 mL, and 4 mL; technical data and operating instructions. Lincoln, UK.
2. Filtron Technology Corporation (1999) Microsep Microconcentrators, operating instructions. Northborough, MA.
3. Schleicher & Schuell (1999) Centrex UF Centrifugal Ultrafilters, operating instructions. Keene, NH.

Detection of Genetic Point Mutations by Peptide Nucleic Acid-Mediated Polymerase Chain Reaction Clamping Using Paraffin-Embedded Specimens

Yvonne Myal*,†,[1] Anne Blanchard,*,† Peter Watson,*,† Michael Corrin,* Robert Shiu,† and Barbara Iwasiow†

**Department of Pathology and †Department of Physiology, Faculty of Medicine, University of Manitoba, 770 Bannatyne Avenue, Winnipeg, Manitoba, R3E 0W3 Canada*

Received March 20, 2000

Peptide nucleic acid (PNA)[2]-mediated PCR clamping is a sensitive molecular assay (1) that can detect protooncogene point mutations in patient-derived tissue samples (1, 2). However, to date, PNA-mediated PCR clamping has only been demonstrated on fresh and frozen tissue. In this study, we demonstrate that PNA-mediated PCR clamping can be successfully used to detect point mutations in DNA derived from Formalin-fixed, paraffin-embedded (ffpe) samples, with no loss in sensitivity.

The PNA molecule is a sequence-specific synthetic oligomer that consists of repeating units of (2-aminoethyl)-glycine linked by amide bonds (2). Because of its unique structure, PNA can mimic DNA but cannot serve as a primer molecule during PCR amplification. The PNA molecule binds tightly to the target sequence and blocks amplification only if the two sequences are fully complementary. Thus, because the PNA is made complementary to the wild-type sequence, only the mutant allele is amplified during the PCR reaction.

Because of the frequency of oncogenic point mutations in many human tumors, PNA-mediated PCR clamping is potentially useful to the surgical pathologist as a means of detecting isolated cancer cells amid a population of normal cells (minimal residual disease, MRD). Currently, standard pathologic procedures usually involve the processing of the primary surgical specimen in Formalin followed by embedding in paraffin blocks to allow accurate assessment of tumor and resection margins. Thus, it would be desirable to determine whether PNA-mediated PCR clamping could be applied to ffpe samples. Also, it should be noted that although existing methods such as immunohistochemistry, denaturing gel electrophoresis, or PCR followed by single-stranded conformational polymorphism have

[1] To whom correspondence should be addressed. Fax: (204) 789-3931. E-mail: myal@ms.umanitoba.ca.

[2] Abbreviations used: PNA, peptide nucleic acid; ffpe, Formalin-fixed, paraffin-embedded; MRD, minimal residual disease.

Analytical Biochemistry **285**, 169–172 (2000)
doi:10.1006/abio.2000.4755
0003-2697/00 $35.00

TABLE 1

Primer Design

Wild type p53 sequence (MCF7)	5′ . . . CCTCAGCAT**C**TTATCCGAGTGG . . . 3′
PNA (15mer)	5′ CCTCAGCAT**C**TTATC 3′
Mutant p53 sequence (T47D)	5′ . . . CCTCAGCAT**T**TTATCCGAGTGG . . . 3′
Mutant forward primer (22mer)	5′ CCTCAGCAT**T**TTATCCGAGTGG 3′
Reverse primer	5′ TTGCAAACCAGACCTCAG 3′

Note. The sequences of the PNA oligomer, the mutant forward primer and the reverse primer are shown. In the T47D human breast cancer cells, the mutant p53 allele contains a T (in bold) instead of a C (also shown in bold) which occurs in the wild-type allele.

been used to detect MRD from ffpe samples, these assays are sometimes unsuccessful either because they are not sensitive enough, resulting in many false negatives or false positives (3–5), or because they require fresh or frozen tissue for efficient PCR. Furthermore, confirmation of the results often requires labor-intensive DNA sequencing protocols. The use of PNA-mediated PCR clamping could address all these limitations.

In testing this application, we developed an *in vitro* assay using serial dilutions of two human breast cancer cell lines, T47D (which carries a p53 gene point mutation at codon 194) and MCF7 (which carries the wild-type gene). The p53 tumor suppressor gene was used as a molecular marker for this study because mutations in this gene constitute the most common genetic change in human cancers. Serial dilutions were generated by mixing the MCF7 cells with increasing numbers of T47D cells. A total of 1×10^7 cells were used for each sample point. Cells were collected in 15-ml tubes and spun at 800 rpm for 5 min. The supernatant was removed and replaced by 1 ml of 4% paraformaldehyde, and the cells quickly dispersed in the fixative. Following a 2-h incubation, the fixed cells were again spun at 800 rpm for 5 min to remove the paraformaldehyde. Two milliliters of molten agar (3%, 43°C) was added to the cell pellets and the mixture was poured into molds (24-well dishes). After 30 min (enough time to allow the agar to set), the molds were placed in embedding cassettes, processed with fixatives [by standard procedures (6)], and followed by infiltration with paraffin. Next, the paraffin blocks were sectioned and used for DNA extraction. For each sample, DNA was extracted from one 5-μm paraffin section in a final volume of 500 μl, according to the method of Smith *et al.* (7). For PNA-mediated PCR amplification, 8 μl of the DNA extract was used per reaction. Although this amount of DNA was too small to measure accurately in all samples, it was the minimum amount of DNA that consistently resulted in a visible PCR product.

The PCR reaction was performed in a total of 50 μl containing 200 μM each of deoxynucleoside triphosphates, 50 mM KCl, 1.5 mM $MgCl_2$, 10 mM Tris–HCl (pH 8.3), 0.2 μM mutant forward primer and reverse primer (Table 1), 2.5 U *Taq* polymerase (Gibco, BRL), and 4–5 μM of PNA primer (Table 1). T_m was an important consideration in primer design. We selected a PNA sequence that had a sufficiently higher T_m than the mutant primer to ensure that the PNA molecule had ample opportunity to anneal to the DNA template. DNA primer PCR amplification consisted of an initial denaturation step of 94°C/5 min, followed by 26 cycles (40 cycles for paraffin-extracted DNA) of 94°C/1 min, 70°C/1 min, 57°C/1 min, and 72°C/1 min, plus an additional final extension cycle at 94°C/1 min and 60°C/10 min. The expected amplified product size was 115 bp.

Figure 1 shows that in the absence of PNA both the mutant and wild-type alleles were amplified. However, in the presence of PNA, only the mutant allele (T47D) was amplified. Amplification of the wild-type p53 allele (in MCF7) was completely inhibited, ruling out the amplification of false positives. Thus, the PNA inhibition of the wild-type p53 gene was indeed allele specific. Higher concentrations of the PNA molecule were no more effective in inhibiting the wild-type allele (data not shown). To rule out nonspecific binding and nonspecific inhibition by the PNA molecule, a 428-bp fragment of the human prolactin-inducible protein (*hPIP*) gene (8) was amplified in the presence and

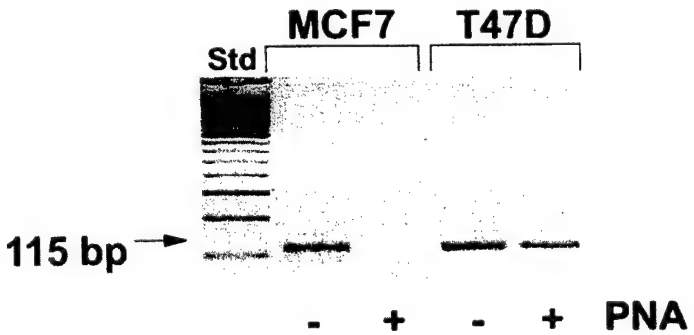

FIG. 1. Inhibition of the wild-type but not the mutant p53 allele by PNA. In the presence of PNA (4 μM), the amplification of the wild-type p53 allele (MCF7 DNA) is inhibited, but the mutant p53 allele (T47D) is not. Samples were usually carried out in triplicates (not shown here). Experiments were also carried out in triplicates. Thirty microliters of each reaction was electrophoresed on a 3% agarose gel and stained with ethidium bromide. The expected amplified 115-bp product is shown.

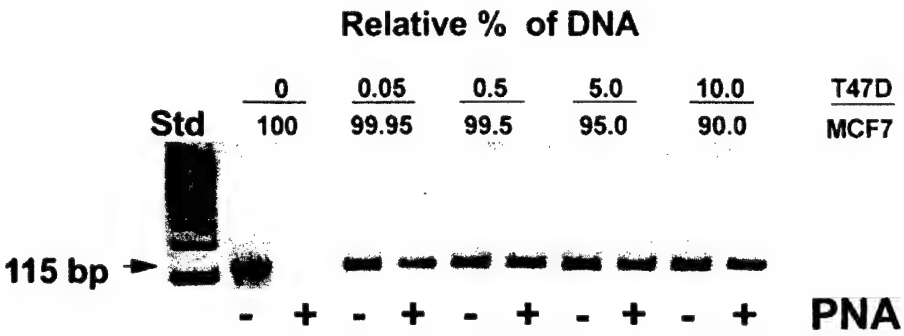

FIG. 2. PNA-mediated PCR clamping of paraffin-embedded cells demonstrates high sensitivity. Cell pellets were fixed (as described in the text) and embedded in paraffin. The percentage of mutant (T47D) alleles to wild type (MCF7) is shown. The total number of cells for each sample was the same but the ratio of T47D to MCF7 cells decreased from right to left. DNA was extracted and PNA-mediated PCR clamping was carried out as described in the text. Thirty microliters of the reaction was electrophoresed on a 3% agarose gel. Suppression of the wild-type alleles by PNA (5 μM) allowed the detection of 0.05% (the lowest limit tested) or 1 mutant allele in a background of 2000 normal alleles.

absence of the PNA molecule (not shown). The PNA failed to inhibit amplification of the *hPIP* control gene, demonstrating that the PNA molecule was gene specific. When PNA-mediated PCR clamping was carried out on DNA isolated from Formalin-fixed paraffin-embedded cells, suppression of the wild-type p53 allele by the PNA molecule allowed us to detect as little as 0.05% mutant alleles in the sample (Fig. 2). The level of sensitivity for this assay achieved by us (1 mutant allele in 2000-fold excess wild-type alleles) using ffpe samples was higher than that reported earlier (1, 2) using fresh or frozen tissue (1 mutant allele in a 200-fold excess of wild type). The reason for this improved sensitivity is not clear but may reflect the purity of the DNA samples. In addition, the sensitivity of this assay could be further enhanced by Southern blot analysis. However, this strategy was omitted because we wanted to develop a nonradioactive and yet sensitive assay that was rapid, practical, and convenient for a clinical laboratory setting.

In summary, we have shown that PNA-mediated PCR clamping can be performed on DNA from samples that have been embedded in paraffin; and that it is specific and sensitive. We have demonstrated a 10-fold increase in sensitivity over that reported earlier for fresh or frozen tissue (1, 2). Our results and those of others (1, 2) also suggest that this assay could be potentially useful for MRD detection, particularly for the screening of "hot spot" oncogenic lesions in histological samples. Improved methods of detection of MRD are clinically important for accurate disease staging of cancer patients (9) and for appropriate therapeutic management. Since the average length of a PNA molecule is 15 bases, theoretically, one PNA molecule could be used to detect 15 point mutations in a single gene. Used in conjunction with current light microscopy techniques, this assay could enhance our ability to more accurately stage cancer, since oncogenic point mutations are associated with poor prognosis for some human cancers (10). The main advantage of this approach is that paraffin-derived samples are convenient, require minimal amounts of tissue, and retrospective studies can be carried out on archival material. Finally, ffpe tissues also represent an easily accessible source of specimens, whereas fresh or frozen tissues are sometimes difficult to obtain.

Acknowledgments. This study was supported by a grant from the Health Sciences Centre Research Foundation, Winnipeg, Manitoba (to Y.M.). P.W. is an MRC Clinician Scientist. M.C. is a Government of Canada Summer Placement Career awardee. The authors thank Sandy Troup and Aihua Huang for their assistance in preparing the histological samples. We also thank Dr. Terry Zelinsky and Ms. Molly Pind for reading the manuscript.

REFERENCES

1. Thiede, C., Bayerdorffer, E., Blasczyk, R., Wittig, B., and Neubauer A. (1996) Simple and sensitive detection of mutations in the ras proto-oncogenes using PNA-mediated PCR clamping. *Nucleic Acids Res.* **24,** 983–984.
2. Behn, M., and Schuermann, M. (1998) Sensitive detection of p53 gene mutations by a 'mutant enriched' PCR-SSCP technique. *Nucleic Acids Res.* **26,** 1356–1358.
3. Fisher, C. J., Gillett, C. E., Vojtesek, B., Barnes, D. M., and Millis, R. R. (1994) Problems with p53 immunohistochemical staining: the effect of fixation and variation in the methods of evaluation. *Br. J. Cancer* **69,** 26–31.
4. Soong, R., Robbins, P. D., Dix, B. R., Grieu, F., Lim,. B, Knowles, S., Williams, K. E., Turbett, G. R., House,. AK., and Iacopetta, B. J. (1996) Concordance between p53 protein overexpression and gene mutation in a large series of common human carcinomas. *Hum. Pathol.* **27,** 1050–1055.
5. Wynford-Thomas, D. (1992) p53 in tumour pathology: can we trust immunocytochemistry? *Pathology* **166,** 329–330.
6. Humanson, G. L. (1967) Animal Tissue Techniques, 2nd ed. Freeman, San Francisco.
7. Smith, S. A., Easton, D. F., Evans, D. G., and Ponder, B. A. (1992) Allele losses in the region 17q12–21 in familial breast and ovarian cancer involve the wild-type chromosome. *Nat. Genet.* **2,** 128–131.

8. Myal, Y., Robinson, D. B., Iwasiow., B. Tsuyuki, D., Wong, P., and Shiu, R. P. (1991) The prolactin-inducible protein (PIP/GCDFP-15) gene: cloning, structure and regulation. *Mol. Cell Endocrinol.* **80,** 165–715.
9. Sidransky, D., Tokino, T., Helzlsouer, K., Zehnbauer, B., Rausch, G., Shelton, B., Prestigiacomo, L. Vogelstein, B., and Davidson, N. (1992) Inherited p53 gene mutations in breast cancer. *Cancer Res.* **52,** 2984–2986.
10. Brennan, J. A., Mao, L., Hruban, R. H., Boyle, J. O., Eby, Y. J., Koch, W. M., Goodman S. N., and Sidransky, D. (1995) Molecular assessment of histopathological staging in squamous-cell carcinoma of the head and neck. *N. Engl. J. Med.* **332,** 429–435.

Pharmacokinetic Study and Determination of Imperialine, the Major Bioactive Component in Antitussive *Fritillaria cirrhosa,* in Rat by High-Performance Liquid Chromatography Coupled with Evaporative Light-Scattering Detector

Shun-Wan Chan,* Song-Lin Li,*† Ge Lin,*[1] and Ping Li†

**Department of Pharmacology, Faculty of Medicine, Chinese University of Hong Kong, Shatin, N.T., Hong Kong, SAR, China; and †Department of Pharmacognosy, China Pharmaceutical University, Nanjing, People's Republic of China*

Received April 6, 2000

Imperialine (Fig. 1) is the major biologically active isosteroidal alkaloid present in the most commonly used antitussive traditional Chinese medicinal herb, Bulbus Fritillaria. It has been identified from several species in genus *Fritillaria,* including *Fritillaria cirrhosa,* the primary plant source for this herbal medicine (1–5). The antitussive effect of imperialine and the crude *fritillaria* alkaloid extracts of various *Fritillaria* spp. has been extensively studied in both *in vitro* and *in vivo* models, and imperialine has been demonstrated to be the most potent *fritillaria* alkaloids (6). However, to date there are no reports on the pharmacokinetic data of imperialine and other *fritillaria* alkaloids. Imposed by the low sensitivity of the chromophore in *fritillaria* alkaloid, a direct HPLC analysis with ultraviolet or fluorescence detection of this type alkaloid is very difficult (7). Consequently, the reported HPLC–UV assay with precolumn derivatization requires extensive sample preparations, and restricted and well-controlled chemical reactions (8). Therefore, the present study attempts to develop a direct HPLC analytical method for the analysis of imperialine in blood samples by using evaporative light scattering detector (ELSD),[2] a universal mass detector that responds to all eluates regardless of their structure and/or chromophore (9, 10). Moreover, the pharmacokinetic profiles of imperialine in rats via intravenous and oral administrative routes were investigated by using the developed HPLC–ELSD analytic method.

Materials and methods. Imperialine was isolated from *F. cirrhosa.* The purity and identity were determined by TLC, HPLC, NMR, and MS analyses. Solanidine was purchased from Sigma Chemical Co. (St. Louis, MO). HPLC-grade solvents were obtained from Labscan Asia Co. (Bangkok, Thailand). HPLC analysis was performed on an HP1100 (Hewlett–Packard) system equipped with an Alltech 500 ELSD (Alltech Associates Inc., Deerfield, IL). A Supelco reversed-phase C_8 analytical column (150 × 4.6 mm, i.d., 3 μ) coupled with a C_8 guard column (20 × 4.0 mm, 5 μ) was utilized with a gradient elution at flow rate of 1 ml/min and column temperature of 28°C. The mobile phase consisted of distilled water (A), acetonitrile (B), and methanol containing 0.6% triethylamine (C) was eluted as follows: 0–6 min A:B:C = 7:35:58; 6–7 min linear increase to A:B:C = 0:42:58 and maintained for 25 min, 25–30 min for returning to the initial conditions. The nitrogen gas flow of 2.22 standard liters per minute and drift tube temperature of 72°C were set for ELSD.

Male Sprague–Dawley rats (180–220 g) supplied by the Laboratory Animal Services Centre at the Chinese University of Hong Kong were fed on a standard laboratory diet with free access to water under the controlled temperature at 20–22°C and relative humidity of 50% with 12-h light/dark cycles prior to the study. Rats were surgically cannulated with polyethylene catheters on the right jugular veins under anesthesia with diethyl ether vapor. The animals recovered in individual metabolic cages and fasted but were allowed to have free access to water overnight. Two groups of conscious cannulated rats with at least five in each group were dosed with the HCl salt of imperialine intravenously (20 mg/kg) and orally (100 mg/kg), respectively. Serial venous blood samples (0.25 ml) were collected from the right jugular vein via the cannulated catheter into heparinized tubes at suitable time intervals up to 360 min after dose. At each blood sampling, an equivalent volume of heparinized normal saline (25% v/v, 0.25 ml) was injected into the animals to maintain a constant blood volume.

[1] To whom correspondence should be addressed. Fax: 852-2603-5139. E-mail: linge@cuhk.edu.hk.

[2] Abbreviation used: ELSD, evaporative light scattering detector.

Analytical Biochemistry **285,** 172–175 (2000)
doi:10.1006/abio.2000.4756
0003-2697/00 $35.00

PERGAMON

European Journal of Cancer 37 (2001) 106–113

European Journal of Cancer

www.ejconline.com

A matrix metalloproteinase inhibitor, batimastat, retards the development of osteolytic bone metastases by MDA-MB-231 human breast cancer cells in Balb C *nu/nu* mice

J. Lee [a], M. Weber [a], S. Mejia [a], E. Bone [b], P. Watson [a], W. Orr [a,*]

[a] *Department of Pathology, University of Manitoba, 770 Bannatyne Avenue, Winnipeg, Manitoba, Canada*
[b] *British Biotech Pharmaceuticals Limited, Oxford, UK*

PERGAMON

European Journal of Cancer 37 (2001) 106–113

European Journal of Cancer

www.ejconline.com

A matrix metalloproteinase inhibitor, batimastat, retards the development of osteolytic bone metastases by MDA-MB-231 human breast cancer cells in Balb C *nu/nu* mice

J. Lee [a], M. Weber [a], S. Mejia [a], E. Bone [b], P. Watson [a], W. Orr [a,*]

[a] *Department of Pathology, University of Manitoba, 770 Bannatyne Avenue, Winnipeg, Manitoba, Canada*
[b] *British Biotech Pharmaceuticals Limited, Oxford, UK*

Received 26 November 1999; received in revised form 17 July 2000; accepted 20 July 2000

Abstract

Bone resorption is a dominant feature of many bone metastases and releases factors from the bone matrix that can promote the expression of the metastatic phenotype in cancer cells. Since proteolytic enzymes, including matrix metalloproteinases (MMPs) contribute to bone destruction by metastatic tumour cells and host cells, we have examined the effect of a MMP inhibitor, batimastat, on the ability of MDA-MB-231 cells to degrade bone *in vitro* and to form bone metastases in BalbC *nu/nu* mice. *In vitro*, the neoplastic cells produced MMP-2 and MMP-9, degraded [^{3}H]-proline-labelled osteoblast matrices, and formed resorption pits in cortical bone. These phenomena were inhibited by $\leqslant 20$ μM batimastat. To induce vertebral and long bone metastases *in vivo*, 1×10^5 MDA-MB-231 cells were injected into the arterial circulation of BalbC *nu/nu* mice. Test groups were also given 30 mg/kg batimastat intraperitoneally (i.p.). After 21 days, the long bone metastases were characterised by a 67% reduction of metaphyseal medullary bone and complete replacement of marrow by tumour. In tumour-bearing mice that had been treated with 30 mg/kg batimastat i.p., the tumour volume decreased 8-fold, osteolysis was inhibited by 35%, and replacement of the bone marrow by tumour was inhibited by 65%. Similar effects were observed in the vertebral metastases. These data provide evidence that MDA-MB-231 cells can degrade osteoblast matrices and mineralised bone *in vitro* and support the hypothesis that MMPs are involved in the pathogenesis of osteolytic bone metastases *in vivo*. They demonstrate that an agent which inhibits proteolysis can retard the development of osteolytic bone metastases in this model.

Keywords: Neoplasm metastasis; Bone, matrix metalloproteinase; Proteinase inhibitor

1. Introduction

Skeletal metastases are common in patients with advanced cancers of the breast, prostate, lung, thyroid and kidney. Bone resorption is a dominant feature of most bone metastases, mediated by osteoclasts [1], tumour-associated macrophages [2], or metastatic cancer cells [3]. Osteolysis [4] contributes to the pathophysiological progression of bone metastases since the local growth factors that are generated and/or released as part of the bone remodelling process can promote the expression of the metastatic phenotype in osteotropic cancer cells [5]. Moreover, by weakening the structural integrity of bone, osteolysis contributes to the clinical features of bone metastases which include pain, pathological fractures, spinal cord compression, and hypercalcaemia [6].

The matrix metalloproteinases are mediators of homeostatic bone growth and remodelling [7] and are likely to contribute to the invasion and metastasis of malignant tumours in bone [8,9]. In experimental models of bone metastasis, there is evidence that osteolysis and colonisation of the bone marrow by the tumour can be reduced by strategies that inhibit the release or production of proteases [10,11] or by overexpressing tissue inhibitors of matrix metalloproteinases in metastatic cells [12]. On this basis, we have postulated and show here that a synthetic inhibitor of matrix metalloproteinases, batimastat (BB-94), inhibits the activity of matrix metalloproteinases expressed by MDA-MB-231 human breast carcinoma cells, and blocks the ability of these cells to degrade osteoblast-like matrices or to form

* Corresponding author. Tel.: +1-204-789-3338; fax: +1-204-789-3931.
E-mail address: worr@cc.umanitoba.ca (W. Orr).

0959-8049/01/$ - see front matter
PII: S0959-8049(00)00363-4

resorption pits in cortical bone. *In vivo*, where more than one cell type may be involved in bone destruction, treatment of tumour-bearing animals with batimastat inhibited tumour-associated osteolysis, tumour growth, and the replacement of marrow by tumour.

2. Materials and methods

2.1. Materials

Dulbecco's Minimal Essential Medium (DMEM) was purchased from GibcoBRL (Edmonton, Alberta, Canada). The MDA-MB-231 cells were a generous gift from G.R. Mundy, University of Texas, San Antonio, TX, USA. The SaOS-2 osteosarcoma cells were purchased from the American Type Culture Collection (Rockville, MD, USA). BalbC *nu/nu* mice weighing 18–20 g were purchased from Charles River (Montreal, Quebec, Canada) and housed according to standards established by the University of Manitoba. Batimastat was supplied by British Biotech Pharmaceuticals Ltd, Oxford, UK.

2.2. *Tumour cell growth* in vitro

4×10^2 MDA-MB-231 human breast cancer cells were seeded into 24 well tissue culture plates and allowed to attach for 2 h. Four replicate wells were then cultured in DMEM with 10% fetal bovine serum, in the presence of batimastat at concentrations ranging from 0 to 50 μM. Daily counts of viable cells were obtained by a haemocytometer.

2.3. *Enzymography*

Enzymography was performed as previously described [4]. Briefly, serum-free conditioned medium was collected over 48 h from confluent cultures of MDA-MB-231 cells. Samples of medium were loaded into 10% sodium dodecyl sulphate–polyacrylamide gel electrophoresis (SDS–PAGE) gels containing 0.3% gelatine and resolved by electrophoresis at 4°C at 100 V overnight. The gel was washed in 2.5% Triton X-100 for 2 h at room temperature and incubated for 48 h at 37°C in substrate buffer containing 50 mM Tris–HCl pH 8.9, and 5 mM $CaCl_2$ with varying concentrations of batimastat. The gel was visualised by staining with Coomassie Blue.

2.4. *Degradation of extracellular matrix*

SaOS-2 (human osteosarcoma) cells were cultured for 5 days in 96-well plates in the presence of 5 μCi/ml [^{3}H]-proline and 25 μg/ml ascorbic acid to form a radiolabelled osteoid-like matrix monolayer on the surface of the tissue culture dish. The osteosarcoma cells were lysed with 20 mM NH_4OH at 37°C for 20 min. The radiolabelled matrices were washed with serum-free DMEM and incubated for 24 h with 1×10^5 MDA-MB-231 tumour cells in the presence of 0–20 μM batimastat. Replicates of 5–6 wells were included for each condition. 100 μl aliquots of medium were collected, added to 6 ml of Beckman ReadySafe™ scintillation fluid, and counted using a Beckman beta counter [4].

2.5. *Resorption of mineralised cortical bone*

Fresh bovine long bone was obtained commercially, the marrow removed, and the bones were washed in methanol [4]. The bone was cut into 2-mm slices using an Isomet low-speed diamond-edged saw. The slices were then polished using fine quality sandpaper, 20 μm grit, and then with 10 μm grit accompanied by intermittent washing in water, using an ultrasonicator for 5-min periods. The slices were then dehydrated, and sterilised with ethylene oxide. Before each experiment, the slices were incubated for 24 h in serum-free medium, then incubated with 1×10^5 MDA-MB-231 cells with or without 20 μM batimastat for 60 min. The non-adhering cells were washed off with serum-free medium. The bone slices were then incubated for 30 days at 37°C in the presence or absence of batimastat. The cancer cells were removed by incubating the slices with 0.1% Triton X-100 for 6 h with 5-min washing in the ultrasonicator and the slices fixed in 100% ethanol. The slices were sputter-coated with gold and mounted for examination in a Scanning Electron Microscope. Bones were cultured in quadruplicate for each experimental condition. Between 30 to 50 random fields on the surface of the bone slices were analysed for each condition. Shallow pits with a diameter of 20–30 μm were marked. The mean number of pits per 0.62 mm^2 field was calculated.

2.6. *Experimental bone metastasis*

Four groups of 3–4 week old BalbC *nu/nu* mice were established from two sets of littermates, as summarised in Table 1. A normal control group consisted of animals that were neither treated with batimastat nor injected with MDA-MB-231 cells. Two groups of animals were

Table 1
Animal groups used to examine the effects of batimastat on the metastasis of MDA-MB-231 cells to bone

Groups	*n*	Batimastat	Tumour	Batimastat
(Time line)		2 days		21 days
Normal control	5	–		–
Batimastat control[a]	6	+	–	+
Tumour only[b]	4	–	+	–
Tumour and batimastat[a,b]	9	+	+	+

[a] 30 mg/kg batimastat injected intraperitoneally (i.p.) daily.
[b] 1×10^5 MDA-MB-231 cells injected.

given daily batimastat injections (30 mg/kg intraperitoneally (i.p.)) for a period of 23 days. Two groups of mice were given a single intracardiac left ventricular injection of 1×10^5 MDA-MB-231 cells 21 days before terminating the experiment. One group received both batimastat (beginning 2 days before injection of the tumour cells) and tumour cells. Intracardiac injections of MDA-MB-231 cells were employed to induce the formation of metastatic bone tumours as described by Yoneda and colleagues [12]. Briefly, under anaesthesia, a left parasternal longitudinal incision was made and the second intercostal space located. A needle was inserted until pulsatile blood was observed. 1×10^5 MDA-MB-231 human breast cancer cells in a total volume of 0.1 ml were injected within 20 s. The animals were allowed to recover and housed for 21 days, receiving a daily injection of batimastat or vehicle. The mice were killed by exposure to atmospheric CO_2. The left femur and the vertebral column were removed and fixed in 10% buffered formalin for 24 h. The vertebrae and femur were decalcified in 10% formic acid for 24 h and then further fixed in formalin for 24 h. The tissues were embedded in paraffin, following standard protocols. A 7-μM thick section of bone was prepared from the centre of the left femur and from the centre of the vertebral column and stained with haematoxylin and eosin. The metaphyseal medullary bone at the distal end of the left femur and the vertebral bodies were systematically scanned with a 40× objective lens. Five microscopic fields were analysed in each vertebral body with metastases. A Merz graticule was used to perform a morphometric analysis of the percentage area of bone, tumour, and marrow for each section [4,13].

2.7. *Batimastat administration*

Batimastat stock solution was prepared for use *in vitro* in absolute ethanol at a concentration of 10 mM and diluted in ethanol before each experiment. For experiments *in vivo*, the solution was prepared at a concentration of 3.0 mg/ml in pyrogen-free phosphate buffered saline (GibcoBRL, Edmonton, Alberta, Canada) with 0.01% Tween 80 (Fisher Scientific) and administered by i.p. injection at a daily dose of 30 mg/kg.

3. Results

3.1. *Experiments* in vitro

Growth curves were obtained to determine if batimastat has an effect on the proliferation of MDA-MB-231

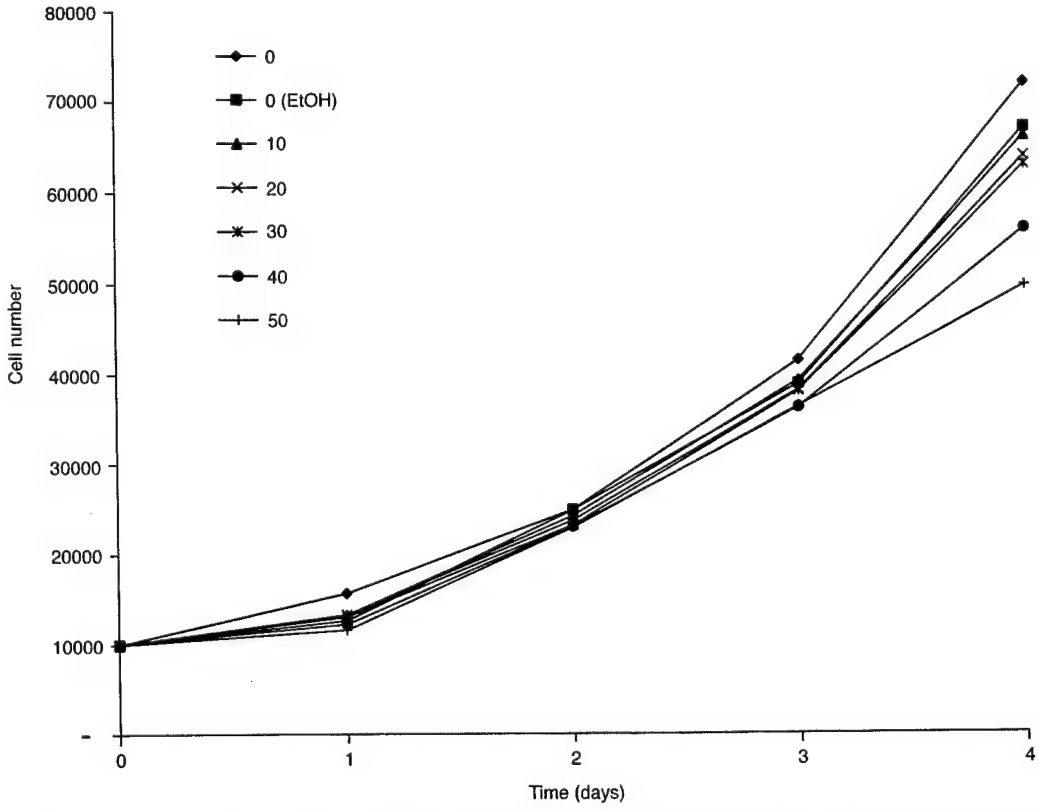

Fig. 1. Effect of batimastat on the growth of MDA-MB-231 human breast cancer cells *in vitro*. 4×10^2 cells were seeded into 24-well tissue culture plates and cultured in the presence of 0–50 μM batimastat. Daily cell counts were obtained by haemocytometer.

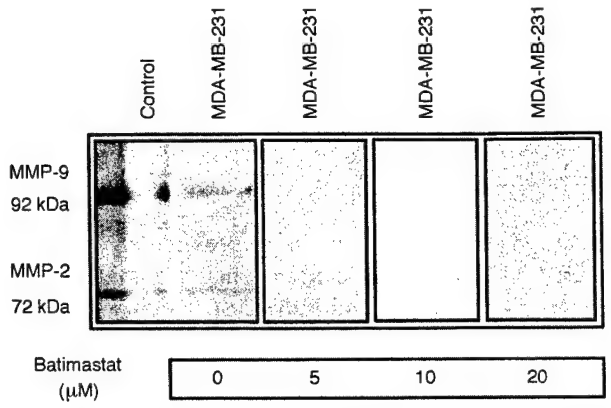

Fig. 2. Effect of batimastat on the expression of MMP-2 and MMP-9 in serum free medium conditioned by MDA-MB-231 cells. Electrophoresis was performed in 10% sodium dodecyl sulphate–polyacrylamide gel electrophoresis (SDS–PAGE) containing 0.3% gelatine. Zymograms were developed over 48 h in substrate buffer containing 0–20 μM batimastat.

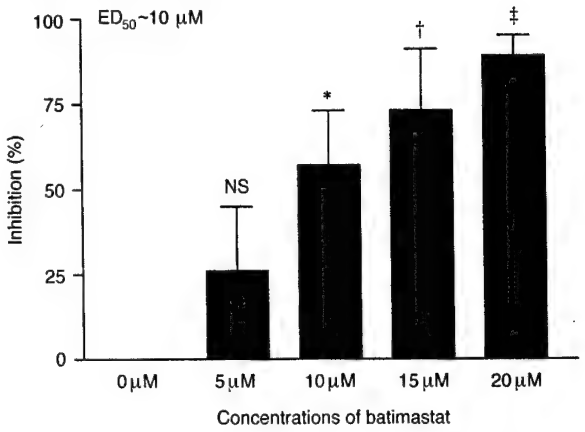

Fig. 3. Effect of batimastat on the degradation of osteoblast-like matrix by MDA-MB-231 cells. MDA-MB-231 cells were cultured on preformed [^{3}H]-proline labelled SaOS-2 osteoblast-like matrix in the presence of 0–20 μM batimastat. Degradation was determined by counting radioactivity released into the culture medium after 24 h. Not statistically significant by standard Student's t-test = NS; Statistically significant = $*P \leqslant 0.05$; $\dagger P \leqslant 0.01$; $\ddagger P \leqslant 0.001$. ED, effective dose.

breast cancer cells *in vitro*. After 4 days culture, the proliferation of the MDA-MB-231 cells was inhibited by approximately 4% in the presence of 10 μM batimastat or the ethanol vehicle and was inhibited up to approximately 30% at concentrations of 50 μM (Fig. 1).

Using enzymography, the serum-free medium of MDA-MB-231 cells, conditioned for 48 h, exhibited enzymatic activities at molecular weights of 92 kDA and 72 kDa, corresponding to the expression of matrix metalloproteinase (MMP)-9 and MMP-2 respectively. These activities were blocked when batimastat was added to the zymographic substrate buffer at concentrations $\geqslant 5$ μM (Fig. 2). Metalloproteinase expression was not inhibited in serum-free conditioned medium, collected from cells that had been cultured to confluence in the presence of 5–20 μM batimastat (data not shown). These results indicated that exposure to batimastat did not alter the expression of MMPs by the neoplastic cells.

Assays to examine the ability of batimastat to inhibit the degradation of non-mineralised bone matrix *in vitro* were performed to model its putative effects on the degradation of non-mineralised osteoid *in vivo*. In three independent experiments, batimastat inhibited the degradation of osteoblast-like matrix by MDA-MB-231 cells in a dose-dependent manner. In all three experiments, matrix degradation was inhibited completely by batimastat at concentrations of 20 μM with an effective dose $(ED)_{50} \cong 10$ μM (Fig. 3).

Assays to examine the effects of batimastat on the ability of MDA-MB-231 cells to directly degrade mineralised bone were performed as previously described [4,14]. MDA-MB-231 cells cultured on devitalised polished slices of bovine cortical bone generated 1.7±0.2 well-defined surface excavations per 0.62 mm^2 field after 30 days. In the presence of 20 μM batimastat, the number of pits decreased by 24% to 1.3±0.2 pits per field ($P \leqslant 0.076$) (Fig. 4). The areas of these pits were not significantly different ($P \leqslant 0.32$) between bones cultured in medium (169±15 μm^2) or in the presence of 20 μM batimastat (148±15 μm^2).

3.2. *Experiments* in vivo

Since metastatic osteolysis can be effected by host-derived osteoclasts and macrophages, as well as by tumour cells, it was important to examine the effects of batimastat *in vivo*. Groups of BalbC *nu/nu* mice were treated according to the protocols described in Table 1. Mice in the tumour-bearing groups were given intracardiac injections of 1×10^5 MDA-MB-231 cells and killed 21 days after tumour cell inoculation. The data obtained by histomorphometric analysis of the distal femoral metaphyses in the two independent experiments are combined in Fig. 5. Compared with non-tumour bearing controls, the non-tumour bearing animals treated with batimastat exhibited a 20% ($P \leqslant 0.3377$) increase in the area of medullary bone. In the tumour-bearing animals, there was a 67% ($P \leqslant 0.0001$) reduction of metaphyseal medullary bone at the distal end of the left femur, compared with normal controls. In tumour-bearing mice treated with batimastat, osteolysis was inhibited by 35% ($P \leqslant 0.02$), compared with untreated tumour-bearing mice. The area of the metaphysis occupied by tumour (tumour burden) was reduced by 68% in tumour-bearing animals treated with batimastat ($P \leqslant 0.0001$). The distance to which the tumour extended into the metaphysis beyond the epiphyseal growth plate was reduced by 75% ($P \leqslant 0.0001$). Overall, the total tumour volume decreased from 5.0±0.3 ($\times 10^{-3}$)

mm^3 in the untreated tumour-bearing animals to 0.6 ± 0.2 ($\times10^{-3}$) mm^3 in the tumour-bearing batimastat-treated mice ($P\leqslant0.0001$). Whereas in normal animals, marrow occupied $85\pm2\%$ of the metaphyseal area, this was reduced to 0% ($P\leqslant0.0001$) in the tumour-bearing animals. Marrow loss was inhibited by 65% ($P\leqslant0.0001$) in tumour-bearing animals treated with batimastat.

In the two experiments, similar results were obtained following analysis of vertebral bone (Table 2). Metastatic tumour was detected in 74% of the vertebral bodies of tumour-bearing animals, but this was reduced to 24% of the vertebral bodies in the tumour-bearing animals treated with batimastat ($P\leqslant0.0001$, data not shown). Batimastat treatment was associated with a 96% inhibition of vertebral bone tumour burden ($P\leqslant0.0001$), complete inhibition of tumour-associated osteolysis ($P\leqslant0.001$), and 53% inhibition of marrow replacement ($P\leqslant0.0001$).

4. Discussion

Bone metastases occur in approximately 80% of patients with late stage cancer. They are characterised by cancer cell growth and bone destruction which contribute to their pathophysiological development and clinical presentation. Since bone metastases are not usually detectable until they have become advanced lesions, they are often incurable. The early stages in their formation are asymptomatic and begin as single micrometastatic cells from the bloodstream. As pre-

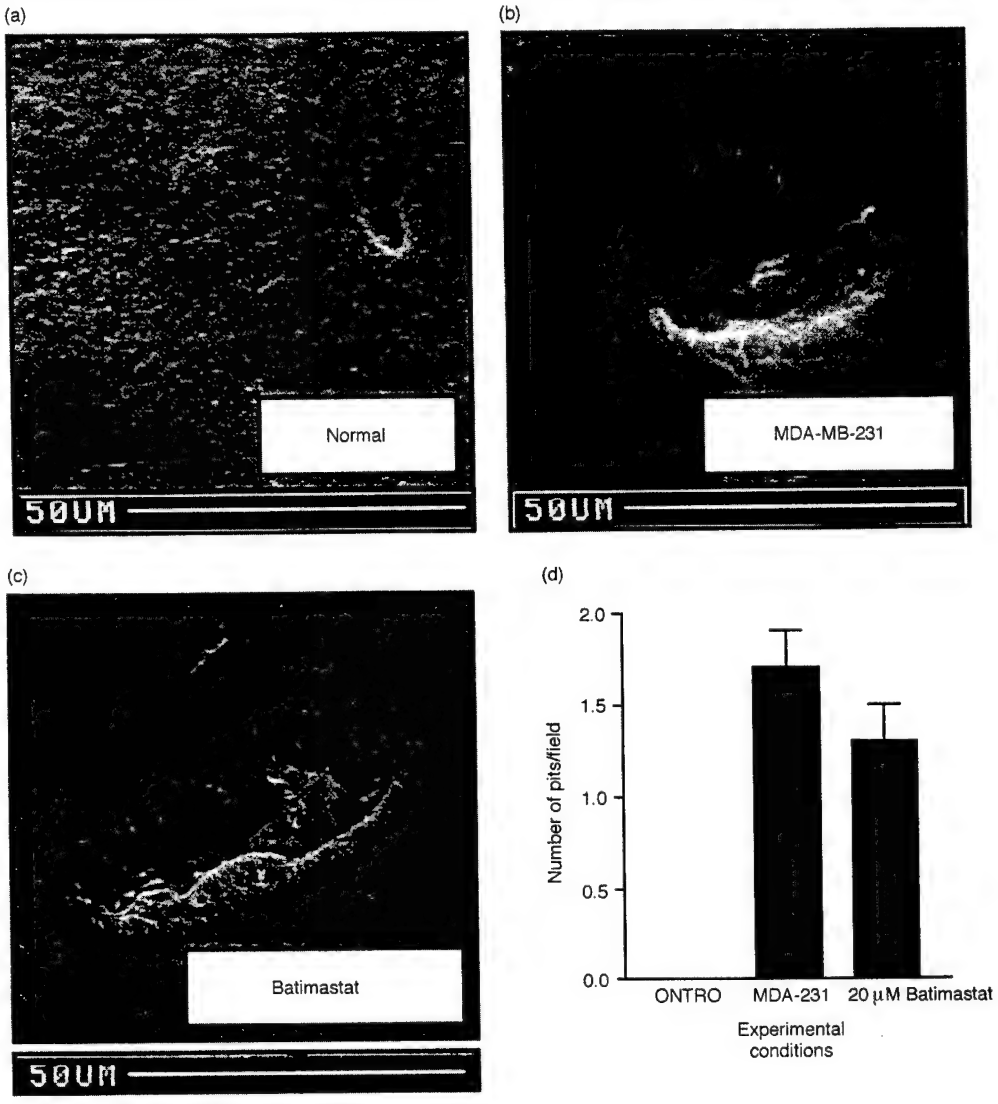

Fig. 4. Effect of batimastat on the formation of cortical bone resorption pits by MDA-MB-231 cells *in vitro*. (a) Appearance of untreated cortical bone after 30 days culture shows an osteocytic lacuna. (b) Resorption pit formed by MDA-MB-231 cells following 30 days coculture with MDA-MB-231 cells. (c) Resorption pit formed by an MDA-MB-231 cell cultured in the presence of batimastat. Scanning electron micrographs ×600. (d) Quantification of pit formation by MDA-MB-231 cells after 30 days incubation in the absence or presence of 20 μM batimastat. Field = 0.62 mm^2.

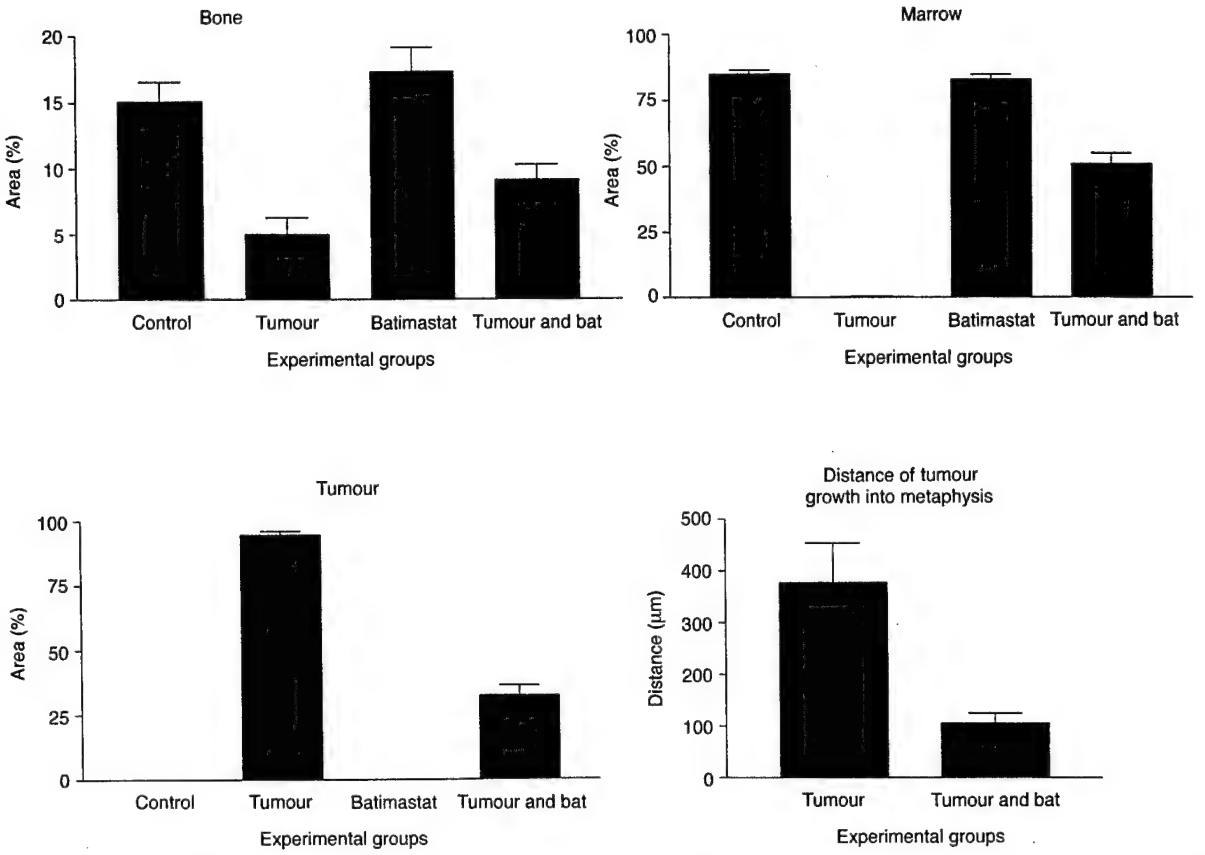

Fig. 5. Effect of batimastat on the development of experimental bone metastases by MDA-MB-231 breast cancer cells in BalbC *nu/nu* mice. Morphometric analysis was performed on histological sections of decalcified left distal femoral metaphysis 21 days after intracardiac injection of tumour cells. The experiment was duplicated to ensure reproducibility. The data presented here are combined from the two independent experiments. Not statistically significant by standard Student's *t*-test = NS; statistically significant by standard Student's *t*-test = $*P \leqslant 0.05$; $\dagger P \leqslant 0.01$; $\ddagger P \leqslant 0.001$. BAT, batimastat.

dicted by Paget [15], it has been established that there is a synergistic relationship between the micrometastatic cells and the bone environment, which creates a favourable condition for the development and growth of disseminated tumour cells [5]. Bone resorption mediates the progression of bone metastases by releasing local matrix-derived factors that can promote the expression of metastatic phenotypes in cancer cells including cancer cell chemotaxis [16], tumour growth [17,18], the expression of cell-surface adhesion molecules for bone matrix [19], and expression of MMPs [20,21]. As proteolytic enzymes, including MMPs, contribute to the mechanisms of osteolysis, we postulated that an MMP inhibitor would block osteolysis and interfere with the formation of lesions in established *in vitro* and *in vivo* models of bone metastasis.

Batimastat, an inhibitor of matrix metalloproteinases, acts by binding the zinc ion in the catalytic site, common to all matrix metalloproteinases. In animal models, batimastat has been reported to inhibit the formation of metastases through its inhibitory effects on tumour growth [22,23], tumour cell invasion of extracellular matrix [23–25] or angiogenesis [23,25–27] and by promoting stromal encapsulation [28]. Batimastat has been shown to reduce the activities of the 72-kDa and 92-kDa MMPs expressed by the human breast cancer cell line MDA-MB-435, to inhibit the local regrowth of resected MDA-MB-435 tumours implanted into athymic nude mice, and to inhibit the formation of lung metastases in these animals [29]. The effects of batimastat on bone metastasis do not appear to have been examined previously.

Table 2
Effect of batimastat on the formation of vertebral metastases by MDA-MB-231 breast cancer cells in BalbC *nu/nu* mice[a]

Groups	Bone (%)	Marrow (%)	Tumour (%)
Normal control	15±2	85±2	0±0
Tumour only	10±2	34±8	56±6
Batimastat control	16±1	84±1	0±0
Tumour and batimastat	20±2†	78±3*	2±1*

[a] Morphometric analysis of decalcified vertebral medullary bone (5 fields/vertebrae, ×200 magnification) was performed 21 days after intracardiac injection of tumour cells. $*P \leqslant 0.0001$ by Student's *t*-test when compared with the untreated (tumour only) group. †($P \leqslant 0.0013$).

In our experiments, batimastat did not inhibit the expression of MMP-2 and MMP-9 by the MDA-MB-231 cells but at concentrations $\geqslant 5$ μM completely inhibited the gelatinolytic activities of secreted MMPs in serum-free medium and concentrations $\geqslant 10$ μM blocked cell-mediated degradation of osteoblast-like matrices. While it is recognised that osteoclastic bone resorption contributes significantly to the osteolytic features of most bone metastases [30], the present experiments confirmed the ability of an osteolytic cancer cell line to induce pit formation in devitalised cortical bone slices in the absence of osteoclasts [4,14]. The ability of a human cancer cell line to cause degradation of mineralised bone was also reconfirmed [14] and was also partially inhibited by batimastat.

The concentrations of batimastat employed in the *in vivo* experiments were based upon precedence from other studies in the literature although they may have exceeded doses required to achieve optimal therapeutic effects. By using histomorphometry to analyse the metastatic lesions, we were able to distinguish between osteolysis, tumour burden, and marrow replacement which can not be accomplished by more conventional radiological measurements. The effects of batimastat treatment on the formation of bone metastases by MDA-MB-231 cells were striking and confirmed in two experiments. The marked osteolytic effects of the tumour were blocked in both femoral and vertebral bone, accompanied by diminished extension of tumour into the medullary long bone, decreased tumour volume, sparing of haematopoietic tissue, and a decrease in the number of metastases found in the vertebral bodies. We were unable to accurately quantify the effects of batimastat on tumour angiogenesis [27,31] as the decalcification procedures we employed appeared to block the ability of established histological markers of angiogenesis to identify blood vessels in our sections. Histomorphometric analysis of the long bones and vertebral bones of non tumour-bearing mice treated with batimastat demonstrated an unexpected increase in the volume of medullary bone, compared with normal untreated controls. An analysis of this phenomenon will be undertaken.

The colonisation of bone marrow by micrometastatic cells is a documented early event in the clinical course of human cancer and is being increasingly regarded as a prognostic factor of clinical significance [32]. Thus, batimastat was administered prior to the injection of tumour cells in order to optimise its potential effects on developing bone metastases rather than to study its actions on established lesions. Given the important contribution of bone resorption to the pathophysiological development of bone metastases, we predict that therapeutic strategies will be most effective if directed at inhibiting the interactions between micrometastatic cells and the bone microcompartment, as opposed to treatment of established lesions.

Acknowledgement

This work was supported by grants to Dr Orr from the Medical Research Council of Canada.

References

1. Mundy GR. Mechanisms of bone metastasis. *Cancer* 1997, **80**, 1546–1556.
2. Quinn JMW, Athanasou NA. Tumour infiltrating macrophages are capable of bone resorption. *J Cell Sci* 1992, **101**, 681–686.
3. Eilon G, Mundy GR. Direct resorption of bone by human breast cancer cells *in vitro*. *Nature* 1978, **276**, 726–728.
4. Sanchez-Sweatman OH, Lee J, Orr FW, Singh G. Direct osteolysis induced by metastatic murine melanoma cells: role of matrix metalloproteinases. *Eur J Cancer* 1997, **33**, 918–925.
5. Orr FW, Lee J, Duivenvoorden WC, Singh G. Pathophysiologic interactions in skeletal metastasis. *Cancer* 2000, **88**, 2912–2918.
6. Rubens RD. Bone metastases — the clinical problem. *Eur J Cancer* 1998, **34**, 210–213.
7. Bord S, Horner A, Hembry RM, Reynolds JJ, Compston JE. Distribution of matrix metalloproteinases and their inhibitor, TIMP-1, in developing human osteophytic bone. *J Anat* 1997, **191**, 39–48.
8. Ueda Y, Imai K, Tsuchiya H, *et al.* Matrix metalloproteinase 9 (gelatinase B) is expressed in multinucleated giant cells of human giant cell tumor of bone and is associated with vascular invasion. *Am J Pathol* 1996, **148**, 611–622.
9. Barille S, Akhoundi C, Collette M, *et al.* Metalloproteinases in multiple myeloma: production of matrix metalloproteinase-9 (MMP-9), activation of proMMP-2, and induction of MMP-1 by myeloma cells. *Blood* 1997, **90**, 1649–1655.
10. Stearns ME, Wang M. Effects of alendronate and taxol on pc 3 ml cell bone metastases in scid mice. *Invas Metast* 1996, **16**, 116–131.
11. Kawakami-Kimura N, Narita T, Ohmori K, *et al.* Involvement of hepatocyte growth factor in increased integrin expression on HepG2 cells triggered by adhesion to endothelial cells. *Br J Cancer* 1997, **75**, 47–53.
12. Yoneda T, Sasaki A, Dunstan C, *et al.* Inhibition of osteolytic bone metastasis of breast cancer by combined treatment with the bisphosphonate ibandronate and tissue inhibitor of the matrix metalloproteinase 2. *J Clin Invest* 1997, **99**, 2509–2517.
13. Kostenuik PJ, Orr FW, Suyama KL, Singh G. Increased growth rate and tumor burden of spontaneously metastatic Walker 256 cancer cells in the skeleton of bisphosphonate-treated rats. *Cancer Res* 1993, **53**, 5452–5457.
14. Sanchez-Sweatman OH, Orr FW, Singh G. Human metastatic prostate PC3 cell lines degrade bone using matrix metalloproteinases. *Invas Metast* 1999, **18**, 297–305.
15. Paget S. The distribution of secondary growths in cancer of the breast. *Lancet* 1889, **1**, 571–573.
16. Orr FW, Millar-Book W, Singh G. Chemotactic activity of bone and platelet-derived TGF-beta for bone-metastasizing rat walker 256 carcinosarcoma cells. *Invas Metast* 1990, **10**, 241–252.
17. Manishen WJ, Sivananthan K, Orr FW. Resorbing bone stimulates tumor cell growth. A role for the host microenvironment in bone metastasis. *Am J Pathol* 1986, **123**, 39–45.
18. Kostenuik PJ, Orr FW, Arsenault L, Millar-Book W, Singh G. Increased expression of c-myc mRNA and protein in walker 256 cancer cells stimulated by bone-derived conditioned media and by transforming factor-B (TGF-B). *Int J Oncol* 1993, **3**, 729–734.
19. Kostenuik PJ, Singh G, Orr FW. Transforming growth factor beta upregulates the integrin-mediated adhesion of human prostatic carcinoma cells to type I collagen. *Clin Exp Metast* 1997, **15**, 41–52.

20. Stearns ME. Alendronate blocks TGF-beta1 stimulated collagen 1 degradation by human prostate PC-3 ML cells. *Clin Exp Metast* 1998, **16**, 332–339.
21. Duivenvoorden WC, Hirte HW, Singh G. Transforming growth factor beta1 acts as an inducer of matrix metalloproteinase expression and activity in human bone-metastasizing cancer cells. *Clin Exp Metast* 1999, **17**, 27–34.
22. Prontera C, Mariani B, Rossi C, Poggi A, Rotilio D. Inhibition of gelatinase A (MMP-2) by batimastat and captopril reduces tumor growth and lung metastases in mice bearing Lewis lung carcinoma. *Int J Cancer* 1999, **81**, 761–766.
23. Tonn JC, Kerkau S, Hanke A, *et al.* Effect of synthetic matrix-metalloproteinase inhibitors on invasive capacity and proliferation of human malignant gliomas *in vitro*. *Int J Cancer* 1999, **80**, 764–772.
24. Kolkhorst V, Sturzebecher J, Wiederanders B. Inhibition of tumour cell invasion by protease inhibitors: correlation with the protease profile. *J Cancer Res Clin Oncol* 1998, **124**, 598–606.
25. Mira E, Manes S, Lacalle RA, Marquez G, Martinez A. Insulin-like growth factor I-triggered cell migration and invasion are mediated by matrix metalloproteinase-9. *Endocrinology* 1999, **140**, 1657–1664.
26. Bergers G, Javaherian K, Lo KM, Folkman J, Hanahan D. Effects of angiogenesis inhibitors on multistage carcinogenesis in mice. *Science* 1999, **284**, 808–812.
27. Wylie S, MacDonald IC, Varghese HJ, *et al.* The matrix metalloproteinase inhibitor batimastat inhibits angiogenesis in liver metastases of B16F1 melanoma cells. *Clin Exp Metast* 1999, **17**, 111–117.
28. Brown PD. Matrix metalloproteinase inhibitors: a novel class of anticancer agents. *Adv Enzyme Regul* 1995, **35**, 293–301.
29. Sledge GW Jr, Qulali M, Goulet R, Bone EA, Fife R. Effect of matrix metalloproteinase inhibitor batimastat on breast cancer regrowth and metastasis in athymic mice. *J Natl Cancer Inst* 1995, **87**, 1546–1550.
30. Guise T. Molecular mechanisms of osteolytic bone metastases. *Cancer* 2000, **88**, 2892–2898.
31. Taraboletti G, Garofalo A, Belotti D, *et al.* Inhibition of angiogenesis and murine hemangioma growth by batimastat, a synthetic inhibitor of matrix metalloproteinases. *J Natl Cancer Inst* 1995, **87**, 293–298.
32. Pantel K, Cote RJ, Fodstad O. Detection and clinical importance of micrometastatic disease. *J Natl Cancer Inst* 1999, **91**, 1113–1124.

[CANCER RESEARCH 61, 2071–2079, March 1, 2001]

Regulation of Growth and Tumorigenicity of Breast Cancer Cells by the Low Molecular Weight GTPase Rad and Nm23[1]

Yu-Hua Tseng, David Vicent, Jianhua Zhu, Yulian Niu, Adewale Adeyinka, Julie S. Moyers, Peter H. Watson, and C. Ronald Kahn[2]

Research Division, Joslin Diabetes Center, Department of Medicine, Harvard Medical School, Boston, Massachusetts 02215 [Y-H. T., D. V., J. Z., J. S. M., C. R. K.]; and Department of Pathology, University of Manitoba, Winnipeg, Manitoba R3E OW3, Canada [Y. N., A. A., P. H. W.]

ABSTRACT

Rad is the prototypic member of a family of novel Ras-related GTPases that is normally expressed in heart, skeletal muscle, and lung and that has been shown to exhibit a novel form of bi-directional interaction with the nm23 metastasis suppressor. In the present study, we have investigated the expression of Rad in normal and neoplastic breast tissues by Western blot and immunohistochemistry and the functional effect of altered Rad expression in breast cancer cell lines. We found that, although Rad is frequently expressed in normal breast tissue (23/30 Rad+ve), expression is usually lost in adjacent invasive carcinoma (8/30 Rad+ve; $P < 0.0001$). However, where Rad expression persists in a small proportion of tumors, it is associated with higher grade, larger size, and extensive axillary nodal involvement ($n = 48$; $P = 0.035$, $P = 0.016$, $P = 0.022$, respectively). Furthermore, Rad is also highly expressed in a breast cancer cell line with high tumorigenic and metastatic potential (MDA-MB231). To further examine the role of Rad in breast cancer, we stably transfected a Rad-ve breast cancer cell line (MDA-MB435). We observed an increase in growth and marked increased colony formation in soft agar *in vitro* ($P < 0.05$) and an increase in tumor growth rate in nude mice ($P < 0.05$). Moreover, coexpression of nm23 with wild-type Rad inhibited the effect of Rad on growth of these cells in culture and markedly inhibited tumor growth *in vivo*. Additional transfection studies with mutated Rad cDNAs revealed that the growth-promoting effects of Rad appeared to be mediated through its NH_2- and COOH-terminal regions, rather than its GTPase domain, and might involve acceleration of cell cycle transition. These findings suggest that Rad may act as an oncogenic protein in breast tissues and demonstrate a potential mechanism by which interaction between Rad and nm23 may regulate growth and tumorigenicity of breast cancer.

INTRODUCTION

Development and progression of breast cancer is a complex process involving both hormonal and genetic factors. Among the several hormones known to stimulate both normal and malignant mammary cell proliferation are steroids, such as estrogen (1) and progesterone (2), and peptide growth factors, such as prolactin (3), insulin (4), and insulin-like growth factor-1 (5). Alterations of a number of genes in breast cancer have also been identified, some of which have been proposed as molecular markers to help predict the prognosis. These include breast cancer susceptibility genes *BRCA-1* and *-2*, p53, Her-2/neu (c-erbB-2), and some regulatory proteins of cell cycle such as cyclin D1 and p27Kip1. Still further altered genes may emerge from investigations centered on chromosomal regions showing loss of heterozygosity (for review, see Ref. 6). Despite the recognition of these factors, the molecular mechanisms of formation of breast cancer still remain unclear, and identification of regulatory genes in the process of tumorigenesis and metastasis is one of the major goals of cancer research.

Rad is a M_r 35,000 small GTPase that was initially cloned by subtractive cloning as a mRNA overexpressed in skeletal muscle of some type-2 diabetic humans and is normally highly expressed in heart and lung (7). It is the prototypic member of a newly emerged Ras-related GTPase family with several unique characteristics, including Gem/Kir, Rem, Rem2 and Ges. Gem/Kir was found by its overexpression in activated T lymphocytes (8) and in v-abl-transformed pre-B cells (9). Rem was cloned as a product of PCR amplification using oligonucleotide primers derived from conserved regions of Rad and Gem/Kir as a mRNA that was repressed by lipopolysaccharide in mice (10). Rem2 mRNA is expressed in rat brain and kidney and possesses a novel cellular localization signal that is different from most Ras-related proteins (11). Ges is expressed in the endothelium and functions as a promoter of cytoskeleton reorganization (12). All of these G proteins possess several structural features that are distinct from other Ras-related GTPases, including major NH_2- and COOH-terminal extensions, a lack of typical prenylation motifs, and several nonconservative changes in the sequence of the GTP-binding domain. The NH_2 terminus of Rad is extended by 88 amino acids, and the COOH-terminus is extended by 31 amino acids as compared with Ras. As a result of the lack of a prenylation motif, Rad is primarily a cytosolic protein that associates with the cytoskeleton in a nonlipid-dependent manner (13). Rad, Gem, and Rem differ from each other and from other Ras-like molecules in the pupative effector (G2) domain. They also contain residues in the G3 consensus sequence for guanine nucleotide binding that are divergent from Ras (7). By expression cloning and coimmunoprecipitation, Rad can be shown to interact with CaM,[3] CaMKII (14), and β-tropomyosin (15). These interactions are enhanced by an increase in calcium influx and favor the GDP-bound form of Rad. Overexpression of Rad in 3T3-L1 adipocytes and C2C12 myocytes causes a marked reduction in insulin-stimulated glucose uptake (16). However, the exact function of Rad is still unknown.

Our laboratory has recently identified a novel form of bi-directional interaction between Rad and nm23 (17). In this complex, nm23 acts as both a GTPase-activating protein and a guanine nucleotide exchange factor for Rad, determining the balance between GTP-Rad and GDP-Rad. The first *nm23* gene (*nm23-M1*) was originally identified by subtractive cloning in murine melanoma cell lines as a putative tumor metastasis suppressor (18). Since then, an additional murine *nm23* gene, *nm23-M2* (19), and five human *nm23* genes, namely *nm23-H1* (20), *nm23-H2* (21), *DR-nm23* (22), *nm23-H4* (23), and *nm23-H5* (24), have been identified. The metastasis suppressor function of nm23 has been demonstrated by both *in vivo* and *in vitro* experiments that show reduced incidence of primary tumor formation and a significant reduction in metastatic potential on transfection of nm23-M1 and nm23-H1 cDNA into highly metastatic murine melanoma cells (25) and human breast cancer cells (26), respectively. In addition,

Received 5/22/00; accepted 1/10/01.

The costs of publication of this article were defrayed in part by the payment of page charges. This article must therefore be hereby marked *advertisement* in accordance with 18 U.S.C. Section 1734 solely to indicate this fact.

[1] Supported by the NIH Grant DK-45935 (to C. R. K.). P. H. W. is supported by a Scientist Award from the Medical Research Council of Canada. The National Cancer Institute of Canada-Manitoba Breast Tumor Bank is funded by the National Cancer Institute of Canada.

[2] To whom requests for reprints should be addressed, at Joslin Diabetes Center, One Joslin Place, Boston, MA 02215. Phone: (617) 732-2635; Fax: (617) 732-2593; E-mail: c.ronald.kahn@joslin.harvard.edu.

[3] The abbreviations used are: CaM, calmodulin, CaMKII, calmodulin-dependent protein kinase II; Wt, wild-type.

nm23 transfection inhibits motility of human and murine tumor cells in response to different factors (27). Nm23 possesses several enzymatic activities, including a nucleoside diphosphate kinase activity (28), a histidine kinase activity (29), and a serine protein kinase activity (30). Rad has been shown to enhance the nucleoside diphosphate kinase activity of nm23 and decrease its autophosphorylation (17).

In addition to its potential function on suppression of tumor metastasis, several reports have suggested that nm23 has a role in cell differentiation and proliferation (for review, see Ref. 31). Nm23 H2 has been found to be identical to the c-myc transcription factor, PuF (32). The homologue of nm23 in *Drosophila* is the Awd (abnormal wing discs) protein (33). Mutation in *awd* causes abnormal structures of imaginal disc during wing development (34). A correlation between increased nm23 expression and cell proliferation has also been suggested by other investigations. The levels of nm23 expression strictly correlate with cell growth rate and DNA synthesis in the human breast epithelial cell line, MCF-10A (35, 36). Overexpression of nm23 in rat pheochromocytoma PC12 cells enhances nerve growth factor-induced sympathetic neuronal cell differentiation by delaying cell cycle transition and increasing neurite outgrowth (37). Nevertheless, the biochemical mechanism of nm23 action is unknown to date.

In this report, we show that Rad is expressed in some human breast cancer and breast cancer cell lines and that expression is related to features of poor prognosis *in vivo*. In cultured cells, overexpression of Rad causes a marked increase in growth and increased colony formation in soft agar, and these effects are inhibited by nm23. Moreover, similar effects are seen when these cells are injected into nude mice. These findings suggest that the Rad-nm23 interaction may regulate growth and tumorigenicity of human breast cancer cells.

MATERIALS AND METHODS

Human Breast Cancer Specimens. All of the breast tumor cases used for this study were selected from the National Cancer Institute of Canada-Manitoba Breast Tumor Bank (Winnipeg, Manitoba, Canada). As described previously (38), tissues are rapidly collected and processed to create matched formalin-fixed-embedded and frozen tissue blocks for each case. The histology of every sample in the bank is uniformly interpreted by a pathologist in H&E-stained sections from the face of the paraffin tissue block. For each case, interpretation data include an estimate of the cellular composition of the section used for study, tumor type, and tumor grade (Nottingham score; Ref. 39). Steroid receptor status was determined for all of the cases by ligand binding assay performed on an adjacent portion of tumor tissue. Tumors with estrogen and progesterone receptor levels above 3 fmol/mg and 15 fmol/mg of total protein, respectively, were considered estrogen-receptor or progesterone-receptor positive.

Two cohorts of tumors were selected. The first cohort comprised a series of 24 invasive ductal tumors selected only to ensure >25% tumor cells/section. Frozen sections from these cases were cut and used for protein extraction and Western blot analysis in our preliminary survey of Rad expression. The second cohort of 48 invasive ductal carcinomas was selected to comprise tumors with approximately equivalent numbers of each tumor grade [low, intermediate, and high (15, 16, and 17 cases, respectively)] and a range of estrogen receptor, progesterone receptor, nodal status, and tumor sizes (Table 1). Additional selection criteria also included high tissue quality, presence of invasive tumor within >25% of the cross-section of the paraffin block, and, where possible, normal ducts or lobules adjacent to the tumor to allow comparison between tumor and normal tissue.

Immunohistochemistry. Immunohistochemistry was performed using polyclonal anti-Rad antibody (1:200 dilution) and the AEC Kit (DAKO Envision System, Toronto, Ontario, Canada) following the manufacturer's instructions. Slides were counterstained with H&E. Rad expression was assessed by brightfield microscopic examination at low (10× objective) magnification with reference to negative control tumor sections run with each batch. Levels of expression were scored semiquantitatively by assessing the average signal intensity (on a scale of 0 to 3) and the proportion of tumor cells showing a positive signal (0, none; 0.1, less than one tenth; 0.5, less than one half; 1.0, greater than one half). The intensity and proportion scores were then multiplied to give an overall score. Tumors with a score equal to or higher than 1.0 were deemed positive.

Table 1 *Rad expression status relative to the clinical-pathological features of the cohort of invasive breast tumors studied*

		Total No.	Rad −ve	Rad +ve	P[a]
ER[b]	+ve	37 (77)[c]	26 (54)	11 (23)	ns[b]
	−ve	11 (23)	8 (17)	3 (6)	
PR[b]	+ve	30 (62.5)	20 (42)	10 (21)	ns
	−ve	18 (37.5)	14 (29)	4 (8)	
Grade	I	15 (31)	15 (31)	0 (0)	0.035
	II	16 (33.5)	8 (17)	8 (17)	
	III	17 (35.5)	11 (23)	6 (12)	
Size[d]	0–2	12 (25)	11 (23)	1 (2)	0.022
	2–5	22 (46)	17 (35.5)	5 (10.5)	
	>5	7 (14.5)	3 (6)	4 (8.5)	
	Unknown	7 (14.5)	4 (8.5)	3 (6)	
NS[b]	0	18 (37.5)	15 (31)	3 (6)	0.016
	+ve (1–2)	9 (19)	8 (17)	1 (2)	
	+ve ≥3	14 (29)	6 (12)	8 (17)	
	Unknown	7 (14.5)	5 (11)	2 (4)	

[a] P, χ^2 test for trend.
[b] ER, estrogen receptor status; PR, progesterone receptor status; NS, nodal status; ns, not significant.
[c] Numbers in parentheses represent approximate percentage values.
[d] Tumor size in cm^2.

Cell Culture and Transfection of Cell Lines. Human breast carcinoma cell lines MDA-MB435 expressing pCMV vector or pCMVnm23-H1 construct (cell lines C-100 and H1–177, respectively; Ref. 26) were generous gifts from Dr. Patricia S. Steeg (National Cancer Institute, Bethesda, Maryland). These cells were transfected with pBabe puromycin resistance vector only (Puro) or expressing full-length human Wt Rad cDNA, the Rad S105N mutant, the Rad N88 mutant, the Rad C249 mutant, or the full-length cDNA of Gem by calcium phosphate method (14, 15). Stable cell lines were established by selection in puromycin-containing media (2 μg/ml). Cells were maintained in DMEM containing 10% fetal bovine serum in a 5% CO_2 environment.

Immunoblotting. Cells grown on a 100-mm dish were washed twice with ice-cold PBS and scraped into 1 ml of lysis buffer as described previously (14). For the preparation of tissue extracts, about 2 mg of normal or tumor human breast tissues from frozen samples were homogenized in 400 μl of lysis buffer. Protein concentrations were determined using the Bradford protein assay (Bio-Rad). Lysates (50 μg) were subjected to SDS-PAGE followed by Western immunoblotting using specific antisera and detection with chemiluminescence (Amersham Pharmacia Biotech, Piscataway, NJ). Rad polyclonal antiserum was used at 1:1000 dilution as described (15). Monoclonal antibody against human nm23 H1 was purchased from Santa Cruz (Catalogue #SC-465; Santa Cruz, CA) and used at 1:500 dilution.

Growth Assays. For anchorage-dependent growth assay, 1×10^4 cells were plated/well in multiple 24-well plates and incubated at 37°C for varying times, and the numbers of cells were determined by trypsinization and counting in a hemocytometer or Coulter particle counter. Soft-agar colonization assay was performed using 3×10^3 cells in 0.5 ml of medium containing 0.3% (w/v) agar over a 0.5 ml plug of medium containing 0.5% (w/v) agar. Colonies were counted after 14 days of incubation. All of the data were obtained from three independent experiments with each group represented by triplicate wells.

Cell Cycle Analysis by Flow Cytometry. Cells (1.5×10^6) were plated in a 60-mm dish and grown for overnight. The cells were washed twice with PBS, kept in serum-deprived medium for 84 h, and then reexposed to 10% fetal bovine serum for 12 or 24 h. Cells were collected by trypsinization followed by centrifugation, washed once with PBS, and resuspended in 0.2 ml of ice-cold PBS. The cells were fixed in 70% ethanol [in 50 mM glycine buffer (pH 2.0)]. After at least 24 h of fixation, DNA was stained with 2.5 μg/ml propidium iodide, and the content was analyzed in a FACScan at the Dana-Farber Cancer Institute flow cytometry facility (Boston, MA).

Tumor Growth Assay. A suspension of 5×10^5 (in 0.2 ml of PBS) MDA-MB435 cells expressing vector alone (Puro), Wt Rad, or Rad S105N in the absence or presence of coexpression of nm23 was injected s.c. into the left hind flank of 5-week-old female NIH Swiss Nude mice (Taconic, German-

town, New York). There were five mice in each treatment group, and the experiments were repeated twice. Tumors were measured with calipers in three dimensions twice weekly. All of the animals were treated in accordance with animal welfare guidelines. The entire experiment was halted after any animal had a visible tumor more than 25 mm in one dimension. At autopsy, all of the organs were examined for gross metastases. Primary tumors, lymph nodes, lungs, spleens, and livers were collected and fixed in 10% formalin. H&E-stained sections were prepared from these formalin-fixed and paraffin-embedded tissues. Slides were reviewed using a light microscope (4× and 20× objectives) and certified by other pathologists.

RESULTS

Rad Was Highly Expressed in a Tumorigenic Breast Cancer Cell Line and a Number of Breast Cancer Tissues. Many small G proteins may act as positive or negative effectors of cell growth; however, the exact function of the small GTPase Rad remains unknown. To explore a possible role for Rad in breast cancer, Western blot analysis was performed on protein extracts of breast tissue samples from a number of patients with breast cancer. This demonstrated a variable level of Rad expression, from very low or undetectable in most cases to very high in a few (Fig. 1*B*). To examine Rad expression further, immunohistochemical analysis was conducted in a second cohort of 48 human breast cancer specimens, selected to allow exploration of the relative cellular expression of Rad in breast. These included normal and neoplastic components in the majority of cases. This revealed that Rad was expressed within both normal breast epithelium and tumor cells. Rad expression was often present and at high levels in normal ductal and lobular epithelium (23/30 cases). By contrast, expression was commonly lost in adjacent invasive carcinoma in the same patient (8/30 Rad+ve; $P < 0.0001$; Wilcoxon matched pairs test). Nevertheless, where persistence of high levels of Rad expression was present in breast tumors, this was associated with higher grade, larger size, and extensive axillary nodal involvement ($n = 48$; $P = 0.035$, $P = 0.016$, $P = 0.022$, respectively; χ^2 test for trend; Fig. 1*C*; Table 1).

In an attempt to find cell models to study Rad action further, several cultured cell lines were screened for Rad expression. Whereas the levels of Rad expression were low in the C2C12 myocytes and in the breast cancer cell line MDA-MB435, Rad was highly expressed in MDA-MB231 breast cancer cells (Fig. 1*A*).

Rad Induces Both Anchorage-dependent and Anchorage-independent Growth in Breast Cancer Cells, and Nm23 Blunts These Effects. Our laboratory has recently demonstrated a novel form of bi-directional interaction between Rad and nm23 (17). To determine whether the Rad-nm23 interaction may have a role in growth of breast cancer cells, we established cell lines overexpressing Wt Rad in the presence or absence of coexpression of nm23 in the MDA-MB435 breast cancer cells, which have a low level of endogenous Rad. Drug-resistant clones were pooled together, and both anchorage-dependent and anchorage-independent growth were monitored in these cells. Rad expression resulted in accelerated cell growth on tissue culture plastics by almost 3-fold, and an increased number of colonies formed in soft agar by almost 2.5-fold (Fig. 2, *A* and *B*). Coexpression of nm23 slightly increased the basal levels of growth in both of these *in vitro* assays, although these increases were not statistically significant. More strikingly, however, nm23 almost completely blocked the growth-promoting effects of Rad. Similar results were obtained from isolated individual clones (data not shown). These data suggested that Rad was able to accelerate both anchorage-dependent and anchorage-independent growth in the breast cancer cells and that this effect may be modified by its interaction with nm23.

The Growth-promoting Effects of Rad Required Its NH_2- and COOH-terminal Regions. To further study the structure-function relationship of Rad on cell growth, we generated several cell lines with either Wt Rad or a series of mutants of Rad in the MDA-MB435

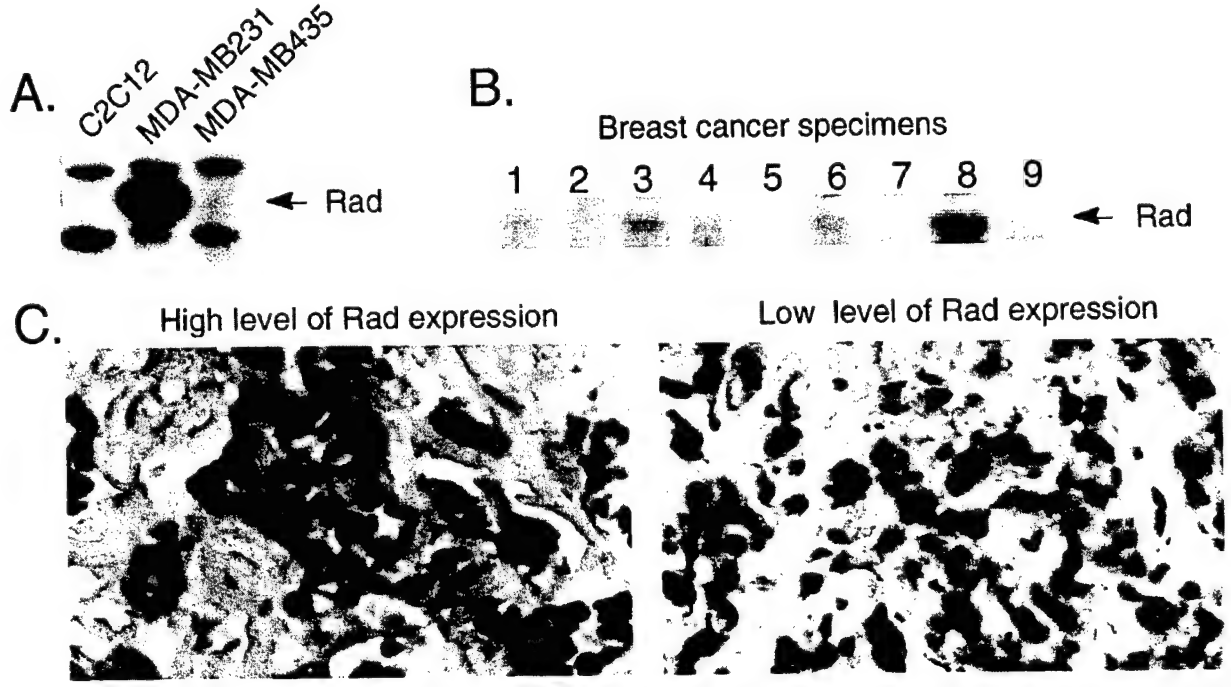

Fig. 1. Rad expression in cell lines and human breast cancer tissues. *A*, Western blot analysis of Rad expression in different cell lines. C2C12 is a murine myocyte line; MDA-MB231 and MDA-MB435 are human breast cancer cell lines. *B*, Western blot analysis of Rad expression in human breast cancer specimens. Protein extracts (50 μg) from randomly selected human breast cancer specimens were analyzed using a polyclonal antibody against human Rad (15). *C*, representative immunohistochemical staining of high (*left panel*) and low (*right panel*) levels of Rad expression in human breast cancer tissues. Cells with red-brown staining in the cytoplasm are considered as positive. Original magnification, ×400.

cells. These mutants included the Rad S105N mutant, the Rad N88 mutant, and the Rad C249 mutant (Fig. 3*A*). The Rad S105N mutant contained a Ser to Asn mutation at position 105, which is analogous to the S17N mutation in Ras and results in a loss of GTP-binding activity favoring GDP binding (15). The other two mutants, Rad N88 and Rad C249, have deletions in the NH_2-terminal 88 amino acids or the COOH-terminal 59 amino acids (residues 249–308), respectively. Both regions have been shown to be important for CaM binding (14). These constructs were transfected into the MDA-MB435 cell with or without coexpression of nm23. Western blotting revealed an over 100-fold overexpression for both Wt Rad and Rad S105N, about a 40-fold increase for Rad C249, and about a 30-fold increase for Rad N88. The extra bands comigrating with Rad C249 and Rad N88 were nonspecific and were not shown when ^{125}I-labeled protein A detection system was used (14). The relatively lower levels of expression of the latter two were consistent with our previous studies demonstrating that the NH_2 terminus and possibly the COOH terminus of Rad may be critical for antibody recognition, protein expression, and/or stability (Ref. 14; Fig. 3*B*).

Analysis in tissue culture revealed that Wt Rad, as well as the Rad S105N mutant, were able to accelerate cell growth (Fig. 3*C*, *Left Panel*). This occurred primarily by shortening the lag time required for entering exponential growth, rather than altering the doubling time (Fig. 3, *D* and *E*). Interestingly, the GDP-bound form of Rad (S105N) had an effect equal to or greater than that of the Wt protein. This is similar to our previous observation that Rad S105N is more potent in interacting with CaM, CaMKII (14), and tropomyosin (15), all of which favor the GDP form of Rad. Cells overexpressing either the NH_2- or COOH-terminal truncation mutant of Rad, in which their interactions with CaM were affected, did not show any change in lag time as compared with the control cells. Similar structure-function relationships were observed in the soft agar colonization assay (Fig. 3*F*). Overall, coexpression of nm23 increased slightly, but not significantly, both anchorage-dependent and anchorage-independent growth as shown in both Fig. 2 and Fig. 3. These data agreed with other investigations on a positive correlation of levels of nm23 expression and cell growth rates (35). Taken together, our data suggested that the growth-promoting effects of Rad might be mediated through its NH_2- and COOH-terminal regions and CaM binding, rather than being dependent on the GTPase activity of Rad. Gem, another member of the Rad family of GTPases that binds CaM (40), was also able to shorten the lag time when transfected into the MDA-MB-435 cells (Fig. 3*D*). However, it was unable to promote colony formation in soft agar (Fig. 3*F*). No significant difference was observed in growth rates of all cell lines during exponential growth (Fig. 3*E*). Again, coexpression of nm23 blunted the growth-accelerating effects of Rad in these cells (Fig. 3, *D–F*).

Rad Promoted Cell Growth by Accelerating Cell Cycle Transitions. Potential mechanisms by which Rad might regulate cell growth *in vitro* include induction of the expression of autocrine factors, increasing plating efficiency, and/or acceleration of cell cycle. To see if Rad induced the expression of autocrine factors, we collected conditioned media from the Puro, Rad Wt, or Rad S105N cultures, added them to control Puro cells, and measured growth. No significant difference was found among these culture media (data not shown). In addition, we treated the cells with mitomycin-C to prevent DNA replication and then replated these cells into tissue culture plates to look for the possibility of changing the plating efficiency of cells by Rad. Again, no difference in plating efficiency was observed among the Puro, Rad Wt, and Rad S105N cells (data not shown). Finally, we determined if Rad had any effect on cell cycle transition. The cells were synchronized by 84 h of serum-starvation (Fig. 4, *A–C*) and then treated with serum for

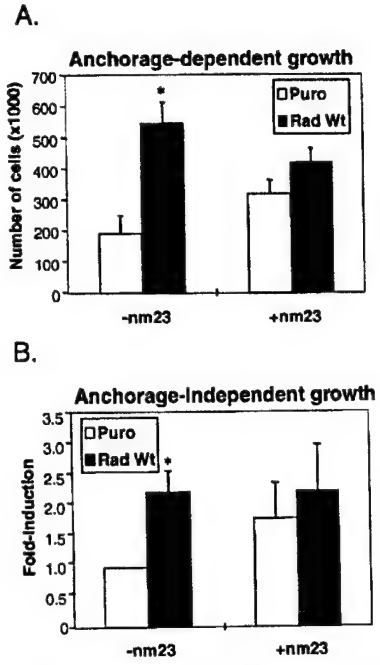

Fig. 2. Effects of Rad and nm23 on anchorage-dependent and anchorage-independent growth. *A*, anchorage-dependent growth of MDA-MB435 cells overexpressing Rad and/or nm23. Cells (1×10^4) were plated/well in multiple 24-well plates and incubated for 6 days, and numbers of cells were determined by trypsinization and counting in a hemocytometer or Coulter particle counter. *B*, soft-agar colonization of MDA-MB435 cells overexpressing Rad and/or nm23. Cells (3×10^3) were plated in 0.5 ml of medium containing 0.3% agar over a 0.5 ml plug of medium containing 0.5% agar. Colonies were counted after 14 days of incubation. In this panel, data are presented as fold-induction by expression of Rad and/or nm23 relative to the Puro control in the absence of nm23 coexpression. All of the data were obtained from three independent experiments with each group represented by triplicate wells. Significance was determined relative to corresponding control by Student's *t* test; * = $P < 0.05$.

12 or 24 h, and cell cycle distributions were determined by flow cytometry of propidium iodide-stained cells. Overexpression of Wt Rad or the S105N mutant caused a large portion of cells to shift into S/G_2M phases after 24 h of serum treatment (Fig. 4, *H* and *I*). This suggests that the mechanism by which Rad promotes cell growth involves, at least in part, induction of cell cycle transitions rather than secretion of some autocrine growth factors or change in plating efficiency.

The Rad-Nm23 Interaction Regulated Tumor Formation in Nude Mice. The above experiments indicate that Rad is able to increase numbers of colonies formed in soft agar, and this effect is blunted in the presence of nm23 (Fig. 2*B* and Fig. 3*F*). To determine whether Rad and/or nm23 could affect the growth of tumors derived from human breast cancer cells *in vivo*, a suspension of 5×10^5 MDA-MB435 cells expressing either Wt Rad or Rad S105N in the absence or presence of coexpression of nm23 was injected s.c. into the left hind flank of 5-week-old, female NIH Swiss Nude mice, and tumor growth was monitored. Mice that received cells overexpressing either Rad Wt or Rad S105N in the absence of nm23 developed larger tumors than mice receiving the control cells (Fig. 5, *A* and *B*). A significant increase was observed in the percentage of Rad Wt or Rad S105N mice that developed detectable tumors at early times after injection (day 33 and day 27; Fig. 5*C*). Furthermore, by day 33 there was a significant increase in the size of tumors in the Rad Wt positive/nm23 negative group relative to the corresponding Puro control (Fig. 5*D*). This is in agreement with the *in vitro* data that also showed Rad affecting the early time points of cell growth (Fig. 3*D*). Interestingly, as in the *in vitro* experiments, the growth-promoting

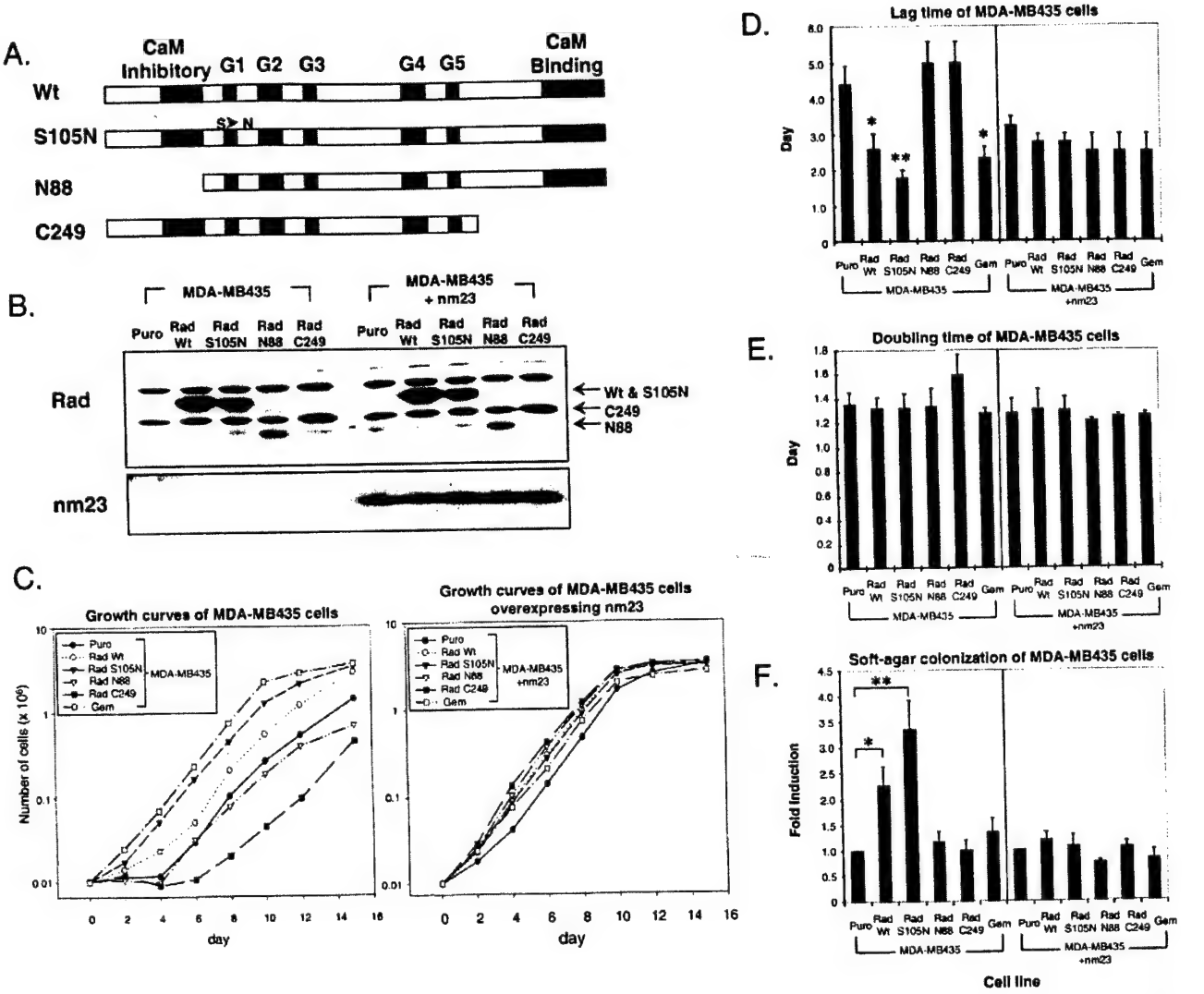

Fig. 3. Structure-function relationship of Rad on growth. *A*, schematic diagram shows the structures of Wt and mutants of Rad. G1-G5 refer to the conserved domains found similar in members of the Ras family of GTPases. Regions that bind or interfere CaM binding were indicated. *B*, Western blot analysis of cells expressing Wt or mutant forms of Rad in the absence or presence of coexpression of nm23. *C*, growth curves of Rad/nm23 overexpressors. *D* and *E*, lag time and doubling time of Rad/nm23-overexpressing cell lines. Lag times were determined by the period of adaptation after subculture before entering exponential growth. Doubling times were determined by calculating growth rates during exponential growth. *F*, soft-agar colonization of Rad/nm23 overexpressors. Data are presented as fold-induction by expression of either Wt Rad or different mutants of Rad or Gem relative to the Puro controls for each nm23 −/+ group. Cells were grown and assayed as described in Fig. 2. Data were obtained from three or four independent experiments. Significance was determined relative to corresponding Puro control using Student's *t* test; * = $P < 0.05$; ** = $P < 0.01$.

effect of Rad was blocked in the cells coexpressing nm23, suggesting that nm23 may play a role as a dominantly negative regulator for Rad in tumor growth (Fig. 5, *A*, *B*, and *D*). Moreover, nm23 caused significant decreases in the probabilities of tumor formation at days 27 and 33, and this effect appeared to be independent of the presence of Rad Wt or Rad S105N (Fig. 5*C*). With only one exception, spontaneous metastases were not evident at 67 days after injection, at which time the mice were sacrificed under animal welfare guidelines, because of the primary tumor sizes of mice.

The histological appearance of tumor resembled typical medullary carcinoma, consistent with the origin of the cells (41). Histological analysis of cross-sections of tumors also revealed that Rad Wt tumors showed a relatively larger area (approximately 30–40% of the cross-section area) with degenerative changes (picnotic nuclei, necrosis, and hemorrhage) as compared with the Puro controls that contain only about 10% of the area involved with degenerative changes (Fig. 6).

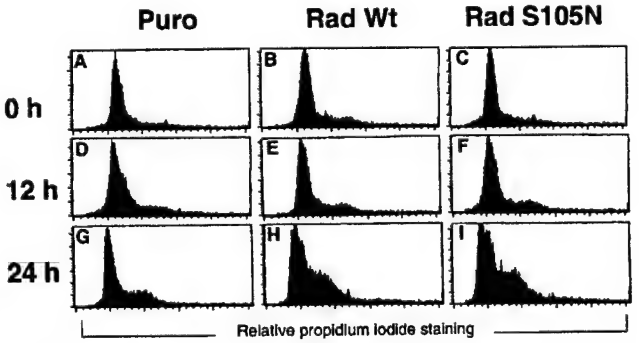

Fig. 4. Effects of Rad on cell cycle distribution. MDA-MB435 cells overexpressing Wt Rad, S105N mutant, or empty vector control (Puro) were serum-starved for 84 h and then treated with 10% serum for 12 and 24 h. DNA content was determined by propidium iodide staining and flow cytometry analysis. The experiments were repeated twice. A representative experiment is shown.

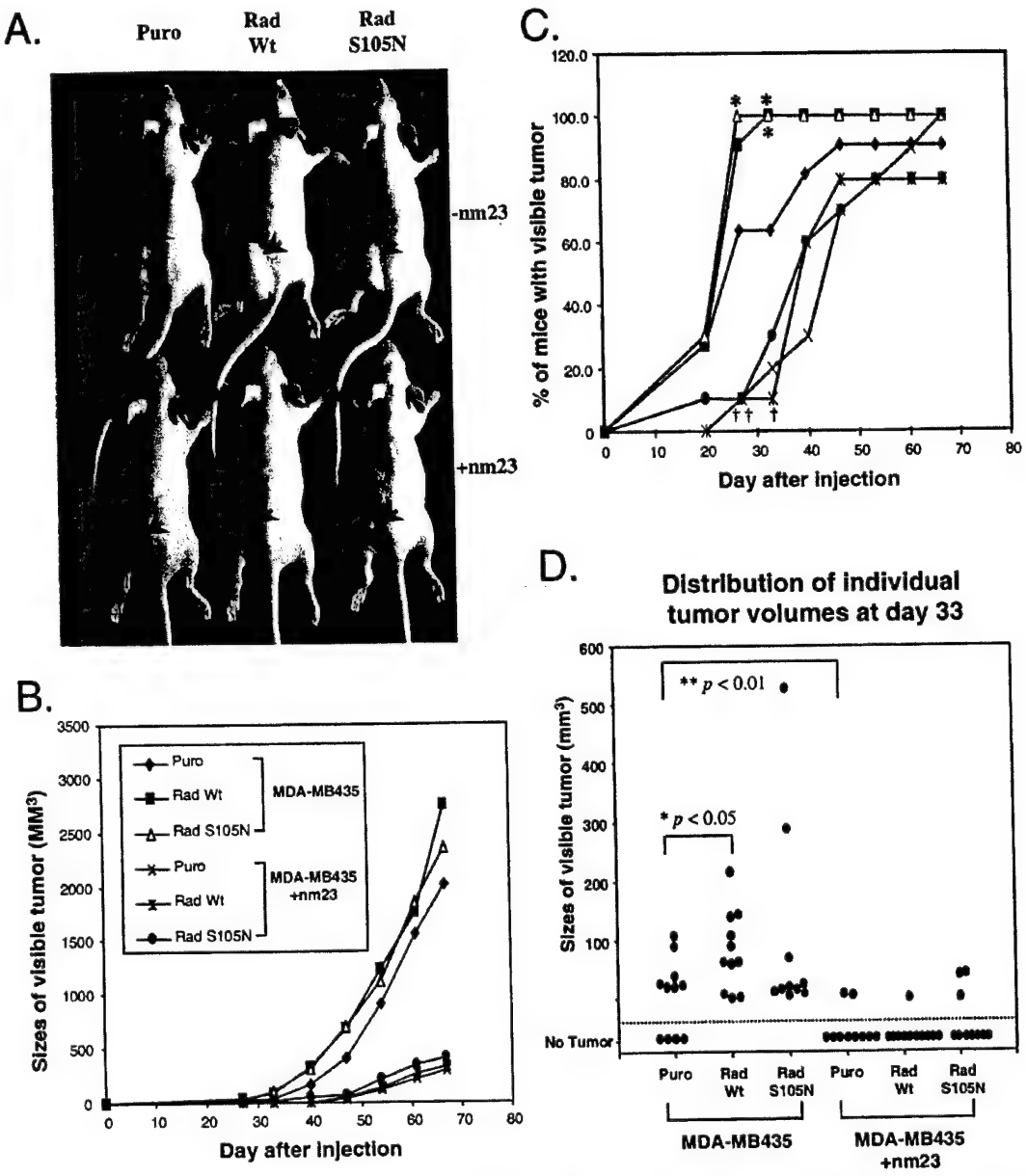

Fig. 5. Effects of Rad and nm23 on tumor growth in nude mice. Five-week old NIH Swiss Nude mice received injections in the left hind flank with 5×10^5 cells expressing either Wt or mutant Rad with or without coexpression of nm23. *A*, shows representative mice from each treatment group at day 67 after injection. *Arrows* indicate tumors. *B*, growth curves of tumors in nude mice. Data are presented as average volume of tumors from mice receiving either control or Rad overexpressors in the presence or absence of coexpression of nm23 ($n = 10$ or 11). *C*, percentage of mice with visible tumors: * = $P < 0.05$ as determined relative to corresponding Puro control, statistical significance was determined using the Fisher's exact test: † = $P < 0.05$; †† = $P < 0.001$ as determined relative to corresponding nm23 negative. *D*, distribution of individual tumor volumes at day 33. Significance was determined relative to the control using a nonparametric Mann-Whitney test; * = $P < 0.05$; ** = $P < 0.01$.

DISCUSSION

Ras-related GTP-binding proteins comprise a superfamily of molecules that play important roles in a wide variety of cellular processes including cell proliferation and differentiation (42), apoptosis (43), intracellular vesicular trafficking (44), cytoskeletal rearrangement (45), cell cycle regulation (46), and glucose transportation in cells (16, 47). Activating mutations of Ras occur in about 30% of all of human tumors, including breast cancer (48, 49). Rad itself has not been implicated in tumor development, although another member of the Rad family, Gem, was originally identified by its overexpression in mitogen-stimulated T lymphocytes and v-abl-transformed pre-B cells (8, 9). In the present study, we have demonstrated not only that Rad is present in some human breast cancers, but also that it is able to accelerate growth of breast cancer cells *in vitro* and increase the tumorigenicity of these cells when injected into nude mice.

Rad was originally identified to be highly expressed in the skeletal muscle of some type-2 diabetic humans and is normally also highly expressed in heart and lung (7). When overexpressed in skeletal muscle, Rad alters contractility and potentiates high fat diet-induced insulin resistance.[4] In transgenic mice with overexpression of Rad in the heart, there is cardiac hypertrophy and an increase in metabolic

[4] J. Ilany, P. J. Bilan, S. Kapur, J. S. Caldwell, M-E. Patti, A. Marette, and C. R. Kahn. Overexpression of Rad in muscle of mice worsens high-fat-diet-induced insulin resistance and glucose intolerance and lowers plasma triglyceride level, manuscript in preparation.

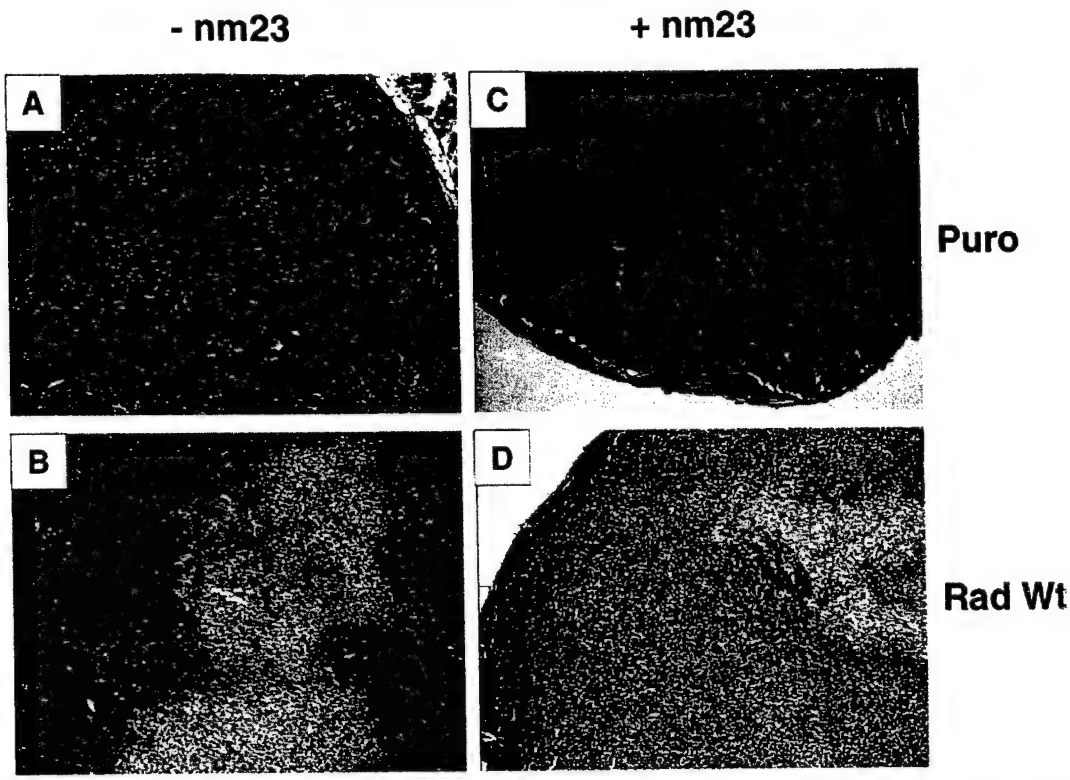

Fig. 6. Histological analysis of tumors from mice that received injections with MDA-MB435 cells. Tumors removed from mice were fixed in 10% formalin and stained with H&E. All of the tumors show typical morphology of medullary breast carcinoma. Lighter staining areas in *B* and *D* show degeneration. Original magnification, ×40.

activity.[5] Moreover, epidemiological evidence has suggested hyperinsulinemia and insulin resistance found in type-2 diabetes mellitus are risk factors for the development of breast cancer (50, 51). *In vivo* experiments using euglycemic, hyperinsulinemic clamps have shown that insulin is able to stimulate Rad expression (52). This raises the possibility that Rad overexpression found in some patients with type-2 diabetes mellitus may be the results of hyperinsulinemia rather than the cause of insulin resistance. Taken together with the data presented in this study, which indicate a growth-accelerating role of Rad in human breast cancer, these data suggest that in type-2 diabetes, Rad may be more closely related to changes in cell growth than changes in cell metabolism.

Studies on the structure-function relationship reveal that the growth-promoting effects of Rad *in vitro* may be mediated through its NH_2- and COOH-terminal regions. Previously (14), we have identified a CaM-binding region in residues 278–297 at the COOH terminus of Rad and a potential negatively regulatory region of Rad-CaM interaction in the NH_2 terminus of Rad which, when removed, increases the binding of Rad to CaM. In the current study, we found that deletions of either the CaM-binding domain (C249) or the CaM-inhibitory domain (N88) of Rad results in losing its growth-promoting effect. Gem, which can also bind CaM (40), also accelerated breast cancer cell growth *in vitro* but differed from Rad in its inability to promote colony formation in soft agar. These data suggest that interaction of these GTPases with CaM through their COOH-terminal extensions may be important for their ability to accelerate anchorage-dependent cell growth, although additional sequences in the NH_2 terminus may also be critical. It has been shown that CaM regulates the G_1-S transition of the cell cycle by increasing the activities of cyclin-dependent kinase 4, cyclin-dependent kinase 2, and retinoblastoma protein phosphorylation (53). In this study, we also found that overexpression of Rad in the MDA-MB435 cells results in acceleration of cell cycle transitions in response to serum stimulation. Taken together, these data suggest that Rad may regulate the growth of breast cancer cells through its interaction with CaM and an acceleration of cell cycle transition.

Another potential mechanism by which Rad may regulate cell growth is related to changes in cytoskeletal adhesion and cell motility. This is suggested by its ability to interact with CaM, CaMKII (14), and β-tropomyosin (15). Tropomyosin clearly plays a role in contraction and cytoskeletal organization, both of which contribute to cell motility (54). CaM and CaMKII have also been shown to be involved in calcium-mediated cell movement (55). Interestingly, there are several lines of well-documented evidence concerning the involvement of small G proteins in cell adhesion and migration (for review, see Ref. 56). Aberrations in these events lead to cell transformation, tumor invasion, and metastasis; *e.g.*, the Rho family proteins, including cdc42, Rac1, and RhoA, have been suggested by multiple studies (57, 58) to play an important role in cytoskeletal rearrangements, cell adhesion, tumor invasion, and metastasis. It seems likely that Rad may regulate growth of tumor cells via similar mechanisms used by the Rho family small G proteins. This is an interesting topic for future studies.

Data from our *in vitro* and *in vivo* studies suggest that nm23 may act as a dominant negative regulator of Rad and that coexpression of nm23 with Rad abolishes its growth-promoting effects. Nm23 possesses several enzymatic activities and mediates a number of biological functions, including proliferation, differentiation, cell motility, and suppression of metastasis (31). We have demonstrated previously (59) a coordinate, bi-directional, and bimolecular interaction between Rad and nm23. In the present study, we find that this interaction appears to play a significant role in control of tumor cell growth. This

[5] L. Field, P. J. Bilan, and C. R. Kahn, manuscript in preparation.

is particularly interesting because the expression of *nm23* gene has been shown to inversely correlate with metastatic potential in several tumor types (60, 61). To date, the exact mechanism of these effects has been unclear. It has been shown that nm23 may mediate part of its effects by altering cell motility (27). Taken together with the fact that Rad may also affect motility via interactions with CaM, CaMKII (14), and β-tropomyosin (15), it is possible that the Rad-nm23 complex acts in a coordinated manner to regulate growth of tumor cells via pathways involved in cytoskeletal organization and cell motility. Furthermore, in this complex, nm23 functions as a GTPase-activating protein and a guanine nucleotide exchange factor for Rad, determining the balance between GTP- and GDP-Rad (17). However, the GTPase activity of Rad does not appear to be critical to its effects on *in vitro* growth of breast cancer cells because this effect appears to favor the GDP-bound form of Rad (the S105N mutant) more than the Wt protein. This is similar to the ability of Rad to interact with CaM, CaMKII, and tropomyosin, all of which favor the GDP form of Rad (14, 15). However, both the Wt Rad and the S105N mutant have similar effects on promoting tumor growth *in vivo*. These phenomena may be explained by having distinct cellular environments between *in vitro* and *in vivo*, which may differentially regulate the activities of Rad and nm23.

In the present study, we have also shown that Rad expression in cell lines significantly increases the tumor growth and the percentage of mice that develop tumors *in vivo* at early times after injection of breast cancer cells. This agrees with the *in vivo* studies where we have observed that high levels of Rad expression are significantly associated with several features indicative of more aggressive tumors, including larger size, higher grade, and more extensive nodal metastasis. Interestingly, the latter features are also those with which loss of nm23 was initially associated (62). However, whereas subsequent investigation has not always confirmed these associations (63), in some of the larger studies, a relationship between persistence of nm23 and longer disease-free and metastasis-free survival has emerged (60, 61). Our current findings, that the positive effects of Rad on tumor growth can be abrogated by interaction with nm23 and the implication that the interaction between these proteins may be significant in prognosis, may be important in resolving the discrepancies between such studies to determine the role of nm23. However, a more extensive study on a much larger cohort of cases than the cohort used in this study will be required to determine the *in vivo* significance in human tumors of an interaction with nm23 and the prognostic significance of Rad expression.

In summary, we have shown that some human breast cancers express the small G protein, Rad, and that Rad is able to regulate growth of breast cancer cells both *in vitro* and in *vivo*. Furthermore, we have shown that this effect of Rad is blocked by coexpression of nm23. These results suggest a novel mechanism by which interaction between Rad and nm23 may play an important role in the regulation of growth and tumorigenicity of breast cancer. Rad may also provide both a new diagnostic test for staging of breast cancer and a new therapeutic target for its treatment.

ACKNOWLEDGMENTS

We thank S. E. Curtis for assistance in injection of cells into nude mice. We are also grateful to T-L. Azar and J. Konigsberg for excellent secretarial assistance.

REFERENCES

1. McManus, M. J., and Welsch, C. W. The effect of estrogen, progesterone, thyroxine, and human placental lactogen on DNA synthesis of human breast ductal epithelium maintained in athymic nude mice. Cancer (Phila.), *54:* 1920–1927, 1984.
2. Papa, V., Hartmann, K. K., Rosenthal, S. M., Maddux, B. A., Siiteri, P. K., and Goldfine, I. D. Progestins induce down-regulation of insulin-like growth factor-I (IGF-I) receptors in human breast cancer cells: potential autocrine role of IGF-II. Mol. Endocrinol., *5:* 709–717, 1991.
3. Clevenger, C. V., Chang, W. P., Ngo, W., Pasha, T. L., Montone, K. T., and Tomaszewski, J. E. Expression of prolactin and prolactin receptor in human breast carcinoma. Evidence for an autocrine/paracrine loop. Am. J. Pathol., *146:* 695–705, 1995.
4. Osborne, C. K., Bolan, G., Monaco, M. E., and Lippman, M. E. Hormone responsive human breast cancer in long-term tissue culture: effect on insulin. Proc. Natl. Acad. Sci. USA, *73:* 4536–4540, 1976.
5. Rasmussen, A. A., and Cullen, K. J. Paracrine/autocrine regulation of breast cancer by the insulin-like growth factors. Breast Cancer Res. Treat., *47:* 219–233, 1998.
6. Dahiya, R., and Deng, G. Molecular prognostic markers in breast cancer. Breast Cancer Res. Treat., *52:* 185–200, 1998.
7. Reynet, C., and Kahn, C. R. Rad. A member of the ras family overexpressed in muscle of type II diabetic humans. Science (Washington DC), *262:* 1441–1444, 1993.
8. Maguire, J., Santoro, T., Jensen, P., Siebenlist, U., Yewdell, J., and Kelly, K. Gem. An induced, immediate early protein belonging to the Ras family. Science (Washington DC), *265:* 241–244, 1994.
9. Cohen, L., Mohr, R., Chen, Y. Y., Huang, M., Kato, R., Dorin, D., Tamanoi, F., Goga, A., Afar, D., Rosenberg, N., and Witte, O. Transcriptional activation of a *ras*-like gene (*kir*) by oncogenic tyrosine kinases. Proc. Natl. Acad. Sci. USA, *91:* 12448–12452, 1994.
10. Finlin, B. S., and Andres, D. A. Rem is a new member of the Rad- and Gem/Kir Ras-related GTP-binding protein family repressed by lipopolysaccharide stimulation. J. Biol. Chem., *272:* 21982–21988, 1997.
11. Finlin, B. S., Shao, H., Kadono-Okuda, K., Guo, N., and Andres, D. A. Rem2, a new member of the Rem/Rad/Gem/Kir family of Ras-related GTPases. Biochem. J., *347:* 223–231, 2000.
12. Pan, J. Y., Fieles, W. E., White, A. M., Egerton, M. M., and Silberstein, D. S. Ges, a human GTPase of the Rad/Gem/Kir family, promotes endothelial cell sprouting and cytoskeleton reorganization. J. Cell Biol., *149:* 1107–1116, 2000.
13. Bilan, P. J., Moyers, J. S., and Kahn, C. R. The Ras-related protein Rad associates with the cytoskeleton in a non lipid-dependent manner. Exp. Cell Res., *242:* 391–400, 1998.
14. Moyers, J. S., Bilan, P. J., Zhu, J., and Kahn, C. R. Rad, and Rad-related GTPases interact with calmodulin and calmodulin-dependent protein kinase II. J. Biol. Chem., *272:* 11832–11839, 1997.
15. Zhu, J., Bilan, P. J., Moyers, J. S., Antonetti, D. A., and Kahn, C. R. Rad, a novel ras-related GTPase, interacts with skeletal muscle β-tropomyosin. J. Biol. Chem., *271:* 768–773, 1996.
16. Moyers, J. S., Bilan, P. J., Reynet, C., and Kahn, C. R. Overexpression of Rad inhibits glucose uptake in cultured muscle and fat cells. J. Biol. Chem., *271:* 23111–23116, 1996.
17. Zhu, J., Tseng, Y. H., Kantor, J. D., Rhodes, C. J., Zetter, B. R., Moyers, J. S., and Kahn, C. R. Interaction of the Ras-related protein associated with diabetes Rad and the putative tumor metastasis suppressor NM23 provides a novel mechanism of GTPase regulation. Proc. Natl. Acad. Sci. USA, *96:* 14911–14918, 1999.
18. Steeg, P. S., Bevilacqua, G., Kopper, L., Thorgeirsson, U. P., Talmadge, J. E., Liotta, L. A., and Sobel, M. E. Evidence for a novel gene associated with low tumor metastatic potential. J. Natl. Cancer Inst. (Bethesda), *80:* 200–204, 1988.
19. Urano, T., Takamiya, K., Furukawa, K., and Shiku, H. Molecular cloning and functional expression of the second mouse nm23/NDP kinase gene, *nm23–M2*. FEBS Lett., *309:* 358–362, 1992.
20. Rosengard, A. M., Krutzsch, H. C., Shearn, A., Biggs, J. R., Barker, E., Margulies, I. M. K., King, C. R., Liotta, L. A., and Steeg, P. S. Reduced Nm23/Awd protein in tumour metastasis and aberrant *Drosophila* development. Nature (Lond.), *342:* 177–170, 1989.
21. Stahl, J. A., Leone, A., Rosengard, A. M., Porter, L., King, C. R., and Steeg, P. S. Identification of a second human *nm23* gene, *nm23–H2*. Cancer Res., *51:* 445–449, 1991.
22. Venturelli, D., Martinez, R., Melotti, P., Casella, I., Peschle, C., Cucco, C., Spampinato, G., Darzynkiewicz, Z., and Calabretta, B. Overexpression of DR-nm23, a protein encoded by a member of the *nm23* gene family, inhibits granulocyte differentiation and induces apoptosis in 32Dc13 myeloid cells. Proc. Natl. Acad. Sci. USA, *92:* 7435–7439, 1995.
23. Milon, L., Rousseau-Merck, M., Munier, A., Erent, M., Lascu, I., Capeau, J., and Lacombe, M. nm23–H4, a new member of the family of human nm23/nucleoside diphosphate kinase genes localized on chromosome 16p13. Hum. Genet., *99:* 550–557, 1997.
24. Munier, A., Feral, C., Milon, L., Phung-Ba Pinon, V., Gyapay, G., Capeau, J., Guellaen, G., and Lacombe, M-L. A new human nm23 homologue (nm23–H5) specifically expressed in testis germinal cells. FEBS Lett., *434:* 289–294, 1998.
25. Leone, A., Flatow, U., King, C. R., Sandeen, M. A., Margulies, I. M. K., Liotta, L. A., and Steeg, P. S. Reduced tumor incidence, metastatic potential, and cytokine responsiveness of *nm23*-transfected melanoma cells. Cell, *65:* 25–35, 1991.
26. Leone, A., Flatow, U., VanHoutte, K., and Steeg, P. S. Transfection of human *nm23–H1* into the human MDA-MB-435 breast carcinoma cell line: effects on tumor metastatic potential, colonization and enzymatic activity. Oncogene, *8:* 2325–2333, 1993.
27. Kantor, J. D., McCormick, B., Steeg, P. S., and Zetter, B. R. Inhibition of cell motility after nm23 transfection of human and murine tumor cells. Cancer Res., *53:* 1971–1973, 1993.
28. Wagner, P. D., and Vu, N. D. Phosphorylation of ATP-citrate lyase by nucleoside diphosphate kinase. J. Biol. Chem., *270:* 21758–21764, 1995.

29. Freije, J. M., Blay, P., MacDonald, N. J., Manrow, R. E., and Steeg, P. S. Site-directed mutation of Nm23-H1. Mutations lacking motility suppressive capacity upon transfection are deficient in histidine-dependent protein phosphotransferase pathways *in vitro*. J. Biol. Chem., *272:* 5525–5532, 1997.
30. MacDonald, N. J., De La Rosa, A., Benedict, M. A., Freije, J. M. P., Krutsch, H., and Steeg, P. S. A serine phosphorylation of nm23, and not its nucleoside diphosphate kinase activity, correlates with suppression of tumor metastatic potential. J. Biol. Chem., *268:* 25780–25789, 1993.
31. Lombardi, D., Lacombe, M. L., and Paggi, M. G. nm23. Unraveling its biological function in cell differentiation. J. Cell. Physiol., *182:* 144–149, 2000.
32. Postel, E. H. NM23/Nucleoside diphosphate kinase as a transcriptional activator of c-myc. Curr. Top. Microbiol. Immunol., *213:* 233–252, 1996.
33. Biggs, J., Hersperger, E., Steeg, P. S., Liotta, L. A., and Shearn, A. A *Drosophila* gene that is homologous to a mammalian gene associated with tumor metastasis codes for a nucleoside diphosphate kinase. Cell, *63:* 933–940, 1990.
34. Rosengard, A. M., Krutzsch, H. C., Shearn, A., Biggs, J. R., Barker, E., Margulies, I. M. K., King, C. R., Liotta, L. A., and Steeg, P. S. Reduced Nm23/Awd protein in tumour metastasis and aberrant *Drosophila* development. Nature (Lond.), *342:* 177–180, 1989.
35. Caligo, M. A., Cipollini, G., Fiore, L., Calvo, S., Basolo, F., Collecchi, P., Ciardiello, F., Pepe, S., Petrini, M., and Bevilacqua, G. *NM23* gene expression correlates with cell growth rate and S-phase. Int. J. Cancer, *60:* 837–842, 1995.
36. Cipollini, G., Berti, A., Fiore, L., Rainaldi, G., Basolo, F., Merlo, G., Bevilacqua, G., and Caligo, M. A. Down-regulation of the *nm23.hl* gene inhibits cell proliferation. Int. J. Cancer, *73:* 297–302, 1997.
37. Gervasi, F., D'Agnano, I., Vossio, S., Zupi, G., Sacchi, A., and Lombardi, D. *nm23* influences proliferation and differentiation of PC12 cells in response to nerve growth factor. Cell Growth Differ., *7:* 1689–1695, 1996.
38. Hiller, T., Snell, L., and Watson, P. H. Microdissection RT-PCR analysis of gene expression in pathologically defined frozen tissue sections. Biotechniques, *21:* 38–40, 1996.
39. Elston, C. W., and Ellis, I. O. Pathological prognostic factors in breast cancer. I. The value of histological grade in breast cancer: experience from a large study with long-term follow-up. Histopathology (Oxf.), *19:* 403–410, 1991.
40. Fischer, R., Wei, Y., Anagli, J., and Berchtold, M. W. Calmodulin binds to and inhibits GTP binding of the Ras-like GTPase Kir/Gem. J. Biol. Chem., *271:* 25067–25070, 1996.
41. Brinkley, B. R., Beall, P. T., Wible, L. J., Mace, M. L., Turner, D. S., and Cailleau, R. M. Variations in cell form and cytoskeleton in human breast carcinoma cells *in vitro*. Cancer Res., *40:* 3118–3129, 1980.
42. Lange-Carter, C. A., and Johnson, G. L. Ras-dependent growth factor regulation of MEK kinase in PC12 cells. Science (Washington DC), *265:* 1458–1461, 1994.
43. Evan, G., and Littlewood, T. A matter of life and cell death. Science (Washington DC), *281:* 1317–1322, 1998.
44. Zerial, M., and Stenmark, H. Rab GTPases in vesicular transport. Curr. Opin. Cell Biol., *5:* 613–620, 1993.
45. Hall, A. Small GTP-binding proteins and the regulation of the actin cytoskeleton. Annu. Rev. Cell Biol., *10:* 31–54, 1994.
46. Yang, J. J., Kang, J. S., and Krauss, R. S. Ras signals to the cell cycle machinery via multiple pathways to induce anchorage-independent growth. Mol. Cell. Biol., *18:* 2586–2595, 1998.
47. Cormont, M., Bortoluzzi, M. N., Gautier, N., Mari, M., Van Obberghen, E., and Le Marchand-Brustel, Y. Potential role of Rab4 in the regulation of subcellular localization of Glut4 in adipocytes. Mol. Cell. Biol., *16:* 6879–6886, 1996.
48. Bos, J. L. *ras* oncogenes in human cancer: a review. Cancer Res., *49:* 4682–4689, 1989.
49. Clark, G. J., and Der, C. J. Aberrant function of the Ras signal transduction pathway in human breast cancer. Breast Cancer Res. Treat., *35:* 133–144, 1995.
50. DeMali, K. A., and Kazlauskas, A. Activation of Src family members is not required for the platelet-derived growth factor β receptor to initiate mitogenesis. Mol. Cell. Biol., *18:* 2014–2022, 1998.
51. Volkers, N. Diabetes and cancer: scientists search for a possible link. J. Natl. Cancer Inst. (Bethesda), *92:* 192–194, 2000.
52. Laville, M., Auboeuf, D., Khalfallah, Y., Vega, N., Riou, J. P., and Vidal, H. Acute regulation by insulin of phosphatidylinositol-3-kinase, Rad, Glut4, and lipoprotein lipase mRNA levels in human muscle. J. Clin. Investig., *98:* 43–49, 1996.
53. Taulés, M., Ruis, E., Talaya, D., López-Girona, A., Bachs, O., and Agell, N. Calmodulin is essential for cyclin-dependent kinase 4 (Cdk4) activity and nuclear accumulation of cyclin D1-Cdk4 during G_1. J. Biol. Chem., *273:* 33279–33286, 1998.
54. Babcoke, G. G., and Fowler, V. M. Isoform-specific interaction of tropomodulin with skeletal muscle and erythrocyte tropomyosins. J. Biol. Chem., *269:* 27510–27518, 1994.
55. Pauly, R. R., Bilato, C., Sollott, S. J., Monticone, R., Kelly, P. T., Lakatta, E. G., and Crowe, M. T. Role of calcium/calmodulin-dependent protein kinase II in the regulation of vascular smooth muscle cell migration. Circulation, *91:* 1107–1115, 1995.
56. Blanchard, J. M. Small GTPases, adhesion, cell cycle control and proliferation. Pathol. Biol., *48:* 318–327, 2000.
57. Mohri, T., Adachi, Y., Ikehara, S., Hioki, K., Tokunaga, R., and Taketani, S. Activated Rac1 selectively up-regulates the expression of integrin α6β4 and induces cell adhesion and membrane ruffles of nonadherent colon cancer Colo201 cells. Exp. Cell Res., *253:* 533–540, 1999.
58. Evers, E. E., Zondag, G. C., Malliri, A., Price, L. S., ten Klooster, J. P., van der Kammen, R. A., and Collard, J. G. Rho family proteins in cell adhesion and cell migration. Eur. J. Cancer, *36:* 1269–1274, 2000.
59. Aprile, J. A., Russo, M., Pepe, M. S., and Loughran, T. P., Jr. Activation signals leading to proliferation of normal and leukemic CD3+ large granular lymphocytes. Blood, *78:* 1282–1285, 1991.
60. Heimann, R., Ferguson, D. J., and Hellman, S. The relationship between nm23, angiogenesis, and the metastatic proclivity of node-negative breast cancer. Cancer Res., *58:* 2766–2771, 1998.
61. Charpin, C., Garcia, S., Bonnier, P., Martini, F., Andrac, L., Horschowski, N., Lavaut, M. N., and Allasia, C. Prognostic significance of Nm23/NDPK expression in breast carcinoma, assessed on 10-year follow-up by automated and quantitative immunocytochemical assays. J. Pathol., *184:* 401–407, 1998.
62. Bevilacqua, G., Sobel, M. E., Liotta, L. A., and Steeg, P. S. Association of low nm23 RNA levels in human primary infiltrating ductal breast carcinomas with lymph node involvement and other histopathological indicators of high metastatic potential. Cancer Res., *49:* 5185–5190, 1989.
63. Sawan, A., Lascu, I., Veron, M., Anderson, J. J., Wright, C., Horne, C. H., and Angus, B. NDP-K/nm23 expression in human breast cancer in relation to relapse, survival, and other prognostic factors: an immunohistochemical study. J. Pathol., *172:* 27–34, 1994.

American Journal of Pathology, Vol. 158, No. 3, March 2001

Expression of the Hypoxia-Inducible and Tumor-Associated Carbonic Anhydrases in Ductal Carcinoma *in Situ* of the Breast

Charles C. Wykoff,* Nigel Beasley,* Peter H. Watson,† Leticia Campo,* Stephen K. Chia,‡ Ruth English,§ Jaromir Pastorek,¶ William S. Sly,‖ Peter Ratcliffe,** and Adrian L. Harris*

From the Institute of Molecular Medicine and the Breast Screening Program,§ John Radcliffe Hospital, Oxford, United Kingdom; the Wellcome Trust Centre for Human Genetics,** Oxford, United Kingdom; the Department of Pathology,† University of Manitoba, Winnipeg, Manitoba, Canada; the Division of Medical Oncology,‡ British Columbia Cancer Agency, Vancouver, British Columbia, Canada; the Institute of Virology,¶ Slovak Academy of Sciences, Bratislava, Slovak Republic; and the Edward A. Doisy Department of Biochemistry,‖ St. Louis University School of Medicine, St. Louis, Missouri*

Carbonic anhydrases (CA) influence intra- and extracellular pH and ion transport in varied biological processes. We recently identified *CA9* and *CA12* as hypoxia-inducible genes. In this study we examined the expression of these tumor-associated CAs by immunohistochemistry in relation to necrosis and early breast tumor progression in 68 cases of ductal carcinoma *in situ* (DCIS) (39 pure DCIS and 29 DCIS associated with invasive carcinoma). CA IX expression was rare in normal epithelium and benign lesions, but was present focally in DCIS (50% of cases) and in associated invasive carcinomas (29%). In comparison, CA XII was frequently expressed in normal breast tissues (89%), in DCIS (84%), and in invasive breast lesions (71%). In DCIS, CA IX was associated with necrosis ($P = 0.0053$) and high grade ($P = 0.012$). In contrast, CA XII was associated with the absence of necrosis ($P = 0.036$) and low grade ($P = 0.012$). Despite this, augmented CA XII expression was occasionally observed adjacent to necrosis within high-grade lesions. Neither CA IX nor CA XII expression was associated with regional or overall proliferation as determined by MIB1 staining. Assessment of mammographic calcification showed that CA XII expression was associated with the absence of calcification ($n = 43$, $P = 0.0083$). Our results demonstrate that induction of CA IX and CA XII occurs in regions adjacent to necrosis in DCIS. Furthermore, these data suggest that proliferation status does not influence expression of either CA in breast tissues, that hypoxia may be a dominant factor in the regulation of CA IX, and that factors related to differentiation, as determined by tumor grade, dominate the regulation of CA XII. The existence of differential regulation and associations with an aggressive phenotype may be important in the development of selective inhibitors of CAs, because the latter have recently been shown to prevent tumor invasion. ***(Am J Pathol 2001, 158:1011–1019)***

The management of pre-invasive ductal carcinoma *in situ* (DCIS) of the breast has become an increasingly significant problem. This is due in part to both the increasing number of these lesions detected by mammography,[1,2] and the impetus provided by the demonstration that invasive breast cancer may be delayed or inhibited by tamoxifen therapy in women at high risk.[3,4] Assessment of DCIS and the risk of progression to invasive disease is complicated by the small size and focal nature of most breast lesions, and has traditionally been based primarily on morphological classification and grading of pre-invasive disease by the pattern of growth into comedo and noncomedo subtypes. Recently, radiological studies have suggested that abnormal patterns of calcification may be associated with high-grade DCIS,[5,6] whereas pathological studies have developed more reproducible and discriminating schema for classification of DCIS lesions.[7] Consequently, the presence of necrosis and nuclear grade[8,9] have emerged as important aspects to consider when assessing breast lesions, although consistent recognition and quantification of both parameters remains problematic.[10]

Necrosis is believed to represent the extreme manifestation of hypoxia within tissues.[11] Interestingly, tumor hypoxia has been shown to be a prognostic indicator for many tumor types, being associated with aggressive growth, metastasis, and poor response to treatment not

Supported by the Imperial Cancer Research Fund and the Wellcome Trust. P. H. W. is supported by a Scientist Award from the Medical Research Council of Canada, an Academic Award from the U. S. Army Medical Research and Materiel Command, and a Research Travel Fellowship from Burroughs Wellcome. S. K. C. is supported by the Shane Fellowship and the Canadian Breast Cancer Foundation.

Accepted for publication December 4, 2000.

Address reprint requests to Dr. Peter Watson, Dept. of Pathology, University of Manitoba, D212-770 Bannatyne Ave., Winnipeg, Manitoba, R3E 0W3, Canada. E-mail: pwatson@cc.umanitoba.ca.

only in patients treated with radiotherapy, but also in those treated with surgery alone.[12–16] Of potential importance for understanding these effects is the role of hypoxia in regulating patterns of gene expression. Studies of gene expression have defined several classes of genes that are up-regulated by hypoxia and demonstrated that activation of the transcriptional complex hypoxia-inducible factor-1 is a key mediator of many of these effects.[17,18] Genes that are up-regulated by microenvironmental hypoxia through hypoxia-inducible factor-1 activation include glucose transporters, glycolytic enzymes, and angiogenic growth factors.

We recently identified the two tumor-associated transmembrane carbonic anhydrases (CA) *CA9*[19–21] and *CA12*[20,22] as being up-regulated by hypoxia in epithelial tumor cell lines.[23] Furthermore, we demonstrated focal perinecrotic expression of CA IX in invasive human tumors, co-localizing with vascular endothelial growth factor mRNA expression and pimonidazole activation.[23]

CA9 and *CA12* are members of a family of catalytically active CAs that share the capacity to catalyze the reversible hydration of carbon dioxide to carbonic acid.[24] CA IX[19,21,25] has been studied extensively in several tumor types including lung, kidney, colon, and cervix, where its expression has been established as a marker of cellular proliferation and early dysplasia.[26–30] CA XII was initially identified in renal carcinoma,[22] and subsequently shown to be associated with colon carcinoma where altered expression occurs in early stages of tumorigenesis.[31] However, the expression of these CAs in breast cancer has not been examined.

We investigated CA IX and CA XII expression in breast cancer in anticipation that their expression might serve as indicators of tissue hypoxia, altered pH, and tumor progression. Specifically we wished to assess the pattern of expression of these genes in DCIS, where the appearance of necrosis and abnormal calcification is associated with a high risk of progression to invasive disease.

Materials and Methods

Tissue Specimens

Sixty-eight pathological specimens containing DCIS of the breast were selected from review of surgical resections collected from 1997 to 1999 at the John Radcliffe Hospital and the Churchill Hospital, Oxford, UK. The cohort comprised 39 cases of pure DCIS (DCIS−) and 29 cases of DCIS associated with invasive carcinoma in the same biopsy (DCIS+), either independent from or directly associated with adjoining invasive carcinoma.

All DCIS lesions were classified into histological grades on the basis of the predominant grade present in the tissue section studied for gene expression according to the Van Nuys grading system.[9,32] The presence of intraductal necrosis within any component of DCIS within the tissue section was evaluated in hematoxylin and eosin-stained sections by light microscopy. The radiological appearance was classified according to the presence and pattern of calcification[5,6] in preoperative mammograms for a subset of cases in which films were available (n = 43). These classifications were performed by a single pathologist (PHW) and radiologist (RE), respectively, without reference to the cohort's immunohistochemical data and outcome. Among the series of cases, the histological grades were as follows: 18 low grade (8 DCIS−, 10 DCIS+), 24 intermediate grade (15 DCIS−, 9 DCIS+), and 26 high grade (16 DCIS−, 10 DCIS+). Intraductal necrosis was present in 51 cases (75%), among which 29 were DCIS− and 22 DCIS+. Mammographic calcifications were present in 35 of 43 cases, among which 27 of 35 were DCIS− and eight of 35 DCIS+. The pattern of calcification was classified as linear type (14 cases) if the presence of any linear calcification was seen, nonlinear type (21 cases), or absent (eight cases).

Cell Lines and Immunoblotting

MDA-MB-231 and ZR-75.1 cell lines were from ATCC (Rockville, MD). Hypoxic conditions were generated in a Napco 7001 incubator (Precision Scientific, Winchester, VA) with 0.1% O_2, 5% CO_2, and balance N_2 for 16 hours. Whole-cell protein extracts were prepared from tissue culture cells by 10 seconds of homogenization in denaturing conditions as described.[33] Whole-cell protein extracts were prepared from tumors by fine section of frozen tissue and 30 seconds of homogenization in denaturing conditions identical to tissue-culture extracts. For Western analysis, aliquots were separated under reducing conditions by sodium dodecyl sulfate-polyacrylamide gel electrophoresis and transferred to Immobilon-P membranes (Millipore, Hertfordshire, UK). CA IX was detected using the mouse monoclonal anti-human CA IX antibody M75 (1:50) as described.[34] CA XII was detected using a rabbit polyclonal anti-human CA XII antibody (1:2000) as described.[22] horseradish peroxidase-conjugated goat-anti-mouse and swine anti-rabbit immunoglobulins (DAKO, Cambridgeshire, UK) (1:2000), respectively, were applied for 1 hour at room temperature. ECL Plus (Amersham Pharmacia, Buckinghamshire, UK) was used for visualization.

Immunohistochemistry (IHC)

Formalin-fixed, paraffin-embedded tissue specimens collected by standard surgical oncology procedures were obtained from the Pathology Department, John Radcliffe Hospital, Oxford, UK. Immunostaining of paraffin sections was performed after dewaxing and rehydrating 5-μm sections. Staining for CA IX, CA XII, and MIB1 was performed on serial sections. Endogenous peroxidase was blocked with 0.5% hydrogen peroxide in water for 30 minutes. Ten percent normal human serum in Tris-buffered saline was applied for 15 minutes at room temperature to block nonspecific protein binding. Primary antibodies: anti-human CA IX murine monoclonal antibody M75 (1:50);[35] anti-human CA XII rabbit polyclonal antibody (1:2000); anti-human Ki67 murine monoclonal antibody MIB1 (1:50) (Immunotech). Primary antibodies were

incubated for 30 minutes at room temperature in Tris-buffered saline with 5% normal human serum, followed by a 30-minute incubation with a peroxidase-conjugated secondary antibody. After each incubation, slides were washed twice with Tris-buffered saline for 5 minutes. Visualization of staining was by diaminobenzidine substrate for 8 minutes. Slides were counterstained with hematoxylin before mounting in Aquamount (BDH). Substitution of primary antibody with PBS was used as a negative control for each antibody. All staining was performed on an automated IHC stainer (MiniPrep 75; Tecan) at room temperature.

Assessment of CA IX, CA XII, and MIB1 Staining

Immunostaining for CA IX and CA XII was assessed by light microscopy and semiquantitative scoring was performed by a single pathologist (PHW), independently of the pathological assessment. Expression and intensity was scored (0, no staining; 1, weak staining; 2, moderate staining; and 3, strong staining), together with the percentage of normal or neoplastic epithelial cells showing expression within the tissue section (0 to 100%). The product of the intensity and the percentage gave a final immunostaining score (0 to 300; IHC score). MIB1 expression was assessed using a Chalkley point array method adapted from methods used to assess vascular density in breast sections.[11] Briefly, MIB1-immunostained section was reviewed at low magnification and five areas showing the highest density of MIB1-positive tumor cells were selected. These hot spots were then assessed at higher magnification (×25 objective) and the number of grid points that coincided with positive and negative tumor cell nuclei was counted. The mean ratio of MIB1-positive/MIB1-negative cells was then calculated. Each hot spot contained between 200 and 1000 tumor cells depending on DCIS histology.

Results

CA IX and CA XII Antibody Specificity

The anti-CA IX and anti-CA XII antibodies used in this study have been previously characterized for immunostaining in many human tissues.[22,31,34,36] However, neither antibody has been applied extensively to breast specimens. Therefore, initial experiments were performed to compare IHC profiles with immunoblotting signals from a set of six invasive breast ductal carcinomas. By IHC, two cases exhibited strong membranous staining for CA IX that was restricted to the invasive ductal carcinoma cells, one was weakly positive, and three were negative (data not shown). Two of the tumors that were either negative or weakly positive for CA IX by IHC exhibited strong membranous staining for CA XII, whereas four cases were negative (data not shown). Immunoblotting for CA IX and CA XII was performed in parallel on protein lysates obtained from the same tumor specimens. As shown in Figure 1A, immunoblotting for CA IX revealed a 54- to 58-kd doublet restricted to the two cases

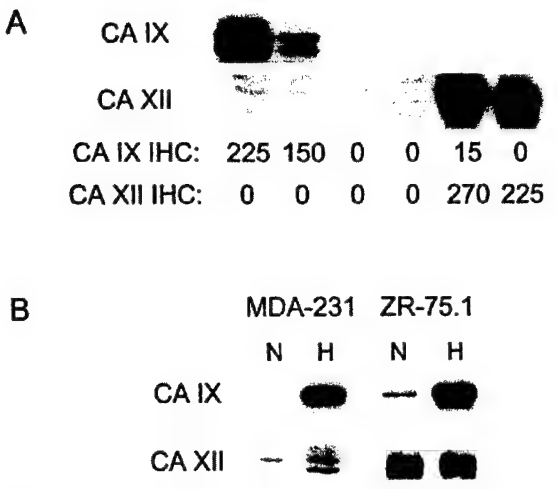

Figure 1. Immunoblotting for CA IX and CA XII. **A:** CA IX and CA XII expression detected by Western blot correlates with the respective immunostaining (IHC) score in invasive breast carcinomas. CA IX and CA XII are detected in tumor extracts that are strongly positive for CA IX or CA XII by IHC in adjacent paraffin sections (IHC score for each CA is indicated). **B:** CA IX and CA XII expression and response to hypoxia in two breast tumor cell lines exposed to either normoxia (N; 20% O_2) or hypoxia (H; 0.1% O_2) for 16 hours.

that were strongly positive by IHC. Similarly, immunoblotting for CA XII revealed a 46- to 48-kd doublet restricted to the two cases that were positive by IHC.

CA IX and CA XII Expression in Breast Cell Lines

We have previously demonstrated wide-spread hypoxic induction of *CA9* and *CA12* mRNA in various tumor cell lines.[23] Here we compared hypoxic induction of CA IX and CA XII in two breast cell lines selected as representative of estrogen receptor (ER)-negative and poorly differentiated (MDA-MB-231), and ER-positive and well-differentiated (ZR-75.1) breast cancer (Figure 1B). CA IX had an undetectable or low basal level of expression and was markedly induced by hypoxia. In comparison, CA XII had a higher level of normoxic expression and was further induced by hypoxia in one of the two cell lines.

CA IX Expression in Breast Tissues

A series of 68 DCIS breast cases were studied for CA IX expression by IHC. Subsets of these cases also contained normal lobular and ductal components (n = 47), and invasive ductal carcinoma components (n = 29). CA IX expression was present in normal epithelium in one of 47 cases (2%), and in this case was limited to focal expression adjacent to the site of a recent biopsy. In many cases, benign breast lesions were present within the tissue section, including cystic changes, apocrine metaplasia, blunt duct, and sclerosis adenosis. No expression was observed in any benign breast lesion. In DCIS lesions, focal membranous CA IX staining, typically adjacent to areas of necrosis, was present in 34 of 68 (50%) cases, including 23 of 39 (59%) pure DCIS and 11 of 29 (38%) DCIS associated with invasive disease. In those cases in which invasive disease was present on the

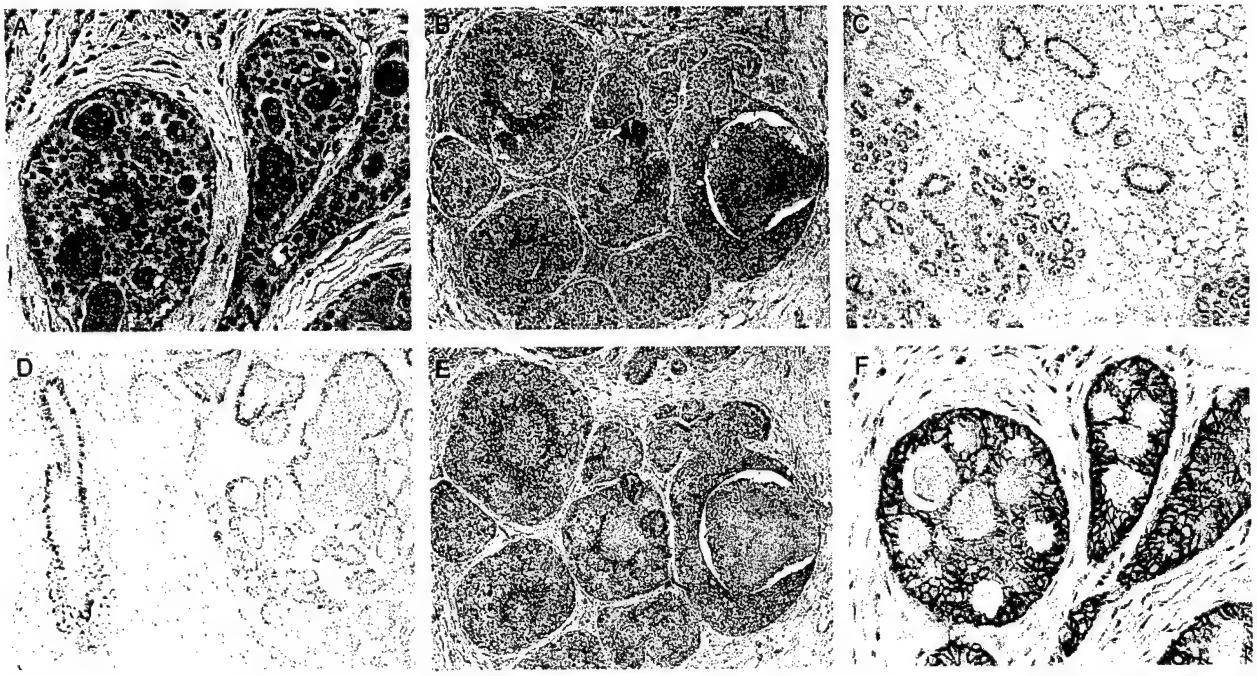

Figure 2. CA IX and CA XII have different expression profiles in non-neoplastic and neoplastic breast tissues. Low levels of CA IX expression are detected in low-grade DCIS (**A**) and more prominently in high-grade DCIS associated with central necrosis (**B**). CA XII expression in normal breast lobules and ducts (**C**), in ductal hyperplasia (**D**), in high-grade DCIS with accentuation adjacent to central luminal necrosis (**E**), and at higher levels in low-grade DCIS (**F**). Original magnifications, ×10 (**B–E**) and ×20 (**A** and **F**).

same tumor section, CA IX was expressed adjacent to regions of necrosis where this was present within the invasive component in four of 14 cases (29%). The presence of CA IX staining in both DCIS and invasive components was correlated ($r = 0.55$, $P = 0.04$). The focal perinecrotic nature of expression was reflected in the distribution of IHC scores with only 13 (19%) tumors scoring >10 (potential range of IHC score was 0 to 300, as described in Materials and Methods). The range of IHC scores was from 0 to 100 (median, 1; mean, 9; and SD, 17). Representative examples of low and high CA IX expression are illustrated in Figure 2, A and B. CA IX was significantly associated with high grade (grade low *versus* intermediate *versus* high; mean (SD), 2 (5), 11 (16), 13 (22), $P = 0.012$ analysis of variance) and the presence of necrosis (necrosis negative *versus* positive; mean (SD), 2 (5), 12 (19), $P = 0.0053$, Mann Whitney; Figure 3 and Table 1).

CA XII Expression in Breast Tissues

The expression of CA XII was assessed by IHC in sections adjacent to CA IX-stained sections for all 68 DCIS cases. Membranous staining of the basal-lateral aspects of breast epithelial cells was present in normal lobular and normal ductal epithelium in 42 of 47 (89%) cases and in every benign breast lesion observed (Figure 2, C and D). In ductal hyperplasia, CA XII expression was predominately limited to basal epithelial cells. In DCIS lesions, widespread membranous CA XII staining was present in 57 of 68 (84%) cases, including 31 of 39 (79%) pure DCIS and 26 of 29 (90%) DCIS associated with invasive disease. In those cases in which invasive disease was present on the same tumor section, CA XII was expressed in 10 of 14 cases (71%). The presence of CA XII staining in both DCIS and invasive components was highly correlated ($r = 0.91$, $P < 0.0001$). Although expression in DCIS was typically homogeneous throughout the tumor section, in intermediate- and high-grade DCIS where CA XII expression tended to be lower, expression was increased adjacent to areas of necrosis (Figure 2E).

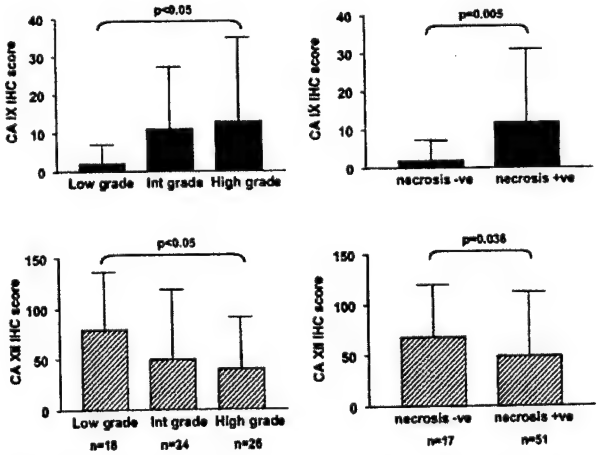

Figure 3. CA IX and CA XII expression are inversely related to grade and the presence of necrosis in DCIS. CA IX expression shown relative to grade (**upper left**) and necrosis (**upper right**) and CA XII expression shown relative to grade (**lower left**) and necrosis (**lower right**). Columns (CA IX, black; CA XII, hatched) represent the mean IHC score with bars showing SD relative to DCIS grade (low, intermediate, high) and necrosis (absent, present).

Table 1. Relationship between CA IX or CA XII Expression and Grade, Necrosis, and MIB1 Staining

DCIS parameter	No.	CA IX			CA XII		
		Negative	Positive		Negative	Positive	
Grade							
Low	18	14	4	$P = 0.0091$	7	11	ns ($P = 0.072$)
Intermediate	24	12	12	$P = 0.0023$ (t)	15	9	$P = 0.025$ (t)
High	26	8	18		19	7	
Necrosis							
Negative	17	14	3	$P = 0.002$	7	10	ns ($P = 0.55$)
Positive	51	20	31		17	34	
MIB1							
Low	13	6	7	ns ($P = 0.42$)	6	7	ns ($P = 0.69$)
High	13	4	9		5	8	

Statistical significance estimated by χ^2 test and χ^2 test for trend (t).

The distribution of IHC scores was wider than for CA IX, with 17 (25%) tumors scoring 60 or more (potential range, 0 to 300). The range of IHC scores was from 0 to 270 (median, 40; mean, 54; and SD, 61). Representative examples of low and high CA XII expression are illustrated in Figure 2, E and F. CA XII was significantly associated with low grade (grade low *versus* intermediate *versus* high; mean (SD), 79(57), 50(69), 40(52), $P = 0.012$ analysis of variance) and the absence of necrosis (necrosis negative *versus* positive; mean (SD), 68(52), 49(64), $P = 0.036$, Mann Whitney; Figure 3 and Table 1).

CA IX and CA XII Expression Relative to the Proliferation Marker MIB1

A correlation between CA IX and proliferation has been suggested previously.[26] We therefore examined the relationship between proliferation and CA IX and CA XII in our breast tissue specimens (Figure 4). Comparison of mitotic rates within positively stained ducts for CA IX and CA XII and within different zones in these ducts (adjacent to the stroma or the lumen), indicated that neither CA IX nor CA XII expression correlated regionally with mitosis. Whereas CA IX expression was typically localized to areas adjacent to necrosis, mitotic figures did not show a similar distribution, being most numerous in the cells adjacent to stroma and farthest removed from necrosis. Similarly, CA XII expression was not restricted to the areas of highest mitotic activity and was typically uniform throughout the intraductal epithelium, with occasional accentuation in luminal cells adjacent to necrosis. To confirm these morphological observations, a random subset of cases ($n = 26$) were immunostained for the proliferation marker MIB1 and the MIB1 score was determined by Chalkley counting. In agreement with previous observations,[37] we found MIB1 to be associated with both grade (low *versus* intermediate *versus* high; mean (SD), 0.16(0.07), 0.4(0.18), 0.56(0.33), $P = 0.0026$ analysis of variance) and the presence of necrosis (necrosis negative *versus* positive; mean (SD), 0.19(0.09), 0.51(0.28), $P = 0.001$ Mann Whitney; Figure 5). However, MIB1 was not significantly related to the expression of either CA IX or CA XII (CA IX negative *versus* positive; MIB1 mean (SD), 0.44(0.37), 0.37(0.21); CA XII negative *versus* positive; MIB1 mean (SD), 0.43(0.31), 0.38(0.26); Table 1). Similarly, when CA IX and CA XII expression were divided into low and high expression using the median IHC score of the series for each (CA IX positive, >1 and CA XII negative, >40), no association was detected between the expression of either CA and MIB1 staining.

CA IX and CA XII Expression Relative to Mammographic Calcification

CA IX and CA XII expression were assessed in relation to the presence and pattern of calcification detected in preoperative mammograms in a subset of cases in which films were available for review ($n = 43$). The presence of calcification was associated with the presence of necrosis ($P = 0.0036$, chi-square) and higher grade ($P = 0.0057$, chi-square) (Table 2). When CA gene expression was classified as low or high on the basis of the median IHC score of the series (CA IX positive, >1 and CA XII positive, >40) a significant relationship was observed between lower CA XII expression and the presence of calcification ($P = 0.0083$, chi-square), as shown in Table 2. The level of CA XII expression was also inversely associated with calcification (calcification absent *versus* present, mean (SD), 94(60), 42(60), $P = 0.03$, Mann Whitney). The pattern of calcification was not significantly different with respect to either CA gene expression. Despite this, comparison of cases with nonlinear *versus* cases with some component of linear calcification revealed a trend toward an increased proportion of CA IX positive cases (8 of 21 *vs.* 9 of 14 or 38% *vs.* 64%), whereas the proportion of CA XII positive cases was no different (6 of 21 *vs.* 3 of 14 or 29% *vs.* 21%). Additionally, cases with linear calcification tended to be associated with higher levels of CA IX expression than cases with nonlinear calcification (CA IX IHC score mean (SD), 9 (12) *vs.* 5 (10), P = n.s.) whereas there was no such trend for CA XII (CA XII IHC score, 41 (69) *vs.* 43 (55), P = n.s.).

Discussion

We have shown that the tumor-associated CAs CA IX and CA XII are both expressed by malignant breast epithelium. CA IX expression was rare in normal ductal and lobular epithelium, and in benign breast lesions, occur-

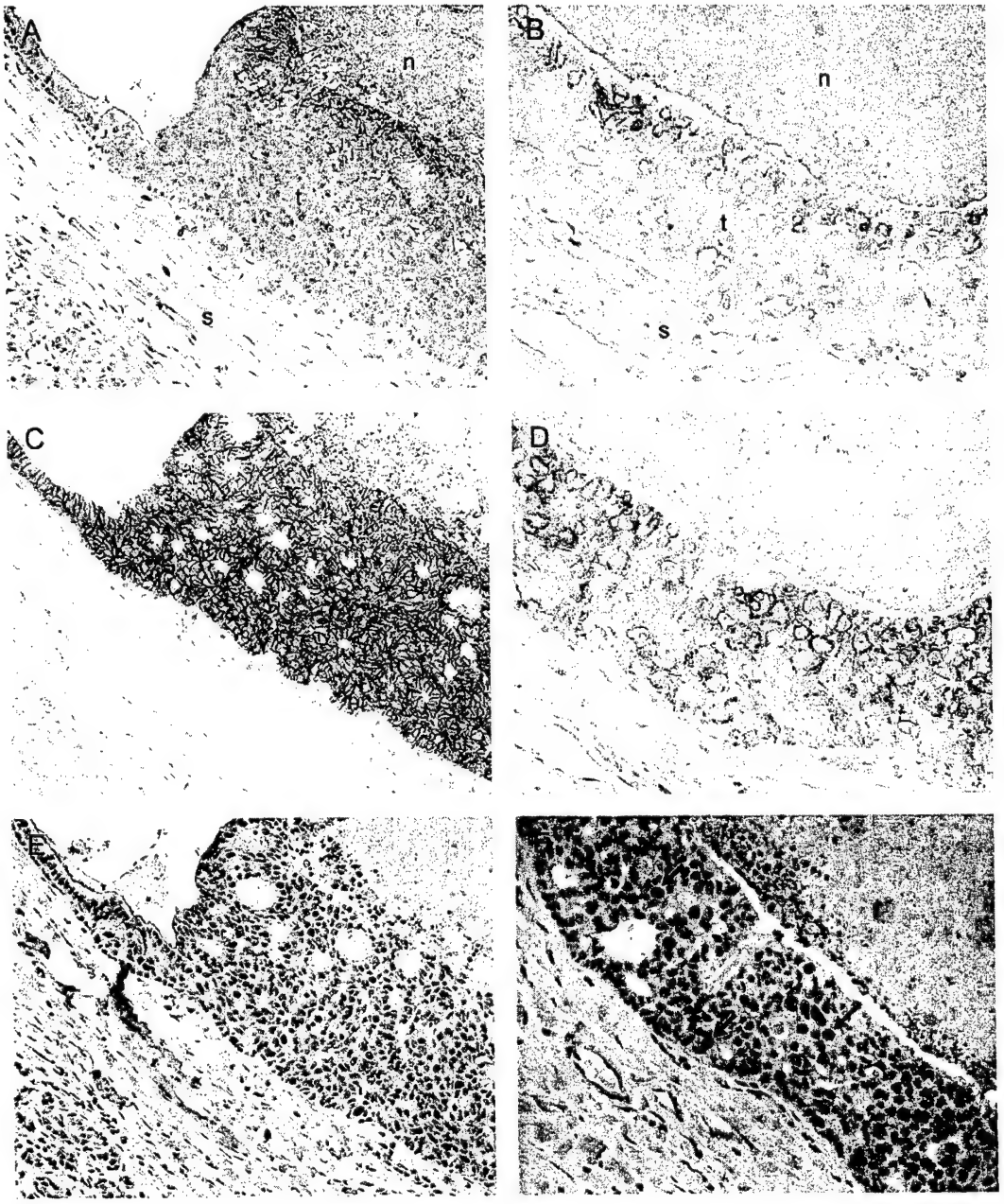

Figure 4. CA IX and CA XII expression is unrelated to MIB1 expression. The pattern of expression of CA IX (**A** and **B**), CA XII (**C** and **D**), and MIB1 (**E** and **F**), was assessed in serial sections from intermediate-grade DCIS (**left column**) and high-grade DCIS (**right column**). CA IX expression is restricted to the inner zone of luminal epithelium adjacent to central necrosis. CA XII expression is present throughout the duct wall, but accentuated adjacent to necrosis in high-grade DCIS, and also in the adjacent portion of non-neoplastic ductal epithelium (**C**, **upper left**). In contrast, MIB1-positive nuclei are distributed throughout the duct in both intermediate- and high-grade DCIS, and are absent from normal epithelium (**E**, **upper left**). **Arrows** within **F** indicate MIB1-positive nuclei. Original magnifications, ×20.

ring primarily in pre-invasive DCIS and invasive breast carcinomas. In DCIS, expression was focal and specifically associated with regions of necrosis and high-grade lesions. In contrast, CA XII was frequently expressed in normal breast tissue as well as in benign, pre-invasive, and invasive breast lesions. In DCIS, expression was typically homogeneous and associated with the absence of necrosis and low-grade lesions. However, focal induction of CA XII was observed in high-grade DCIS adjacent to necrosis. The finding that both CA IX and CA XII are induced *in vivo* in breast tumor cells adjacent to regions of necrosis suggests that these CAs may be important components of the breast epithelial cellular response to hypoxia. This observation is compatible with our recent findings in a variety of tissue-culture cell lines,[23] where both *CA9* and *CA12* are induced by hypoxia, and that at least for *CA9* this induction is hypoxia-inducible factor-1-dependent. However, future studies to establish co-localization of CA expression with hypoxia-inducible factor-1 in tissue sections will be important to confirm *in vivo*.

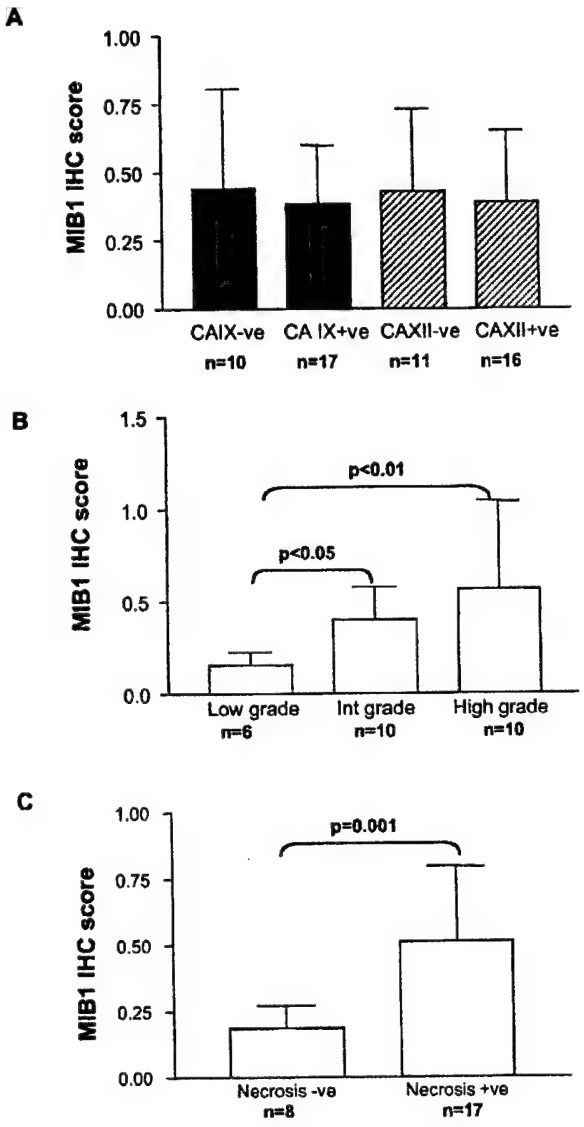

Figure 5. MIB1 expression relative to CA IX or CA XII expression, DCIS grade, and the presence of necrosis. Columns (CA IX, black; CA XII, hatched; MIB1, clear) represent the mean MIB1 IHC score with bars showing SD relative to CA IX or CA XII expression (negative, positive), DCIS grade (low, intermediate, high), and necrosis (absent, present).

CAs have been studied in a spectrum of tumor types in relation to their potential role as diagnostic and prognostic markers. Earlier studies focusing on CAs I, II, and IV revealed no clear relationships with tumorigenesis.[26] More recently, *CA9* has been identified as overexpressed in multiple tumor cell lines and in several human tumor types. In various studies, *CA9* has been found to be associated with aspects of early tumorigenesis,[20,26,30,35,38] and it has therefore been proposed to serve as a biomarker for dysplasia. In accordance with these findings, we have shown that whereas CA IX expression is rare in normal or benign breast lesions, CA IX expression occurs in pre-invasive DCIS of the breast where it is limited to malignant epithelium. In the breast specimens examined, CA IX expression was not related to proliferation and was strongly associated with necrosis, indicating that hypoxia may be an important pathway for induction of CA IX in breast tumors *in vivo*.

CA12 was initially identified as a renal carcinoma-associated gene[20,22] and has subsequently been found to be expressed in a range of normal tissues including endometrium, pancreas, and colon.[31,39,40] Interestingly, in the normal colon CA XII is expressed highly by the differentiated surface epithelium relative to the cells of the crypt base, and whereas no change in the surface expression occurs with tumorigenesis, increased basal/deep mucosal expression is associated with increasing dysplasia and invasive tumor stage.[31] Similarly, and in striking contrast to CA IX expression, we have observed constitutive expression of CA XII in normal breast epithelium and benign ductal hyperplasia. This suggests that CA XII may play a role in the control of pH in normal breast tissue. The function of this membrane-associated extracellular CA may be coupled to that of an intracellular CA such as CA II, as has been hypothesized for other secretory/excretory organs such as the salivary glands, pancreas, and kidney.[40] Clearly, a detailed examination of the interplay between the many CAs is warranted. We have also shown that CA XII expression persists in malignant pre-invasive DCIS. Although focal induction of CA XII was observed in areas adjacent to necrosis, the differentiation status of the DCIS lesion (as indicated by grade) had a more dominant role in determining CA XII

Table 2. Relationship in DCIS between the Presence of Calcification and CA IX or CA XII Expression, Necrosis, and Grade

DCIS parameter	No.	Mammogram calcification		
		Negative	Positive	
CA IX				
Negative	21	3	18	ns (P = 0.477)
Positive	22	5	17	
CA XII				
Negative	28	2	26	P = 0.0083
Positive	15	6	9	
Necrosis				
Negative	10	5	5	P = 0.0036
Positive	33	3	30	
Grade				
Low	9	5	4	P = 0.0057,
Intermediate	15	1	14	P = 0.0137 (t)
High	19	2	17	

Statistical significance estimated by χ^2 test and χ^2 test for trend (t).

expression, which was reflected in the pattern of expression observed in the ER-negative and ER-positive cell lines examined. Of note, differentiation has been proposed to play a role in the expression of other CAs, including CA I whose induction is association with differentiation in the colon,[41] and CA II whose expression is associated with differentiation in pancreatic cell lines under the influence of tumor necrosis factor-α.[42]

An abnormal pattern of calcification in a breast mammogram is an important indicator of DCIS.[5] In particular, the presence of linear type calcification is associated with high-grade DCIS and may predict outcome of associated small invasive tumors.[5,6,43,44] Calcification is believed to reflect a disruption of the normal vascular architecture caused by abnormal proliferation within the intraductal epithelium.[45] This leads to a reduction in luminal pH, changes in the equilibria of many ions, and resulting calcification.[46] Inherited alteration and deficiency of CA II activity causes metabolic acidosis and ectopic tissue calcification.[47] Similarly, changes in extracellular pH influenced by CA IX and CA XII expression may affect the extent and pattern of calcification in DCIS of the breast. In the current series, increased mammographically detectable calcification was associated with reduced CA XII expression, as well as the presence of high-grade DCIS and necrosis, as previously reported.[48] Our inability to demonstrate a relationship between calcification and CA IX staining could relate to the fact that CA IX staining was only present very focally. Therefore, the tissue block assessed for CA IX expression may not correspond to the status of the area of the mammogram assessed for calcification, which encompassed the entire biopsy. Furthermore, our results suggest that whereas overall loss of CA XII expression is important in the development of calcification, local gain of CA IX expression adjacent to the ductal lumen may influence the pattern of calcification. However the significance of these observations awaits confirmation by larger studies as this subset of cases is small and includes a disproportionate number of cases with calcification present, reflecting the fact that calcification is a key factor in detection of tumors by mammography.[5]

The effect on local pH and the significance for breast tumor progression of reciprocal changes in the expression of these CAs remains to be determined. However, there is additional evidence to suggest that a switch in pH regulatory pathways may occur in breast tumor progression. Although a decrease in the activity of the Na^+/H^+ exchanger was noted in response to serum deprivation in nontumor breast cells, stimulation of this exchanger and an increased capacity for extracellular acidification was observed in tumor cells.[49] In terms of tumor progression, maintenance of high levels of CA XII may be important for both the function and survival of the ductal epithelium in normal tissue. Loss of CA XII expression with progression to higher grade DCIS may reflect the acquisition of alternative cellular responses to ameliorate the effects of disruption of tissue architecture, altered pH, and hypoxia.[18,50] One facet of this adaptation may be provided by the induction of other CAs such as CA IX to modulate the effects of local hypoxia. This view predicts that overall loss of CA XII and/or gain of CA IX expression may be associated with a high risk of progression to invasive disease and therefore be of prognostic significance. Interestingly, inhibition of CA activity has recently been demonstrated to suppress invasion of some tumor cell lines.[51]

In conclusion, we have shown that CA IX and CA XII are expressed in breast tissues, and that the profile of expression of these CAs in DCIS suggests that whereas hypoxia may be a dominant factor in the regulation of CA IX, the regulation of CA XII is dominated by other factors related to cellular differentiation.

References

1. Ernster VL, Barclay J, Kerlikowske K, Grady D, Henderson C: Incidence of and treatment for ductal carcinoma in situ of the breast. JAMA 1996, 275:913–918
2. Ernster VL, Barclay J: Increases in ductal carcinoma in situ (DCIS) of the breast in relation to mammography: a dilemma. J Natl Cancer Inst Monogr 1997, 22:151–156
3. Fentiman IS: Trials of treatment for non-invasive breast cancer. Recent Results Cancer Res 1998, 152:135–142
4. Fisher B: Highlights from recent National Surgical Adjuvant Breast and Bowel Project studies in the treatment and prevention of breast cancer. CA Cancer J Clin 1999, 49:159–177
5. Holland R, Hendriks JH: Microcalcifications associated with ductal carcinoma in situ: mammographic-pathologic correlation. Semin Diagn Pathol 1994, 11:181–192
6. Tabar L, Chen HH, Duffy SW, Yen MF, Chiang CF, Dean PB, Smith RA: A novel method for prediction of long-term outcome of women with T1a, T1b, and 10–14 mm invasive breast cancers: a prospective study. Lancet 2000, 355:429–433
7. Shoker BS, Sloane JP: DCIS grading schemes and clinical implications. Histopathology 1999, 35:393–400
8. Fisher ER, Costantino J, Fisher B, Palekar AS, Redmond C, Mamounas E: Pathologic findings from the National Surgical Adjuvant Breast Project (NSABP) Protocol B-17. Intraductal carcinoma (ductal carcinoma in situ). The National Surgical Adjuvant Breast and Bowel Project Collaborating Investigators. Cancer 1995, 75:1310–1319
9. Silverstein MJ, Lagios MD, Craig PH, Waisman JR, Lewinsky BS, Colburn WJ, Poller DN: A prognostic index for ductal carcinoma in situ of the breast. Cancer 1996, 77:2267–2274
10. Schnitt SJ, Harris JR, Smith BL: Developing a prognostic index for ductal carcinoma in situ of the breast. Are we there yet? Cancer 1996, 77:2189–2192
11. Leek RD, Landers RJ, Harris AL, Lewis CE: Necrosis correlates with high vascular density and focal macrophage infiltration in invasive carcinoma of the breast. Br J Cancer 1999, 79:991–995
12. Wetzels RH, Kuijpers HJ, Lane EB, Leigh IM, Troyanovsky SM, Holland R, van Haelst UJ, Ramaekers FC: Basal cell-specific and hyperproliferation-related keratins in human breast cancer. Am J Pathol 1991, 138:751–763
13. Vaupel P, Hoeckel M: Predictive power of the tumor oxygenation status. Adv Exp Med Biol 1999, 471:533–539
14. Dachs GU, Chaplin DJ: Microenvironmental control of gene expression: implications for tumor angiogenesis, progression, and metastasis. Semin Radiat Oncol 1998, 8:208–216
15. Brizel DM, Sibley GS, Prosnitz LR, Scher RL, Dewhirst MW: Tumor hypoxia adversely affects the prognosis of carcinoma of the head and neck. Int J Radiat Oncol Biol Phys 1997, 38:285–289
16. Walenta S, Wetterling M, Lehrke M, Schwickert G, Sundfor K, Rofstad EK, Mueller-Klieser W: High lactate levels predict likelihood of metastases, tumor recurrence, and restricted patient survival in human cervical cancers. Cancer Res 2000, 60:916–921
17. Maxwell PH, Dachs GU, Gleadle JM, Nicholls LG, Harris AL, Stratford IJ, Hankinson O, Pugh CW, Ratcliffe PJ: Hypoxia-inducible factor-1 modulates gene expression in solid tumors and influences both angiogenesis and tumor growth. Proc Natl Acad Sci USA 1997, 94: 8104–8109

18. Zhong H, De Marzo AM, Laughner E, Lim M, Hilton DA, Zagzag D, Buechler P, Isaacs WB, Semenza GL, Simons JW: Overexpression of hypoxia-inducible factor 1alpha in common human cancers and their metastases. Cancer Res 1999, 59:5830–5835
19. Grabmaier K, Vissers JL, De Weijert MC, Oosterwijk-Wakka JC, Van Bokhoven A, Brakenhoff RH, Noessner E, Mulders PA, Merkx G, Figdor CG, Adema GJ, Oosterwijk E: Molecular cloning and immunogenicity of renal cell carcinoma-associated antigen G250. Int J Cancer 2000, 85:865–870
20. Ivanov SV, Kuzmin I, Wei MH, Pack S, Geil L, Johnson BE, Stanbridge EJ, Lerman MI: Down-regulation of transmembrane carbonic anhydrases in renal cell carcinoma cell lines by wild-type von Hippel-Lindau transgenes. Proc Natl Acad Sci USA 1998, 95:12596–12601
21. Opavsky R, Pastorekova S, Zelnik V, Gibadulinova A, Stanbridge EJ, Zavada J, Kettmann R, Pastorek J: Human MN/CA9 gene, a novel member of the carbonic anhydrase family: structure and exon to protein domain relationships. Genomics 1996, 33:480–487
22. Tureci O, Sahin U, Vollmar E, Siemer S, Gottert E, Seitz G, Parkkila AK, Shah GN, Grubb JH, Pfreundschuh M, Sly WS: Human carbonic anhydrase XII: cDNA cloning, expression, and chromosomal localization of a carbonic anhydrase gene that is overexpressed in some renal cell cancers. Proc Natl Acad Sci USA 1998, 95:7608–7613
23. Wykoff C, Beasley NJP, Watson PH, Turner KJ, Pastorek J, Sibtain A, Wilson GD, Turley H, Talks K, Maxwell PH, Pugh CW, Ratcliffe PJ, Harris AL: Hypoxia inducible expression of tumor associated carbonic anhydrases. Cancer Res 2000, 60:7075–7083
24. Jiang W, Gupta D: Structure of the carbonic anhydrase VI (CA6) gene: evidence for two distinct groups within the alpha-CA gene family. Biochem J 1999, 344:385–390
25. Pastorek J, Pastorekova S, Callebaut I, Mornon JP, Zelnik V, Opavsky R, Zat'ovicova M, Liao S, Portetelle D, Stanbridge EJ: Cloning and characterization of MN, a human tumor-associated protein with a domain homologous to carbonic anhydrase and a putative helix-loop-helix DNA binding segment. Oncogene 1994, 9:2877–2888
26. Nogradi A: The role of carbonic anhydrases in tumors. Am J Pathol 1998, 153:1–4
27. Liao SY, Stanbridge EJ: Expression of the MN antigen in cervical Papanicolaou smears is an early diagnostic biomarker of cervical dysplasia. Cancer Epidemiol Biomarkers Prev 1996, 5:549–557
28. Liao SY, Aurelio ON, Jan K, Zavada J, Stanbridge EJ: Identification of the MN/CA9 protein as a reliable diagnostic biomarker of clear cell carcinoma of the kidney. Cancer Res 1997, 57:2827–2831
29. Liao SY, Stanbridge EJ: Expression of MN/CA9 protein in Papanicolaou smears containing atypical glandular cells of undetermined significance is a diagnostic biomarker of cervical dysplasia and neoplasia. Cancer 2000, 88:1108–1121
30. Vermylen P, Roufosse C, Burny A, Verhest A, Bosschaerts T, Pastorekova S, Ninane V, Sculier JP: Carbonic anhydrase IX antigen differentiates between preneoplastic malignant lesions in non-small cell lung carcinoma. Eur Respir J 1999, 14:806–811
31. Kivela A, Parkkila S, Saarnio J, Karttunen TJ, Kivela J, Parkkila AK, Waheed A, Sly WS, Grubb JH, Shah G, Tureci O, Rajaniemi H: Expression of a novel transmembrane carbonic anhydrase isozyme XII in normal human gut and colorectal tumors. Am J Pathol 2000, 156:577–584
32. Silverstein MJ, Poller DN, Waisman JR, Colburn WJ, Barth A, Gierson ED, Lewinsky B, Gamagami P, Slamon DJ: Prognostic classification of breast ductal carcinoma-in-situ. Lancet 1995, 345:1154–1157
33. Wiesener MS, Turley H, Allen WE, Willam C, Eckardt KU, Talks KL, Wood SM, Gatter KC, Harris AL, Pugh CW, Ratcliffe PJ, Maxwell PH: Induction of endothelial PAS domain protein-1 by hypoxia: characterization and comparison with hypoxia-inducible factor-1alpha. Blood 1998, 92:2260–2268
34. Pastorekova S, Zavadova Z, Kostal M, Babusikova O, Zavada J: A novel quasi-viral agent, MaTu, is a two-component system. Virology 1992, 187:620–626
35. Saarnio J, Parkkila S, Parkkila AK, Haukipuro K, Pastorekova S, Pastorek J, Kairaluoma MI, Karttunen TJ: Immunohistochemical study of colorectal tumors for expression of a novel transmembrane carbonic anhydrase, MN/CA IX, with potential value as a marker of cell proliferation. Am J Pathol 1998, 153:279–285
36. Saarnio J, Parkkila S, Parkkila AK, Waheed A, Casey MC, Zhou XY, Pastorekova S, Pastorek J, Karttunen T, Haukipuro K, Kairaluoma MI, Sly WS: Immunohistochemistry of carbonic anhydrase isozyme IX (MN/CA IX) in human gut reveals polarized expression in the epithelial cells with the highest proliferative capacity. J Histochem Cytochem 1998, 46:497–504
37. Zafrani B, Leroyer A, Fourquet A, Laurent M, Trophilme D, Validire P, Sastre-Garau X: Mammographically-detected ductal in situ carcinoma of the breast analyzed with a new classification. A study of 127 cases: correlation with estrogen and progesterone receptors, p53 and c-erbB-2 proteins, and proliferative activity. Semin Diagn Pathol 1994, 11:208–214
38. Turner JR, Odze RD, Crum CP, Resnick MB: MN antigen expression in normal, preneoplastic, and neoplastic esophagus: a clinicopathological study of a new cancer-associated biomarker. Hum Pathol 1997, 28:740–744
39. Karhumaa P, Parkkila S, Tureci O, Waheed A, Grubb JH, Shah G, Parkkila A, Kaunisto K, Tapanainen J, Sly WS, Rajaniemi H: Identification of carbonic anhydrase XII as the membrane isozyme expressed in the normal human endometrial epithelium. Mol Hum Reprod 2000, 6:68–74
40. Nishimori I, Fujikawa Adachi K, Onishi S, Hollingsworth MA: Carbonic anhydrase in human pancreas: hypotheses for the pathophysiological roles of CA isozymes. Ann NY Acad Sci 1999, 880:5–16
41. Sowden J, Leigh S, Talbot I, Delhanty J, Edwards Y: Expression from the proximal promoter of the carbonic anhydrase 1 gene as a marker for differentiation in colon epithelia. Differentiation 1993, 53:67–74
42. Franz MG, Winkler BC, Norman JG, Fabri PJ, Gower Jr WR: Tumor necrosis factor-alpha induces the expression of carbonic anhydrase II in pancreatic adenocarcinoma cells. Biochem Biophys Res Commun 1994, 205:1815–1821
43. Evans AJ, Pinder SE, Snead DR, Wilson AR, Ellis IO, Elston CW: The detection of ductal carcinoma in situ at mammographic screening enables the diagnosis of small, grade 3 invasive tumours. Br J Cancer 1997, 75:542–544
44. Holland R, Hendriks JH, Vebeek AL, Mravunac M, Schuurmans Stekhoven JH: Extent, distribution, and mammographic/histological correlations of breast ductal carcinoma in situ. Lancet 1990, 335:519–522
45. Engels K, Fox SB, Whitehouse RM, Gatter KC, Harris AL: Distinct angiogenic patterns are associated with high-grade in situ ductal carcinomas of the breast. J Pathol 1997, 181:207–212
46. Stubbs M, Rodrigues L, Howe FA, Wang J, Jeong KS, Veech RL, Griffiths JR: Metabolic consequences of a reversed pH gradient in rat tumors. Cancer Res 1994, 54:4011–4016
47. Sly WS, Sato S, Zhu XL: Evaluation of carbonic anhydrase isozymes in disorders involving osteopetrosis and/or renal tubular acidosis. Clin Biochem 1991, 24:311–318
48. Evans AJ, Pinder S, Ellis IO, Sibbering M, Elston CW, Poller DN, Wilson R: Screening-detected and symptomatic ductal carcinoma in situ: mammographic features with pathologic correlation. Radiology 1994, 191:237–240
49. Reshkin SJ, Bellizzi A, Albarani V, Guerra L, Tommasino M, Paradiso A, Casavola V: Phosphoinositide 3-kinase is involved in the tumor-specific activation of human breast cancer cell Na(+)/H(+) exchange, motility, and invasion induced by serum deprivation. J Biol Chem 2000, 275:5361–5369
50. Tannock IF, Rotin D: Acid pH in tumors and its potential for therapeutic exploitation. Cancer Res 1989, 49:4373–4384
51. Parkkila S, Rajaniemi H, Parkkila AK, Kivela J, Waheed A, Pastorekova S, Pastorek J, Sly WS: Carbonic anhydrase inhibitor suppresses invasion of renal cancer cells in vitro. Proc Natl Acad Sci USA 2000, 97:2220–2224

[CANCER RESEARCH 61, 5262–5267, July 1, 2001]

Carbonic Anhydrase IX, an Endogenous Hypoxia Marker, Expression in Head and Neck Squamous Cell Carcinoma and its Relationship to Hypoxia, Necrosis, and Microvessel Density

Nigel J. P. Beasley, Charles C. Wykoff, Peter H. Watson, Russell Leek, Helen Turley, Kevin Gatter, Jaromir Pastorek, Graham J. Cox, Peter Ratcliffe, and Adrian L. Harris[1]

Oxford Centre for Head and Neck Oncology, Radcliffe Infirmary, Oxford OX2 6HE, United Kingdom [N. J. P. B., G. J. C.]; ICRF Molecular Oncology Group, Institute of Molecular Medicine [C. C. W., P. H. W., R. L., H. T., A. L. H.] and Nuffield Department of Clinical Laboratory Sciences [K. G.], John Radcliffe Hospital, Oxford OX3 9DU, United Kingdom; Institute of Virology, Slovak Academy of Sciences, Bratislava, Slovak Republic [J. P.]; and Welcome Trust Centre for Human Genetics, Oxford OX3 7BN, United Kingdom [P. R.]

ABSTRACT

Carbonic anhydrase IX (CA IX) is a transmembrane glycoprotein with an active extracellular enzyme site. We have shown previously that it was hypoxia inducible and may therefore be an endogenous marker of hypoxia. It is overexpressed in some tumors, particularly renal cell carcinoma. The aim of this study was to examine the expression and localization of CA IX in head and neck squamous cell carcinoma (HNSCC) and relate this to the location of tumor microvessels, angiogenesis, necrosis, and stage. Expression of CA IX was determined by immunoblotting in three HNSCC cell lines grown in normoxia and hypoxia (pO_2 0.1%) and three paired tumor and normal tissue samples of HNSCC. Archived paraffin sections (79) of HNSCC were immunostained with antibodies to CA IX and CD34 to determine microvessel density (MVD). By double staining sections with CA IX and CD34, the distance between blood vessels and the start of CA IX expression and necrosis was calculated. CA IX was induced by hypoxia in all three HNSCC cell lines and overexpressed in HNSCC tumor tissue. Overexpression was localized to the perinecrotic area of the tumor on immunostaining, and the percentage area of the tumor expressing CA IX was significantly higher with more tumor necrosis ($P = 0.001$), a high MVD ($P = 0.02$), and advanced stage ($P = 0.033$) on univariate analysis and necrosis ($P = 0.0003$) and MVD ($P = 0.0019$) on multivariate analysis. The median distance between a blood vessel and the start of CA IX expression was 80 μm (range, 40–140 μm). CA IX is overexpressed in HNSCC because of hypoxia and is a potential biomarker for hypoxia in this tumor. Overexpression may help to maintain the intracellular pH, giving tumor cells a survival advantage and enhancing resistance to radiotherapy and chemotherapy. CA IX is a potential target for future therapy in HNSCC.

INTRODUCTION

Carbonic anhydrases are encoded by three independent gene families: α-CA, β-CA, and γ-CA. *CA9*[2] is one of the α-CA isoenzymes. Carbonic anhydrases catalyze the reversible conversion of carbon dioxide to carbonic acid and are involved in respiration, calcification, acid-base balance, and the formation of aqueous humor, cerebrospinal fluid, saliva, and gastric acid. The different carbonic anhydrases have different tissue distribution, subcellular localization, biological function, kinetic properties, and susceptibility to inhibitors (1).

CA9 is a novel member of the carbonic anhydrase family which codes for a transmembrane glycoprotein that possesses an extracellular catalytic domain with weak enzymatic activity. It has homology also to basic helix-loop-helix domain proteins. Transfection into murine fibroblast NIH mouse fibroblast cells promotes proliferation, and it may be involved in control of cell proliferation and oncogenesis (1, 2).

There is abundant expression of CA IX protein in normal human upper GI mucosa and GI-associated structures, such as pancreas, gallbladder, and liver (3–5). Expression is most prominent on the basolateral surfaces of the crypt enterocytes in the duodenum and jejunum. This suggests that it might serve as a ligand or a receptor for another protein that regulates intercellular communication or cell proliferation (6). Interestingly, expression is lost in gastric adenocarcinoma (5). Normal human heart, lung, kidney, prostate, peripheral blood, brain, placenta, and muscle do not express CA IX (3).

CA IX overexpression has been identified in a number of solid tumors, including renal carcinoma and particularly clear cell adenocarcinoma (7–10), cervical squamous carcinoma (11, 12), ovarian carcinoma (13), colorectal carcinoma (14), esophageal carcinoma (15), bladder carcinoma (16), and non-small cell lung carcinoma (17). In some epithelial tissues, expression has been observed in areas of severe dysplasia, *e.g.*, cervix (12), but in most, no expression is present until malignant invasion occurs, where it is often an early indicator of malignancy, *e.g.*, lung carcinoma (17). There appears to be an inverse correlation between CA IX expression and stage and grade in some tumors (7, 11, 14, 15), and low expression of CA IX has been correlated with poor prognostic factors, such as lymph node metastases and depth of invasion (11, 14, 15).

Clear cell renal carcinoma where CA IX expression is particularly high is almost always associated with mutation of the VHL tumor suppressor gene and loss of function of pVHL (18). CA IX is also overexpressed in mutant VHL renal cell carcinoma cell lines. This overexpression is reversed by transfection of the wt VHL gene back into the cell (19).

After the recent description of VHL regulation of HIF-1α (20), we investigated the hypoxic regulation of CA IX and have shown it is inducible by hypoxia. A HIF binding site in the 5′ promoter region of *CA9* was found, and we showed that a hypoxia response element and HIF-1α were essential for *CA9* transcription under hypoxia.

HNSCC is known to be a particularly hypoxic tumor with the degree of hypoxia having a significant impact on its response to radiotherapy chemotherapy and prognosis (22–25). The aim of this study was to examine the induction of CA IX by hypoxia in HNSCC cells lines and to analyze its expression and localization in HNSCC. Expression has been examined in relation to MVD as a measure of angiogenesis and necrosis as an indicator of the effects of hypoxia. Additionally, the distance of CA IX expression from blood vessels was analyzed as a surrogate assessment of the relation to hypoxia.

Received 1/16/01; accepted 4/24/01.

The costs of publication of this article were defrayed in part by the payment of page charges. This article must therefore be hereby marked *advertisement* in accordance with 18 U.S.C. Section 1734 solely to indicate this fact.

[1] To whom requests for reprints should be addressed, at ICRF Molecular Oncology Group, Institute of Molecular Medicine, John Radcliffe Hospital, Oxford OX3 9DU, United Kingdom. E-mail: aharris.lab@icrf.icnet.uk.

[2] The abbreviations used are: *CA9*, carbonic anhydrase 9 (gene); CA IX, carbonic anhydrase IX (protein); HIF-1α, hypoxia inducible factor 1 α; HNSCC, head and neck squamous cell carcinoma; MVD, microvessel density; TBS, Tris-buffered saline; VHL, von Hippel Lindau; MoAb, monoclonal antibody; wt, wild type; pHi, intracellular pH; pHe, extracellular pH; GI, gastrointestinal.

MATERIALS AND METHODS

Cell Lines. Human HNSCC lines UM-SCC22A, UM-SCC22B (courtesy of Dr. T. Carey, University of Michigan; Ref. 26), and SCC-25 (American Type Culture Collection) were maintained in DMEM with 10% heat-inactivated FCS and 2 mM fresh glutamine. Cells were exposed to normoxia or hypoxia (94.9% N_2, 5% CO_2, and 0.1% O_2) for 16 h. Cells were harvested on ice and homogenized in lysis buffer [8 M urea, 10% glycerol, 10 mM Tris-HCl (pH 6.8), 1% SDS, 5 mM phenylmethylsulfonyl, 1 μg/ml aprotinin, 10 μg/ml pepstatin, and 10 μg/ml leupeptin] using an IKA Ultra-Turrax T8 homogenizer (Janke & Kinkel, Staufen, Germany) for 30 s at full speed.

Primary renal adenocarcinoma cell lines expressing pVHL (RCC4/VHL) or empty vector (RCC4) were a gift from C. H. C. M. Buys (University of Groningen) and used as positive and negative controls as described (20). Cells were maintained in DMEM, 10% heat-inactivated FCS, 2 mM fresh glutamine, and 1 mg/ml G418 (G418 was removed from the medium 24 h before collection of samples). Cells were harvested on ice and prepared in 8 M urea lysis buffer as above. Whole cell preparations for immunostaining were harvested and fixed in 10% neutral buffered formalin overnight. Cell pellets were embedded in paraffin and sectioned onto silanized glass slides.

Fresh Tissue Samples. Three paired tumor and normal tissue samples from primary HNSCC were snap frozen in liquid nitrogen. Tissue samples were frozen sectioned and stained with H&E to ensure that material contained normal or tumor tissue as appropriate. Samples were sectioned on ice and homogenized in 8 M urea lysis buffer as above.

CA IX Immunoblotting. Cell and tissue extracts were protein quantified using the Bio-Rad detergent-compatible protein assay (Bio-Rad, UK) to ensure even protein loading between lanes. Samples were diluted in phosphate buffered saline to give 50 μg of protein/well. RCC4 and RCC4/VHL extracts were used as positive and negative controls, respectively. Proteins were resolved in NuPage Bis Tris 4–12% gels (Novex, UK) and transferred with a wet blotter (Novex) to Immobilon-P membrane (Millipore, Bedford, MA) in 25 mM Tris base, 190 mM glycine, and 15% methanol. Membranes were developed using the Western Breeze chemiluminescent immunodetection system (Novex) with mouse MoAb M75, as described (27), at a dilution of 1:50 in assay diluent.

Archived Tumor Specimens. Previously untreated patients (79) with HNSCC presented to the Oxford Center for Head and Neck Oncology between 1995 and 1999 were studied (Table 1). All had surgery as their first line of management, with some receiving postoperative radiotherapy. Specimens of complete resections rather than biopsies were selected so that both normal and tumor tissue were present on each slide. Seven samples of lymph node metastases from patients in this series were also selected.

H&E-stained sections of all of the specimens were examined at low (×40) and medium (×100) power by two observers (N. B. and P. W.). Tumors were graded as well, moderate or poorly differentiated. The margin of tumor invasion into surrounding normal tissue was identified as either pushing or infiltrating. A pushing margin is recognized when there is a defined border between tumor and stroma; an infiltrating margin when there is no clearly defined border to the tumor and invasion occurs in thin filaments (28). The whole tumor area was examined, and the degree of necrosis was divided into three categories 0 < 5%, 5.1 < 25%, and >25.1%.

Immunostaining. Sections (4 μm) of formalin-fixed, paraffin-embedded tissue were cut onto silanized glass slides. They were cleared of paraffin in Citroclear (HD Supplies, UK) and rehydrated through graded alcohol baths. After a rinse in tap water, they were placed in 3% hydrogen peroxide for 15 min.

CA IX. Slides were blocked in 10% normal human serum for 15 min, then incubated with 1:50 MoAb M75, as described (27), in TBS and 5% normal human serum for 30 min. They were rinsed twice in TBS and then developed using the Horse Radish Peroxidase Envision System (DAKO). Slides were counterstained with hematoxylin (Sigma Chemical Co. diagnostics, St. Louis, MO) and mounted with Aquamount (BDH, Poole, UK). Slides were examined at low (×40) and medium (×100) power by two observers (P. W. and N. B.). The percentage of tumor cells positive for CA IX in the whole tumor section was determined. Formalin-fixed, paraffin-embedded RCC4 and RCC4/VHL cell pellets were used as positive and negative controls, respectively.

CD34. Slides were pressure cooked for 3 min in Tris/EDTA lysis buffer (pH 9.0) and incubated with 1:100 MoAb Qbend 10 (DAKO) in TBS for 60 min. After two rinses in TBS, they were incubated with goat antimouse IgG (PO447, DAKO) for 30 min, washed in TBS, and then incubated with alkaline phosphatase anti-alkaline phosphatase for 30 min. The last two steps were repeated twice with 10-min incubations as described (29). New Fucsin Red substrate was applied for 15 min, and slides were counterstained with hematoxylin and mounted with Aquamount. MVD was determined in tumor microvessel hotspots using a Chalkley point counting grid at high power (×250) by two observers (R. L. and N. B.). The average of the vessel counts in the three most vascular areas per section was taken (30).

Table 1 *Patient and tumour characteristics by category and CA IX expression*

	n	CA IX expression[a] Median (range)
Age (yr) (median, 62) (range, 17–92)		
>62	39	20% (0–80%)
<62	40	20% (0–90%)
Sex		
Male	54	20% (0–90%)
Female	25	15% (0–90%)
Site		
Oral cavity	31	20% (0–90%)
Oropharynx	23	30% (0–75%)
Larynx	16	7.5% (0–80%)
Hypopharynx	9	25% (0–75%)
Stage		
T_1	9	5% (0–20%)
T_2	20	20% (0–75%)
T_3	18	27.5% (0–90%)
T_4	32	20% (0–90%)
Nodal stage		
N_0	38	20% (0–90%)
N+	41	20% (0–80%)
Grade		
Well differentiated	12	25% (0–75%)
Moderately differentiated	57	20% (0–90%)
Poorly differentiated	10	10% (0–60%)
Margin		
Pushing	49	30% (0–90%)
Infiltrating	27	15% (0–80%)
Unable to assess	3	
Necrosis (median, 5%) (range, 0–75%)		
Low (<5%)	46	15% (0–75%)
Moderate (5–25%)	26	30% (0–90%)
High (>25%)	7	60% (5–90%)
MVD (median, 6%) (range, 0–7)		
Low (<5.7)	46	10% (0–90%)
High (>6)	30	35% (0–90%)

[a] As a percentage of the tumour area involved.

Double Staining CA IX, CD34. Two representative slides demonstrating overexpression of CA IX and areas of necrosis were selected. CA IX immunostaining was carried out as above using the Horse Radish Peroxidase Envision System (DAKO) without counterstaining. Slides were then washed for 15 min in TBS, and immunostaining for CD34 was carried out as above. Slides were counterstained and mounted as above.

The distance from blood vessels marked with CD34 to the start of CA IX expression and necrosis was assessed using an eyepiece graticule calibrated against a graduated slide. Measurements were taken from both tumors in three different areas carefully selected to represent cross sections of a tumor cord, avoiding oval or longitudinal sections. Measurements were done in three different directions from a single vessel.

Statistics. Correlation between the level of CA IX expression in sections of primary tumor and nodal metastases was examined using Spearman's rank correlation. The difference in CA IX expression with age (two categories at the median age), MVD (two categories at the highest third), percentage of tumor necrosis (three categories: 0–5%, 5–25%, and >25%), sex, T stage (T_{1-4}), N stage (N_0 and N+), grade of tumor, and margin of invasion was compared using a Mann-Whitney *U* test or Kruskall Wallis test as appropriate. The difference in necrosis score with MVD (two categories at the highest third) was examined using the Mann-Whitney *U* test. For multivariate analysis, bivariate logistic regression was used and an odds ratio calculated. For this test, CA IX expression was divided at the median into two categories of high expression (>20%) and low expression (≤20%), necrosis into two categories present (>5%) or absent (≤5%), and T stage into early ($T_{1/2}$) and advanced ($T_{3/4}$). All statistics were done using SPSS software v9.0.

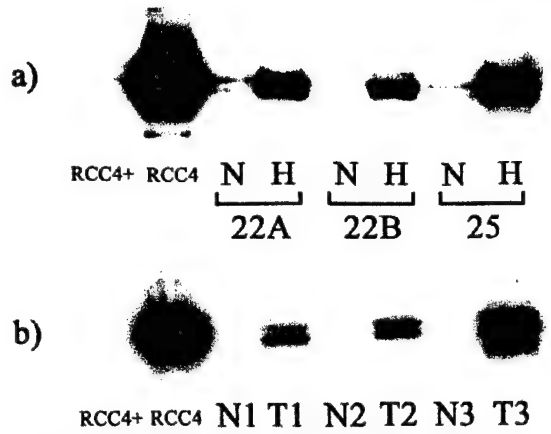

Fig. 1. *RCC4/VHL* (wt VHL), negative control; *RCC4* (empty vector), positive control. *a*, expression of CA IX in HNSCC cell lines (UM-SCC22A, UM-SCC22B, and SCC-25) on Western blotting in normoxia and hypoxia. *N*, normoxia; *H*, hypoxia (pO_2 0.1%). *b*, expression of CA IX in paired tumor and normal tissue from 3 patients with HNSCC. *T*, tumor tissue; *N*, paired normal tissue.

RESULTS

Expression of CA IX on Western Blotting in HNSCC Cell Lines and Tissue Samples. Because VHL mutation constitutively up-regulates HIF-1α, controls for CA IX expression were extracts from the renal cell line RCC4 with VHL mutation. They showed marked up-regulation of CA IX in normoxia, in contrast to the control RCC4/VHL cell line transfected with wt VHL, where CA IX was minimal in normoxia. It appeared as two bands related to glycosylation. CA IX was up-regulated in all three head and neck cell lines exposed to hypoxia (0.1% O_2 for 16 h) with little or no expression in normoxia (Fig. 1*a*). CA IX expression was clearly up-regulated in tumor samples compared with paired normal tissue taken at operation from patients with HNSCC (Fig. 1*b*).

Localization of CA IX Expression in HNSCC. CA IX was overexpressed in 71 of 79 HNSCC tumor sections examined; expression was confined to the perinecrotic region of these tumors (Fig. 2*a*). It was absent or very low in the normal epithelium overlying tumor tissue (Fig. 2*b*). Expression was confined to the cell membrane (Fig. 2*c*). In the eight tumor sections where no CA IX expression was seen, these was little or no tumor necrosis observed (0% necrosis in four cases, 5% necrosis in two cases, 20% necrosis in two cases). The level of expression was similar in both the primary and lymph node metastases from the same patient in all seven cases, although no significant correlation could be demonstrated because of the small numbers [primary median CA IX 50% (range, 5–60%), secondary median CA IX 35% (range, 20–80%), $n = 7$, $P = 0.093$, Spearman's correlation].

Distance between Blood Vessel and Necrosis and CA IX Expression. The median distance from a blood vessel to the start of necrosis was 130 μm (range, 80–200 μm; $n = 18$), and the median distance between a blood vessel and the start of CA IX expression was 80 μm (range, 40–140 μm; $n = 18$), as shown in Fig. 2*f*. Using a formula published by Tomlinson and Gray (31), which makes assumptions about oxygen diffusion and consumption on the basis of experiments done on squamous cell carcinoma of the lung, the partial pressure of oxygen at a given distance from the nearest vessel can be

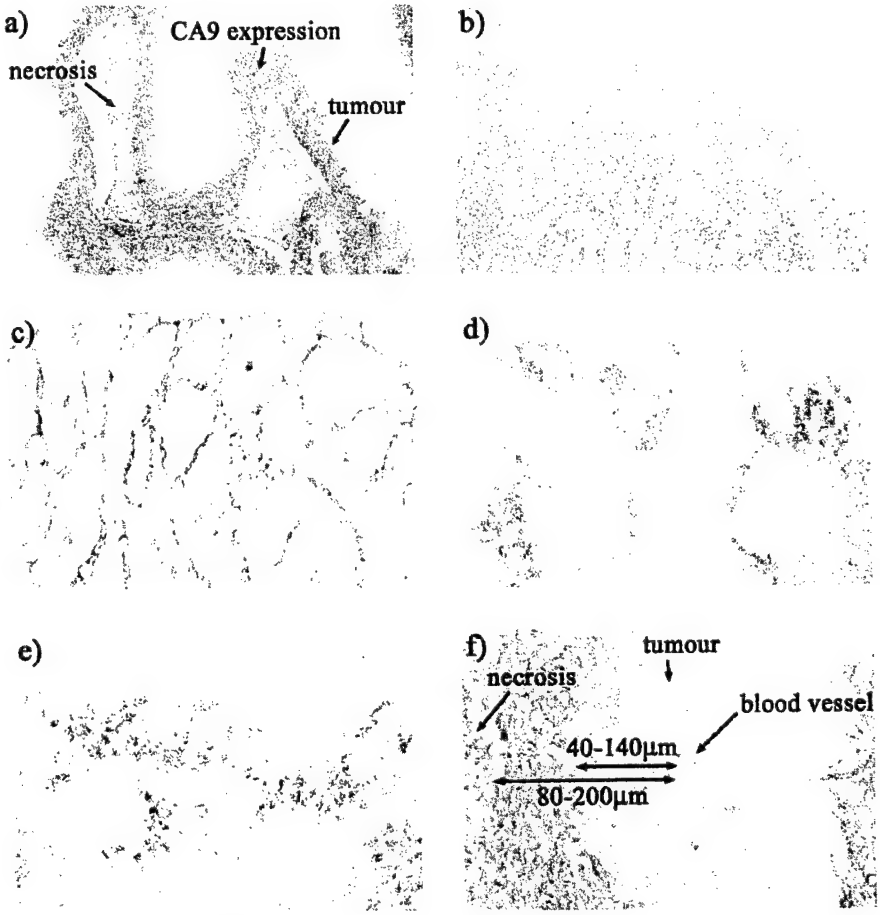

Fig. 2. Expression of CA IX on immunostaining in HNSCC. *a*, perinecrotic expression of CA IX (×100). *b*, overlying normal squamous epithelium (×100). *c*, membrane expression of CA IX (×1000). Expression of CA IX is shown in paired primary (*d*) and lymph node metastases (e; ×100). *f*, range of distances between a blood vessel labeled with CD34 MoAb and the start of CA IX expression and necrosis (×250).

calculated (Fig. 3). In the HNSCC sections examined here, the median distance from a blood vessel to the start of CA IX expression of 80 μm (range, 40–140 μm) gives a tissue pO_2 of 1% (range, 0–2.8%). These results are only approximate because of the shrinkage of tissue on formalin fixation, the variation in sectioning of the tumor, and the assumptions made about oxygen diffusion and consumption.

Difference in CA IX Expression with MVD, Necrosis Score, and T Stage. CA IX expression was higher in tumors with a MVD in the top third of the range (P = 0.02, Mann-Whitney; Table 1), as shown in Fig. 4. CA IX expression was also higher as the percentage of tumor necrosis increased (P = 0.001, Kruskall Wallis; Table 1), as shown in Fig. 5. There was a significantly higher level of CA IX expression in more advanced tumors (T_{2-4}) compared with T_1 tumors (P = 0.033, Kruskall Wallis; Table 1). There was no significant difference in CA IX expression between categories of age, sex, N-stage, grade, or margin of invasion (Table 1). There was no significant difference in percentage of tumor necrosis with increasing T stage (P = 0.37, Kruskall Wallis, data not shown) or high and low MVD (P = 0.47, Mann-Whitney, data not shown).

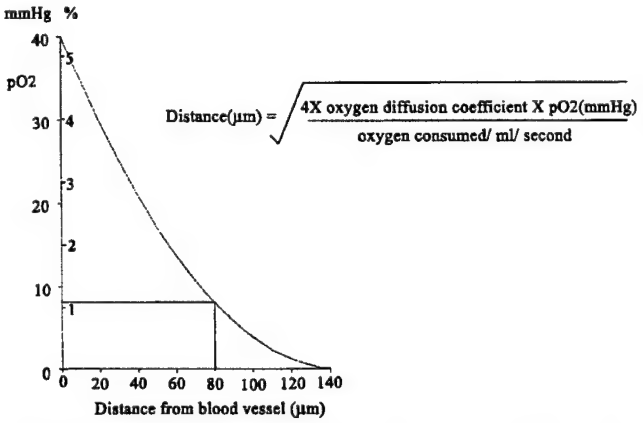

Fig. 3. Formula for the calculation of the oxygen tension at distances from a blood vessel (31). Shown is pO_2 (vertical axis) in mmHg and percentage of O_2. The median distance from a blood vessel, 80 μm, and lower end of the range, 40 μm, are shown with their corresponding pO_2.

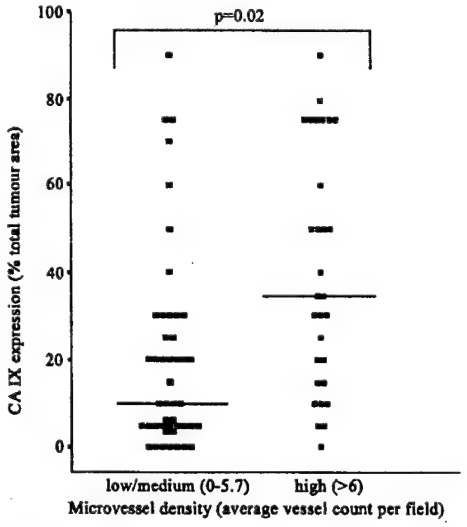

Fig. 4. Difference in CA IX expression with MVD measured by Chalkley vessel counting in HNSCC, n = 76. The percentage of total tumor area positive for CA IX is plotted against categories of MVD, low/medium (<5.7) and high (>6%). There is a significant difference between the two categories, P = 0.02, Mann-Whitney U test.

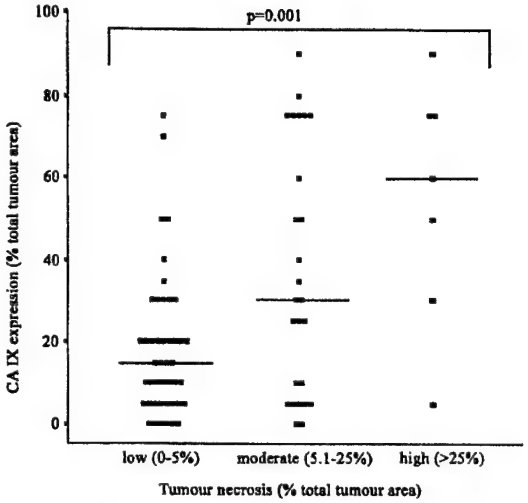

Fig. 5. Difference in CA IX expression with percentage area of tumor necrosis in HNSCC, n = 79. The percentage of total tumor area positive for CA IX is plotted against categories of necrosis, low (<5%), moderate (5.1–25%), and high (>25%). There is a significant difference between the three categories, P = 0.001, Kruskall Wallis test.

When the difference in CA IX expression between high and low groups of MVD, categories of necrosis, and T stage was examined using multivariate analysis, percentage of tumor necrosis (P = 0.0003; odds ratio, 10.0) and MVD (P = 0.0019; odds ratio, 7.3) remained significant factors associated with CA IX expression. The effect of T stage on CA IX expression was no longer seen.

DISCUSSION

Hypoxic regions are common within solid tumors because of disorderly vasculature, shunting of blood, and oxygen consumption out of balance with oxygen supply as rapid growth outstrips the blood supply (32–35). Tumor hypoxia has been shown to be important in resistance to radiotherapy and chemotherapy (25, 36–38) and has a significant effect on disease free and overall survival in HNSCC (22, 23, 37).

This study demonstrates that CA IX is overexpressed in HNSCC. It was clearly induced by hypoxia in cell lines *in vitro*, and on immunostaining expression, it was clearly localized to the perinecrotic regions of the tumor, which are known to be hypoxic. CA IX expression was seen at a median distance from blood vessels of 80 μm correlating with a calculated pO_2 in the range of 1% at the edge nearest the blood vessels. At the edge nearest the area of necrosis, the pO_2 would be ~0.1%, which *in vitro* also gave strong induction of CA IX. There was a significant increase in CA IX expression as tumor necrosis increased. These observations suggest that CA IX is regulated by hypoxia *in vivo*. There was variability between tumors in distance from blood vessels to necrosis, which may reflect the susceptibility of the tumor cells to hypoxia-induced death, the heterogeneity of oxygen distribution within the tumor (39), or O_2 consumption by the tumor contributing to the final effect of necrosis. However, these variations also appear to affect CA IX expression concomitantly. CA IX expression was only seen in the cell membrane on immunostaining. It is a transmembrane glycoprotein that makes CA IX a potentially useful indicator of tissue hypoxia, as the protein cannot diffuse away from its point of origin. This is in contrast to vascular endothelial growth factor, which does not correlate with biomarkers of hypoxia, such as Pimonidazole (40). Although secreted proteins may be useful peripheral blood markers of hypoxia (41), CA IX is induced at the same oxygen tension at which HIF-1α and its downstream

target genes are induced and provides a measure of the percentage of the tumor population that is hypoxic (42).

The correlation between CA IX and MVD is likely to be attributable to the overexpression of CA IX at the same oxygen tension as hypoxia-induced proangiogenic cytokines, such as vascular endothelial growth factor. The lack of correlation between MVD and necrosis may be because necrosis indicates both severe hypoxia, metabolic O_2 consumption by the tumor, and the ability of a cell to withstand hypoxia rather than being a simple measure of hypoxia, although one study in breast carcinoma did find a correlation between MVD and necrosis (43).

Tumor cells can undergo apoptosis in hypoxia, and therefore, there is strong selection for pathways to escape this fate, *e.g.*, p53 mutation (44). Selection of these cells in the hypoxic microenvironment is an important mechanism for malignant progression (45). Hypoxic apoptosis is substantially mediated by an acidotic pHe, which occurs because of the switch from aerobic to anaerobic metabolism in hypoxia, *in vitro* studies (46). In that study, buffering the pH changes in hypoxia either by changing the medium or more concentrated buffers allowed cell survival under hypoxia. Thus, induction of genes able to regulate extracellular or pHi may help hypoxic cells survive. Several mechanisms exist at a cellular level to generate an acidotic pHe and maintain the pHi. It has been proposed that increased activity of the mitogen-sensitive Na^+/H^+ exchanger, increased function or expression of H^+ pumping ATPases, or an interaction between the tumor cell and its immediate environment may maintain the pHi at a normal level while lowering the pHe. Carbonic anhydrases have been suggested as one mechanism whereby the cell could maintain a difference in pH across its membrane (19, 47, 48).

Carbonic anhydrases catalyze the reversible conversion of H_2O and CO_2 to carbonic acid. During aerobic metabolism, CO_2 is generated. This moves out of the cell down a diffusion gradient as the extracellular CO_2 is maintained at a lower level by conversion to carbonic acid, which dissociates into H^+ and $HCO3^-$. The bicarbonate ions are pumped back into the cell in exchange for chloride ions while the H^+ ions remain in the extracellular environment and lower the pHe. The induction by hypoxia of CA IX with its active extracellular enzyme site could theoretically help to lower the extracellular CO_2 and maintain the pHi at a normal level, preventing apoptosis and giving the cell a major survival advantage. A reduction in the pHe has advantages to tumor cells as it helps in the breakdown of the extracellular matrix, migration and invasion of tumor cells, induction of expression of growth factors, and reduction of the viability of nearby cells (49). This potential ability of hypoxia-induced CA IX to affect the pHi and pHe *in vitro* and *in vivo* is currently under investigation. The pH of a tumor is one of the most significant factors in mathematical models of tumor survival. (50). Chronic lowering of the pHi by inhibitors of the Na^+/H^+ exchanger or Na^+-dependent $HCO3^-/Cl^-$ exchanger is directly cytotoxic to tumor cells and inhibits tumor growth (48).

The pH of a tumor may significantly alter the uptake of chemotherapy drugs, particularly if they are weak electrolytes (51). Chlorambucil and 5FU, both weak acids, have increased toxicity and are retained in tumors cells when there is a low pHe (52, 53). Doxorubicin and mitoxantrone, both weak bases, have reduced intracellular accumulation with low pHe (54, 55). Doxorubicin toxicity has been enhanced in an animal model by raising the pHe with bicarbonate in the drinking water (49).

Carbonic anhydrase inhibitors have been shown to inhibit tumor cell invasion *in vitro* (47), and in xenograft experiments, carbonic anhydrase inhibitors as part of a chemotherapy regimen enhanced the effect of chemotherapy drugs and helped delay tumor growth (56).

Thus, our demonstration of up-regulation of CA IX *in vivo* in a perinecrotic pattern suggests this may be an important pathway in hypoxia, possibly regulating pHe to allow survival of a viable rim of cells under hypoxic conditions. This subpopulation of cells may be a suitable target for inhibitors of carbonic anhydrase. Use of CA IX as a target for radioimmunotherapy with MoAbs or use of CA IX to convert a pro-drug to an active drug may have potential problems because of its abundant expression normal human upper GI mucosa and GI-associated structures.

CA IX expression correlates with the oxygen diffusion distance and is expressed in a perinecrotic manner; this may be a marker for hypoxia in HNSCC. It is induced by hypoxia in HNSCC cells and is up-regulated in HNSCC. Up-regulation correlates with tumor necrosis and MVD. Overexpression may help to maintain the pHi, give tumor cells a survival advantage, and enhance resistance to radiotherapy and chemotherapy. CA IX provides a potential target for future therapy.

REFERENCES

1. Opavsky, R., Pastorekova, S., Zelnik, V., Gibadulinova, A., Stanbridge, E. J., Zavada, J., Kettmann, R., and Pastorek, J. Human *MN/CA9* gene, a novel member of the carbonic anhydrase family: structure and exon to protein domain relationships. Genomics, *33:* 480–487, 1996.
2. Pastorek, J., Pastorekova, S., Callebaut, I., Mornon, J. P., Zelnik, V., Opavsky, R., Zat'ovicova, M., Liao, S., Portetelle, D., Stanbridge, E. J., *et al.* Cloning and characterization of MN, a human tumor-associated protein with a domain homologous to carbonic anhydrase and a putative helix-loop-helix DNA binding segment. Oncogene, *9:* 2877–2888, 1994.
3. McKiernan, J. M., Buttyan, R., Bander, N. H., Stifelman, M. D., Katz, A. E., Chen, M. W., Olsson, C. A., and Sawczuk, I. S. Expression of the tumor-associated gene *MN*: a potential biomarker for human renal cell carcinoma. Cancer Res., *57:* 2362–2365, 1997.
4. Nishimori, I., FujikawaAdachi, K., Onishi, S., and Hollingsworth, M. A. Carbonic anhydrase in human pancreas: hypotheses for the pathophysiological roles of CA isozymes. Ann. N. Y. Acad. Sci., *880:* 5–16, 1999.
5. Pastorekova, S., Parkkila, S., Parkkila, A. K., Opavsky, R., Zelnik, V., Saarnio, J., and Pastorek, J. Carbonic anhydrase IX, MN/CA IX: analysis of stomach complementary DNA sequence and expression in human and rat alimentary tracts. Gastroenterology, *112:* 398–408, 1997.
6. Saarnio, J., Parkkila, S., Parkkila, A. K., Waheed, A., Casey, M. C., Zhou, X. Y., Pastorekova, S., Pastorek, J., Karttunen, T., Haukipuro, K., Kairaluoma, M. I., and Sly, W. S. Immunohistochemistry of carbonic anhydrase isozyme IX (MN/CA IX) in human gut reveals polarized expression in the epithelial cells with the highest proliferative capacity. J. Histochem. Cytochem., *46:* 497–504, 1998.
7. Uemura, H., Nakagawa, Y., Yoshida, K., Saga, S., Yoshikawa, K., Hirao, Y., and Oosterwijk, E. MN/CA IX/G250 as a potential target for immunotherapy of renal cell carcinomas. Br. J. Cancer, *81:* 741–746, 1999.
8. Liao, S. Y., Aurelio, O. N., Jan, K., Zavada, J., and Stanbridge, E. J. Identification of the MN/CA9 protein as a reliable diagnostic biomarker of clear cell carcinoma of the kidney. Cancer Res., *57:* 2827–2831, 1997.
9. McKiernan, J. M., Buttyan, R., Bander, N. H., de la Taille, A., Stifelman, M. D., Emanuel, E. R., Bagiella, E., Rubin, M. A., Katz, A. E., Olsson, C. A., and Sawczuk, I. S. The detection of renal carcinoma cells in the peripheral blood with an enhanced reverse transcriptase-polymerase chain reaction assay for MN/CA9. Cancer (Phila.), *86:* 492–497, 1999.
10. Murakami, Y., Kanda, K., Tsuji, M., Kanayama, H., and Kagawa, S. *MN/CA9* gene expression as a potential biomarker in renal cell carcinoma. BJU Int., *83:* 743–747, 1999.
11. Brewer, C. A., Liao, S. Y., Wilczynski, S. P., Pastorekova, S., Pastorek, J., Zavada, J., Kurosaki, T., Manetta, A., Berman, M. L., DiSaia, P. J., and Stanbridge, E. J. A study of biomarkers in cervical carcinoma and clinical correlation of the novel biomarker MN. Gynecol. Oncol., *63:* 337–344, 1996.
12. Liao, S. Y., and Stanbridge, E. J. Expression of the MN antigen in cervical papanicolaou smears is an early diagnostic biomarker of cervical dysplasia. Cancer Epidemiol. Biomarkers Prev., *5:* 549–557, 1996.
13. Zavada, J., Zavadova, Z., Pastorekova, S., Ciampor, F., Pastorek, J., and Zelnik, V. Expression of MaTu-MN protein in human tumor cultures and in clinical specimens. Int. J. Cancer, *54:* 268–274, 1993.
14. Saarnio, J., Parkkila, S., Parkkila, A. K., Haukipuro, K., Pastorekova, S., Pastorek, J., Kairaluoma, M. I., and Karttunen, T. J. Immunohistochemical study of colorectal tumors for expression of a novel transmembrane carbonic anhydrase, MN/CA IX, with potential value as a marker of cell proliferation. Am. J. Pathol., *153:* 279–285, 1998.
15. Turner, J. R., Odze, R. D., Crum, C. P., and Resnick, M. B. MN antigen expression in normal, preneoplastic, and neoplastic esophagus: a clinicopathological study of a new cancer-associated biomarker. Hum. Pathol., *28:* 740–744, 1997.
16. Uemura, H., Kitagana, H., Hirso, Y., Okajama, E., DeBruyne, F., Coaterwijk, E. Expression of tumour-associated antigen MN/G250 in urologic carcinoma:potential therapeutic target. J. Urol., *157* (Suppl.): 377, 1997.
17. Vermylen, P., Roufosse, C., Burny, A., Verhest, A., Bosschaerts, T., Pastorekova, S., Ninane, V., and Sculier, J. P. Carbonic anhydrase IX antigen differentiates between preneoplastic malignant lesions in non-small cell lung carcinoma. Eur. Respir. J., *14:* 806–811, 1999.

18. Iliopoulos, O., and Kaelin, W. The molecular basis of von Hippel-Lindau disease. Mol. Med. Today, *3:* 289–293, 1997.
19. Ivanov, S. V., Kuzmin, I., Wei, M. H., Pack, S., Geil, L., Johnson, B. E., Stanbridge, E. J., and Lerman, M. I. Down-regulation of transmembrane carbonic anhydrases in renal cell carcinoma cell lines by wild-type von Hippel-Lindau transgenes. Proc. Natl. Acad. Sci. USA, *95:* 12596–12601, 1998.
20. Maxwell, P., Weisner, M. S., Chang, G. W., Clifford, S. C., Vaux E. C., Cockman, M. E., Wykoff, C. C., Pugh, C. W., Maher, E. R., Ratcliffe, P. J. The tumour suppressor protein VHL targets hypoxia-inducible factors for oxygen-dependent proteolysis. Nature (Lond.), *399:* 271–275, 1999.
21. Wykoff, C., Beasley, N., Watson, P., Turner, L., Pastorek, J., Wilson, G., Turley, H., Maxwell, P., Pugh, C., Ratcliffe, P., and Harris, A. Hypoxia-inducible regulation of tumor-associated carbonic anhydrases. Cancer Res., *60:* 7075–7083, 2000.
22. Brizel, D. M., Dodge, R. K., Clough, R. W., and Dewhirst, M. W. Oxygenation of head and neck cancer: changes during radiotherapy and impact on treatment outcome. Radiother. Oncol., *53:* 113–117, 1999.
23. Stadler, P., Becker, A., Feldmann, H. J., Hansgen, G., Dunst, J., Wurschmidt, F., and Molls, M. Influence of the hypoxic subvolume on the survival of patients with head and neck cancer. Int. J. Radiat. Oncol. Biol. Phys., *44:* 749–754, 1999.
24. Sundfor, K., Lyng, H., and Rofstad, E. K. Tumour hypoxia and vascular density as predictors of metastasis in squamous cell carcinoma of the uterine cervix. Br. J. Cancer, *78:* 822–827, 1998.
25. Vaupel, P., and Hoeckel, M. Predictive power of the tumor oxygenation status. Adv. Exp. Med. Biol., *471:* 533–539, 1999.
26. Carey, T. Head and neck tumor lines. *In:* R. Hay, A. Gazdar, and J-G. Park (eds.), Atlas of Human Tumor Cell Lines, pp. 79–120. Orlando, FL: Academic Press, Inc., 1994.
27. Pastorekova, S., Zavadova, Z., Kostal, M., Babusikova, O., and Zavada, J. A novel quasi-viral agent, MaTu, is a two-component system. Virology, *187:* 620–626, 1992.
28. Crissman, J. D., Liu, W. Y., Gluckman, J. L., and Cummings, G. Prognostic value of histopathologic parameters in squamous cell carcinoma of the oropharynx. Cancer (Phila.), *54:* 2995–3001, 1984.
29. Cordell, J. L., Falini, B., Erber, W. N., Ghosh, A. K., Abdulaziz, Z., MacDonald, S., Pulford, K. A., Stein, H., and Mason, D. Y. Immunoenzymatic labeling of monoclonal antibodies using immune complexes of alkaline phosphatase and monoclonal anti-alkaline phosphatase (APAAP complexes). J. Histochem. Cytochem., *32:* 219–229, 1984.
30. Fox, S. B. Tumour angiogenesis and prognosis. Histopathology, *30:* 294–301, 1997.
31. Tomlinson, R., and Gray, L. The histological structure of some human lung cancers and the possible implications for radiotherapy. Br. J. Cancer, *9:* 539–549, 1955.
32. Dewhirst, M. W., Secomb, T. W., Ong, E. T., Hsu, R., and Gross, J. F. Determination of local oxygen consumption rates in tumors. Cancer Res., *54:* 3333–3336, 1994.
33. Secomb, T. W., Hsu, R., Dewhirst, M. W., Klitzman, B., and Gross, J. F. Analysis of oxygen transport to tumor tissue by microvascular networks. Int. J. Radiat. Oncol. Biol. Phys., *25:* 481–489, 1993.
34. Secomb, T. W., Hsu, R., Ong, E. T., Gross, J. F., and Dewhirst, M. W. Analysis of the effects of oxygen supply and demand on hypoxic fraction in tumors. Acta Oncol., *34:* 313–316, 1995.
35. Kimura, H., Braun, R. D., Ong, E. T., Hsu, R., Secomb, T. W., Papahadjopoulos, D., Hong, K., and Dewhirst, M. W. Fluctuations in red cell flux in tumor microvessels can lead to transient hypoxia and reoxygenation in tumor parenchyma. Cancer Res., *56:* 5522–5528, 1996.
36. Moulder, J. E., and Rockwell, S. Tumor hypoxia: its impact on cancer therapy. Cancer Metastasis Rev., *5:* 313–341, 1987.
37. Gatenby, R. A., Kessler, H. B., Rosenblum, J. S., Coia, L. R., Moldofsky, P. J., Hartz, W. H., and Broder, G. J. Oxygen distribution in squamous cell carcinoma metastases and its relationship to outcome of radiation therapy. Int. J. Radiat. Oncol. Biol. Phys., *14:* 831–838, 1988.
38. Teicher, B. A. Hypoxia and drug resistance. Cancer Metastasis Rev., *13:* 139–168, 1994.
39. Helmlinger, G., Yuan, F., Dellian, M., and Jain, R. K. Interstitial pH and pO2 gradients in solid tumors *in vivo:* high-resolution measurements reveal a lack of correlation. Nat. Med., *3:* 177–182, 1997.
40. Raleigh, J. A., Calkins-Adams, D. P., Rinker, L. H., Ballenger, C. A., Weissler, M. C., Fowler, W. C., Jr., Novotny, D. B., and Varia, M. A. Hypoxia and vascular endothelial growth factor expression in human squamous cell carcinomas using pimonidazole as a hypoxia marker. Cancer Res., *58:* 3765–3768, 1998.
41. Koong, A. C., Denko, N. C., Hudson, K. M., Schindler, C., Swiersz, L., Koch, C., Evans, S., Ibrahim, H., Le, Q. T., Terris, D. J., and Giaccia, A. J. Candidate genes for the hypoxic tumor phenotype. Cancer Res., *60:* 883–887, 2000.
42. Jiang, B. H., Semenza, G. L., Bauer, C., and Marti, H. H. Hypoxia-inducible factor 1 levels vary exponentially over a physiologically relevant range of O2 tension. Am. J. Physiol., *271:* C1172–C1180, 1996.
43. Leek, R., Landers, R., Harris, A., and Lewis, C. Necrosis correlates with high vascular density and focal macrophage infiltration in invasive carcinoma of the breast. Br. J. Cancer, *79:* 991–995, 1999.
44. Graeber, T. G., Osmanian, C., Jacks, T., Housman, D. E., Koch, C. J., Lowe, S. W., and Giaccia, A. J. Hypoxia-mediated selection of cells with diminished apoptotic potential in solid tumours. Nature (Lond.), *379:* 88–91, 1996.
45. Hockel, M., Schlenger, K., Aral, B., Mitze, M., Schaffer, U., and Vaupel, P. Association between tumor hypoxia and malignant progression in advanced cancer of the uterine cervix. Cancer Res., *56:* 4509–4515, 1996.
46. Schmaltz, C., Hardenbergh, P. H., Wells, A., and Fisher, D. E. Regulation of proliferation-survival decisions during tumor cell hypoxia. Mol. Cell. Biol., *18:* 2845–2854, 1998.
47. Parkkila, S., Rajaniemi, H., Parkkila, A. K., Kivela, J., Waheed, A., Pastorekova, S., Pastorek, J., and Sly, W. S. Carbonic anhydrase inhibitor suppresses invasion of renal cancer cells *in vitro*. Proc. Natl. Acad. Sci. USA, *97:* 2220–2224, 2000.
48. Yamagata, M., and Tannock, I. F. The chronic administration of drugs that inhibit the regulation of intracellular pH: *in vitro* and anti-tumour effects. Br. J. Cancer, *73:* 1328–1334, 1996.
49. Raghunand, N., He, X., van Sluis, R., Mahoney, B., Baggett, B., Taylor, C. W., Paine-Murrieta, G., Roe, D., Bhujwalla, Z. M., Gillies, R. J. Enhancement of chemotherapy by manipulation of tumour pH. Br. J. Cancer. *80:* 1005–1011, 1999.
50. Gatenby, R. A. The potential role of transformation-induced metabolic changes in tumor-host interaction. Cancer Res., *55:* 4151–4156, 1995.
51. Gerweck, L. E. Tumor pH: implications for treatment and novel drug design. Semin. Radiat. Oncol., *8:* 176–182, 1998.
52. Kozin, S. V., and Gerweck, L. E. Cytotoxicity of weak electrolytes after the adaptation of cells to low pH: role of the transmembrane pH gradient. Br. J. Cancer, *77:* 1580–1585, 1998.
53. Ojugo, A. S., McSheehy, P. M., Stubbs, M., Alder, G., Bashford, C. L., Maxwell, R. J., Leach, M. O., Judson, I. R., and Griffiths, J. R. Influence of pH on the uptake of 5-fluorouracil into isolated tumour cells. Br. J. Cancer, *77:* 873–879, 1998.
54. Gerweck, L. E., Kozin, S. V., and Stocks, S. J. The pH partition theory predicts the accumulation and toxicity of doxorubicin in normal and low-pH-adapted cells. Br. J. Cancer, *79:* 838–842, 1999.
55. Vukovic, V., and Tannock, I. F. Influence of low pH on cytotoxicity of paclitaxel, mitoxantrone, and topotecan. Br. J. Cancer, *75:* 1167–1172, 1997.
56. Teicher, B. A., Liu, S. D., Liu, J. T., Holden, S. A., and Herman, T. S. A carbonic anhydrase inhibitor as a potential modulator of cancer therapies. Anticancer Res., *13:* 1549–1556, 1993.

Prognostic Significance of a Novel Hypoxia-Regulated Marker, Carbonic Anhydrase IX, in Invasive Breast Carcinoma

By Stephen K. Chia, Charles C. Wykoff, Peter H. Watson, Cheng Han, Russell D. Leek, Jaromir Pastorek, Kevin C. Gatter, Peter Ratcliffe, and Adrian L. Harris

Purpose: **To assess the frequency of expression and the prognostic significance of a hypoxia-regulated marker, carbonic anhydrase IX (CA IX), in a cohort of patients with invasive breast cancer.**

Patients and Methods: **CA IX expression was evaluated by immunohistochemistry with a murine monoclonal antibody, M75, in a series of 103 women treated surgically for invasive breast cancer. The majority of patients were treated with adjuvant hormonal or chemotherapy. The frequency of CA IX expression, its association with recognized prognostic factors, and the relationship with outcome was evaluated by univariate and multivariate statistical analyses.**

Results: **CA IX expression was present in 49 (48%) of 103 cases. The level of CA IX expression was found to be significantly associated with tumor necrosis ($P < .001$), higher grade ($P = .02$), and negative estrogen receptor status ($P < .001$). Furthermore, CA IX expression was associated with a higher relapse rate ($P = .004$) and a worse overall survival ($P = .001$). By multivariate analysis, CA IX was also shown to be an independent predictive factor for overall survival (hazard ratio, 2.61; 95% confidence interval, 1.01 to 6.75, $P = .05$).**

Conclusion: **CA IX expression was associated with worse relapse-free survival and overall survival in an unselected cohort of patients with invasive breast carcinoma. The potential role of CA IX as a marker of hypoxia within breast carcinomas was also indicated by a significant association with necrosis. Further work assessing its prognostic significance in breast cancer is warranted, particularly interactions with radiotherapy and chemotherapy resistance.**

J Clin Oncol 19:3660-3668.

THE BENEFITS OF adjuvant chemotherapy and hormonal therapy for the treatment of invasive breast cancer are now well proven.[1,2] However, many women still undergo treatment without necessarily achieving benefit. Much work has been directed at identifying prognostic factors that will improve our capability to predict the risk of breast cancer relapse and death in women after the diagnosis of primary breast cancer. The value of factors such as axillary lymph node status, tumor size, tumor grade, and hormonal receptor status are well established.[3-6] However, earlier diagnosis and changes in clinical practice have made it more difficult to apply all of these factors because the majority of women now present with small, node-negative tumors. Further work is required to refine relapse risk in order to determine the group of women most in need of adjuvant treatment and to spare those whose prognosis is favorable further therapy. Also, it is important to identify factors that may modify the effectiveness of therapy because these may provide new targets for modification of resistance.

Hypoxia has been implicated as an important component in tumor progression and spread. The degree of tumor hypoxia has been shown to be inversely correlated with response to treatment and overall survival.[7] This is partly related to radiation resistance but is also independently a risk factor for poor outcome.[8,9] Hypoxia is also a vital factor in the etiology of tumor necrosis, and the latter parameter has also been demonstrated, although perhaps not widely appreciated, to be a prognostic factor for a worse relapse-free and overall mortality rate in both node-negative and node-positive breast cancer.[10] A correlation has been established between the degree of tumor necrosis and angiogenesis.[11,12] Last, the degree of angiogenesis, as quantified by

From the Division of Medical Oncology, British Columbia Cancer Agency, Vancouver, British Columbia; Department of Pathology, University of Manitoba, Winnipeg, Manitoba, Canada; Imperial Cancer Research Fund Molecular Oncology Laboratory, University of Oxford, Institute of Molecular Medicine and Nuffield Department of Clinical Laboratory Sciences, John Radcliffe Hospital, and Welcome Trust, University of Oxford, Churchill Hospital, Oxford, United Kingdom; and Institute of Virology, Slovak Academy of Sciences, Slovak Republic.

Submitted September 26 2000; accepted May 8, 2001.

S.K.C. is supported by the Shane Fellowship and the Canadian Breast Cancer Foundation, British Columbia/Yukon Chapter. P.H.W. is the recipient of a Medical Research Council of Canada Scientist Award, an Academic Award from the United States Army Research and Material Command, and travel awards from Burroughs Welcome Trust and the Royal College of Physicians and Surgeons of Canada.

Address reprint requests to Adrian L. Harris, MD, Imperial Cancer Research Fund Molecular Oncology Laboratory, University of Oxford, Institute of Molecular Medicine, John Radcliffe Hospital, Oxford, OX3 9DU, United Kingdom; email: aharris.lab@lcrf.lcnet.uk.

0732-183X/01/1916-3660/$20.00

microvessel density and analysis of angiogenic factors such as vascular endothelial growth factor in tumor tissue samples, has been found to be prognostic for relapse-free survival (RFS) and overall survival (OS) in cohorts of women with node-positive and node-negative breast carcinoma.[13-18] Taken together, it may be plausible that hypoxia, tumor necrosis, and angiogenesis are potentially associated biologically and prognostically in breast carcinoma.

We have recently identified the carbonic anhydrase 9 (*CA 9*) gene to be hypoxia-inducible in several epithelial cell lines via a hypoxia response element in its 5' promoter. Furthermore, the upregulation of this enzyme was dependent on hypoxia inducible factor 1.[19] Carbonic anhydrase 9 protein (CA IX) belongs to the family of zinc metalloenzymes responsible for the reversible conversion of carbon dioxide and water to carbonic acid. Members of the mammalian alpha-CA family play a variety of roles in many physiologic processes, in particular serving to maintain pH, water, and ion equilibrium.[20,21] CA IX, originally identified in HeLa cells (a human cervical carcinoma cell line), was also found to be a tumor marker in human ovarian, endometrium, and cervical cancer specimens, and was named MN.[22] Subsequently, the MN cDNA was cloned and the transmembrane protein product showed structural and functional homology with other alpha-CA isoenzymes[23,24] and was subsequently renamed *CA 9*.[25] CA IX is normally expressed in the alimentary tract and associated organs.[26,27] Further work has shown that CA IX is expressed in renal cell carcinoma,[28,29] esophageal carcinoma,[30] non–small-cell lung carcinoma,[31] and colorectal tumors.[32] These studies have also revealed that the expression of this biomarker is restricted to transformed, dysplastic, and malignant epithelial cells and is rarely expressed in benign tumors or normal tissue.

To date, we are unaware of any extensive reports investigating the presence of CA IX in human breast cancer or on the relationship of CA IX expression to outcome in any human cancer series. Therefore, in light of our recent findings that CA IX may be a marker for hypoxia in vivo, the aims of this study were to assess the expression of CA IX in invasive breast carcinoma in relation to tumor necrosis and to determine whether this novel biomarker is an independent prognostic factor for breast cancer relapse and death.

PATIENTS AND METHODS

Patients and Tissues

We assessed a series of 103 surgically resected available invasive breast carcinomas treated at the John Radcliffe Hospital and the Churchill Hospital, Oxford, from 1989 to 1994 with a median follow-up of 6.2 years. The majority of the cohort underwent either modified radical mastectomy or lumpectomy with breast irradiation. Axillary lymph node status was confirmed histologically. If lymph node involvement was found, then adjuvant radiotherapy to the axilla was delivered. Adjuvant systemic treatment consisted of tamoxifen at 20 mg daily for 5 years for postmenopausal women regardless of hormonal receptor status and six cycles of intravenously administered cyclophosphamide, methotrexate, and fluorouracil delivered every 3 weeks for premenopausal women. All patients were assessed at follow-up every 3 months for the first 18 months and every 6 months thereafter. Treatment for confirmed recurrent disease was by endocrine manipulation for soft tissue or skeletal metastasis or by chemotherapy for visceral disease and failed endocrine therapy. The clinicopathologic characteristics of the entire cohort are summarized in Table 1.

Table 1. Patient Demographics

Characteristic		No. of Patients (N = 103)
Age, years		
Median	59	
Range	28-82	
< 50 years		27
≥ 50 years		76
Surgical treatment		
Lumpectomy		5
Lumpectomy + RT		63
Mastectomy		35
Tumor size, cm		
Median	2.4	
Range	0.8-8.0	
< 2 cm		43
≥ 2 cm		58
Node status		
Positive		58
Range of positive nodes	1-16	
Negative		45
Grade		
1		15
2		48
3		40
ER status		
Positive		70
Negative		33
EGFR status		
Positive		56
Negative		46
Adjuvant therapy		
Chemotherapy		27
Hormonal therapy (tamoxifen)		80
Duration follow-up, years		
Median	6.2	
Range	0.4-10.1	
Relapses		41
Deaths		32

Abbreviations: ER, estrogen receptor; EGFR, epidermal growth factor receptor; RT, radiotherapy.

Immunohistochemistry

Immunohistochemical staining for CA IX was performed on 5-μm serial sections on coated slides from paraffin-embedded blocks. Paraffin was first removed from all slides by means of standard techniques; slides were then placed in 0.5% hydrogen peroxide for 15 minutes to saturate endogenous peroxidases. Incubation with 10% normal human serum in Tris-buffered saline (TBS) for 15 minutes was then performed to block nonspecific uptake of the antibody. The murine monoclonal antibody M75 at a dilution of 1:50 in TBS with 5% normal human serum for 30 minutes was used to assess expression of CA IX. This antibody has previously been characterized with Western blot analysis to confirm its specificity.[27] We have also further confirmed its ability to specifically detect CA IX expression in tissue sections by direct correlation with Western blot analysis in human breast tumor specimens.[33] Known positive and negative controls for CA IX expression from this direct correlation were then used with each immunohistochemistry (IHC) procedure batch to ensure quality control of staining. Next, a 30-minute incubation with a peroxidase conjugated to goat anti-mouse immunoglobulins (Dako EnVision + System, peroxidase, mouse; Dako, Carpinteria, CA) was performed. Slides were then stained with 3,3'-diaminobenzidine chromogen solution for 8 minutes, then counterstained with hematoxylin and mounted with Aquamount. All staining was performed on an automated immunohistochemical stainer (Miniprep 75; Tecan, Reading, United Kingdom) at room temperature. After successive incubations (except the normal human serum block), the slides were washed twice with TBS for 5 minutes.

Assessment of CA IX Expression

Immunostaining was quantified for CA IX by light microscopy and semiquantitative scoring by a single pathologist (P.H.W.) blinded to the patients' clinical data and outcome. In brief, a score of 0 to 3 for the intensity of staining in the majority of the entire section with invasive carcinoma was given (0, no staining; 1, weak staining; 2, moderate staining; 3, strong staining). All slides were evaluated by light microscopy, and the percentage of tumor cells throughout the section that were stained positive was estimated. The product of the intensity staining and the percentage of tumor then produced a final immunostaining score (IHC score) of 0 to 300.

Tumor Hormone Receptor Status

Estrogen receptor (ER) analysis was performed using an enzyme-linked immunosorbent assay technique (Abbott Laboratories, North Chicago, IL). Tumors with cytoplasmic estrogen levels greater than 10 fmol/mg protein were considered positive. Epidermal growth factor receptor (EGFR) was determined by a ligand binding assay as previously described.[34] Tumors with an EGFR level of $\geq$ 20 fmol/mg membrane protein were considered positive.

Assessment of Tumor Grade and Necrosis

Tumor grade and necrosis was scored by a single pathologist (P.W.H.), independent from the IHC analysis and blinded to the patients' clinical data and outcome, on hematoxylin-and-eosin–stained sections adjacent to those sections subjected to IHC. Tumor grade was assessed with the Nottingham scoring system.[35] The entire section was assessed, and the percentage of necrosis within the invasive tumor component was scored. Necrosis within in situ carcinoma components was not scored. For statistical analysis, the percentage of necrosis was either categorized into four categories of levels (negative, low, medium, or high) or divided into negative or positive (where the presence of any necrosis was considered positive), as previously described.[11]

Statistical Analysis

For statistical analysis, CA IX expression was evaluated as both a continuous and a discontinuous variable. In the latter case, the median IHC score for the entire series was used as a cutpoint (ie, an IHC score $\geq$ 1, corresponding to the presence of any staining, was considered as positive for CA IX expression). CA IX was evaluated in relation to a range of established prognostic variables by the Mann-Whitney test and Kruskal-Wallis tests where appropriate. The association with RFS and OS was assessed by univariate analysis (log-rank test and Kaplan-Meier method) and multivariate analysis (Cox regression model). All tests were performed using Stata statistical analysis software version 5.0 (Stata Corp, College Station, TX).

RESULTS

The clinicopathologic features of this unselected cohort of 103 women with invasive breast cancer are described in detail in Table 1. Among these patients, the median age was 59 years, the median tumor size was 2.4 cm, 58% had axillary node-positive disease, and 68% were positive for ER. Necrosis was present in 50 patients, and among this subset, marked necrosis ($\geq$ 25% of tumor) was present in 14 patients. The mean percentage necrosis was 17% (SD, $\pm$ 16%). The majority, 90 cases, were invasive ductal carcinomas; 11 were invasive lobular carcinomas, and two were tubular carcinomas. The median duration of follow-up for the entire cohort was 6.2 years; to date, 41 members (40%) of the cohort have relapsed and 32 (31%) have died.

CA IX Expression in Relation to Clinicopathologic Variables

The specificity of the M75 antibody for detection of CA IX expression in breast tissue sections was initially confirmed by comparison of IHC scores with the detection of the 58-kd and 54-kd bands corresponding to the CA IX protein in Western blots performed on the same tumor specimens.[33]

CA IX expression was detectable in 48% of cases as strong membranous staining within epithelial tumor cells. The pattern of expression was predominantly focal within the tumor and typically limited to tumor cells immediately adjacent to areas of necrosis. Expression was also occasionally seen adjacent to areas of dense collagenous stromal scar within the central regions of some tumors. The focal nature of expression was reflected in the distribution of IHC scores (range, 0 to 225; median, 0; mean, 23), with only 14% of tumors having an IHC score greater than 50. Representative examples of tumors showing low, moderate, and high CA IX expression are illustrated in Fig 1.

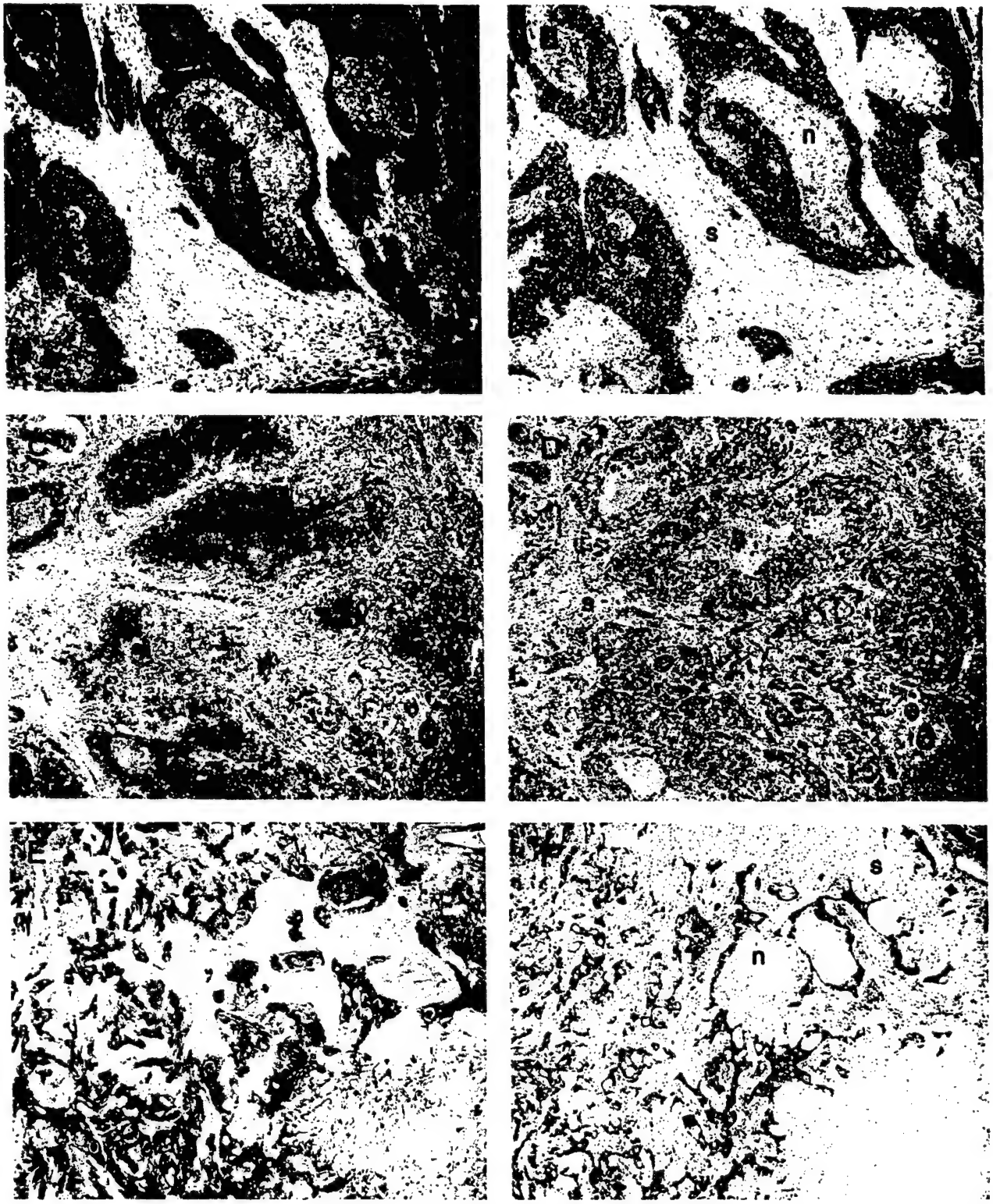

Fig 1. Representative immunohistochemical expressions of CA IX with the corresponding hematoxylin-and-eosin (H&E)–stained slides: (A) low expression of CA IX; (B) H&E slide corresponding to A; (C) moderate expression of CA IX; (E) H&E slide corresponding to C; (E) high expression of CA IX; (F) H&E slide corresponding to E. Abbreviations: n, necrosis; s, stroma; t, tumor.

Table 2. Association Between CA IX Expression and Other Prognostic Parameters

Variable	CA IX IHC Score Mean	SD	P
Grade			
1	8	14	
2	19	43	
3	33	47	.02
ER			
Negative	50	59	
Positive	10	24	< .001
Necrosis			
Negative	9	25	
Positive	38	52	< .001

Abbreviations: CA IX, carbonic anhydrase IX; IHC, immunohistochemistry.

CA IX expression was compared with several established clinicopathologic prognostic variables (Table 2). Within the entire cohort, significant associations were found between the presence and level of CA IX expression and the presence of necrosis ($P < .001$), higher tumor grade ($P = .02$), and negative ER status ($P < .001$). There were no apparent relationships with other prognostic variables such as age, nodal status, tumor size, tumor type, and EGFR status. Necrosis was also assessed in relation to ER status and grade and was significantly associated with ER-negative status ($P = .002$) and high grade ($P < .0001$).

Relationship of CA IX to RFS and OS

Univariate analysis of established prognostic factors and their relationship to survival confirmed that nodal status, grade, and ER status were all significantly related to both RFS (P values, $< .001$, $= .04$, and $= .03$, respectively) and OS (P values, $< .001$, $= .04$, and $= .02$, respectively). Tumor size was also predictive of RFS ($P = .04$), and patient age was found to be predictive of OS ($P = .05$). The presence of CA IX expression showed a significant association with a shorter RFS ($P = .004$) and a poorer OS ($P = .001$) (Fig 2). Similarly, the level of CA IX expression was also significant in terms of RFS ($P = .04$) and OS ($P < .001$). Interestingly, the presence of necrosis was also significantly associated with OS ($P = .03$).

In multivariate Cox proportional hazards analysis, where nodal status, ER status, tumor size, grade, and necrosis were considered together with the CA IX status, positive lymph node involvement was an independent predictor of RFS (hazard ratio, 2.90, $P = .006$). Although statistically insignificant, the presence of CA IX expression trended for a worse RFS (hazard ratio, 2.13, $P = .06$). When these same factors were analyzed for their impact on overall survival, only positive lymph node status and CA IX presence were significant independent predictors of OS ($P = .004$ and $P = .05$, respectively) (Table 3). The presence of any CA IX staining was found to be an independent poor prognostic factor for overall survival, with a hazard ratio of 2.61 ($P = .05$, 95% confidence interval, 1.01 to 6.75). Moreover, quantitatively, every 10-unit increase in CA IX IHC score was associated with a hazard ratio of 1.16 ($P = .002$, 95% confidence interval, 1.06 to 1.27). Thus, not only the presence but also the extent of CA IX expression is independently associated with a poorer outcome in this cohort of patients with breast cancer.

Table 3. Cox Multivariate Analysis for Overall Survival

Variable	Odds Ratio	95% CI	Significance
Nodal status	3.78	1.52-9.44	.004
CA IX	2.61	1.01-6.75	.05
Grade	1.43	0.64-3.23	NS
Size	1.43	0.65-3.18	NS
ER	0.71	0.29-1.75	NS
Necrosis	0.94	0.35-2.53	NS

Abbreviations: CI, confidence interval; NS, not significant.

DISCUSSION

We have recently shown a marked upregulation of *CA 9* mRNA and protein in cancer cell lines exposed to hypoxia.[19] In this current study, we have extended our previous observation to show that CA IX is expressed in invasive breast carcinoma in vivo, with expression being virtually restricted to regions directly adjacent to areas of necrosis. Furthermore, we have demonstrated that CA IX is associated with several poor prognostic factors, including high tumor grade, ER-negative status, and the presence of necrosis. Finally, CA IX expression is predictive for reduced RFS and OS in univariate analysis and is an independent factor for overall survival in multivariate analysis. Though CA IX was not statistically an independent predictive factor for RFS in multivariate analysis, a trend for a worse RFS was seen ($P = .06$). Because this is what is to our knowledge the first published study describing a possible relationship to outcome for this carbonic anhydrase, further work in larger cohorts of patients is warranted to confirm these findings.

CA IX was first identified in a human cervical carcinoma (HeLa) cell line and was subsequently found to be present in human carcinoma cell lines and clinical tumor specimens, but not in the corresponding normal tissue.[22] Further evidence for a role in tumorigenesis came with the acquisition of many of the features of a transformed phenotype by

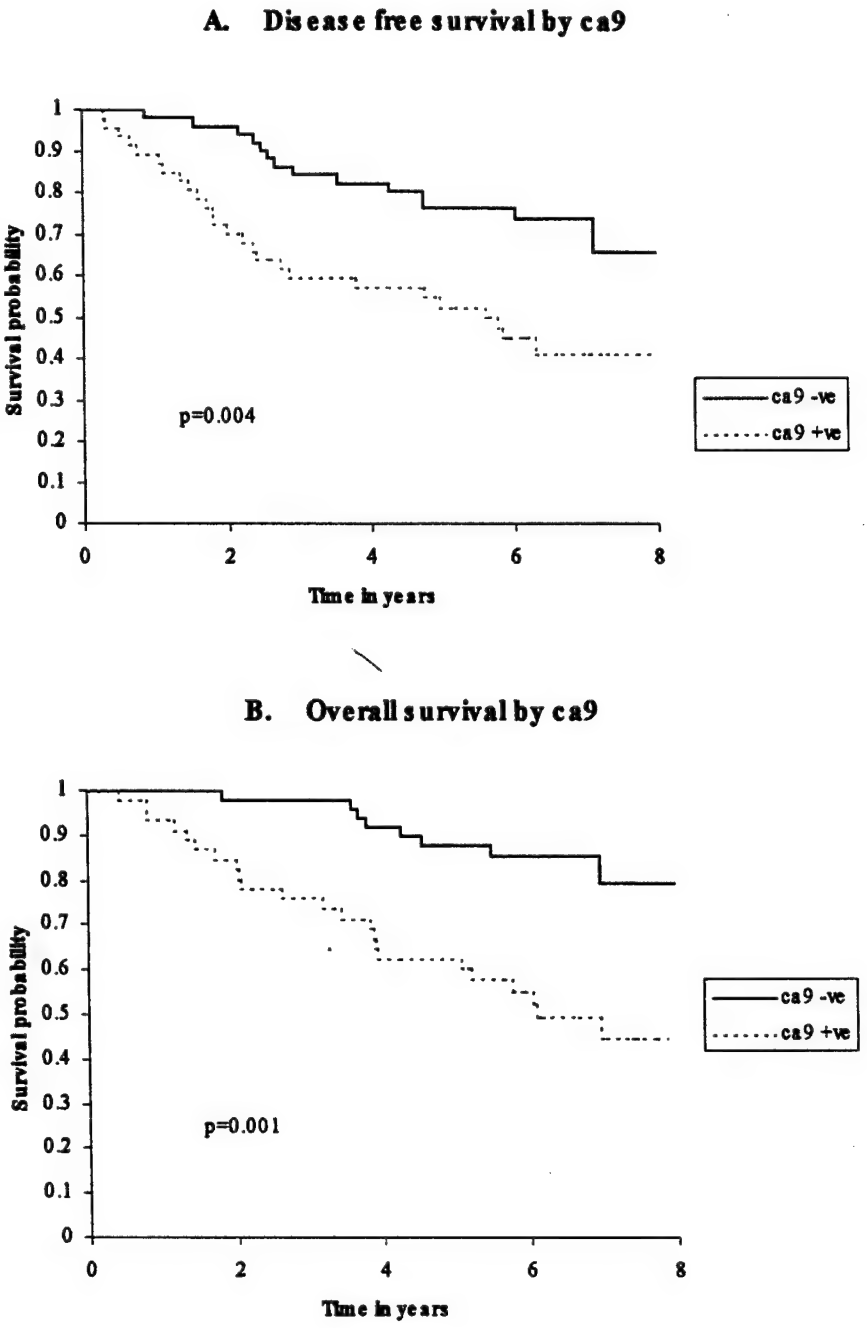

Fig 2. Disease-free survival and overall survival for expression of CA IX. Kaplan-Meier estimates of disease-free survival (A) and overall survival (B) according to presence or absence of CA IX expression.

stable transfection of NIH 3T3 cells with the MN cDNA (altered morphology, enhanced DNA synthesis with shorter doubling times, and capacity for anchorage-independent growth).[23] Cloning of MN identified four distinct domains: an *N*-terminal region with structural features suggesting a role in extracellular matrix interactions, a second extracellular domain with close homology to the catalytic domain of other members of the alpha-CA gene family, a transmembrane region, and an intracytoplasmic C terminus.[23,24]

In the current study, CA IX expression was closely correlated with the presence of necrosis, believed to be an indicator of local hypoxia, within invasive breast tumors. In a recent study, conducted on a similarly sized cohort of invasive breast cancers, we found that the presence of

necrosis correlated with high vascular density, high tumor grade, and ER-negative status.[11] However, necrosis was not related to RFS or OS. In the present cohort, we have also confirmed that necrosis is associated with ER-negative and high-grade tumors, but necrosis also showed a significant relationship with poor overall survival, but not with RFS, in univariate analysis. The explanation for this difference is not clear; however, it is of potential relevance that the current cohort has longer follow-up (74 months *v* 63 months).

Previous work on CA IX has identified a similar pattern of membranous expression on malignant cells, with rare expression in normal or benign tissue (most prevalent in the gastrointestinal tract and associated organs).[28-32] In a study of 65 non–small-cell lung carcinoma specimens, the frequency of positive immunostaining was 80%, with no correlation with histologic subtype or tumor differentiation.[31] In a series of 147 renal cell carcinomas, IHC demonstrated strong staining in 87% of tumors. Interestingly, there was a significant inverse relationship between MN/CA IX staining and tumor grade and stage, with a greater proportion of malignant cells staining positive in the lower-grade and -stage tumors.[36] This inverse correlation of level of CA IX expression and histologic grade and other poor prognostic factors (eg, depth of invasion, lymph node metastasis) has also been shown in studies with cervical carcinoma,[37] colorectal carcinoma,[32] and esophageal cancer.[30] This is different from the results of our study, where there is a positive correlation between the level of CA IX expression and the tumor grade, as indicated by both histologic grade and ER status. The reason for this difference is unknown. However, one possibility is that although hypoxia associated with visible necrosis seems to be a dominant factor in the regulation of CA IX in breast tissues, there may be other factors involved in the regulation CA IX expression in other tissues and related tumor types. Certainly an association between CA IX expression and areas of necrosis has not been described in these other studies.

An explanation for the association seen in breast tumors between CA IX expression and poor prognosis may lie in the nature of its involvement in pH regulation in breast tissue. Evidence exists that the extracellular pH of solid tumors is often more acidic than that of normal tissue,[38,39] whereas the intracellular pH in tumors is similar to normal cells.[39-41] It is thought that this altered cellular pH gradient may have implications for resistance to certain chemotherapeutic agents, in particular weakly basic drugs such as doxorubicin, because of reduced permeability and cell uptake. In fact, a recent study has demonstrated enhanced efficacy for doxorubicin in human breast cancer cells in vitro and in vivo when the pH is raised from 6.8 to 7.4.[42] Because carbonic anhydrases exert their enzymatic effect by catalyzing the reversible interconversion of carbonic acid to carbon dioxide, expression of CA IX may reflect an adaptive cellular response to extremes of pH and therefore may indicate those tumors with regions of very low extracellular pH that may then contribute to chemotherapeutic and radiation resistance. Alternatively, it has been proposed that expression of CA IX may positively contribute to reduction of extracellular pH and thereby contribute as a causal factor to increased malignancy and invasiveness.[43]

Last, the utility of CA IX as a biomarker may have both diagnostic and therapeutic implications. Besides its specificity by IHC for malignant cells, a recent study has shown that reverse transcriptase–polymerase chain reaction detection of *CA 9* can be highly specific for detecting circulating renal carcinoma cells.[44] Likewise, work has already been performed on a radiolabeled antibody to CA IX (mAbG250) for scintigraphic diagnosis of renal cell carcinoma,[45] and this same antibody has also been shown to exert antitumor effects on a renal cell carcinoma xenograft model.[46] However, the specific functions of CA IX on the growth of breast cancer remain to be established.

In conclusion, we have shown that CA IX expression is closely associated with necrosis in invasive breast carcinoma, complementing previous work demonstrating that CA IX is regulated by hypoxia in vitro. We have also shown that this biomarker has prognostic significance for a shorter RFS and a worse OS in an unselected series of invasive breast carcinomas. It remains to be determined whether the expression of CA IX in breast cancers in vivo is simply an indicator of response to necrosis caused by local hypoxia or whether it actively contributes to the process of tumor progression. Confirmation of the prognostic significance of CA IX expression in larger randomized studies is clearly warranted to explore this relationship further.

REFERENCES

1. Early Breast Cancer Trialists' Collaborative Group: Polychemotherapy for early breast cancer. Lancet 352:930-942, 1998

2. Early Breast Cancer Trialists' Collaborative Group: Tamoxifen for early breast cancer: An overview of the randomized trials. Lancet 351:1451-1467, 1998

3. Fisher B, Bauer M, Wickerham DL, et al: Relation of number of positive axillary nodes to the prognosis of patients with primary breast cancer: An NSABP update. Cancer 52:1551-1557, 1983

4. Davies BW, Gelber D, Goldhirsh A, et al: Prognostic significance of tumor grade in clinical trials of adjuvant therapy for breast cancer with axillary lymph node metastasis. Cancer 58:2662-2670, 1986

5. Koscielny S, Tubiana M, Le MG, et al: Breast cancer: Relationship between the size of the primary tumor and the probability of metastatic dissemination. Br J Cancer 49:709-715, 1984

6. Clark GM, McGuire WL: Steroid receptors and other prognostic factors in primary breast cancer. Semin Oncol 15:20-25, 1988 (suppl 1)

7. Hockel M, Schlenger K, Aral B, et al: Association between tumor hypoxia and malignant progression in advanced cancer of the uterine cervix. Cancer Res 56:4509-4515, 1996

8. Fyles AW, Milosevic M, Wong R, et al: Oxygenation predicts radiation response and survival in patients with cervix cancer. Radiother Oncol 48:149-156, 1998

9. Nordsmark M, Overgaard M, Overgaard J: Pretreatment oxygenation predicts radiation response in advanced squamous cell carcinoma of the head and neck. Radiother Oncol 41:31-39, 1996

10. Fisher ER, Anderson S, Redmond C, et al: Pathologic findings from the National Surgical Adjuvant Breast Project protocol B-06: 10 year pathologic and clinical prognostic discriminants. Cancer 71:2507-2514, 1993

11. Leek RD, Landers RJ, Harris AL, et al: Necrosis correlates with high vascular density and focal macrophage infiltration in invasive carcinoma of the breast. Br J Cancer 79:991-995, 1999

12. Kato T, Kimura T, Miyakawa R, et al: Clinicopathologic study of angiogenesis in Japanese patients with breast cancer. World J Surg 21:49-56, 1997

13. Weidner N, Semple JP, Welch WR, et al: Tumor angiogenesis and metastasis-correlation in invasive breast carcinoma. N Engl J Med 324:1-8, 1991

14. Horak ER, Leek R, Klenk N, et al: Angiogenesis, assessed by platelet/endothelial cell adhesion molecule antibodies, as indicator of node metastasis and survival in breast cancer. Lancet 340:1120-1124, 1992

15. Fox SB, Leek RD, Smith K, et al: Tumor angiogenesis in node-negative breast carcinomas: Relationship with epidermal growth factor receptor and survival. Breast Cancer Res Treat 29:109-116, 1994

16. Gasparini G, Weidner N, Bevilacqua P, et al: Tumor microvessel density, p53 expression, tumor size and peritumoral lymphatic vessel invasion are relevant prognostic markers in node-negative breast carcinoma. J Clin Oncol 12:454-466, 1994

17. Gasparini G, Toi M, Gion M, et al: Prognostic significance of vascular endothelial growth factor protein in node-negative breast carcinoma. J Natl Cancer Inst 89:139-147, 1997

18. Linderholm B, Grankvist K, Wilking N, et al: Correlation of vascular endothelial growth factor content with recurrences, survival, and first relapse site in primary node-positive breast carcinoma after adjuvant treatment. J Clin Oncol 18:1423-1431, 2000

19. Wykoff CC, Beasley NJP, Watson PH, et al: Hypoxia inducible expression of tumor associated carbonic anhydrases. Cancer Res 60:7075-7083, 2000

20. Maren TH: Carbonic anhydrase: Chemistry, physiology and inhibition. Physiol Rev 47:595-781, 1967

21. Tashian RE: The carbonic anhydrases: Widening perspectives on their evolution, expression and function. Bioessays 10:186-192, 1989

22. Zavada J, Zavadova Z, Pastorekova S, et al: Expression of MaTu-MN protein in human tumor cultures and in clinical specimens. Int J Cancer 54:268-274, 1993

23. Pastorek J, Pastorekova S, Callebaut I, et al: Cloning and characterization of MN, a human tumor-associated protein with a domain homologous to carbonic anhydrase and a putative helix-loop-helix DNA binding segment. Oncogene 9:2877-2888, 1994

24. Opavsky R, Pastorekova S, Zelnik V, et al: Human MN/CA 9 gene, a novel member of the carbonic anhydrase family: Structure and exon to protein domain relationships. Genomics 33:480-487, 1996

25. Hewett-Emmett D, Tashian RE: Functional diversity, conservation, and convergence in the evolution of the alpha-, beta- and gamma-carbonic anhydrase gene families. Mol Phylogenet Evol 5:50-77, 1996

26. Pastorekova S, Parkkila S, Parkkila AK, et al: Carbonic anhydrase IX, MN/CA IX: Analysis of stomach complementary DNA sequence and expression in human and rat alimentary tracts. Gastroenterology 112:398-408, 1997

27. Saarnio J, Parkkila S, Parkkila AK, et al: Immunohistochemistry of carbonic anhydrase isozyme IX (MN/CA IX) in human gut reveals polarized expression in the epithelial cells with the highest proliferative capacity. J Histochem Cytochem 46:497-504, 1998

28. Liao SY, Aurelio ON, Jan K, et al: Identification of the MN/CA 9 protein as a reliable diagnostic biomarker of clear cell carcinoma of the kidney. Cancer Res 57:2827-2831, 1997

29. McKiernan JM, Buttyan R, Bander NH, et al: Expression of the tumor-associated gene MN: A potential biomarker for human renal cell carcinoma. Cancer Res 57:2362-2365, 1997

30. Turner JR, Odze RD, Crum CP, et al: MN antigen expression in normal, preneoplastic, and neoplastic esophagus: A clinicopathological study of a new cancer associated biomarker. Hum Pathol 28:740-744, 1997

31. Vermylen P, Roufosse C, Burny A, et al: Carbonic anhydrase IX antigen differentiates between preneoplastic malignant lesions in non–small cell lung carcinoma. Eur Respir J 14:806-811, 1999

32. Saarnio J, Parkkila S, Parkkila AK, et al: Immunohistochemical study of colorectal tumors for expression of a novel transmembrane carbonic anhydrase, MN/CA IX, with potential value as a marker of cell proliferation. Am J Pathol 153:279-285, 1998

33. Wykoff CC, Beasely NJP, Watson PH, et al: Expression of the hypoxia inducible and tumor associated carbonic anhydrases in ductal carcinoma in situ (DCIS) of the breast. Am J Pathol 158:1011-1019, 2001

34. Fox FB, Smith K, Hollyer J, et al: The epidermal growth factor receptor as a prognostic marker: Results of 370 patients and review of 3009 patients. Breast Cancer Res Treat 29:41-49, 1994

35. Elston CW, Ellis IO: Pathological prognostic factors in breast cancer: The value of histological grade in breast cancer—Experience from a large study with long term follow-up. Histopathology 19:403-410, 1991

36. Uemura H, Nakagawa Y, Yoshida K, et al: MN/CA IX/G250 as a potential target for immunotherapy of renal cell carcinomas. Br J Cancer 81:741-746, 1999

37. Brewer C, Liao SY, Wilczynski SP, et al: A study of biomarkers in cervical carcinoma and clinical correlation of the novel biomarker MN. Gynecol Oncol 63:337-344, 1996

38. Wike-Hooley JL, Haveman J, Reinhold HS: The relevance of tumour pH to the treatment of malignant disease. Radiother Oncol 2:343-366, 1984

39. Gerweck LE, Seetharaman K: Cellular pH gradient in tumor versus normal tissue: Potential exploitation for the treatment of cancer. Cancer Res 15:1194-1198, 1996

40. Griffiths JR: Are cancer cell acidic? Br J Cancer 64:425-427, 1991

41. Negendank W: Studies of human tumours by MRS: A review. NMR Biomed 5:303-324, 1992

42. Raghunand N, He X, van Sluis R, et al: Enhancement of chemotherapy by manipulation of tumour pH. Br J Cancer 80:1005-1011, 1999

43. Ivanov SV, Kuzmin I, Wei M-H, et al: Down regulation of transmembrane carbonic anhydrases in renal carcinoma cell lines by wild-type von Hippel-Lindau transgenes. Proc Natl Acad Sci U S A 95:12596-12601, 1998

44. McKiernan JM, Buttyan R, Bander NH, et al: The detection of renal carcinoma cells in the peripheral blood with an enhanced reverse transcriptase–polymerase chain reaction assay for MN/CA 9. Cancer 86:492-497, 1999

45. Steffens MG, Boerman OC, Oosterwijk-Wakka JC, et al: Targeting of renal cell carcinoma with iodine-131–labeled chimeric monoclonal antibody G250. J Clin Oncol 15:1529-1537, 1997

46. Van Dijk J, Uemura H, Beniers AMJC, et al: Therapeutic effects of monoclonal antibody G250, interferons and tumor necrosis factor, in mice with renal cell carcinoma xenografts. Int J Cancer 56:262-268, 1994

[CANCER RESEARCH 61, 6669–6673, September 15, 2001]

Advances in Brief

HIF-1-dependent Regulation of Hypoxic Induction of the Cell Death Factors BNIP3 and NIX in Human Tumors[1]

Heidi M. Sowter, Peter J. Ratcliffe, Peter Watson, Arnold H. Greenberg, and Adrian L. Harris[2]

Institute of Molecular Medicine, John Radcliffe Hospital, Oxford, OX3 9DS [H. M. S., A. L. H.], Welcome Trust Centre for Human Genetics, Oxford, OX3 7BN [P. J. R.], United Kingdom; University of Manitoba, Winnipeg, Manitoba, R3E 0W3 Canada [P. W., A. H. G.]

Abstract

Solid tumors contain regions of hypoxia, a physiological stress that can activate cell death pathways and, thus, result in the selection of cells resistant to death signals and anticancer therapy. Bcl2/adenovirus E1B 19kD-interacting protein 3 (BNIP3) is a cell death factor that is a member of the Bcl-2 proapoptotic family recently shown to induce necrosis rather than apoptosis. Using cDNA arrays and serial analysis of gene expression, we found that hypoxia induces up-regulation of BNIP3 and its homologue, Nip3-like protein X. Analysis of human carcinoma cell lines showed that they are hypoxically regulated in many tumor types, as well as in endothelial cells and macrophages. Regulation was hypoxia inducible factor-1-dependent, and hypoxia inducible factor-1 expression was suppressed by von Hippel-Lindau protein in normoxic cells. Northern blotting and *in situ* hybridization analysis has revealed that these factors are highly expressed in human tumors compared with normal tissue and that BNIP3 is up-regulated in perinecrotic regions of the tumor. This study shows that genes regulating cell death can be hypoxically induced and are overexpressed in clinical tumors.

Introduction

Solid tumors are poorly oxygenated compared with normal tissues and contain regions of hypoxia. Induction of apoptosis by hypoxia is one mechanism by which stress-damaged cells can be destroyed, and most tumor cells retain the ability to undergo apoptosis in response to hypoxic stress (1). However, hypoxia increases the mutation rate of cells (2), resulting in the selection of mutations that make cells more resistant to apoptosis and less responsive to cancer therapy (3, 4). HIF-1[3] is a heterodimeric transcription factor consisting of an oxygen-regulated α subunit (Hif-1α) and a stable nuclear factor, Hif-1β/ARNT, and has been well characterized as a mediator of hypoxic response (reviewed in Ref. 5). Under normoxic conditions, Hif-1α is rapidly degraded by the proteosome after being targeted for ubiquitination, a process that is dependent on the pVHL (6). Under hypoxic conditions, degradation of Hif-1α is suppressed, and transcription of mRNAs encoding hypoxically responsive genes can occur. HIF-1 has been shown to be a factor mediating hypoxia-induced apoptosis; hypoxia increases apoptosis in Hif-1α++ embryonic stem cells and CHO cells, but this process is strikingly reduced in the same cells in which the gene has been disrupted (7). We screened for genes induced by hypoxia in a breast carcinoma cell line (T47D) using gene expression arrays and detected an up-regulation of BNIP3. Also, using the SAGE map website,[4] virtual subtraction of genes expressed by a glioblastoma cell line (H247) under normoxic and hypoxic conditions revealed up-regulation of NIX in hypoxia (8). BNIP3 is a proapoptotic mitochondrial protein that was isolated through its interaction with E1B 19K and Bcl-2 (9). Overexpression of BNIP3 and its homologue NIX (10–12) in Rat-1 fibroblasts and MCF-7 breast carcinoma cells induces cell death within 12 h. BNIP3 and NIX are expressed ubiquitously in most human tissues as assessed by Northern blotting (12), although it is not known which cell types express BNIP3 and NIX or if their pattern of expression differs in malignant tissue. A recent study has shown that BNIP3 mRNA levels increase in response to hypoxia in a CHO cell line and that this effect is mediated via Hif-1α (13). We have characterized the response of BNIP3 and NIX to hypoxia in human cell lines and shown that BNIP3 and NIX are overexpressed in human tumors compared with normal tissue.

Materials and Methods

Cell Culture. Human cell lines were obtained from the Imperial Cancer Research Fund cell service and grown in DMEM, RPMI 1640, or Hams F-12 supplemented with 10% FCS (Globepharm), L-glutamine (2 μM), penicillin (50 IU/ml), and streptomycin sulfate (50 μg/ml). The human cell lines investigated were: SKBr, T47D, MDA468, MCF7, and MDA231 (breast cancer); SKOV3 (ovarian cancer); HT1080 (fibrosarcoma), MKN45 (stomach cancer); C32 and LS174T (colon cancer); EJ (bladder cancer); DU145 (prostate cancer); U937 and THP-1 (macrophage); RZM (Epstein-Barr virus-transformed normal human lymphocytes); HUVEC (endothelial). RCC4 (renal cancer) cell lines expressing pVHL or empty vector have been described previously (6). The CHO cell lines used were KA13 (mutated to be defective for Hif-1α) and C4.5 (the parent cell line) and have been described previously (14). Parallel incubations were performed on flasks of cells approaching confluence in normoxia (humidified air with 5% CO_2) or hypoxia [hypoxic conditions were generated in a Napco 7001 incubator (Precision Scientific) with 0.1% O_2, 5% CO_2, and balance N_2].

Western Blotting. Cells were homogenized in a lysis buffer containing 8 M urea, 10% SDS, 1 M DTT, and protease inhibitors. Proteins were electrophoresed on a 10% SDS-PAGE gel and transferred onto a polyvinylidene difluoride membrane (Millipore). BNIP3 protein was detected using a mouse antihuman BNIP3 monoclonal antibody (10) followed by goat antimouse horseradish peroxidase (Dako) and enhanced chemiluminescence developing reagents (Amersham). Blots were exposed to film from 30 s to 2 min.

Immunohistochemistry. Formalin-fixed paraffin-embedded tissue (John Radcliffe Hospital pathology archives) or cell pellets (created by washing and centrifuging cell lines, which had been scraped from tissue culture flasks) was sectioned onto 3-aminopropyltriethoxy-silane (Sigma Chemical Co.) -coated slides. Sections were dewaxed and rehydrated before being blocked in 10% horse serum. A rabbit polyclonal antibody to BNIP3, which has been described previously (15), or a mouse monoclonal antibody to human CD68 (Dako) was applied to the sections at 1:500 and 1:10. Biotinylated horse antimouse IgG or goat antimouse IgG (1:200) and avidin-biotin complex AP conjugate were applied consecutively for 30 min each at room temperature and visualized using AP substrate (Vectastain).

Probe Production. Regions of BNIP3 and NIX selected to avoid areas of homology were amplified by reverse transcription-PCR from cDNA synthesized from MCF-7 cells subjected to hypoxia. BNIP3 cDNA was amplified between bp 277 and 431 using 5′-ACCAACAGGGCTTCTGAAAC-3′ as the

Recevied 3/27/01; accepted 8/1/01.

The costs of publication of this article were defrayed in part by the payment of page charges. This article must therefore be hereby marked *advertisement* in accordance with 18 U.S.C. Section 1734 solely to indicate this fact.

[1] Supported by the Imperial Cancer Research Fund.

[2] To whom requests for reprints should addressed, at Institute of Molecular Medicine, John Radcliffe Hospital, Oxford, OX3 9DS, United Kingdom. E-mail: harrisa@icrf.icnet.uk.

[3] The abbreviations used are: HIF, hypoxia-inducible factor; VHL, von Hippel-Lindau; pVHL, product of the von Hippel-Lindau gene; CHO, Chinese hamster ovary.

[4] Internet address: http://www.ncbi.nlm.nih.gov/SAGE.

upstream primer and 5′-GAGGGTGGCCGTGCGC-3′ as the downstream reverse complement primer. NIX cDNA was amplified between bp 716 and 798 using 5′-AGTAGCTTATTTGAACTTGAGACCATTG-3′ as the upstream primer and 5′-TGAGGGTTACTGGAATTGGATATGTA-3′ as the downstream reverse complement primer. The purified PCR products were labeled for Northern blotting with [^{32}P]dCTP (T7 Quickprime kit; Pharmacia), and unincorporated label was separated from the probe by running the mixture through a NICK column (Pharmacia) followed by precipitation in 5 M ammonium acetate and ethanol using yeast tRNA as a carrier. For *in situ* hybridization the purified PCR products were cloned into pCR-script SK (Stratagene, Cambridge, United Kingdom) and sequenced to confirm their identity and orientation. Riboprobes were transcribed (MAXIscript *in vitro* transcription kit, Ambion AMS Ltd., Witney, Oxon, United Kingdom) from linearized plasmids with [^{33}P]UTP (Amersham) before phenol extraction and ethanol precipitation.

RNA Preparation and Northern Blotting. Total RNA was prepared according to Chomczynski and Sacchi (16) and assessed by absorbance at 260/280 nm. Aliquots (20 μg) were electrophoresed in 1% agarose gels containing formaldehyde and transferred to Hybond N membranes by capillary blotting in 10 × SSC [1 × SSC consists of 150 mM sodium chloride and 15 mM tri-sodium citrate (pH 7.0)]. After fixation, blots were incubated overnight at 68°C with ^{32}P-labeled cDNA probes and washed in several changes of 1 × SSC/0.1% SDS before exposing to X-ray film for ≤7 days. The consistency of RNA loading and transfer was assessed by staining of the 28S rRNA with ethidium bromide.

***In Situ* Hybridization.** The *in situ* hybridization protocol used in this study has been described previously (17). Briefly, the riboprobes were diluted to 30,000 cpm/μl in hybridization buffer [50% deionized formamide, 0.3 M sodium chloride, 10 mM Tris (pH 6.8), 10 mM sodium phosphate (pH 6.8), 5 mM EDTA (pH 8.0), 1× Denhardt's solution, 10% dextran sulfate, 50 mM DTT, and 1 mg/ml yeast tRNA] and incubated on the sections for 18 h at 55°C. The slides were then washed and treated with RNase A before being coated with autoradiographic emulsion and exposed to film for 21 days at 4°C.

Results

Expression of BNIP3 Protein in Human Cell Lines. The 18 human cell lines described above, representing epithelial tumors, sarcomas, endothelium, lymphocytes, and macrophages, were subjected to 0.1% hypoxia or normoxia for 16 h before making protein extractions. Western blot analysis for BNIP3 revealed that an increase of both the M_r 30,000 and 60,000 forms of BNIP3 protein occurred after hypoxia in 15 of the 18 cell lines (results from 6 cell lines are shown in Fig. 1*A*). The induction was concordant for both protein forms. Of these cell lines, 12 were derived from carcinomas (SKBR, T47D, MDA468, MDA231, MCF7, SKOV3, EJ, MKN45, C32, LS174T, RCC4, and DU145), 2 from macrophages (U937 and THP-1) and 1 from endothelial cells (HUVEC). The RZM (lymphocyte) and HT1080 (fibrosarcoma) cell lines expressed very low levels of BNIP3 protein under normoxic conditions, but protein levels did not increase in response to hypoxia (Fig. 1*A*). Additional analysis of the MCF7 cell line revealed that BNIP3 protein production was up-regulated within 8 h of exposure to hypoxia and persisted for ≥24 h in the continued presence of hypoxia (data not shown).

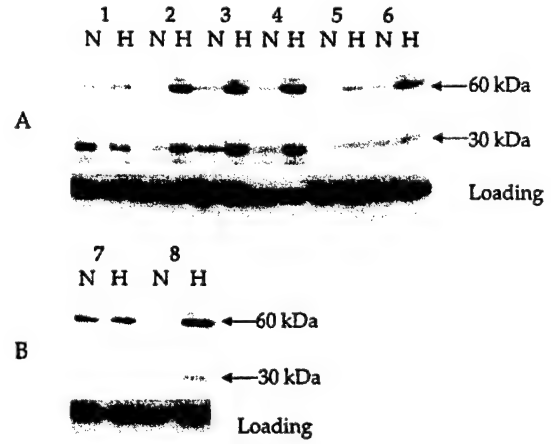

Fig. 1. Western blot analysis of protein extracted from various cell lines after treatment with normoxia (*N*) or hypoxia (*H*) for 16 h. Blots were probed with an antibody to BNIP3 (*top panel*) or β-tubulin (*bottom panel*). *A*, cell lines shown are: HT1080 (*1*); EJ (*2*); MKN45 (*3*); HUVEC (*4*); LS174T (*5*); and DU145 (*6*). *B*, cell lines shown are RCC4 (*7*) and RCC4-VHL (*8*).

Hif-1α-dependent Induction of BNIP3 Protein. The RCC4 cell line, which is derived from renal carcinoma cells defective for VHL, showed constitutive up-regulation of BNIP3 under normoxic conditions (Fig. 1B). When VHL was reintroduced into this cell line, levels of BNIP3 in normoxia were suppressed and became inducible by hypoxia (Fig. 1*B*). To additionally check the role of Hif-1α in BNIP3 induction, CHO KA13 and C4.5 cells were subjected to normoxia or hypoxia for 16 h before being analyzed immunohistochemically for BNIP3 protein. Neither cell line expressed BNIP3 protein under normoxic conditions, although after treatment with hypoxia, BNIP3 expression was markedly increased in the C4.5 cells. The KA13 cells, which are defective for Hif-1α, showed little, if any, increase in BNIP3 protein after hypoxia (Fig. 2).

Expression of NIX and BNIP3 mRNA in Human Cell Lines. The HT1080 cell line and 4 of the cell lines showing increased protein levels under hypoxia (EJ, T47D, MDA231, and MDA468) were subjected to normoxia or hypoxia for 16 h before extracting total RNA. Northern blot analysis identified transcripts of 4.5 kb and 1.4 kb (NIX) and 5 kb and 1.7 kb (BNIP3), which, in concordance with the BNIP3 protein expression, increased under hypoxia in all of the cell lines except HT1080 (Fig. 3). The increase in expression was concordant for both transcripts of NIX and BNIP3.

Expression of NIX and BNIP3 mRNA in Human Normal Breast and Breast Tumor Tissue. RNA was extracted from tumor and distant normal breast obtained from mastectomy samples and analyzed for NIX and BNIP3 expression using Northern blotting. Levels of NIX and BNIP3 mRNA were higher in the tumor samples compared with normal tissue in 5/5 and 3/5 cases respectively (Fig. 3). The expression of BNIP3 mRNA in the remaining 2 cases was unchanged. Both transcripts of NIX mRNA were present in human tissue, but the 5-kb transcript of BNIP3 was only detected in the tumor sample of 1 of the cases.

Localization of BNIP3 mRNA in Human Tumors. To localize BNIP3-expressing cells in human tissue, formalin-fixed blocks of normal breast and tumor from 2 of the patients described above, as well as blocks from various other types of human epithelial tumors, were subjected to *in situ* hybridization analysis. BNIP3 mRNA was detectable in 5/9 tumors, consisting of 1/2 SSC head and neck carcinomas, 1/2 ovarian carcinomas, 1 pancreas carcinoma, and 2 breast carcinomas. BNIP3 expression was not detected in 1 lung carcinoma, 1 lymphoma, and 2 case of normal breast tissue. BNIP3 mRNA was expressed on epithelial carcinoma cells in perinecrotic areas of the tumor (Fig. 4) in all of the samples except 1 breast carcinoma, where hybridization was seen in epithelial cells from a well-vascularized area of the tumor (data not shown). No specific hybridization was detected when the sections were hybridized with the sense control probe for BNIP3 (Fig. 4).

Discussion

In this study we have demonstrated that the cell death factors BNIP3 and NIX are hypoxically inducible in a wide range of human epithelial, endothelial, and macrophage cell lines but not in

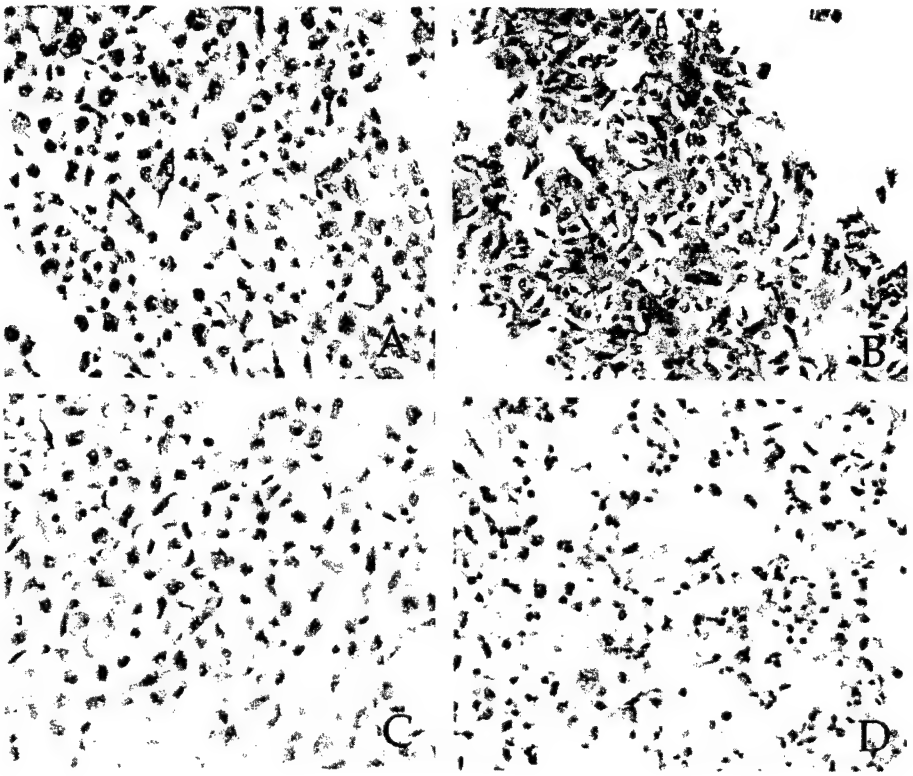

Fig. 2. Immunohistochemical analysis of BNIP3 expression by C4.5 cells (*A* and *B*) and KA13 cells (*C* and *D*) after treatment with normoxia (*A* and *C*) and hypoxia (*B* and *D*).

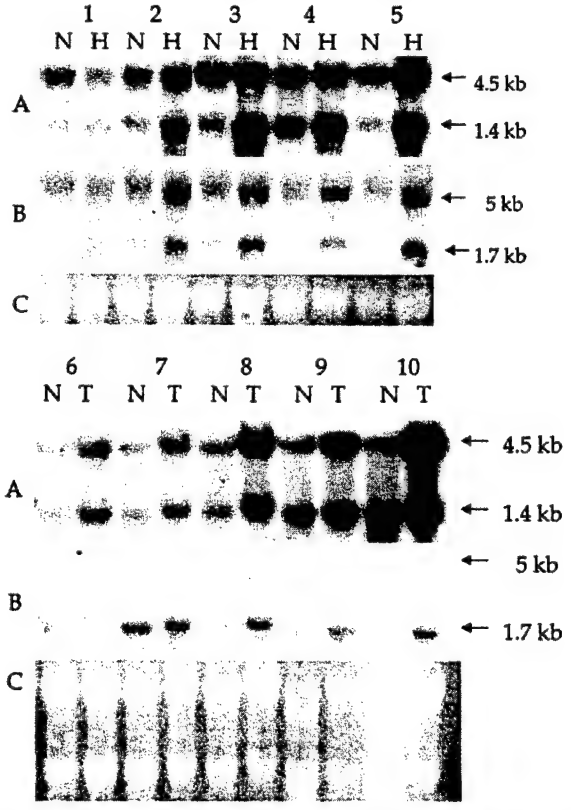

Fig. 3. Northern blot analysis of RNA extracted from HT1080 (*1*), EJ (*2*), T47D (*3*), MDA231 (*4*), and MDA468 (*5*) cell lines after 16 h treatment with normoxia (*N*) or hypoxia (*H*), and RNA extracted from normal (*N*) and tumorous (*T*) breast tissue from 5 patients (*6–10*). Blots were probed for NIX (*A*) and BNIP3 (*B*). The positions of ethidium bromide labeled 28 S and 18 S rRNA were used to estimate the size of the transcripts; one or both of these bands are shown in *C* as a loading control.

lymphocyte or fibrosarcoma cell lines. This result has been confirmed at the protein level for BNIP3 and at the mRNA level for both BNIP3 and NIX. Time course studies in a breast carcinoma cell line indicated that BNIP3 protein markedly increased after 8 h of hypoxia; this result demonstrates that induction is relatively rapid in tumor cells and contrasts with a recent study where BNIP3 protein was only detectable in a CHO-K1 cell line after 4 days of hypoxic culture (13).

It is probable that the hypoxic induction of BNIP3 in human cells is mediated via Hif-1α, because RCC4 cells lacking wild-type pVHL have high levels of BNIP3 protein under both normoxic and hypoxic conditions. Reintroduction of pVHL to this cell line restores degradation of Hif-1α under normoxic conditions (6) and reduces BNIP3 expression. In addition, BNIP3 protein is not markedly induced under hypoxic conditions in CHO cells defective for Hif-1α. These results confirm recent data that suggested a HIF-1-dependent response based on mutational analysis of the BNIP3 promoter (13).

Importantly, our study has also demonstrated that mRNAs encoding NIX and in most cases BNIP3 are expressed at higher levels in clinical material from human breast tumors when compared with normal breast tissue. This result is consistent with up-regulation of the HIF-1 pathway in human tumors but somewhat surprising in light of other studies that have shown down-regulation of BNIP3 in keloid cells compared with normal tissue (18) and human T-cell leukemia virus type I injected cells (19). These differences may relate to different patterns of microenvironmental hypoxia. In our material, *in situ* hybridization analysis of RNA expression in human tumors revealed that it is expressed by perinecrotic areas of tumor, which result from hypoxic stress.

Areas of necrosis are commonly found in solid tumors and correlate with poor prognosis. Also, cell death by necrosis is seen more commonly than apoptosis in hypoxic tumors. BNIP3 activates caspase-independent necrosis-like cell death as a consequence of opening the

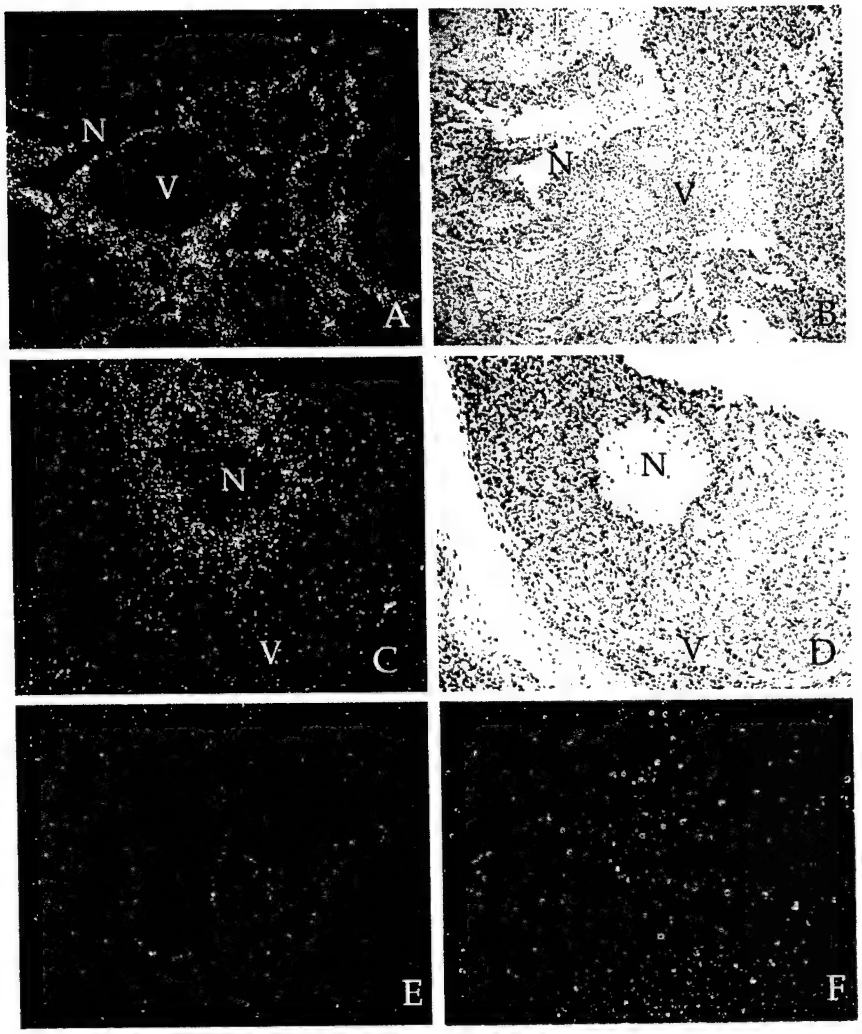

Fig. 4. *In situ* hybridization analysis of BNIP3 mRNA in human tissue. Hybridization, visualized as silver granules under dark field conditions, was detected in perinecrotic areas of tumor. *N*, necrotic areas of tissue; *V*, vascularized areas of the tissue. *A* and *B*, a section of an ovarian carcinoma hybridized with BNIP3 antisense probe shown under dark-field (*A*) and bright-field (*B*) conditions. *C* and *D*, a section of a SSC head and neck carcinoma hybridized with BNIP3 antisense probe shown under dark-field (*C*) and light-field (*D*) conditions. *E*, a section of normal breast tissue hybridized with BNIP3 antisense probe and shown under dark field conditions. *F*, a section of an ovarian carcinoma hybridized with BNIP3 sense probe shown under dark-field conditions.

mitochondrial permeability transition pore (20) and may be the pathway mediating hypoxia-induced necrotic cell death in cancer. HIF-1 activation regulates many pathways advantageous to tumor growth such as angiogenesis, glycolysis, and glucose uptake (5), although our results suggest that activation of HIF-1 during the evolution of cancer also coselects pathways such as BNIP3/NIX that have the potential for antitumor effects.

Most tumor cells retain the ability to undergo apoptosis in response to hypoxic stress (1), although paradoxically, this loss of apoptotic-sensitive cells leads to the selection of viable cells that are more resistant to treatment and contribute to tumor relapse (3). Hockel *et al.* (21) have determined that a subset of hypoxic cervical carcinomas have a low apoptotic index and that these tumors are highly aggressive. The mechanism by which hypoxia selects for cells resistant to apoptosis is unclear. Striking upregulation of the BNIP3/NIX gene products by hypoxia and enhanced expression in clinical tumors suggests that additional analysis of this pathway in normal and tumor tissue may be helpful in understanding this important process.

Note Added in Proof

Since this work was submitted, Guo *et al.* (22) have demonstrated the induction of BNIP3 by hypoxia in rat cardiomyocytes. This shows that this pathway can also be regulated by hypoxia in non-carcinoma tissue.

References

1. Shimizu, S., Eguchi, Y., Kamiike, W., Itoh, Y., Hasegawa, J., Yamabe, K., Otsuki, Y., Matsuda, H., and Tsujimoto, Y. Induction of apoptosis as well as necrosis by hypoxia and predominant prevention of apoptosis by Bcl-2 and Bcl-XL. Cancer Res., *56:* 2161–2166, 1996.
2. Reynolds, T. Y., Rockwell, S., and Glazer, P. M. Genetic instability induced by the tumor microenvironment. Cancer Res., *56:* 5754–5757, 1996.
3. Schmaltz, C., Hardenbergh, P. H., Wells, A., and Fisher, D. E. Regulation of proliferation-survival decisions during tumor cell hypoxia. Mol. Cell. Biol., *18:* 2845–2854, 1998.
4. Graeber, T. G., Osmanian, C., Jacks, T., Housman, D. E., Koch, C. J., Lowe, S. W., and Giaccia, A. J. Hypoxia-mediated selection of cells with diminished apoptotic potential in solid tumours. Nature (Lond.), *379:* 88–91, 1996.
5. Semenza, G. L. Regulation of mammalian O2 homeostasis by hypoxia-inducible factor 1. Annu. Rev. Cell Dev. Biol., *15:* 511–578, 1999.
6. Maxwell, P. H., Wiesner, M., Chang, G-W., Clifford, S., Vaux, E., Cockman, M., Wycoff, C., Pugh, C., Maher, E., and Ratcliffe, P. The tumour suppressor protein VHL targets hypoxia-inducible factors for oxygen-dependent proteolysis. Nature (Lond.), *399:* 271–275, 1999.
7. Carmeliet, P., Dor, Y., Herbert, J-M., Fukumura, D., Brusselmans, K., Dewerchin, M., Neeman, M., Bono, F., Abramovitch, R., Maxwell, P., Koch, C. J., Ratcliffe, P., Moons, L., Jain, R. K., Collen, D., and Keshet, E. Role of HIF-1α in hypoxia-mediated apoptosis, cell proliferation and tumour angiogenesis. Nature (Lond.), *394:* 485–490, 1998.
8. Lal, A., Lash, A. E., Altschul, S. F., Velculescu, V., Zhang, L., Mclendon, R. E., Marra, M. A., Prange, C., Morin, P. J., Polyak, K., Papadopoulos, N., Vogelstein, B., Kinzler, K. W., Strausberg, R. L., and Riggins, G. J. A public database for gene expression in human cancers. Cancer Res., *59:* 5403–5407, 1999.
9. Boyd, J. M., Malstrom, S., Subramanian, T., Venkatesh, L. K., Scheper, U., Elangovan, B., D'Sa-Eipper, C., and Chinnadurai, G. Adenovirus E1B 19 kDa and Bcl-2 proteins interact with a common set of cellular proteins. Cell, *79:* 341–351, 1994.

10. Matsushima, M., Fujiwara, T., Takahashi, E-I., Minaguchi, T., Eguchi, Y., Tsujimoto, Y., Suzumori, K., and Nakamura, Y. Isolation, mapping and functional analysis of a novel human cDNA (*BNIP3L*) encoding a protein homologous to human BNIP3. Genes, Chromosomes Cancer, *21:* 230–235, 1998.
11. Chen, G., Cizeau, J., Vande Velde, C., Hoon Park, J., Bozek, G., Bolton, J., Shi, L., Dubik, D., and Greenberg, A. H. NIX and BNIP3 form a subfamily of pro-apoptotic mitochondrial proteins. J. Biol. Chem., *274:* 7–10, 1999.
12. Yasuda, M., Han, J-W., Dionne, C. A., Boyd, J., and Chinnadurai, G. BNIP3α: a human homologue of mitochondrial proapoptotic protein BNIP3. Cancer Res., *59:* 533–537, 1999.
13. Bruik, R. K. Expression of the gene encoding the proapoptotic BNIP3 protein is induced by hypoxia. Proc. Natl. Acad. Sci. USA, *97:* 9082–9087, 2000.
14. Wood, S. M., Wiesener, M. S., Yeates, K. M., Okada, N., Pugh, C. W., Maxwell, P. H., and Ratcliffe, P. J. Selection and analysis of a mutant cell line defective in the hypoxia-inducible factor-1α-subunit (HIF-1α). J. Biol. Chem., *273:* 8360–8368, 1998.
15. Ray, R., Chen, G., Vande Velde, C., Cizeau, J., Hoon Park, J., Reed, J. C., Gietz, R. D., and Greenberg, A. H. BNIP3 heterodimerises with Bcl-2/Bcl-Xl and induces cell death independent of a Bcl-2 homology 3 (BH3) domain at both mitochondrial and nonmitochondrial sites. J. Biol. Chem., *275:* 1439–1448, 2000.
16. Chomczynski, P., and Sacchi, N. Single-step method of RNA isolation by acid guanidium thiocyanate-phenol-chloroform extraction. Anal. Biochem., *162:* 156–159, 1987.
17. Clark, D. E., Smith, S. K., Sharkey, A. M., Sowter, H. M., and Charnock-Jones, D. S. Hepatocyte growth factor/scatter factor and its receptor c-Met: localization and expression in the human placenta throughout pregnancy. J. Endocrinol., *151:* 459–467, 1996.
18. Sayah, D. N., Soo, C., Shaw, W. W., Watson, J., Messadi, D., Longaker, M. T., Zhang, X., and Ting, K. Downregulation of apoptosis-related genes in keloid tissues. J. Surg. Res., *87:* 209–216, 1999.
19. Harhaj, E. W., Good, L., Xiao, G., and Sun, S-C. Gene expression profiles in HTLV-I-immortalized T cells: deregulated expression of genes involved in apoptosis regulation. Oncogene, *18:* 1341–1349, 1999.
20. Vande Velde, C., Cizeau, J., Dubik, D., Alimonti, J., Brown, T., Israels, S., Hakem, R., and Greenberg, A. H. BNIP3 and genetic control of necrosis-like cell death through the mitochondrial permeability transition pore. Mol. Cell. Biol., *20:* 5454–5468, 2000.
21. Hockel, M., Schlenger, K., Hockel, S., and Vaupel, P. Hypoxic cervical cancers with low apoptotic index are highly aggressive. Cancer Res., *59:* 4525–4528, 1999.
22. Guo, K., Searfoss, G., Krolikowski, D., Pagnoni, M., Franks, C., Clark, K., Yu, K. T., Jaye, M., and Ivashchenko, Y. Hypoxia induces the expression of the pro-apoptotic gene *BNIP3*. Cell Death Differ. *8:* 367–376, 2001.

Human Molecular Genetics, 2001, Vol. 10, No. 18 1907–1913

Genetic model of multi-step breast carcinogenesis involving the epithelium and stroma: clues to tumour–microenvironment interactions

Keisuke Kurose[1,2], Stacy Hoshaw-Woodard[3], Adewale Adeyinka[4], Stanley Lemeshow[3], Peter H. Watson[4] and Charis Eng[1,2,5,*]

[1]Clinical Cancer Genetics and Human Cancer Genetics Programs, Comprehensive Cancer Centre, and Division of Human Genetics, Department of Internal Medicine, [2]Division of Human Cancer Genetics, Department of Molecular Virology, Immunology and Medical Genetics and [3]Center for Biostatistics, Comprehensive Cancer Centre, The Ohio State University, Columbus, OH 43210, USA, [4]Department of Pathology, University of Manitoba Health Sciences Centre, Winnipeg, Manitoba R3E 0W3, Canada and [5]CRC Human Cancer Genetics Research Group, University of Cambridge, Cambridge CB2 2QQ, UK

Received April 18, 2001; Revised and Accepted June 21, 2001

ABSTRACT

Although numerous studies have reported that high frequencies of loss of heterozygosity (LOH) at various chromosomal arms have been identified in breast cancer, differential LOH in the neoplastic epithelial and surrounding stromal compartments has not been well examined. Using laser capture microdissection, which enables separation of neoplastic epithelium from surrounding stroma, we microdissected each compartment of 41 sporadic invasive adenocarcinomas of the breast. Frequent LOH was identified in both neoplastic epithelial and/or stromal compartments, ranging from 25 to 69% in the neoplastic epithelial cells, and from 17 to 61% in the surrounding stromal cells, respectively. The great majority of markers showed a higher frequency of LOH in the neoplastic epithelial compartment than in the stroma, suggesting that LOH in neoplastic epithelial cells might precede LOH in surrounding stromal cells. Furthermore, we sought to examine pair-wise associations of particular genetic alterations in either epithelial or stromal compartments. Seventeen pairs of markers showed statistically significant associations. We also propose a genetic model of multi-step carcinogenesis for the breast involving the epithelial and stromal compartments and note that genetic alterations occur in the epithelial compartments as the earlier steps followed by LOH in the stromal compartments. Our study strongly suggests that interactions between breast epithelial and stromal compartments might play a critical role in breast carcinogenesis and several genetic alterations in both epithelial and stromal compartments are required for breast tumour growth and progression.

INTRODUCTION

Breast cancer is the most common and second most lethal cancer in women in Western countries. Numerous studies have focused on the role of chromosome abnormalities and gene mutations in sporadic breast cancer, but to date no clear model of the critical events or delineation of primary abnormalities has emerged. Various chromosome arms have been observed to be affected by a high frequency of structural or numerical abnormalities (1–5). Although several of these chromosome arms appear to be the sites of putative tumour suppressor genes (TSGs), the number and identity of TSGs relevant for mammary carcinogenesis is unknown. At the molecular level, several somatic mutations in genes residing in these regions have been described (1,6–9). Despite this abundance of data, the relevance, role and timing of most of the described genetic abnormalities in sporadic breast cancer are still unclear. It is also not known whether specific mutations play relevant roles as causative factors or are the consequence of the general genomic instability and progression in breast tumours.

A few studies have previously demonstrated that loss of heterozygosity (LOH) identified at various chromosomal loci at high frequency in invasive cancer is already present in *in situ* carcinoma, atypical ductal hyperplasia, non-atypical hyperplasia of the breast, and perhaps adjacent normal epithelial cells, although these studies predated laser capture microdissection (LCM), hence, contamination from clearly malignant tissue cannot be excluded (10–15). These observations are also found in colonic adenomas (16), Barrett oesophageal metaplasia

*To whom correspondence should be addressed at: Human Cancer Genetics Program, The Ohio State University Comprehensive Cancer Centre, 420 West 12th Avenue, Room 690C TMRF, Columbus, OH 43210, USA. Tel: +1 614 292 2347; Fax: +1 614 688 3582; Email: eng-1@medctr.osu.edu

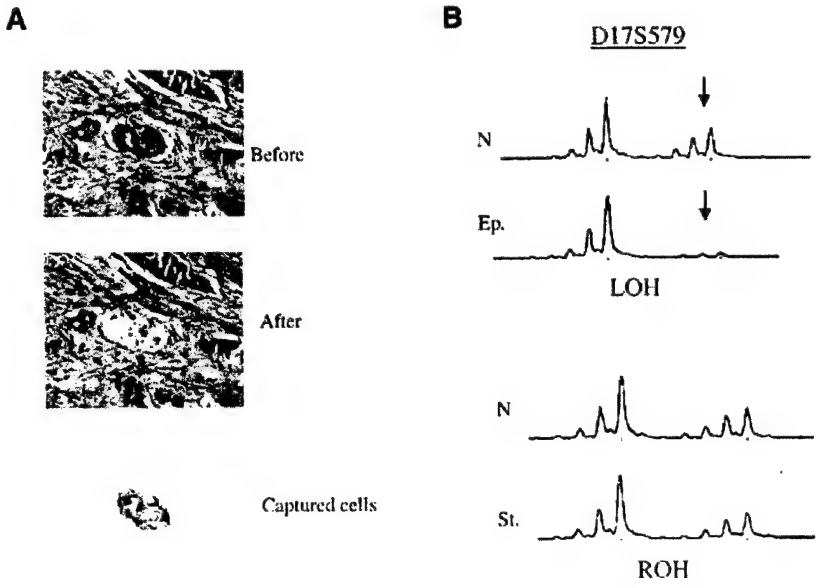

Figure 1. (**A**) LCM from breast cancer specimen. Captured cells are the neoplastic epithelial component. The surrounding stromal fibroblasts are immediately adjacent to the removed cells (arrow). (**B**) Illustrative examples of LOH (arrows) and retention of heterozygosity (ROH) at D17S579. N, normal cells; Ep., epithelial cells; St., stromal cells.

(17,18) and lung hyperplasias (19). These reports indicate that the majority of premalignant or precursor lesions share their LOH phenotypes with invasive disease in the same organs, providing novel biologic evidence that they are genetically and perhaps evolutionarily related. Nonetheless, until recently, any cancer such as breast cancer was treated as a single amorphous entity. Most such genetic studies were uniformly performed on the entire tumour without regard to its components, despite the fact that a few groups were quite aware of both epithelial and stromal components of tumours, and the cell biology of the tumour 'microenvironment' has been described for the last 20 years. Thus, until now, when a genetic alteration, be it intragenic mutation, regional amplification or deletion manifested by LOH, is attributed to a breast cancer, it is unclear if the alteration is actually occurring in the epithelial compartment, the surrounding stromal compartment or both.

The effects of the metabolism of the tumour stroma, locally as well as systemically, are largely unknown. Although the stroma has generally been considered a silent bystander during epithelial carcinogenesis, the concept that the microenvironment is central to maintenance of cellular function and tissue integrity provides the rationale for the idea that its disruption can contribute to neoplasia (20). Several studies performed *in vivo* and *in vitro* indicated that the growth and invasive potentials of carcinoma cells are influenced through interactions with host stromal cells (21–23). Despite these progressive cell biological studies, the precise genetic mechanisms leading to tumour progression remain unclear. Even less clear is the role of differential genetic alterations in the epithelial neoplastic component and its surrounding stroma.

Recently, Moinfar *et al.* (5) reported the high frequency of LOH in the mammary stroma with breast cancer. They examined 11 patients with ductal carcinoma *in situ*, including five cases with invasive ductal carcinoma, and found LOH in the stromal cells. Although these investigators identified frequent genetic alterations in the mammary stroma, each component of the breast carcinoma was manually microdissected; thus cross-contamination cannot be excluded. Further, they examined a limited number of samples and a limited number of microsatellite markers on only five chromosome arms. In this present study, we sought to systematically examine for genetic alterations in the epithelial and stromal components of invasive adenocarcinomas of the breast with the DNA extracted from cells from each compartment obtained by LCM. We found frequent LOH in both epithelial and/or stromal components of breast cancer and identified associations among LOH at various chromosomal regions, suggesting that genetic alterations in the epithelial and surrounding stromal cells are involved in the breast tumorigenesis through concurrent and independent pathways.

RESULTS

LCM of each specimen was performed to selectively obtain normal epithelial or stromal cells, carcinomatous epithelial cells and stromal cells surrounding the epithelial carcinoma (e.g. Fig. 1A). LOH at each of the 13 chromosomal regions was detected in epithelial and/or stromal compartments among the 41 invasive adenocarcinomas of the breast (e.g. Fig. 1B). Table 1 summarizes the frequencies of LOH observed at 13 loci in neoplastic epithelial and surrounding stromal cells. Among the 13 microsatellite markers examined, the LOH frequency ranged from 25% (9/36) at D3S1581 (3p14–q21) to 69% (22/32) at D17S796 (17p13) in the neoplastic epithelial compartment, and from 17% (6/36) also at D3S1581 to 61% (20/33) at D2S156 (2q34) in the surrounding stromal

Table 1. LOH frequencies and distribution in the epithelial and stromal cells

Chromosomal region	Marker	Cases with LOH in Ep[a]/informative cases	Cases with LOH in St[b]/informative cases	Cases with LOH in either Ep or St/ informative cases	Cases with LOH only in Ep	Cases with LOH only in St	Cases with LOH in both Ep and St	McNemar's test *P*-value (exact *P*-value)
1p36	D1S228	16/34 (47%)	10/34 (29%)	21/34 (62%)	11	5	5	0.1336 (0.2101)
2q34	D2S156	16/33 (48%)	20/33 (61%)	26/33 (79%)	6	10	10	0.3173 (0.4545)
3p14.2–p21.2	D3S1581	9/36 (25%)	6/36 (17%)	11/36 (31%)	5	2	4	0.2568 (0.4531)
3p24.3–p25.1	D3S1286	17/37 (46%)	14/37 (38%)	23/37 (62%)	9	6	8	0.4386 (0.6072)
6q25.3	D6S437	14/29 (48%)	15/29 (52%)	20/29 (69%)	5	6	9	0.7630 (1.000)
8p23.2	D8S264	21/32 (66%)	18/32 (56%)	25/32 (78%)	7	4	14	0.3657 (0.5488)
10q23.3	D10S1765	15/36 (42%)	10/32 (31%)	16/32 (50%)	6	5	5	0.7630 (1.000)
11q23	D11S912	19/37 (51%)	16/37 (43%)	25/37 (68%)	9	6	10	0.4386 (0.6072)
13q14	D13S155	18/33 (55%)	16/33 (48%)	23/33 (70%)	7	5	11	0.5637 (0.7744)
16q24.3	D16S413	20/31 (65%)	13/32 (41%)	23/31 (74%)	11	3	9	0.0325 (0.0574)
17p13	D17S796	22/32 (69%)	14/32 (44%)	24/32 (75%)	10	2	12	0.0209 (0.0386)
17q21	D17S579	17/32 (53%)	11/32 (34%)	21/32 (66%)	10	4	7	0.1088 (0.1796)
22q12.2–q13.1	D22S277	15/37 (41%)	15/37 (41%)	21/37 (57%)	6	6	9	1.000 (1.000)

[a]Ep, epithelium; [b]St, stroma.

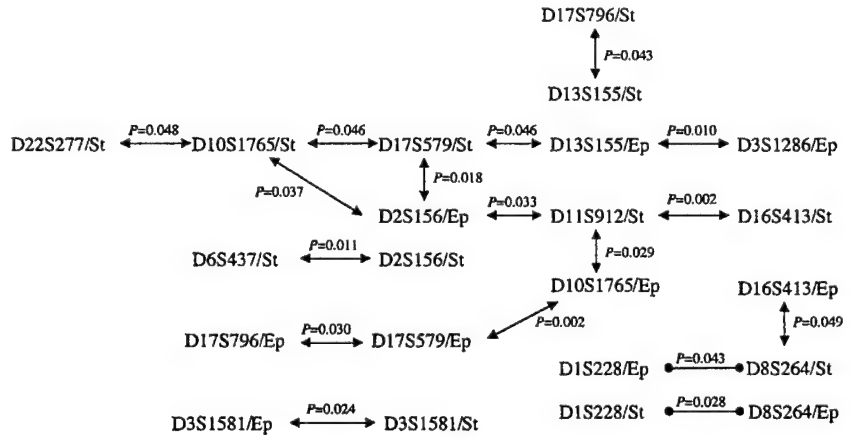

Figure 2. Positive and negative associations between markers in epithelial and stromal compartments of adenocarcinomas of the breast. Double-headed arrows denote positive correlations while double-knobbed lines denote negative correlations. Numbers above the arrows or lines are *P*-values (Fisher's exact test). Ep, epithelial cells; St, stromal cells.

component (Table 1). D2S156 (2q34) and perhaps D6S437 (6q25) were the only two markers demonstrating a higher frequency of LOH in the surrounding stromal compartment compared with the neoplastic epithelial cells. In contrast, the great majority of markers showed a higher frequency of LOH in the neoplastic epithelial compartment compared with the surrounding stromal cells (Table 1).

On further inspection of the differential LOH data, it can be noted that for certain markers, LOH predominates in the neoplastic epithelial compartment, for others, LOH predominates in the stromal compartment, and for yet other markers, it occurs in both compartments (Table 1). For instance, LOH at 16q24.3 (D16S413) was identified more frequently in only the neoplastic epithelial cells (11 tumours) than in only the stromal cells (three tumours; $P = 0.0325$, McNemar's test). The number of tumours that showed LOH at 17p13 (D17S796) only in stromal cells (two tumours) was significantly fewer than that having LOH at 17p13 in both epithelial and stromal cells or only in the neoplastic epithelial cells (12 or 10 tumours; $P = 0.0209$, McNemar's test).

We then looked for pair-wise associations of dependency or independency of particular genetic alterations with one another in either epithelial or stromal compartments (Fig. 2). We found that there were statistically significant associations in 17 pairs

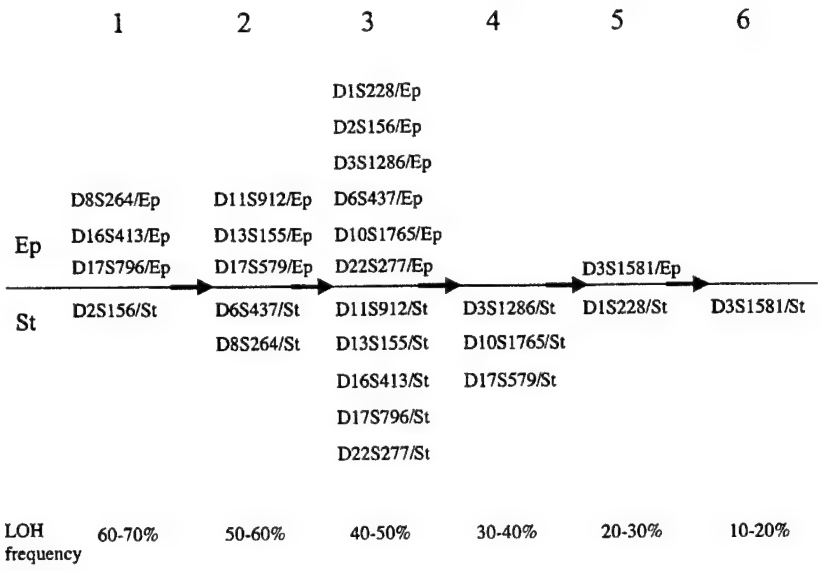

Figure 3. Proposed genetic model of multistage, stepwise carcinogenesis in the breast involving the epithelial and stromal compartments. Ep, epithelial cells; St, stromal cells.

(17/325; 5.3%) of markers (Fig. 2). Fifteen pairs (15/17; 88%) showed positive associations and two pairs (2/17; 12%) showed negative associations (Fig. 2). LOH at four markers, D10S1765, D11S912 and D17S579 in the surrounding stromal compartment and D2S156 in the neoplastic epithelial compartment, were associated with three or more sites of LOH (Fig. 2). Of note, LOH at D10S1765 in the stromal compartment was associated with LOH at D17S579 and D22S277 in the stromal compartments and also with LOH at D2S156 in the neoplastic epithelial compartments. LOH at D17S579 in the stromal compartment, in turn, was found to be associated with LOH at D2S156 and D13S155 in the neoplastic epithelial compartment and at D10S1765 in the surrounding stromal compartment. In contrast, LOH at D8S264 (8p23.2) in the neoplastic epithelial cells is negatively correlated with LOH at D1S228 (1p36) in the surrounding stromal cells. Interestingly, LOH at D8S264 in the surrounding stromal compartment is negatively correlated with LOH at D1S228 in the neoplastic epithelial compartment.

DISCUSSION

In this present study, we have found frequent LOH in both neoplastic epithelial and surrounding stromal cells of invasive adenocarcinomas of the breast. In our series of 41 breast cancer samples, we identified LOH in the neoplastic epithelial compartment, ranging from 25% (9/36) to 69% (22/32), and in the stromal compartment, ranging from 17% (6/36) to 61% (20/33), respectively. Of note, the great majority of markers demonstrated a higher frequency of LOH in the neoplastic epithelial compartment compared with the surrounding stromal cells (Table 1). Further inspection of the differential LOH data indicated that the frequency of LOH only in the stromal compartment occurred among fewer tumours than that in both neoplastic epithelial and surrounding stromal compartments, or that in only the neoplastic epithelial cells (Table 1). In the field of human cancer genetics, it has been shown that markers with the highest frequency of LOH represent those with the earliest genetic alterations, the so-called first 'hits', and the one with the lowest frequency of LOH represents the latest 'hit' in carcinogenesis (16). Thus, under this assumption, from our data, we can propose a genetic model of multistage, stepwise carcinogenesis in the breast, according to the relative frequencies of LOH in the epithelial and stromal compartments (Fig. 3). Our proposed model encompasses data that shows a higher frequency of LOH in breast epithelial cells occurs earlier than in the stromal compartment (Fig. 3). Although Moinfar *et al.* (5) worked without the advantage of LCM and used markers representing only five chromosomal regions and a sample size of 11, their observations of relative frequencies of LOH in the neoplastic epithelium (occurring in 1/4 to 3/3 tumours) compared with presumably surrounding stroma (occurring in 1/4 to 4/5 tumours) might be interpreted as concurrent with ours. These data together with our observations suggest that genetic alterations in the epithelial compartment, at least in some chromosomal regions, precede the genetic changes in the surrounding stromal cells. If in fact we may extrapolate that each region of LOH represents at least one putative TSG, then it is possible that the same putative gene involved in epithelial carcinogenesis plays some role in the stroma at a later stage, with the possible exception of D2S156. In our study, the earliest genetic alterations occurred at D8S264, D16S413 and D17S796 in the epithelium as well as D2S156 in the stroma (Fig. 3). It is almost certain that the D17S796 marker represents *TP53*, and indeed, *TP53* alterations have been noted amongst the most frequent and earliest somatic alterations in prior studies involving 'whole' breast carcinomas (24,25). The regions of D8S264 and D16S413 have yet to yield convincing TSGs involved in breast carcinogenesis. Our data would strongly support the existence of one or more TSGs residing in these two regions which when

mutated participate in the initiation of cancer within the breast epithelium. Of interest, LOH at D2S156 in the stromal cells is also scored as an early event (Fig. 3). This has not been a region noted to have LOH in whole breast cancers. Nonetheless, our data suggest that there will be at least one important gene residing in that interval which plays a prominent role in the initiation of breast carcinogenesis, possibly from a micro-environmental or 'landscaper' point of view (26). The genetic model proposed (Fig. 3) assumes for simplicity that frequency of occurrence reflects temporal sequence. This in turn assumes an equivalent effect on tumorigenesis and early progression between all alterations. However, it is recognized that an alternative possibility is that some alterations may be dominant while others may require the cooperation of parallel or multiple complex alterations at other sites to facilitate progression, and that this would influence the prevalence of the alteration in advanced tumours. In the case of these different assumptions, a lower frequency of stromal alterations could reflect the fact that stromal alterations are not dominant and only exert an indirect effect on the adjacent epithelium, or only exert an effect in collaboration with others, to influence the overall process of tumorigenesis.

The apparent asynchronous LOH at each marker between epithelium and stroma might suggest that while the neoplastic epithelium is clonal, as is the stroma, these observations may support one viewpoint that epithelium and stroma derive from different cellular origins. However, there are advocates of a common cellular origin of both epithelium and stroma (27). If this latter is true, then in the context of our observations, the LOH in epithelium and stroma occurred after the divergence of epithelial and stromal cell from the presumed common cell.

Despite a relatively small sample size, we were able to examine pair-wise associations between regions and compartments where LOH occurred (Fig. 2). For example, LOH at D17S579 in the neoplastic epithelial cells was associated with LOH at D17S796 and D10S1765 in the neoplastic epithelial compartments. These chromosomal loci contain several putative TSGs. The polymorphic markers, D17S579 (17q21), D17S796 (17p13) and D10S1765 (10q23.3), are in proximity to the *BRCA1*, *TP53* and *PTEN* genes, respectively. Previous reports have identified that there are significant associations between LOH of *BRCA1* and *TP53* (28,29) or *PTEN* gene (28) in sporadic heterogeneous breast cancer samples. Crook *et al.* (30) found a high proportion of 'whole' breast and ovarian tumours from *BRCA1* mutation carriers had *TP53* mutations. Our proposed genetic model does suggest that LOH at D17S796 in the neoplastic epithelial cells is the earliest hit, LOH at D17S579 in the neoplastic epithelial cells is the second one, then LOH at D10S1765 in the neoplastic epithelial cells is the third hit in these consequences (Table 1 and Fig. 3). The association between LOH of *BRCA1* and *PTEN* is, therefore, one of the genetic alterations that might be expected to occur as a consequence of the loss of *BRCA1* and *TP53*. LOH at D2S156 in the neoplastic epithelial compartment was associated with LOH at three markers, D10S1765, D11S912 and D17S579, in the surrounding stromal compartments. The reciprocal interaction between epithelial and stromal cells plays a key role in the morphogenesis, proliferation and differentiation of epithelial cells (31–33). Most of the intercellular substances, extracellular matrix (ECM) molecules that are required for tumour growth and progression are produced by the stromal cells (34). It is well demonstrated that altered gene expression occurs between normal and neoplastic breast stroma (35) and that stromal cells play a critical role in the production and possible dissolution of the ECM (36,37). Thus, genetic alterations in the stromal cells may change the interaction between epithelial cells and ECM molecules and influence the tumour invasion and dissemination (22,23). Our results suggest that LOH at 2q34 (D2S156) might precede LOH of three chromosomal loci in the stromal compartments (Figs 2 and 3). Therefore, we hypothesized that loss of a putative TSG on 2q34 might play an important role in genetic alterations of stromal compartments, which in turn might influence tumour invasion and dissemination through ECM remodelling. If this hypothesis is correct, then we can further hypothesize that genetic alterations in the stroma might predict for poorer prognosis due to increased tumour invasiveness.

In summary, we have found frequent LOH in both neoplastic epithelial and surrounding stromal compartments in invasive adenocarcinomas of the breast and statistically significant associations among the LOH at various chromosomal regions. We also propose a multi-step genetic model of breast carcinogenesis involving epithelium and stroma, which can help build further hypotheses and guide future studies of reciprocal interactions between breast neoplastic epithelial and stromal cells in tumour initiation, progression, invasion and metastases. Such studies might eventually lead to novel therapeutic strategies, which selectively target epithelium or stroma.

MATERIALS AND METHODS

Breast cancer samples

Forty-one archival (formalin-fixed and paraffin-embedded) tissues that were distinct cases of clinically sporadic primary invasive adenocarcinomas of the breast were used. Twenty-six samples were obtained from the National Cancer Institute of Canada Manitoba Breast Tumour Bank and 15 were from the Department of Pathology of The Ohio State University.

Microdissection of tissue and DNA extraction

Microdissection of carcinomatous epithelial cells, surrounding stromal cells, and normal epithelial or stromal cells from fixed, paraffin-embedded sections of breast was performed using an Arcturus PixCell II Laser Capture microdissecting microscope (Arcturus Engineering Inc., Mountain View, CA). This system utilizes a transparent thermoplastic film applied to the surface of the tissue section on standard histopathology slides. The breast cancer epithelial, surrounding stromal, and normal epithelial or stromal cells to be microdissected were identified and targeted through a microscope, and a narrow (~15 uM) carbon dioxide laser-beam pulse specificity activated the film above these cells. The resulting strong focal adhesion allowed selective procurement of only the targeted cells (38) (Fig. 1A). The cells removed in Figure 1A are the neoplastic epithelial component. The surrounding stromal fibroblasts are immediately adjacent to the removed cells (Fig. 1A, arrow). It is acknowledged that while LCM minimizes cross-contamination of cell types, it does not guarantee against it. However, the very 'clean' LOH (virtually all or none) which we have obtained does suggest that any cross-contamination is not significant.

DNA from microdissected tissue was extracted in 50 µl of solution containing 0.04% proteinase K, 1% Tween-20, 10 mM Tris–HCl (pH 8.0), and 1 mM EDTA at 37°C overnight followed by heat inactivation at 95°C for 10 min.

LOH analysis

For purposes of this study, genomic DNA, extracted from paraffin embedded tissues, served as template for PCR amplification of 13 microsatellite markers selected from a comprehensive genetic map of the human genome (39). Fluorescent-labelled polymorphic markers, including D1S228 (1p36), D2S156 (2q34), D3S1581 (3p14.2–p21.2), D3S1286 (3p24.3–p25.1), D6S437 (6q25.3), D8S264 (8p23.2), D10S1765 (10q23.3), D11S912 (11q23), D13S155 (13q14), D16S413 (16q24.3), D17S796 (17p13), D17S579 (17q21) and D22S277 (22q12.2–q13.1), were used for this analysis. All subsequent PCRs were carried out using 0.5 µM each of forward and reverse primer in 1× PCR buffer (Qiagen, Valencia, CA), 1.5 mM $MgCl_2$ (Qiagen), 1× Q-buffer (Qiagen), 1.25 U of HotStar Taq polymerase (Qiagen) and 200 µM of each dNTP (Gibco, Gaithersburg, MD) in a final volume of 25 µl. After a denaturation at 95°C for 14 min, reactions were subjected to 40 cycles of 94°C for 1 min, 55–60°C for 1 min, and 72°C for 1 min followed by 10 min at 72°C. PCR reactions and genotyping were repeated at least a second time to confirm the data. Amplified PCR products were separated by electrophoresis through 6% denaturing polyacrylamide gels, and the signal was detected with an Applied Biosystems model 377×l semi-automated DNA sequencer (Applied Biosystems, Perkin-Elmer Corp., Norwalk, CT). The results were analysed by automated fluorescence detection using the GeneScan collection and analysis software (GeneScan, Applied Biosystems). Scoring of LOH was initially performed by inspection of the GeneScan analysis output. A conservative ratio of peak heights of alleles between germline DNA and somatic DNA ≥1.9:1 were used to define LOH in this study (40).

Statistical analysis

Comparisons for statistical significance were performed by using either the standard Fisher's exact test (2-tailed) or the McNemar's test for matched pairs at the $P = 0.05$ level of significance. McNemar's test was used when interest focused on differences in proportions of patients with LOH in either stromal or epithelial cells, but not both. This test determines whether, in these cases of discordance, there are a disproportionate number of patients with LOH in one of the two sites. McNemar's test is used in recognition of the fact that the stromal and epithelial cells are taken from the same breast tissue and, hence, are matched. However, the Fisher's exact test was also employed because it is unclear from a biological point of view whether each data point (i.e. LOH at any one marker) is dependent on the next (i.e. LOH at other markers).

ACKNOWLEDGMENTS

We thank Fred Wright and Sandya Liyanarchchi for providing statistical assistance. Part of this work was performed in the Laser Capture Microdissection core facility in the Tissue Procurement Shared Resources Service of the Comprehensive Cancer Centre. This work was supported in part by the Jimmy V Golf Classic Award for Basic and Clinical Cancer Research from the V Foundation (to C.E.) and a grant from the National Cancer Institute, Bethesda, MD (P30CA16058 to The Ohio State University Comprehensive Cancer Centre).

REFERENCES

1. Devilee, P. and Cornelisse, C.J. (1994) Somatic genetic changes in human breast cancer. *Biochim. Biophys. Acta*, **1198**, 113–130.
2. Bieche, I. and Lidereau, R. (1995) Genetic alterations in breast cancer. *Genes Chromosomes Cancer*, **14**, 227–251.
3. Kerangueven, F., Noguchi, T., Coulier, F., Allione, F., Wargniez, V., Simony-Lafontaine, J., Longy, M., Jacquemier, J., Sobol, H., Eisinger, F. *et al.* (1997) Genome-wide search for loss of heterozygosity shows extensive genetic diversity of human breast carcinomas. *Cancer Res.*, **57**, 5469–5474.
4. O'Connell, P., Pekkel, V., Fuqua, S.A., Osborne, C.K., Clark, G.M. and Allred, D.C. (1998) Analysis of loss of heterozygosity in 399 premalignant breast lesions at 15 genetic loci. *J. Natl Cancer Inst.*, **90**, 697–703.
5. Moinfar, F., Man, Y.G., Arnould, L., Bratthauer, G.L., Ratschek, M. and Tavassoli, F.A. (2000) Concurrent and independent genetic alterations in the stromal and epithelial cells of mammary carcinoma: implications for tumorigenesis. *Cancer Res.*, **60**, 2562–2566.
6. Li, J., Yen, C., Liaw, D., Podsypanina, K., Bose, S., Wang, S.I., Puc, J., Miliaresis, C., Rodgers, L., McCombie, R. *et al.* (1997) PTEN, a putative protein tyrosine phosphatase gene mutated in human brain, breast, and prostate cancer. *Science*, **275**, 1943–1947.
7. Done, S.J., Arneson, N.C., Ozcelik, H., Redston, M. and Andrulis, I.L. (1998) p53 mutations in mammary ductal carcinoma *in situ* but not in epithelial hyperplasias. *Cancer Res.*, **58**, 785–789.
8. Feilotter, H.E., Coulon, V., McVeigh, J.L., Boag, A.H., Dorion-Bonnet, F., Duboue, B., Latham, W.C., Eng, C., Mulligan, L.M. and Longy, M. (1999) Analysis of the 10q23 chromosomal region and the PTEN gene in human sporadic breast carcinoma. *Br. J. Cancer*, **79**, 718–723.
9. Negrini, M., Monaco, C., Vorechovsky, I., Ohta, M., Druck, T., Baffa, R., Huebner, K. and Croce, C.M. (1996) The FHIT gene at 3p14.2 is abnormal in breast carcinomas. *Cancer Res.*, **56**, 3173–3179.
10. Rosenberg, C.L., de las Morenas, A., Huang, K., Cupples, L.A., Faller, D.V. and Larson, P.S. (1996) Detection of monoclonal microsatellite alterations in atypical breast hyperplasia. *J. Clin. Invest.*, **98**, 1095–1100.
11. Lakhani, S.R., Collins, N., Stratton, M.R. and Sloane, J.P. (1995) Atypical ductal hyperplasia of the breast: clonal proliferation with loss of heterozygosity on chromosomes 16q and 17p. *J. Clin. Pathol.*, **48**, 611–615.
12. Lakhani, S.R., Slack, D.N., Hamoudi, R.A., Collins, N., Stratton, M.R. and Sloane, J.P. (1996) Detection of allelic imbalance indicates that a proportion of mammary hyperplasia of usual type are clonal, neoplastic proliferations. *Lab. Invest.*, **74**, 129–135.
13. Jensen, R.A., Page, D.L. and Holt, J.T. (1994) Identification of genes expressed in premalignant breast disease by microscopy-directed cloning. *Proc. Natl Acad. Sci. USA*, **91**, 9257–9261.
14. Noguchi, S., Motomura, K., Inaji, H., Imaoka, S. and Koyama, H. (1994) Clonal analysis of predominantly intraductal carcinoma and precancerous lesions of the breast by means of polymerase chain reaction. *Cancer Res.*, **54**, 1849–1853.
15. Deng, G., Lu, Y., Zlotnikov, G., Thor, A.D. and Smith, H.S. (1996) Loss of heterozygosity in normal tissue adjacent to breast carcinomas. *Science*, **274**, 2057–2059.
16. Fearon, E.R. and Vogelstein, B. (1990) A genetic model for colorectal tumorigenesis. *Cell*, **61**, 759–767.
17. Blount, P.L., Galipeau, P.C., Sanchez, C.A., Neshat, K., Levine, D.S., Yin, J., Suzuki, H., Abraham, J.M., Meltzer, S.J. and Reid, B.J. (1994) 17p allelic losses in diploid cells of patients with Barrett's esophagus who develop aneuploidy. *Cancer Res.*, **54**, 2292–2295.
18. Zhuang, Z., Vortmeyer, A.O., Mark, E.J., Odze, R., Emmert-Buck, M.R., Merino, M.J., Moon, H., Liotta, L.A. and Duray, P.H. (1996) Barrett's esophagus: metaplastic cells with loss of heterozygosity at the APC gene locus are clonal precursors to invasive adenocarcinoma. *Cancer Res.*, **56**, 1961–1964.
19. Hung, J., Kishimoto, Y., Sugio, K., Virmani, A., McIntire, D.D., Minna, J.D. and Gazdar, A.F. (1995) Allele-specific chromosome 3p deletions occur at an early stage in the pathogenesis of lung carcinoma. *J. Am. Med. Assoc.*, **273**, 558–563.

20. Bissell, M.J. and Barcellos-Hoff, M.H. (1987) The influence of extracellular matrix on gene expression: is structure the message? *J. Cell Sci.* (suppl.), **8**, 327–343.
21. Picard, O., Rolland, Y. and Poupon, M.F. (1986) Fibroblast-dependent tumorigenicity of cells in nude mice: implication for implantation of metastases. *Cancer Res.*, **46**, 3290–3294.
22. Grey, A.M., Schor, A.M., Rushton, G., Ellis, I. and Schor, S.L. (1989) Purification of the migration stimulating factor produced by fetal and breast cancer patient fibroblasts. *Proc. Natl Acad. Sci. USA*, **86**, 2438–2442.
23. Camps, J.L., Chang, S.M., Hsu, T.C., Freeman, M.R., Hong, S.J., Zhau, H.E., von Eschenbach, A.C. and Chung, L.W. (1990) Fibroblast-mediated acceleration of human epithelial tumor growth *in vivo*. *Proc. Natl Acad. Sci. USA*, **87**, 75–79.
24. Coles, C., Condie, A., Chetty, U., Steel, C.M., Evans, H.J. and Prosser, J. (1992) p53 mutations in breast cancer. *Cancer Res.*, **52**, 5291–5298.
25. Buchholz, T.A., Weil, M.M., Story, M.D., Strom, E.A., Brock, W.A. and McNeese, M.D. (1999) Tumor suppressor genes and breast cancer. *Radiat. Oncol. Investig.*, **7**, 55–65.
26. Kinzler, K.W. and Vogelstein, B. (1998) Landscaping the cancer terrain. *Science*, **280**, 1036–1037.
27. Pierce, G.B. and Speers, W.C. (1988) Tumors as caricatures of the process of tissue renewal: prospects for therapy by directing differentiation. *Cancer Res.*, **48**, 1996–2004.
28. Hanby, A.M., Kelsell, D.P., Potts, H.W., Gillett, C.E., Bishop, D.T., Spurr, N.K. and Barnes, D.M. (2000) Association between loss of heterozygosity of BRCA1 and BRCA2 and morphological attributes of sporadic breast cancer. *Int. J. Cancer*, **88**, 204–208.
29. Tong, D., Kucera, E., Schuster, E., Schmutzler, R.K., Swoboda, H., Reinthaller, A., Leodolter, S. and Zeillinger, R. (2000) Loss of heterozygosity (LOH) at p53 is correlated with LOH at BRCA1 and BRCA2 in various human malignant tumors. *Int. J. Cancer*, **88**, 319–322.
30. Crook, T., Crossland, S., Crompton, M.R., Osin, P. and Gusterson, B.A. (1997) p53 mutations in BRCA1-associated familial breast cancer. *Lancet*, **350**, 638–639.
31. Cunha, G.R., Bigsby, R.M., Cooke, P.S. and Sugimura, Y. (1985) Stromal-epithelial interactions in adult organs. *Cell Differ.*, **17**, 137–148.
32. Donjacour, A.A. and Cunha, G.R. (1991) Stromal regulation of epithelial function. *Cancer Treat. Res.*, **53**, 335–364.
33. Hom, Y.K., Young, P., Wiesen, J.F., Miettinen, P.J., Derynck, R., Werb, Z. and Cunha, G.R. (1998) Uterine and vaginal organ growth requires epidermal growth factor receptor signaling from stroma. *Endocrinology*, **139**, 913–921.
34. Hanahan, D. and Folkman, J. (1996) Patterns and emerging mechanisms of the angiogenic switch during tumorigenesis. *Cell*, **86**, 353–364.
35. Leygue, E., Snell, L., Dotzlaw, H., Hole, K., Hiller-Hitchcock, T., Roughley, P.J., Watson, P.H. and Murphy, L.C. (1998) Expression of lumican in human breast carcinoma. *Cancer Res.*, **58**, 1348–1352.
36. Wolf, C., Rouyer, N., Lutz, Y., Adida, C., Loriot, M., Bellocq, J.P., Chambon, P. and Basset, P. (1993) Stromelysin 3 belongs to a subgroup of proteinases expressed in breast carcinoma fibroblastic cells and possibly implicated in tumor progression. *Proc. Natl Acad. Sci. USA*, **90**, 1843–1847.
37. Noel, A., Hajitou, A., L'Hoir, C., Maquoi, E., Baramova, E., Lewalle, J.M., Remacle, A., Kebers, F., Brown, P., Calberg-Bacq, C.M. *et al.* (1998) Inhibition of stromal matrix metalloproteases: effects on breast-tumor promotion by fibroblasts. *Int. J. Cancer*, **76**, 267–273.
38. Emmert-Buck, M.R., Bonner, R.F., Smith, P.D., Chuaqui, R.F., Zhuang, Z., Goldstein, S.R., Weiss, R.A. and Liotta, L.A. (1996) Laser capture microdissection. *Science*, **274**, 998–1001.
39. Dib, C., Faure, S., Fizames, C., Samson, D., Drouot, N., Vignal, A., Millasseau, P., Marc, S., Hazan, J., Seboun, E. *et al.* (1996) A comprehensive genetic map of the human genome based on 5 264 microsatellites. *Nature*, **380**, 152–154.
40. Marsh, D.J., Zheng, Z., Zedenius, J., Kremer, H., Padberg, G.W., Larsson, C., Longy, M. and Eng, C. (1997) Differential loss of heterozygosity in the region of the Cowden locus within 10q22–23 in follicular thyroid adenomas and carcinomas. *Cancer Res.*, **57**, 500–503.

British Journal of Cancer (2002) 86, 1276–1282

www.bjcancer.com

The hypoxia-inducible genes VEGF and *CA9* are differentially regulated in superficial *vs* invasive bladder cancer

KJ Turner[1,2], JP Crew[1,2], CC Wykoff[1], PH Watson[3], R Poulsom[4], J Pastorek[5], PJ Ratcliffe[6], D Cranston[2] and AL Harris*[,1]

[1]ICRF Molecular Oncology Laboratory and Angiogenesis Group, Institute of Molecular Medicine, John Radcliffe Hospital, Oxford OX3 9DU, UK; [2]Department of Urology, Churchill Hospital, Oxford OX3 7LJ, UK; [3]Department of Pathology, University of Manitoba, D212-770 Bannatyne Ave, Winnipeg, Manitoba R3E 0W3, Canada; [4]ICRF In Situ Hybridisation Service, 44 Lincoln's Inn Fields, London WC2A 3PX, UK; [5]Institute of Virology, Slovak Academy of Sciences, 84246 Bratislava, Slovak Republic; [6]Wellcome Trust Centre for Human Genetics, Oxford OX3 7BN, UK

Regulation by hypoxia may underlie the expression of vascular endothelial growth factor in bladder cancer. We have compared the distribution of vascular endothelial growth factor mRNA with a hypoxia marker, carbonic anhydrase 9 (CA IX). vascular endothelial growth factor mRNA was analysed by *in situ* hybridisation and CA IX by immunochemistry in 22 cases of bladder cancer. The relationship of microvessels to the distribution of CA IX was determined. In a separate series of 49 superficial tumours, CA IX immunostaining was compared with clinico-pathological outcome. In superficial and invasive disease there was overlap in the expression of vascular endothelial growth factor and CA IX, CA IX being more widespread. Both were expressed predominantly on the luminal surface, and surrounding areas of necrosis (invasive tumours). Expression of both factors was greater in superficial disease. Expression was absent within ~80 μm of microvessels. Unlike vascular endothelial growth factor, CA IX did not predict outcome in superficial disease. Differential responses to reoxygenation provide one explanation: vascular endothelial growth factor mRNA declined rapidly, while CA IX expression was sustained for >72 h. Expression of vascular endothelial growth factor mRNA in bladder tumours is consistent with hypoxic regulation and suggests differential regulation in superficial *vs* invasive disease. The expression of CA IX on the luminal surface justifies investigation of its utility as a therapeutic target/prognostic indicator.
British Journal of Cancer (2002) **86,** 1276–1282. DOI: 10.1038/sj/bjc/6600215 www.bjcancer.com

Keywords: bladder neoplasms; angiogenic factors; carbonic acid; cell hypoxia

Tumour growth and metastasis are dependent upon angiogenesis (Folkman, 1990). VEGF (vascular endothelial growth factor) is a key regulator of this process (Ferrara and Davis-Smyth, 1997). Expression of VEGF is an indicator of stage and outcome in a number of tumour types and functional studies have confirmed its central role in angiogenesis and tumour growth (Zhang *et al*, 1995; Borgstrom *et al*, 1998). Previously we demonstrated that expression of VEGF mRNA varies widely in human superficial bladder cancer and that the level of expression is predictive of relapse and stage progression (Crew *et al*, 1997). The mechanisms by which some superficial tumours express VEGF mRNA at low levels and others considerably higher (up to 345-fold more) remain undetermined. An understanding of these mechanisms may shed light on factors influencing a more angiogenic and therefore more aggressive phenotype, and could provide new therapeutic or prognostic approaches. Interestingly there are differences between superficial and invasive tumours in this regard. For example, expression of the angiogenic factor thymidine phosphorylase (TP) is significantly higher in invasive than in superficial bladder tumours (O'Brien *et al*, 1995). In contrast, expression of VEGF mRNA is four-fold higher in superficial than in invasive tumours though expression of VEGF protein does not differ (O'Brien *et al*, 1995). This is indicative of differential regulation at the translational level and we have shown that expression of the eukaryotic initiation factor-4E (eIF-4E) correlates with VEGF protein : mRNA ratios in bladder tumours (Crew *et al*, 2000).

The regulation of VEGF by hypoxia has received considerable attention. Tumour hypoxia is associated with rapid proliferation, increased risk of metastasis and poor outcome (Brizel *et al*, 1996). Regulation of gene expression by hypoxia may explain these effects. Genes regulated by hypoxia include those that facilitate anaerobic metabolism of glucose (Firth *et al*, 1994; Ebert *et al*, 1996), and genes that enhance vascularity and oxygen delivery such as VEGF (Schweiki *et al*, 1992). The transcription factor complexes HIF-1 (hypoxia inducible factor 1) and HIF-2 have emerged as key mediators of the hypoxic upregulation of these genes (Semenza, 1999).

Hypoxia is usually associated with acidic pH which may promote tumour growth (Martinez-Zaguilan *et al*, 1996). Carbonic anhydrases are important for regulation of pH and we demonstrated recently that the tumour associated carbonic anhydrase 9 (*CA9*) is tightly regulated by the HIF-1 pathway (Wykoff *et al*, 2000). (*CA9* refers to the carbonic anhydrase 9 gene including any genomic sequence and mRNA, CA IX refers to the corresponding protein). CA9 is induced strongly by hypoxia in a number of tumour cell lines and the *CA9* gene has a HIF-1 hypoxia response

*Correspondence: Professor AL Harris; ICRF Molecular Oncology Group, Weatherall Institute of Molecular Medicine, John Radcliffe Hospital, Headington, Oxford OX3 9DS, UK; E-mail: aharris.lab@icrf.icnet.uk
Received 7 August 2001; revised 16 January 2002; accepted 24 January 2002

element (HRE) immediately 5′ to its transcriptional start site. Expression of CA IX was compared with that of the bioreductive hypoxia marker pimonidazole in a series of bladder transitional cell carcinomas. The distribution of the two factors was strikingly similar although staining for CA IX was less extensive. Both CA IX and pimonidazole were detected at the luminal surface of papillary tumours and around areas of necrosis.

Because pathways of both pH regulation (*CA9*) and angiogenesis (VEGF) are regulated by hypoxia, we have compared the expression patterns of CA IX and VEGF in superficial and invasive bladder cancers. Expression of VEGF was evaluated at the level of mRNA for two reasons. First, VEGF protein is secreted and therefore VEGF mRNA is a superior marker of the localisation of VEGF production and regulation. Second, knowledge of the localisation of the mRNA might facilitate understanding of the mechanisms of VEGF mRNA upregulation in bladder cancer, which have not been studied previously.

We demonstrate that VEGF mRNA is expressed most strongly on the luminal surface of bladder tumours, and surrounding areas of necrosis. This expression co-localises with areas of tumour hypoxia as defined by expression of CA IX in both superficial and invasive bladder tumours. We also show that expression of CA IX is greater in superficial than invasive tumours, consistent with previous observations on the expression of VEGF mRNA (O'Brien *et al*, 1995). These observations highlight differences between superficial and invasive bladder cancer, suggesting that different pathways may regulate angiogenesis in superficial and invasive disease with the possibility that hypoxia is the driver of angiogenesis in papillary tumours.

MATERIALS AND METHODS

Immunohistochemistry

Formalin-fixed, paraffin-embedded tissue specimens collected by standard surgical oncology procedures were obtained from the Pathology Department, John Radcliffe Hospital, Oxford, UK. Samples of normal bladder were taken from cadaveric organ donors at the time of nephroureterectomy. CA IX immunostaining using monoclonal antibody M75 was as described (Wykoff *et al*, 2000). Slides were viewed by two observers (K Turner and P Watson). The CA IX score was derived from the product of (i) the percentage of tumour cells staining for CA IX and (ii) the average intensity of that staining on a scale of 1 (least intense) to 3. M75 antibody was from Pastorek (Pastorek *et al*, 1994).

Double staining for CA IX and CD34

CA IX immunostaining was as described with omission of counterstaining (Wykoff *et al*, 2000). Sections were then incubated with 1:100 MoAb QBEnd10 (DAKO) (30 min) and then with goat anti-mouse IgG (PO447, DAKO) (30 min) followed by APAAP (30 min). The last two steps were repeated twice with 10 min incubations. Visualisation was by New Fuchsin Red substrate (DAKO). The distance from vessels to the edge of regions of CA IX staining was assessed using an eyepiece graticule calibrated against a graduated slide. Vessels that lay obliquely to the plain of the section were excluded.

In situ mRNA hybridisation

Specific localisation of VEGF mRNA was accomplished by *in situ* hybridisation using an antisense riboprobe as described (Wykoff *et al*, 2000).

CA IX and VEGF mRNA were studied in serial tissue sections. In the majority of cases CA IX expression was more widespread than expression of VEGF mRNA. For this reason, the percentage of the tumour expressing VEGF mRNA that was also positive for CA IX was quantified in each section. Sections were viewed by two observers (K Turner and P Watson) and a consensus reached.

Effect of reoxygenation on hypoxically induced CA IX protein/VEGF mRNA tissue culture

The A549 lung carcinoma cell line was obtained from ECACC (European Collection of Animal Cell Cultures, UK). Cells were grown in DMEM (Sigma) supplemented with 10% foetal calf serum (Globepharm), L-glutamine (2 μM), penicillin (50 IU ml^{-1}), and streptomycin sulphate (50 $\mu g\ ml^{-1}$). Studies of gene expression were performed on cells approaching confluence in normal growth medium. Parallel incubations were performed on aliquots of cells in normoxia (humidified air with 5% CO_2) and hypoxia. Hypoxic conditions were generated in a Napco 7001 incubator (Precision Scientific) with 0.1% O_2, 5% CO_2, and balance N_2. Re-oxygenation experiments were performed by exposure of cells to hypoxia for 16 h followed by a return to normoxia for the indicated time.

RNA analysis

Total RNA was extracted by a modified acid/guanidinium thiocyanate/phenol/chloroform method (RNAzol B; Cinna/Biotec Laboratories), dissolved in hybridisation buffer (80% formamide, 40 mM PIPES, 400 mM sodium chloride, and 1 mM EDTA, pH 8) and analysed by RNase protection assay (RPA). RPAs for vascular endothelial growth factor-A (VEGF-A) and *CA9* were performed using ^{32}P-labelled RNA probes transcribed using SP6 RNA polymerase from the previously described DNA templates (Maxwell *et al*, 1999; Wykoff *et al*, 2000). RPAs were performed on 30 μg total RNA using an internal control assay for U6 small nuclear RNA as described (Maxwell *et al*, 1999).

Cell lysis and immunoblotting

Whole cell protein extracts were prepared from tissue culture cells by 10 s homogenisation in denaturing conditions as described (Wiesener *et al*, 1998). For Western analysis, aliquots were separated by SDS-polyacrylamide gel electrophoresis and transferred to Immobilon-P membranes. CA IX was detected using the mouse monoclonal anti-human CA IX antibody M75 (1:50) as described (Pastorekova *et al*, 1992). HRP-conjugated goat-anti-mouse immunoglobulin (DAKO) (1:2000) was applied for 1 h at room temperature (RT). ECL Plus (Amersham Pharmacia) was used for visualisation.

RESULTS

Expression of VEGF mRNA in bladder cancer

Expression of VEGF mRNA was examined by *in situ* hybridisation in 22 cases of bladder cancer selected to represent the range of stage and grade in human bladder tumours (Table 1), and in two samples of normal bladder. Expression of a control mRNA (β-actin) was verified in each case as a marker of mRNA preservation (data not shown). Neither of the samples of normal bladder showed any expression of VEGF mRNA (data not shown). There was considerable inter-tumour variation in VEGF with no expression detected in four cases (one case of isolated carcinoma *in situ* (CIS), two TaG1 tumours, and one T3G3 tumour). In the remaining cases expression was most intense on the luminal surface of tumours. This expression was patchy, with areas of strong and weak luminal expression within the same resected chip. Enhanced luminal expression was particularly marked in superficial tumours: intense staining of the outer half of the transitional cell epithelium was typical (approximately 50 μm from luminal surface to core) (Figure 1). Increased luminal expression was also noted in all chips of invasive tumour that contained surface epithelium. However, this staining was substantially less intense and widespread than in superficial tumours (Figure 2). In several cases of invasive

Table 1 Expression of CA IX protein and VEGF mRNA in human bladder cancer

Patient	Tumour stage/grade	VEGF *in situ* hybridisation	CA IX immunostaining	>50% overlap
1	CIS	−ve	−ve	na
2	Ta G1	−ve	luminal	na
3	Ta G1	−ve	luminal	na
4	Ta G2	luminal	luminal	y
5	T1 G1	luminal	luminal	y
6	T1 G2	luminal	luminal	y
7	T1 G2	luminal	luminal	y
8	T1 G2	luminal	luminal	y
9	T1 G2	luminal	luminal	y
10	T2 G2	luminal, and perinecrotic	luminal, and perinecrotic	y
11	T2 G2	luminal and invasive tumour	luminal and invasive tumour	y
12	T2 G3	luminal	luminal	y
13	T2 G3	luminal	luminal	y
14	T2 G3	luminal, and perinecrotic	luminal but sparse	n
15	T2 G2, CIS in separate biopsy	perinecrotic CIS −ve	perinecrotic CIS −ve	y
16	T2 G2, CIS in separate biopsy	perinecrotic CIS weakly positive	perinecrotic CIS weakly positive	y
17	T2 G2	luminal and perinecrotic	luminal and perinecrotic	y
18	T2 G3	luminal and perinecrotic	luminal and perinecrotic	y
19	T2 G3	invasive tumour	invasive tumour	y
20	T2 G3, CIS in separate biopsy	luminal and perinecrotic CIS −ve	luminal and perinecrotic CIS −ve	y
21	T3 G3	−ve	−ve	na
22	T4 G3, CIS in separate biopsy	luminal, CIS weakly positive	luminal, CIS weakly positive	y

In a series of 22 human bladder tumours of a range of stage and grade the location of expression of VEGF was assessed by *in situ* hybridisation of mNRA. In serial sections expression of CA IX was assessed by immunochemistry using monoclonal antibody M75. In each case the percentage of the tumour expressing VEGF mRNA that was also positive for CA IX (i.e. the overlap) was quantified. y=yes; n=no; na=not applicable.

tumour, in addition to luminal expression, there was enhanced expression of VEGF within the invasive portion of the tumour. This expression was observed primarily around areas of necrosis (Figure 2). Of the four cases of invasive bladder cancer in which there was CIS in a separate biopsy, the CIS did not express VEGF in two cases and was weakly positive in the remaining two cases.

Expression of CA IX

CA IX expression was evaluated by immunochemistry in the same 22 cases on serial sections. In 17 out of 18 cases in which VEGF mRNA was detected, at least 50% of the areas that expressed VEGF mRNA also expressed CA IX. Furthermore, the distribution of CA IX and VEGF expression was strikingly similar (Figures 1 and 2). Like VEGF mRNA, CA IX was expressed maximally on the luminal surface of tumours and around regions of necrosis in invasive tumours. In addition, whilst both superficial and invasive tumours showed luminal enhancement, this was much more marked in superficial tumours. Expression of CA IX in the sections of CIS from patients with invasive tumours matched that of VEGF. CA IX was not detected in the normal bladder specimens, nor was it detected in samples from the patient with isolated CIS.

In addition to these 22 cases, CA IX immunostaining was performed on a further five cases of isolated CIS, three normal bladders and four normal ureters. Of these, one case of CIS showed very weak luminal staining, but the remainder of the CIS cases and all sections of normal urothelium were negative for CA IX expression. In summary, in a total of 10 cases of CIS, immunostaining for CA IX was weak in three, and absent in seven.

Relationship of CA IX to microvessels

In order to elucidate factors that might influence the expression of CA IX in bladder cancer, we examined the relationship between expression of CA IX and tumour microvessels. The distribution of CD 34 staining (as a marker of blood vessels) was compared to that of CA IX staining in the same sections for a subset of cases (52 vessels were assessed in 12 different cases, Figure 3). In superficial and invasive tumours, CA IX expression was typically detected in regions of the tumour that were a mean distance of 80 μm from a blood vessel (standard deviation=44 μm).

Relationship of CA IX expression in superficial bladder cancer to other clinical and prognostic factors

We have demonstrated previously that VEGF mRNA expression on RNAse protection was predictive of recurrence and stage progression in a series of 55 superficial bladder tumours (Ta/T1, G1/G2) (Crew *et al*, 1997). Given the association between CA IX and VEGF expression, we aimed to establish whether CA IX expression was also predictive of outcome in these cases. Therefore, sections from 49 of these previously studied cases were stained for CA IX and expression was scored semi-quantitatively (range=0–225, median=30, cases were split into 'low' CA IX (i.e. score <median (n=22), and 'high' CA IX (i.e. score >median (n=27)). Comparisons were made between CA IX expression and other factors that we had determined previously including expression of VEGF mRNA (by RNAse protection), tumour grade, risk of recurrence, time to recurrence, and risk

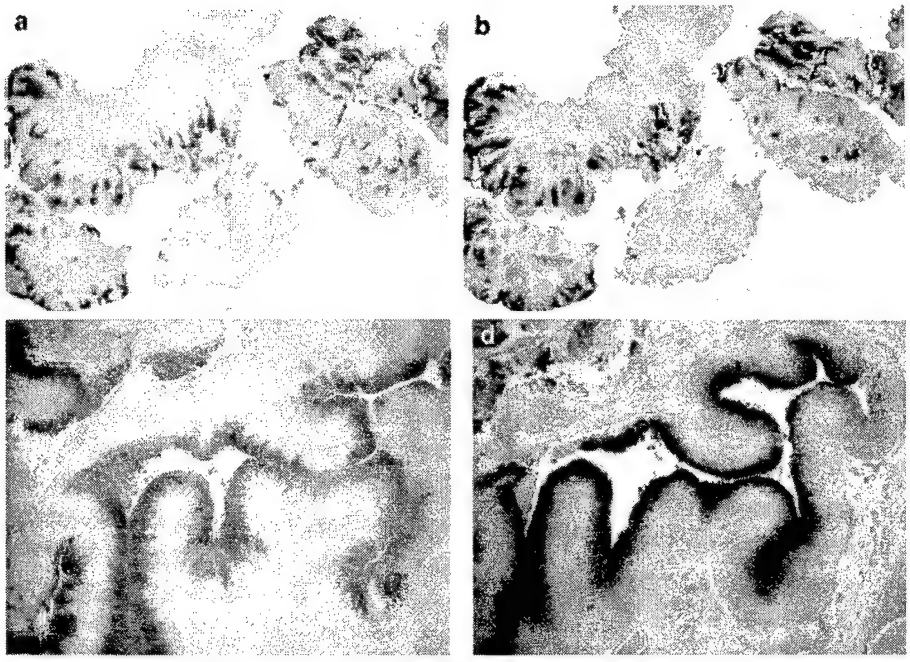

Figure 1 Expression of CA IX protein (**A**,**C**) and VEGF mRNA (**B**,**D**) in superficial bladder cancer at low power (reduced from × 10) (**A**,**B**) and high power (reduced from × 40) (**C**,**D**).

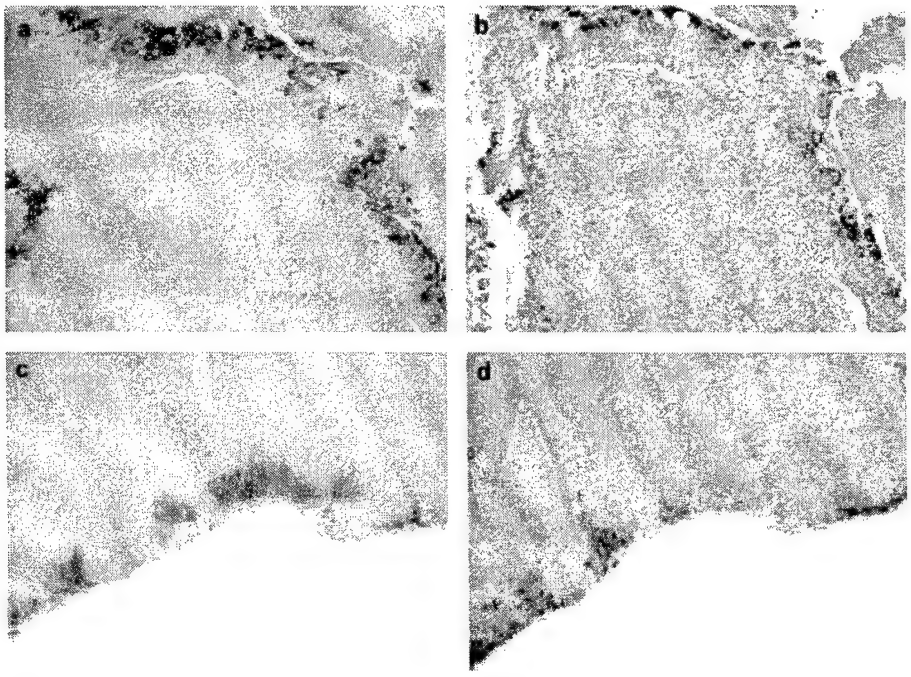

Figure 2 Expression of CA IX protein (**A**,**C**) and VEGF mRNA (**B**,**D**) in invasive bladder cancer showing perinecrotic (**A**,**B**) and luminal expression (**C**,**D**). Reduced from × 40.

of stage progression (Table 2). Although we had observed concordance of the focal staining pattern in superficial tumours, the total level of VEGF mRNA as assessed by RNAse protection did not correlate statistically with the CA IX score in these cases. No significant associations were found between CA IX staining and any other of these parameters when assessed by both continuous and cutpoint analysis.

Temporal relationship of CA IX/VEGF expression to hypoxia and reoxygenation

Though there was striking overlap in the expression of CA IX and VEGF, there were differences in the extent of the expression of these two factors. Specifically, CA IX was generally expressed over a greater area of the tumour than VEGF mRNA, and VEGF but not

CA IX was predictive of time to recurrence and risk of stage progression in Ta/T1 disease. We therefore investigated any differences in regulation that might underlie these observations. In particular we investigated the temporal relationship between expression of CA IX/VEGF and hypoxia and reoxygenation. To our knowledge, there are no currently available cell lines derived from superficial human bladder tumours. Previously we had been unable to detect hypoxic induction of CA IX in invasive bladder cancer cell lines (Wykoff *et al*, 2000), which is consistent with the low level of CA IX expression observed in invasive tumours in this study. For these reasons the A549 lung carcinoma cell line, which shows marked hypoxic induction of both VEGF and *CA9*, was chosen for these studies. Interestingly, whilst *CA9* mRNA and CA IX protein, and VEGF mRNA were induced by hypoxia, they differed markedly in their response to reoxygenation (Figure 4). Detection of CA IX protein remained constant for at least 72 h but both *CA9* mRNA and VEGF mRNA declined rapidly, reaching normoxic levels of expression within 8 h.

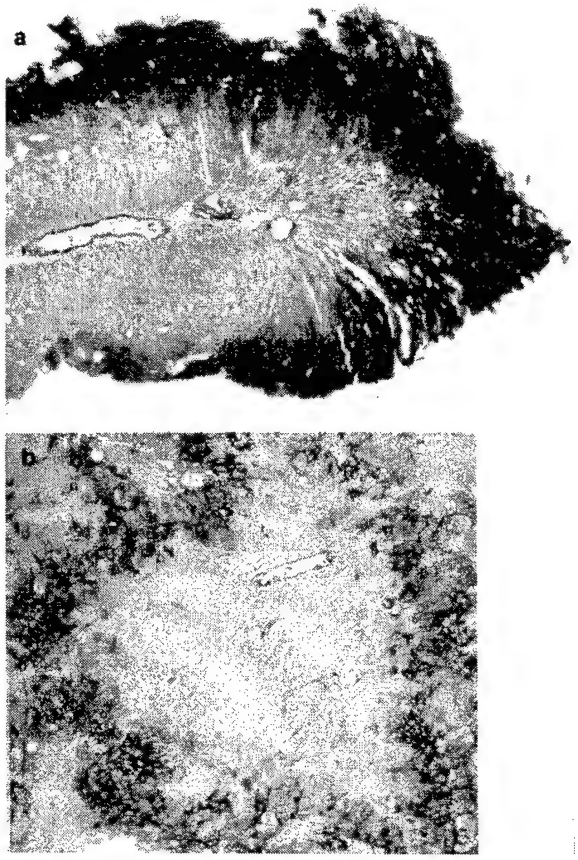

Figure 3 Relationship of CA IX expression to microvessels in superficial (**A**) and invasive bladder cancer (**B**). Reduced from x 40.

DISCUSSION

Angiogenesis plays a key role in the pathogenesis of bladder cancer: microvessel density is a prognostic indicator in invasive bladder cancer (Bochner *et al*, 1995; Jaeger *et al*, 1995), expression of the angiogenic factors bFGF (basic fibroblast growth factor), TGFβ (transforming growth factor β), midkine, and HGF (hepatocyte growth factor) is elevated in patients with bladder cancer (reviewed in Jones and Fujiyama, 1999) and VEGF expression is predictive of stage progression and relapse in superficial tumours (Crew *et al*, 1997).

Current attention is focused on the upstream events that govern expression of angiogenic mediators. Hypoxia has emerged as a potent stimulus in this regard, with hypoxia inducible transcription factors regulating many aspects of this hypoxic response, including expression of VEGF. The activity of the HIF pathway can also be modulated by genetic influences such as mutations in the VHL gene and other oncogenes (Maxwell *et al*, 1999), and by growth factors (Semenza, 2000).

In this study we have investigated the relationship between expression of VEGF and CA IX, having shown previously that

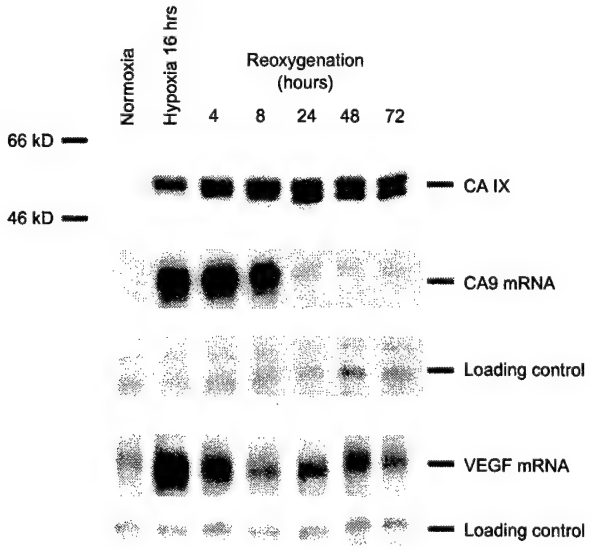

Figure 4 Expression of CA IX protein (by Western blotting), and VEGF mRNA/*CA9* mRNA (by RNAse protection) in A549 lung carcinoma cells after growth under hypoxic conditions and then subsequent reoxygenation.

Table 2 Relationship of CA IX expression in human bladder cancer to other clinicopathological parameters

	VEGF mRNA[a] Median (range)	Grade (% G1)	Recurrence at 6 months (%)	Time to recurrence in months Mean (s.d.)	Progression (% progressed)	Mean time to progression in months Mean (s.d.)
Low CA IX score	62.5 (4–242)	27	55	6.8 (6.7)	27	9.3 (5.8)
High CA IX score	91 (1–345)	19	48	5.7 (4.9)	19	6.4 (3.5)

Expression of CA IX was determined in a series of 49 superficial (Ta/T1, G1/G2) bladder tumours by immunohistochemistry using antibody M75. The CA IX score was derived from the product of (i) the percentage of tumour cells staining for CA IX and (ii) the average intensity of that staining on a scale of 1 (least intense) to 3. Cases were split into 'low' CA IX (i.e. score < median (n=22)), and 'high' CA IX (i.e. score > median (n=27)). Comparisons were made between CA IX expression and other factors that we had determined previously including expression of VEGF mRNA (by RNAse protection), tumour grade, risk of recurrence, time to recurrence, and risk of stage progression. There were no significant differences in the variables between tumours with high and low CA IX scores. [a]Arbitrary units.

CA 9 is upregulated by HIF. We demonstrate that expression of VEGF mRNA localises to areas of the tumour that also express CA IX in both superficial and invasive bladder cancers. These observations suggest that expression of VEGF in human bladder cancer is determined by tumour hypoxia and may be mediated via the HIF pathway.

Expression of both VEGF and CA IX was most intense on the luminal surface of tumours. Malignant transitional epithelium is many times thicker than transitional cell epithelium in normal bladder. The reduced oxygen tension that is associated with this increased distance from vessels may enhance expression of VEGF.

Increasingly, superficial and invasive bladder cancers are regarded as distinct pathological entities and a two-pathway model for bladder tumour development has been proposed (see Lee and Droller, 2000 for review). In keeping with this, superficial and invasive bladder tumours differ in their expression of angiogenic mediators. For example, expression of VEGF is four-fold higher in superficial tumours than in invasive tumours but expression of thymidine phosphorylase is 33 times higher in invasive tumours (O'Brien *et al*, 1995). In concordance with these results, we show here that expression of VEGF mRNA is more widespread in superficial tumours than in invasive tumours.

The localisation, shown here for the first time, of VEGF mRNA on the luminal surface of bladder tumours explains the strong relationship we have found previously between urinary and tumour VEGF protein, and the relationship of urinary VEGF to recurrence (Crew *et al*, 1999). Expression of CA IX/VEGF mRNA at the luminal surface of invasive tumours was markedly less than that on the luminal surface of superficial tumours, even in regions of equivalent distance from vessels. In addition, expression of CA IX/VEGF mRNA was observed around areas of necrosis in invasive tumours, a phenomenon that we have observed in tumours of the breast, ovary, and head and neck (Wykoff *et al*, 2000). This perinecrotic expression of CA IX/VEGF was also markedly less intense than that observed on the luminal surface of superficial tumours, even though microenvironmental hypoxia is the likely precipitant. These data therefore suggest that there is relatively less activation of hypoxia regulated transcription pathways in invasive tumours. This apparent difference between the two tumour types adds to the evidence that superficial and invasive bladder cancer represent different disease processes.

Support for this hypothesis comes from our observations in CIS, which is currently regarded as a progenitor of the invasive rather than superficial phenotype (Lee and Droller, 2000). Like invasive tumours, expression of VEGF/CA IX in CIS was substantially less than that seen in superficial bladder cancer, even though the transitional epithelium in CIS was equivalent in thickness to superficial bladder cancer.

Expression of CA IX was generally more widespread than that of VEGF mRNA, and VEGF but not CA IX was predictive of relapse and stage progression in our series of superficial bladder tumours. There are several potential explanations for this discrepancy. First, the difference in distribution may reflect different temporal responses to cellular hypoxia. Whilst both factors were strikingly induced by 16 h of hypoxia in tissue-culture cells, the level of VEGF mRNA declined rapidly upon reoxygenation (in accordance with a previous description (Schweiki *et al*, 1992)) whereas CA IX protein levels remained high during reoxygenation for at least 72 h. Therefore, the expression of VEGF mRNA observed in bladder tumours may reflect current hypoxia, whereas expression of CA IX may represent more chronic hypoxia. Second, whilst expression of CA IX may facilitate survival under adverse pH, expression of VEGF enhances growth and implantation. Hypoxia stimulates the expression of both factors, but the level of expression of each factor will vary and the factor that most favours tumour growth or implantation is most likely to correlate with adverse outcome. Third, in addition to regulation by HIF, *CA9* and VEGF most likely have other dissimilar mechanisms of regulation. For instance, VEGF expression in hypoxia is also influenced by the RNA binding protein HuR that stabilises VEGF mRNA (Levy *et al*, 1998).

This study emphasises the importance of hypoxia in defining the patterns of gene expression in bladder cancer. It also adds to the growing body of evidence that superficial and invasive bladder cancer exhibit significant biological differences. In particular, the former demonstrate a much more marked luminal expression of hypoxia inducible genes. Expression of extracellular carbonic anhydrases is likely to affect microenvironmental pH and in doing so may promote tumour growth (Martinez-Zaguilan *et al*, 1996). Carbonic anhydrase inhibitors inhibit the invasion of renal cancer cells *in vitro* and synergise with chemotherapeutic agents in animal models (Teicher *et al*, 1993; Parkkila *et al*, 2000). The high frequency and marked enhancement of CA IX expression in superficial bladder cancer reported here, combined with the relative absence in normal transitional epithelium, suggests that investigation into the utility of CA IX as a therapeutic target in this context is warranted. Furthermore, since CA IX is a transmembrane protein, measurement of shed protein in the urine could be a potential marker of recurrence.

REFERENCES

Bochner BH, Cote RJ, Weidner N, Groshen S, Chen SC, Skinner DG, Nichols PW (1995) Angiogenesis in bladder cancer: relationship between microvessel density and tumor prognosis. *J Natl Cancer Inst* **87:** 1603–1612

Borgstrom P, Bourdon MA, Hillan KJ, Sriramarao P, Ferrara N (1998) Neutralising anti vascular endothelial growth factor antibody completely inhibits angiogenesis and growth of human prostate cancer microtumors in vivo. *Prostate* **35:** 1–10

Brizel DM, Scully SP, Harrelson JM, Layfield LJ, Bean JM, Prosnitz LR, Dewhirst MW (1996) Tumor oxygenation predicts for the likelihood of distant metastases in human soft tissue sarcoma. *Cancer Res* **56:** 941–943

Crew JP, Fuggle S, Bicknell R, Cranston DW, de Benedetti A, Harris AL (2000) Eukaryotic initiation factor-4E in superficial and muscle invasive bladder cancer and its correlation with vascular endothelial growth factor expression and tumour progression. *Br J Cancer* **82:** 161–166

Crew JP, O'Brien T, Bicknell R, Fuggle S, Cranston D, Harris AL (1999) Urinary vascular endothelial growth factor and its correlation with bladder cancer recurrence rates. *J Urol* **161:** 799–804

Crew JP, O'Brien T, Bradburn M, Fuggle S, Bicknell R, D. C, Harris AL (1997) Vascular endothelial growth factor is a predictor of relapse and stage progression in superficial bladder cancer. *Cancer Res* **57:** 5281–5285

Ebert BL, Gleadle JM, O'Rourke JF, Bartlett SM, Poulton J, Ratcliffe PJ (1996) Isoenzyme-specific regulation of genes involved in energy metabolism by hypoxia: similarities with the regulation of erythropoietin. *Biochem J* **313:** 809–814

Ferrara N, Davis-Smyth TD (1997) The biology of vascular endothelial growth factor. *Endocr Rev* **10:** 4–25

Firth JD, Ebert BL, Pugh CW, Ratcliffe PJ (1994) Oxygen-regulated control elements in the phosphoglycerate kinase 1 and lactate dehydrogenase A genes: Similarities with the erythropoietin 3' enhancer. *Proc Natl Acad Sci USA* **91:** 6496–6500

Folkman J (1990) What is the evidence that tumors are angiogenesis dependent. *J Natl Cancer Inst* **82:** 4–6

Jaeger TM, Weidner N, Chew K, Moore DH, Kerschmann RL, Waldman FM, Carroll PR (1995) Tumour angiogenesis correlates with lymph node metastases in invasive bladder cancer. *J Urol* **154:** 69–71

Jones A, Fujiyama C (1999) Angiogenesis in urological malignancy: prognostic indicator and therapeutic target. *Br J Urol* **83:** 553–556

Lee R, Droller MJ (2000) The natural history of bladder cancer. *Urologic Clinics of North America* **27:** 1–13

Levy NS, Chung S, Furneaux H, Levy AP (1998) Hypoxic stabilization of vascular endothelial growth factor mRNA by the RNA-binding protein HuR. *J Biol Chem* **273:** 6417–6423

Martinez-Zaguilan R, Seftor EA, Seftor RE, Chu YW, Gillies RJ, Hendrix MJ (1996) Acidic pH enhances the invasive behavior of human melanoma cells. *Clin Exp Metastasis* **14:** 176–186

Maxwell PH, Wiesener MS, Chang G-W, Clifford SC, Vaux EC, Cockman ME, Wykoff CC, Pugh CW, Maher ER, Ratcliffe PJ (1999) The tumour suppressor protein VHL targets hypoxia-inducible factors for oxygen-dependent proteolysis. *Nature* **399:** 271–275

O'Brien T, Cranston D, Fuggle S, Bicknell R, Harris AL (1995) Different angiogenic pathways characterize superficial and invasive bladder cancer. *Cancer Res* **55:** 510–513

Parkkila S, Rajaniemi H, Parkkila A-K, Kivela J, Waheed A, Pastorekova S, Pastorek J, Sly W (2000) Carbonic anhydrase inhibitor suppresses invasion of renal cancer cells in vitro. *Proc Natl Acad Sci USA* **97:** 2220–2224

Pastorek J, Pastorekova S, Callebaut I, Mornon JP, Zelnik V, Opavsky R, Zat'ovicova M, Liao S, Portetelle D, Stanbridge EJ (1994) Cloning and characterization of MN, a human tumor-associated protein with a domain homologous to carbonic anhydrase and a putative helix-loop-helix DNA binding segment. *Oncogene* **9:** 2877–2888

Pastorekova S, Zavadova Z, Kostal M, Babusikova O, Zavada J (1992) A novel quasi-viral agent, Ma Tu, is a two-component system. *Virology* **187:** 620–626

Schweiki D, Itin A, Soffer D, Keshet E (1992) Vascular endothelial growth factor induced by hypoxia may mediate hypoxia initiated angiogenesis. *Nature* **359:** 843–845

Semenza GL (1999) Regulation of mammalian O2 homeostasis by hypoxia-inducible factor 1. *Annu Rev Cell Dev Biol* **15:** 551–578

Semenza GL (2000) HIF-1 and human disease: one highly involved factor. *Genes Dev* **14:** 1983–1991

Teicher BA, Liu SD, Liu JT, Holden SA, Herman TS (1993) A carbonic anhydrase inhibitor as a potential modulator of cancer therapies. *Anticancer Res* **13:** 1549–1556

Wiesener MS, Turley H, Allen WE, William C, Eckardt KU, Talks KL, Wood SM, Pugh CW, Ratcliffe PJ, Maxwell PH (1998) Induction of endothelial PAS domain protein-1 by hypoxia: Characterisation and comparison with hypoxia-inducible factor-1α. *Blood* **92:** 2260–2268

Wykoff CC, Beasley NJP, Watson PW, Turner KJ, Pastorek J, Sibtain A, Wilson GD, Turley H, Talks K, Maxwell PH, Pugh CW, Ratcliffe PJ, Harris AL (2000) Hypoxia inducible expression of tumor associated carbonic anhydrases. *Cancer Res* **60:** 7075–7083

Zhang H-T, Craft P, Scott PAE, Ziche M, Weich HA, Harris AL, Bicknell R (1995) Enhancement of tumor growth and vascular density by transfection of vascular endothelial growth factor into MCF-7 human breast carcinoma cells. *J Natl Cancer Inst* **87:** 213–218

[CANCER RESEARCH 62, 2736–2740, May 15, 2002]

Advances in Brief

Identification of a Novel Breast- and Salivary Gland-specific, Mucin-like Gene Strongly Expressed in Normal and Tumor Human Mammary Epithelium[1]

Richard J. Miksicek,[2,3] Yvonne Myal,[2] Peter H. Watson, Christina Walker, Leigh C. Murphy, and Etienne Leygue

Department of Physiology, Michigan State University, East Lansing, Michigan 48824 [R. J. M.]; Department of Pathology, University of Manitoba, Winnipeg, Manitoba, R3E 0W3 Canada [Y. M., P. H. W.]; Department of Biochemistry and Medical Genetics and Manitoba Institute of Cell Biology, University of Manitoba, Winnipeg, Manitoba, R3E 0W3 Canada [P. H. W., C. W., L. C. M., E. L.]

Abstract

Expression profiling using the public expressed sequence tag (EST) and serial analysis of gene expression (SAGE) databases resulted in the identification of a putative breast-specific mRNA that we have termed small breast epithelial mucin (SBEM). Hybridization analysis performed on 43 normal human tissues revealed that the *SBEM* gene was only expressed in mammary and salivary glands. Further reverse-transcription PCR analyses confirmed SBEM expression in most of established human breast epithelial cell lines analyzed (7 of 8) but not in cell lines of non-breast origin (0 of 6). *SBEM* mRNA expression was detected in >90% of invasive ductal carcinomas and correlated with the expression of a previously characterized breast-specific gene, mammaglobin-1 ($n = 54$; Spearman $r = 0.34$, $P = 0.011$). Interestingly, a higher SBEM:mammaglobin-1 ratio was observed in primary tumors with axillary lymph node metastasis than in node-negative tumors ($n = 46$; Mann-Whitney, $P = 0.04$). In a subset of 20 primary breast tumors and their matched axillary lymph nodes, a high concordance (Fisher's exact test, $P < 0.001$) was seen between PCR detection of *SBEM* mRNA in lymph node tissue and their histopathological status, indicating that SBEM mRNA expression is conserved in nodal metastasis. The *SBEM* gene is predicted to code for a putative low molecular weight, secreted sialoglycoprotein, potentially useful for the diagnosis of metastatic breast cancer.

Introduction

Early detection remains a central goal in breast cancer treatment to enable intervention at a localized and potentially curable stage and to maximize the opportunity for breast conservation. The 5-year survival rate for women with breast cancer increases dramatically when it can be diagnosed at an early stage, from >95% in patients with a localized tumor to ~75% with regional disease and <25% in women with disseminated cancer (1). Nevertheless, only 60% of all breast cancers are diagnosed at a local stage, and any improvement in early detection would have a significant impact on reducing overall breast cancer mortality.

Improving the diagnosis and clinical management of breast cancer requires access to a wider range of biomarkers able to reflect the molecular phenotype of breast tissue. A special need exists to identify novel genes whose expression is restricted to the mammary epithelium, because these genes have the greatest potential to enhance detection of micrometastatic disease and the potential to report on proliferative changes in the breast, analogous to the ability of elevated serum prostate-specific antigen levels to indicate the presence of hyperplasia or cancer of the prostate gland (2).

The identification of new tissue-specific markers has benefited especially from expansion of public and private databases for ESTs[4] (3, 4) and by large-scale efforts to profile patterns of gene expression using techniques such as serial analysis of gene expression (5). Using sequence analysis software and web-based tools developed for molecular profiling, we have identified a novel putative breast-specific gene, belonging to a recently regrouped cluster (UniGene identifier Hs.348419),[5] which represents an attractive candidate for a breast tumor marker with obvious potential for cancer diagnostics.

Materials and Methods

Database and Sequence Analysis. The cDNA xProfiler tool[6] was used to search for novel breast-specific ESTs. Protein sequence analysis used the SignalP algorithm[7] to search for the presence of a signal sequence (6) and the NetOGlyc algorithm[8] to predict sites of potential glycosylation (7).

RNA Hybridization Analysis for Tissue Specificity. A ^{32}P-labeled SBEM probe, generated using the cloned SBEM PCR product (396 bp) and the RadPrime DNA labeling system (Life Technologies, Inc., Burlington, Ontario, Canada), was hybridized to a commercially available RNA Master Blot (Clontech, Palo Alto, CA), containing poly(A)+ RNA (100–500 ng) isolated from a variety of adult and fetal human tissues, according to the manufacturer's instructions.

Cell Culture and RNA Preparation. Cell lines were obtained from the American Type Culture Collection or other sources and were cultured as follows: DMEM with 10% fetal bovine serum (MCF7, MCF10AT1, MCF10AT3c, SK-UT-1B, and HepG2); DMEM with 10% calf serum (MDA MB-231, Hec 1A, and HeLa); DMEM:Ham's F12 (1:1) with 10% fetal bovine serum (ZR-75-1 and RL95-2); RPMI 1640 with 10% fetal bovine serum (T-47D and LNCaP); or MSU-1 medium (8) with 5% fetal bovine serum (M13SV-1). All media were supplemented with penicillin (50 units/ml), streptomycin (50 μg/ml), HEPES (pH 7.4; 5 mM), and glutamine (2 mM). MCF7, T-47D, and ZR-75-1 cells also received bovine insulin (10 μg/ml). Media and sera were obtained from Life Technologies, Inc. (Life Technologies, Inc., Grand Island, NY). RNA was extracted from cultured cells using guanidinium isothiocyanate, followed by centrifugation through a 5.7 M cesium chloride cushion as described (9). RNA from cultured primary HMECs obtained by reduction mammoplasty was a kind gift from P. Ervin (Biotherapies, Inc., Ann Arbor, MI).

Breast Tumors and Axillary Lymph Nodes. Fifty-four invasive ductal carcinomas were selected from the Manitoba Breast Tumor Bank (Winnipeg, Manitoba, Canada). Cases spanned many ER (0–298 fmol/mg protein) and PR (0–1199 fmol/mg protein) levels, as determined by ligand binding assay. Tumors also spanned many grades (Nottingham grade scores from 5 to 9). For

Received 11/8/01; accepted 3/28/02.

The costs of publication of this article were defrayed in part by the payment of page charges. This article must therefore be hereby marked *advertisement* in accordance with 18 U.S.C. Section 1734 solely to indicate this fact.

[1] Supported by R21 CA094943-01 (to R. J. M.), NSERC (to Y. M.), and BC000577 (to E. L.).

[2] These authors contributed equally to this work.

[3] To whom requests for reprints should be addressed, at Department of Physiology, Michigan State University, East Lansing, MI 48824-1101. Phone: (517) 355-6475, extension 1285; Fax: (517) 355-5125; E-mail: miksicek@msu.edu.

[4] The abbreviations used are: EST, expressed sequence tag; SBEM, small breast epithelial mucin; HMEC, human mammary epithelial cell; ER, estrogen receptor-α; PR, progesterone receptor; RT-PCR, reverse transcription-PCR; GAPDH, glyceraldehyde phosphate dehydrogenase; MUC1, mucin 1.

[5] Internet address: http://www.ncbi.nlm.nih.gov/UniGene/. UniGene is a system for automatically partitioning GenBank sequences, including ESTs, into a nonredundant set of gene-oriented clusters.

[6] Internet address: http://cgap.nci.nih.gov/CGAP/Tissues/xProfiler.

[7] Internet address: http://www.cbs.dtu.dk/services/SignalP/.

[8] Internet address: http://www.cbs.dtu.dk/services/NetOGlyc/.

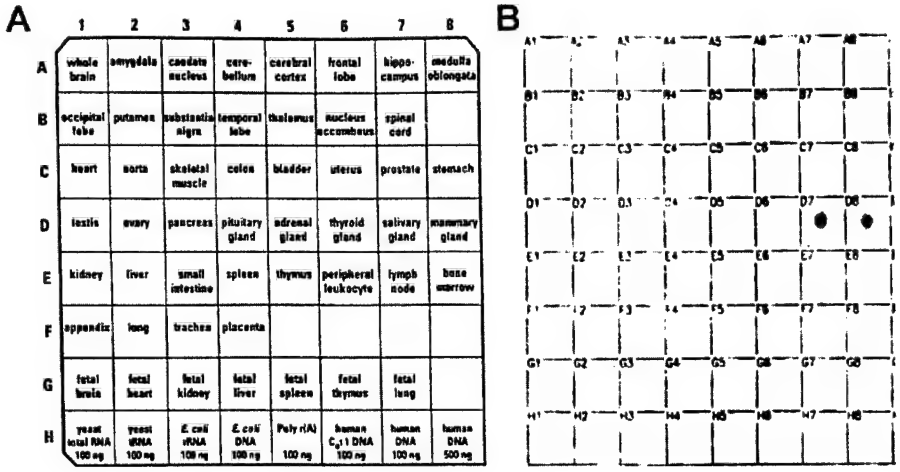

Fig. 1. Tissue expression of *SBEM* mRNA. An RNA Master Blot (Clontech Laboratories, Palo Alto, CA) containing poly(A)+ RNAs from different human tissues (*A*) was screened with ^{32}P-labeled SBEM probe as described in "Materials and Methods." The SBEM transcript (*B*) was expressed in the human salivary (*D7*) and mammary gland (*D8*).

46 tumors, pathological axillary lymph node status (presence or absence of metastasis) was known.

In a subset of cases (n = 20), frozen primary human breast tumor samples and their matched frozen lymph nodes containing (n = 14) or not (n = 6) histologically detectable metastatic cancer cells were available from the Manitoba Breast Tumor Bank. For the primary tumor samples, the ER levels, determined by ligand binding assays, ranged from 2.3 fmol/mg protein to 298 fmol/mg protein, whereas PR levels ranged from 10.1 fmol/mg protein to 112 fmol/mg protein.

RNA Analysis by RT-PCR. Total RNA was extracted from 20-μm frozen tissue sections (five sections/tumor) and reverse transcribed as described previously (10). The primers used for SBEM amplification consisted of SBEM-U (5′-CTTTGAAGCATTTTTGTCTGTG-3′; sense) and SBEM-L (5′-AAGGTAAGTAGTTGGATGAAAT-3′; antisense). PCR amplifications were performed, and PCR products were analyzed as described previously (11), with minor modifications. Briefly, aliquots of each reverse transcription mixture (2 μl for Fig. 2 and 0.8 μl for Fig. 3) were amplified in a final volume of 20 μl, in the presence of 20 mM Tris-HCl (pH 8.4), 50 mM KCl, 1.5 mM $MgCl_2$, 200 μM of each deoxynucleotide triphosphate, 5 ng/μl of each SBEM primer, and 0.5 unit of Taq DNA polymerase. Each PCR consisted of 35 cycles (15 s at 94°C, 30 s at 58°C, and 60 s at 74°C).

Primers used for mammaglobin-1 were: Mam-1 (5′-CCGACAGCAGCAGCCTCAC-3′, sense strand) and Mam-2 (5′-TCCGTAGTTGGTTTCTCAC-3′, antisense strand). Primers for the ubiquitously expressed *GAPDH* gene were GAP-1 (5′-ACCCACTCCTCCACCTTTG-3′, sense strand) and GAP-2 (5′-CTCTTGTGCTCTTGCTGGG-3′, antisense strand). To amplify cDNA corresponding to mammaglobin-1 and GAPDH, 30 cycles of PCR were used (30 s at 94°C, 30 s at 55°C, and 30 s at 72°C). All buffers were the same as for SBEM PCR, except that 2 mM $MgCl_2$ was used when amplifying mammaglobin-1 cDNA. PCR products were then separated on a 1.5% agarose gel. After electrophoresis, the gels were stained with ethidium bromide (0.5 μg/ml).

Quantification and Statistical Analysis. Three independent PCRs were performed for tumor specimens using SBEM, mammaglobin-1, and GAPDH primers and signals, visualized with UV irradiation on a GelDoc2000/Chemi-Doc System (Bio-Rad), were quantified by densitometry using the Quantity One software (version 4.2; Bio-Rad). SBEM and mammaglobin-1 expression was normalized to GAPDH expression as described previously (11). Correlation between SBEM expression and tumor characteristics or mammaglobin-1 expression was tested by calculation of the Spearman coefficient r. Differences between tumor subgroups were tested using the Mann-Whitney two-tailed test or Fisher's exact test.

***In Situ* Analysis of SBEM mRNA Expression.** *In situ* hybridization was performed on adjacent paraffin-embedded breast tumor tissue sections corresponding to a case shown to express high levels of *SBEM* mRNA by RT-PCR, using SBEM ^{32}P-labeled sense and antisense probes, as described previously (12).

Results

Identification of a Putative Novel Breast-specific Gene. The cDNA xProfiler tool (see "Materials and Methods") was used to identify tissue-restricted cDNAs with preferential representation in libraries prepared from normal breast tissue and breast tumors. This search identified a new cluster of ESTs now grouped under the UniGene identifier number Hs.348419. Of the 30 ESTs found in this cluster, 15 are ascribed to breast cDNA libraries, 9 were isolated from random activation of gene expression or pooled tissues, 5 were isolated from fetal sources (fetal heart and fetal skin), and 1 came from a head and neck tumor cDNA library. Alignment of these ESTs led to the construction of a 500-bp consensus cDNA sequence containing a 90-amino acid open reading frame in which the initiating methionine is framed by a nearly perfect consensus motif for translation initiation (5′-CCACCATGA-3′; Ref. 13). Further database analysis showed that this sequence, interrupted by three introns, is present on chromosome 12q13.2. Primers were designed to span the open reading frame, and we cloned a 396-bp fragment from both MCF-7 cells and breast tissue, which we called SBEM (GenBank accession number AF414087). The presence of a hydrophobic signal peptide (residues 1–19; Ref. 6) within the protein sequence (GenBank accession number AAL02119) suggests that SBEM is a secreted protein subject to proteolytic processing. The NetOGlyc glycosylation algorithm (7) further predicts this protein to be *O*-glycosylated on most of its 16 threonine residues. The SBEM protein contains three tandem copies of a neutral octapeptide core repeat (ThrThrAlaAlaXxxThrThrAla, where Xxx corresponds to Ala, Pro, or Ser). The NH_2 and COOH termini of the processed polypeptide are otherwise charged and fairly polar. These features suggest strong similarity to many sialomucins, although this protein lacks a transmembrane domain and is substantially shorter than most other known epithelial mucins (14, 15).

Expression of *SBEM* mRNA Is Restricted to the Mammary and Salivary Glands. Database searches suggested that SBEM expression was mainly restricted to breast tissue. To confirm this prediction, we performed hybridization analysis with an RNA MasterBlot containing highly purified polyadenylated RNA from 43 adult and 7 fetal human tissues arrayed on a nylon membrane. A *SBEM* cDNA probe hybridized exclusively to mRNA from the mammary and salivary glands (Fig. 1). Of note, no expression was observed in colon, lung, uterus, ovary, liver, pancreas, kidney, or prostate, all of which represent common primary tumor sites. Additionally, no hybridization to any of the fetal RNAs was observed.

***SBEM* mRNA Is Expressed in Breast Cancer Cell Lines but not in Cell Lines of Non-Breast Origin.** The profile of *SBEM* mRNA expression was further assessed using RT-PCR, followed by PCR amplification, in a panel of human breast and non-breast cell lines. A SBEM PCR product of the expected size (396 bp) was readily detected in MCF7 and ZR-75-1 breast tumor cells (data not shown). Lower but reproducible expression was also observed in primary HMECs and in several established breast epithelial cell lines including T-47D, M13SV-1 (8), MCF10AT1, and MCF10AT3c (16). MDA MB-231 breast tumor cells were negative for SBEM expression, as were six tumor cell lines of non-breast origin (uterus: RL95-2, SK-UT-1B, Hec 1A; cervix: HeLa; prostate: LNCaP; and liver: HepG2). As controls, we also examined the expression of a housekeeping gene (*GAPDH*) and mammaglobin-1, an established mammary-specific gene that is being independently investigated as a promising marker for breast tumor diagnosis and nodal metastasis (12, 17). Of the cell lines tested, only HMEC and ZR-75-1 cells expressed mammaglobin-1, consistent with published reports.

Analysis of *SBEM* mRNA in Human Breast Tumors. Northern blot analyses performed on a small series of 10 cases revealed that *SBEM* mRNA was 600 bp long and differentially expressed from one sample to another (data not shown). To determine whether *SBEM* mRNA was widely expressed in human breast tumor tissue, 54 human breast tumors, spanning many ER and PR levels as well as tumor grade and nodal status, were selected from the Manitoba Breast Tumor Bank. Total RNA was extracted from frozen tissue sections and reverse transcribed. PCR amplification of *GAPDH* (control), *mammaglobin-1*, and *SBEM* cDNA was then performed. A PCR product, 396-bp long was detected in all but three tumors (data not shown) when using SBEM-specific primers. After cloning and sequencing, this product was shown to correspond to *SBEM* cDNA. Quantification of the *SBEM* signal relative to the *GAPDH* signal was performed as described in "Materials and Methods." No correlation was found between SBEM expression and tumor characteristics such as ER ($n = 54$; Spearman $r = -0.01$, $P = 0.89$) and PR ($n = 54$; Spearman $r = -0.03$, $P = 0.77$) levels or tumor grade ($n = 44$; Spearman $r = -0.06$, $P = 0.68$). Interestingly, however, the *SBEM* signal correlated positively with *mammaglobin-1* expression ($n = 54$; Spearman $r = 0.340$, $P = 0.011$). Subgroup comparison of *SBEM* and *mammaglobin-1* expression confirmed our previous observation[9] that *mammaglobin-1* expression is higher in ER-positive and low-grade tumors (Table 1). Interestingly, although not statistically significant ($P = 0.09$), higher SBEM expression was found in lymph node-positive compared with node-negative tumors. Also of interest is the fact that the SBEM:mammaglobin-1 ratio is significantly ($n = 46$; Mann-Whitney, $P = 0.04$) higher in these lymph node-positive tumors.

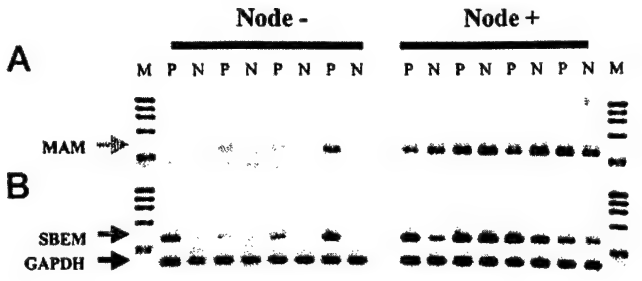

Fig. 2. RT-PCR analysis of *mammaglobin-1*, *SBEM*, and *GAPDH* mRNA expression in primary breast tumors (*P*) and their corresponding axillary lymph nodes (*N*), histologically shown to contain (*Node +*) or not to contain (*Node −*) metastases. *Mammaglobin-1* (*MAM*) PCR products were run separately (*A, dotted arrow*), whereas *SBEM* and *GAPDH* PCR products were mixed before separation on 2% agarose gels prestained with ethidium bromide (*B*). *Gray arrow*, product corresponding to SBEM; *black arrow*, product corresponding to *GAPDH*. *M*, molecular weight markers (Φ;x174 RF DNA/Hae III fragments; Life Technologies, Inc., Grand Island, NY). *N*, negative control, no cDNA added during the PCR reaction.

***SBEM* mRNA Expression in Primary Breast Tumors and Their Corresponding Axillary Nodes.** We next investigated the possibility that *SBEM* mRNA could be a tissue marker of axillary lymph node metastasis. Twenty independent cases were selected, including 14 tumors that were axillary lymph node positive and 6 that were node negative. Total RNA was extracted from frozen primary tumor sections and frozen node sections of corresponding axillary lymph nodes. The histological status of all tissues was confirmed in paraffin sections cut from adjacent mirror image paraffin tissue blocks that had been processed in parallel to the frozen blocks. These RNAs were reverse-transcribed and analyzed by RT-PCR using *SBEM*-specific primers. PCR was performed three times, giving the same result. A representative experiment is shown in Fig. 2. A signal corresponding to *SBEM* was detected in all lymph nodes containing metastatic cells by histopathological assessment (14 of 14 cases). In contrast, no signal was detectable in lymph nodes from cases without histologically detectable tumor cells (0 of 6 cases). RT-PCR detection of *SBEM* mRNA in axillary lymph nodes is therefore strongly associated (Fisher's exact test, $P < 0.001$) with the histopathological detection of lymph node metastases. The higher sensitivity afforded by RT-PCR detection therefore indicates that *SBEM*, perhaps together with *mammaglobin-1*, represents an excellent marker for the detection or confirmation of occult breast tumor metastasis, where histopathology may not be definitive.

***SBEM* mRNA Is Expressed in Mammary Epithelial Tumor Cells *in Vivo*.** To further establish whether *SBEM* was expressed by mammary epithelial cells *in vivo*, paraffin breast tumor tissue sections corresponding to a case shown to strongly express *SBEM* mRNA by RT-PCR were studied by *in situ* hybridization. No signal was detectable when using a sense probe (Fig. 3*A*). In contrast, a signal was observed in epithelial tumor cells when using an antisense probe (Fig. 3*B*). *SBEM* mRNA was not detected in stromal or inflammatory cells in any of the sections studied.

[9] E. Leygue, L. C. Murphy, and P. H. Watson, unpublished results.

Table 1 *Median values (arbitrary units) of SBEM expression, mammaglobin-1 (Mam) expression, and SBEM:mammaglobin-1 ratio in different tumor subgroups*

Tumors	*n*	SBEM	*P*	Mam	*P*[a]	SBEM: Mam	*P*[a]
ER +	34	2.29	0.66	0.63	**0.04**	3.39	0.22
ER −	20	2.15		0.34		4.44	
PR +	34	2.30	0.63	0.59	0.27	3.56	0.50
PR −	20	1.97		0.38		3.58	
Node +	36	2.30	0.09	0.45	0.62	3.97	**0.04**
Node −	10	1.96		0.70		2.42	
Grades 5–7	24	2.05	0.84	0.59	**0.03**	3.33	0.10
Grades 8–9	20	2.24		0.34		4.02	

ER +, >3 fmol/mg of protein; ER −, ≤3 fmol/mg of protein; PR +, >10 fmol/mg of protein; PR −, ≤10 fmol/mg of protein, as determined by ligand binding assay. Node +, confirmed metastasis in axillary lymph nodes; Node −, absence of metastasis in analyzed axillary lymph nodes. Grade, Nottingham grading system. Subgroup comparison was performed using the Mann-Whitney two-tailed test.

[a] Bold face *P* values correspond to statistically significant differences between tumor subgroups ($P < 0.05$).

Discussion

This article reports the identification, cloning, and preliminary characterization of a cDNA encoding a novel mucin-like protein that displays an unusually narrow pattern of expression. Hybridization analysis revealed that *SBEM* mRNA was only detectable in two normal tissues, breast and salivary gland. Interestingly, the tissue-

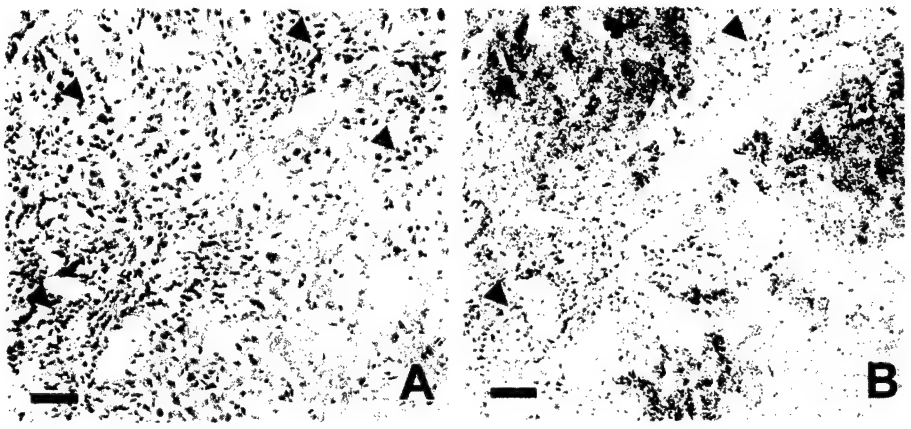

Fig. 3. Expression of *SBEM* mRNA in a primary breast tumor studied by *in situ* hybridization. These plates illustrate consecutive sections from a single breast tumor and show H&E-stained paraffin section treated with a sense probe (*A*) and *SBEM* mRNA expression in epithelial cells detected using an antisense probe (*B*). *Mauve* and *black arrowheads* show tumor epithelial cells and regions of stroma with inflammation, respectively. *Bar*, 30 μm.

specific expression that we observed experimentally directly reflects the distribution of ESTs within the Hs.348419 cluster. Indeed, as mentioned above, only two adult tissues (breast and head/neck tumors) have been shown to express SBEM-related ESTs. The fact that SBEM is also expressed in salivary tissue does not undermine the possible use of SBEM as a marker of breast cancer, because tumors of the salivary gland are less common and can readily be distinguished clinically.

Among the primary breast tumors examined in this study (representing mostly invasive ductal carcinoma), *SBEM* mRNA was observed by RT-PCR analysis in the majority (>90%) of cases. Despite a significant overall correlation between the expression of *SBEM* and *mammaglobin-1* mRNA, a significantly higher SBEM:mammaglobin-1 ratio was observed in primary tumors associated with positive axillary lymph nodes as compared with node-negative tumors. This was mostly attributable to a trend toward higher SBEM expression in node-positive tumors. Although further analysis of a larger number of tumors will be required to confirm these observations, this may suggest differences in the biology of these tumors and also a possible role of SBEM and mammaglobin-1 in the mechanisms involved in tumor metastasis. Our findings indicate, however, that SBEM expression is a common feature of breast cancer and can furthermore serve as a useful marker for breast nodal metastasis, both for detection of micrometastatic cells within lymph nodes as well as in the differential diagnosis of the primary origin of an unknown metastasis. This potential is enhanced by the conserved SBEM expression in high grade and ER/PR-negative tumors that are most likely to metastasize.

The potential diagnostic relevance of SBEM is also increased by its predicted biochemical structure. The *SBEM* cDNA sequence codes for a 90-amino acid polypeptide that contains a distinctive tandem repeat, rich in alanine and threonine residues, that represents a probable target for *O*-glycosylation. Consistent with such posttranslational modification is the presence of a well-defined signal peptide, leading us to predict that SBEM is likely to be processed at the apical surface of luminal epithelial cells and to be secreted into the alveolar or ductal lumen. Further study is needed to ascertain whether higher SBEM expression occurs in association with tumors.

Secreted (or transmembrane) proteins that contain internally repeated, densely glycosylated neutral core motifs such as this are characteristic of mucins, which are typically expressed by the surface epithelium of secretory mucosae and by exocrine glands (14, 15). The role of mucins is primarily one of hydrating and lubricating epithelial linings, although several mucins have been implicated in modulating both cell adhesion and growth factor signaling (18, 19). Furthermore, mucins have a well-established link to cancer, best illustrated by the product of the *MUC1* gene. *MUC1* is overexpressed in a variety of epithelial tumors including breast cancer and gives rise to several well-characterized tumor antigens including CA15.3 and CA27.29 (20, 21). Combined with the loss of cell polarity and changes in glycosylation patterns observed in transformed epithelial cells, overexpression of *MUC1* results in the appearance of mucin-derived tumor antigens in the sera of cancer patients that are not seen in normal controls (14, 22). We hypothesize that a similar situation may hold for SBEM expression in the human mammary epithelium and in human breast tumors. However, *MUC1* displays relatively broad expression among epithelial tissues including the colon, breast, pancreas, ovary, prostate, tracheobronchial tree, stomach, and uterus. For this reason, *MUC1*-derived tumor antigens have relatively poor specificity for individual tumor types, and their clinical utility is limited to monitoring the efficacy of cancer therapy and warning of tumor relapse or malignant spread (21–23).

Parallels between SBEM and known epithelial mucins such as *MUC1*, together with its more narrowly restricted pattern of expression, suggest that this novel gene represents an attractive candidate for a breast biomarker with potential for cancer diagnostics, as well as being a possible future target for the development of a breast tumor vaccine. Moreover, the absence of *SBEM* expression in normal lymph node tissue suggests that this gene could also be used to detect breast micrometastases in axillary lymph nodes.

References

1. Breast Cancer Facts and Figures, 2001–2002, pp. 5–6. Atlanta: American Cancer Society, 2001.
2. Stenman, U. H., Leinonen, J., Zhang, W. M., and Finne, P. Prostate-specific antigen. Semin. Cancer Biol., *9:* 83–93, 1999.
3. Schuler, G. D. Pieces of the puzzle: expressed sequence tags and the catalog of human genes. J. Mol. Med., *75:* 694–698, 1997.
4. Hatey, F. Expressed sequence tags for genes: a review. Genet. Sel. Evol., *30:* 521–541, 1998.
5. Velculescu, V. E., Zhang, L., Vogelstein, B., and Kinzler, K. W. Serial analysis of gene expression. Science (Wash. DC), *270:* 484–487, 1995.
6. Nielsen, H., Engelbrecht, J., Brunak, S., and von Heijne, G. Identification of prokaryotic and eukaryotic signal peptides and prediction of their cleavage sites. Protein Eng., *10:* 1–6, 1997.
7. Hansen, F. E., Lund, O., Tolstrup, N., Gooley, A. A., Williams, K. L., and Brunak, S. NetOglyc: prediction of mucin type *O*-glycosylation sites based on sequence context and surface accessibility. Glycoconj. J., *15:* 115–130, 1998.
8. Kang, K-S., Morita, I., Cruz, A., Jeon, Y. J., Trosko, J. E., and Chang, C. C. Expression of estrogen receptors in a normal human breast epithelial cell type with luminal and stem cell characteristics and its neoplastically transformed cell lines. Carcinogenesis (Lond.), *18:* 251–257, 1997.
9. Ausbubel, F. M., Brent, R., Kingston, R. E., Moore, D. D., Seidman, J. G., Smith J. A., and Struhl, K. (eds.). Short Protocols in Molecular Biology, Ed. 2, pp. 4.5–4.6. New York: John Wiley & Sons, 1992.
10. Leygue, E. R., Watson, P. H., and Murphy, L. C. Estrogen receptor variants in normal human mammary tissue. J. Natl. Cancer Inst., *88:* 284–290, 1996.
11. Dotzlaw, H., Leygue, E., Watson, P. H., and Murphy, L. C. Estrogen receptor β mRNA expression in human breast tumor biopsies: relationship to steroid receptor status and regulation by progestins. Cancer Res., *59:* 529–532, 1999.

12. Leygue, E., Snell, L., Dotzlaw, H., Hole, K., Troup, S., Hiller-Hitchcock, T., Murphy, L. C., and Watson, P. H. Mammaglobin, a potential marker of breast cancer nodal metastasis. J. Pathol., *189:* 28–33, 1999.
13. Kozak, M. Initiation of translation in prokaryotes and eukaryotes. Gene (Amst.), *234:* 187–208, 1999.
14. Marth, J. D., and Varki, A. *O*-Glycans *In:* A. Varki (ed.), Essentials of Glycobiology, pp. 101–106 and 537–549. New York: Cold Spring Harbor Laboratory, 1999.
15. Moniaux, N., Escande, F., Porchet, N., Aubert, J. P., and Batra, S. K. Structural organization and classification of the human mucin genes. Front. Biosci., *6:* 1192–1206, 2001.
16. Dawson, P. J., Wolman, S. R., Tait, L., Heppner, G. H., and Miller, F. R. MCF10AT: a model for the evolution of cancer from proliferative breast disease. Am. J. Pathol., *148:* 313–319, 1996.
17. Fleming, T. P., and Watson, M. A. Mammaglobin and its utility as a breast cancer marker. Ann. NY Acad. Sci., *923:* 78–89, 2000.
18. Satoh, S., Hinoda, Y., Hayashi, T., Burdick, M. D., Imai, K., and Hollingsworth, M. A. Properties of pancreatic *MUC1* gene encoding an anti-adhesion molecule. Int. J. Cancer, *88:* 507–518, 2000.
19. Carraway, K. L., Price-Schiavi, S. A., Komatsu, M., Jepson, S., Perez, A., and Carraway, C. A. Muc4/sialomucin complex in the mammary gland and breast cancer. J. Mammary Gland Biol. Neoplasia, *6:* 323–337, 2001.
20. Zimmerman, R. L., Fogt, F., and Goonewardene, S. Diagnostic value of a second generation CA 15-3 antibody to detect adenocarcinoma in body cavity effusions. Cancer (Phila.), *90:* 230–234, 2000.
21. Cheung, K. L., Graves, C. R., and Robertson, J. F. Tumour markers in the diagnosis and monitoring of breast cancer. Cancer Treat. Rev., *26:* 91–102, 2000.
22. Burchell, J. M., Mungul, A., and Taylor-Papadimitriou, J. *O*-Linked glycosylation in the mammary gland: changes that occur during malignancy. J. Mammary Gland Biol. Neoplasia, *6:* 355–364, 2001.
23. Baruch, A., Hartmann, M., Zrihan-Licht, S., Greenstein, S., Burstein, M., Keydar, I., Weiss, M., Smorodinsky, N., and Wreschner, D. H. Preferential expression of novel MUC1 tumor antigens and their tumor-potentiating function. Int. J. Cancer, *71:* 741–749, 1997.

Advances in Brief

Activated Mitogen-activated Protein Kinase Expression during Human Breast Tumorigenesis and Breast Cancer Progression[1]

Adewale Adeyinka, Yulian Nui, Tracy Cherlet, Linda Snell, Peter H. Watson, and Leigh C. Murphy[2]

Departments of Biochemistry and Medical Genetics [Y. N., T. C., L. C. M.] and Pathology [A. A., L. S., P. H. W.], Faculty of Medicine, University of Manitoba, Winnipeg, Manitoba, R3E 0W3 Canada

Abstract

Purpose: **The purpose of this study is to address the hypothesis that activated mitogen-activated protein kinase (MAPK; extracellular signal-regulated kinases 1 and 2) has a role in breast tumorigenesis, breast cancer progression, and the development of tamoxifen resistance.**

Experimental Design: **H-score analysis and a specific antibody for the immunohistochemical detection of activated MAPK in formalin-fixed, paraffin-embedded tissue sections were used to compare expression in: (*a*) human breast tumors and their matched adjacent normal breast tissue; (*b*) primary human breast tumors and their matched lymph node metastases; and (*c*) primary breast tumors from patients who later proved to be sensitive or resistant to tamoxifen treatment.**

Results: **Active MAPK expression was detected in 48% of primary human breast tumors and was significantly increased in tumors compared with adjacent normal breast (Wilcoxon test, $P = 0.027$). A significant positive association (χ^2, $P = 0.02$; $n = 55$) was obtained between active MAPK and the presence of lymph node metastases. Moreover, increased active MAPK (Wilcoxon test, $P = 0.0098$) was found in concurrent lymph node metastases compared with primary breast tumors. No significant difference in active MAPK was found in primary tumors of patients who later responded to tamoxifen or did not respond to tamoxifen.**

Conclusions: **These data suggest that active MAPK is a marker of breast cancer metastasis and has a role in the metastatic process. However, active MAPK is unlikely to be a marker of endocrine sensitivity or involved in *de novo* tamoxifen resistance.**

Introduction

Ligand-independent activation of ERs[3] has been extensively documented in experimental models (1). Consequently, it has been speculated that such a mechanism could, in part, underlie estrogen-independent activation of ERs and, therefore, may be associated with altered ER activity that is thought to underlie the altered estrogen action that occurs during human breast tumorigenesis (2) and/or breast cancer progression, in particular, the development of antiestrogen resistance (1). Previously, we had developed an estrogen-independent (as defined by loss of growth responsiveness to estradiol) ER+ human breast cancer cell line (T5-PRF) by long-term growth in estrogen-depleted media (3). Among other changes (3, 4), these estrogen-independent cells contained a significant increase in activated MAPK (5), as well as an increased apparently ligand-independent activity of the endogenous ER (4). Recently, increased activated MAPK was found in another cell line model of apparently estrogen-independent proliferation (6). MAPK has been implicated in the ligand-independent activation of ERα because it can directly phosphorylate ERα on serine 118, leading to ligand-independent ER activation and the loss of tamoxifen inhibition of ER-mediated transcriptional activation (7). Furthermore, treatment of cells with EGF or IGF-I that activates the Ras/Raf/MAPK pathway also activates the ERs in a ligand-independent fashion, and this is accompanied by serine 118 phosphorylation of ERs (7). These data suggest the possibility that increased activated MAPK in estrogen target tissues *in vivo* could effect estrogen and antiestrogen responsiveness. Interestingly, an increased expression and activity of MAPK in human breast tumors compared with normal breast tissues were reported (8), although only one breast tumor case was matched to its own adjacent normal breast tissue, all others were independent samples. If confirmed, this observation suggests that increased MAPK during human breast tumorigenesis, especially in ER+ breast tumorigenesis, could also contribute to the altered estrogen action that occurs during this process (9, 10). However, the relationship of activated MAPK to steroid receptor status to other known prognostic variables in breast cancer and to breast cancer progression, in particular antiestrogen sensitivity and resistance, has not been documented. In this study, we have investigated the expression of activated MAPK in human breast tissues directly *in vivo* using immunohistochem-

Received 8/29/01; revised 2/26/02; accepted 3/13/02.

The costs of publication of this article were defrayed in part by the payment of page charges. This article must therefore be hereby marked *advertisement* in accordance with 18 U.S.C. Section 1734 solely to indicate this fact.

[1] Supported by grants from the Canadian Institutes for Health Research/Medical Research Council of Canada and the U. S. Army Medical Research and Materiel Command (USAMRMC). The Manitoba Breast Tumor Bank is supported by funding from the National Cancer Institute of Canada. P. H. W. is a Medical Research Council of Canada Scientist. A. A. is funded by a Susan Komen Breast Cancer Foundation Fellowship and a USAMRMC postdoctoral award. T. C. is funded by a USAMRMC predoctoral studentship.

[2] To whom requests for reprints should be addressed, at Manitoba Institute of Cell Biology, University of Manitoba, 675 McDermot Avenue, Winnipeg, Manitoba, R3E OV9 Canada. Phone: (204) 787-4071; Fax: (204) 787-2190; E-mail: lcmurph@cc.umanitoba.ca.

[3] The abbreviations used are: ER, estrogen receptor; MAPK, mitogen-activated protein kinase; EGF, epidermal growth factor; IGF, insulin-like growth factor; PR, progesterone receptor; ERK, extracellular signal-regulated kinase; TBS, Tris-buffered saline; NEB, New England Biolabs.

istry and assessed the relationship of activated MAPK expression with known prognostic variables and progression in human breast cancer.

Materials and Methods

Human Breast Tissues. All breast samples used for this study were selected from the National Cancer Institute of Canada/Manitoba Breast Tumor Bank (Winnipeg, Manitoba, Canada). As was previously described (11), tissues are given to the Bank from cases at multiple centers within Manitoba, rapidly collected and processed to create matched formalin-fixed, paraffin-embedded and frozen tissue blocks for each case with the mirror image surfaces oriented by colored inks. The histology of every sample in the Bank is uniformly interpreted by a pathologist in H&E-stained sections from the face of the paraffin tissue block. This information is available in a computerized database along with relevant pathological and clinical information and was used as a guide for selection of specific paraffin and frozen blocks from cases for this study. For each case, interpretation included an estimate of the cellular composition (including the percentage of invasive epithelial tumor cells and stroma), tumor type, and tumor grade (Nottingham score). Steroid receptor status was determined for all primary tumor samples by a ligand-binding assay performed on an adjacent portion of tumor tissue. Tumors with ER levels $>$ 3 fmol/mg of total protein were considered ER+, and tumors with PR levels $>$ 10 fmol/mg of total protein were considered PR+.

Cohort 1. Twenty-six primary human breast tumor biopsies were selected. For each case, matched adjacent normal and tumor tissue blocks were available. The quality of each block and the relative cellular composition were determined by the histopathological assessment of sections from adjacent mirror image paraffin-embedded tissue blocks as described previously (11). The presence of normal ducts and lobules as well as the absence of any atypical lesion was confirmed in all normal tissue specimens. In three cases, the normal tissue sections did not contain normal glands and, therefore, were excluded from the normal *versus* tumor analysis, leaving 23 cases. The ER levels ranged from 0.8 to 83 fmol/mg protein. Five tumors were ER− and 18 were ER+. The PR levels ranged from 2.2 to 112 fmol/mg protein. Fifteen tumors were PR+ and 8 tumors were PR−. The tumors spanned a range of grades (grade scores 5–9) as determined by the Nottingham grading system.

Cohort 2. To identify cases that responded divergently to tamoxifen, a review of 1000 consecutive cases identified 490 cases that were ER+ and node negative. Among these cases, 196 were identified that had been treated with adjuvant tamoxifen after surgery ± local radiation. From these cases, a subset of 15 was selected that had shown progression of disease (either dead or alive with recurrent disease, referred to as tamoxifen-resistant cases). A similar control subset (n = 14) was specifically selected to comprise cases with similar lengths of follow-up (resistant, 34 months *versus* sensitive, 39 months), ER status, tumor grade, and tumor histology but that showed no progression of disease (referred to as tamoxifen-sensitive cases). The ER levels for the tamoxifen-sensitive cases ranged from 4.4 to 146 fmol/mg protein, and the PR levels ranged from 9.5 to 216 fmol/mg protein. One of these tumors were PR− and the rest were PR+. The ER levels for the tamoxifen-resistant cases ranged from 4.6 to 107 fmol/mg protein, and the PR levels ranged from 8.8 to 143 fmol/mg protein. One of these tumors was PR− and the rest were PR+. There were no significant differences between the two groups with respect to ER levels or grade scores, however, there was a significantly statistical difference between the groups with respect to PR levels. The tamoxifen-sensitive group had a significantly (P = 0.0064, Mann-Whitney test, two-tailed) higher median PR level (40.5 fmol/mg protein) than the tamoxifen-resistant group (14.8 fmol/mg protein).

Cohort 3. Sections from 21 primary human breast tumor samples and their matched lymph node metastases were selected. For the primary tumor samples, the ER levels, determined by ligand-binding assays, ranged from 0 to 298 fmol/mg protein. Seventeen tumors were ER+ and 4 were ER−. PR levels determined by ligand-binding assays ranged from 2.7 to 323 fmol/mg protein. Fourteen tumors were PR+ and 7 were PR−.

Antibodies. The following antibodies specific for dually phosphorylated (active) forms of the MAPK isoforms, ERK1 and ERK2 (p44/42), were used in this study: (*a*) phospho-p44/42 MAPK (Thr202/Tyr204) rabbit polyclonal antibody (9101S; New England Biolabs, Beverly, MA); (*b*) phospho-p44/42 MAPK (Thr202/Tyr204) E10 monoclonal antibody (9106L; New England Biolabs); and (*c*) antiactive MAPK rabbit polyclonal antibody (V8031; Promega, Madison, WI). The antibodies used for immunohistochemistry were validated by the following method. Estrogen-depleted MCF-7 breast cancer cells were treated for 3 h with 50 μM of the MAPK kinase 1 inhibitor, PD98059 (Calbiochem, La Jolla, CA), or vehicle (DMSO) alone. Half of the cells from each group was extracted and analyzed by Western blotting. The remainder was embedded in 3% agar, formalin fixed, paraffin embedded, and processed for immunohistochemistry (12). Western blot analysis (Fig. 1) showed a significant decrease in the M_r 44,000/M_r 42,000 ERK 1/2 MAPK bands of the PD98059-treated cell extracts compared with the vehicle alone-treated cells using an antibody that recognized only the dually phosphorylated (active) MAPK isoforms ERK1 and ERK2. No change in total MAPK levels was seen when the blot was stripped and reprobed with an antibody recognizing total MAPK [ERK1(C-16) catalog no. sc93-G; Santa Cruz Biotechnology], supporting the conclusion that inhibition of the MAPK kinase 1 that activates ERK1 and ERK2 led to decreased detection of active MAPK with no effect on total MAPK levels, which were equivalent between the two treatment groups. Immunohistochemistry, using two different antibodies (polyclonal NEB 9101S and monoclonal NEB 9106L antibodies) to active MAPK, showed the presence of nuclear and some cytoplasmic staining in some but not all cells. The cell pellet sections were assessed by semiquantitative scoring using an H-score system, as described previously (13). Importantly, the intensity and the percentage of cell staining were significantly reduced in the PD98059-treated cells compared with the vehicle alone-treated cells (Fig. 2). The immunohistochemistry results were therefore consistent with the Western blot analysis. The polyclonal antibody (Fig. 2, *B* and *E*) gave a better signal immunohistochemically and was used on randomly selected human breast tumor sections. The results showed little if any

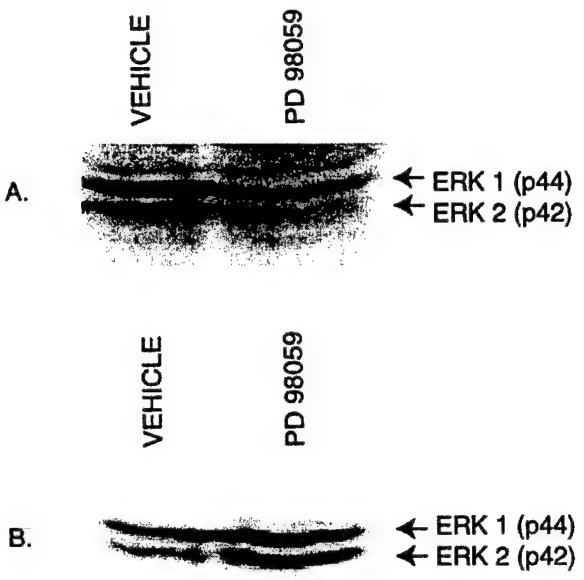

Fig. 1 Western blot analysis of T-5 human breast cancer cells with and without PD98059 treatment. T-5 human breast cancer cells were exposed to 50 mM PD98059 for 3 h and proteins extracted (14). Proteins were resolved by 10% PAGE/SDS as described in the "Materials and Methods" section. *A*, expression of active MAPK visualized using antiactive MAPK rabbit polyclonal antibody (V8031; Promega) and chemiluminescence. *B*, blots from *A* were stripped and reprobed with goat anti-ERK1 (total MAPK; Santa Cruz Biotechnology) and visualized via chemiluminescence.

background staining in these tissue sections, and positive nuclear staining was seen in some of the epithelial tumor cells (Fig. 2, *A* and *D*). Therefore, this antibody was used for additional immunohistochemical analysis of activated MAPK in formalin-fixed, paraffin-embedded sections of human breast tissues.

Western Blot Analysis. Estrogen-depleted MCF-7 cells that had been treated or not treated with PD98059, as described above, were extracted using Buffer J [0.5 M Tris-HCl (pH 6.8), 4% SDS, 20% glycerol, and 0.2 M DTT] containing 1 tablet/10 ml complete protease inhibitor mixture tablets (Roche, Mannheim, Germany) that were optimized to inhibit proteolysis and phosphatases, as described previously (14). Aliquots of the extracts were analyzed using 10% SDS-PAGE with a 4% stacking gel at 200V for 45 min at room temperature according to the Laemmli method (15). Gels were transferred to nitrocellulose using 3-(cyclohexylamino)propanesulfonic acid transfer buffer [10 mM 3-(cyclohexylamino)propanesulfonic acid (pH 11.0) and 20% methanol] and transferred for 1 h at 120V at 4°C. Blots were blocked overnight at 4°C in 0.2% (w/v) I-block (Tropix, Foster City, CA) in TBS. Blots were incubated with rabbit antiactive-MAPK antibody (Promega, 1/1000 in 0.2% I-block in TBS containing 0.5% Tween-20) overnight at 4°C, followed by goat antirabbit antibody conjugated to horseradish peroxidase (Bio-Rad, 1/5000) for 1 h at room temperature. Detection was carried out using the enhanced chemiluminescence detection system according to the manufacturer's instructions (Amersham, Buckinghamshire, United Kingdom). The membrane was then stripped [0.2 M glycine, 0.1% SDS, 1% Tween-20 (pH 2.2)] for 1 h at room temperature and blocked for 1 h at room temperature with 0.2% I-block in TBS. The membrane was then probed with 1/1000 dilution of goat anti-ERK1 (total MAPK; Santa Cruz Biotechnology) in 0.2% I-block overnight at 4°C, followed by incubation with 1/5000 donkey antigoat antibody conjugated to horseradish peroxidase for 1 h at room temperature. Detection was with the enhanced chemiluminescence detection system as described above.

Immunohistochemistry. In all cases, tissue samples had been fixed for 18–24 h in 10% buffered formalin before routine embedding in paraffin wax. Five-μm thick sections were cut, mounted on Superfrost/Plus slides (Fisherbrand), dried overnight at 37°C, dewaxed in xylene (4 min), and rehydrated in graded alcohol. DAKO EnVision System peroxidase (DAKO Diagnostics Canada, Inc.) was used for immunohistochemistry staining. After an initial pilot study using both the monoclonal (NEB 9106L) and polyclonal (NEB 9101S) antibodies, subsequent staining of human breast tissues was done using the polyclonal antibody to active MAPK. Blocking steps included peroxidase blocking reagent (0.03% hydrogen peroxide containing sodium azide) for 5 min to block endogenous peroxidase and Universal Blocker (DAKO Diagnostics Canada, Inc.) for 15 min to prevent nonspecific staining with antibody from both mouse and rabbit. Tissue sections were incubated overnight at 4°C with the primary antibody (1:250 dilution in antibody diluting buffer; DAKO Diagnostics Canada, Inc.) after an initial incubation with the same antibody at 37°C for 30 min. After the overnight incubation, slides were treated with labeled polymer (goat antirabbit and goat antimouse immunoglobulin in Tris-HCl buffer containing carrier protein and antimicrobial agent) for 30 min at room temperature. Finally, slides were incubated for 10 min with substrate 3-amino-9-ethylcarbazole. Each incubation step was followed by a 2-min TBS wash twice. The slides were counterstained with hematoxylin, immersed in a bath of ammonia water, rinsed in distilled water, and a coverslip applied using an aqueous mounting medium.

Levels of expression were scored semiquantitatively under the light microscope by assessing the average signal intensity (on a scale of 0–3) and the proportion of cells showing a positive signal (0, none; 0.1, less than one tenth; 0.5, less than one half; and 1.0 greater than one half). The intensity and proportion scores were then multiplied to give an H-score (13).

Statistical Analysis. Differences between normal samples and their matched tumors were tested using the Wilcoxon matched pairs test, two-tailed. Correlation between activated MAPK expression and tumor characteristics was tested by calculation of the Spearman coefficient *r*. A χ^2 test was used to determine statistical significance of the association between active MAPK and nodal status. Fisher's exact test was used to test for differences in frequency of detection of active MAPK between groups.

Results

Activated MAPK Expression Is Increased during Human Breast Tumorigenesis. To confirm and extend previous data suggesting that activated MAPK expression is increased in breast tumors compared with normal breast tissue, we used a

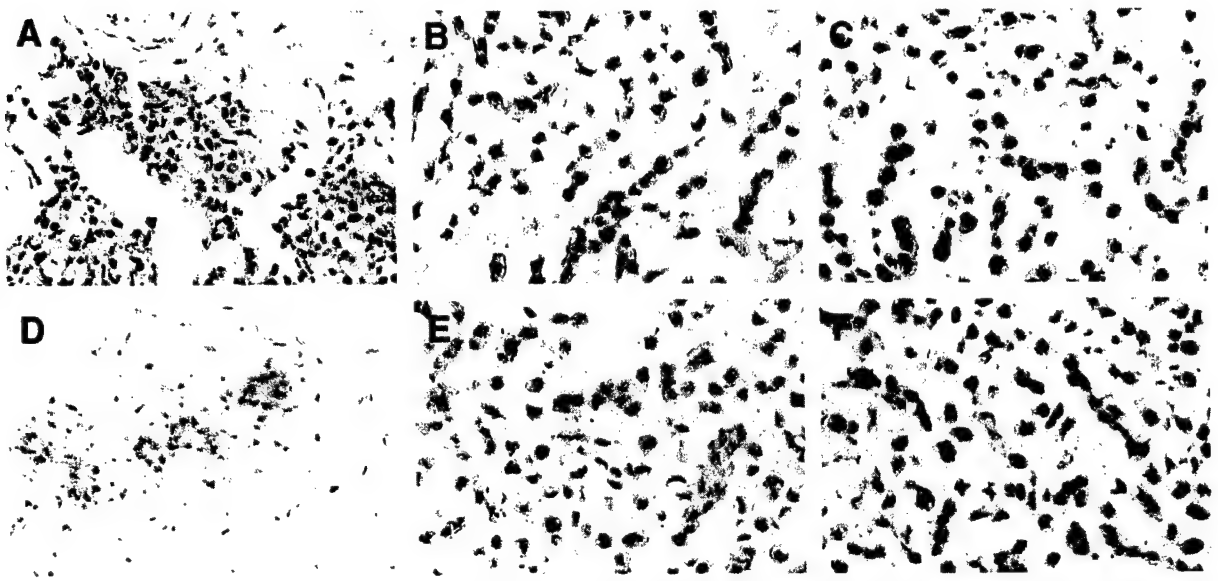

Fig. 2 Active MAPK expression in primary invasive breast tumors and matched adjacent normal breast tissues determined immunohistochemically. *A*, active MAPK expression in an invasive breast tumor detected using rabbit polyclonal antibody (9101S; New England Biolabs). *B*, active MAPK expression in vehicle alone-treated T-5 cells using rabbit polyclonal antibody (9101S; New England Biolabs). *C*, active MAPK expression in vehicle alone-treated T-5 cells using E10 monoclonal antibody (9106L; New England Biolabs). *D*, active MAPK expression in the matched adjacent normal breast tissue using rabbit polyclonal antibody (9101S; New England Biolabs). *E*, active MAPK expression in PD98059 treated T-5 cells using rabbit polyclonal antibody (9101S; New England Biolabs). *F*, active MAPK expression in PD98059 treated T-5 cells using E10 monoclonal antibody (9106L, New England Biolabs). ×200.

polyclonal antibody recognizing only active MAPKs ERK1/ERK2 as described and validated above to compare active MAPK expression in 23 breast tumor samples with their matched adjacent normal breast tissues containing normal ductal epithelium. Interestingly, of the 23 samples studied, only 11 (48%) had detectable staining in the tumor epithelium. There did not appear to be any relationship of frequency of detection of activated MAPK expression and ER status, although in this cohort only 6 of the tumors were ER−. The tissue sections were subjected to semiquantitative H-score analysis using sections obtained from agar-embedded cell pellets of PD98059-treated and -untreated cell lines as controls (Fig. 2, *B* and *E*). An example of activated MAPK staining in a human breast tumor and its matched adjacent normal breast tissue is shown in Fig. 2, *A* and *D*, respectively. The data were analyzed by a Wilcoxon matched pairs statistical test. The expression of active MAPK seen in breast tumors (median for all 23 tumors, 0.1; median for the 12 tumors with detectable staining only, 0.6) was significantly increased ($P = 0.027$, $n = 23$; $P = 0.027$, $n = 12$) compared with their adjacent matched normal breast tissue (median for all 23 normal tissues, 0.0; median for the 12 normal samples whose corresponding tumor had detectable staining, 0.0).

Activated MAPK Expression Is Not Altered between Breast Tumors That Are Tamoxifen Sensitive or Tamoxifen Resistant. Ligand-independent activation of ERs is thought to be, at least in part, a possible mechanism associated with tamoxifen resistance in ER+ breast tumors. To determine whether activated MAPK expression could be a predictor of tamoxifen sensitivity in primary breast cancers, tumors described under cohort 2 were examined immunohistochemically as described above for activated MAPK expression. The tumors were all ER+ and node negative and were the primary tumors obtained from patients who were later treated with tamoxifen (as described above) and remained disease free (tamoxifen-sensitive cases, $n = 14$) or relapsed (tamoxifen-resistance cases, $n = 15$). Tumor characteristics are detailed in Table 1. It should be noted that there were no statistically significant differences between the sensitive and resistant groups with respect to ER levels, tumor grade, age, or time of follow-up. However, a statistically

Table 1 Characteristics of the primary tumors of patients who relapsed (tamoxifen resistant) or remained disease free (tamoxifen sensitive) after tamoxifen adjuvant therapy

	ER (fmol/mg protein)	PR (fmol/mg protein)	Grade[a]	Age (yr)	Follow-up (mo)
Tamoxifen sensitive					
Median	30	40.5[b]	6	72.5	39
Max[c]	146	216	9	87	76
Min[d]	4.4	9.5	4	47	13
Tamoxifen resistant					
Median	14.2	14.8[b]	6	67	32
Max	107	143	9	89	63
Min	4.6	8.8	5	49	9

[a] Nottingham score.
[b] Significant difference, $P = 0.0064$ (Mann-Whitney rank sum test, two-sided), between the two subgroups for this parameter.
[c] Maximum value observed in cohort.
[d] Minimum value observed in cohort.

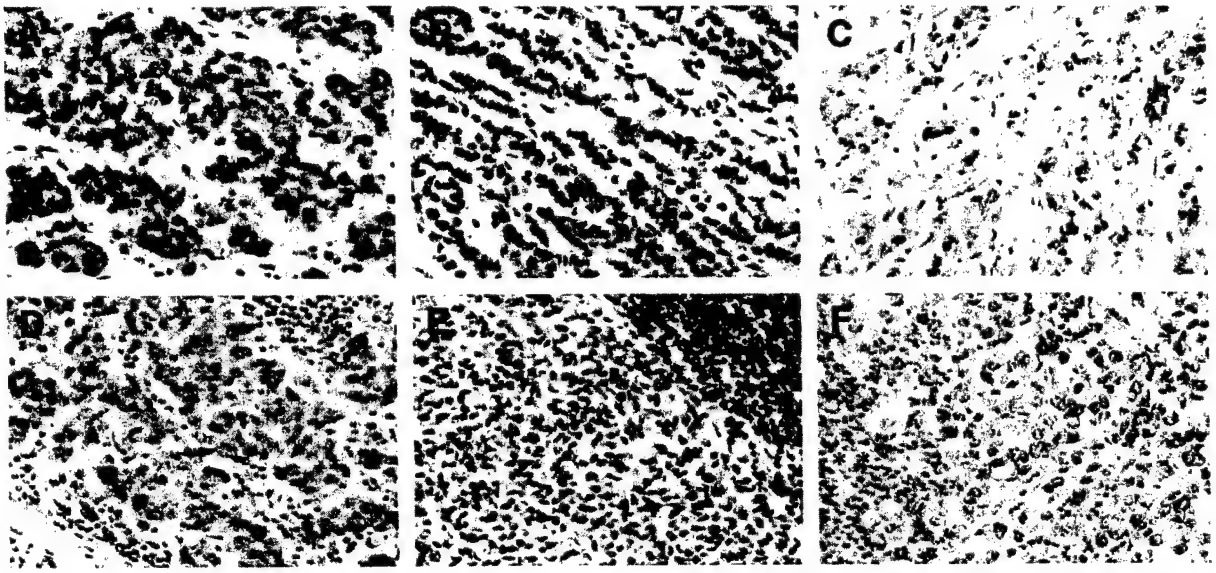

Fig. 3 Active MAPK expression in primary breast tumors and matched concurrent lymph node metastases. Immunohistochemistry with rabbit polyclonal antibody (9101S; New England Biolabs) on primary tumors (*A–C*) and their matched lymph node metastases (*D–F*, respectively), showing no staining (*A* and *D*), moderate staining (*B* and *E*), and intense staining (*C* and *F*) for MAPK. **, lymphocytes. ×200.

significant difference was observed between the level of PRs in the primary tumors of the sensitive and resistant cases (Mann-Whitney rank sum test, $P = 0.0064$). Higher levels of PRs were observed in the primary tumors of tamoxifen-sensitive cases (median, 40.5; $n = 14$) *versus* tamoxifen-resistant cases (median, 14.8; $n = 15$).

Ten of 29 tumors had detectable active MAPK staining (7 of 14 sensitive and 3 of 15 resistant); using Fisher's exact test, there was no statistically significant difference ($P = 0.128$) between the two groups in terms of the frequency of detection of active MAPK. When active MAPK was quantified using H-score analysis, there was no statistically significant difference in active MAPK expression between the two groups (sensitive median, 0.05 *versus* resistant median, 0.0; Mann-Whitney rank sum test, $P = 0.1$). It was concluded that activated MAPK as measured in primary breast tumors before beginning tamoxifen treatment was unlikely to be a marker of endocrine sensitivity.

Activated MAPK Expression Is Associated with Lymph Node Metastases. Correlation between activated MAPK expression and tumor characteristics was tested by calculation of the Spearman coefficient r using active MAPK H-scores obtained from all tumors in both cohorts 1 and 2. No statistically significant correlations were found with grade, cellular composition, ER level, or PR level. However, a significant positive association was obtained between active MAPK expression and the presence of lymph node metastases (χ^2, $P = 0.02$). This suggested that active MAPK may be a marker of metastases and could be associated with progression in human breast cancer.

To investigate this further, an additional cohort of 21 primary human breast tumor samples and their matched lymph node metastases (cohort 3) were provided by the National Cancer Institute of Canada/Manitoba Breast Tumor Bank. Nineteen of 21 primary tumors (90%) had detectable active MAPK expression, and 19 of 21 lymph node metastases (90%) had detectable active MAPK expression. This increased frequency of detection of active MAPK expression as compared with the original cohort 1 (48%), where there was a mixture of node positive and node negative primary breast tumors, is consistent with the statistically significant association of active MAPK expression and lymph node involvement identified in cohort 1. This difference in frequency of detection between the two cohorts is significant ($P = 0.0034$, Fisher's exact test). Also, the pattern of active MAPK detection seemed to be conserved between each primary and its matched lymph node metastasis, *i.e.*, if the primary tumors (19 of 21) had detectable active MAPK, so did its matched lymph node metastases (19 of 21); if the primary tumor did not have detectable active MAPK (2 of 21), then its matched lymph node metastasis was also negative (2 of 19).

Activated MAPK Expression Is Increased in Lymph Node Metastases Compared with the Primary Breast Tumor. When the level of active MAPK expression was semiquantified using H-score analysis as described in the "Materials and Methods" section, a statistically significant increase (Wilcoxon matched pairs test, $P = 0.0098$) in active MAPK expression was found in the lymph node metastases (median score, 1.0; $n = 21$) *versus* the primary breast tumor (median score, 0.2; $n = 21$). Examples of increased expression of active MAPK in lymph node metastases compared with their matched primary breast tumor are shown in Fig. 3. These data suggest that not only is active MAPK expression a potential marker of metastasis but that it is also increased during breast cancer progression.

Discussion

There are several studies *in vitro* using breast cancer cell lines that suggest a role of activated MAPK in human breast cancer and possibly altered estrogen/antiestrogen responsiveness (5, 6, 16–18). The data presented here confirm and extend previous data that suggested increased expression of active MAPKs ERK1 and ERK2 occurs during human breast tumorigenesis *in vivo* (8). Using multiple samples of human breast tumors and their matched adjacent normal breast tissues together with immunohistochemical detection of dually phosphorylated (active) MAPK, our data provide unequivocal evidence that increased active MAPK expression occurs in ~50% of primary breast tumors compared with their adjacent normal breast tissues. Conclusions reached from previously published data were derived from comparisons between breast tumors and independent cases of normal breast tissue and benign breast lesions. In only one case was the sample matched from the same patient. The combined data suggest that increased expression of active MAPK frequently occurs during human breast tumorigenesis and, in part, may play a role in this process. The reasons for increased active MAPK expression are unknown, although it may, in part, be because of increased total expression of MAPK (8) in addition to increased activity of growth factor receptor-induced cell proliferation pathways (19, 20).

In examining the relationship of active MAPK expression in primary human breast tumors with known prognostic variables, increased active MAPK expression was unrelated to tumor type, tumor grade, or steroid receptor status. However, a positive association of active MAPK detection with the presence of lymph node metastases was observed. This suggests that active MAPK may be a marker of nodal metastases and poor prognosis. Furthermore, the level of active MAPK in lymph node metastases was significantly increased above that found in their matched primary tumors, suggesting the possibility that increased active MAPK may have a mechanistic role in the metastatic progression of breast tumors. Receptor tyrosine kinase activation of signal transduction pathways often includes activation of the ERK 1/2 MAPKs. Several growth factor receptor pathways are known to be deregulated in breast tumors; in particular, the c-erbB2 receptor is amplified and associated with a poor prognosis in ~30% of human breast cancers (21). Both EGF and IGF-I receptor pathways are often increased in human breast tumors, and increased EGF receptor activity is also associated with a poor prognosis (22). In contrast, increased IGF receptor levels are usually associated with a good prognosis (23). Alterations in the extracellular environment (*e.g.*, extracellular matrix components), which occurs during tumorigenesis and metastasis, can also affect MAPK activity (19). Therefore, it is possible that the increased active MAPK seen in lymph node metastases may be due, in part, to increased and/or deregulated activity of such receptor tyrosine kinase pathways, altered extracellular environment, as well as an increased level of expression of total MAPK (8). Therefore, multiple mechanisms are likely to be responsible for the increased active MAPK seen during breast tumorigenesis and breast cancer progression. Irrespective of the mechanism(s) by which active MAPK is increased, our data suggest that it may be an excellent marker for predicting micrometastases and identifying a subgroup of node negative breast cancers with a poor prognosis. However, this requires additional investigation.

The data presented here suggest that active MAPK is increased in breast tumors compared with their matched adjacent normal breast tissues, suggesting that active MAPK is increased during breast tumorigenesis and may have a role in breast tumorigenesis. A more detailed study of preneoplastic breast lesions would be necessary to support this hypothesis and identify the stage at which this increase occurs. However, in ER+ breast tumorigenesis, such an increase in activated MAPK may have a role in the deregulated and altered action of estrogen thought to occur during this process (2). Although our data suggest that increased active MAPK expression was unrelated to steroid hormone receptor status in primary breast tumors, we have found a proportion (41%) of ER+ tumors that can contain increased active MAPK expression. Because active MAPK is able to directly phosphorylate ERα (7) and apparently induce ligand-independent activation of the receptor, the hypothesis has been suggested that this may underlie, in part, the development of tamoxifen resistance. To address this issue, we compared the expression of active MAPK in primary tumors of patients that later were classified as tamoxifen sensitive or resistant. These breast tumors were all ER+ and node negative. We found no significant differences in either the frequency of detection or the level of active MAPK expression between the primary tumors from patients that subsequently were shown to be tamoxifen sensitive and the primary tumors from patients that subsequently were shown to be tamoxifen resistant. These data suggest that active MAPK expression in ER+ primary human breast tumors is not a marker of endocrine responsiveness and is unlikely to be involved in *de novo* tamoxifen resistance. We cannot, however, exclude the possibility that altered active MAPK expression may be involved in acquired tamoxifen resistance. In this study, we have only measured active MAPK in the primary tumors of ER+ patients as yet unexposed to any form of adjuvant treatment. Previous data and our current data show that not all ER+ breast cancers will respond to tamoxifen treatment despite never having seen tamoxifen before. This type of resistance is referred to as *de novo* resistance. To study acquired tamoxifen resistance, it would be necessary in future studies to acquire biopsy material from breast cancer metastases that develop in patients whose original breast cancer responded to tamoxifen and then disease recurrence occurred during tamoxifen treatment and/or use xenograft mouse model systems of acquired tamoxifen-resistant human breast cancer cells (16).

In summary, we have investigated the expression of the active MAPKs ERK1 and ERK2 during human breast tumorigenesis and breast cancer progression. Significantly increased active MAPK was found in primary breast tumors compared with their adjacent matched normal breast tissues, was correlated with nodal metastasis when detected in primary breast tumors, and was significantly increased in lymph node metastases compared with their matched primary breast tumors. These data suggest that not only is active MAPK a marker of progression in human breast cancer but may also have a role in both breast cancer progression as well as breast tumorigenesis.

References

1. Katzenellenbogen, B. S. Estrogen receptors: bioactivities and interactions with cell signaling pathways. Biol. Reprod., *54:* 287–293, 1996.

2. Murphy, L. Mechanisms of hormone independence in human breast cancer. In Vivo, *12:* 95–106, 1998.

3. Coutts, A., Davie, J., Dotzlaw, H., and Murphy, L. Estrogen regulation of nuclear matrix-intermediate filament proteins in human breast cancer cells. J. Cell. Biochem., *63:* 174–184, 1996.

4. Coutts, A., Leygue, E., and Murphy, L. Altered oestrogen receptor-α variant mRNA expression in estrogen independence. J. Mol. Endocrinol., *23:* 325–336, 1999.

5. Coutts, A., and Murphy, L. Elevated mitogen-activated protein kinase activity in estrogen nonresponsive human breast cancer cells. Cancer Res., *58:* 4071–4074, 1998.

6. Jeng, M., Yue, W., Eischeid, A., Wang, J., and Santen, R. Role of MAPK in the enhanced cell proliferation of long-term estrogen deprived human breast cancer cells. Breast Cancer Res. Treat., *62:* 167–175, 2000.

7. Kato, S., Endoh, H., Masuhiro, Y., Kitamoto, T., Uchiyama, S., Sasaki, H., Masushige, S., Gotoh, Y., Nishida, E., Kawashima, H., Metzger, D., and Chambon, P. Activation of the estrogen receptor through phosphorylation by mitogen-activated protein kinase. Science (Wash. DC), *270:* 1491–1494, 1995.

8. Sivaraman, V., Wang, H., Nuovo, G., and Malbon, C. Hyperexpression of mitogen-activated protein kinase in human breast cancer. J. Clin. Investig., *99:* 1478–1483, 1997.

9. Anderson, E., Clarke, R., and Howell, A. Estrogen responsiveness and control of normal human breast proliferation. J. Mammary Gland Biol. Neopl., *3:* 23–35, 1998.

10. Clarke, R., Howell, A., Potten, C., and Anderson, E. Dissociation between steroid receptor expression and cell proliferation in the human breast. Cancer Res., *57:* 4987–4991, 1997.

11. Hiller, T., Snell, L., and Watson, P. Microdissection/RT-PCR analysis of gene expression. Biotechniques, *21:* 38–44, 1996.

12. Riera, J., Simpson, J., Tamayo, R., and Battifora, H. Use of cultured cells as a control for quantitative immunohistochemical analysis of estrogen receptor in breast cancer. Am. J. Clin. Pathol., *111:* 329–335, 1999.

13. Al-haddad, S., Zhang, Z., Leygue, E., Snell, L., Huang, A., Niu, Y., Hiller-Hitchcock, T., Hole, K., Murphy, L., and Watson, P. Psoriasin (S100A7) expression and invasive breast cancer. Am. J. Pathol., *155:* 2057–2066, 1999.

14. Joel, P., Traish, A., and Lannigan, D. Estradiol-induced phosphorylation of serine 118 in the estrogen receptor is independent of p42/p44 mitogen-activated protein kinase. J. Biol. Chem., *273:* 13317–13323, 1998.

15. Laemmli, U. Cleavage of structural proteins during the assembly of the head of bacteriophage T4. Nature (Lond.), *227:* 680–685, 1970.

16. Hilsenbeck, S., Friedrichs, W., Schiff, R., O'Connell, P., Hansen, R., Osborne, C., and Fuqua S. A. Statistical analysis of array expression data as applied to the problem of tamoxifen resistance. J. Natl. Cancer Inst. (Bethesda), *91:* 453–459, 1999.

17. Kurokawa, H., Lenferink, A., Simpson, J., Pisacane, P., Sliwkowski, M., Forbes, J., and Arteaga, C. Inhibition of HER2/neu (erbB-2) and mitogen-activated protein kinases enhances tamoxifen action against HER2-overexpressing, tamoxifen-resistant breast cancer cells. Cancer Res., *60:* 5887–5894, 2000.

18. Oh, A., Lorant, L., Holloway, J., Miller, D., Kern, F., and El-Ashry, D. Hyperactivation of MAPK induces loss of ERα expression in breast cancer cells. Mol. Endocrinol., *15:* 1344–1359, 2001.

19. Roovers, K., and Assoian, R. Integrating the MAPK signal into the G_1 phase cell cycle machinery. Bioessays, *22:* 818–826, 2000.

20. Ethier, S. Growth factor synthesis and human breast cancer progression. J. Natl. Cancer Inst. (Bethesda), *87:* 964–973, 1995.

21. Dowsett, M., Cooke, T., Ellis, I., Gullick, W., Gusterson, B., Mallon, E., and Walker, R. Assessment of HER2 status in breast cancer: why, when, and how? Eur. J. Cancer, *367:* 170–176, 2000.

22. Fox, S., and Harris, A. The epidermal growth factor receptor in breast cancer. J. Mammary Gland Biol. Neopl., *2:* 131–141, 1997.

23. Papa, V., Gliozzo, B., Clark, G., McGuire, W., Moore, D., Fujita-Yamaguchi, Y., Vigneri, R., Goldfine, I., and Pezzino, V. Insulin-like growth factor I receptors are overexpressed and predict a low risk in human breast cancer. Cancer Res., *53:* 3736–3740, 1993.

Chapter in "Expression Genetics: Differential Display". Editors Arthur and Michael McClelland, Eaton Publishing. 1999

Watson P. H., Hiller-Hitchcock T., Snell L., [1] Hole K., Murphy L.C., Leygue E.T., and Dotzlaw H.[2], Roughley P.J. [3]

Department of Pathology [1] and Department of Biochemistry and Molecular Biology [2], University of Manitoba, Winnipeg, Manitoba, R3E OW3, Canada, and Genetics Unit, Shriners Hospital for children, Montreal, Quebec, H3G 1A6. [3]

Update to : Hiller T, Snell L, Watson P. "Microdissection/RT-PCR analysis of gene expression in pathologically defined frozen sections" Biotechniques, 21, 38-44, 1996.

We have continued to utilize this approach in our research program (1) to pursue the specific goal of identification of genes that influence the acquisition of the invasive phenotype in human breast cancer. Assessment of risk of progression to invasive breast cancer has recently become an increasingly recognizable and defined problem in clinical management. This is partly due to the increasing number of patients who present with pre-invasive ductal carcinoma in-situ, (DCIS) (2). More recently, the demonstration that breast cancer can be delayed or inhibited by tamoxifen therapy in women at high risk as defined in the NSABP trial has also provided a new focus and impetus to improve the accuracy of risk determination (3). But although there is clearly a need for better predicators of biological potential and there has also been an impressive growth in the knowledge of genes involved in tumor invasion and metastasis (4), the importance of most of these factors in the development of the invasive phenotype in the complex heterogeneous disease of human breast cancer has been difficult to establish (5,6). This is partly because many of these genes (including cell adhesion molecules, proteases and motility factors) were first identified in tumor cell lines and systems other than epithelial breast carcinoma. This in turn reflects a lack of suitable breast specific models or breast cell lines that are representative of the pre-invasive, in-situ stage of cancer.

To address this critical issue in the biology of early breast tumor progression, many groups have based their studies on human tissues and begun to survey DCIS lesions with microsatellite markers in search of regions of loss of heterozygosity (LOH) that may harbor tumor invasion suppressor genes. This approach has yielded some interesting loci but not specific genes as yet (7). In contrast, our approach as outlined previously, has been to directly study differential gene expression within histologically defined breast tissues, in order to identify potential 'invasion' genes (1).

This approach has been crucially dependent on the design and maturation of the NCIC-Manitoba Breast Tumor Bank resource to allows selection and dissection of histologically defined frozen breast tissues (8). To date we have identified a number of cDNAs that are differentially expressed between DCIS and invasive tumor components. To rapidly determine the potential of this approach we have initially focused on 6 known cDNAs identified in other systems. We have confirmed amongst these, real differential expression (3 cDNA's, see below), differential expression attributable to differences in local regional composition (1 cDNA) and false positives (2 cDNA's) by in-situ hybridization and RT-PCR. Consideration of the patterns of expression amongst the 3 differentially expressed cDNA's has encouraged us to pursue the potential role of two of these, psoriasin (9) and lumican (10) in invasion.

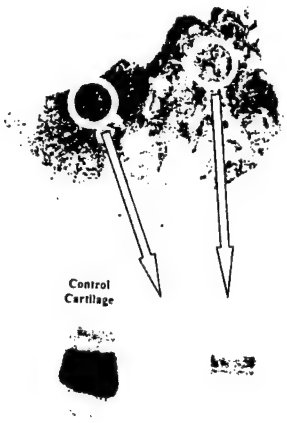

Fig 1. Microdissection and Western blot analysis of lumican protein expression within 1-2mm diameter regions within a frozen breast tumor section that shows discordance with the high (left) and low (right) levels of mRNA expression in eacl region (indicated by density of black grains), as determined by in-situ hybridization applied to a paraffin section of a mirror image block (shown above).

Psoriasin (S100 A7), a member of the S100 calcium binding protein family (11) is differentially expressed in DCIS vs invasive epithelial components. Expression is relatively low or undetectable in normal & proliferative lesions, high in DCIS, but low in invasive carcinomas (9). Furthermore, its potential capability to influence cell motility (12) is compatible with the hypothesis that altered expression may be a marker of invasiveness. Lumican is a small leucine-rich proteoglycan (13), that we have also found overexpressed in the stromal component of invasive breast cancer (14). We have gone on recently to show that it is the most abundant proteoglycan within its

stromal gene family, using an adaptation of our previous techniques to extract protein from microdissected frozen sections. We have also applied microdissection coupled to Western blot to frozen tissue sections to compare lumican protein expression within regions that show different levels of mRNA expression, as determined by in-situ hybridization applied to adjacent mirror image paraffin sections (figure 1). This has clearly shown that altered lumican expression in tumors also involves abnormal protein deposition within subregions of breast tumors. Although not previously studied in tumor progression, its known role in cross linking of collagen (15) supports the hypothesis that such changes in lumican expression may influence invasiveness.

REFERENCES

1. Hiller T., L. Snell L and P. H. Watson. "Microdissection/RT-PCR analysis of gene expression" Biotechniques, 1996, 21, 38-44.
2. Kerlikowske K, Barclay J, Grady D, Sickles EA, Ernster V J Comparison of risk factors for ductal carcinoma in situ and invasive breast cancer. Natl Cancer Inst 1997, 1;89(1):76-82
3. NSABP Website http://www.nsabp.pitt.edu/BCPT_Area.html
4. Dickson, R.B. and Lippman, M.E., Molecular determinants of growth, angiogenesis and metastasis in breast cancer. Semin. Oncol., 1992, 19:286-298
5. Friedrichs K, Franke F, Lisboa BW, Kugler G, Gille I, Terpe HJ, Holzel F, Maass H, Gunthert U. CD44 isoforms correlate with cellular differentiation but not with prognosis in human breast cancer. Cancer Res 1995 15;55(22):5424-5433
6. Hole A, Belkhiri A, Snell L, Watson P. "CD44 variant expression and estrogen receptor status in breast cancer" Breast Cancer Research & Treatment, 1997, 43, 165-173,
7. O'Connell P, Pekkel V, Fuqua SA, Osborne CK, Clark GM, Allred DC Analysis of loss of heterozygosity in 399 premalignant breast lesions at 15 genetic loci. J Natl Cancer Inst 1998 6;90(9):697-703
8. Watson P.H., L. Snell and M. Parisien. "The Role of a Tumor Bank in Translational Research" Canadian Medical Association Journal, 1996,155, 281-283.
9. Leygue E., L. Snell, T. Hiller, H. Dotzlaw, K. Hole, L.C. Murphy and P.H. Watson. "Differential expression of Psoriasin Messenger mRNA between in-situ and invasive human breast carcinoma" Cancer Research, 1996, 56, 4606-4609.
10. Leygue E, Snell L, Dotzlaw H, Hole K, Hiller T, Roughley P, Watson P, Murphy L, "Expression of Lumican in human breast carcinoma" Cancer Research 1998, 58(7): 1348-1352
11. Watson PH, Leygue ER, Murphy LC. Psoriasin (S100A7). Int J Biochem Cell Biol 1998, 30(5):567-571
12. Jinquan T, Vorum H, Larsen CG, Madsen P, Rasmussen HH, Gesser B, Etzerodt M, Honore B, Celis JE, Thestrup-Pedersen K J. Psoriasin: a novel chemotactic protein. Invest Dermatol 1996 , 107(1):5-10
13. Iozzo RV: The family of the small leucine-rich proteoglycans: key regulators of matrix assembly and cellular growth. Crit Rev Biochem Mol Biol 1997, 32: 141-174
14. Chakravarti S, Magnuson T, Lass JH, Jepsen KJ, LaMantia C, Carroll H: Lumican regulates collagen fibril assembly: skin fragility and corneal opacity in the absence of lumican. J Cell Biol 1998, 141: 1277-1286

ENDOCRINE ONCOLOGY

Edited by

STEPHEN P. ETHIER, PHD

Department of Radiation Oncology,
University of Michigan Cancer Center,
Ann Arbor, MI

HUMANA PRESS
TOTOWA, NEW JERSEY

999 Riverview Drive, Suite 208
Totowa, New Jersey 07512

For additional copies, pricing for bulk purchases, and/or information about other Humana titles, contact Humana at the above address or at any of the following numbers: Tel: 973-256-1699; Fax: 973-256-8341; E-mail: humana@humanapr.com; Website: http://humanapress.com

Cover design by Patricia F. Cleary

This publication is printed on acid-free paper. ♾
ANSI Z39.48-1984 (American National Standards Institute)
Permanence of Paper for Printed Library Materials.

Due diligence has been taken by the publishers, editors, and authors of this book to assure the accuracy of the information published and to describe generally accepted practices. The contributors herein have carefully checked to ensure that the drug selections and dosages set forth in this text are accurate and in accord with the standards accepted at the time of publication. Notwithstanding, as new research, changes in government regulations, and knowledge from clinical experience relating to drug therapy and drug reactions constantly occurs, the reader is advised to check the product information provided by the manufacturer of each drug for any change in dosages or for additional warnings and contraindications. This is of utmost importance when the recommended drug herein is a new or infrequently used drug. It is the responsibility of the treating physician to determine dosages and treatment strategies for individual patients. Further it is the responsibility of the health care provider to ascertain the Food and Drug Administration status of each drug or device used in their clinical practice. The publisher, editors, and authors are not responsible for errors or omissions or for any consequences from the application of the information presented in this book and make no warranty, express or implied, with respect to the contents in this publication.

The Publisher

Printed in the United States of America. 10 9 8 7 6 5 4 3 2 1

2 Multiple Facets of Estrogen Receptor in Human Breast Cancer

Leigh C. Murphy, PHD, Etienne Leygue, PHD, Helmut Dotzlaw, PHD, Amanda Coutts, PHD, Biao Lu, MSC, Aihua Huang, MSC, and Peter H. Watson, MB

CONTENTS

INTRODUCTION
ERα AND ITS VARIANTS
ERβ AND ITS VARIANTS
EXPRESSION OF OTHER STEROID HORMONE RECEPTORS AND THEIR VARIANTS IN HUMAN BC
CONCLUSIONS AND CONTROVERSIES
ACKNOWLEDGMENTS
REFERENCES

INTRODUCTION

Estrogen is a major regulator of mammary gland development and function, and affects the growth and progression of mammary cancers *(1,2)*. In particular, the growth responsiveness of breast cancer (BC) cells to estrogen is the basic rationale for the efficacy of the so-called endocrine therapies, such as antiestrogens. Estrogens mediate their action via the estrogen receptor (ER), which belongs to the steroid/thyroid/retinoid receptor gene superfamily *(3)*. The protein products of this family are intracellular, ligand-activated transcription factors regulating the expression of several gene products, which ultimately elicit a target tissue-specific response *(4)*. Indeed, ER, together with progesterone receptor (PR), expression in human breast tumors, are important prognostic indicators, as well as markers of responsiveness to endocrine therapies *(5,6)*. However, although the majority of human BCs are thought to be initially hormone-responsive, it is well appreciated that alterations in responsiveness to estrogen occurs during breast tumorigenesis. During BC progression, some ER-positive BCs are *de novo* resistant to endocrine therapies, and of those that originally respond to antiestrogens, many develop resistance. This progression from hormonal dependence to independence is a significant clinical problem,

From: *Contemporary Endocrinology: Endocrine Oncology*
Edited by: S. P. Ethier © Humana Press Inc., Totowa, NJ

because it limits the useful of the relatively nontoxic endocrine therapies, and is associated with a more aggressive disease phenotype *(7)*. This occurs despite the continued expression of ER, and often PR *(8,9)*. The ER is pivotal in estrogen and antiestrogen action in any target cell, but the nature of the ER is clearly multifaceted.

Until recently, it was thought that only one ER gene existed. However, a novel ER, now referred to as ERβ, has recently been cloned and characterized *(10,11)*. Moreover, it has recently been shown that ERβ mRNA is expressed in both normal and neoplastic human breast tissue *(12–14)*. This suggests that ERβ may have a role in estrogen action in both normal and neoplastic human breast tissue. Furthermore, it has now become apparent that several variant mRNA species of both the classical ERα and ERβ can be expressed in human breast tissues, and may therefore have roles in estrogen and antiestrogen signal transduction *(13,15–18)*. The current data suggest that an evaluation of estrogen interaction with human breast tissue needs to include ERα, ERβ, and any variant forms of these receptors that may be expressed. The following chapter focuses on the multifaceted nature of the ER in human breast tissues.

ERα AND ITS VARIANTS

Identification of ERα Variant mRNAs in Human Breast Tissues

A large body of data has accumulated supporting the existence of ERα variants *(19,20)*. The majority of the data supporting the expression of ERα variants has been at the mRNA level. Two main structural patterns of ERα variant mRNAs have been consistently identified: the truncated ERα mRNAs *(21)* and the exon-deleted ERα mRNAs *(22)*. The truncated ERα mRNAs were originally identified, by Northern blot analysis, as fairly abundant smaller-sized mRNA species in some human BC biopsy samples *(23)*. The cDNAs of several truncated ERα mRNAs have been cloned and found to contain authentic polyadenylation signals followed by poly(A) tails. The exon-deleted ERα mRNAs have been identified mostly from reverse transcription polymerase chain reaction (RT-PCR) products, using targeted primers.

Multiple ERα variant mRNAs are often detected in individual tumor specimens. In order to determine the relative frequency and pattern of variant expression in a particular sample, an RT-PCR approach was developed that allowed the simultaneous detection of all deleted ERα variant mRNAs containing the primer annealing sites in exons 1 and 8, at levels that represent their initial relative representation in the RNA extract. Since truncated transcripts do not have exon 8 sequences, they will not be measured by this technique. Examples of the results obtained are shown (Fig. 1), and serve to illustrate that

Fig. 1. Top panel. Schematic representation of WT ERα (WT-ER) cDNA and primers allowing co-amplification of most of the described exon-deleted ERα variants. ERα cDNA contains eight different exons coding for a protein divided into structural and functional domains (A–F). Region A/B of the receptor is implicated in transactivating function (AF-1). The DNA-binding domain is located in the C region. Region E is implicated in hormone binding and another transactivating function (AF-2). 1/8U and 1/8L primers allow amplification of 1381-bp fragment corresponding to WT ERα mRNA. Co-amplification of all possible exon-deleted or -inserted variants, which contain exon 1 and 8 sequences, can occur. Amplification of the previously described ERα variant mRNAs deleted in exon 3 (D3-ER), exon 4 (D4-ER), exon 7 (D7-ER), both exons 3 and 4 (D3–4-ER), exons 2 and 3 (D2–3-ER), exons 4 and exon 7 (D4/7-ER), would generate 1264-, 1045-, 1197-, 928-, 1073-, and 861-bp fragments, respectively. **Bottom panel.** Co-amplification of WT ERα and deleted variant mRNAs in breast tumor samples. Total RNA extracted from ER-positive (+) and ER-negative (–) breast tumors was reverse-transcribed and PCR-amplified, as described *(24)*, using 1/8U

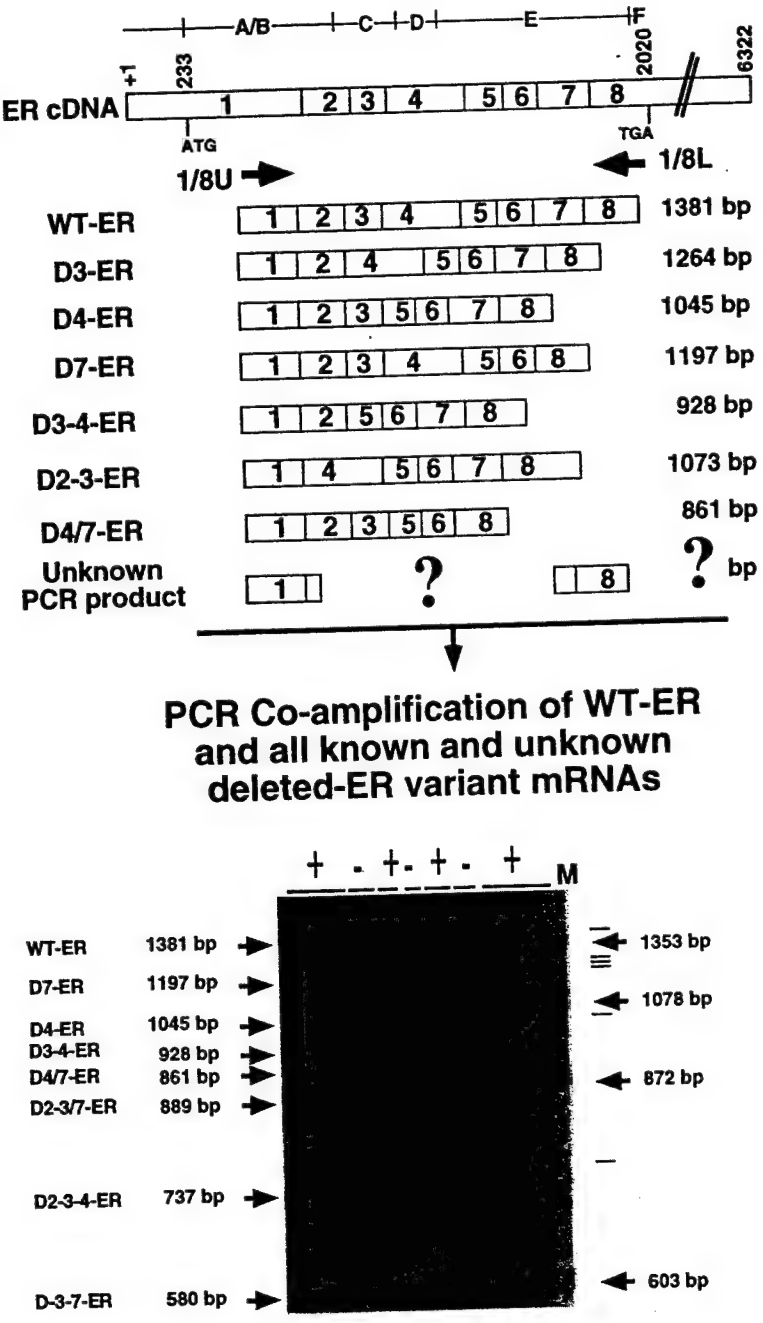

and 1/8L primers. Radioactive PCR products were separated on a 3.5% acrylamide gel, and visualized by autoradiography. Bands reproducibly obtained within the set of tumors studied, and which migrated at 1381, 1197, 1045, 928, 889, 861, 737, and 580 bp, were identified as corresponding to WT-ER mRNA and variant mRNAs deleted in exon 7 (D7-ER), exon 4 (D4-ER), both exons 3 and 4 (D3–4-ER), exons 2, 3, and 7 (D2–3/7-ER), both exons 4 and 7 (D4/7-ER), exons 2, 3, and 4 (D2–3–4-ER), and within exon 3 to within exon 7 (D-3–7-ER), respectively. PCR products indicated by dashes (-), barely detectable within the tumor population, i.e., present in less than or equal to three particular tumors, have not yet been identified. M, Molecular weight marker (phi174, Gibco-BRL, Grand Island, NY). Adapted with permission from ref. *24*.

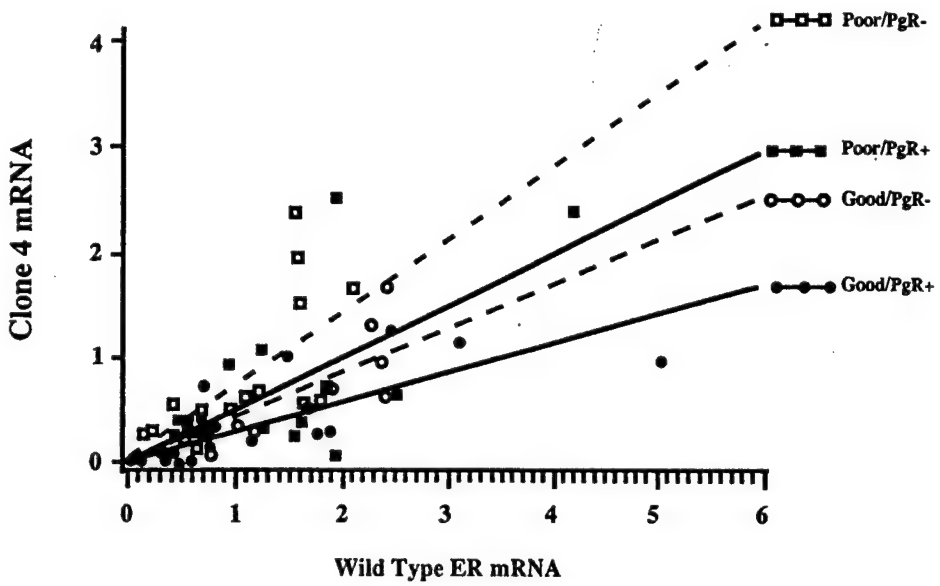

Fig. 2. Linear regression analysis of the relationship between the clone-4-truncated ERα mRNA and the WT ERα mRNA in the various groups. Closed circles represent the good prognosis/ER-positive–PR-positive group; open circles represent the good prognosis/ER-positive–PR-negative group; closed squares represent the poor prognosis/ER-positive–PR-negative group; open squares represent the poor prognosis/ER-positive–PR-negative group. Good vs Poor, $P = 0.0004$; PR-negative vs PR-positive. $P = 0.011$. Reproduced with permission from ref. *25*.

a complex pattern of exon-deleted variant ERα transcripts are expressed in any one tumor, that the pattern and relative frequency of detection of ERα variant mRNAs may vary between tumors, and that, in some cases, the relative frequency of detection of individual ERα variant mRNAs may be correlated with known prognostic markers *(24)*.

An example of such a correlation is shown in Fig. 2 *(25)*. The expression of the truncated clone-4 ERα variant mRNA was measured relative to the wild-type (WT) ERα mRNA in a group of breast tumors. The relative expression of the clone-4 variant was significantly increased in those tumors with characteristics of poor prognosis, compared to those tumors with good prognostic characteristics, i.e., clone-4 expression was higher in large tumors with high S-phase fraction, and from patients with nodal involvement, compared to small tumors with low S-phase fraction from patients without nodal involvement. Also, in this group, the relative expression of clone-4 was significantly higher in PR-negative tumors vs PR-positive tumors, suggesting a correlation of increased truncated variant expression and markers of endocrine resistance.

Data support the possibility that ERα variant proteins exist, and that their pattern and frequency are different from different individuals. In some cases, the expression of single ERα variant mRNA species was correlated with known markers of prognosis and endocrine sensitivity. This, in turn, suggested the hypothesis that altered expression of ERα variants may be a mechanism associated with progression to hormone independence.

Putative Biological Significance of ERα Variant mRNAs

Expression of ERα Variant mRNAs in Normal and Neoplastic Human Breast Tissue

Most studies investigating ERα variant mRNAs have used human BC tissues or cell lines *(19)*. However, it is now known that both truncated and exon-deleted ERα variant

mRNAs can be detected in other tissues, including normal tissues *(19)*. In particular, ERα variant mRNAs have been identified in normal human breast tissue and cells *(26–29)*. Therefore, ERα variant mRNAs are not tumor-specific, are not found in the complete absence of the WT ERα mRNA, and are probably generated by alternative splicing mechanisms.

These observations raised the question of whether the expression of ERα variant mRNAs is altered during breast tumorigenesis and/or progression. When the level of expression of individual variant ERα mRNAs was measured relative to the level of the WT ER transcript, differences between normal and breast tumor tissues were found. The relative expression of clone-4-truncated ERα variant mRNA and the exon-5-deleted ERα variant mRNA, but not the exon-7-deleted ERα variant mRNA, was significantly increased in breast tumors, compared to normal breast tissues obtained from both reduction mammoplasties and normal tissues adjacent to breast tumors *(26,27)*. Preliminary data suggests that this is also true for samples of ER-positive breast tumors and their matched, adjacent normal tissues *(29a)*; there is also evidence suggesting that an exon-3-deleted ERα variant mRNA is decreased in BCs, compared to normal human breast epithelium *(29)*. Because this ERα variant mRNA encodes a protein that can inhibit WT ERα transcriptional activity *(30)* and causes growth suppression when stably overexpressed in ER-positive MCF-7 human BC cells *(29)*, it was concluded that the exon-3-deleted ERα variant may function to attenuate estrogenic effects in normal mammary epithelium. This function is markedly reduced via decreased exon-3-deleted ERα expression during breast tumorigenesis. In preliminary studies of ER-positive human breast tumor samples and their matched adjacent normal tissues, a statistically significant decreased relative expression of the exon-3-deleted ERα mRNA in the tumor, compared to the normal breast tissues, was noted *(29a)*.

The available data provide evidence for an extensive and complex pattern of alternative splicing associated with the ERα gene, which may be altered during breast tumorigenesis.

Specificity of ERα Splice Variants in Human Breast Tumors

It is unlikely that the mechanisms generating alternatively spliced forms of ERα result from a generalized deregulation of splicing processes within breast tumors, since similar variants for the glucocorticoid receptor *(16,28)*, the retinoic acid receptors-α and -γ *(28)*, and vitamin D_3 receptor *(16)* have not been found in breast tumor tissues. However, similar splice variants of PR (*see* subheading Expression of Other Steroid Hormone Receptors, below) were found in both normal and neoplastic breast tissues *(31,32)*.

Expression of ERα Variant mRNAs During BC Progression

As described above, the relative expression of at least one ERα variant mRNA, i.e., clone-4-truncated ERα mRNA, is significantly higher in primary breast tumors with characteristics of poor prognosis (including the presence of concurrent lymph node metastases), compared to primary tumors with good prognostic markers (including lack of concurrent lymph node metastases) *(25)*. An increased relative expression of exon-5-deleted ERα mRNA has been found in locoregional BC relapse tissue (in the same breast as the original primary tumor, but no lymph node metastases) obtained from patients following a median disease-free interval of 15 mo, compared to both the corresponding primary breast tumor *(33)* and the primary breast tumor tissue of patients who did not relapse during this period. Although the difference did not reach statistical significance,

these same authors reported a trend toward higher relative expression of exon-5-deleted ERα mRNA in primary tumors of women who relapsed, compared to primary tumors of those that did not relapse. Together, these data suggest that, in addition to altered expression of ERα variant mRNA, which occurs during breast tumorigenesis, further changes in ERα variant expression may occur during BC progression. However, another study *(34)* has recently found no significant differences in the relative expression of clone-4-truncated, exon-5-deleted, and exon-7-deleted ERα mRNAs, between a series of primary breast tumors and their matched concurrent lymph node metastasis, suggesting that altered expression of ERα variant mRNAs probably occurs prior to the acquisition of the ability to metastasize, and therefore may be a marker of future metastatic potential. This hypothesis remains to be tested.

Expression of ERα Variant mRNAs and Endocrine Resistance

The hypothesis that altered forms of ERα may be a mechanism associated with endocrine resistance has been suggested for some time. Moreover, the identification of ERα variant mRNAs in human breast biopsy samples *(23,35,36)* provided good preliminary data for the hypothesis. In addition, preliminary functional data of the recombinant exon-5-deleted ERα protein suggested that it possessed constitutive, hormone-independent transcriptional activity that was about 15% that of the WT ER *(36)*. The data using a yeast expression system were also consistent with the correlation of relatively high levels of exon-5-deleted ERα mRNA in several human BC biopsy samples classified as ER-negative and PR-positive and/or pS2-positive *(36–38)*. It was also found that the exon-5-deleted ERα mRNA was often co-expressed at relatively high levels with the WT ERα in many human BC that were ER-positive *(38)*. It has been observed that transiently expressed exon-5-deleted ERα has an inhibitory effect on endogenously expressed WT ERα in MCF-7 human BC cells *(39)*, although it does not decrease the WT activity to the same extent as hydroxytamoxifen. In contrast, in human osteosarcoma cells, exon-5-deleted ERα was shown to have little effect alone, but significantly enhanced estrogen-stimulated gene expression by transiently co-expressed WT ERα *(40)*. The limitations of transient expression analysis were addressed by two groups who stably overexpressed the exon-5-deleted ERα in MCF-7 human BC cells *(41,42)*. However, different phenotypes were obtained by the two groups. No effect of the recombinant exon-5-deleted ERα on growth or estrogen/antiestrogen activity in MCF-7 cells was found in one study *(41)*; in the other study *(42)*, the overexpression of recombinant exon-5-deleted ERα in MCF-7 cells was associated with estrogen-independent and antiestrogen-resistant growth. The reasons for the differences between the two studies are unclear, but may be the result of different MCF-7 variants, or changes that could have occurred in the transfectants in addition to transgene expression. The transgene in the Rea and Parker study *(41)* was episomally maintained; in the study by Fuqua et al. *(42)*, the transgene was presumably integrated into the host chromosomes in a random fashion.

Several laboratories have developed cell culture models of estrogen independence and antiestrogen resistance. Variable results have been obtained when the association of altered ERα variant mRNA expression with estrogen/antiestrogen responsiveness was investigated. An increased relative expression of an exon-3 + 4-deleted ERα variant mRNA was found in an estrogen-independent MCF-7 cell line (T5-PRF) derived by long-term growth in estrogen-depleted medium *(43,44)*. However, this cell line was still sensitive to antiestrogens *(43)*. Although one cell line that was tamoxifen (TAM)-resistant had

differential expression of an exon-2-deleted ERα and an exon-5-deleted ERα mRNA, compared to the parental cell line *(45)*, other independently derived antiestrogen-resistant clones showed no major differences in the expression of ERα variant mRNAs *(46,47)*.

Investigation of ERα splice variants, using clinical tissue samples, has also led to variable conclusions. The relative expression of the clone-4-truncated ERα variant mRNA was significantly increased in primary breast tumors with characteristics of poor prognosis, compared to tumors with good prognostic characteristics *(25)*. Similarly, the relative expression of clone 4 was significantly higher in PR-negative vs PR-positive tumors, suggesting a correlation of increased truncated variant expression and markers of endocrine resistance *(25)*. Furthermore, an increased frequency of detection of ERα variant mRNAs deleted in exons 2–4 and 3–7 was associated with high tumor grade, but an increased detection of an exon-4-deleted ERα variant mRNA was associated with low tumor grade *(24)*. The presence of exon-5-deleted ERα mRNA was found in one study *(39)* to be associated with increased disease-free survival. However, no difference in the relative expression of an exon-5-deleted ERα variant mRNA was found between all TAM-resistant tumors and primary control breast tumors *(37)*, although, in the subgroup of TAM-resistant tumors that were ER-positive/pS2-positive, the relative expression of the exon-5-deleted ERα was significantly greater than the control TAM-sensitive group.

Although increased expression of any one ERα variant does not correlate with TAM resistance of BCs overall, its association with, and therefore possible involvement in, endocrine resistance in some tumors cannot be excluded. Moreover, the presence of multiple types of ERα variant mRNAs in any one tumor or normal tissue sample has been well documented *(24,28)*, but no data have been published in which total ERα splice variant expression has been analyzed in relationship to endocrine resistance and prognosis. Although mutations have been found in the ERα gene in human breast tumors, they are rare and are not more frequent in TAM-resistant tumors *(48)*.

Identification of ERα Variant Proteins

The detection of proteins that correspond to ERα variant mRNAs remains an important issue. It is relevant, therefore, to understand the structure of these proteins. The predicted proteins of some of the most frequently detected ERα variant transcripts are shown schematically in Fig. 3. All of the variant transcripts would encode ERα proteins missing some structural/functional domains of the WT ERα. Although the ERα variant transcripts encode several different types of protein, there are some common themes that emerge. A common feature of these putative proteins is the universal presence of the A/B region, which is known to contain the cell and promoter specific AF-1 function. Exon-4-deleted and exon-3 + 4-deleted ERα mRNAs are in frame and encode proteins that do not bind ligand. However, the majority of the most abundantly expressed variant transcripts, i.e, exon-7-deleted, an exon-4 + 7-deleted, and the clone-4-truncated ERα mRNAs, encode proteins that are C-terminally truncated, and cannot bind ligand. Thus, a common feature of these variants is the inability to bind ligand. The results obtained, in which recombinant techniques were used to measure the function of individual ERα variants in vitro, are variable, and often depend on co-expression of the WT receptor. It is difficult to make general conclusions, but many recombinant ERα variant proteins have been observed to modulate the activity of the WT receptor. However, the relevance of the relative levels of expression of WT and variant ERα proteins that are achieved under the experimental conditions used is unclear, because limited data have been published on the

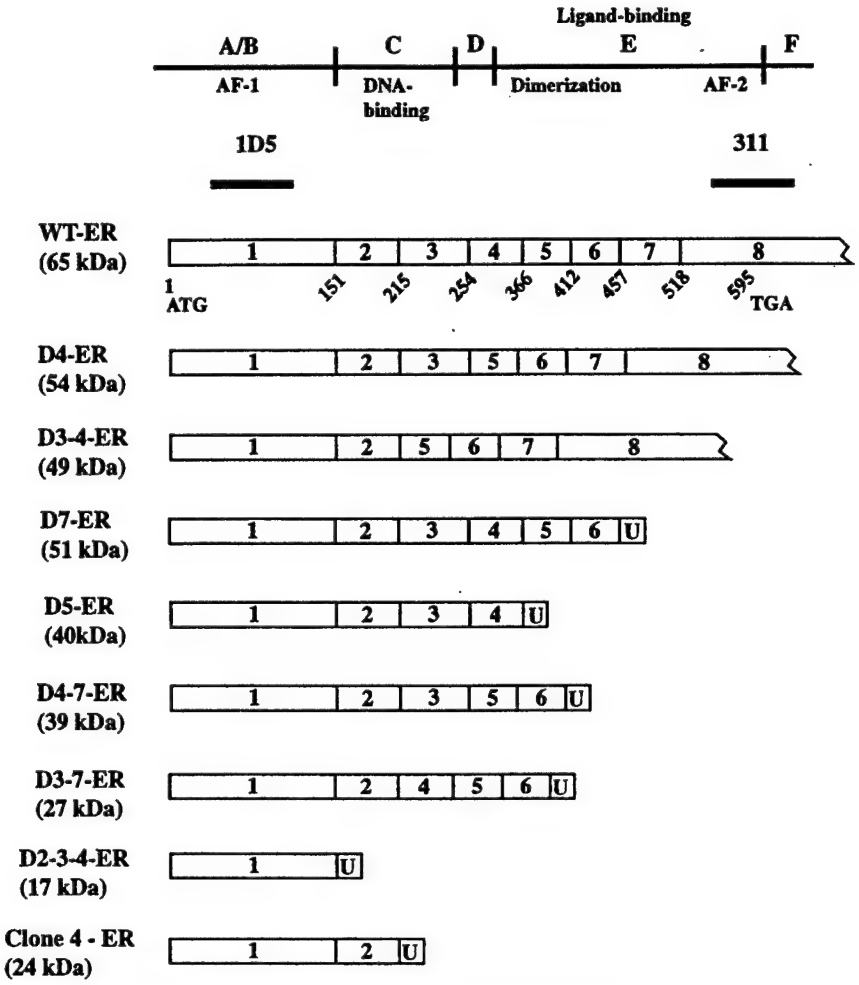

Fig. 3. Schematic representation of the ERα variant proteins predicted to be encoded by ERα variant mRNAs. Identical sequence is depicted by numbered exons. U, amino acid sequence unrelated to WT human ERα amino acid sequence. U sequences are unique to any particular variant. The position of N- and C-terminal epitopes, recognized by 1D5 and AER311 Abs, respectively, are indicated.

detection of ERα variant proteins encoded by known ERα variant mRNAs in tissues or cells in vivo.

From a different perspective, the prediction that the majority of ERα variant proteins are C-terminally truncated has implications for the determination of clinical ER status. Early detection, and changes in clinical practice, have resulted in smaller amounts of breast tumor tissue being available for assay. For this and other reasons, the use of immunohistochemistry (IHC) methods to assess ER status is becoming more common. Therefore, depending on the antibodies (Abs) used, the presence of C-terminally truncated ERα variant proteins could theoretically influence determination of ER status of the tumor sample. The authors have tested this experimentally, by transiently transfecting WT ERα and clone-4-truncated ERα expression vectors into Cos-1 cells, and determining ER status of the cells, using Abs either to the N-terminus of the ERα (Fig. 3, 1D5, Dako) or Abs to the C-terminus (Fig. 3, AER311, Neomarkers). Preliminary data, using

different combinations of WT ERα and variant ERα expression vectors transfected into Cos-1 cells, indicate that the signals (expressed as H-scores, which take into account the intensity of staining and the number of positively staining cells) obtained with the N-terminal and C-terminal Abs, become increasing discrepant (N-terminal > C-terminal signal) with increasing variant expression, presumably because of increased ERα-like proteins containing the N-terminal region, but not the C-terminal region. These preliminary data suggest that increased expression of C-terminally truncated ERα variant proteins could interfere with the IHC determination of ER status.

This possibility was investigated in human breast tumor tissues *(49)*. A series of breast tumors was assayed for ERα, using the set of Abs described above, and the H-scores from each Ab were compared for each tumor. The tumors fell into two distinct groups: one in which the H-scores obtained with each Ab were consistent and not significantly different from each other; and another group, in which the H-scores obtained with each Ab were inconsistent and significantly different from each other. Further, in all but one case, the H-score was higher for the N-terminal Ab, compared to the C-terminal Ab *(50)*. In preliminary experiments using a subset of the original tumor set, the authors found similar results, using another set of N-terminal and C-terminal ERα Abs. Together with the previous experimental data, one interpretation of the tumor data would be that the discrepant tumors had higher levels of C-terminally truncated ERα-like proteins.

To address the hypothesis that the C-terminally truncated ERα-like proteins could correspond to proteins encoded by ERα variant transcripts, the authors compared expression of ERα variant mRNAs in the consistent and inconsistent tumors. The results show a significantly higher relative expression and detection of ERα variant mRNAs that would encode C-terminally truncated proteins in the inconsistent vs the consistent tumors *(50)*. These results suggest that, irrespective of function, the expression of significant amounts of C-terminally truncated ERα variant proteins could interfere with the IHC determination of ER status, which, in turn, might underlie some of the inconsistencies between ER status and clinical response to endocrine therapy. These data are consistent with the hypothesis that ERα variant mRNAs may be stably translated in vivo. However, such data are indirect, and other mechanisms, e.g., altered epitope detection, increased proteolytic activity, and so on, may underlie the discrepant ERα H-scores found in some human breast tumors.

More recently, data published from several independent groups support the detection of ERα-like proteins in cell lines and tissues in vivo, which could correspond to those predicted to be encoded by previously identified ERα variant mRNAs. The presence of an exon-5-deleted ERα protein was demonstrated immunohistochemically in some human breast tumors, using a monoclonal Ab specific to the predicted unique C-terminal amino acids of the exon-5-deleted ERα protein *(39)*. However, although there was a correlation between IHC detection and presence or absence of exon-5-deleted ERα mRNA determined by RT-PCR, the group was unable to detect any similar protein by Western blotting, suggesting either very low levels, compared to WT ERα, or differential stability of the variant protein relative to the WT ERα during the extraction procedure. In addition, an ERα-like protein, consistent with that predicted to be encoded by the exon-5-deleted ER mRNA, is expressed in some BT 20 human BC cell lines, as determined by Western blot analysis *(51)*. Western blotting of ovarian tissue has identified both a 65-kDa WT ERα protein and a 53-kDa protein recognized by ERα Abs to epitopes in the N-terminus and C-terminus of the WT protein, but not with an Ab recognizing an epitope encoded

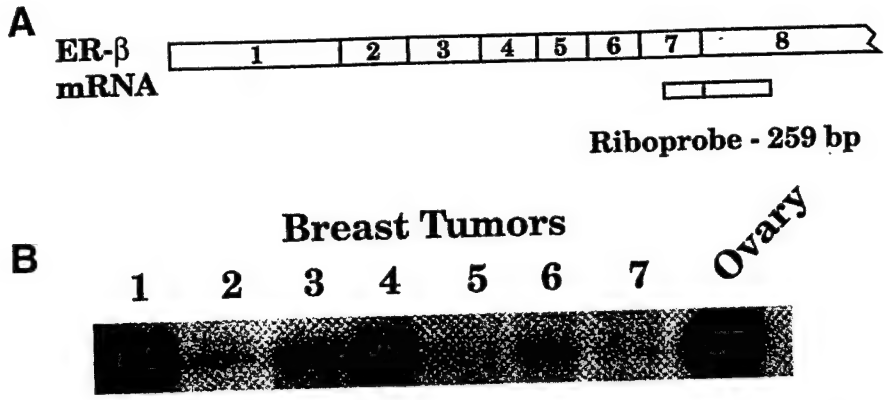

Fig. 4. Detection of ERβ mRNA in human breast tumors by RNase protection assay. (**A**) Schematic representation of hERβ mRNA showing various exon sequences, and identifying the riboprobe position and size of the expected protected fragment (259 bp). (**B**) Total RNA was isolated from seven breast tumor samples, and 25 μg was used in an RNase protection assay, as previously described *(21)*. Ovarian RNA was used as a positive control.

by exon 4 *(52)*. These results correlated with the presence of both WT and exon-4-deleted ERα mRNAs in these tissues, and suggested that the 53-kDa protein was derived from the exon-4-deleted ERα mRNA.

More recently, a 61-kDa ERα-like protein and a more abundant 65-kDa WT ERα protein were identified in MCF-7 cells *(29)*. The 61-kDa protein is thought to be encoded by an exon-3-deleted ERα mRNA expressed at low levels in these cells, and its co-migration, both before and after dephosphorylation with the recombinant exon-3-deleted ERα protein, when expressed at higher levels after stable transgene expression in another MCF-7 clone, was thought to strongly suggest its identity with the recombinant exon-3-deleted ERα protein.

There is accumulating evidence suggesting that variant ERα proteins, which correspond to those predicted to be encoded by some of the ERα variant mRNAs, can be detected by conventional technologies in clinical specimens.

ERβ AND ITS VARIANTS

Identification of ERβ mRNA in Human Breast Tissues

With the discovery of ERβ, which had properties similar to, yet distinct from, ERα *(10, 11,53,54)*, and can interact with the ERα *(55,56)*, it became important to know whether ERβ was expressed in human breast tumors, and, if so, what role it plays in estrogen/antiestrogen action.

The authors have detected the presence of ERβ mRNA, both by RT-PCR *(12,14)* and by RNase protection assay (Fig. 4; *14*), in some human BC biopsy samples and some human BC cell lines. *In situ* hybridization analysis suggested that expression of ERβ mRNA could be detected in the BC cells of a human BC biopsy sample *(14)*. Using an RT-PCR approach to analyze both ERβ and ERα mRNA expression in a range of breast tumors *(12)*, the following was observed: There was no correlation between ERβ expression and ERα expression in breast tumors; in some cases, both ERβ and ERα mRNA were expressed in the same tumor; in those tumors in which both ER mRNAs were expressed,

the relative expression appeared to vary widely among tumors. Furthermore, ERβ mRNA can be detected in normal human breast tissues by RT-PCR *(13)* and RNase protection assay *(14)*. Although there are no data reporting the expression of ERβ protein(s) in human breast tissues as yet, the available information suggest that ERβ may be expressed in both normal and neoplastic human breast tissues, and may have a role in these tissues.

Expression of ERβ mRNA During Breast Tumorigenesis

The demonstration of ERβ mRNA expression in both human breast tumors and normal human breast tissue suggests that the well-documented role of estrogen in breast tumorigenesis *(1,57)* may involve both receptors. Using a multiplex RT-PCR approach, it has been shown that the ERα:ERβ ratio in a small group of ER-positive human breast tumors was significantly higher than the ratio in their adjacent normal breast tissues *(58)*. The increase in ERα:ERβ ratio in breast tumors was primarily the result of a significant upregulation of ERα mRNA in all ER-positive tumors, in conjunction with a lower ERβ mRNA expression in the tumor, compared to the normal compartment in some, but not all, ER-positive cases. Preliminary data suggest that the level of ERβ mRNA in breast tumors may be correlated with the degree of inflammation (unpublished data). Because *in situ* hybridization data suggest that expression of ERβ mRNA could be detected in the cancer cells of a human BC biopsy sample *(14)*, and that human lymphocytes in lymph nodes can also express ERβ mRNA *(14)*, it is possible that the cell type contributing to the expression of ERβ mRNA may be heterogeneous, depending on the tumor characteristics. If the RNA studies reflect the protein levels of the two ERs, results to date provide evidence to suggest that the role of ERα- and ERβ-driven pathways, and/or their interaction, probably changes during breast tumorigenesis.

Identification of ERβ Variant mRNAs in Human Breast Tissues

The presence of multiple ERα variant mRNAs in both normal and neoplastic human breast tissues has led to the question of the expression of ERβ variant mRNAs. Several ERβ variant mRNAs have been detected. The authors have identified an exon-5 + 6-deleted ERβ mRNA in human breast tumors *(59)*. This transcript is in-frame, and would be expected to encode an ERβ-like protein deleted of 91 amino acids within the hormone binding domain. A human ERβ variant mRNA, deleted in exon 5, was identified in MDA-MB231 human BC cells and in some human breast tumor specimens *(18)*. Although that group was unable to detect an exon-5-deleted ERβ mRNA in normal human breast tissue, the authors have detected both exon-5-deleted ERβ mRNA and an exon-6-deleted ERβ mRNA, as well as an an exon-5 + 6-deleted ERβ mRNA, in normal human breast tissue samples *(13)*, and in some human breast tumors. The exon-5-deleted ERβ mRNA and the exon-6-deleted ERβ mRNA are out-of-frame and predicted to encode C-terminally truncated ERβ-like proteins, which would not bind ligand.

More recently, several exon-8-deleted human ERβ mRNAs have been identified *(17)* from a human testis cDNA library, and by RT-PCR from the human BC cell line MDA-MB435. These variants have been named human ERβ2–5. It should be noted that human ERβ2 is not the equivalent of the ERβ variant mRNA with an in-frame insertion of 54 nucleotides between exons 5 and 6 identified in rodent tissues *(13,60,61)*, and also named ERβ2. The authors have been unable to detect an equivalent of the rodent ERβ2 mRNA in any normal or neoplastic human tissue so far studied *(13)*.

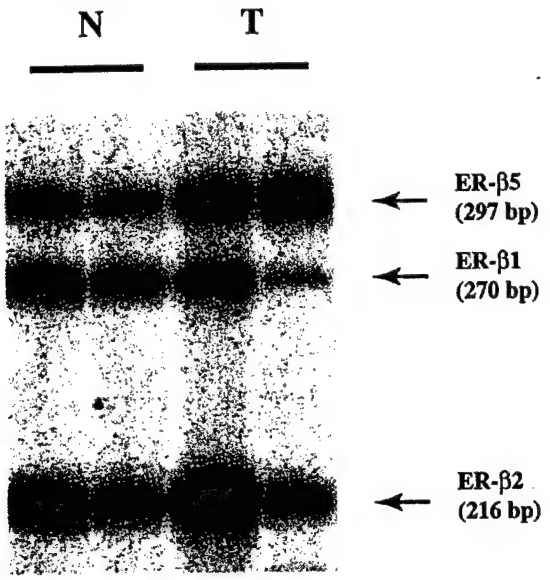

Fig. 5. RT-triple primer PCR analysis *(26)* of the relative expression of human ERβ1, human ERβ5, and human ERβ2 mRNAs in normal (N) and breast tumor (T) tissue samples.

Several of the human ERβ variants deleted in exon 8, specifically hERβ2 and hERβ5, can be detected in normal human mammary gland and in several human BC cell lines *(17)*. The predominant type of hERβ exon-8-deleted mRNA present varies among the different cell lines. The authors have confirmed the presence of the hERβ2 and the hERβ5 variant mRNAs in several normal human breast tissue samples from both reduction mammoplasties and normal tissue adjacent to breast tumors (Fig. 5; unpublished data). Moreover, the authors have identified both hERβ2 and the hERβ5 variant mRNAs in several human breast tumor samples (Fig. 5; unpublished data). Using a semiquantitative RT-triple primer PCR approach *(26)*, which simultaneously measures the relative expression of the WT hERβ1 and the two variant hERβ2 and hERβ5 mRNAs, it appears that, in most, but not all, cases, the level of the variant mRNA species exceeds that of the WT hERβ1 (Fig. 5; unpublished data) in both normal and neoplastic human breast tissues. The known sequence of all human ERβ-like transcripts is shown schematically in Fig. 6; also shown in this figure are the proteins predicted to be encoded by these variant hERβ mRNAs. All the hERβ variant mRNAs identified to date are predicted to encode proteins that are altered in the C-terminus in some fashion, and are unlikely to bind ligand *(62)*. However, published data *(17)* suggest that some of these variant receptors can form homo- or heterodimers among themselves and with WT hERβ and hERα, and may preferentially inhibit hERα DNA-binding transcriptional activity *(62)*.

Putative Role of ERβ and Its Variants in Breast Cancer

Transient transfection studies have provided data which suggest that ERβ1, i.e., the WT ERβ, can only mediate an antagonist response when bound to TAM-like agents, in contrast to the TAM-bound WT ERα, which can mediate either an antagonist or agonist activity on a basal promoter linked to a classical estrogen response element *(53,63)*. This suggests the possibility that altered relative expression of the two ERs may underlie

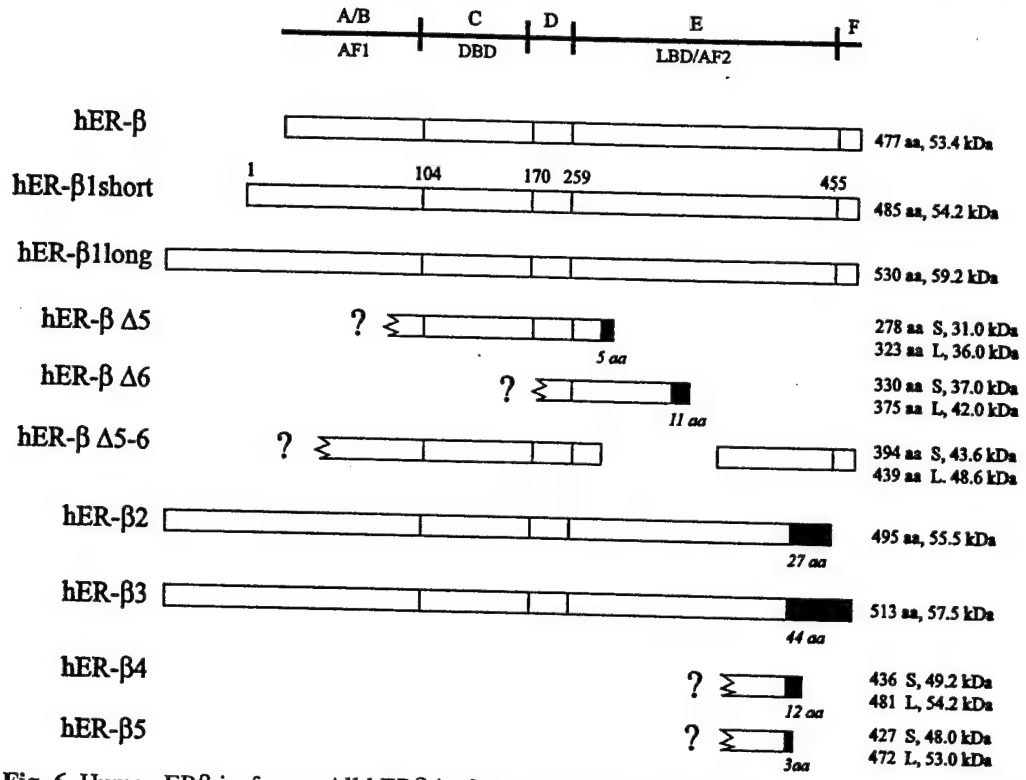

Fig. 6. Human ERβ isoforms. All hERβ isoforms are aligned. White boxes indicate identity of amino acid between sequences. Amino acid positions of the different structural domains are indicated for the hERβ1 short *(14)*, which contains eight extra N-terminal amino acids, compared to the first hERβ described *(10)*. hERβ1 long (Genbank AF051427) contains 45 additional N-terminal amino acids. hERβ1Δ5 *(13,18)*, hERβ1Δ6 *(13)*, hERβ2 (Genbank AF051428, AB006589cx), hERβ3 (Genbank AF060555), hERβ4 (Genbank AF061054), and hERβ5 (Genbank AF061055) are truncated, and contain different C-terminal amino acids (black boxes). hERβΔ5–6 *(13)* (Genbank AF074599) is missing 91 amino acids within the LBD/AF-2 domain. For each receptor, the length (aa) and the calculated molecular mass (kDa), when known or corresponding to the short (S) or the long (L) forms of the putative proteins, are given. Broken boxes and question marks indicate that flanking amino acid sequences are unknown.

altered responses to antiestrogens, and could be a mechanism of altered responsiveness to antiestrogens in human BC. The activity of the estrogen-bound ERβ1 on activating protein 1 (AP-1)-containing promoters is inhibitory, in contrast to that of estrogen-bound ERα, which stimulates transcription *(54)*. Furthermore, antiestrogens of all types demonstrated marked transcriptional activity through ERβ1 on promoters that contained AP-1 sites *(54)*. A nonligand-binding hERβ variant protein, encoded by the variant hERβ2 (also named hERβcx), can heterodimerize with ERβ1, but preferentially heterodimerizes with ERα, and shows a dominant-negative activity only against ERα-mediated transactivation *(17,62)*. It is possible, therefore, that ERβ1 and its variants could have a direct regulatory role on ERα activity. Since the authors have observed an increased ratio of ERα:ERβ mRNA in human breast tumors, compared to their adjacent matched normal tissues, which primarily results from increased expression of ERα mRNA in the breast tumor component *(58)*, it is possible that this may translate into unregulated ERα activity and unregulated growth responses mediated through ERα.

However, there are several issues that must be addressed before anyone can begin to develop rational pathophysiologically relevant hypotheses regarding the role of ERβ and/or its variants in human breast tissues. First, it is not yet known whether ERβ and ERα are expressed together in the same breast cells, or separately in different normal or neoplastic cell populations. Second, studies so far have only measured mRNA levels. No studies of ERβ protein expression in human breast have been published to date. Therefore, the pathophysiological relevance of the relative levels of ERβ and ERα expression achieved in transient expression studies, and the resulting functional outcome, are unknown. Third, some in vitro studies have been done using an N-terminally truncated ERβ1 *(64)*, and the functional impact of this is also unknown.

EXPRESSION OF OTHER STEROID HORMONE RECEPTORS AND THEIR VARIANTS IN HUMAN BC

The observation that the PR gene showed a complex pattern of alternative splicing similar to, although not as extensive as, that of ERα, led to the further characterization of PR variants *(16,31,32)*. Two commonly expressed variant transcripts identified in human breast tumors and normal human breast tissue were cloned and sequenced. Variant PR mRNAs with either a precise deletion of exon 6 or exon 4 were identified in most breast tumors examined. PR transcripts deleted in exon 2, exons 3 + 6, or exons 5 + 6, were also found in a few breast tumors *(31,32)*. The exon-6-deleted transcript was the most abundant and frequently expressed PR variant mRNA in the human breast tumors examined, and specific PCR primers were designed to determine the expression of this transcript, relative to the WT PR, using RT-PCR analysis *(27)*. Altered expression of ERα variant mRNAs was observed previously between normal and neoplastic breast tissue; therefore, it was of interest to determine if exon-6-deleted PR mRNA expression was altered during breast tumorigenesis. Using an approach similar to that described previously *(27)*, the relative expression of the exon-6-deleted variant PR mRNA to the WT PR mRNA was examined in 10 normal reduction mammoplasty samples and 17 breast tumors. The relative expression of the exon-6-deleted PR variant to the WT PR mRNA was found to be significantly lower ($P < 0.01$) in normal breast tissues (median = 4.8%) than in breast tumors (median = 13.9%) (unpublished data).

The exon-2-deleted PR mRNA encodes a C-terminally truncated PR-like protein without a DNA or a ligand-binding domain *(32)*. The exon-4-deleted PR mRNA is in-frame, but encodes a protein deleted in exon 4 sequences, missing a nuclear localization signal, and the recombinant protein representing exon-4-deleted PR-A did not bind DNA and had little effect on WT PR-A function *(32)*. Exon-6-deleted PR variant mRNA is out-of-frame and encodes a C-terminally truncated PR-like protein lacking the hormone-binding domain, and the exon-5 + 6-deleted PR variant mRNA is in-frame, but encodes a protein deleted in exon 5 + 6 sequences of the hormone-binding domain *(32)*. Richter et al. *(32)* have demonstrated that recombinant proteins, representing the exon-6-deleted PR-A and the exon-5 + 6-deleted PR-A are dominant-negative transcriptional inhibitors of both the WT PR-A and PR-B *(32)*. It is possible, therefore, that the presence of PR variant proteins encoded by the identified PR variant mRNAs could modify WT PR activity and influence responses to endocrine therapies. Small, variant PR-like proteins have been identified by Western blotting in some breast tumors *(32,65,66)*, which correspond in size to some of the proteins predicted to be encoded by some of the exon-deleted PR mRNAs. However,

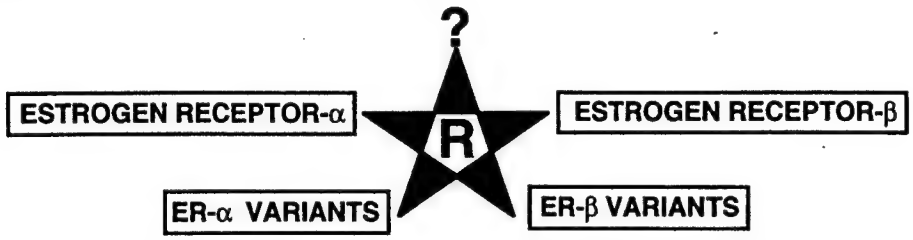

Fig. 7. Schematic representation of the known and unknown (?) multiple facets of the estrogen receptor (R).

some data *(66)* suggest that the presence and abundance of PR variant mRNAs may not correlate with the detection of these smaller-sized PR immunoreactive species in human breast tumors.

The measurement of PR is an important tool in clinical decision-making with respect to prognosis and treatment of human BC. Furthermore, the level of PR expression provides important clinical information *(67)*. As the use of enzyme-linked immunosorbent assays and IHC assays for PR detection increases, it is likely that variant PR expression will interfere with these assays, whatever their function. PR Ab (AB-52 Ab) used in such assays detect epitopes in the N-terminal region of the WT molecule, which is shared by truncated PR-like molecules. If any or all of the deleted PR variant mRNAs so far identified are translated into stable proteins, they will be co-detected with the WT PR in such assays. Presence of PR variants may also be a factor contributing to discrepancies between biochemical measurement and immunological detection of PR. Indeed, the potential for ERα variant expression to interfere with the IHC assessment of ER status has been documented *(49,50,68)*.

CONCLUSIONS AND CONTROVERSIES

The multifaceted nature of the ER is suggested by the expression of ERα mRNA, ERβ mRNA, and their variant mRNAs in both normal and neoplastic human breast tissues (Fig. 7). There is a large body of molecular data that support at least the potential for the multifaceted nature of the ER, and therefore estrogen/antiestrogen signaling in both normal and neoplastic human breast tissues. Alterations in the relative expression of several ER-like mRNAs have been shown to occur during breast tumorigenesis, and the relative frequency of detection and expression of individual ER-like mRNAs can be correlated with different prognostic characteristics in BC. This, in turn, suggests a possible role in breast tumorigenesis and possibly hormonal progression in BC. However, there are still major gaps that need to be filled before there can be a clear idea of the pathophysiological and functional relevance of the experimental results so far in hand. Unequivocal data are required to support the in vivo detection of variant ERα, variant ERβ, and WT ERβ proteins, which correspond to the variant ERα, variant ERβ, and WT ERβ mRNA species, respectively. There is a need to experimentally determine putative function, using expression levels that reflect pathophysiological levels of expression. There is a need to know if the two WT ERs and/or their variants are co-expressed in the same cells within heterogeneous normal and neoplastic breast tissues. Further, given the detection of multiple forms of variant ER-like species in any one breast tissue sample, the limitations in interpreting data from experimental systems, in which only one variant species is considered in the presence or absence of WT protein, needs to be understood.

ACKNOWLEDGMENTS

This work was supported by grants from the Canadian BC Research Initiative (CBCRI) and the U.S. Army Medical Research and Materiel Command (USAMRMC). The Manitoba Breast Tumor Bank is supported by funding from the National Cancer Institute of Canada (NCIC). LCM is a Medical Research Council of Canada (MRC) Scientist, PHW is a MRC Clinician-Scientist, EL is a recipient of a USAMRMC Postdoctoral Fellowship, AC is a recipient of a Manitoba Health Research Council (MHRC) Studentship.

REFERENCES

1. Vorherr H. Breast Cancer. Urban & Schwarzenberg, Baltimore, 1980.
2. Clarke R, Skaar T, Baumann K, Leonessa F, James M, Lippman M, et al. Hormonal carcinogenesis in breast cancer: cellular and molecular studies of malignant progression. Breast Cancer Res Treat 1994;31: 237–248.
3. Green S, Kumar V, Krust A, Walter P, Chambon P. Structural and functional domains of the estrogen receptor. Cold Spring Harbor Symp Quant Biol 1986;51:751–758.
4. Tsai MJ, O'Malley BW. Molecular mechanisms of action of steroid/thyroid receptor superfamily. Annu Rev Biochem 1994;63:451–486.
5. Horwitz KB, McGuire WL, Pearson OH, Segaloff A. Predicting response to endocrine therapy in human breast cancer: a hypothesis. Science 1975;189:726,727.
6. Horwitz K, Koseki Y, McGuire W. Estrogen control of progesterone receptor in human breast cancer: role of estradiol and antiestrogen. Endocrinology 1978;103:1742–1751.
7. Murphy L. Mechanisms associated with the progression of breast cancer from hormone dependence to independence. Pezcoller Foundation J 1995;2:6–16.
8. Taylor R, Powles T, Humphreys J, Bettelheim R, Dowsett M, Casey A, Neville A, Coombes R. Effects of endocrine therapy on steroid-receptor content of breast cancer. Br J Cancer 1982;45:80–84.
9. Katzenellenbogen B. Antiestrogen resistance: mechanisms by which breast cancer cells undermine the effectiveness of endocrine therapy. J Natl Cancer Inst 1991;83:1434,1435.
10. Mosselman S, Polman J, Dijkema R. ER-beta: identification and characterization of a novel human estrogen receptor. FEBS Lett 1996;392:49–53.
11. Kuiper G, Enmark E, Pelto-Huikko M, Nilsson S, Gustafsson J-A. Cloning of a novel estrogen receptor expressed in rat prostate and ovary. Proc Natl Acad Sci USA 1996;93:5925–5930.
12. Dotzlaw H, Leygue E, Watson P, Murphy L. Expression of estrogen receptor-beta in human breast tumors. J Clin Endocrinol Metab 1997;82:2371–2374.
13. Lu B, Leygue E, Dotzlaw H, Murphy LJ, Murphy LC, Watson PH. Estrogen receptor-beta mRNA variants in human and murine tissues. Mol Cell Endocrinol 1998;138:199–203.
14. Enmark E, Pelto-Huikko M, Grandien K, Lagercrantz S, Lagercrantz J, Fried G, Nordenskjold M, Gustafsson J-A. Human estrogen receptor β gene structure, chromosomal localization and expression pattern. J Clin Endocrinol Metab 1997;82:4258–4265.
15. Murphy L, Leygue E, Dotzlaw H, Douglas D, Coutts A, Watson P. Oestrogen receptor variants and mutations in human breast cancer. Ann Med 1997;29:221–234.
16. Murphy L, Dotzlaw H, Leygue E, Coutts A, Watson P. The Pathophysiological role of estrogen receptor variants in human breast cancer. J Steroid Biochem Mol Biol 1998;65:175–180.
17. Moore J, McKee D, Slentz-Kesler K, Moore L, Jones S, Horne E, et al. Cloning and characterization of human estrogen receptor β isoforms. Biochem Biophys Res Commun 1998;247:75–78.
18. Vladusic E, Hornby A, Guerra-Vladusic F, Lupu R. Expression of estrogen receptor β messenger RNA variant in breast cancer. Cancer Res 1998;58:210–214.
19. Murphy L, Dotzlaw H, Leygue E, Douglas D, Coutts A, Watson P. Estrogen receptor variants and mutations: a review. J Steroid Biochem Mol Biol 1997;62:363–372.
20. McGuire WL, Chamness GC, Fuqua SA. Estrogen receptor variants in clinical breast cancer. Mol Endocrinol 1991;5:1571–1577.
21. Dotzlaw H, Alkhalaf M, Murphy LC. Characterization of estrogen receptor variant mRNAs from human breast cancers. Mol Endocrinol 1992;6:773–785.
22. Fuqua SA, Allred DC, Auchus RJ. Expression of estrogen receptor variants. J Cell Biochem 1993; 17G(Suppl):194–197.

23. Murphy LC, Dotzlaw H. Variant estrogen receptor mRNA species detected in human breast cancer biopsy samples. Mol Endocrinol 1989;3:687–693.
24. Leygue E, Huang A, Murphy L, Watson P. Prevalence of estrogen receptor variant messenger RNAs in human breast cancer. Cancer Res 1996;56:4324–4327.
25. Murphy LC, Hilsenbeck SG, Dotzlaw H, Fuqua SAW. Relationship of clone 4 estrogen receptor variant messenger RNA expression to some known prognostic variables in human breast cancer. Clin Cancer Res 1995;1:155–159.
26. Leygue E, Murphy L, Kuttenn F, Watson P. Triple primer polymerase chain reaction. A new way to quantify truncated mRNA expression. Am J Pathol 1996;148:1097–1103.
27. Leygue ER, Watson PH, Murphy LC. Estrogen receptor variants in normal human mammary tissue. J Natl Cancer Inst 1996;88:284–290.
28. Pfeffer U, Fecarotta E, Vidali G. Coexpression of multiple estrogen receptor variant messenger RNAs in normal and neoplastic breast tissues and in MCF-7 cells. Cancer Res 1995;55:2158–2165.
29. Erenburg I, Schachter B, Lopez RM, Ossowski L. Loss of an estrogen receptor isoform (ER-alpha deleted 3) in breast cancer and the consequences of its reexpression: interference with estrogen-stimulated properties of malignant transformation. Mol Endocrinol 1997;11:2004–2015.
29a. Leygue E, Dotzlaw H, Watson PH, Murphy LC. Altered expression of estrogen receptor-α variant messenger RNAs between adjacent normal breast and breast tumor tissues. Breast Cancer Res 1999;51:2–10.
30. Wang Y, Miksicek RJ. Identification of a dominant negative form of the human estrogen receptor. Mol Endocrinol 1991;5:1707–1715.
31. Leygue E, Dotzlaw H, Watson PH, Murphy LC. Identification of novel exon-deleted progesterone receptor variant mRNAs in human breast tissue. Biochem Biophys Res Commun 1996;228:63–68.
32. Richter J, Lange C, Wierman A, Brooks K, Tung L, Takimoto G, Horwitz KB. Progesterone receptor variants found in breast cells repress transcription by wild type receptors. Breast Cancer Res Treat 1998; 48:231–241.
33. Gallacchi P, Schoumacher F, Eppenberger-Castori S, Landenberg EV, Kueng W, Eppenberger U, Mueller H. Increased expression of estrogen receptor exon 5 deletion variant in relapse tissues of human breast cancer. Int J Cancer 1998;79:44–48.
34. Leygue E, Hall R, Dotzlaw H, Watson P, Murphy L. Estrogen receptor-alpha variant mRNA expression in primary human breast tumors and matched lymph node metastases. Br J Cancer 1999;79:978–983.
35. Garcia T, Lehrer S, Bloomer WD, Schachter B. A variant estrogen receptor messenger ribonucleic acid is associated with reduced levels of estrogen binding in human mammary tumors. Mol Endocrinol 1988; 2:785–791.
36. Fuqua SA, Fitzgerald SD, Chamness GC, Tandon AK, McDonnell DP, Nawaz Z, O'Malley BW, McGuire WL. Variant human breast tumor estrogen receptor with constitutive transcriptional activity. Cancer Res 1991;51:105–109.
37. Daffada AA, Johnston SR, Smith IE, Detre S, King N, Dowsett M. Exon 5 deletion variant estrogen receptor messenger RNA expression in relation to tamoxifen resistance and progesterone receptor/pS2 status in human breast cancer. Cancer Res 1995;55:288–293.
38. Zhang QX, Borg A, Fuqua SA. An exon 5 deletion variant of the estrogen receptor frequently coexpressed with wild type estrogen receptor in human breast cancer. Cancer Res 1993;53:5882–5884.
39. Desai A, Luqmani Y, Coope R, Dagg B, Gomm J, Pace P, et al. Presence of exon 5 deleted oestrogen receptor in human breast cancer: functional analysis and clinical significance. Br J Cancer 1997;75: 1173–1184.
40. Chaidarun S, Alexander J. A tumor specific truncated estrogen receptor splice variant enhances estrogen stimulated gene expression. Mol Endocrinol 1998;12:1355–1366.
41. Rea D, Parker MG. Effects of an exon 5 variant of the estrogen receptor in MCF-7 breast cancer cells. Cancer Res 1996;56:1556–1563.
42. Fuqua SA, Wolf DM. Molecular aspects of estrogen receptor variants in breast cancer. Breast Cancer Res Treat 1995;35:233–241.
43. Coutts A, Davie J, Dotzlaw H, Murphy L. Estrogen regulation of nuclear matrix-intermediate filament proteins in human breast cancer cells. J Cell Biochem 1996;63:174–184.
44. Coutts A, Leygue E, Murphy L. Mechanisms of hormone independence in human breast cancer cells. Abstract. 1998. In: 88th Annual Meeting of the American Association for Cancer Research pp. 296, San Diego, CA, 1997.
45. Madsen MW, Reiter BE Lykkesfeldt AE. Differential expression of estrogen receptor mRNA splice variants in the tamoxifen resistant human breast cancer cell line, MCF-7/TAMR-1 compared to the parental MCF-7 cell line. Mol Cell Endocrinol 1995;109:197–207.

46. Madsen MW, Reiter BE, Larsen SS, Briand P, Lykkesfeldt AE. Estrogen receptor messenger RNA splice variants are not involved in antiestrogen resistance in sublines of MCF-7 human breast cancer cells. Cancer Res 1997;57:585–589.
47. Brunner N, Boysen B, Jirus S, Skaar T, Holst-Hanson C, Lippman J, et al. MCF7/LCC9: an antiestrogen resistant MCF 7 variant in which acquired resistance to the steroidal antiestrogen ICI 182780 confers an early cross resistance to the nonsteroidal antiestrogen tamoxifen. Cancer Res 1997;57:3486–3493.
48. Karnik PS, Kulkarni S, Liu XP, Budd GT, Bukowski RM. Estrogen receptor mutations in tamoxifen-resistant breast cancer. Cancer Res 1994;54:349–353.
49. Huang A, Pettigrew N, Watson P. Immunohistochemical assay for oestrogen receptors in paraffin wax sections of breast carcinoma using a new monoclonal antibody. J Pathol 1996;180:223–227.
50. Huang A, Leygue E, Snell L, Murphy L, Watson P. Expression of estrogen receptor variants mRNAs and determination of estrogen status in human breast cancer. Am J Pathol 1997;150:1827–1833.
51. Castles CG, Fuqua SA, Klotz DM, Hill SM. Expression of a constitutively active estrogen receptor variant in the estrogen receptor-negative BT-20 human breast cancer cell line. Cancer Res 1993;53:5934–5939.
52. Park W, Choi J, Hwang E, Lee J. Identification of a variant estrogen receptor lacking exon 4 and its coexpression with wild type estrogen receptor in ovarian carcinomas. Clin Cancer Res 1996;2:2029–2035.
53. Tremblay G, Tremblay A, Copeland N, Gilbert D, Jenkins N, Labrie F, Giguere V. Cloning, chromosomal localization, and functional analysis of the murine estrogen receptor β. Mol Endocrinol 1997;11: 353–365.
54. Paech K, Webb P, Kuiper G, Nilsson S, Gustafsson JA, Kushner PJ, Scanlan TS. Differential ligand activation of estrogen receptors ER alpha and ER beta at AP1 sites. Science 1997;277:1508–1510.
55. Cowley S, Hoare S, Mosselman S, Parker M. Estrogen receptors alpha and beta form heterodimers on DNA. J Biol Chem 1997;272:19,858–19,862.
56. Pettersson K, Grandien K, Kuiper GG, Gustafsson JA. Mouse estrogen receptor beta forms estrogen response element-binding heterodimers with estrogen receptor alpha. Mol Endocrinol 1997;11:1486–1496.
57. Colditz G. Relationship between estrogen levels, use of hormone replacement therapy, and breast cancer. J Natl Cancer Inst 1998;90:814–823.
58. Leygue E, Dotzlaw H, Watson P, Murphy L. Altered estrogen receptor alpha and beta mRNA expression during human breast tumorigenesis. Cancer Res 1998;58:3197–3201.
59. Leygue E, Dotzlaw H, Hare H, Watson P, Murphy L. Expression of estrogen receptor beta variant mRNAs in human breast tumors. Breast Cancer Res Treat 1997;46,48(Abstract).
60. Chu S, Fuller P. Identification of a splice variant of the rat estrogen receptor β gene. Mol Cell Endocrinol 1997;132:195–199.
61. Petersen D, Tkalcevic G, Koza-Taylor P, Turi T Brown T. Identification of estrogen receptor β2, a functional variant of estrogen receptor β expressed in normal rat tissues. Endocrinology 1998;139:1082–1092.
62. Ogawa S, Inoue S, Watanabe T, Orimo A, Hosoi T, Ouchi Y, Muramatsu M. Molecular cloning and characterization of human estrogen receptor βcx: potential inhibitor of estrogen action in human. Nucleic Acids Res 1998;26:3505–3512.
63. Watanabe T, Inoue S, Ogawa S, Ishii Y, Hiroi H, Ikeda K, Orimo A, Muramatsu M. Agonistic effect of tamoxifen is dependent on cell type, ERE-promoter context and estrogen receptor subtype: functional differences between estrogen receptors α and β. Biochem Biophys Res Commun 1997;236:140–145.
64. Leygue E, Dotzlaw H, Lu B, Glor C, Watson P, Murphy L. Estrogen receptor-beta: mine is longer than yours? J Clin Endocrinol Metab 1998;83:3754–3755.
65. Graham J, Yeates C, Balleine R, Harvey S, Milliken J, Bilou M, Clarke C. Characterization of progesterone A and B expression in human breast cancer. Cancer Res 1995;55:5063–5068.
66. Yeates C, Hunt S, Balleine R, Clarke C. Characterization of a truncated progesterone receptor protein in breast tumors. J Clin Endocrinol Metab 1998;83:460–467.
67. Clark GM, McGuire WL, Hubay CA, Pearson OH, Marshall JS. Progesterone receptors as a prognostic factor in stage II breast cancer. N Engl J Med 1983;309:1343–1347.
68. Huang A, Leygue E, Dotzlaw H, Murphy L, Watson P. Estrogen receptor-α mRNA variants influence the determination of estrogen receptor status in human breast cancer. Breast Cancer Res Treat 1999; 58:219–225.

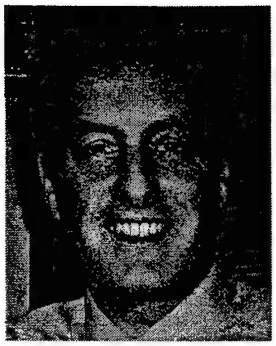

Peter Watson
Department of Pathology, University of Manitoba, D212-770 Bannatyne Ave, Winnipeg, MB R3E 0W3, Canada
Tel.: +1 204 789 3435
Fax: +1 204 789 3931
pwatson@cc.umanitoba.ca

The importance of tumor banking: bridging no-mans-land in cancer research

'A tumor bank is a collection of processed and characterized human tissues... collected and processed at the outset for and organized in such a way as to facilitate research.'

Expert Rev. Anticancer Ther. 2(1), 1–3 (2002)

Our understanding of the biology of cancer has expanded dramatically, with advances in molecular technology that enable us to accurately dissect the intracellular circuits of cell lines and animal models in the laboratory. However, these technologies have now evolved still further – in conjunction with progress in bioinformatics – such that we now have the capability to explore the genetic machinery of complex human tumors on a dramatic scale. Foremost amongst these technologies is gene structure and expression microarray. However other technologies, such as laser dissection, tissue arrays and automated immunostainers further augment the capabilities for sharply focused and high-throughput analysis that allows us to study comprehensive expression profiles peculiar to single cells or specific tumor components. The potential of these technologies is clearly applicable across a wide spectrum of cancer research. The approaches and tools of what was once considered as the separate realm of translational research have become the domain of many fields with the emergence of new areas, such as molecular diagnostics and pharmacogenomics [1,2].

However, these advances have also brought recognition of new issues. One is the urgent need to improve the access to tissue resources and the linkage between these and clinical data. Another issue is the complexity of heterogeneous tissue samples. Where once a cube of tissue labelled 'tumor' might have been an acceptable substrate, histologically defined sections and isolated cell clusters are now sought after, as research has begun to appreciate the value of exploration of subcomponents of tumors and the fine scale of some of the most important pathologies. This of course raises the human challenge of incorporating new skills into research teams and training new scientists who have the expertise to analyse tissue composition and pathology. It also raises the resource challenge of obtaining suitable tissue for research, with respect to known cellular composition, quality of tissue, and quality and maturity of associated clinical data. This challenge is perhaps all the more urgent as continued evolution in clinical practice has led to a reduction in the scope of surgery (e.g., small tissue cores instead of open biopsies) and an increase in the extent of surgical pathology examination (e.g., margin assessment) in conjunction with a changing 'ethical landscape'.

To address these resource problems we need both improved tools and public debate. Partially defined tissue samples recovered from freezers or retrospective searches through the storage facilities of clinical pathology departments for 'representative blocks' are clearly inadequate for the pace of discovery and potential advance that we now contemplate. Tumor banks are perhaps the best tool to address these challenges. A tumor bank is a collection of processed and characterized human tissues, associated pathological data

 ISSN 1473-7140

and associated or linked clinical patient data, collected and processed at the outset for and organized in such a way as to facilitate research [3]. The samples may include tumor, as well as adjacent normal tissues and blood samples and are associated with a spectrum of information obtained by analysis at the time of accrual into the bank. This information may encompass the collection time and quality, the tissue composition (histology) and the alterations within that reflect the type and stage of disease (pathology), as well as clinical information about the patient including treatment, response and ensuing state of health. Different tumor banks can and should vary in their emphasis on the spectrum of pathologies and related histological data, or the selection and consistency of the patient cohort, to serve different levels of research [4]. However, an inherent property of a tumor bank is that case material is accrued for the primary purpose of research, into a recognized and accredited structure that can provide a secure, confidential insulation and interface between the patient and the researcher. At the research interface, case material can be anonymous and untraceable, while on the clinical interface individual case material can be identifiable within the bank, allowing for maturation of the case over time by additional of essential clinical outcome information.

'A tumor bank provides a resource tool that can efficiently address the limitations of other tissue resources and can accelerate and improve the quality of cancer research'

It is important to recognize that a 'tumor bank' is different from both hospital-based 'clinical archives' and 'research study collections'. The clinical archive comprises tissues in all pathology departments and together with the clinical patient records can serve as the basis for research encompassing well developed questions and tools, such as the application of antibodies recognizing known gene targets to tissue arrays. However, access to and study of such material can be limited by the inability to efficiently select appropriate samples and cases by research criteria, the lack of standardization of pathology reporting, poor linkage between specimens and patient-related outcome data, ethical and consent issues, as well as case by case conflicts with clinical priorities. Although it is possible to transform this archive into a tumor bank or tissue array, the restricted nature of the tissue processing remains a limitation [5]. Alternatively, large prospective collection systems can been implemented to acquire and distribute fresh tissues [101]. However, without a processing and storage element these systems are necessarily limited in their capability for case selection by detailed research criteria, such as tissue composition and the capacity to add value through linked clinical data. The 'research study collection' comprises a data set designed to answer a specific research question. These are often unique collections but a major limitation stems from the fact that these are usually created without the need to commit to, or consider, a design to facilitate other applications or incorporate the capacity to release material to others. Subsequent secondary use often raises issues of ownership, oversight and accountability that are inefficient to deal with on a post-hoc basis. Research collections – as individual endeavors – can also lack the consistent involvement of the necessary clinical expertise to enhance the data quality of the resource. By contrast, a tumor bank provides a resource tool that can efficiently address the limitations of other tissue resources and can accelerate and improve the quality of cancer research.

Public debate can also address these challenges. Both clinical advances and ethical changes have been adopted to benefit individuals. However, perhaps we have not given appropriate consideration or encouraged a wider public debate, to weigh up the costs and the balance of individual *versus* collective benefit in every instance. One clinical practice example is that of new clinical guidelines for the examination of breast tissue biopsies suspected of harboring preinvasive cancer. These now encourage the processing of an entire pathological specimen into formalin-fixed paraffin-embedded tissue blocks to enhance clinical pathology examination, primarily to reduce the odds of missing a small focus of invasive cancer. However, clinical management may not necessarily be significantly altered by the additional information of a microinvasive element and examination of every 3 mm deep tissue block is still limited, by practical convention, to a single thin section from the face of the tissue block. On the other hand, the cost to the collective is to severely constrain our ability to study this critical stage of the disease of breast cancer by limiting the availability of fresh or frozen tissue specimens that might be harvested and often consigning the remaining invaluable paraffin-embedded tissue to gather dust. Similarly, new ethical standards may be necessary for the pursuit of better protection for the privacy of individuals but the balance between this benefit and the collective cost may warrant further informed debate [6,7].

Improvement in tumor bank resources is an urgent issue. However, it remains an activity that is prioritized in common with its nature, to a no-mans-land between healthcare and basic research. As a result tumor bank initiatives have for the most part emerged as time-limited isolated projects funded by research agencies and driven by research groups and end-user scientists. This format has provided most of the resources that we use today. However, these banks often suffer from lack of scale and standardization, high costs of maintaining small standalone collection systems and databases and a limited ability to capture those tissue samples related to multicenter clinical trials. Perhaps the importance of tumor banks may now be sufficient to warrant a more concentrated effort and comprehensive approach to building a better resource. For this it would seem that a far better path might lie in directly engaging the healthcare sector and specifically the discipline of clinical pathology, to incorporate tumor banking activity into the routine daily practice and mandate of term value to healthcare. It would also

require the adoption of a sustainable funding mechanism to stimulate this integration, founded on formal funding partnerships with those interested more directly in the product. The task is not trivial but the benefits of equivalent efforts to build a far-reaching resource can be seen every day within the frames of our internet browsers.

References

1 Ross JS, Greene B. Targeted therapy in oncology: the agony and ecstasy of personalized medicine. *Expert Rev. Anticancer Ther.* 1(3), 321–322 (2001).

2 Poste G. Molecular diagnostics: a powerful new component of the healthcare value chain. *Expert Rev. Mol. Diagn.* 1(1), 1–5 (2001).

3 Watson PH, Snell L, Parisien M. The NCIC-Manitoba Breast Tumor Bank: a resource for applied cancer research. *CMAJ* 155, 281–283 (1996).

4 Watson PH. Tumor tissue and clinical databanks – a review of the importance, role and future of tumor banks. *Cancer Strategy* 6, 1–6 (1999).

5 Glass AG, Donis-Keller H, Mies C *et al.* The Co-operative Breast Cancer Tissue Resource: archival tissue for the investigation of tumor markers. *Clin. Cancer Res.* 7(7), 1843–1849 (2001).

6 Dowsett M. New hurdles for translational research. *Breast Cancer Res.* 2, 241–243 (2000).

7 Prime W, Sobel ME, Herrington CS. Utilization of human tissue in breast cancer research. *Breast Cancer Res.* 2, 237–240 (2000).

Website

101 Co-operative Human Tissue Network (CHTN). http://www-chtn.ims.nci.nih.gov

Affiliation

- *Peter Watson*
  Professor and Director of the Manitoba Breast Tumor Bank
  Department of Pathology,
  University of Manitoba,
  D212-770 Bannatyne Ave,
  Winnipeg, MB R3E 0W3, Canada
  Tel.: +1 204 789 3435
  Fax: +1 204 789 3931
  pwatson@cc.umanitoba.ca

Biomed Pharmacother 2002 ; 56 : 65-77

S0753332201001573/FLA

Dossier: Steroid receptors

Steroid receptors in human breast tumorigenesis and breast cancer progression

L.C. Murphy[1]*, P. Watson[2]

[1]Manitoba Institute of Cell Biology, Dept of Biochemistry and Medical Genetics, University of Manitoba, Canada , R3E 0V9; [2]Manitoba Institute of Cell Biology, Dept of Pathology, and Medical Genetics, University of Manitoba, Winnipeg, Manitoba, Canada , R3E 0V9

(Received 17 December 2001; accepted 18 December 2001)

Summary – Steroid hormones, in particular estrogen and progesterone, play important roles in normal and neoplastic breast development. Alterations in both estrogen signaling and progesterone signaling likely occur during breast tumorigenesis and breast cancer progression. This is demonstrated by alteration of estrogen (ER) and progesterone (PR) receptor isoform expression as well as other factors such as coregulators, that can affect the activity, directly or indirectly, of in particular ER signal transduction pathways during breast tumorigenesis and breast cancer progression. A commonly emerging theme is the marked alteration of estrogen action that occurs during these processes. Since targeting ER signaling previously was successful, a better knowledge of all the molecular players involved in regulating estrogen signaling pathways and identifying changes that occur in vivo, seems critical to further exploit this previously successful approach and identify new targets for prevention and treatment of human breast cancer. © 2002 Éditions scientifiques et médicales Elsevier SAS

breast / estrogen / review

Normal development of the mammary gland is critically dependent on the ovarian steroid hormones, estrogen and progesterone [12, 37]. In addition, important roles for ovarian steroid hormones in the development of breast cancer (breast tumorigenesis) as well as the subsequent course of the disease (breast cancer progression) [35], have been assumed since it was first shown by George Beatson at the end of the 19th century that ovariectomy was useful in the treatment of premenopausal, metastatic breast cancer [8], and more recently that the antiestrogen, tamoxifen, is an effective treatment for both early and advanced breast cancer [87] and may prevent invasive breast cancer [27]. Furthermore, other steroid hormones such as androgens and vitamin D may influence breast cancer development and progression [29, 70].

*Correspondence and reprints.
E-mail address: lcmurph@cc.umanitoba.ca (L.C. Murphy).

However, changes in steroid hormone action, in particular estrogen action, occur during breast tumorigenesis and breast cancer progression. These are important clinical problems, which need to be addressed, since they impact on the effectiveness of targeting the estrogen receptor pathway, in both the prevention and treatment of breast cancer, e.g., the development of tamoxifen resistance.

Despite the importance of steroid hormones in both normal and neoplastic mammary development, and the enormous increase in basic knowledge concerning molecular mechanisms of steroid hormone action, our understanding of steroid hormone action in normal and neoplastic human mammary glands is relatively poor. This review is aimed at summarizing what is currently known about steroid receptor pathways (in particular those associated with estrogen and progesterone action) in human mammary tissues and changes that occur in these pathways during breast

tumorigenesis and breast cancer progression. Such information is necessary to yield a better understanding of alternative approaches to target estrogen signaling pathways in the prevention and treatment of breast cancer.

A GENERAL MODEL OF STEROID HORMONE ACTION IN TARGET CELLS

Steroid receptors, e.g., estrogen receptor (ER), are members of the nuclear receptor super family, many of which are ligand-responsive transcription factors, that share similarities with respect to their structural and functional properties. As shown in *figure 1*, each member of the steroid receptor family possesses a modular structure composed of i) an N-terminal region containing ligand-independent transcriptional activating functions (collectively referred to as AF-1); ii) a centrally located DNA binding domain having two zinc finger motifs; iii) a hinge region which contains signal elements for nuclear localization, possible transactivation function and coregulator binding; and iv) a ligand-binding domain in the C-terminal region of the protein containing a ligand-dependent transcriptional activating function (called AF-2) as well as a dimerization domain, a nuclear localization function and cofactor-binding domains. AF1 and AF2 can function independently or synergistically depending on the gene promoter and/or the cell type [89]. Between members of the family of steroid receptors, the N-terminal region has the highest degree of amino acid sequence variability whereas the DNA-binding domain has the most shared homology.

A schematic overview of how steroid hormones regulate function of target cells at a molecular level is shown in *figure 2*. The steroidal ligand generally enters the cell by passive diffusion and binds directly to most often an intracellular steroid receptor protein. However, the presence of membrane and possibly mitochondrially-localized steroid hormone receptors in addition to the usually cytoplasmic and/or nuclear-localized steroid receptors, has received increasing investigation and experimental support over the last few years [43]. The intracellular steroid receptor complex undergoes an activation step involving conformational changes, allowing it to dimerize and bind to specific DNA motifs called hormone-responsive elements (HRE) found in the promoters of hormone-regulated genes [89]. Activated steroid receptors may also interact indirectly with promoter regions of target genes via protein-:protein binding to other transcription factors directly bound to their specific DNA binding motifs; an example of such a transcription factor is AP-1 [38]. In turn, the receptor-DNA complexes dynamically associate with coactivators and basal transcriptional components to enhance the transcription of genes, whose mRNAs are translated into proteins that elicit specific biological responses [64]. It is likely that receptors that are not bound to their ligands, or those bound to antagonists, but also in some cases agonist-bound receptors, form complexes with co-repressors and/or other transcription factors to inhibit the transcription of specific genes [64]. Coregulators are thought to have a major role in chromatin remodeling due to either their own ability to covalently modify histones or other proteins, as well as by recruiting other integrators which have the ability to covalently modify histones and/or other proteins. In particular acetylation and deacetylation functions are thought to be important in this regard [64].

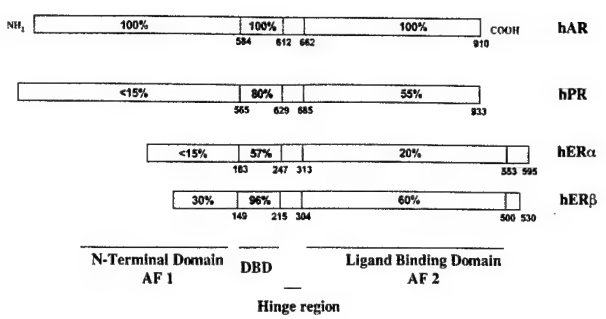

Figure 1. A comparison of the relative amino acid sequence homology within the functional domains of several members of the family of steroid hormone receptors. It should be noted that the relative amino acid sequence homology (shown by the % in the boxes) for hERβ is in reference to hERα, whereas hPR and hERα are relative to hAR. AF = transactivating function; DBD = DNA binding domain; ER = estrogen receptor; AR = androgen receptor; PR = progesterone receptor.

A MODEL OF HUMAN BREAST TUMORIGENESIS AND BREAST CANCER PROGRESSION

Clinical management and research investigation hinges on a serial model of breast tumorigenesis. This assumes that invasive carcinoma arises from the accumulation of multiple genetic defects, and that

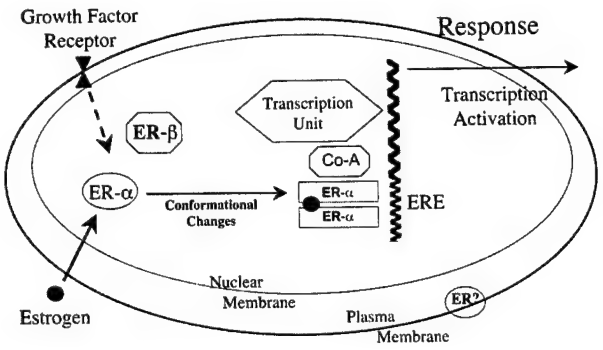

Figure 2. Schematic pathway for the molecular action of estradiol in a target cell. Both ligand (estrogen, antiestrogen)- and non-ligand (growth factor receptor pathways)-dependent activation of ER have been described. Non-genomic actions of estrogen may also be mediated via membrane-associated estrogen receptor. ER = estrogen receptor; Co-A = coactivator; Co-R = corepressor; ERE = estrogen response element.

these genetic alterations are paralleled by a series of pathological lesions that herald increasing risk of progression to invasive disease. The classification of the wide spectrum of preneoplastic and pre-invasive lesions that can be found in human breast tissue into nonproliferative disease (NPD), proliferative disease without atypia (PDWA), proliferative disease with atypia (ADH), and pre-invasive disease (DCIS), has been very useful for investigation of this model *(figure 3)* [2].

However, several limitations can be identified for consideration, as the model is reexamined in the light of new data, which may offer additional concepts to improve on the classification. First, it is clear that within ductal carcinoma in-situ (DCIS) and probably

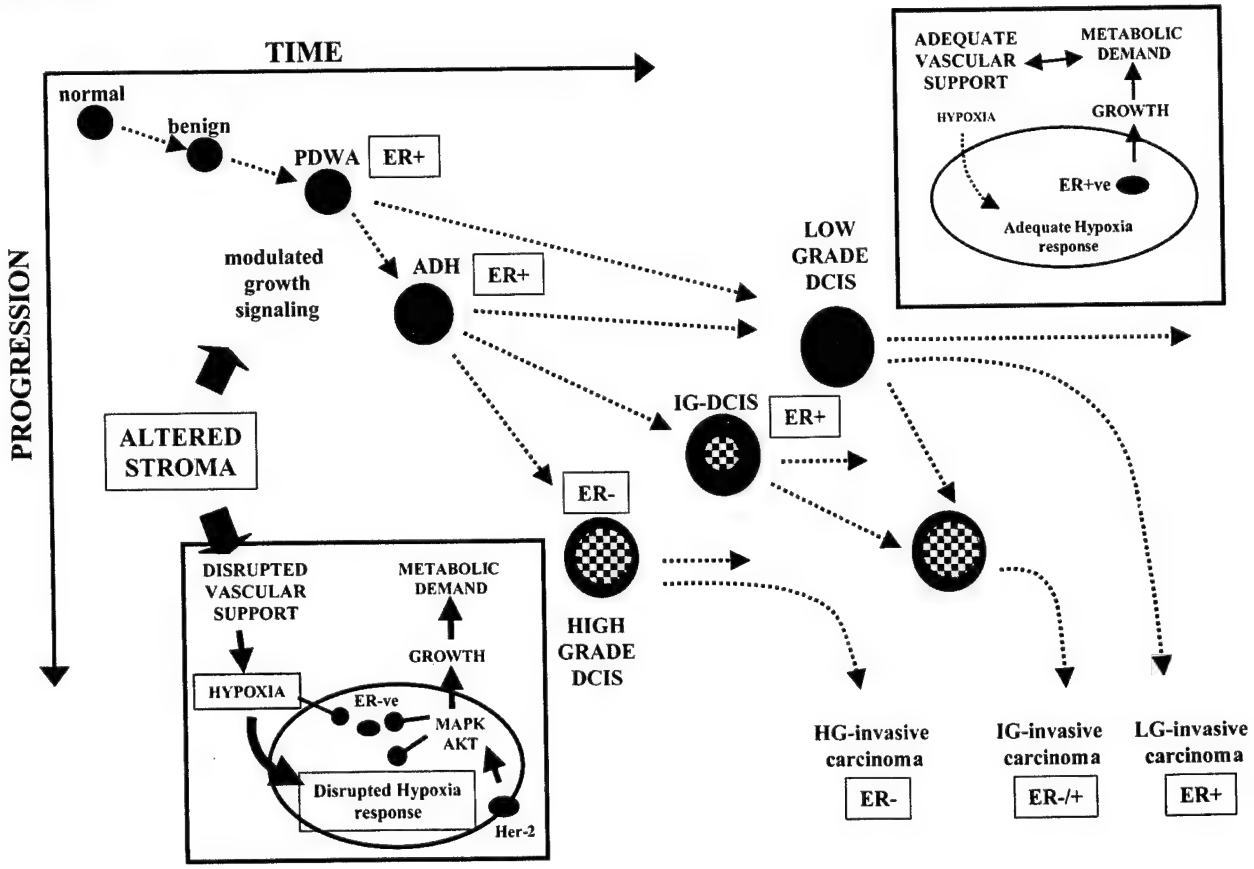

Figure 3. Model of early stages of breast tumorigenesis and the potential role of newly recognized factors, altered stroma, hypoxia, and Her2 amplification. A series of lesions defined morphologically and histopathologically are thought to represent the evolution of a normal breast epithelial cell to an invasive breast cancer = breast tumorigenesis. Other events occur after the development of invasive breast cancer that lead to breast cancer metastasis = breast cancer progression. In normal breast tissue only a minority of cells are ER-alpha positive (ER+) and estrogen action is indirect. In invasive breast cancer approximately 70% of tumors are ER+ and estrogen action is direct. LG = low grade; IG = intermediate grade; HG = high grade.

other categories, morphologically similar lesions can exhibit different biologies, providing impetus into identification of biological markers that might enhance morphological assessment [2], such as the expression of the Her-2 receptor. Second, the recognition of pathological lesions has previously focused principally on the changes within the epithelial cell component of the terminal duct lobular unit [2]. This is consistent with the central role of this cellular component and because this is the principal target of accumulated risk of invasive carcinoma. But recent work has highlighted the potential role of other cellular components that are not routinely assessed in the current pathology classification. These include the myoepithelial cells, which may exert a barrier or controlling influence [71]; the stromal fibroblasts, which are responsible for the production of many components of the extracellular matrix which can directly influence epithelial cell biology [56, 77]; and the endothelium and microvasculature, which is responsible for ensuring adequate support for metabolism [26].

For example, alteration of the extracellular matrix is a recognized component of most breast pathologies, from the fibrosis within low-risk benign non-proliferative lesions encompassed by the term 'fibrocystic changes' through typical PDWA and atypical ADH proliferative disease to the 'stromal reaction' with in-situ and invasive carcinoma. The importance of this aspect is indicated by the value of mammographic density as an independent risk factor for breast cancer, which correlates closely with increased collagenous stroma in the tissue biopsy [31]. While these stromal alterations are usually assumed to constitute a 'host reaction' to changes in adjacent epithelial cells (and influenced by paracrine interactions), stromal fibrosis and other changes also occur in the absence of defined epithelial lesions. Furthermore, specific genetic alterations may occur within breast stroma independent of those in the epithelium [48].

Alteration in the capacity of the stroma to support epithelial metabolism may also be a significant factor in the development of hypoxia in high-risk lesions (manifested by necrosis). Amongst the widespread effects of hypoxia may be a direct influence on progression and risk of invasion [22]. However, a difference also apparently often exists between the capacity of epithelial cells to survive the predicted hypoxic conditions within the central zones of large-diameter ducts of marked intraductal hyperplasia and low grade DCIS and the typical failure to survive and succumb to necrosis within the central zones of proliferations within much smaller-diameter ducts of high-grade DCIS [15, 95]. This difference in capacity to survive stress is associated with an apparent increase in local microvasculature and stimulation of angiogenesis commonly associated with high-grade DCIS with necrosis [26], so that paradoxically increased angiogenesis is associated with necrosis.

In terms of the analysis of the role of ER in early breast tumor progression, some of these additional factors may be important in interpretation of the underlying biology. In particular, there is evidence that hypoxia may have significant epigenetic effects on the ER-alpha pathway, capable of influencing both ER-alpha expression and activity in invasive breast cancer cells [47]. It is therefore possible that the loss of ER-alpha expression in high-grade comedo-type DCIS may be closely linked to the emergence of hypoxia within high-risk breast lesions. This effect may supercede the increased expression of ER-alpha and coexpression of proliferative markers in the same cells, which may characterize increasing risk in earlier stage lesions [79].

Thus, the current working model and the interpretation of molecular data might be improved in the future as the influence and capability to assess each of these additional factors is considered.

ESTROGEN SIGNALING PATHWAYS

The ER signal transduction system is of particular significance in human breast cancer. Primarily due to the successful use of the antiestrogen, tamoxifen, in the treatment of both early and advanced breast cancer [87, 88], and to the high potential of Selective Estrogen Receptor Modulators (SERMs) in the prevention of breast cancer [27]. However, given the observed changes in estrogen action during breast tumorigenesis, that approximately 50% of ER-alpha-positive breast cancers are de novo resistant to tamoxifen and that many breast cancers acquire tamoxifen resistance during progression despite the continued expression of ER-alpha, our understanding of this pathway and its regulation needs to be expanded. The following is a review of current knowledge of the estrogen signaling pathway in human breast tissues.

Estrogen receptor

The nature of ER is clearly multifaceted [32, 68], with two distinct genes encoding an estrogen receptor, i.e., ER-alpha and ER-beta, and the possible expression of several variant isoforms of each receptor generated via alternative splicing mechanisms. Available data provide evidence that ER-alpha and ER-beta have both distinct functions as well as overlapping and interactive/cooperative functions in a range of target tissues [19]. The functions of putative ER variant isoforms remain however unclear .

Estrogen receptor-alpha

One reason that estrogen action is thought to change during breast tumorigenesis is that in normal breast epithelium expression of ER-alpha protein is infrequent, with detection in the minority of ductal epithelial cells (7–17%) [74], while 70% and greater of all invasive breast cancers are ER-alpha-positive, determined by classical ligand-binding assays and immuno-assays [34]. Therefore, the expression of ER-alpha is significantly upregulated in the majority of breast cancers. How and why this occurs is unknown. In normal breast tissue no expression of ER-alpha is detected in myoepithelial cells, and until recently, and in contrast to the rodent mammary gland [21], no expression was detected in human mammary stromal cells except for one study where ER-alpha was detected in some human mammary fibroblasts enriched from reduction mammoplasties from very young women and were grown in culture for a few passages [61]. Recently the presence of ER-alpha was clearly identified immunohistochemically in a small number of human mammary extralobular (non-specialized) fibroblasts and adipocytes in breast tissue obtained from young teenage girls and pregnant woman [45]. Discrepancies with previously published data may be due to the very young age of the individuals from which the tissue came in the latter studies, since it was observed that numbers of ER-alpha-positive fibroblasts diminished with increasing complexity of the glandular tissue which occurs with increasing reproductive age [14, 45]. The expression of ER-alpha in ductal epithelial cells varies during the menstrual cycle, and generally is lower in premenopausal breast tissue than postmenopausal tissue. ER-alpha expression therefore increases with age [80], reaching a plateau after the menopause [80]. In normal breast epithelial cells, ER-alpha expression is negatively correlated with and most often not detected in the proliferating cells [18], suggesting that ER-alpha-positive cells do not proliferate or that ER-alpha is downregulated during proliferation. The data also support the concept that the proliferative effects of estrogen are indirect in the normal mammary gland [3]. This is in contrast to many ER-alpha-positive breast cancer cells where estrogen is directly mitogenic [18, 58]. However, although ER-alpha expression increases and the number of proliferating cells (Ki67-positive) decreases with increasing age, the percentage of ER-alpha-positive proliferating cells increases with age [79]. Interestingly, the expression of ER-alpha is greater in normal tissue from women with breast cancer compared to those without breast cancer [44] and is higher in breast tissue of Australian Caucasian women (high incidence of breast cancer) than Japanese women (low incidence of breast cancer) [51], both suggesting that increased ER-alpha expression in normal breast tissue is a risk factor for breast cancer.

The consistent observation that ER-alpha is markedly increased during breast tumorigenesis is supported by matched breast tumor and adjacent normal tissue studies [69] (see *figure 4*), and suggests that its expression is deregulated at some time during this process. But when does this occur? Recently data have emerged documenting ER-alpha expression in breast lesions thought to represent the evolution towards invasive breast cancer (see previous section). The percentage of cells expressing ER-alpha is moderately increased in PDWA and the relationship of ER-alpha expression to age is maintained [80]. However, ER-alpha expression is highly expressed in the majority of cells of most, if not all, ADH lesions and there is no variation with age [2, 80]. Around 75% of DCIS express ER-alpha in the majority of cells but expression is inversely correlated with increasing grade, and there is no variation of expression with age [2, 80]. As well, greater than 90% of LCIS express ER-alpha in the majority of cells [2]. The loss of age variation of ER-alpha expression in precancerous lesions that have increasing risks of breast cancer indicates increasing autonomy and altered regulation of ER-alpha expression during breast tumorigenesis [93]. The increased expression of ER-alpha in precancerous breast lesions with increasing risk of breast cancer is also correlated with increased percentage of dually

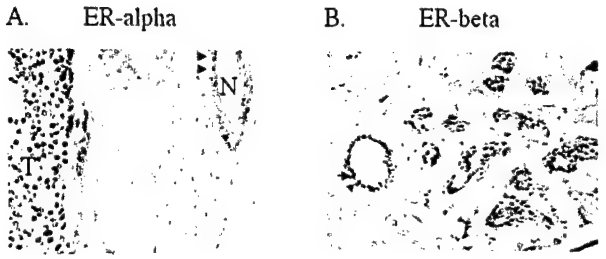

Figure 4. Estrogen receptor expression in human breast tissues using immunohistochemistry. **A.** Specific antibodies (6F11 Neomarkers) to ER-alpha were used to detect expression in a biopsy sample containing adjacent normal (N) and invasive breast cancer (T). The pink/brown staining represents ER-alpha protein, and arrows show ER+ normal breast epithelial cells. **B.** Specific antibodies to total ER-beta [76] were used to detect expression in a sample of normal human breast. Arrows show ER-beta staining in myoepithelial cells. Blue color represents counterstaining.

ER-alpha positive and Ki67-positive (proliferating) cells [79], again supporting the deregulation of estrogen action during breast tumorigenesis.

Approximately 70% of human breast tumors are ER-positive as determined by ligand binding and specific immunoassay [34]. The former assay does not distinguish between ER-alpha and -beta, but the latter assays use specific ER-alpha antibodies, which do not cross-react with ER-beta. Since there is a good correlation of ER determined by ligand binding and immunoassays [34] as well as with ER-alpha mRNA determination [6], ER-positive in most cases is due to estrogen receptor-alpha expression. However, only about 50% of the ER-positive tumors respond to endocrine therapies [73] and most are considered de novo resistant to such treatments, e.g., tamoxifen. Furthermore, of those tumors that originally respond to antiestrogen therapy, most will eventually acquire resistance to antiestrogen/endocrine therapies [73]. This occurs despite the continued expression of ER-alpha. Acquired and de novo resistance is unlikely to be due to mutations of ER-alpha, since they occur rarely and are not correlated with tamoxifen resistance [41]. Indeed, ER status of breast cancers usually does not change during progression from preinvasive DCIS to primary invasive breast cancer to metastatic breast cancer [75]. It is therefore rare that ER-negative tumors evolve from ER-positive tumors. When this occurs it is uncertain if ER expression has been extinguished in originally ER-positive breast cancer cells or whether an ER-negative population previously contained in a heterogeneous mix of ER-positive and ER-negative cells in the primary tumor, has been selected for.

Estrogen receptor-beta

Data concerning ER-beta expression during breast tumorigenesis and breast cancer progression are beginning to emerge. So far the data suggest that while expression of ER-alpha is upregulated during breast tumorigenesis, ER-beta is downregulated; however, maintenance of ER-beta expression in invasive breast cancer may be associated with proliferation markers and recurrence.

In normal human mammary epithelium ER-beta appears to be widely if not ubiquitously expressed [39, 76], consistent with previous studies in the rodent mammary gland [78]. ER-beta can be detected in most luminal epithelial cells and possibly some of the myoepithelial cells as well *(figure 4B)*. These data are consistent with studies in which ER-beta mRNA measured by RT-PCR was detected in all types of mammary epithelial cells obtained from reduction mammoplasty tissue, and sorted by flow cytometry using specific epithelial markers *(figure 5)*. In contrast and as expected, ER-alpha mRNA was infrequently detected in any of the sorted normal mammary epithelial cells *(figure 5)*. These data suggest that in normal mammary epithelium the minority of cells coexpress ER-alpha and ER-beta. However, the majority of normal human breast epithelial cells express ER-beta only. The function of ER-beta expression independent of ER-alpha is unknown, although when both receptors are coexpressed it has been speculated that ER-beta isoforms may negatively modulate ER-alpha activity [33, 72, 94] possibly via mechanisms involving heterodimerization [20, 72].

However, recent data comparing ER-positive breast tumors and their matched adjacent normal breast tissues suggest that the relative expression of ER-alpha mRNA and ER-beta mRNA is significantly different, due to a marked increase in ER-alpha expression and a decreased expression of ER-beta mRNA in tumors compared to normal tissue [52]. This supports, therefore, the hypothesis that altered expression of ER occurs during breast tumorigenesis, and may play a role in altered estrogen action occurring during this process.

More recently, the reduced expression of ER-beta in breast tumors compared to normal breast tissue

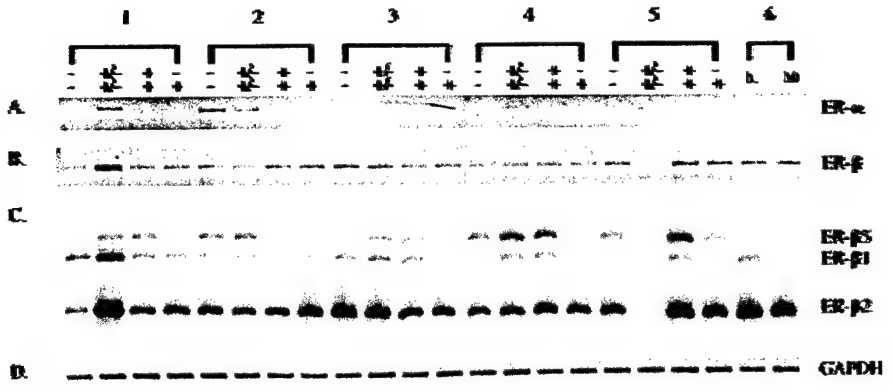

Figure 5. Normal human mammary epithelial cells obtained from reduction mammoplasties. 1–6 are cells isolated from six different patients. The cells were sorted by flow cytometry (sorted cells provided by J. Stingl) [86] on the basis of differential expression of markers alpha-6 integrin (top line), CALLA/CD10 (bottom line), as well as epithelial-specific antigen (ESA), shown to identify different epithelial populations as determined by phenotypic and functional characterization. L = luminal; M = myoepithelial enriched. RNA was extracted and analyzed for ER expression by RT-PCR using primers specific for each ER = estrogen receptor. A. ER-alpha; B. ER-beta; C. ER-beta isoforms were measured by RT and TP-PCR [53]; D. GAPDH was used as a control for equal loading of RNA amongst different samples.

has been confirmed at the protein level [76]. ER-beta protein was identified in normal breast luminal and myoepithelial cells, as well as in some of the stromal fibroblasts. ER-beta has also been detected in the stromal cells of both primary and recurrent breast cancers [40], suggesting that ER-beta may be the major ER in human breast stromal cells.

ER-beta expression in breast lesions with increasing risk of breast cancer has recently been determined [76]. As expected, the expression of total ER-beta protein, determined immunohistochemically, is high in normal and nonproliferative benign breast lesions. However, marked downregulation of ER-beta protein compared to normal tissue is seen in lesions such as PDWA, ADH and DCIS. In particular there is a significant decrease in ER-beta protein levels in high-grade DCIS compared to low-grade DCIS. ER-beta protein expression was inversely correlated with proliferation as determined by Ki67 staining. Furthermore, the ratio of ER-alpha to ER-beta expression increased in the various lesions with increasing proliferation and increasing risk of invasive breast cancer. The data provide evidence that the expression of ER-beta and ER-alpha is altered significantly and in opposite directions during breast tumorigenesis. Since it has been suggested that ER-beta isoforms may have a negative modulatory effect on ER-alpha [33, 72, 94], the downregulation of this family during breast tumorigenesis may represent a reduction of negative modulation of ER-alpha during this time.

The data available suggest that ER-beta expression varies amongst individual breast tumors. Indeed, there appear to be four classes of breast tumor: i) both estrogen receptor-beta and estrogen receptor-alpha are expressed; ii) only estrogen receptor-beta is expressed; iii) only estrogen receptor-alpha is expressed; and iv) neither receptor is expressed [24, 39, 40]. The relationship of ER-beta expression to prognostic markers remains controversial, but may reside in the different methods for determining ER-beta expression, which include protein versus RNA levels and antibodies, which detect only wild-type ER-beta [39] versus antibodies that detect total ER-beta [40, 76, 82], which includes both the wild-type protein and its various putative isoforms. In some reports ER-beta has been suggested to be correlated to good prognostic markers in breast tumors [39, 82], and in others poor prognostic markers [23, 40, 85]. Since ER-beta and ER-alpha respond differentially to antiestrogens in a cell type and promoter-specific fashion, it was speculated that altered levels of ER-beta could be associated with antiestrogen resistance in vivo. One report has suggested that total ER-beta RNA is significantly increased in a small group of tumors that later proved to be resistant to tamoxifen [84]. However, our unpublished data in a larger cohort of tumors show that the ratio of ER-alpha to ER-beta RNA is not significantly different between tamoxifen-resistant and -sensitive tumors, nor is the relative expression of any variant

isoform RNA to the wild-type RNA, and preliminary analysis suggests that these data are confirmed at the protein level using immunohistochemistry.

Estrogen receptor variant isoforms

Variant isoform expression for both ERs has mainly been investigated at the RNA level, and the expression of several variant isoform mRNAs relative to the wild-type mRNA also changes in breast tumors compared to normal breast tissue [28, 55, 57, 72]. Therefore, one aspect of estrogen signaling, i.e., the types of ERs, is significantly altered during human breast tumorigenesis, and may play a role in altered estrogen action during this process.

The mechanisms and factors regulating expression of ERs are poorly understood, therefore what mechanisms/factors are responsible for altered ER expression during breast tumorigenesis are important gaps in our knowledge to be filled, and could possibly provide alternative targets for breast cancer prevention.

Coregulators

Factors that enhance and repress receptor activity directly, namely coactivators and corepressors, are now considered to be important in mediating steroid receptor transcriptional activity [64]. As well, experimental modulation of levels of these two classes of coregulators was shown to alter steroid receptor transcriptional activity [64]. Therefore, factors other than ER-alpha levels might also be altered during breast tumorigenesis, which could enhance or deregulate ER-alpha signaling, and which may underlie alterations of estrogen responsiveness from indirect in normal breast epithelium to direct in ER-alpha positive breast tumor cells.

Several factors that can coactivate ERs are upregulated in human breast tumors compared to their matched normal breast tissues. These include SRA [69], AIB1 [59, 69], PELP1 [91], TIF2 [46] and CBP [46]. However, expression levels of a specific repressor of ER activity, REA [65], is not altered between normal breast tissues and ER-positive breast tumors [69]. Furthermore, since prothymosin-alpha is increased in breast tumors compared to normal tissues [90], and it decreases REA activity [63], REA activity is likely markedly reduced in breast tumors compared to normal breast tissue. There is also other evidence suggesting that N-CoR, another potential corepressor of the nuclear receptor family, may also be downregulated in invasive breast tumors compared to normal breast tissue [46]. Another factor which can negatively impact on ER-alpha, and which is often downregulated in breast tumors compared to normal breast tissue, is BRCA1 [97]. These studies support an upregulation of potential coactivators of ER with little change and possibly downregulation of activity of some known ER corepressors, during human breast tumorigenesis, which again could underlie altered estrogen action occurring during this process.

The altered expression of coactivators and corepressors has been shown experimentally to altered target cell responses to estrogen and antiestrogens [83]. Furthermore, reduced expression of the corepressors N-CoR and SMRT was found in an experimental model of tamoxifen resistance compared to the tamoxifen-sensitive breast cancer [50]. These findings suggested the hypothesis that altered expression of coactivators and corepressors in human breast tumors may be associated with and have a role in progression of the disease and development of antiestrogen resistance. The expression of several coactivators and corepressors has been measured in human breast tumor samples. Levels of the coregulators vary amongst tumors and in some cases can be correlated with various prognostic markers [54]. For example, REA mRNA levels are positively correlated with ER levels and negatively correlated with tumor grade [81], AIB1 mRNA levels are correlated with high grade, absence of ER or PR, high HER2/neu and p53 staining [13], although AIB1 gene amplification is more likely associated with ER/PR-positive tumors [7]. Despite these correlations there is little data on specific alterations of coregulators or the ratio of coactivators/corepressors and the prediction of antiestrogen resistance in vivo. Our own unpublished data have found no differences in the expression of SRA mRNA or AIB1 mRNA relative to REA mRNA in a small cohort of breast tumors later found to respond or not respond to tamoxifen. Interestingly, one study has identified higher levels of SRC-1 mRNA in breast tumors which later responded to tamoxifen versus those which did not respond to tamoxifen [9]. These data require parallel studies where relevant protein expression is determined. However, they also do not exclude the possibility that

altered coactivator and corepressor expression may be a mechanism associated with acquired tamoxifen resistance.

Non-classical estrogen receptors

There is increasing evidence that not all effects of steroid hormones are mediated via the regulation of genomic or transcriptional events [43]. Transcription-independent effects of estrogen manifest themselves often as rapid responses in target cells of the order of seconds to a few minutes, and are thought to be mediated by membrane-associated ERs. Little is known about such receptors in the development and progression of human breast cancer in vivo. However, such receptors were identified in MCF7 breast cancer cells in culture and growing as xenografts in nude mice. Further, data were presented that suggested they may contribute to estrogen-induced growth and survival [62]. But any contribution of membrane-associated ER to estrogen signaling in human breast tumorigenesis and progression remains to be determined.

PROGESTERONE RECEPTORS

Progesterone has a fundamental role in the normal development and function of the mammary gland [36] although its role in breast tumorigenesis and breast cancer progression is less clear [17]. It is, however, quite clear that progesterone receptors (PR) play a pivotal role in the mechanisms by which progestins effect target cells and tissues. In general, there are two isoforms of PR, PRA and PRB, generated by alternative promoter usage from the same gene, and therefore showing differential regulation of expression. PRB is identical to PRA except it contains 164 extra amino acids in its N-terminal region, which contains extra functional domains [17].

Similar to ER-alpha expression, PR expression in normal breast epithelium is detectable in only a small proportion of cells. In normal mammary epithelium, often ER-alpha and PR are coexpressed, but these cells are almost uniformly non-proliferating cells [18]. In contrast to ER-alpha expression, PR expression in the normal mammary gland does not change significantly throughout the menstrual cycle [5]. Although estrogen does induce PR expression in the epithelial component of human breast tissue implanted into nude mice [49], and PR levels appear to be decreased in postmenopausal normal breast compared to premenopausal breast tissues. Little data are available regarding PR expression in preneoplastic breast lesions but those available suggest that similar to ER-alpha expression PR expression increases in preneoplastic breast lesions [5]. One study suggests that both PR isoforms are expressed in close to 100% of PDWA and ADH breast lesions, but frequency and level of expression decreases somewhat in DCIS (65% for PRA and 75% for PRB) and invasive breast cancer (66% for PRA and 55% for PRB) [4]. This latter observation agrees with previously reported estimates of PR positivity in invasive breast cancers of 50–70% [5]. These data also suggest that the relative levels of PRA and PRB may change during breast tumorigenesis. This is an interesting observation given that PRA can function as a dominant repressor for PRB [92] and other steroid hormone receptors including ER-alpha [5], and supports the hypothesis that alteration of factors that modify ER-alpha activity occurs during human breast tumorigenesis and may have a role in altered estrogen action occurring during that process. A more recent study also demonstrates the expression of PRA and PRB in normal as well as in PDWA, ADH and DCIS breast lesions [66]. These studies demonstrate a loss of the coordinate expression of PRA and PRB in ADH, DCIS, and invasive breast cancer, with often a predominance of PRA. Further, they demonstrate a significant cell-to-cell heterogeneity of PR isoform expression in ADH and DCIS. This heterogeneity appears to precede the predominance of an isoform's expression, and in turn suggests that a marked alteration of regulation of PR isoform expression occurs during breast tumorigenesis and the possibility that altered PR isoform ratios may have a role in breast tumorigenesis.

In invasive breast cancer, PR expression is generally regarded as a marker of an intact ER signaling pathway, a better prognosis and those patients whose tumors express both ER-alpha and PR have the highest chance of responding to endocrine therapies [5]. Further those primary breast tumors that are PR-negative have a higher likelihood of metastasis, and therefore lack of PR expression is associated with more aggressive breast cancer [5]. Of interest is the observation that in PR-positive breast tumors the relative expression of PRA and PRB varies widely, with a significant proportion of tumors expressing predominantly one isoform [30]. Furthermore, other isoforms of PR distinct from PRA and PRB have been

detected in human breast tumors in vivo [30], although the significance of isoforms, distinct from PRA and PRB, remains unclear. An important impact of altered PR isoform expression in target cells is the possibility that they confer altered hormone responsiveness, which may have a role in both the development and progression of breast cancer.

OTHER STEROID HORMONE RECEPTORS AND ORPHAN RECEPTORS

Androgen receptors (AR) are expressed in normal mammary gland [21], which is also an androgen target tissue. Androgens often antagonize the effects of estrogen in mammary gland development, and could be considered to be endogenous antiestrogens under some circumstances. Interestingly, it has recently been reported that women who have AR alleles that encode for short polyglutamine tracts in the AR protein have a reduced risk of developing breast cancer [29]. Experimental studies with AR containing short polyglutamine repeats tend to show higher transcriptional activity and sensitivity to androgen [16]. Therefore, women who have such AR may be more sensitive to androgens, and since androgens have negative modulatory effects on estrogen action and growth in the breast, it is possible these more active ARs have a functional role in the protective effect against breast cancer. Interestingly, AR can be detected in the majority of human breast tumors and is strongly correlated with ER-alpha and PR expression [11]. There does not appear to be a general pattern of altered AR expression during breast tumorigenesis [10]; however, structural changes in AR have been reported to occur in some human breast tumors [11]. Androgens can both stimulate and inhibit the growth of human breast cancer cells in culture; however the mechanisms that determine these effects are not completely understood. The data are intriguing and suggest roles for AR in modulating breast tumorigenesis, and possibly breast cancer progression. However, as yet there is no clear-cut consensus concerning these roles or their mechanism.

Recent studies suggest that other steroid hormone receptors such as vitamin D receptor [70] and orphan receptors such as estrogen-receptor-related receptors [96] and PXR [25] are expressed in breast tissues and may influence estrogen and/or antiestrogen action in these tissues. However, the interactions and exact roles of these other receptors in breast tumorigenesis and breast cancer progression remain to be determined.

LIGAND-INDEPENDENT AND CROSS-TALK MECHANISMS

Ligand-independent activation of steroid hormone receptors can occur through cross-talk pathways with a variety of growth factors [32]. Growth factors such as EGF and/or IGF-1 bind to their respective tyrosine kinase receptors located in the plasma membrane of target cells and activate signal transduction pathways involving activation of other kinases. This action can lead to phosphorylation of steroid receptors and ligand-independent activation. One enzyme activated by growth factor signaling that can directly phosphorylate both ERs as well as AR is Mitogen Activated Protein Kinase (MAPK) [1, 42]. Similarly, other kinases have been shown to directly phosphorylate several steroid hormone receptors including ER-alpha and ER-beta in the absence of the appropriate steroid ligand [32]. These growth factor/phosphorylation pathways can also influence steroid hormone receptor pathways via their ability to modulate the activity of co-activators by phosphorylation [60]. Such alternative pathways for regulation of ER and other steroid hormone receptor activity could have a profound influence on breast tumorigenesis as well as the emergence of hormone independence in tumors that have not lost their steroid hormone receptors. Indeed, recent data show clearly that the active form of some of these kinases are markedly upregulated during human breast tumorigenesis and continue to be increased during breast cancer progression [67].

CONCLUSIONS

Several steroid hormones are likely to be involved in both normal and neoplastic breast development. However, estrogen signaling and therefore ERs in particular play a critical role. This is adequately supported by the clinical findings that inhibiting estrogen signaling, in particular by blocking the ER, has proved to be efficacious in both the treatment and prevention of breast cancer. It is clear however, that the current approaches are far from perfect. Further, there is evidence that estrogen action changes in breast tumorigenesis and breast cancer progression.

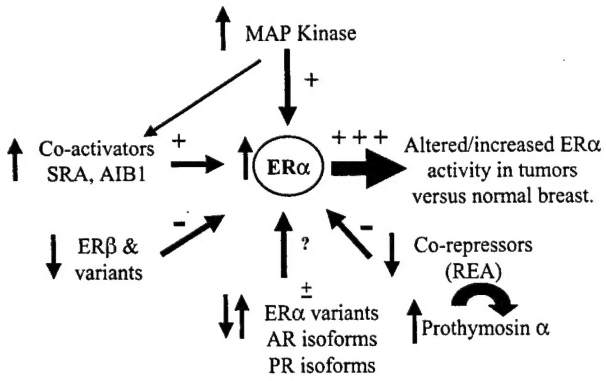

Figure 6. Summary of changes in factors that can modulate ER-alpha activity in breast tumors versus matched normal breast tissues, and therefore may have a role in altered estrogen action that occurs during breast tumorigenesis. Alterations in expression and/or activity of some of these same factors may also occur during breast cancer progression, and may have a role in that process. Upward pointing arrows represent increased expression and/or activity; downward pointing arrows represent decreased expression and/or activity.

Indeed, a common pattern that is emerging, at least during breast tumorigenesis, is that many factors are upregulated in breast tumors that have the potential to increase the activity or deregulate the activity of ER-alpha, whereas there is either no change or a decrease in factors that can negatively modulate ER-alpha activity *(figure 6)*. It is unclear how this occurs or why multiple alterations for upregulating ER-alpha activity are necessary. However, understanding all the molecular players involved in directly and indirectly regulating and modulating estrogen signaling pathways, and identifying changes that occur in vivo would seem to be critical to further exploit this previously successful approach and identify new targets for prevention and treatment of human breast cancer.

REFERENCES

1 Abreu-Martin M, Chari A, Palladino A, Craft N, Sawyers C. Mitogen-activated protein kinase 1 activates androgen receptor-dependent transcription and apoptosis in prostate cancer. Mol Cell Biol 1999 ; 19 : 5143-54.

2 Allred D, Mohsin S, Fuqua S. Histological and biological evolution of human premalignant breast disease. Endocr-Rel Cancer 2001 ; 8 : 47-61.

3 Anderson E, Clarke R, Howell A. Estrogen responsiveness and control of normal human breast proliferation. J Mammary Gland Biol Neoplasia 1998 ; 3 : 23-35.

4 Ariga A, Suzuki T, Kinura M, Onoue T, Ohuchi N, Sasano H. Progesterone receptor A and B isoforms in the human breast and its disorders. Jpn J Cancer Res 2001 ; 92 : 302-8.

5 Balleine R, Mote P, Hunt S, McGowan E, Clarke C. Progesterone receptors in normal and neoplastic breast. In: Ethier S, Ed. Endocrine oncology. Totawa, New Jersey: Humana Press; 2000. p. 35-47.

6 Barrett-Lee P, Travers M, McClelland R, Luqmani Y, Coombes R. Characterization of estrogen receptor messenger RNA in human breast cancer. Cancer Res 1987 ; 47 : 6653-9.

7 Bautista S, Valles H, Walker R, Anzick S, Zeillinger R, Meltzer P, et al. In breast cancer, amplification of the steroid receptor coactivator gene AIB1 is correlated with estrogen and progesterone receptor positivity. Clin Cancer Res 1998 ; 4 : 2925-9.

8 Beatson G. On the treatment of inoperable cases of carcinoma of the mammary gland: suggestions for a new method of treatment with illustrative cases. Lancet 1869 ; 2 : 104-7.

9 Berns E, Staveren Iv, Klign J, Foekens J. Predictive value of SRC-1 for tamoxifen response of recurrent breast cancer. Breast Cancer Res Treat 1998 ; 48 : 87-92.

10 Bieche I, Parfait B, Tozlu S, Lidereau R, Vidaud M. Quantitation of androgen receptor gene expression in sporadic breast tumors by real-time RT-PCR: evidence that MYC is an AR-regulated gene. Carcinogenesis 2001 ; 22 : 1521-6.

11 Birrell S, Hall R, Tilley W. Role of the androgen receptor in human breast cancer. J Mammary Gland Biol Neoplasia 1998 ; 3 : 95-103.

12 Bocchinfuso W, Korach K. Mammary gland development and tumorigenesis in estrogen receptor knockout mice. J Mammary Gland Biol Neoplasia 1997 ; 2 : 323-34.

13 Bouras T, Southey M, Venter D. Overexpression of the steroid receptor coactivator AIB1 in breast cancer correlates with the absence of estrogen and progesterone receptors and positivity for p53 and HER2/neu. Cancer Res 2001 ; 61 : 903-7.

14 Boyd M, Hildebrandt R, Bartow S. Expression of the estrogen receptor gene in developing and adult human breast. J Steroid Biochem Mol Biol 1996 ; 37 : 243-51.

15 Bussolati G, Bongiovanni M, Cassoni P, Sapino A. Assessment of necrosis and hypoxia in ductal carcinoma in situ of the breast: basis for a new classification. Virchows Arch 2000 ; 437 : 360-4.

16 Chamberlain N, Driver E, Miesfeld R. The length and location of CAG trinucleotide repeats in the androgen receptor N-terminal domain affect transactivation function. Nucleic Acids Res 1994 ; 22 : 3181-6.

17 Clarke C, Sutherland R. Progestin regulation of cellular proliferation. Endocr Rev 1990 ; 11 : 266-301.

18 Clarke R, Howell A, Potten C, Anderson E. Dissociation between steroid receptor expression and cell proliferation in the human breast. Cancer Res 1997 ; 57 : 4987-91.

19 Couse J, Korach K. Estrogen receptor null mice: what have we learned and where will they lead us? Endocr Rev 1999 ; 20 : 358-417.

20 Cowley S, Hoare S, Mosselman S, Parker M. Estrogen receptors alpha and beta form heterodimers on DNA. J Biol Chem 1997 ; 272 : 19858-62.

21 Cunha G, Young P, Hom Y, Cooke P, Taylor J, Lubahn D. Elucidation of a role for stromal steroid hormone receptors in mammary gland growth and development using tissue recombinants. J Mammary Gland Biol Neoplasia 1997 ; 2 : 393-402.

22 Denko N, Giaccia A. Tumor hypoxia, the physiological link between Trousseau's syndrome (carcinoma-induced coagulopathy) and metastasis. Cancer Res 2001 ; 61 : 795-8.

23 Dotzlaw H, Leygue E, Watson P, Murphy L. Estrogen receptor-ß messenger RNA expression in human breast tumor biopsies: relationship to steroid receptor status and regulation by progestins. Cancer Res 1999 ; 59 : 529-32.

24 Dotzlaw H, Leygue E, Watson P, Murphy L. Expression of estrogen receptor-beta in human breast tumors. J Clin Endocrinol Metabol 1997 ; 82 : 2371-4.

25 Dotzlaw H, Leygue E, Watson P, Murphy L. The human orphan receptor PXR messenger RNA is expressed in both normal and neoplastic breast tissue. Clin Cancer Res 1999 ; 5 : 2103-7.
26 Engels K, Fox S, Whitehouse R, Gatter K, Harris A. Distinct angiogenic patterns are associated with high-grade in situ ductal carcinomas of the breast. J Pathol 1997 ; 181 : 207-12.
27 Fisher B, Constantino J, Wickerham D, Redmond C, Kovanah M, Cronin W, et al. Tamoxifen for the prevention of breast cancer: report of the National Surgical Adjuvant Breast and Bowel Project P-1 study. J Natl Cancer Inst 1998 ; 90 : 1371-88.
28 Fuqua S, Schiff R, Parra I, Friedrichs W, Su J, McKee D, et al. Expression of wild-type estrogen receptor beta and variant isoforms in human breast cancer. Cancer Res 1999 ; 59 : 5425-8.
29 Giguere Y, Dewailly E, Brisson J, Ayotte P, Laflamme N, Demers A, et al. Short polyglutamine tracts in the androgen receptor are protective against breast cancer in the general population. Cancer Res 2001 ; 61 : 5869-74.
30 Graham JD, Yeates C, Balleine RL, Harvey SS, Milliken JS, Bilous AM, et al. Characterization of progesterone receptor A and B expression in human breast cancer. Cancer Res 1995 ; 55 : 5063-8.
31 Guo Y, Martin L, Hanna W, Banerjee D, Miller N, Fishell E, et al. Growth factors and stromal matrix proteins associated with mammographic densities. Cancer Epidemiol Biomarkers Prev 2001 ; 10 : 243-8.
32 Hall J, Couse J, Korach K. The multifaceted mechanisms of estradiol and estrogen receptor signaling. J Biol Chem 2001 ; 276 : 36869-72.
33 Hall J, McDonnell D. The estrogen receptor beta-isoform (ERbeta) of the human estrogen receptor modulates ER alpha transcriptional activity and is a key regulator of the cellular response to estrogens and antiestrogens. Endocrinology 1999 ; 140 : 5566-78.
34 Harvey J, Clark G, Osborne C, Allred D. Estrogen receptor status by immunohistochemistry is superior to the ligand binding assay for predicting response to adjuvant endocrine therapy in breast cancer. J Clin Oncol 1999 ; 17 : 1474-81.
35 Horwitz K, Clarke C. Estrogens and progestins in mammary development and neoplasia. J Mammary Gland Biol Neoplasia 1998 ; 3 : 1-103.
36 Humphreys R, Lydon J, O'Malley B, Rosen J. Mammary gland development is mediated by both stromal and epithelial progesterone receptors. Mol Endocrinol 1997 ; 11 : 801-11.
37 Humphreys R, Lydon J, O'Malley B, Rosen J. Use of the PRKO mice to study the role of progesterone in mammary gland development. J Mammary Gland Biol Neoplasia 1997 ; 2 : 343-54.
38 Jakacka M, Ito M, Weiss J, Chien PY, Gehm B, Jameson J. Estrogen receptor binding to DNA is not required for its activity through the nonclassical AP1 pathway. J Biol Chem 2001 ; 276 : 13615-21.
39 Jarvinen T, Pelto-Huikko M, Holli K, Isola J. Estrogen receptor beta is coexpressed with ER alpha and PR and associated with nodal status, grade, and proliferation rate in breast cancer. Am J Pathol 2000 ; 156 : 29-35.
40 Jensen E, Cheng G, Palmieri C, Saji S, Makela S, Noorden Sv, et al. Estrogen receptors and proliferation markers in primary and recurrent breast cancer. Proc Natl Acad Sci U S A 2001 ; e-pub : 1-6.
41 Karnik PS, Kulkarni S, Liu XP, Budd GT, Bukowski RM. Estrogen receptor mutations in tamoxifen-resistant breast cancer. Cancer Res 1994 ; 54 : 349-53.
42 Kato S, Endoh H, Masuhiro Y, Kitamoto T, Uchiyama S, Sasaki H, et al. Activation of the estrogen receptor through phosphorylation by mitogen activated protein kinase. Science 1995 ; 270 : 1491-4.
43 Kelly M, Levin E. Rapid actions of plasma membrane estrogen receptors. Trend Endocrinol Metab 2001 ; 12 : 152-6.
44 Khan SA, Rogers MA, Obando JA, Tamsen A. Estrogen receptor expression of benign breast epithelium and its association with breast cancer. Cancer Res 1994 ; 54 : 993-7.
45 Koerner F, Oyama T, Kurosumi M, Maluf H. Ovarian hormone receptors in human mammary stromal cells. J Steroid Biochem Mol Biol 2001 ; 78 : 285-320.
46 Kurebayashi J, Otsuki T, Kunisue H, Tanaka K, Yamamoto S, Sonoo H. Expression levels of estrogen receptor-α, estrogen receptor-ß, coactivators and corepressors in breast cancer. Clin Cancer Res 2000 ; 6 : 512-8.
47 Kurebayashi J, Otsuki T, Moriya T, Sonoo H. Hypoxia reduces hormone responsiveness of human breast cancer cells. Jpn J Cancer Res 2001 ; 92 : 1093-101.
48 Kurose K, Hoshaw-Woodard S, Adeyinka A, Lemeshow S, Watson P, Eng C. Genetic model of multi-step breast carcinogenesis involving the epithelium and stroma: clues to tumour-microenvironment interactions. Hum Mol Genet 2001 ; 10 : 1907-13.
49 Laidlaw I, Clarke R, Howell A, Owen A, Potten C, Anderson E. The proliferation of normal human breast tissue implanted into athymic nude mice is stimulated by estrogen but not progesterone. Endocrinology 1995 ; 136 : 164-71.
50 Lavinsky R, Jepsen K, Heinzel T, Torchia J, Mullen T, Schiff R, et al. Diverse signaling pathways modulate nuclear receptor recruitment of N-CoR and SMRT complexes. Proc Natl Acad Sci U S A 1998 ; 95 : 2920-5.
51 Lawson J, Field A, Champion S, Ishikura H, Trichopoulos D. Low oestrogen receptor alpha expression in normal breast tissue underlies low breast cancer incidence in Japan. Lancet 1999 ; 354 : 1787-8.
52 Leygue E, Dotzlaw H, Watson P, Murphy L. Altered estrogen receptor alpha and beta mRNA expression during human breast tumorigenesis. Cancer Res 1998 ; 58 : 3197-201.
53 Leygue E, Dotzlaw H, Watson P, Murphy L. Expression of estrogen receptor beta1, beta2, and beta5 messenger RNAs in human breast tissue. Cancer Res 1999 ; 59 : 1175-9.
54 Leygue E, Dotzlaw H, Watson P, Murphy L. Expression of the steroid receptor RNA activator (SRA) in human breast tumors. Cancer Res 1999 ; 59 : 4190-3.
55 Leygue E, Hall R, Dotzlaw H, Watson P, Murphy L. Estrogen receptor-alpha variant mRNA expression in primary human breast tumors and matched lymph node metastases. Br J Cancer 1998 in press.
56 Leygue E, Snell L, Dotzlaw H, Hole K, Hiller-Hitchcock T, Murphy L, et al. Lumican and decorin are differentially expressed in human breast carcinoma. J Pathol 2000 ; 192 : 313-20.
57 Leygue ER, Watson PH, Murphy LC. Estrogen receptor variants in normal human mammary tissue. J Natl Cancer Inst 1996 ; 88 : 284-320.
58 Lippman M, Bolan G. Oestrogen responsive human breast cancer in long term tissue culture. Nature 1975 ; 256 : 592-3.
59 List H, Reiter R, Singh B, Wellstein A, Riegel A. Expression of the nuclear coactivator AIB1 in normal and malignant breast tissue. Breast Cancer Res Treat 2001 ; 68 : 21-8.
60 Lopez G, Turck C, Schaufele F, Stallcup M, Kushner P. Growth factors signal to steroid receptors through mitogen-activated protein kinase regulation of p160 coactivator activity. J Biol Chem 2001 ; 276 : 22177-82.
61 Malet C, Gompel A, Yaneva H, Cren H, Fidji N, Mowszowicz I, et al. Estradiol and progesterone receptors in cultured normal human epithelial cells and fibroblasts: immunocytochemical studies. J Clin Endocrinol Metab 1991 ; 73 : 8-17.
62 Marquez D, Pietras R. Membrane-associated binding sites for estrogen contribute to growth regulation of human breast cancer cells. Oncogene 2001 ; 20 : 5420-30.

63 Martini P, Delage-Mourroux R, Kraichely D, Katzenellenbogen B. Prothymosin alpha selectively enhances estrogen receptor transcriptional activity by interacting with a repressor of estrogen receptor activity. Mol Cell Biol 2000 ; 20 : 6224-32.
64 McKenna N, Lanz R, O'Malley B. Nuclear receptor coregulators: cellular and molecular biology. Endocr Rev 1999 ; 20 : 321-44.
65 Montano M, Ekena K, Delage-Mourroux R, Chang W, Martini P, Katzenellenbogen B. An estrogen receptor-selective coregulator that potentiates the effectiveness of antiestrogens and represses the activity of estrogens. Proc Natl Acad Sci U S A 1999 ; 96 : 6947-52.
66 Mote P, Bartow S, Tram N, Clarke C. Loss of coordinate expression of progesterone receptor A and B is an early event in breast carcinogenesis. Breast Cancer Res Treat ; in press.
67 Murphy L, Adenyinka A, Nui Y, Cherlet T, Snell L, Watson P. Activated mitogen-activated protein kinase (ERK1/2) expression during human breast tumroigenesis and breast cancer progression. In: The endocrine society's 83rd annual meeting. Denver: 2001. p. P2-611.
68 Murphy L, Leygue E, Dotzlaw H, Coutts A, Lu B, Huang A, et al. Multiple facets of the estrogen receptor in human breast cancer. In: Ethier S, Ed. Endocrine oncology. Totowa, New Jersey: Humana Press; 2000. p. 17-34.
69 Murphy L, Simon S, Parkes A, Leygue E, Dotzlaw H, Snell L, et al. Altered relative expression of estrogen receptor coregulators during human breast tumorigenesis. Cancer Res 2000 ; 60 : 6266-71.
70 Narvaez C, Zinser G, Name JW. Functions of 1alpha,25-dihydroxyvitamin D(3) in mammary gland: from normal development to breast cancer. Steroids 2001 ; 66 : 301-8.
71 Nguyen M, Lee M, Wang J, Tomlinson J, Shao Z, Alpaugh M, et al. The human myoepithelial cell displays a multifaceted anti-angiogenic phenotype. Oncogene 2000 ; 19 : 3449-59.
72 Ogawa S, Inoue S, Watanabe T, Orimo A, Hosoi T, Ouchi Y, et al. Molecular cloning and characterization of human estrogen receptor bcx: potential inhibitor of estrogen action in human. Nucleic Acids Res 1998 ; 26 : 3505-12.
73 Osborne C, Elledge R, Fuqua S. Estrogen receptors in breast cancer therapy. Science Med 1996 ; 3 : 32-41.
74 Ricketts D. Estrogen and progesterone receptors in normal female breast. Cancer Res 1991 ; 51 : 1817-22.
75 Robertson J. Oestrogen receptor: a stable phenotype in breast cancer. Br J Cancer 1996 ; 73 : 5-12.
76 Roger P, Sahla M, Makela S, Gustafsson JA, Baldet P, Rochefort H. Decreased expression of estrogen receptor beta protein in proliferative preinvasive mammary tumors. Cancer Res 2001 ; 61 : 2537-41.
77 Roskelley C, Bissell M. Dynamic reciprocity revisited: a continuous, bidirectional flow of information between cells and the extracellular matrix regulates mammary epithelial cell function. Biochem Cell Biol 1995 ; 73 : 391-7.
78 Saji S, Jensen E, Nilsson S, Rylander T, Warner M, Gustafsson J- A. Estrogen receptors α and ß in the rodent mammary gland. Proc Natl Acad Sci U S A 2000 ; 97 : 337-42.
79 Shoker B, Jarvis C, Clarke R, Anderson E, Hewlett J, Davies M, et al. Estrogen receptor-positive proliferating cells in the normal and precancerous breast. Am J Pathol 1999a ; 155 : 1811-5.
80 Shoker B, Jarvis C, Sibson D, Walker C, Sloane J. Oestrogen receptor expression in the normal and precancerous breast. J Pathol 1999 ; 188 : 237-44.
81 Simon S, Parkes A, Leygue E, Dotzlaw H, Snell L, Troup S, et al. Expression of REA in human breast tumors: relationship to some known prognostic markers. Cancer Res 2000 ; 60 : 2796-9.
82 Skliris G, Carder P, Lansdown M, Speirs V. Immunohistochemistry detection of ER-beta in breast cancer: towards more detailed receptor profiling? Br J Cancer 2001 ; 84 : 1095-6.
83 Smith C, Nawaz Z, O'Malley B. Coactivator and corepressor regulation of the agonist/antagonist activity of the mixed antiestrogen, 4-hydroxytamoxifen. Mol Endocrinol 1997 ; 11 : 657-66.
84 Speirs V, Malone C, Walton D, Kerin M, Atkin S. Increased expression of estrogen receptor beta mRNA in tamoxifen-resistant breast cancer patients. Cancer Res 1999 ; 59 : 5421-4.
85 Speirs V, Parkes A, Kerin M, Walton D, Carleton P, Fox J, et al. Coexpression of estrogen receptor alpha and beta: poor prognostic factors in human breast cancer? Cancer Res 1999 ; 59 : 525-8.
86 Stingl J, Eaves C, Kuusk U, Emerman J. Phenotypic and functional characterization in vitro of a multipotent epithelial cell present in the normal adult human breast. Differentiation 1998 ; 63 : 201-13.
87 Trialists EBC. Systemic treatment of early breast cancer by hormonal, cytotoxic, or immune therapy. 133 randomised trials involving 31,000 recurrences and 24,000 deaths among 75,000 women. Early Breast Cancer Trialists' Collaborative Group. Lancet 1992 ; 339 : 1-15.
88 Trialists EBC. Tamoxifen for early breast cancer: an overview of the randomised trials. Early Breast Cancer Trialists' Collaborative Group. Lancet 1998 ; 351 : 1451-67.
89 Tsai MJ, O'Malley BW. Molecular mechanisms of action of steroid/thyroid receptor superfamily. Annu Rev Biochem 1994 ; 63 : 451-86.
90 Tsitsiloni O, Stiakakis J, Koutselinis A, Gogas J, Markopoulos G, Yialouris P, et al. Expression of alpha-thymosins in human tissues in normal and abnormal growth. Proc Natl Acad Sci U S A 1993 ; 90 : 9504-7.
91 Vadlamudi R, Wang R, Mazumdar A, Kim Y, Shin J, Sahin A, et al. Molecular cloning and characterization of PELP1, a novel human coregulator of estrogen receptor alpha. J Biol Chem 2001 ; 276 : 38272-9.
92 Vegeto E, Shahbaz MM, Wen DX, Goldman ME, O'Malley BW, McDonnell DP. Human progesterone receptor A form is a cell- and promoter-specific repressor of human progesterone receptor B function [see comments]. Mol Endocrinol 1993 ; 7 : 1244-55.
93 Walker R. Oestrogen receptor and its potential role in breast cancer development. J Pathol 1999 ; 188 : 229-30.
94 Weihua Z, Saji S. Estrogen receptor (ER) ß, a modulator of ERα in the uterus. Proc Natl Acad Sci U S A 2000 ; 97 : 5936-41.
95 Wykoff C, Beasley N, Watson P, Campo L, Chia S, English R, et al. Expression of the hypoxia-inducible and tumor-associated carbonic anhydrases in ductal carcinoma in situ of the breast. Am J Pathol 2001 ; 158 : 1011-9.
96 Yang C, Zhou D, Chen S. Modulation of aromatase expression in the breast tissue by ERR alpha-1 orphan receptor. Cancer Res 1998 ; 58 : 5695-700.
97 Zheng L, Annab L, Afshari C, Lee W, Boyer T. BRCA1 mediates ligand-independent transcriptional repression of the estrogen receptor. Proc Natl Acad Sci U S A 2001 ; 98 : 9587-92.